CHAPTER ONE

INTRODUCTION

1.1 BACKGROUND OF THE STUDY

In the last few decades, industrial wastewater and effluent treatment gained much importance. This is not unconnected with increased concern about the environmental quality. The presence of contaminants in some water bodies used for domestic and industrial processes and coupled with the strict national and international regulations on water pollution makes it imperative that industrial wastewater should be treated prior to discharge to water bodies and environs. High concentrations of contaminants like heavy metals, organic compounds, sulphates, etc, in surface water are generally associated with industrial effluents. Some of these contaminants are of special concern because they are non biodegradable, and therefore persist in the environment. Heightened awareness of the deleterious effects of industrial effluents on the environment and particularly, water bodies has resulted in an intensive research effort to identify efficient methods of effluent treatment so as to minimize the impacts. Generally, the techniques employed for the removal of pollutants include, precipitation, coagulation and flocculation, lime softening, sorption/adsorption, ion exchange and reverse osmosis or electro dialysis. Although all these techniques afford moderate to efficient industrial pollutants removal, coagulation - flocculation and adsorption or sorption on solid substrate materials (adsorbents) are preferred because of their high efficiency, easy handling, and cost-effectiveness, as well as the availability of different coagulants and adsorbents (Prasad, *et al*, 2000). The two techniques (Coag-flocculation and adsorption) will be employed simultaneously as non of them can singly achieve the required purity.

Coag-flocculation techniques are very important in wastewater treatment operations. It is employed to separate suspended solids from water. Finely dispersed solids (colloids) contained in wastewater are stabilized by electric charges on their surface, causing them to repel each other. These charges prevent the particles from colliding to form large masses called flocs. Coagulation is the destabilization of

colloids by neutralizing the forces that keep them apart. These colloids may include organic and inorganic particles (O'Melia *et al*, 1978). Several factors influence the operations between the colloids, such as attractive and repulsive forces respectively. These forces may affect the colloids in different ways depending on variation of the operation conditions like (pH, temperature, salt concentration, etc) surrounding them. The rate at which two particles approach each other depends on their static and dynamic properties (Suidan, 1988).

The most frequently occurring forces between colloids are; Van der Waal's forces, electrostatic forces and forces due to adsorbed macromolecules. In addition, specific forces may act in specific cases. For instance, magnetically or chemical bond may be found between the colloids (O'Melia et al, 1978). Some of these forces are active at long range such that their impacts are felt over several tens of nanometers. It is on this phenomenon that the fundamental principle of colloids stability is based. Chemical bonds are short range and therefore can only come into effect in the absence of long-range repulsion.

The flocculation of particles in a liquid depends on the rate of collision between particles, caused by their relative motion. This relative motion may be caused by Brownian force resulting in fluid movement, giving rise to velocity gradient or by particle motion due to an external force (e.g gravity). The rate of flocculation is determined by the collision frequency induced by the relative motion. When this collision is caused by Brownian force/movement, it is referred to as perikinetic flocculation. But, if it is by velocity gradient it is called orthokinetic flocculation. If there is no surface repulsion between the particles, then every collision leads to aggregation and the process is called rapid flocculation. If a significant repulsion exists, then only a fraction of the collision results in aggregation and in this case it is called slow flocculation.

Coagulation includes two separate and sequential stages, a collision stage followed by attachment stage (WST, 2005). The collision stage could be a product of Brownian motion, fluid shear or differential sedimentation. Brownian motion, only affecting the movement of particles (< l μ m) is the random motion of particles caused by the thermal energy surrounding liquids. Fluids shear, either laminar or turbulent, is caused by velocity gradient that occur in all real flow fluids. Differential

sedimentation is produced at a rate associated with the gravity and buoyancy forces. In this process aggregated dense and large particles can settle faster than smaller or less dense ones. (Lentech, *et al*, 2005; Thomas, *et al*, 1999).

Adsorption is an important step in many industrial processes mainly in products purification and effluents treatment. Adsorption is the adhesion of atoms, ions, or molecules from a gas, liquid or dissolved solid to a surface as a result of some attractive forces between the adsorbing surface and the substance adsorbed. This occurs only when the substance is in contact with the adsorbing surface. The substance thus adsorbed on the surface is called the adsorbate and the substance on which is adsorbed is known as adsorbent.

The extent of adsorption is largely dependent on the characteristics of the adsorbent such as surface area, particle size, porosity, residual electric charges on the adsorbent and adsorbate, capacity for aggregation, and degrees of dissociation, solubilization, and ionization. Also, the nature of transport medium which may include concentration, temperature, pH, presence of foreign ions etc, greatly influence the process of adsorption.

Based on the prevailing forces, adsorption processes can be classified as either physical (Van der Waal's adsorption) or chemisorption (activated adsorption). In physical adsorption, the individuality of the adsorbate and the adsorbent are preserved. In chemisorption, there is transfer or sharing of electron or breakage of the adsorbate into atoms or radicals which are bound separately.

The possibilities of using natural coag-flocculants and adsorbents in a view to reduce/remove organic/inorganic loads from pharmaceutical and refined vegetable oil wastewaters have been studied. This will serve as a link to improved ecological and environmental sustainability.

1.2 STATEMENT OF THE PROBLEM.

Industrial wastewater has been posing a serious threat to the world, especially the African continent where the industrial wastwater treatment technology has not been fully developed and implemented by the industrialists. The industrialists are more concerned with how to maximize profits from the investment; hence little or no attention is paid to the wastewater generated, which causes a lot of havoc to the environment. This problem is compounded by the attitudes of the

regulatory agencies to enforce the legislation. The regulatory agencies and/or the enforcement arms of the agencies have done little or nothing to enforce these laws. It could be that they lack resources or do not know the authorities and powers conferred on them by the law. It is against this backdrop, that this work was embarked upon.

Some industries are aware of the enormous environmental degradation caused by wastewater on the immediate environment to the extent that serious plans are in progress towards setting-up a wastewater treatment plant (FEPA, 1992).

The havoc caused by wastewater includes, deterioration of the soil (which makes it erosion proned), pollution of water bodies, emission of gases with pungent odor, among others. The impacts of wastewater to the environs cannot be over-emphasized in that, the drainage channels through which the wastewater passes is usually reconstructed every four months as a result of the impacts of the wastewater on the environment. This is an indication, that the nature of the wastewater is either very acid or basic (Muhammad, 2007). This work is set out to study the potentials for using different natural coag-flocculants and adsorbents in the removal/reduction of pollutants from pharmaceutical and refined vegetable oil wastewaters. The effectiveness of these natural materials will save the environment from further deterioration by the wastewaters.

1.3 AIM AND OBJECTIVES OF THE STUDY

The aim of this work is to investigate the potentials for using different local coag-flocculants and adsorbents in the removal/reduction of pollutants(Total dissolved and suspended solids-TDSS) from vegetable oil and pharmaceutical industry wastewaters. The objectives are as follows:

1. Characterization of wastewaters, coag-flocculants and adsorbents
2. Evaluation of effects of process parameters on coag-flocculation and adsorption.
3. Determination of coag-flocculation and adsorption kinetic parameters
4. Statistical modeling of coag-flocculation and adsorption via 2^3 central composite design (CCD)
5. Evaluation of adsorption isotherm and thermodynamic parameters

1.4 IMPORTANCE OF THE STUDY

Indiscriminate discharge of untreated or inadequately treated wastewater into the immediate evironment has resulted to dwindling state of our environmental health. This unwholesome act led to detrioration of the soil, destruction of the drianage systems, pollution of water bodies, emission of gases with pungent odor etc. Although, many other methods such as oxidation, solvent extraction, filtration, reverse osmosis etc, have been used for wastewater treatment, yet the health and environmental concern of synthetic organic and inorganic chemical associated with these conventional methods have made them ineffective. Thus, this brings to fore, the need to modify some agricultural waste that usually litter the streets to be employed in the areas of wastewater treatment.

Futhermore, commercially activated carbon is usually expensive because they are not produced in large quantities in Nigeria. Therefore, producing activated carbons from agricultural wastes for this purpose will definetly reduce the cost of importing them into the country as well as conserving our foreign earnings and providing an alternative means of waste reduction and reuse.

Information available from this work would promote improved efficiency in some aspects of water treatment and as well, serving as a data base for the design of relevant water treatment equipments.

1.5 SCOPE OF THE STUDY

The coag-flocculants employed for this study were sourced from seed/tuber powder of *Corchorus olitorus, Mucuna pruriens, Telfairia occidentalis, Pleurotus tuberregium sclerotium* and Shell powder of snail (*Archatinata marginata*).The availability and biodegradability nature of the materials make the usage imperative for the study. It is the supernatant from the process that is subjected to adsorption process.

The adsorbents were sourced from activated carbon derived from nuts of *Magnifera indica, seed shells of Treculia africana and Oryza sativa,* together with activated *kaolinite* and Laterite. The abundance and environmental friendliness of these materials supports their potentials for large scale utilization.

The experimental thrust is on the reduction/removal of TDSS in refined vegetable oil and pharmaceutical industry wastewaters of known characteristics via coag-flocculation and adsorption methods.

CHAPTER TWO
LITERATURE REVIEW

2.1. Theoretical Background

2.1.1. Coagulation/flocculation

In water and wastewater treatment, Coagulation/flocculation is the most conventional technique in conjunction with sedimentation and filtration to remove dissolved organic matter and for making colloids aggregate. Coagulation, is normally carried out with metal salts such as aluminum and iron salts, and much has already been done to optimize this process. The interest in the use of polymers to partially or completely replace inorganic coagulants as primary coagulants in water /waste water treatment arises from the significant inherent advantages of polymers. This is mainly based on high treatment efficiency, final coagulant dosage requirement, the reduced voluminous sludge, facilitation of filtration, health benefits and reduced level of aluminum in treated water (Gang, 2007; Bolto, 1995; Mallevialle, et al, 1984). In colloid chemistry, it is common to restrict the term coagulation to case where aggregates tend to be small and dense; flocculation is then restricted to the case where aggregates tend to be larger and more open in structure. However, in water/wastewater treatment practice, coagulation is the destabilization of colloidal particles brought about by the addition of a chemical reagent (coagulant) such that the charged particles are neutralized to enable the particles attract one another and aggregate (AWWA, 1984; Jiang and Graham, 1998; Yan, 2005, WST, 2005).

In wastewater treatment practice, the term coagulation and flocculation are not synonymous. Coagulation is used to describe the initial process whereby the original colloid dispersion is destabilized, principally by charge neutralization. It takes place in rapid mix or flash mix basins, making it very rapid . The primary function of rapid mix basin is to disperse the coagulant so that it contacts all the wastewater.Two theories have been advanced to explain basic mechanisms involved in the stability and instability of colloid systems.

Chemical theory assumes that colloids are aggregates of defined chemical structural units; it occurs because of specific chemical reactions between colloidal particles and the chemical coagulant added.

Physical theory proposes that reduction of forces tending to keep colloids apart occurs through the reduction of electrostatic forces, such as the Zeta potential. Good coagulation/flocculation and sedimentation is difficult to be achieved in wastewater treatment with the presence of high zeta potential

whilst flocculation is the agglomeration of destabilized-n-particles into micro flux and then into bulky floccules which can be called flocs. While the coagulation process destabilizes particles through chemical reactions between the coagulants and the suspended colloids, flocculation is the transport step that causes the necessary collisions, between the destabilized particles and subsequent floc aggregations or floc break up (Jin, 2005; Roussy, et al., 2004).

The purpose of flocculation is to form aggregates or flocs from the finely divided matter. The flocculation of wastewater by mechanical or air agitation may be worthy of consideration when it is desired to:

Increase the removal of suspended solids and BOD_5 in primary settling facilities.
Condition wastewater containing certain industrial wastes.
Improve the performance of secondary settling tanks, especially the activated sludge process also to increase the collisions of coagulated solids, hey agglomerate to form settleable or filterable solids. It is accomplished by prolonged agitation of coagulated particles in order to promote an increase in size and density.
It can be carried out in a separate basin of an integral part of the clarifier structure. Air flocculation is employed, the air supply system should be adjusted so that the flocculation energy level can be varied throughout the tank. In both mechanical and air agitation flocculation systems, it is a common practice to taper the energy input so that flocs initially formed will not be broken as they leave the flocculation facilities (Hutchison and Healy, 1990)

Polymers are broadly divided into three Categories based on their ionic nature: Cationic, anionic and non-ionic. Principally cationic polymers are used as primary coagulants for water treatment; anionic and nonionic polymers have gained wide acceptance as flocculants aids. Cationic can be thought of as double acting because they act in two ways: charge neutralization and bridging.

The water-soluble polymers with many repeating units or monomers, referred to as polyelectrolyte's. Polyelectrolyte's are organic macromolecules which could be synthetic organic compounds or natural organic material- as original extracts from certain plants or animals.

2.1.2 . Mechanism of coagulation/flocculation

Coagulation process is associated with different mechanisms that bring about the destablization of charged stable water medium. The various mechanisms are discussed below:

2.1.2.1. Double-layer compression

The mechanism of double-layer compression relies on compressing the diffuse layer surrounding a colloid. This is accomplished by increasing the ionic strength of the solution through the addition of an indifferent electrolyte. The added electrolyte increases the charge density in the diffuse layer. The diffused layer is compressed towards the particle surface reducing the thickness of the layer. This ensures that the Zeta potential (Zp), significantly decreased to encourage aggregation (Reynolds and Richards, 1996).

2.1.2.2. Adsorption and charge neutralization:

This mechanism holds when coagulant with opposite charge to that of colloids is brought in contact with the colloids such that the charged colloids adsorb the coagulant and thus the colloids are neutralized to initiate the aggregation of these colloids (Reynolds and Richards, 1996).

The coagulant dosage should be proportional to the quantity of colloids present. The effect of the adsorption is that it leads to a reduction of Zeta potential (Zp), to a level where the colloids are destabilized (Sanks, 1977; O'melia 1987). Typical example include the following reaction $Fe^{3+} + H_20 \rightleftarrows Fe\ (OH)^{2+} + H^+$. This complex ($Fe\ (OH)^{2+}$) possess a high positive charge and are adsorbed onto the surface of the negative colloids.

2.1.2.3. Enmeshment by precipitate (*Sweep-floc coagulation*)

This is common with coagulants that have the ability to form precipitate. Typical examples are $AL_2\ (SO_4)_3$, $FeCl_3$ and Lime. The precipitate physically entraps the suspended colloidal particles as they settle. Also, this mechanism holds when the colloidal particle themselves serve as nuclei for the formation of the precipitate, which is

the hub for the formation of floc that gives rise to sweep-floc coagulation. This mechanism is also brought about by over dosing the colloidal solution with coagulants, associated with precipitation (Bagwel et. al, 2001; Sanks, 1979; Swift, et. al., 1964).

2.1.2.4. Inter particle bridging

Bagwel, et.al (2001) was able to demonstrate that bridging occurs when coagulants forms threads or fibres which attach several colloids, capturing and binding them together. In organic, primary coagulants and organic polyeletrolytes both have the capability of bridging. Also WSSA, (1992), was able to collaborate that higher molecular weights result in longer molecules and more effective bridging.

Bridging is often used in conjunction with charge neutralization to grow fast settling and/or shear resistance flocs. The implication is that charge neutralization (under rapid mixing) is followed by bridging. Practically, this is achieved by introducing low molecular weight polymer (e.g. Alum) and followed by the introduction of high molecular weight polymer (Thomas, et. al., 1999; Yan, 2005).

2.1.3 Coagulation/flocculation transport mechanism

Coagulation transport mechanisms are classified based on the driving force of the process.

2.1.3.1. Perikinetic flocculation/coagulation.

This is the aggregation of particles caused by random thermal propelled motion (Brownian diffusion). This accounts for the fast irreversible coagulation proposed by Smoluchowski's theory. The driving force for particle movement is thermal energy of the fluid (Han, and Lawer, 1992).

2.1.3.2. Orthokinetic coagulation

The driving force behind orthokinetic coagulation is body force such as gravity and centrifugal forces. Generally, the particles or colloids are of different sizes, which necessitate the rising or sedimentation of the particles/colloids depending on whether their mass density are smaller or greater than that of the continuous phase (Han and Lawer, 1992). Owing to this movement, the destabilized particles follow the streamlines and eventually result in interparticle contacts and ultimately to aggregation. Han and

Lawer (1992) indicated in their work that orthokinetic flocculation's most likely to occur when both particles are greater than 1μm diameter and fairly similar in size.

2.1.3.3. Differential settling

This is caused by different settling velocities of particles. Because the settling velocity of particles which have similar densities is proportional to the particle size, the sedimentation of differential particles in heterogeneous suspension provides an additional transport for promoting flocculation. It most likely occurs when at least one of the particles is larger than 10nm in diameter and the other is significantly different in size (Han and Lawer., 1992; Thomas, et. al, 1999). The collision frequency, Beta, for these transport mechanims is given by Fridriskhsberg (1984).

$$\beta_{DS}(i,j) = \frac{\pi \Delta\rho g \alpha}{72\mu}(d_i + d_j)^3 (d_i - d_j) \qquad (2.1)$$

Where

i and j are particles sizes

$\Delta\rho$ - difference in density between the particle and the fluid (kg/m^3)

g – gravitational constant $9.806 m/s^2$ (Zhang, et. al, 2003).

2.1.4 Classification of coagulants

Coagulants can be classified into two groups namely: organic and inorganic (Aqua Ben Co, 2001)

2.1.4.1 Organic coagulants (polyelectrolytes)

These are water-soluble organic polymers that are used as both primary coagulants and coagulant aids. Polyelectrolytes are organic macromolecules. Polyelectrolytes may be made up of one or more basic monomers (usually two) Baarlsurd and Henriskens (1994). Polyelectrolyte are classified as non-ionic, anionic or cationic depending in the residual charges on the polymer in solution.

2.1.4.2 Non-ionic polyelectrolytes

These are polymers with a very low charge density. Non-ionics are used to flocculate solids through bridging. A typical non-ionic is a polyacrylamide (Stochi, 1990, and WST, 2005).

2.1.4.3. Anionic Polyelectrolytes

These are negatively charged polymers and anonics are normally used for bridging to flocculate solids. These are manufactured with various charge densities, through the intermediate charge densities are usually the most useful. Typical example is the acrylamide based anionics.

2.1.4.4 Cationic polyelectrolytes

These are positively charged polymers and cone in a cride range of families, charge densities and molecular weights. Cationics can be thought of as double acting because they act in two ways: Charge neutralization and natural organic polymers (alignates): Artificial organic polymers (amide derivatives, cellulose derivatives); synthetic organic polymer (quarternary salt of polyvinyl pyridine) (WST, 2005).

2.1.5.1 Inorganic coagulant

The use of inorganic metal salts as coagulants is well established. The three main inorganic coagulants include the following:

(a) Aluminum derivatives;

(b) Iron derivatives;

(c) Lime.

With the exception of aluminate, all common iron and aluminum coagulants are acid salts and therefore their addition lowers the pH of the treated water. An alkali may be required to counteract the pH depression of the coagulant. This is important because pH affects both particle surface charge and floc precipitation during coagulation.

When an inorganic coagulant is introduced into water, it dissociates into its constituents which may take part in various reactions with water or other solutes present. The nature of the resulting aqueous species largely determines the effect of the coagulant on colloidal stability and particle distribution (Terlizzi, 1994; Jiang and Graham, 1998).

Among possible types of aqueous species are the following (Terlizzi, 1994).

- Simple hydrated ions: Na^+, k^+, CL^-, SO_4^-
- Hydrolyzed species: $MgOH^+$, $Al(OH)_2^+$
- Metal-anion complexes: $ALSO_4^+$, $FeHPO_4^+$
- Aluminum sulphate (Alum); $AL_2(SO_4)_3.18H_2O$
- Sodium Aluminate: $Na_2AL_2O_4$
- Poly aluminum chloride (PAC): $AL_{13}(OH)_{20}(SO_4)_2$
- Ferric sulphate $Fe_2(SO_4)_3$
- Ferric chloride: $FeCL_3.6H_2O$.
- Ferrous sulphate: (Copperas): $FeSO_4.7H_2O$.
- Lime $Ca(OH)_2$

2.1.6. Factors Influencing Coagulation

2.1.6.1. Effect of pH

The pH range in which coagulation occurs may be the most important factor in proper coagulation. The great majority of coagulation problems are related to improper pH levels. Whenever possible coagulation should be conducted in the optimum pH zones. When this is not done, lower coagulation efficiency results, generally giving rise to waste of chemicals and lowered water quality (WST, 2005).

Each of the inorganic salt coagulants has its own characteristic optimum pH range in some water plants, the acidic reactions of the inorganic salts are taken advantage of when the raw water pH levels are higher.

2.1.6.2. Effect of Salt Species

Natural waters contain various levels of cations, and anions such as calcium, sodium, magnesium, sulphate, chloride, phosphates and others. Some of these ions may affect the efficiency of coagulation.

Generally, mono and divalent cations such as sodium, calcium and magnesium have little or no effect on the coagulation process. In most instance, trivalent cations do not have adverse effect in the process. In fact, significant concentration of naturally occurring ion in water supply has resulted in the ability to feed lower than normal dosage of inorganic salt coagulants.

Changes in the concentration and species of these ions affect the pH of the water medium. The resulting changes in the pH in turn affect the coagulation process.

2.1.6.3. Effect of Temperature

Low water temperature causes low turbidity removal efficiency and poor effluent quality. Jiang and Graham (1998) indicated that low temperatures had a pronounced detrimental effect on flocculation kinetics, slowing down the rate of flocculation.

As water temperature approach freezing temperatures, almost all chemical reactions occur more slowly. It can be more difficult therefore to evenly disperse the coagulants into the water. As a result, the coagulation process becomes less efficient, and higher coagulant dosages are generally used to compensate for the effects. In addition, the settling characteristics became poor due to the higher density of the water in the non-freezing temperature range.

2.1.6.4. Velocity Gradient

High velocity gradient provides more opportunities for collision, but the shear force from too high a velocity gradients can break up larger floc and will limit the maximum floc size (Yan, 2005). The velocity gradient in full scale flocculation basin can be created by a variety of mechanism, including baffle chambers, rotating paddles, reciprocating blade and turbine-type mixers. The efficiency of mechanical system should be judged by its ability to produce a uniform distribution of eddy currents throughout the basin.

2.1.6.5. Effect of Dosage

Dosage is a vital factor in coagulation efficiency. For effective coagulation, the dosage must be optimum. Normally, with increasing dosage, turbidities destabilization occurs Reynolds and Richards, 1996). This process is dominated by adsorption and charge neutralization mechanism. The optimum dosage often corresponds to Zeta potential which is approximately zero.

It is important to note that above the optimum dosage, restablization can take place due to charge reversal on the colloids. It is important therefore, that the coagulant dosage should be proportional to the quantity of colloids present (WSSA, 1992).

2.2. NATURAL MATERIALS AS COAG-FLOCCULANTS

Natural materials have been used in water treatment since ancient times. But lack of knowledge on the exact nature and mechanism by which they work has impeded their wide spread application and they have been unable to compete with the commonly used chemicals (Ghebremichael, 2004). At present, it becomes imperative to use natural materials due to cost and associated health and environmental concerns of synthetic organic polymers and inorganic chemicals.

Besides the natural materials under investigation in this work, a number of effective coagulants have been identified from plant and animal origins. Some of the common ones include *moringa olelifera* (Jahn, 2001), nirmali (Tripathi, et al., 1976), okra (AI-Samawi and Shokrala., 1996), *Cactus latifaira* and *prosopis juliflora* (Diaz, et al., 1999), tannin from valonia (Ozacar and Sengil, 2000) apricot, peach kernel and beans (Jahn, 2001). And the natural coagulants from animal origin is chitosan (Fernandez-Kim, 2004; Knorr, 1991). By using natural coagulants, considerable savings in chemicals and sludge handling cost may be achieved. Apart from being less expensive, natural coagulants produced readily biodegradable and less voluminous sludge (Ndabigengesere, et al., 1995). Presented below are details on the natural materials employed as coag-flocculants in this work.

2.2.1. Mucuna Pruriens Seed

General description and uses

Mucuna pruriens is a tropical legume known as velvet beans and by other common names; Devil beans (English-Nigeria),Agbala seed(Igbo),Werepe or Yerepe(Yoruba), Inyelekpe (Igala), native to Africa and Asia .The plant is notorious for extreme itchiness it produces on contact, particularly with the young foliage and the seed pods. It has value in agricultural and horticultural use and has a range of medicinal properties.

The plant is an annual climing shrub with long vines that can reach over 15m length. When the plant is young, it is almost completely covered with fuzzy hairs, but when

older, it is almost completely free of hairs. The Leaves are tripinnate, ovate, rhombous-shaped or widely ovate. The side of the leaves are often heavily grooved and sides of the leaves have hairs. The stems of the leaflets are two to three millimeters long. Additional adjacent leaves are present and are about 5mm long.

The flowers heads take the form of axially arrayed particles. They are 15 to 32cm long and have two or three or many flowers. The accompanying leaves are about 12.5mm long; the flower stand axes are from 2.5 to 5mm. The bell is 7.5 to 9mm long and silky. The sepals are longer or of the same length as the shuttles. The crown is purplish or white. The flag is 1.5mm long. The wings are 2.5 to 3.8cm long.

In the fruit ripening stage, a 4 to 13cm long, 1 to 2cm-wide, unwinged, leguminous fruit develops. There is a ridge along the length of the fruit. The husk is very hairy and carries up to seven seeds. The seeds are flattened uniform ellipsoids, 1 to 1.9cm long, 0.8 to 1.3cm wide and 4 to 6.5cm thick. The hilum, the base of the funiculus (connection between plancenta and plant seeds) is surrounded by a significant arillus (fleshy seed shell). M. pruriens bears white, lavender, or purple flavors. Its seed pods are about 10cm log and are covered in loose, orange hairs that cause a severe itch if they come in contact with skin. The chemical compounds responsible for the itch are a protein, mucunain and serotonin (Reddy, 2008) The seeds are shiny black or brown drift seeds.

In many parts of the world, mucuna pruriens is used as important forge, fallow and green manure crop (Reddy, 2008). Since the plant is a legume, it fixes nitrogen and fertilizes soil.

M. pruriens is a widespread fodder plant in the tropics. To that end, the whole plant is fed to animals as silage, dried hay or dried seeds. M. pruriens silage contains 11-23% crude protein. It also has use in the countries of Benin and Vietnam as a biological for problematic imperata cylindrica grass (Reddy, 2008). M. pruriens is sometimes used as a coffee substitute called "Nescafe". (not to be confused with the commercial brand Nescafe). These require that they be socked from at least 30minutes to 48hours in advance of cooking or the water change up to several times during cooking, since otherwise the plant can be toxic to humans. The seed of M. puriens have been used for the prophylactic treatment of snakebites. The dried bears of M. pruriens are used for treating Parkinson's disease (Katzenchlager, et.al, 2004).

2.2.2. Telfairia Occidentalis Seed

General description and uses

Telfairia occidentalis is a tropical vine grown in West Africa as a leaf vegetable and for its edible seeds. Common name for the plant include fluted gourd, fluted pumpkin, and Ugu. Telfairia occidentalis is a member of the curcurbitacae family and is indigenous to Southern Nigeria (Akoroda, 1990). The fluted gourd grows in many nations of West Africa but is mainly cultivated in Nigeria, used primarily in soups and herbal medicine (Nwanna, 2008). Although the fruit is inedible, the seeds produced the gourd are high in protein and fat, and can therefore contribute to a well-balanced diet. The plant is a drought tolerant, dioecious perennial that is usually grown trellised.

Telfairia occedentalis is traditionally used by an estimated 30 to 35million people, indigeneous people in Nigeria, including the Efik, Ibibo and Urhobo (Akoroda, 1990). However, it is predominantly used by the Igbo tribe, who continue to cultivate the gourd for food sources and traditional medicines (Okoli and Mgbeogu, 1983). A recurring subject in the Igbo's folklore, the fluted gourd is noted to have healing properties and was used as a blood tonic, to be administered to the weak or ill (Akoroda, 1990). It is endemic to Southern Nigeria, and was an asset to international food trades of the Igbo tribe (Akoroda, 1990). The edible seeds of Telifairia occidentalis can be boiled and eaten whole or fermented and added to "Ogili" (Badifu, 1993). The fluted gourd has been traditionally utilized by indigenous tribes as a blood tonic, likely due to its high protein content (Akoroda, 1990) .Flour produced from the seeds can be used for high protein breads, although more research is needed to fulfill this potential food source (Giami, 2003) furthermore, the shoots and leaves can be consumed as vegetable.

2.2.3. Pleurotus Tuberregium Sclerotium

Description and Uses

Pleurotus tuber-regium is a tropical sclerotial mushroom which has been gaining some interest in the U.S. Being sclerotial, the mushroom produces a sclerotium, or underground tuber as well as a mushroom. Both the sclerotium and the mushroom are edible. The mushroom looks somewhat like an oyster mushroom (Pleurotus Ostreatus) except that, when mature, the cap curves upward to spherical, to a void and can be quite large-up to 30cm (11.8 inches) or larger in diameter (Isikhuemhem and Okhuoya,1996). It is dark brown

on the outside and white on the inside. As far as we have been able to determine, no one is commercially cultivating this species although research being conducted in Nigeria is aimed at encouraging cultivation in that country. According to Ralph Arnold, members of the Oregon Mycological Society are getting good results with fried they have been running.

In Nigeria P. tuber-reguium is used as both a food and a medicinal. The sclerotium, which is hard is peeled and ground for use in melon soup (Isikhuemhem and Okhuoya, 1996). It may also be dried for future use. Nigeria native doctor's use various combination of herbs and other ingredients in their medicine. P. tuber-regium is used in some of those combination that are intended to cure headache, stomach ailments, and high blood pressure (Isikhuemhem and Okhuoya, 1996). On study (Ogundana and fagade, 1981) indicates that the dry matter, 7.4% is crude fibre, 14.6% is crude protein and 4.48% is fat and oil protein protein levels compare to shiitake at 18%, P. Ostreatu at up to 30%, wheat at 13% and milk at 25% (all based upon dry weight). Fat levels are comparable to other mushroom species. Total sugar content is about 18.6% with high concentrations of galactose and low concentrations of glucose and maltose. Levels of oxalic acid, which can reduce the food value were low as were levels of hydrocyanic acid which can toxic. The mushroom also contained low levels of vitamin C.

2.2.4. Corchorus Olitorius Seed

Description and uses

Corchorus is a genus of about 40-100 species of flowering plant in the family malvaceae, native to tropical and subtropical regions throughout the world(Stewart, 2011).Different common names are used in different context, with jute applying to the fiber produced from the plant and mallow-leaves for the leaves used as a vegetable.The plants are tall, usually annual herbs reaching a height of 2-4m, unbranched or with only a few side branches. The leaves are alternate, simple, lanceolate, 5-15cm long, with an acuminate tip and a finely serrated or lobed margin. The flowers are small (2-3cm diameter) and yellow, with five petals, the fruit is a many seeded capsule. It thrives almost anywhere, can be grown year round.

Corchorus leave are consumed in the cuisines of various countries. Corchorus olitorius is used mainly in the cuisine of southern Asia, the middle East, and North Africa. Corchorus is capsularis in Japan and china. It has a mucilaginous (somewhat "Simy") texture,

similar to okra, when cooked. The seeds are used as a flavoring and a herbal tea is made from the dried leaves. The leaves of corchorus are rich betacarotene, iron, calcium and vitamin C. The plant has an antioxidant activity with a significant α-tocopherol equivalent Vitamin (Whittock, et al, 2003). In Nigeria cuisine especially amongst the Yorubas, it is commonly used in a stew known as ewedu, a condiment to other starch-based foods such as amala. The Hausa people of Nigeria and the Fulani neighbours call it rama. They use it to produce soup (taushe) or boil the leaves and mix it with kuli-kuli (groundnut cake) to form a dish known as kwado in Hausa. And Fulani peoples also use Jute leaves to treat some diseases.

2.2.5. *Archatinata marginata* Shell

Description and Uses

Achatina is a species of land snail is family Achatinidae, known commonly as the giant African snail or giant African land snail (Rowson, et.al, 2010). Outside of it native range it thrives in many types of habitat in area with mild Climates; It feeds voraciously and is a vector for plant pathogens, causing severe damage to agricultural crops and native plants. It competes with native snail taxa, it is a nuisance pest of urban areas, and it spreads human disease (Lv, et.al, 2009). It is listed as one of the top 100 invasive species in the world (Lv, et.al, 2009) .

The adult snail is around 7cm (2.8in) in height and 20cm (7.9in) or more in length. The shall has a conical shape, being about twice as high as it is broad. Either clockwise (dextral) or counter-clockwise (sinistral) direction can be observed in the coiling of the shell, although the right-hand (dextral) cone is more common. Shell colouration is light variable, and dependent on diet. Typically, brown is the predominant colour and the shell is banded (Skelley, etal, 2011). The shell is particularly tough and has the highest heave metal content of any snail species (Jatto, 2013). Achatina are used by some practioners of candomble for religious purposes in Brazil as an offering to the deity oxala. The snail substitute for a closely related species, the African giant snail (*Maginata achatina*) normally offered in Nigeria. They are also edible if cooked properly.

2.3. Adsorption Phenomenon and Process

Adsorption is the process of accumulating substances that are in solution on a suitable interface. It is a mass transfer operation in that a constituent in the liquid phase is transferred to the solid phase (Tchobanoglous,et.al, 2003).

Adsorption involves in general the accumulation (or depletion) of soluble molecules at an interface (including gas- liquid – interface as in foam fractionation, and liguid—liquid interface as in detergency) (Perry, et. al, 1999).

In adsorption, molecules diffuse from the bulk of the fluid to the surface of the solid adsorbent forming a distinct adsorbed phase. Adsorption is effective in removing trace components from a liquid phase and may be used either to recover the component or simply to remove a noxious substance from an industrial effluent. Adsorption occurs when molecules diffusing in the phase are held for a period of time by forces emanating from an adjacent surface. The surface represents a gross discontinuity in the structure of the solid and atoms at the surface have a residual of molecular forces which are not satisfied by surrounding atoms such as those in the body of the structure.

The residual or van der waal's forces are common to all surfaces and the only reason why certain solids are designated "adsorbents" is that they can be manufactured in a highly porous form given rise to a large internal surface. Adsorption is of two major types namely: physical and chemical.

2.3.1. TYPES OF ADSORPTION

Based on the energy associated with adsorption and types of bond responsible for the accumulation of the adsorbate on the adsorbent, adsorption can be classified into two types:

(a) Physical adsorption (physisorption)

(b) Chemical adsorption (Chemisorption)

2.3.1.1. Physical Adsorption

This occurs due to the intermolecular forces of attraction (Van der Waals forces) between the molecules of the adsorbent and that of the adsorbate. This process is weakly exothermic and can be reversed by heat, physical stripping, replacement with a compound having a higher affinity than the adsorbate, or some

combination of these methods. The chemical composition of physically adsorbed adsorbate generally is not changed by the adsorption/desorption process (Cronin, 1998; Menkiti, 2010).

Generally, the physical adsorption process begins as an adsorbate molecule is transported from the bulk adsorbate phase to the surface of the adsorbent. Thereafter, the molecules diffuse into the pore and physically bonds with the surface. Heat is usually evolved, making adsorption an exothermic process.

2.3.1.2. Chemical Adsorption

Chemical adsorption involves a chemical interaction between the adsorbate and adsorbent. The process is more exothermic than physical adsorptions, almost irreversible, hence, after desorption the adsorbate may be chemically different from its original form (Cronin, 1998).

The chemical bond involved is usually covalent and the adsorbent tends to find sites that will maximize its co-ordination number with substrate. Chemical adsorption is specific and involves forces which are stronger than those associated with physiosorption. Therefore the heat of adsorption is high and of the same order of heat of reaction. This process requires generally high temperature, hence the adsorbing material is heated to higher temperatures to remove the adsorbed materials. Unlike physical adsorption, where multilayer coverage is feasible, chemical adsorption does not exceed monolayer coverage. This is because the valence force holding the molecules on the adsorbent surface varnishes rapidly with distance. Generally, chemical adsorption is linked to the porosity and surface chemistry of the carbon, since it is associated with the number of active sites and carbon surface (Okoye, 2009). Although there are significant differences between physical and chemical adsorption, but there are instances in which it is hard to assign the adsorption definitely to one of these types.

2.3.2. Adsorption Factors

There are various factors that influences adsorption processes namely:

2.3.2.1. Surface Area

This is an important parameter to consider when creating or selecting an adsorbent. In an ideal adsorption situation – where all other conditions (such as

pore size, surface chemistry and adsorbent – adsorbate interactions) are optimal for contaminant removal – the surface area would serve as the limiting factor for the adsorption process. In this case, as the activated adsorbents surface area increased, so would the adsorption of the target contaminant. Manufacturers of activated carbon for example attempts to increase the surface area of the adsorbent with the hope of enhancing the carbons removal efficiency likewise enhanced by applying chemical activation on them. Typically, the surface area of activated carbon for example reaches a maximum around 1500 m^2/g.

The activated carbon surface area is commonly found using a theory developed by Braunauer, Emmett and Teller (BET) for physical adsorption. While the BET theory is inadequate as a universal equation for physical adsorption, it has been adapted to describe surface area (Dabrowski, 2001). BET surface area is determined by flowing nitrogen gas at 77K through a sample of activated carbon, allowing the N_2 to enter the pores of the carbon. From the amount of N_2 that adsorbs to the pores, the surface area is deduced. It should be noted that BET surface area can at times be misleading when attempting to directly correlate it to the adsorption capacity of an activated carbon (Pope, 2003). Since nitrogen gas molecules are much smaller than many target contaminants, the size of the contaminant itself should be considered with respect to the pore size distribution of the carbon.

2.3.2.2. Pore Size Distribution

Another essential parameter to consider for an adsorbent is its pore size distribution (PSD), pore size distribution is usually expressed as a graphical relationship, using pore width (A^o) as the independent variable and cumulative pore volume (CC/g) as the dependant variable. Pore widths that fall under $20A^o$ are considered to be micropores, from 20 to $500A^o$ are mesopores and above 500 A^o are macropores. The variation of pore width in an activated carbon for example is dependent upon the activation process. Theoretically, any precursor can have any desired PSD, yet, the degree of distribution may require more manipulation of the activation environment, and hence may be more energy (and cost) intensive.

2.3.2.3. Potential Hydrogen (pH)

When the parameter pH is discussed in an experiment, commonly it is used as a descriptor to express the ionic condition of a given aqueous system. However, in the case of activated carbon adsorption, it is important to take into account the pH of the carbon surface and internal pore in addition to the aqueous medium. An internal measurement of the activated carbon is expressed through the point of zero charge (PZC). The PZC is the point at which the carbon surface has no detectable charge.

The PZC is the point at a solution pH below 7, the carbon surface is positively charged and a solution pH above 7 will promote a negatively charged carbon surface. PZC is an important characteristic when predicting or describing the process of adsorption, yet is only a dominant factor when the target contaminant is close to the adsorption site. For example (assuming the contaminant is in range of the adsorption site), if the target contaminant was a cation, a solution PH greater than 7 would be desired for the PZC. Conversely, if the target contaminant is an anion, a solution P^H below 7 would be desired.

The Zeta potential, a measurement of external charge, governs the attraction of the target contaminant to the activated carbon. Zeta potential is the measurement of electric potential at the shearing plane-the "space" between the activated carbon surface and the adjacent water molecules (Adamson, 1990).

2.3.2.4. Surface Chemistry

The structure of activated carbon is graphitic in nature, consisting of molecular layers of carbon, which can be viewed, according to Coughlin and Ezra, much like a poly nuclear aromatic molecule (Coughlin and Ezra, 1968). These layers contain carbon atoms that are bonded together with three sigma bonds and one pi- bond having Sp^2 hybridization. It is also possible for Sp^3 hybridization (tetrahedron) to occur, which may result in cross- linking among the graphite layers (Coughlin and Ezra, 1968). The carbon within this structure is microcrystalline and is held together with the graphite layers through van der Waals forces. When other atoms are bound within this system, they can be present within the layers, forming "heterocyclic" rings, or at the edges of the microcrystalline carbon molecules, thus forming functional groups (Coughlin and Ezra, 1968). Edges sites located between the graphic layers are very reactive and are therefore prominent sites for functional groups and adsorption. It is

asserted by Coughlin and Ezra (1968), that the basal face of the benzene ring can weakly adsorb through II- interactions.

A discussion of activated carbon surface chemistry should also include a thorough examination of electron interactions, including electron density, electrostatics, attraction and repulsion, as well as dispersive forces and the influence of functional groups located on both the adsorbent and the adsorbate. Numerous discussions in the literature center around speculation of these interactions and many of these theories have not yet been sufficiently disproven. It is hoped that a deeper understanding of the activated carbon surface chemistry will provide the keys for unlocking the mechanisms of the adsorption process.

2.3.2.5. Solubility of the adsorbate

The rate of adsorption of a solute is inversely proportional to the solvent solubility. The greater the solubility, the stronger the solute- solvent bond, and therefore, the smaller the rate of adsorption. This theorem is referred to as the lundeluis rule.

2.3.2.6 Temperature

In physical adsorption, temperature increase will reduce adsorption due to increased solubility of adsorbate when the assumption of instantaneous equilibrium is not valid. If the instantaneous equilibrium is not valid then the equilibrium is the sole criteria. The adsorption reaction is written below.

$$A + X \rightleftharpoons A.X \qquad 2.2$$

Where

X - Active adsorbent site

A – Adsorbate.

From Chateliers principle, the adsorption, that is forward reaction will increase the temperature of the reaction and favour the backwards reaction (desorption), this is exothermic reaction, also this increase in temperature reduces the rate of adsorptions since desorption is the opposite of adsorption.

2.3.3. Adsorption Isotherm

The adsorption isotherm a function which connects the amount of adsorbate on the adsorbent, with its pressure (for gas) or concentration (for liquid) expressed at constant temperature. It can also be expreesed as a set of data which represents constant temperature measurements of the quantities of adsorbate adsorbed by a unit weight of adsorbent in equilibrium wioth each of a number of different activities (concentration for liquids and partial pressure for gases) of the mobile phase.
Isotherms indicate the affinity of adsorbent for the adsorbate but do not relate the contact time or the amount required to reduce the adsorbate from one concentration to another.

In general the amount of an adsorbate adsorbed in moles per gram solid is a function of the activity of the adsorbate , the temperature of the system, the pH of the solution, the amount of contact between the adsorbate and adsorbed. In specific terms the factors affecting adsorption capacity are the characteristics of the adsorbate (particularly molecule size and polarity), characteristics of the system (temperature, pressure of the adsorbate, and presence of competing adsorbates) and the characteristics of the adsorbent, where the most important parameters are surface area and pore size distribution.

2.3.4 Adsorption Models

Since adsorption involves complex molecular – level interactions that are not completely understood, there is currently no general "theory of adsorption" that can be used to accurately predict adsorption capacity given independently determined characteristics of an adsorbate and adsorbent (Gregg, et.al, 1982). In view of this, numerous equations based on empirical observations or theoritical models have been proposed over the years in an effort to predict adsorptive behavior. While none serves as a general theory of adsorption; these equations can be useful in predicting adsorption under circumstances appropriate for the underlying assumptions they are based on.

The following equations can be used to express isotherm models: Langmuir, Freundlich, Temkin, and BET etc.

2.3.4.1. Langmuir Isotherm

The Langmuir isotherm is an empirical isotherm derived from a proposed kinetic mechanism. It is based on the following assumptions:

1. The surface of the adsorbents is uniform; that is, all the adsorption sites are equivalent and similar
2. Adsorbed molecules do not interact. They do not react
3. All adsorption occurs through the same mechanism
4. At the maximum adsorption, only a mono layer is formed: Molecules of adsorbates do not deposit on other, already adsorbed molecules of adsorbate, only on the free surface of the adsorbent.

The four assumption are not all true. The fourth assumption is the most troublesome, but it is also addressed by BET isotherm. The Langmuir isotherm is usually better for chemisorption.

Consider the reaction.

$A + S \underset{K_{-A}}{\overset{K_A}{\rightleftharpoons}} A.S$ which is simply the reversible adsorption of A on a catalyst surface. This is case of a molecule. A being adsorbed on a single site, S on the catalyst surface. Rate of adsorption $V_A = K_A C_A C_V$ (2.3)

Rate of desorption, $r_A = K_A C_{AS}$ (2.4)

The rate of adsorption, $r_{ads} = K_A C_A C_V - K_A C_{AS}$ (2.5)

Where K_A and K_A are rate constants for forward and reverse reaction.

$K_A C_A C_V$ and C_{AS} are concentrations of specie A, concentration of vacant site and concentration of occupied sites, respectively.

Where C_t is summation of vacant and occupied sites.

Site Balance: $C_t = C_V + C_{AS}$

Replacing the intermediate complex, C_{AS} in eqn (2.5)

$K_A C_V C_{AS}$ or $C_V = C_t - C_{AS}$

Eqn (2.5) becomes

$K_A C_V (C_t - C_{AS}) - K_A C_{AS}$ (2.6)

Equilibrium, r_{net} = 0

$K_A C_V\ (C_t - C_{AS}) - K_A C_{AS}$

$K_A C_V C_t - K_A C_V C_{AS} = K_A C_{AS}$

$K_A C_{AS} + K_A C_{AS} = K_A C_A C_t$ (2.7)

Divide both sides of equation (2.7) by K_A and equating $K_A/K_A = K_{ads}$

Where K_{ads} is equilibrium constant

$K_A C_V C_{AS} + C_{AS} = K_{ads} C_A C_t$

$K_A\ (K_{ads} C_A + 1) = K_{ads} C_A C_t$

$$K_{ads} = \frac{K_A C_A C_t}{1 + K_A C_A} \quad (2.8)$$

Putting $C_{AS}/C_1 = 0$, equations (2.8) becomes

$$0 = \frac{K_A C_A}{1 + K_{ads} C_A} = \frac{K_A P_A}{1 + K_{ads} P_A} \quad (2.9)$$

Equation (2.9) is the Langmuir isotherm

For liquid isotherm, however, the Langmuir isotherms are usually expressed as follows:

$q_e = (K_L q_{max}\ C_e)/\ (1+K_L C_e)$ (2.10)

Where q_e is the equilibrium value of adsorbate per unit mass of adsorbent (mg/g), q_{max} is the maximum amount of adsorption corresponding to mono layer coverage (mg/g), C_e is the equilibrium concentration of the adsorbate, K_L is the langmiur's constant and is related to the measure of affinity of adsorbate for the adsorbed l/mg(Patel and Suresh, 2008; menkiti, 2010). For correlation purpose, the equation is rearranged as follows

$1/q_e = (1/K_L - q_{max})\ 1/C_e + (1/q_{max})\ ]$ (2.11)

A linear plot of $1/q_e$ against $1/C_e$ yield a straight line graph which has a slope and intercept corresponding to ($1/K_L$- q_{max}) and ($1/q_{max}$), respectively, from which the q_{max} and K_L can be calculated.

To confirm the favorability of an adsorption process to Langmuir isotherm, the essential features of the isotherm can be expressed in terms of a dimensionless constant, separation factor or equation parameter, R_L, which can be calculated by the following equation.

$$R_L = 1/(1 + K_L C_O) \quad (2.12)$$

Where, C_O is the initial adsorbate concentration. The value of R_L indicates whether the isotherm a irreversible ($R_L = 0$), favourable ($0 < R_L < 1$), linear ($R_L = 1$) or unfavourable ($R_L > 1$) (Radirvelu and Namasivayam, 2003).

2.3.4.2 Freunlich Isotherm

The Freundlich equation is an empirical expression used to describe adsoption isotherm where there is a linear response for adsorption capacity as a function of a adsorbate concentration (or partial pressure) when this function is plotted on log-log scales. The valid concentration range for the Freudlich equation varies according to the adsorbate-adsobent combination.

The major assumptions of Freudlich isotherm are:

1. Heat of adsorption falls logarithmically as fractional coverage, θ increases.
2. Heat of adsorption, ΔH is exponentially dependent on θ, the fractional coverage.

The model assumes that different site with several adsorption energies are involved in the process of adsorption (Pimental, 2008).

The derivation of Freudlich isotherm proceed from the Langmuir isotherm expressed is equation (2.9) can be re-written as

$$\theta + \theta KP = KP \quad (2.13)$$

$$\theta (1 + KP) = KP$$

$$\theta = (KP - \theta KP)$$

$$\theta = KP (1 - \theta)$$

$$\frac{\theta}{1 - \theta} = KP \quad (2.14)$$

$K_e = K_e^{\Delta H/RT}$ (2.15)

$\Delta H = \Delta H_m \ln\theta$ (2.16)

Where T is temperature in Kelvin

R is universal gas constant

K_a/K_d (2.17)

Where K_a/K_d are the rate constants for forward and backward reactions.

Combining (2.15) and (2.16) yields

$$\frac{\theta}{1-\theta} = KPe^{\Delta H/RT} \quad (2.18)$$

Combing (3.6C) and (3.5C), it yields

$$\frac{\theta}{1-\theta} = \frac{K_a}{K_d} P \exp(\Delta H_m \ln \theta / RT) \quad (2.19)$$

Taking logarithm of both sides of equation (2.19)

$$\ln \frac{\theta}{1-\theta} = \ln\left(\frac{K_a}{K_d}\right) + \ln P + \frac{\Delta H_m \ln \theta}{RT} \quad (2.20)$$

It is assumed that $\frac{\ln \theta}{1-\theta} = 0$, then for non-dissociative gases

$$\frac{\Delta H_m \ln\theta}{} = -\ln\left(\frac{K_a}{K_d} P\right)$$

$= -\ln(a_o P)$ (2.21)

Where $\frac{K_a}{K_d} = a_0$

$$\ln\theta = -\frac{RT}{\Delta H_m} \ln(a_o P) \quad (2.22)$$

$\theta = (a_o P)^{RT/\Delta H_m}$

But $q_m = -\Delta H_m$

$$\theta = (a_o P)^{RT/\Delta H_m} \quad (2.23)$$

Equation (2.23) transforms to

$$g/g_m = (a_o P)^{RT/q_m} \quad (2.24)$$

Where g_m is the amount of adsorbate adsorbed by adsorbent completely covered with a monolayer of adsorbing specie.

g is the amount of adsorbate adsorbed by adsorbent

Equation (2.24) is the Freundlich Isotherm. For liquid isotherm eqn. (2.24) can be re-written as shown below:

$$q = k_1 C_e^{1/n} \quad (2.25)$$

Where 1/n is a heterogeneity factor which is a measure of intensity of adsorption or affinity of the absorbate for the adsorbent (Faust and Asman, 1987) and is less than 1 if the adsorption process is favourable, K_1 is the freundlich constant which is a measure of adsorption capacity (mg/g). The freundlich equation is useful in cases where the actual identity of the adsorbate is not known (Treybals, 1980)

On lineraizing equation (2.25) a plot of log C (on the abscissa) against log q_e (on the ordinate) provides value for K_1 and n corresponding to the y-intercept and slope, respectively. The linear form is

$$\text{Log } q_e = \log K_1 + 1/n \log C_e \quad (2.26)$$

2.3.4.3 Temkin Isotherm

Temkin attempted to modify Langmuir isotherm to conform to a large experimental data. It is considered that, most systems obey a linear decrease instead of the logarithmic decrease of heat of adsorption with coverage as proposed by Freundlich isotherm, while incorporating the concept of heterogeneity of active sites. In an attempt to modify this principle and ensure isotherm that accommodates large experimental data resulted in the proposition of Temkin isotherm.

For the Temkim Isotherm, the derivation of the model proceeds from:

$$\theta/ (1-\theta) = (K_a/K_d) P \exp (\Delta H/RT) \quad (2.27)$$

Equation (2.27) is transformed to elementary Temkin Isotherm for gases as shown in equation (2.28):

$$\text{In}(1-\theta) = \ln P + (\Delta H_o \alpha \theta)/ RT + \ln A_o \quad (2.28)$$

$$\text{Where } A_o = a_o \exp (q/RT) \quad (2.29)$$

α is positive constant

$a_o = k_a/k_d$

However Temkin isotherm is known to apply in the middle region of coverage ($0.2 < \theta < 0.8$ because in many cases, it is found that it is between limits that heat of adsorption falls linearly rather logarithmically as proposed by the Freundlich Isotherm. Hence the variation of ln [$\theta/(1- \theta)$] becomes eligible. Thus,

$\ln P + (\Delta H_o \alpha \theta)/ RT + \ln A_o = 0$ (2.30)

Equation (2.30) can be rearranged in the form of equation (2.31)

$\theta = (RT/q_o\alpha) \ln (A_oP)$ (2.31)

Where $q_o = -\Delta H_o$ (2.32)

ΔH_o is the heat of adsorption at zero coverage

For correlation purpose, the isotherm is expressed as follows:

$g= (g_mRT/q\alpha) [\ln a_o + (q_o/RT)] + (g_mRT/q_o\alpha)\ln p$ (2.33)

A plot of g versus ln P gives a straight line graph where slope is $(g_mRT/q_o\alpha)$, from which q_o can be calculated.

For liquid adsorbates, the Temkin isotherm model is shown below

$q_e =[(RT)/b_T] \ \ln k_T + (RT)/ b_T \ InC_e]$ (2.34)

Where b_T indicates the adsorption potential of the adsorbent and K_T is the Temkin constant (Horsfall and spiff, 2005).

A plot of q_e versus $\ln C_e$ gives a straight line graph from which the values of K_T and b_T can be calculated.

2.3.4.4 Brunauer, Emmet and Teller (BET) Model

BET theory (Brunauer, et.al, 1938) is based on a kinetic model of adsorption roposed by Langmuir in 1916 and portrays a solid surface as an array of adsorption sites. Equilibrum occurs when the rate at which molecules arriving from the gas phase and condensing or adsorbing onto unoccupied adsorption sites is equal to the rate at which molecules evaporate or desorbed from occupied sites.

Assuming multiple adsorption layers, the BET equilibrium adsorption equation is produced.

$$\frac{n}{n_c} = \frac{c\,(P/P_o)}{(1-P/P_o[1+(C-1)(P/P_o)]} \quad (2.35)$$

Where

$$c=\exp \frac{(p_t-q_l)}{RT} \quad (2.36)$$

P_O is the saturation vapour pressure of the adsorbate: (q_t-q_L) is the net heat of adsorption; R is the ideal gas law constant and T is the temperature in Kelvin (Greg and Sing, 1982).

Because adsorption experiments frequently measure volume adsorbed, rather than moles adsorbed equation (2.35) transform to

$$\frac{V}{V_m} = \frac{c\,(P/P_O)}{(1-P/P_O)[1+(C-1)\,(P/P_O)]} \quad (2.37)$$

2.4 **BATCH ADSORPTION KINETICS**

Various kinetic models are used in determining the mechanism of an adsorption process and the potential rate controlling steps. Models used in this work are presented below:

2.4.1 Bhattacharya–Venkobachar Model (BVM)

The Bhattacharya – Venkobachar equation is shown as follows:

$$\ln [1 - (U)\,T] = (K_B)t \quad (2.38)$$

Where $(U)\,T = (C_0 - C_1)/ (C_0 - C_e)$ (2.39)

K_B is the Bhattacharya venkobachar's constant (min^{-1})

C_0 is the initial concentration (mg/l)

C_t is the concentration at time t, (mg/l)

C_e is the concentration at equilibrium (mg/l)

A plot of ln [1 – (U)T] versus t should yield a straight line, if the adsorption process obeys the model. From the shape of the plot, K_B can be determined.

2.4.2 Pseudo First Order Model

The langergren pseudo first order equation is generally expressed as follows:

$$\frac{dq_t}{dt} = K_1(q_{e-}q_t) \quad (2.40)$$

Where $\mathbf{q_e}$ and $\mathbf{q_t}$ are the adsorption capacity at equilibrium and at time t, respectively (mg/l) and $\mathbf{K_1}$ is a constant of pseudo first order adsorption (min^{-1}). Integrating equation (2.40) within the specified limits, it yields

$$\int_0^{q_t} \frac{dq_t}{q_e - q_t} = \mathbf{K_1} \int_0^t dt \qquad (2.41)$$

Equation (2.41) can be transformed to

$$\mathbf{ln}\ (q_e - q_t) = \mathbf{ln}\ (q_e) - K_1\mathbf{t}) \qquad (2.42)$$

A plot of $\mathbf{ln}\ (q_e - q_t)$ versus **t** should give a straight line, if the adsorption is controlled by this model. K_1 and can be determined form the slope and intercept of the plot, respectively. The experimental $\mathbf{q_e}$ should be with the estimated one. Generally, higher values of K_1 suggest greater adsorption (Igwe and Abia, 2007).

The major disadvantage with this model is that in most cases, the equation does not fit well for experimental data over the entire range of contact time (Ho and Mckay, 1999).

2.4.3 Pseudo Second Order Model

The pseudo second order adsorption kinetic rate equation as expressed by Ho (2000) is presented as

$$\frac{\mathbf{dq_t}}{\mathbf{dt}} = \mathbf{K_2}(q_e - q_t)^2 \qquad (2.43)$$

Where k_2 is the rate constant of pseudo second order adsorption (g mg^{-1} min^{-1}). On integrating equation (2.43) as shown below

$$\int_0^{q_t} \frac{dq_t}{q_e - q_t} = \mathbf{K_2} \int_0^t dt \qquad (2.44)$$

It transforms to the following linear equation (2.45)

$$\frac{t}{q_t} = \left(\frac{1}{K_2 q_e 2}\right) + \frac{1}{q_e} \qquad (2.45)$$

A plot of $\frac{\mathbf{t}}{\mathbf{q_t}}$ versus **t** should give a straight line, if this model is obeyed by the adsorption process $\mathbf{q_e}$ and $\mathbf{K_2}$ are determined from the slope and intercept of the plots respectively. The experimental q_e should tally with the estimated one. Decrease in the values of $\mathbf{k_2}$, suggests increased adsorption (Debnath and Ghosh, 2008).

The main assumptions of the pseudo-second order kinetic model is that rate limiting step is chemical sorption involving bond formation through sharing or exchange of

electron between adsorbate and adsorbent. It also assumes that adsorption follows the Langmuir equation (Ho and Mckay, 2000).

2.4.4 Elovich Model

Elovich model in generic form is expressed as:

$$\frac{dq_t}{dt} = \alpha \exp(-\beta q_t) \quad (2.46)$$

Where, α is the initial adsorption rate (mg g^{-1} min^{-1}) and β is desorption rate constant (mg g^{-1} min^{-1}) during anyone experiment. To simplify the Elovich equation, Chien and Clayton (1980), assumed $\alpha\beta t >> t$ and by applying the boundry conditions q_t = 0 at t = 0 and q_t = q at t = t, equation (2.46) becomes

$$q_t = (1/\beta) \ln(\alpha\beta) + (1/\beta) \ln(t) \quad (2.47)$$

Thus, a plot of $\mathbf{q_t}$ versus **ln (t)** should yield a linear relationship with a slope of $(1/\beta)$ and an intercept of $(1/\beta)$ ln $(\alpha\beta)$, if the adsorption process fits the Elovich model.

2.4.5 THERMODYNAMIC EQUATIONS

$$\Delta G = RT \ln K_L \quad (2.48)$$

$$\ln \frac{K_{L1}}{K_{L2}} = \frac{-\Delta H}{R}\left(\frac{1}{T_2} - \frac{1}{T_1}\right) \quad (2.49)$$

$$\Delta G = \Delta H - T\Delta S \quad (2.50)$$

Where; ΔG is change in gibb's free energy; K_L is the Langmuir's constant; ΔH is change in enthalpy; ΔS is change in entropy; R is universal gas constant

2.5 Activated Carbon

Activated carbon is amorphous, hydrophobic and non-polar class of substance with high carbon content which have undergone the process of activation. Soleimani and Kaghazach (2008) asserts that activated carbon is a commercial name for an artificial activated carbonaceous adsorbent that has high porous structure and large surface area. A generalized definition is that activated carbons are non-hazardous, processed, carbonaceous product having a high degree of porosity and an extended inter-particulate surface area. Based on these properties, they adsorb a wide variety of substances.

Due to the amorphooous nature of activated carbon, it is irregular atomic structure unlike other allotropes of elemental carbon such as diamond, fullerence and or nanotubes (Okoye, 2009).

Activated carbon (AC) typically comes in three general types: granular or natural grains, pellets and powders. AC with a concentration of small pores tends to adsorb smaller molecules than the large pored carbons. Nevertheless, one of its main limltations is that it is combustible.

2.5.1. Feedstock For Production Of Activated Carbon

Activated carbon can be produced from both synthetic and natural feedstocks. The raw natural feedstocks are mainly the carbonaceous substances, such as young fossil material (Coal wood, peat, lignin), vegetable matter (sawdust, nutshells, fruit nuts, leaves), animal matter (bones) and petroleum wastes. Commercially, the most readily feedstocks are peat, lignite, wood and nutshells.

The phase of application of an activated carbon also determine the type of feeedstocks to be employed in the production of the carbon. For vapour phase application, carbon from lignin and wood, which are low density materials and high volatile content are not suitable because they have large pore volume but low density. However, the quality of the carbon can be improved by densification, reconstitution or compression during carbonization. On the other hand, carbons from fruits pits, semi-hard coals and nutshells, which have higher density than wood and posses high volatile content are hard and granular with large micropore volumes. Therefore, they are quite suitable for solution as well as a vapour application (Okoye,2009).

2.5.2. Characteristics Of Good Feedstock For Activated Carbon Production

1. The feedstock should have low ash content(i.e low inorganic content)
2. The feedstock should have high workability, high shelf life and sufficient volatile content.
3. The feedstock should have high density and structural strength to avoid excessive crumbling under use.

2.5.3 Production Of Activated Carbon

The processing technique to be used for the production of activated carbon depends on the nature and types of raw material available as well as the desired physical form of the avctivated carbon. The production of activated carbon involves the following steps:

1. Preparation of raw materials.
2. Carbonization
3. Activation

2.5.3.1 Preparation Of Raw Material

The following procedure was carried out on the raw materials to put them in a form suitable for carbonization

i. *Sizing* – The involves breaking down of the raw materials into lumps or granules of approdpriate sizes, which can be hanled effectively in subsequent operations.

ii. *Sieving* – This is done using wire gauze in the case of materials with fibre or fluffy particies in order to remove these particles and leave the desired material for carbonization. Agitation followed by blowing could also be carried out along side the sieving.

iii. *Reconstitution*- This involves pulverization of the raw materials followed by agglomeration by extrucsion or briquetting. It is usually done on low-densitry materials in order to improve their quality.

2.5.3.2 Carbonization

This is a high temperature thermal conversion of carbonaceous raw material into carbon in the absence of air using murfle fumace/rotary kiln operated between 4oo^{o}c and 800^{o}c (Hassler, 1988). This is a procedure carried out under time schedule to remove the volalie or non-carbon entities. This leads to the formation of a head carbon mass, possessing a partially developed or rudimentary pre structure. In the work of Hassler (1988). It was held that basic micro structure of carbon is formed at 500^{o}C, although there may be blockages of the micro pores by pyrolytic products, which can only volatilize at higher temperatures.

Two stages, softening and hardening during carbonization are of great importance to the quality of activated carbon produced. The softening stage occurs first, its temperature determining to a large extent the nature of the char formed. The hardening stage then follows and it is this stage that the char hardens and shrinks. Shrinkage of the char plays a very important role in the pore development.

2.5.3.3 Activation

This is the process of transforming inert carbon into highly adsorbent material by conferring on it a porous material structure and large specific surface area (Austine, 1984). The objective is to enhance the volume and enlarge the pores, which were created during the carbonization process, and also to create new pores. Two types of carbonization exit: physical and chemical.

2.5.3.4 Properties of Activated Carbon

Activated carbon is not a pure carbon. It contains other elements in various proportions depending on the source material and in the mechanism of its production. Such other elements which are chemically combined with carbon atoms include hydrogen, oxgen, nitrogen, sulphur etc. The adsorptive and catalytic power of the activated carbon are traced to the presence of those elements in the carbon. The morphology of an activated carbon observed by an microscopy is greatly determined by the raw material is directly reflected in the final production. This is as a result of the fact the nature of starting material is directly reflected in the final product. The properties of commercially available activated carbons are responsible for their use as either gas-phase or liquid phase adsorbents. These properties are grouped into two broad classes: physical properties and chemical properties.

2.5.3.5 Physical Properties Of Activated Carbon

i. *Ash Content and Percentage Fixed Carbon*

The ash content of an activated carbon is used to determine the raw material used to produce the activated carbon. Almost all shell carbon contains 10% - 20% ash content and coal based contains 6% - 16% ash content. The ash content reduces the efficiency of reactivation. It also reduces the overall activity coefficient. The metals (Fe_2O_3) can leach out of activated carbon resulting in

discoloration – acid/water soluble ash content. The remaining content apart from the amount of the inorganic material or the carbonaceous material in the activated carbon is the percentage fixed carbon. The ash content is also known as loss on ignition. When a sample of known weight is heated in the furnace at the specified temperature for a given time, the weight obtained after heating corresponds to the ash content while the weight loss corresponds to the volatile solids (Okiemimen, et. al, 2007). The percentage fixed carbon is assumed to be approximately 58% of the volatile matter (Dioha, et. al, 2005).

ii. *pH of The Carbon*

The pH is the measure of the surface acidity or basicity o the oxygen containing group. This measurement is used to predict hydophilicity and anionic or cationic adsorptive preference of the carbon. The p^H of the carbon particle determines the materials ironic or cationic preference .The pH can be measured by using the pH meter or a litmus paper and compared with the pH chart.

iii. *Apparent Density and Bulk Density*

Higher density provides greater volume activity and normally indicates better quality activated carbon. The apparent density is equal to the mass (weight) of a quantity of carbon divided by the volume it occupies (including pore volume and inter particle voids, adjusted for the moisture content). Generally, bituminous – based GAC has a density between 28-- 40 pounds per cubic foot (PCF), liqnite-based GAC has a density of approximately 22-26 PCF, and wood-based GAC has a density of 15 – 19 PCF (Department of the Army Engineering US. Army Corps of Engineers and Adsorption Design Guide, 2001). The bulk density of activated carbon and its specific adsorptive capacity for a given substance is used in determining the grade of carbon needed for existing systems. The bulk density of the unit weight of the carbon within the adsorber. Generally, the bulk density of the liquid phase applications is 80 - 95% of the apparent density and for vapor phase applications, it is 80 – 100% of the apparent density. Decolorized carbon has bulk density of around 0.5g/ml. apparent density is used to determine the volumetric carbon usage rate since the carbon usage rate is typically stated in mg.contaminant removal/ gram of carbon.

iv. *Particle Size Distribution*

The finer the particle size of an activated carbon, the better access to the surface area and the faster the rate of adsorption kinetics. For smaller particle sizes the rate of diffusion of an organic into the pore and its subsequent adsorption is significantly increased. The particle size that will be used in a filter. However, particle size may not be that important in all cases, as the porous nature of the carbon particle results in large surface areas in all sizes of carbon particles. Head loss through a carbon bed increases and as the uniformity increases (Department of the Army Corps of Engineers and Engineering Design Adsorption Guide, 2001).

The particle size distribution can be carried out in the laboratory using the mesh/sieve analysis. This is done using a rest of sieves of different mesh sizes. The sieves may be mounted vibrator, which should be designated to give a degree of vertical movement in addition to the horizontal vibration, or may be hand shaken (Richardson, et. al, 2003). Careful consideration of particle size distribution can provide significant operating benefits.

v. *Pore Volume*

Activated carbon has a large volume of small pores which create a large surface area. This large surface area is a result of the space created by crystallites of micro porous structures with large internal surface area. Activated carbon has surface areas ranging from 250 m^2/g to 2500m^2/g. These internal pores are classified based on sizes in micropores (10A^o to 1000A^o). Adsorption occurs primarily in the micropores with macropore acting conduits. The relative proportions of these pores depend on the raw material used. However, particle size may not be that important in all cases as the nature of the pore of the carbon results in large surface area in all sizes of carbon particles. The pore volume is a measure of the total pore volume within the carbon particles in cubic centimeters per gram (cm^3/g).

vi *Molasses Number*

Molasses number or molasses efficiency refers to the milligrams of molasses adsorbed during the standard test. It is also a measure of the macropore content of the activated carbon (greater than 28A^o in diameter or larger than 2nm) by

adsorption of molasses from solution ahigh molasses efficiency is reported as a percentage.

A carbon with a high percentage of this pore size is suitable for adsorbing high molecular weight substances such as color bodies or other colloids – carbons with a high molasses number are generally only used in color removal applications, and is not a valid specification requirement for water treatment. This is a preparatory test, and should not be used in specifying granular activated carbon (GAC) (US. Army Corps Engineers and Engineering design Adsorption Guide, 2001).

vii. *Hardness/Abrasion Number*

The abrasion number measures the ability of carbon to withstand handling and slurry transfer and to resist attrition. It is important indicator of activated carbon to maintain its physical integrity and withstand frictional forces imposed to backwashing. There are large differences in the hardness of activated carbon, depending on the raw material and activity level. Two different tests are used, based on the type of carbon material. A Ro tap abrasion test is used for bituminous – coal based on GAC, and a stirring abrasion test is used for the softer, liqnite – coal based GAC. The abrasion number is the ratio of the final average (mean) particle diameter to the original mean particle diameter (determined by sieve analysis) multiplied by 100. The desired average particle size of the GAC retained should be greater than or equal to 70%. This is of limited value because measuring techniques are not reproducible.

viii *Oil Composition*

This is also called the percentage oil yield. The oil is separated from the activated carbon by the use of extraction. The solvent used must be immisible with the other components but the oil must be more soluble in the selected solvent. The extraction may have to be repeated several times to effect complete separation. Solvents that may be used for extraction include hexane, ether, dichloromethane, amongst others.

2.5.3.6. Chemical Properties Of Activated Carbon

i. *Surface Area*

This is the carbon particle area available for adsorption. The larger the adsorption capacity, the more the solute uptake, however, this surface area needs to be effective. And a high degree of the area needs to be in the "adsorption pore" region,

as well as being accessible to the contaminant with an effective "transport pore" structure, for the capacity to be useful. This is measured by determining the amount of nitrogen adsorbed by the carbon and reported as square meters per gram (commonly between 500 and 2000m^2/g). The American Society for testing Material, ASTM D3037 identifies the procedure for determining the surface area using the nitrogen BET (Brumauer, Emmett, and Teller) method. Nitrogen is used because of its small size, which allows it to access the micropores within the carbon particle. The surface area of activated carbon can be determined by the iodine adsorption method (Egwaikhide, et al, 2007). The amount of iodine adsorbed from aqueous solution was estimated by titrating a blank with standard thiosulphate solution and compared with titrating against iodine containing the sample.

ii. *Iodine Number/content*

This is the most fundamental property used to characterize activated carbon performance. Iodine number refers to the milligrams of 0.02 normal iodine solution adsorbed during a standard test. The iodine number is a measure of the volume present in pores form 10 to 29A^o (10^{-10}m) in diameter by adsorption of iodine from solution. It is also a measure of acidity level higher iodine number indicates higher degree of activation, often reported in mg/g (typical range 500 – 1200mg/g). It is equivalent to surface area of activated carbon between 900m^2/g and 1100m^2/g. It is a measure of the micropore content of activated carbon, adsorptions occur primarily in the micropores with macropores acting as conduits. Carbons with a high percentage of pore sizes in this range would be suitable for adsorbing lower molecular weight substances from water. Carbons with a high iodine number are the most suitable for use as vapor phase carbons, as water molecules tend to effectively block off and isolate pore sizes less than 28A^o. This restricts mass transfer in the micropores, resulting in poor carbon utilization and excessive cost. Virgin liquid phase carbons generally have an iodine number of 1000. Reactivated liquid phase carbon has an iodine number between 800 and 900.

2.6 Rice Husk (*Oryza Sativa Husk*)

General Description and Uses

Oryza sativa husk (rice husk) are the hard protecting covering of grains of rice. In addition to protecting rice during the growing season, rice hulls or husks can be put to use as building material, fertilizer insulation material, or fuel. The hull is formed from hard materials including opaline silica and lignin. The hull is mostly indigestible to humans. Winnowing used to separate the rice from hulls, is to put the while rice into a pan and throw it into the air while the wind blows. The light hulls are blown away while the heavy rice falls back into the pan.

Combustion of rice hulls affords rice husk ash (RHA). This ash is a potential source of amorphous reactive silica, which has variety of applications in materials science. Most of the ash is used in the production of Portland cement (Otto, 2008) when burnt completely the ash can have a blaine number of as much as 3,600 compared to the blaine number of cement between 2,800 to 3,000, meaning it is finer than cement. A number of possible use of RHA include absorbents for oils and chemical, soil ameliorants, a source of silicon, insulation powder in steel mills, as repellents in the form of "Vinegar-tar" release agent in the ceramics industry, as an insulation material. More specialized applications include the use of this material as a catalyst support (Chumee, 2008). In kerala, India, Rice husks (umikari in Malayalam) were universally, used for over centuries in cleaning teeth, before toothpast replaced it. Rice hulls can be used in brewing beer to increase lantering ability of a mash. Rice hulls (rich in lignin) are inexpensive by product of human food processing, serving as a source of fiber that is considered a filler ingredient in cheep pet foods (Otto, 2008).

2.7. Breadfruit husk (*Treculia africana* Husk)

Description and uses

Treculia Africana, the African bread fruit, is a tree species in the genus Treculia. It is used as a food plant. The fruits are hard and fibrous, can be the size of a volleyball and weight up to 8.5kg (19 lb). Chimpanzees have been observed to use tools to break the fruits into small piece that they can eat (Walker, 2009). The fruits contain polyphenols (Lawal, 1992).

Many tribal names are given to this species but the most common name is "Ukwa" (Nuga and Ofodile, 2010).The geographical distribution of *Treculia Africana* extender through west and central Africa. The species can grow below attitude of 1,500m (4,900ft) (Nuga and Ofodile, 2010). *Treculia Africana* is a large tree and is part of the family *Moraceae*. It grows in wet areas and forests. The species can grow up to a height of 30m (98ft). The girth of the stem can attain 6m (20ft). The bark is grey and discharges a cream latex. The leaves are large and dark green above and light below. The flowering period is from October until February. The fruit is bid round and greenish yellow. The texture of the fruit is spongy when it is ripe and it contains abundant seeds.

Based on detailed field observations, three varieties are distinguished within the subspecies; *Treculia Africana var. Africana* (extending from Senegal to Southern Sudan and South to Angola, Central Mozambiqe and Principe and Sao Tome Island); *Treculia Africana Var. Inverse* (Anambra State, Edo and Delta State, more abundantly on the eastern State of Nigeria) and *Treculia Africana Var. Mollis* (isolated localities in Edo and Delta State of Nigeria, Cameroun, DR. Congo, Gabon and Cabinda). Their taxonomic differences are based mainly on the size of the fruit head (infructence) and the hairness of branchlets and leaves.

African breadfruit is an edible traditional fruit, consumed, for example in Nigeria, where it is eaten because of their high nutrition value. Fresh seeds contain 38.3% carbohydrate, 17.7 crude proteins and 15.9% fat. It is known that African breadfruit a good adjunct in brewing because it is a source of fermentable sugar (Nwabueze and Uchendu, 2011). Different parts of the plant are used for medicine: the roots, the bark and the leaves. The tree is used to treat malaria, worms, cough and digestive disorders:

2.8. Mango Seed (*Magnifera Indica* Seed)

Description and uses

The Mango is a Juicy stone fruit belonging to the genus *Magnifera*, consisting of numerous tropical fruiting trees, cultivated mostly for edible fruit. The majority of these species are found in nature as wild mangos. They all belong to the flowering

plant family *Anacardiaceae*. The mango is native to South and Southeast Asia, from where it has been distributed worldwide to become one of the most cultivated fruits in the tropics. The highest concentration of Magnifera genus is in the western part of Malesia (Sumata, Java and Borneo) and in Burma and India. While other *Magniferea* species (e.g horse mango. M.foetide) are also grown on a more localized basis, *Magnifera Indica*- The "common mango" or "Indian mango" – is the only mango tree commonly cultivated in many tropical and subtropical regions. It originated in Indian subcontinent (present day india and pakistan) and Burma (kostermans and Bompard, 1993) it is the national fruit of India, Pakistan, and the Philippines, and the national tree of Bangladesh.

In several cultures, its fruit and leaves are ritually used as floral decorations at weddings, public celebrations, and religious ceremonies.

Mango trees grow up to 35-40m (115-131ft) tall, with a crown radius of 10m (33ft): The trees are long-lived, as some specimens still fruit after 300years. The flowers are produced in terminal panicles 10-40cm (3.9-15.7 in) long; each flower is small and white with five petals 5-10mm (0.20-0.39in) long, with a mild, sweet odor suggestive of lily of the valley. Over 400 varieties of mango are known, many of which ripen in summer, while some give double crop. The English word "Mango" (plural "Mangoes" or "Mangos") originated from the Malayalam word Via Ludovico di Varthema in Italian in 1510, as mango.

Mangoes are generally sweet, although the test and texture of the flesh varies across cultivars; some have a soft, pulpy texture familiar to an overripe plum, while others are firmer, like a cantaloupe or avocado, and some may have fibrous texture. The skin of unripe, picked, or cooked mango can be consumed, but has the potential to cause contact dermatitis of the lips, gingiva, or tongue in susceptible people. Mangoes are widely used in cuisine; sour, unripe mangoes are used in chutneys, ethane Pickies (Devika, 1995), side dishes or may be eaten raw with salt, chili, or soy sauce. A summer drink called aam panna comes from mangoes. Mango pulp made into jelly or cooked with red gram ethai and green chilies may be severed with cooked rice. Mango lassi is popular throughout South Asia (Ajila and prasada, 2008), prepared by mixing ripe mangoes or mango pulp with buttermilk and sugar. Ripe mangoes are also used to make curries. Mangoes are used in preserves such as

Movamba, amchur (dried and powdered unripe mango) and pickies, including a spicy mustard-oil pickies and alcohol. Mango is used to make juice, smoothies, ice cream, fruit bars etc.

2.9. Ukpor Clay *(Kaolinite)*

Kaolinite is a clay mineral with the chemical composition $AL_2Si_2O_5(OH)_4$. It is a layered silicate material, with one tetrahedral sheet linked through oxygen atoms to one tetrahedral sheet of alumina octahedral. Rocks that are rich in kaolinite are known as china clay or kaolin.The name is derived from Gaolin, ("High Hill") in Jingdezhen, Jiangxi province, China.

Kaolinite is one of the most common minerals; it is mined, as kaolin, in Brazil, France, United Kingdom, Germany, India, Australia, Korea, the people's Republic of China, and the USA. Kaolinite has a low shrink-swell capacity and a low cation exchange capacity (1- 15meq/100g). It is soft, earth, usually white mineral (dioctahedral phyllosilicate clay), produced by the chemical weathering of aluminum silicate minerals like feldspar. In many parts of the world, it is colored pink-orange-red by iron oxide, giving it a distinct rust appearance. Lighter concentrations yield white, yellow or light orange colors. In Nigeria, kaolinite is mined as Ukpor clay in Nnewi south, Anambra State. There, it is minded and pulverized and then sold for as adsorbent, component for local medicines and other industrial uses as follows:

i. In paper industry: The largest single user of kaolin is the paper industry. Because kaolin is used, paper products print better and are made whiter and smother. Kaolin used as a filler in the interstices of the sheet adds ink receptivity and opacity to the paper sheet. Kaolin used to coat the surface of the paper sheet makes possible sharp photographic illustrations and bright printed colours. The significant properties of kaolin of greatest value to the paper industry are whiteness, low viscosity, non-abrasiveness, controlled particle sizes, and flat hexagonal plates.

ii. In Rubber Industry: Kaolin is used as a filler in many rubber goods. It adds strength, abrasion resistance, and rigidity to both natural and synthetic rubber products. In general, most rubber products extrude more easily after kaolin filler is added.

iii. In ceramics industry: Kaolin is used in ceramic whiteware products, insulators, and refractories. In whiteware, Kaolin aids accurate control of molding properties, and adds dry and fired strength, dimensional stability, and a smooth surface finish to the ware.

iv. In paint industry: Kaolin is used in paint because it is chemically inert and insoluble in the paint system, has a high covering power, gives the paint desirable flow properties, and is low in cost.

v. In plastic industry: The addition of kaolin to thermosetting and thermoplastic mixes gives smoother surfaces, a more attractive finish, good dimensional stability and high resistance to chemical attack.

Finally, kaolinites can be used in the treatment of wastewater, because it has favourable properties such as fine particle size, non-abrasiveness, chemical stability, it is soft and has low viscosity at high solid's content in many systems. It is readily wet and dispersed in water and some organic systems which place it in a better position to be used as an adsorbent which is in agreement with previous work (Murray, 1959).

Table 2.1: Clay Characteristics

Category	Mineral
Chemical formula	$AL_2Si_2O_5(OH)_4$
Colour	white, sometimes red, blue or brown tints from impurities.
Crystal system	triclinic
Cleavage	perfect on (0.01)
Hardness (mols)	
Scale	2 – 2.5
Luster	Dull and earthly
Refractive index	α : 1.553 – 1.565; α : 1.559 – 1.569, α : 1.569 – 1.590
Specific index	2.16 - 2.68

2.10. Laterite (Red Mud)

Laterite is a surface formation in hot and wet tropical areas which is rich in iron and aluminum and develops by intensive and long lasting weathering of the underlying parent rock. Nearly all kinds of rocks can be deeply decomposed by the action of high rainfall and elevated temperatures. The percolating rainwater causes dissolution of primary rock minerals and decrease of easily soluble elements as sodium, potassium, calcium, magnesium and silicon. This gives rise to a residual concentration of more insoluble elements predominantly iron and aluminum.

Laterite consists mainly of the mineral kaolinites, goethite, hematite and gibbsite which form in the course of weathering. Moreover, many laterites contain quartz as relatively stable relic mineral from the parent rock. The iron oxides goethite and hematite cause the red-brown colour of laterite.

Laterization is economically most important for the formation of laterite ore deposit. Bauxite which is an aluminum – rich laterite variety can be formed from various parent rocks if the drainage is most intensive thus leading to a very strong leaching of silica and equivalent enrichment of aluminum hydroxides and above all gibbsite.

The mineralogical and chemical composition of red mud has been previously studied (Altundogen, et al., 2000). Several studies have been reported in the literature, where red mud is used for water and wastewater treatment via adsorption. The adsorption of both cations and anions onto red mud and its conditioned forms has been successfully carried out.

CHAPTER THREE

MATERIALS AND METHOD

3.1. COAGULATION/FLOCCULATION

3.1.1. Sample Collection

Two samples each, of pharmaceutical and refined vegetable oil wastewater were collected from local pharmaceutical and vegetable oil waste line, during the month of April 2009. Twelve black Jericans of thirty- litre capacity each were filled to the brim with the wastewater in order to expel entrapped air within the Jericans. The Jericans were corked and remained sealed until the commencement of the analysis (Menkiti, 2010; Wright and Hordon,1993).

The samples were refrigerated at 4^0C as required by test method (APHA and AWWA; 1985) in order to avoid microbial action leading to chemical changes.

The raw materials: *Telfairia occidental's* seed, *Maginata achatina*, *Pleurotus tuberregium sclerotium* were sourced from Nkwo market Enugwu-Ukwu Anambra state; while C*orchorus olitorius* seed and *Mucuna Pruriens* seed were obtained from Dugbe market, Ibadan, Oyo state and Oye Oba market Nsukka, Enugu State, respectively for the production of bio-coagulants during the month of June 2009.

3.1.2. Production of Biocoagulants

3.1.2.1. Animal tissue derived biocoagulants

The snail was obtained from Nkwo market Enugu-Ukwu Anambra State. Upon receipt, the snail was washed with tap water and rinsed with distilled water to remove debris and soluble organics. Subsequently, it was boiled for 20minutes. The shells and the edible parts were separated and the former kept in a container at ambient temperature. The shells were then dried in the laboratory oven (Quimis model Q-317B) at 60^oC for 36hours to make sure that completely dried shells were obtained (Jatto, et al.,2010). To obtain a uniform size product, the dried shell was ground through a centrifugal grinding mill (model No DR 64857-Retsch/Brinkamann ZW-1 westbury, New york) and sieved with 0.5mm sieve. Dried ground shell was placed in opaque plastic bottles and stored at ambient temperature for use.

3.1.2.2. Plants seed derived biocoagulants

The seeds of the various plant raw materials were obtained after dehulling. The obtained seeds were sundried between 3-4 days, powered using kitchen blender (model 248, moulinex, Japan) and sieved through 0.5mm sieve and stored in opaque plastic bottles at ambient temperature ready for use (Gunaratna, et al.,2007).

3.1.2.3. Plants tuber derived biocoagulants

The tubers of *pleurotus tuberregnium sclerotium* plant was sourced from Nkwo market Enugwu-Ukwu, Anambra State. The back of the tubers was scraped with kitchen knife to remove debris. The obtained tubers were sundried for 3-4 days, powdered using kitchen blenders (model, 248,moulinex, Japan) and sieved with 0.5mm sieve, stored in plastic bottles at ambient temperature.

3.1.3. Coag-flocculation test

The coagulation/flocculation experiment was carried out using a jar test procedure on a stirring apparatus at room temperature. The stirring apparatus was equipped with a six- place paddle stirrer of model No 300, Phipps and bird Inc. virgins USA.

A series of 250ml each of the effluents were separately poured into appropriate measuring cylinders and dosed with appropriate amount of the bio-coagulants. Rapid mixing was performed on the dosed effluents at 120 rpm for 2 minutes to destabilize the suspension, followed by slow mixing for 20 minutes at 10 rpm to facilitate floc agglomeration.

The samples were then left to settle for 40 mintues. At specified time intervals after the commencement of the settling period, samples were withdrawn using pipette from the top 2cm depth of the 250ml effluents contained in the beaker. The withdrawn samples were analyzed for turbidity using lab-tech turbidimeter (model 212R) at intervals of 2-40minutes. The turbidity value in NTU is digitally read off when the withdrawn supernatant (treated) effluent is emptied into a curvette, which is in turn inserted into a hole provided for it in the turbidimeter. In this work, the effects of dosage and pH on the coagulation process were studied via changes in turbidity values.

3.1.4. Characterization procedure for coag-flocculants

This presents standarded methods used in characterizing the biocoagulants as contained in Table 3.1

Table 3.1: Characterization parameters for coag-flocculants

Parameters	Procedure(AOAC;1989)(Menkiti,2010)
Moisture	AOAC- PA (100)
Ash content	AOAC- PA (103)
Lipid	AOAC- PA (105)
Crude protein	AOAC- PA (109)
Carbohydrate	AOAC- PA (115)
Crude fibre	AOAC- PA (118)

3.2. **ADSORPTION**

3.2.1. Sample Collection

he husks or shells of bread fruit (*Treculia Africana*), rice (O*ryza sativa*) and mango seed nuts (*Magnifera indica*) were sourced from Otuocha-Aguleri environs. Ukpor clay (*kaolinite*) and laterite were sourced from Ukpor (in Nnewi, South L.G.A) and Awka respectively.

3.2.2 Production of Adsorbents

3.2.2.1 Production of Bioadsorbents (activated carbon)

The raw materials samples were thoroughly screened /cleaned to remove debris and sundried for 5-14days. Before then mango seeds were dehulled to get the nuts. The cleaned/screened samples of bread fruit husks, rice husks and mango nuts were ground using domestic blender. The samples were then put in earthen ware and placed in muffle furnace (model KCO 80750120 kgyn Budapest) set at different temperature. Bread fruits husks, rice husks and mango nuts samples were set 300-400^{o} for 2hrs, 400-600^{o}c for 3hrs and 600-900^{o}c for 3hrs holding time respectively. After the carbonization, the samples were allowed to cool. The three samples were soaked in 60% solution of H_2S0_4 in the ratio of 1:1 in each case. The impregnated samples were left at room temperature for 24hrs. After impregnation the excess

solutions were filtered off and the sample washed with distilled water until the pH of the leachate is approximately 7. After washing, the sample were dried in an oven at temperature of 80^0C before sieving commenced. The sieved samples passed through 0.3mm and retained 0.15mm sieved mesh size.

3.2.2.2. Production of non-carbon adsorsorbents

Laterite and Ukpor clay (kaolinite) were obtained from construction site at Awka and Ukpor town respectively. The samples were ground using mortar and pestle and sieved through 1mm to retained 0.5mm sieved mesh size and the same procedure of H_2S0_4 impregnation and sample sieving was followed as in the production of bioadsorbents.

3.2.3. Characterization procedure for adsorbents

The standard methods used in characterizing the bioadsorbents are as presented in Table 3.2

Table 3.2: Characterization of parameter for adsorbents

Parameters	Procedure
% yield	Aloko and Adebayo(2007) ; ASTMD 2865(1994)
%weight loss	ASTMD 2865(1994)
Surface Area	D2864 (1994)
Total pore volume	ASTM D2862
Moisture content	ASTM D2866(1994)
Ash contents	ALOKO and ADEBAYO(2007)
Bulk density	ASTM D2867(1994)
Iodine number	AOAC (1993)
Oil content	AOAC((1993)

3.2.4. Batch Adsorption

Five different adsorbent masses of 0.2, 0.4, 0.6, 0.8 and 1.0g were weighted and placed in five different plastic test tubes containing 20ml of supernatant effluent from coagulation process. The tubes (containing the supernatant effluent) were subsequently

placed in the centrifuge (model Sum 800D England) and stirred at 20rev/min for period of 5, 10, 20, 25, 30, 35, 40, 50 and 60minutes. The procedure was repeated for both pharmaceutical and vegetable oil effluents using H_2S0_4 impregnated adsorbents of *magnifera indica, treculia Africana, oryza sativa*, *kaolinite* and laterite. At the end of the agitation, the adsorbents were removed by filtration using ash-less and fine crystal filter paper Whatman No 42. The filtrate poured in a uv-curvette was then put in a fitting hole in the spectrophotometer, that displays concentration level of the particles in the filtrate. The adsorption capacity and percentage quantity adsorbents were calculated from equations (3.1) and (3.2)

$$q_t = \frac{[C_o - C_t]}{W} \quad (3.1)$$

$$\% \text{ q} = \frac{[C_o - C_t]}{C_o} \text{ x } 100 \quad (3.2)$$

Where C_o and C_t (mg/l) are the liquid phase concentration of particles at initial and any time t, respectively, w is the mass concentration of the dry adsorbent used(g/l). C_o is constant for each batch of effluent.

3.3. TEMPERATURE DEPENDENCY

Five 1g mass of adsorbents were weighed out and put in five different 250ml beakers containing 20ml of the supernatant effluent from coag-flocculation process. The contents of the beakers labeled A,B,C,D,E were subjected to magnetic stirring at 25^{o}c for 5,10,15, 20,30minutes respectively. At the end of each interval of stirring, spectrophotometric absorbance of the filtrate was read off and recorded. The same procedure was repeated at 35^{o}C for the supernatants effluents from PIE and VIE.

3.4 STATISTICAL MULTI VARIABLE POLYNOMIAL MODEL DEVELOPMENT

The statistical design of experiments (DOE) is an efficient procedure for planning experiments so that data obtained can be analysed to yield valid and objective conclusions. It involves the laying out of a detailed experimental plan prior to doing the experiment.

For the purpose of this work, standard CCD with a 2^3 full factorial design was employed. The standard CCD is usually constructed from a 2^{m-1} design for the cube portion, which is augmented with centre points and star points. The procedure for the generation of the optimum composite plan is shown below.

No of experimental points for CCD, N is

$$N=k^{m-1} + 2m + N_0 \quad (3.3)$$

Where k is the level of the experiment (here = 2)

m is the no of variables (here 3:$X_1X_2X_3$)

t is the degree of fractionality (t = 0, since m<4)

N_0 is the centre point (this is chosen to be 3)

Therefore $N = 2^3 + 2 (3) + 3$

$= 8 + 6 + 3 = 17$ runs

The levels are the lower limit (-1) and upper limited (+1). The base level is denoted by (0). It describes the point at the centre of the plan.

The table showing the experimental plan is known as model or analysis matrix. It is arranged in columns and rows. In general, the i^{-th} column (X_1) starts with 2^{i-1} repeats of -1 followed by 2^{i-1} repeats of +1.

The model matrix of CCD full 2^3 factorial design, start points and centre points are constructed as shown below; No of runs = 17, No of centre points = 3, No of star points = 6, No of variables = 3.

Table 3.3: Experimental Plan for CCD.

S/N	X_1	X_2	X_3
1.	0	0	0
2	-1	-1	-1
3.	1	-1	-1
4.	-1	1	-1
5.	1	1	-1
6.	0	0	0
7.	-1	-1	1
8.	1	-1	1
9.	-1	1	1
10	1	1	1
11.	0	0	0
12.	-1	0	0
13.	1	0	0
14.	0	-1	0
15.	0	1	0
16.	0	0	-1
17.	0	0	1

Table 3.4: Upper, Lower and base level of the variables

	Variables	Lower Limit (-1)	Base level (0)	Upper Limit (+1)
1.	X_1	(-1)	X_1 (0)	x_1 (+1)
2.	X_2	(-1)	X_2 (0)	x_2 (+1)
3.	X_3	(-1)	X_3 (0)	x_3 (+1)

Lower and upper limits are chosen.

Base level = $(X_{-1} + X_{+1})/2$ (3.4)

The model equation for the experiment is proposed as shown below:

$$Y = b_0+b_1X_1+b_2X_2+b_3X_3+b_{12}X_1X_2+b_{13}X_1X_3+b_{23}X_2X_3+b_{11}X^2_1+b_{22}X^2_2+b_{33}X^2_3 \quad (3.5)$$

A second order (quadratic) model typically used in response surface DOE's with suspected curvature does not include the three way interaction terms ($b_{123}X_1X_2X_3$) but adds three more terms to linear model namely $b_{11}X^2_1 + b_{22}X^2_2 + b_{33}X^2_3$.

A model could include many cross-products (or interactions) terms involving X_1's. However, in general these terms are not needed and most DOE software defaults the model.

The coefficients of the model shown in equation (3.5) can be evaluated using the following formulae:

$$b_o = a\sum^{M}_{u=i} Y_u + P\sum^{M}_{j=i} = \sum^{M}_{u=i} X^2_{ju} \quad (3.6)$$

For the coefficients of linear terms

$$b_i = e\sum^{N}_{u=i} X_{iu} + Y_u \quad (3.7)$$

For the coefficients of interactions

$$b_{ij} = g\sum^{N}_{u=i} X_{iu} + X_{tu}Y_u \quad (3.8)$$

For the coefficients of the terms of the 2nd order

$$b_{ij} = c\sum^{N}_{u=i} X^2_{ju} Y_u + d\sum^{M}_{j=i} \sum^{N}_{u=i} X^2_{ju} + p\sum^{N}_{u=i} Y_u \quad (3.9)$$

The constants e.g c, d and p are determined from statistical table.

If $(b_i) \leq \sqrt{e}\ (s_z)\ t\ (\alpha, Y_z)$: the b_i is insignificant

If $F < F_{table}$: the model is adequate.

The inter value conversion equation for the DOE is given below:

$X_R - X_b = X_c (X_u - X_b)$

$X_R = X_b + X_c (X_u - X_b)$

X_R = the real value expected to be determined

X_b = Real base value

X_u = Real upper limit

X_c = Known coded value

3.4.1. The variable parameters for statistical experimental design

The independent variables for the CCD are as follows:

a. For coag-flocculation: pH, Dosage, Settling time.

b. For adsorption: pH, adsorbent mass, settling time. The output responses (dependent variable) for coag-flocculation and adsorption is removal efficiency in percentage.

$$\% \text{ Removal Efficiency} = \frac{[C_o - C_t]}{C_o} X\ 100 \qquad (3.10)$$

Experimental range and levels are shown as follows:

Table 3.5: Independent variables set for Coag-flocculation: pH, dosage, settling time.

Variable	Lower limit(-1)	Base level(0)	Upper limit(+1)
pH	1.0000	7.000	13.000
dosage	0.1000	0.4000	0.7
Settling time	2.0000	22.0000	40

Table 3.6: Independent variables set for Adsorption: pH, adsorbent mass, stirring time

Variable	Lower limit(-1)	Base level (0)	Upper limit(+1)
pH	2.0000	6.0000	10
Adsorbent	0.2000	0.6000	1.0
mass	5.0000	32.5000	60
Stirring time			

3.5Characterization of PIE and VIE WasteWaters

The following standarded procedures were employed for the characterization process

Table 3.7: Characterization procedures for PIE and VIE WasteWaters

S/N	Parameters	Referred Standard Methods
1.	pH	APHA, AWWA, 423-1985
2.	Total suspended solid(TSS)	APHA, AWWA,209C-1985
3.	Total Dissolved solid(TDS)	APHA,AWWA, 209B-1985
4.	Total solid(TS)	APHA,AWWA, 209A-1985
5.	Biochemical oxygen Demand(BOD_5)	Digital BOD kit application
6.	Electrical conductivity(EC)	APHA, AWWA, 205-1985
7.	Turbidity	APHA, AWWA, 214-1985
8.	Nitrate $N0_3$	APHA, AWWA,418A-1985
9.	Iron	APHA,AWWA, 315B-1985
10.	Chemical Oxygen Demand(COD)	Tchobanoglous and Schroeder
11.	Total hardness	1985
12.	Calcium content	APHA, AWWA,314B- 1985
13.	Magnesium content	APHA, AWWA, 311C-1985
14.	Chloride	APHA, AWWA, 318C-1985
15.	Total acidity	APHA, AWWA, 407, 1985
16.	Total Alkalinity	APHA, AWWA,1985
17.	Total viable count	APHA, AWWA, 403 1985
18.	Total coliform count	Cooper 2001 Mair, et al 2000
19.	Feacal count	APHA, AWWA, 907B 1985
20.	Clostridium perfrigens	Cooper 2001& Mair, et al 2000
		Cooper, 2001; Mair. et al

Table 3.8: Equipment used and models

The equipemt employed in the work are listed in the table below

EQUIPMENT	**MODEL**
MAGNETIC STIRRER	Gallenhamp Magnetic Stirrer England APP No 6886644A
OVEN	Nemmert oven Din 40050-1p20
pH METER	Hand pH meter Havanar
FURNACE	Model KCO 80750120 kygn budapest(furnace)
VISCO METER	Model cat No 9721-R-56, cannon instrument corp. USA
BLENDER	Model- 248 moulinex
STIRRER	Six paddle stirrer model No.300, Phipps and Bird Inc. Virginia, USA.
TURBIDIMETER	Mc Turbidimeter Lab tech model 212R
CENTRIFUGAL GRINDING MILL	Model No DR 64857 Retsh/Brinkmann
BOD KIT	Spectroquant NOVA 60 BT
FTIR	Diffuse reflectance infrared fourier transform (DRIFT)
SEM	Spectrometer (perkin-Elmer, model spectrum one, USA. Electron probe micro Analyzer(model Jeol- JXA 840A, Japan
ELETRIONIC THERMOSTAT WATER BATH	HH-W21-Cr 4211(England)
WEIGHING BALANCE	"KERRO Lab Digital scale KA-3002C(Taiwan)
CENTRIFUGE	Sum 800D England

CHAPTER FOUR

RESULTS AND DISCUSSION

4.1. RESULT AND DISCUSSION ON COAG-FLOCCULATION

4.1.1. Characterization Results of the WasteWaters (PIE and VIE) and Coag-flocculants

The characterization results of the wastewaters (before and after coagulation) and coag-flocculants of organic derivatives are presented in tables 4.1 and 4.2.

The characterization results of the PIE, before and after coag-flocculation indicate parameter reduction from 3.87 to 5.98, 1256.00 to 794.00mg/l, 22.55 to 20.50mg/l, 620.00 to 155.00mg/l, 90.00 to 0.00mg/l and 57.25 to 5.75mg/l, 880.00 to 295.00mg/l for PH, turbidity, TSS, BOD, TVC,TDS and COD respectively and for the VIE 4.99 to 4.92, 102.00 to 38.00 NTU, 140.00 to 2.50mg/l, 651.60 to 220.00mg/l, 238.33 to 0.00mg/l, 2126.25 to 550.00mg/l for pH, turbidity, TSS,BOD, TVC and COD respectively. However, for VIE there is increase from 0.00 to 45.00mgL for TDS. The reduction in the parameters observed in table 4.1 justified the effectiveness of the organic derived coag-flocculant employed for the treatment. The generally low pH values obtained after treatment in the effluent samples, might be due to the high levels of free CO_2 prevalent in them, which may consequently affect the bacterial counts as reported by Edema, et al(2001). This phenomenon supports the results of bacteriology analysis posted in table 4.1, which indicate that all the values are nil except TCC in PIE effluent sample. The general implication is that life may not be sustained in acidic media. However, the result of TCC in PIE, indicates that about 10% of living organisms can survive in varying effluent media conditions. This occurrence points to the fact that the coag-flocculated effluent may not be suitable for agricultural and other applications without further treatment (tertiary treatment). Table 4.1, show relative increase in electrical conductivity values 1.73 to 8.74 $\mu m/m^2$ for VIE and 8.17 to 10.46 $\mu m/m^2$ for PIE. The values obtained indicate that the effluents contain charged ions, suggesting that it can conduct electricity. Also the level of nutrients (Ca, Mg) and absence of heavy metals, make the post effluent to be recycled for agricultural purposes (as a soil conditioner). Besides, tables 4.1 and 4.2, indicate that a number of parameters do not meet up with WHO standard for drinking water, an indication of the need for further treatment of the coag-flocculated effluents.

The presence of COD, BOD, turbidity and other chemical parameters in the effluents accounts for inherently natural organic materials prevalent in VIE and PIE. This is an indication that both effluents are basically endowed with organic matter known for imparting color to water. Also from the table 4.2, both PIE and VIE has low BOD values to compare with the COD values, this might be as a result of low biodegradability of the organic matter. Similarly, table 4.3, shows the composition of the organic derived coag-flocculants. Among all the parameters studied, crude protein, a water-soluble cationic peptide is responsible for the coagulating property inherent in them and other natural coagulants of this type (Gassenschmidt, et al. 1993). The percentage protein contents of MPSC, SSC, PTSC, COSC and TOSC are 40.75%, 38.50%, 43.70%, 29.57% and 27.00% respectively.

The best optimized value of TDSS reduction are recorded at 1.6847e+003,1.4582+003,1.73173+003,1.2066e+003 and 1.1071e+003mg/l for MPSC, SCC, PTSC, COSC and TOSC respectively. The optimized value gave support to the fact that protein content of these substrates is the coag-flocculation agent in them. This is justified by the results presented in tables 4.133 to 4.134, where the substrates with the highest values of protein content had the best particle removal performance.

Table 4.1: Characterization of VIE and PIE before and after coag-flocculation

Parameter	Beforecoag-Flocculation		After coag-flocculation		WHO Standard
	PIE	**VIE**	**PIE**	**VIE**	
PH	3.87	4.99	5.98	4.92	7.00 – 8.00
Temperature (^oC)	28.00	28.17	26.50	27	
Electrical conductivity (No/m^2)	8.17	1.73	10.46	8.74	1250.00
Phenol (mg/l)	nil	nil	nil	nil	
Total Hardness (mg/l)	6000	65	3730.00	45	500.00
Ca hardness (mg/l)	3344.00	15.83	200.00	12.5	200.00
Mg hardness (mg/l)	2656.00	49.17	3530.00	32.5	100.00
Chlorides CL^- (mg/l)	100.00	36.67	5.50	25.00	200
Dissolved oxygen (mg/l)	20.00	54.42	2.95	4.62	nil
Turbidity (NTU)	1256.00	102.00	794.00	38.00	5.00

Iron fe^{2-} (mg/l)	nil	0.04	nil	0.03	0.03
Nitrate No_3^{2-} (mg/l)	nil	nil	nil	nil	3.00
Total acidity (mg/l)	250.00	10.83	0.02	1.10	nil
TDS (mg/l)	57.25	nil	5.75	45.00	50.00
TSS (mg/l)	225.50	140.00	20.50	2.50	50.00
Oil & grease (mg/l)	nil	50.00	nil	nil	nil
Total viable count (cfu/ml)	90.00	238.33	nil	nil	nil
Total coliform count (cfu/ml)	10.00	40.50	1.00	nil	3/100ml
Pseudomonas aeruginosa(MPN/ml)	nil	nil	nil	nil	nil

Table 4.2: Characterization of COD and BOD for VIE and PIE before and after coag-flocculation

Parameter		Beforecoag-Flocculation		After coag-flocculation		WHO Standard
		PIE	**VIE**	**PIE**	**VIE**	
COD	(mg/l)	880.00	2125.25	295.00	550.00	50.00
BOD	(mg/l)	620.00	651.60	155.00	220.00	20.00

Table 4.3: Characterization Results of coag-flocculants

Parameter	MPSC	SSC	PTSC	COSC	TOSC
Moisture Content (%)	20.00	10.00	10.00	10.00	0.01
Ash content (%)	12.00	10.00	6.00	10.00	2.00
Lipid content (%)	7.50	11.00	9.00	8.00	53.00
Crude protein (%)	40.75	38.50	43.70	29.57	27.00
Carbohydrate (%)	5.25	20.50	5.51	22.43	15.00
Crude fibre (%)	8.50	10.00	11.00	20.00	3.00

4.1.2. Primary Jar Test Results For Varying Dosage and pH

The primary jar test results for variable dosages and pH are presented in this section. Both variables pH and dosage results are presented for PIE and VIE in the following order.

(a) Removal efficiency profile for varying coag-flocculant dosage at constant pH.

(b) Removal efficiency profile for pH varying effluent and constant coag-flocculant dosage

4.1.2.1 Removal efficiency for varying coag-flocculant dosage at constant PIE pH

The results are graphically presented in figures 4.1 to 4.30. These figures actually indicated that the reactive effectiveness of the coag-flocculants to remove soluble reactive TDSS from the predominantly negatively charged PIE effluent is time dependent. This phenomenon is justified because early stage of coagulation witnessed dispersing of the coag-flocculating agent in the effluent and at this point less sites are available for adsorption of the TDSS particles. Hence sorption capacity of the coag-flocculants increases with time due to increases in adsorptive sites. This is supported by the results obtained from the figures which indicate that best performances are recorded at maximum coag-flocculating time of 40minutes. The general features observed in figures 4.1-4.30, show that efificiency of the coag-flocculants increases with time, but the magnitude differ for a particular pH. General overview of the coag-flocculants performance show that many of the coag-flocculants recorded efficiency (E%> 80%) at the time of 40 mins, an indication that the study conformed to the principles of rapid coag-flocculation. High level of efficiency recorded confirms the high potency of these coag-focculants in removal of turbidity.

In specific terms, the activity behaviour of SSC coag-flocculant displayed in figs. 4.1- 4.6, follow the same pattern with the exception of figures. 4.2 and 4.3. The important features of these figures. 4.1, 4.4, 4.5 and 4.6 confirm that the best performance is recorded for SSC at pH of 13 and 1, though the performance recorded for pH of 7 and 10 is satisfactory. This behavior obtained in these figures is suggestive of the fact that coag-flocculant dosage has negligible influence on the efficiency, implying that any of the dosages could be used to achieve a good performance. Whereas, the poor performance recorded in figures. 4.2 and 4.3 for pH

of 3 and 5, could be attributed to low degree of solubility of SSC- coag-flocculant in relatively weak acidic medium which gave rise to the provision of few adsorptive sites for particles attachments on the coag-flocculants polymers.

In case of COSC-coag-flocculant behaviour shown in figures. 4.7 - 4.12, critical observation of the figures shows that maximum TDSS removal is recorded at the pH of 7 for all doses, followed by pH of 10 and 13. In general terms, it can be deduced from the figures that increasing COSC - coag-flocculant dosage has insignificant effect on TDSS removal efficiency here .

The performance of TOSC-coag-flocculant is illustrated in figures. 4.13 - 4.18. The figures show similar trend but with different percentage removal for a particular pH. Figure 4.18 show that over 89% of TDSS removal is achieved at pH of 13 and 0.1 g/l TOSC dosage, an indication that increase in dosage could have led to returbidization of the waste water sample (PFRA, 2003). The good performances in alkaline medium as observed could be due to adsorption of TDSS inherent in the waste water onto hydroxide flocs or that the positive charges on the TOSC surface significantly decreased as medium OH^- increases. The contribution by charge neutralization of the TOSC to destabilize the particles became less important as the pH increased (Sanghi and Bhattacharya, 2005).

PTSC-Coag-flocculant activity as shown in figures. 4.19 - 4.24, indicates that the efficiency values recorded for pH of 1 and 13, are very closely followed by decrease in efficiency obtained for pH of 3, 5, 7 and 10. The results recorded at pH of 13 is above 95% efficiency. This is an indication that sorption capacity of PTSC is optimum at that pH, an evidence that electrostatic interaction of PTSC cations with anions in the medium is at maximum.

In case of MPSC-Coag-flocculant, demonstrated in figures.4.25 – 4.30, it is shown that the efficiency values recorded for pH of 7, 10 and 13 are satisfactory (figures. 4.28, 4.29 and 4.30). This is an indication that MPSC-Coag-flocculant is more soluble in alkaline medium; then ensuring greater cationic and anionic interactions which is optimum at the pH of 13. Also, it can be observed that coag-flocculant dosage (MPSC) has slight influence on efficiency.

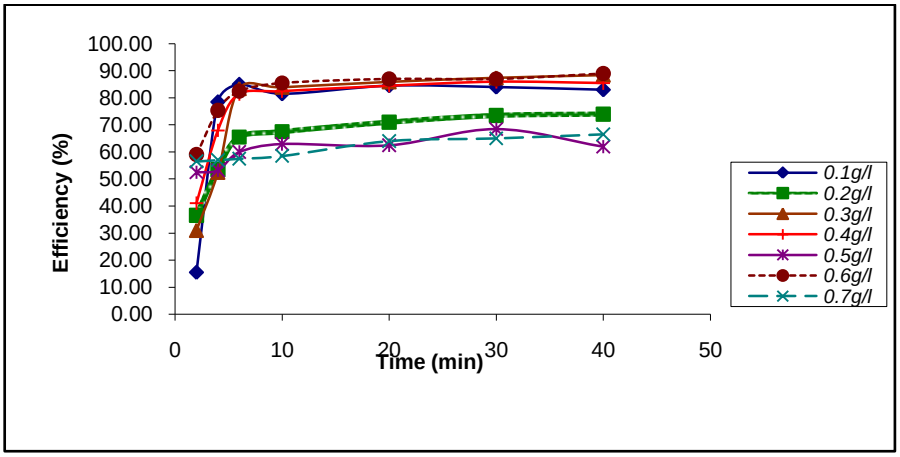

Fig.4.1: Removal efficiency as a function of time and ssc dosage for PIE pH 1

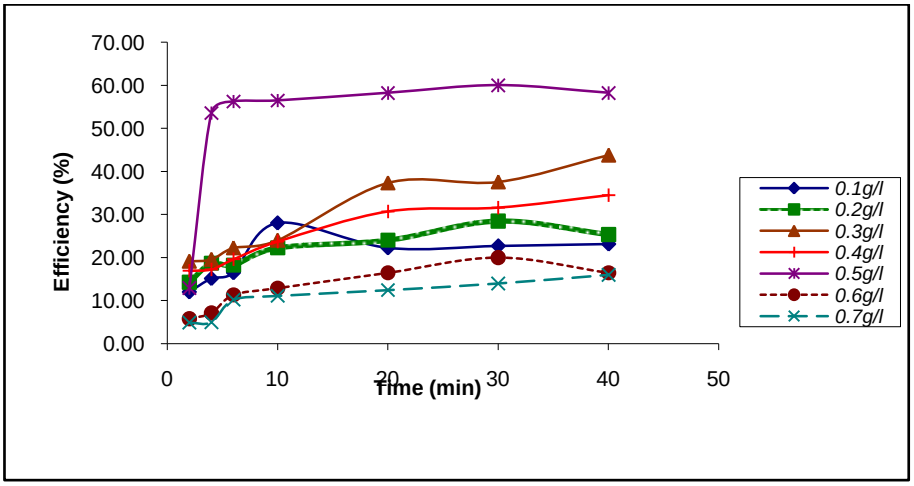

Fig.4.2: Removal efficiency as a function of time and ssc dosage for PIE pH 3

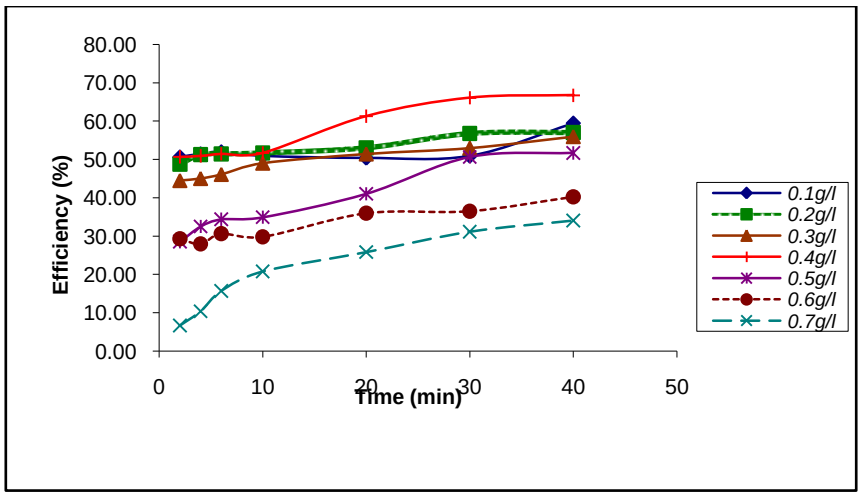

Fig.4.3: Removal efficiency as a function of time and ssc dosage PIE at pH 5

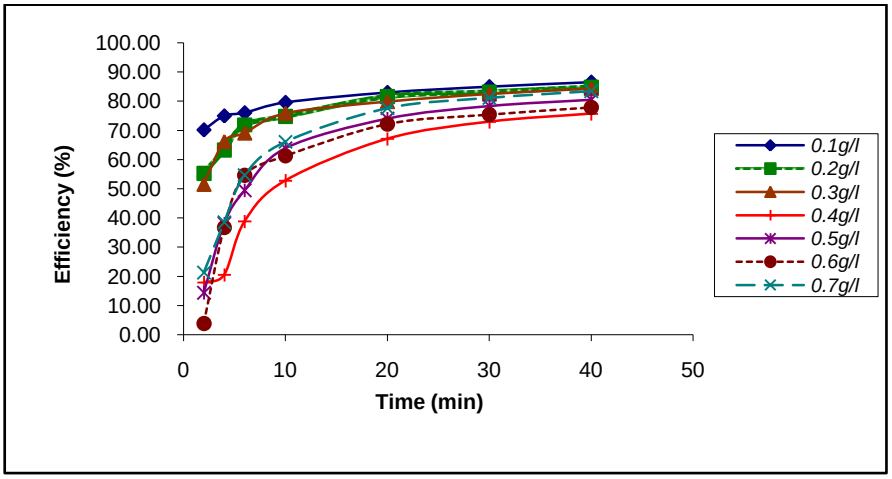

Fig.4.4: Removal efficiency as a function of time and ssc dosage for PIE at pH 7

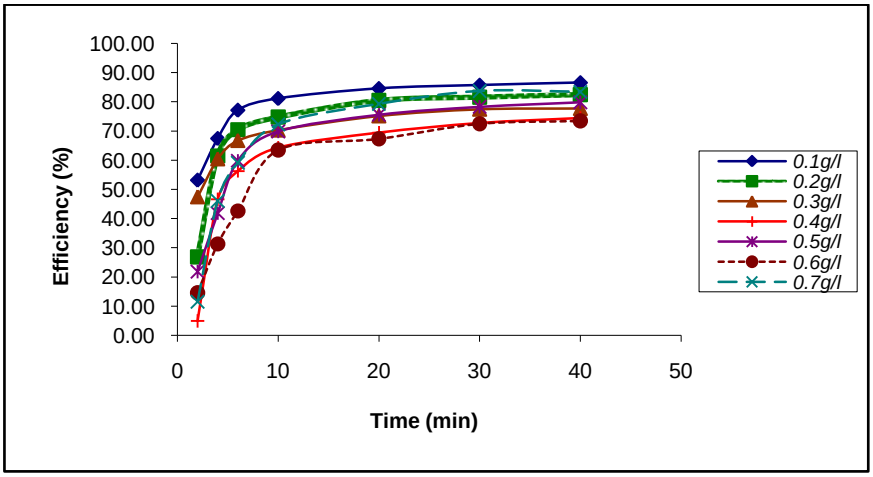

Fig.4.5. Removal efficiency as a function of time and ssc dosage for PIE Ph 10

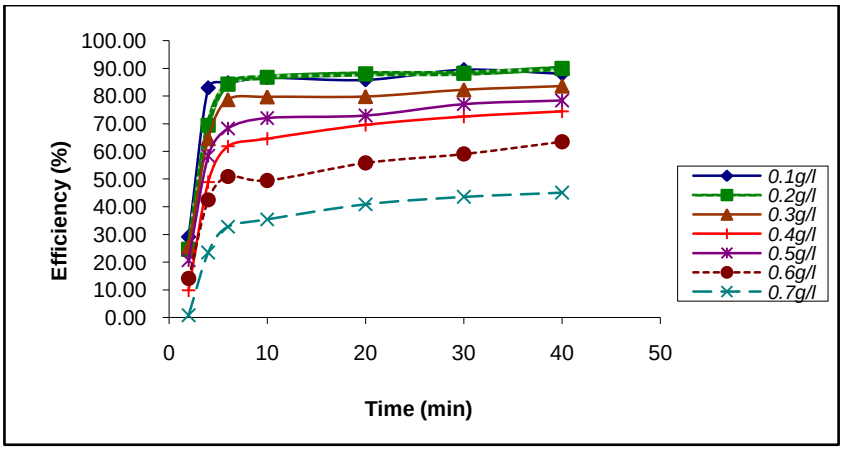

Fig.4.6: Removal efficiency as a function of time and ssc dosage for PIE at pH 13

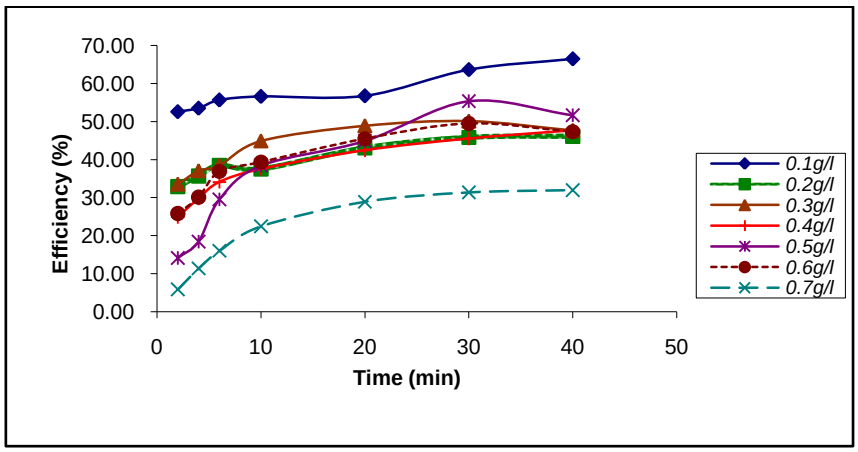

Fig.4.7: Removal efficiency as a function of time and cosc daosage for PIE pH 1

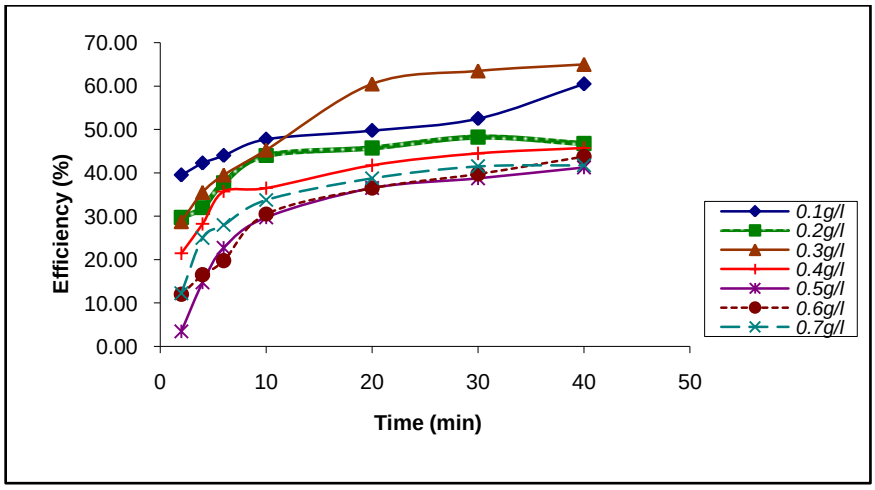

Fig.4.8: Removal efficiency as a function of time and cosc daosage for PIE pH 3

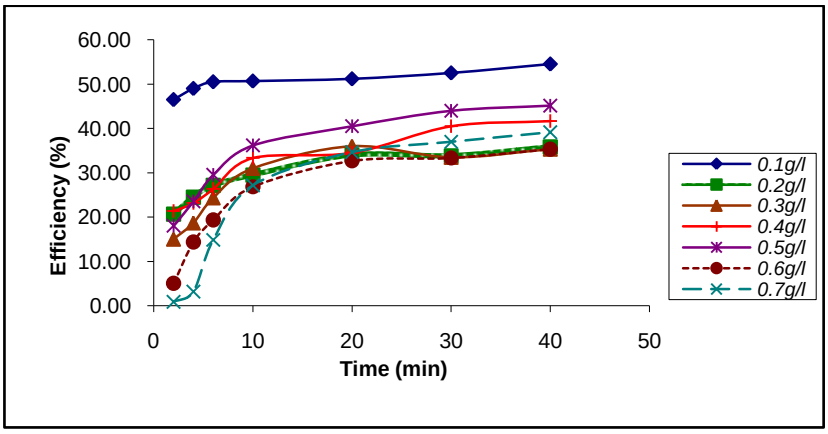

Fig.4.9: Removal efficiency as a function of time and cosc daosage for PIE at pH 5

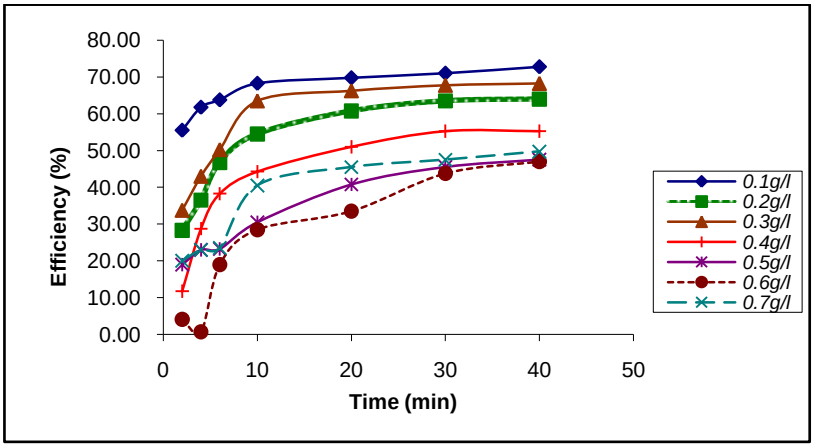

Fig.4.10: Removal efficiency as a function of time and cosc dosage for PIE at pH 7

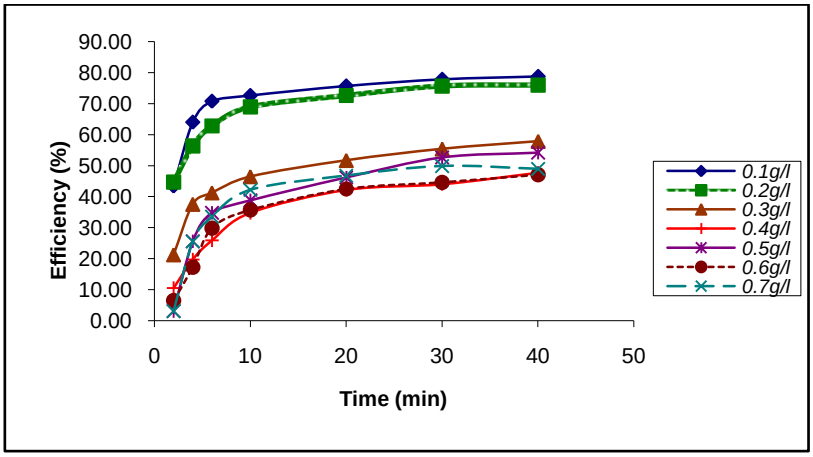

Fig. 4.11: Removal efficiency as a function of time and cosc dosage for PIE at pH 10

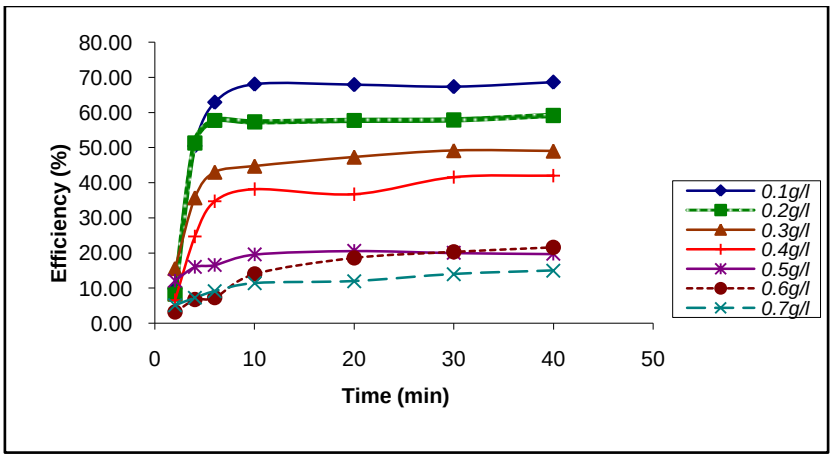

Fig.4.12: Removal efficiency as a function of time and cosc dosage for PIE at pH 13

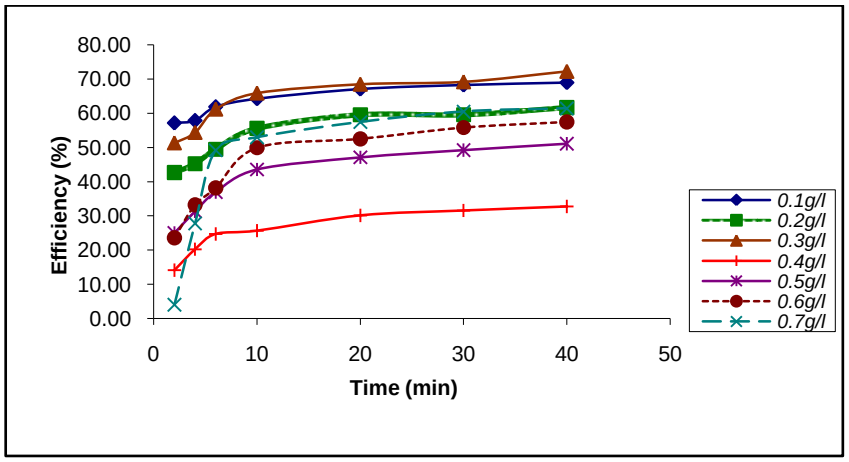

Fig.4.13: Removal efficiency as a function of time and tosc dosage for PIE at pH 1

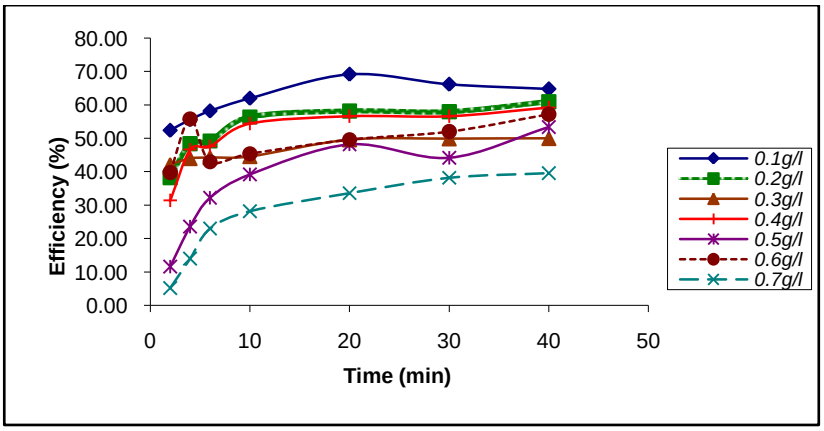

Fig.4.14: Removal efficiency as a function of time and tosc dosage for PIE at pH 3

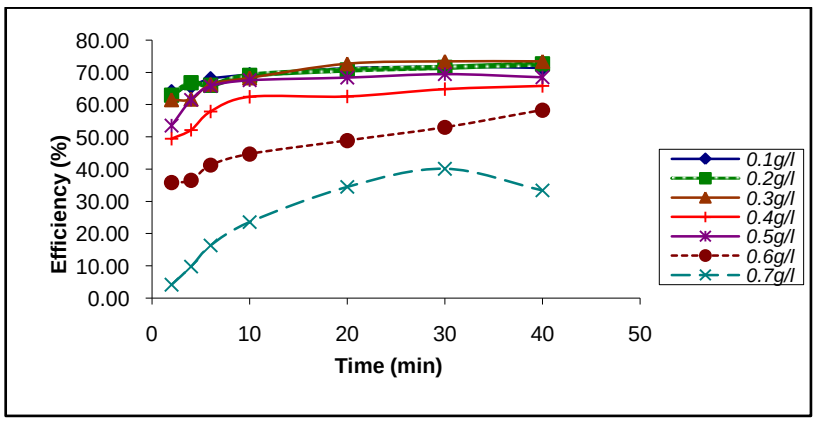

Fig.4.15: Removal efficiency as a function of time and tosc dosage for PIE at pH 5

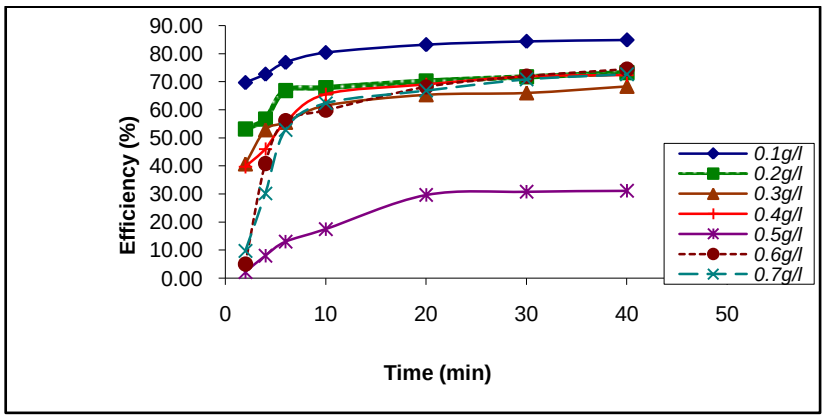

Fig.4.16: Removal efficiency as a function of time and tosc dosage for PIE at pH 7

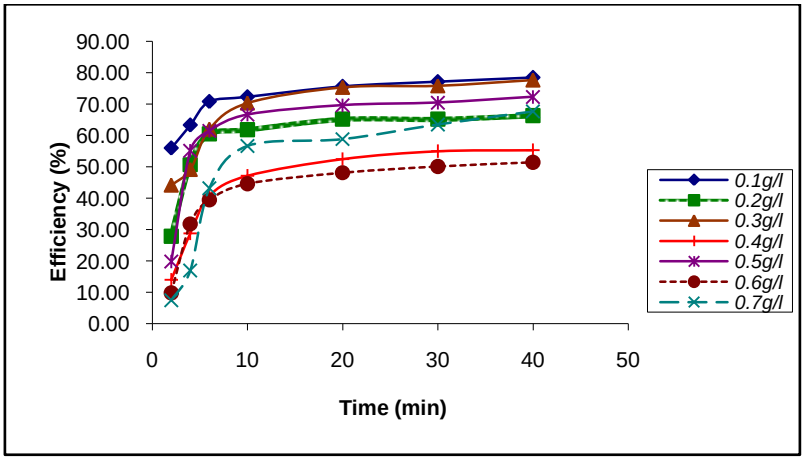

Fig.4.17 Removal efficiency as a function of time and tosc dosage for PIE at pH 10

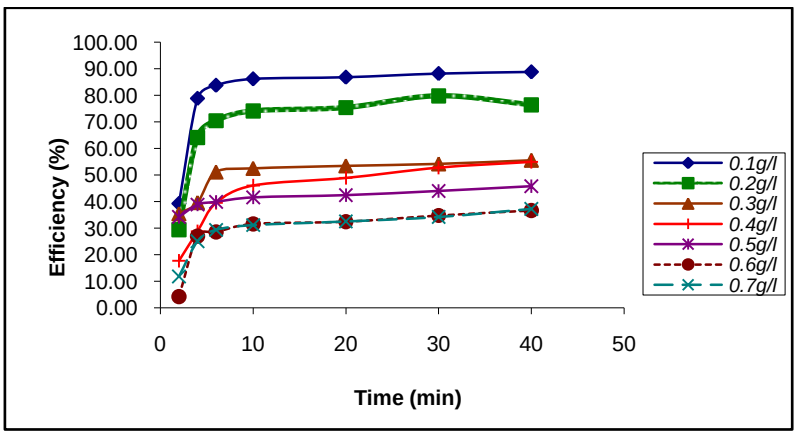

Fig.4.18 Removal efficiency as a function of time and tosc dosage for PIE at pH 13

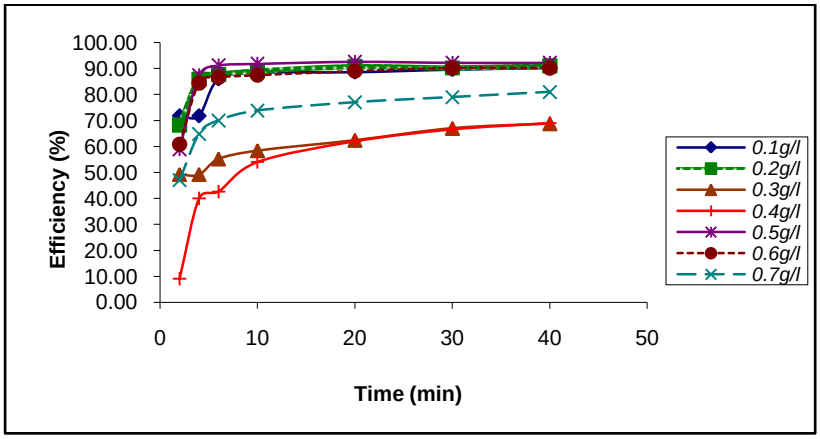

Fig.4.19: Removal efficiency as a function of time and tosc dosage for PIE at pH 1

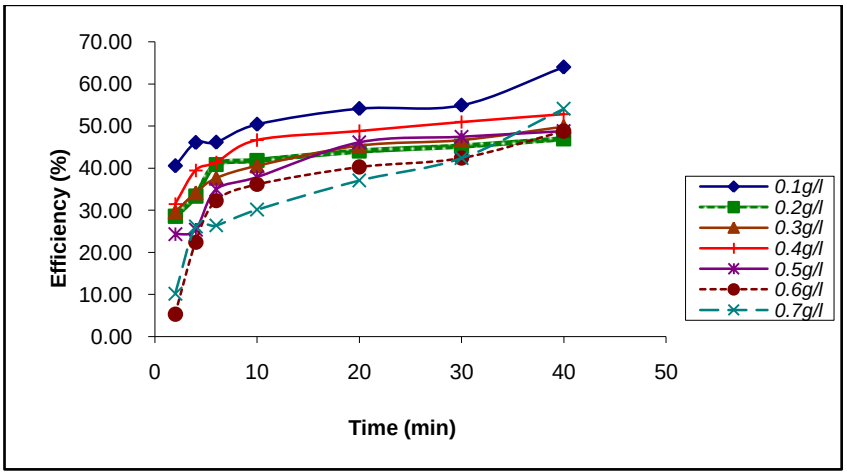

Fig.4.20: Removal efficiency as a function of time and ptsc dosage for PIE pH 3

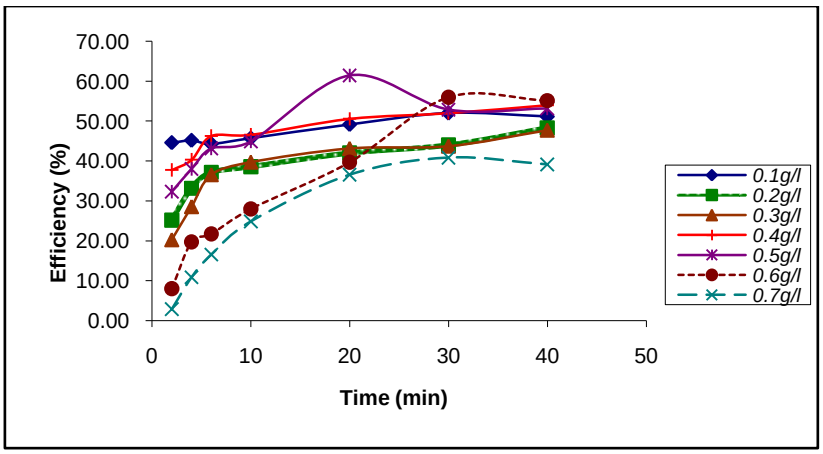

Fig.4.21: Removal efficiency as a function of time and ptsc dosage for PIE pH 5

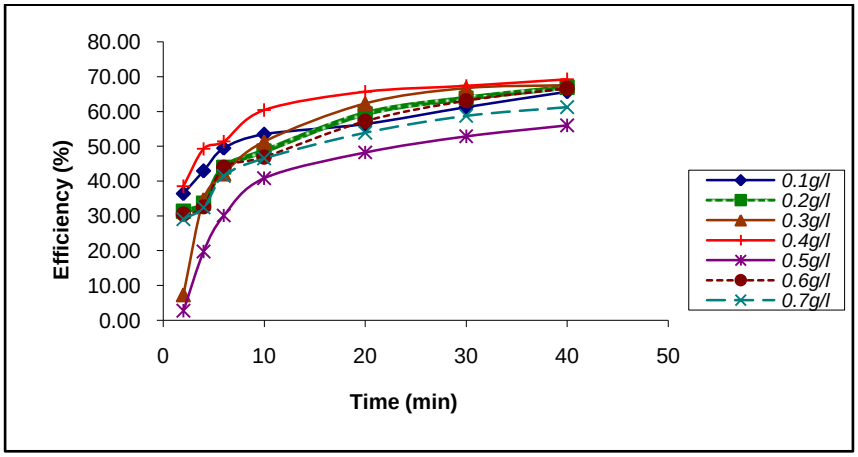

Fig.4.22: Removal efficiency as a function of time and ptsc dosage for PIE at pH 7

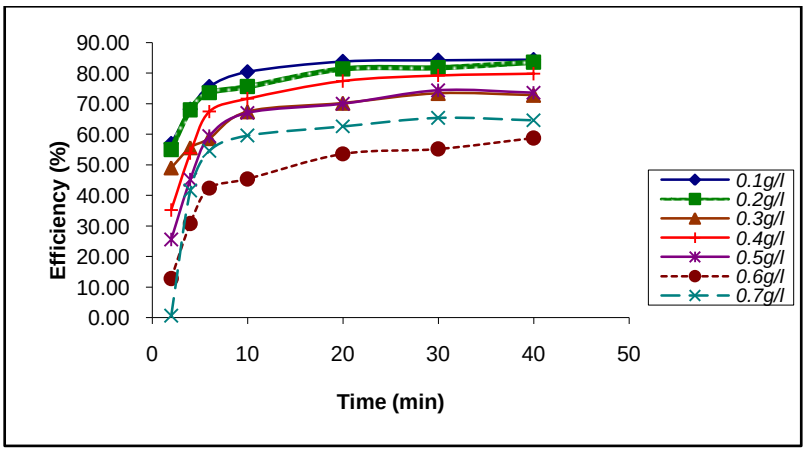

Fig.4.23: Removal efficiency as a function of time and ptsc dosage for PIE at pH 10

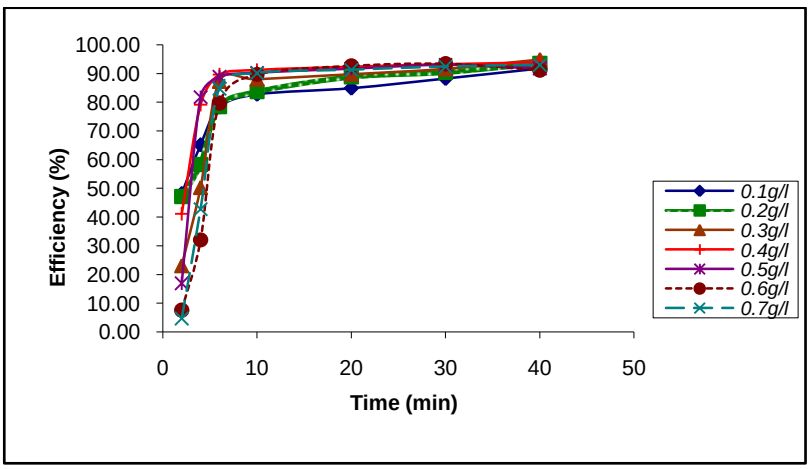

Fig.4.24: Removal efficiency as a function of time and ptsc dosage for PIE at pH 13

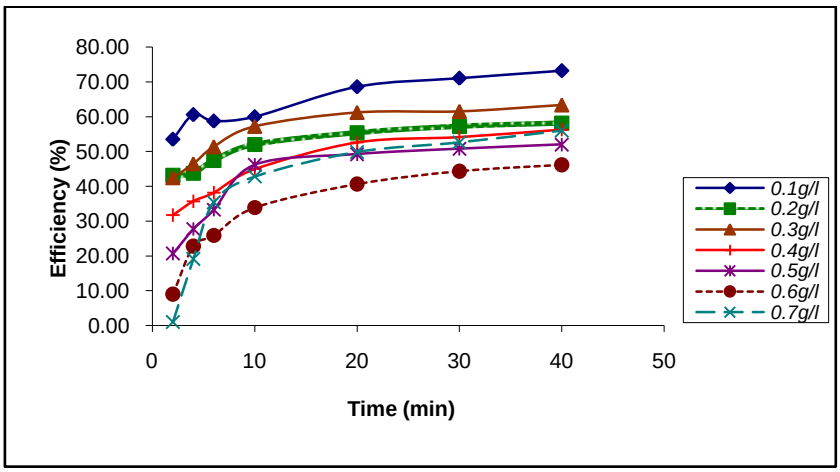

Fig.4.25: Removal efficiency as a function of time and mpsc dosage for PIE at pH 1

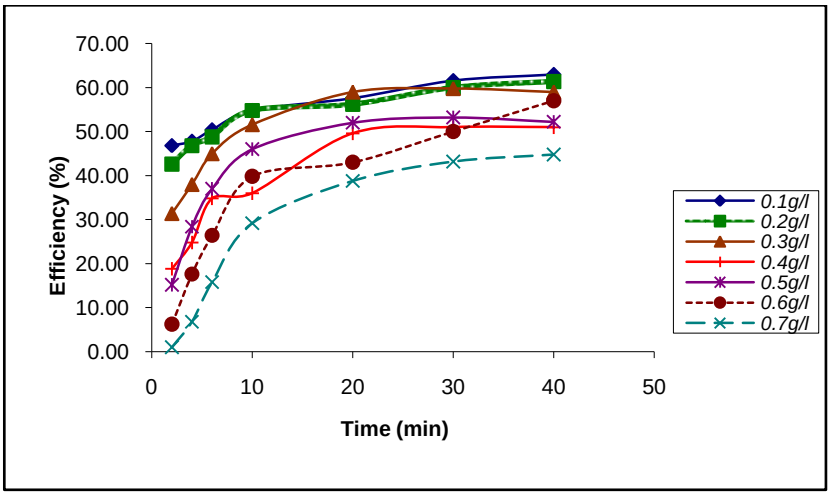

Fig.4.26: Removal efficiency as a function of time and mpsc dosage for PIE at pH 3

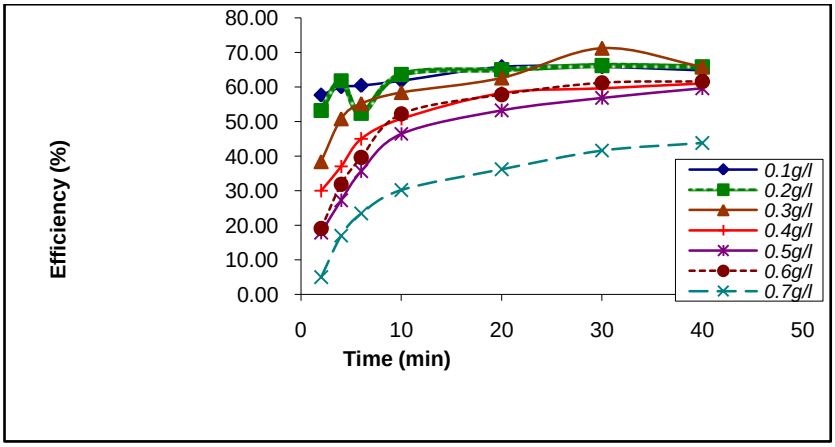

Fig.4.27: Removal efficiency as a function of time and mpsc dosage for PIE at pH 5

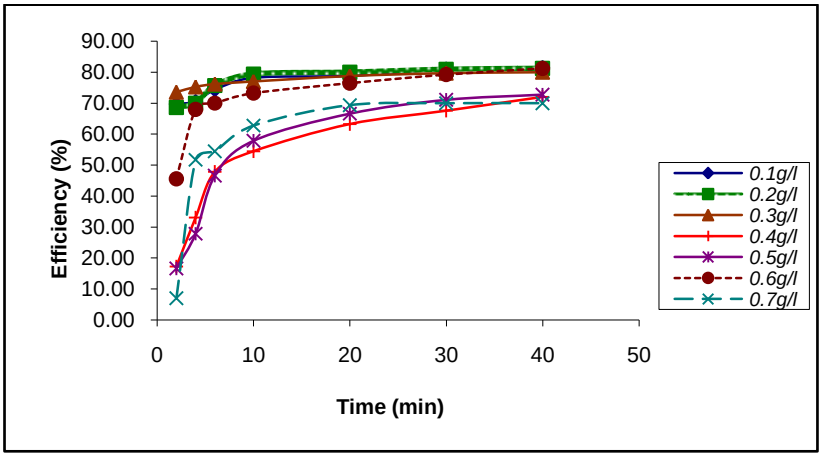

Fig.4.28: Removal efficiency as a function of time and mpsc dosage for PIE at pH 7

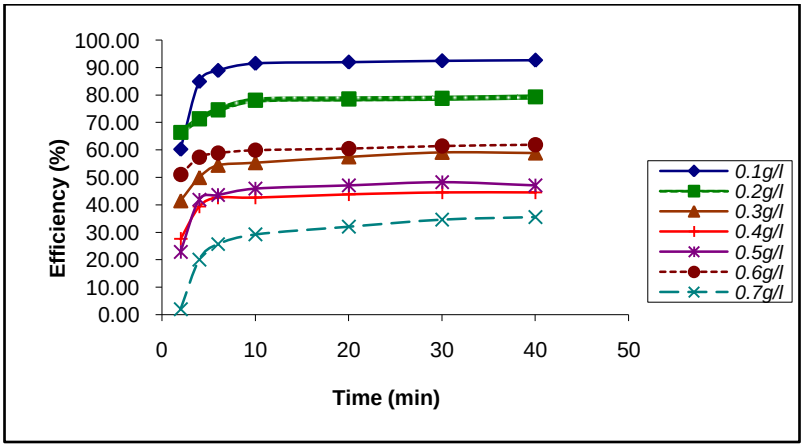

Fig.4.29: Removal efficiency as a function of time and mpsc dosage for PIE at pH 10

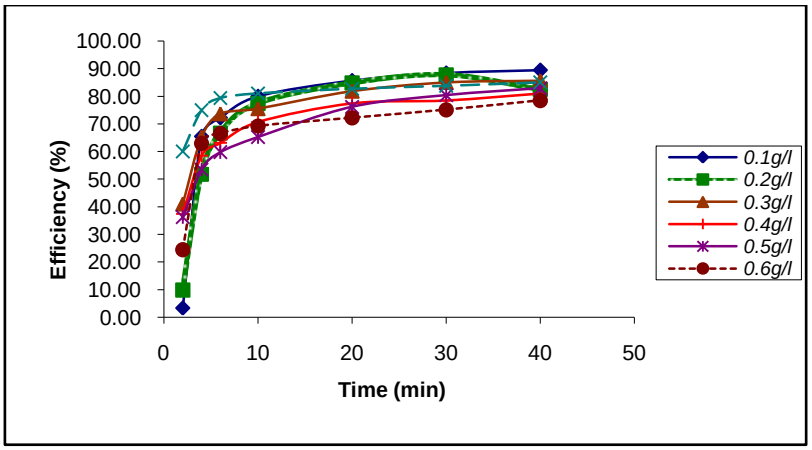

Fig.4.30: Removal efficiency as a function of time and mpsc dosage for PIE at pH 13

4.1.2.2 Removal efficiency for pH varying medium at constant coag-flocculant dosage in PIE.

The coag-flocculation behavior of the coag-flocculants in PIE are illustrated in the graphs presented in figs.4.31 to 4.65. The general observable trend in the figures, indicate that efficiency E(%) increases with time, similar to figs.4.1-4.30. The implication is that at longer settling time more ions/particles are adsorbed onto the coag-flocculants. Thus, confirming that coag-flocculation process employed is mainly controlled by surface charge neutralization and bridging mechanism (Holthof, et al., 1996).

In specific terms, consideration of the coag-flocculants indicate that the optimal conditions for SSC are pH of 13, dosage of 0.2g/l and settling time of 40min, while that of COSC are pH of 10, dosage of 0.1g/l and settling time of 40min. In the case of TOSC, the majority of the optimal performance are achieved at the pH of 13, dosage of 0.1g/l and settling time of 40 mins. Though the performance recorded from 6 – 40min settling time for pH 13 and all the dosages considered are satisfactory. For MPSC, the optimal performance is recorded at pH of 10 for 0.1g/l dosage and 40min. However, the result obtained at pH of 13 from 10 – 40mins for all the dosages studied are satisfactory. This is an indication that for practical purposes the optimal performance of MPSC lies between pH of 10 and 13.

Overall results, from the figures, indicate that majority of the optimum performance recorded for the coag-flocculants is at pH of 13. The implication is that the coag-flocculation process for these coag-flocculants in PIE are more efficient in alkaline medium, following high degree of solubility.

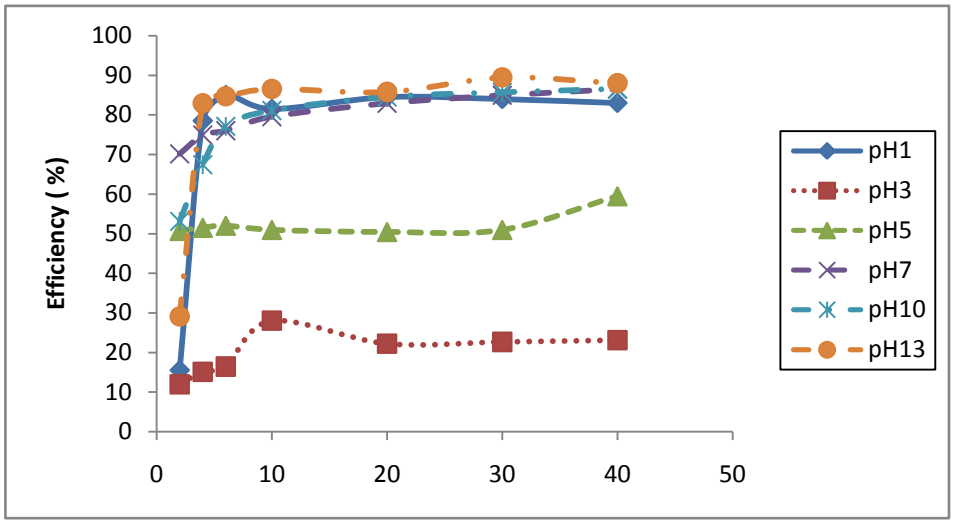

Fig.4.31: Removal efficiency as a function of time for pH varying PIE at 0.1g/l ssc

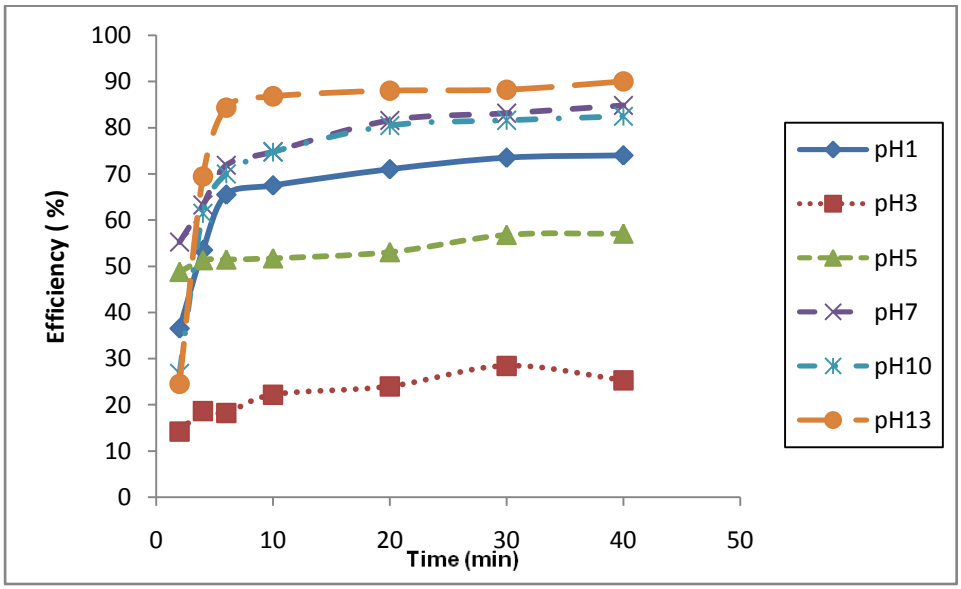

Fig.4.32:Removal efficiency as a function of time for pH varying PIE at 0.2g/l ssc

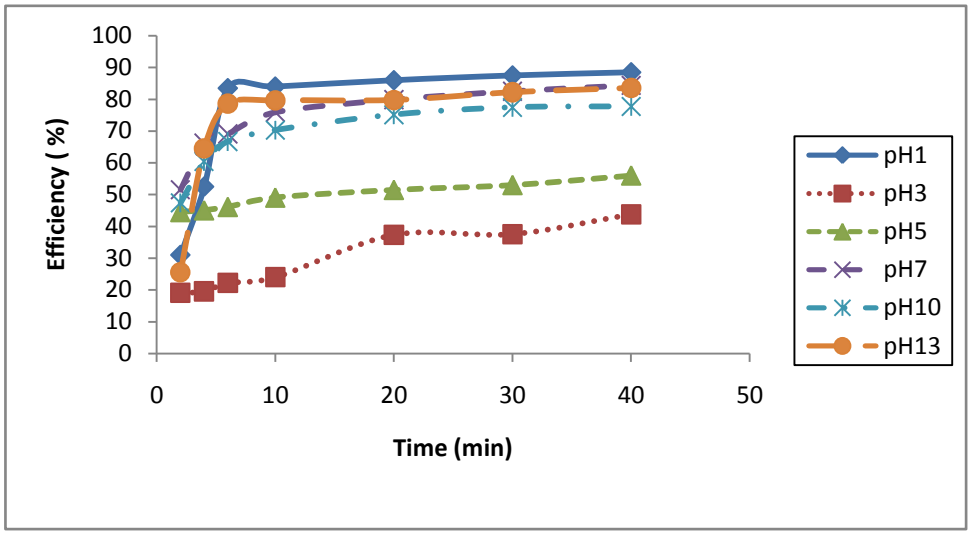

Fig.4.33:Removal efficiency as a function of time for pH varying PIE at 0.3g/l ssc

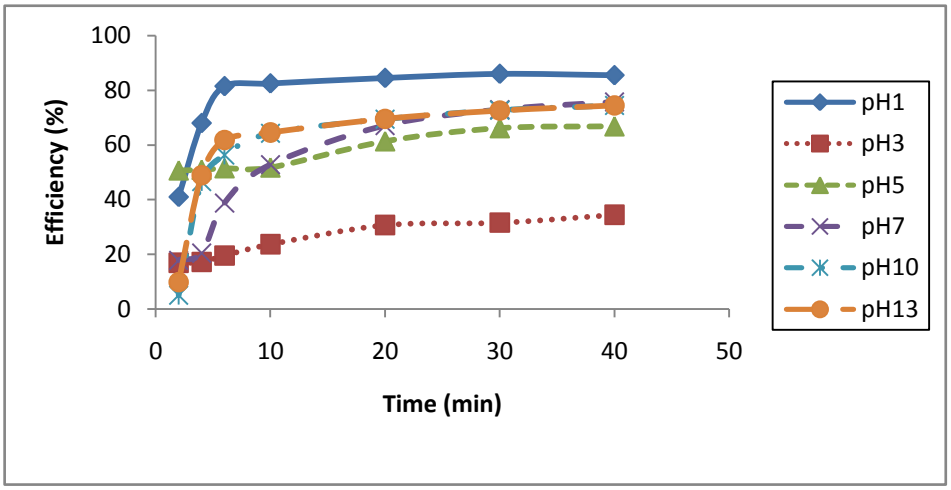

Fig.4.34:Removal efficiency as a function of time for pH varying PIE at 0.4g/l ssc

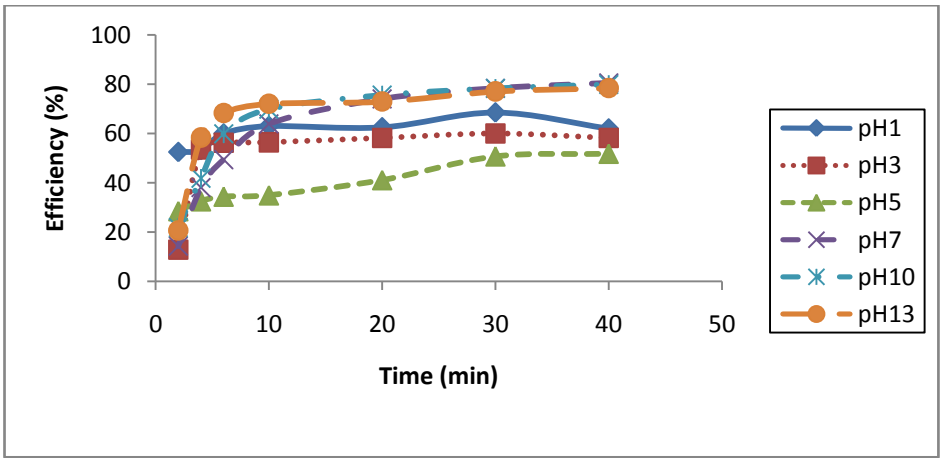

Fig.4.35:Removal efficiency as a function of time for pH varying PIE at 0.5g/l ssc

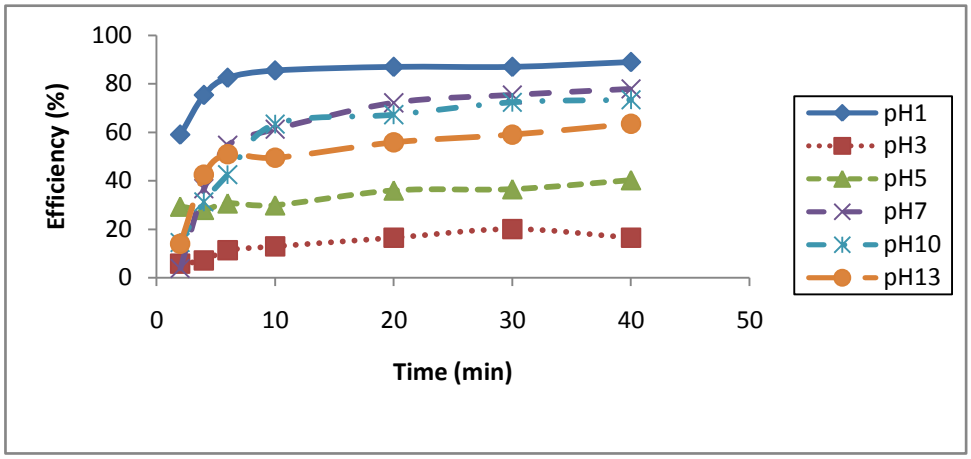

Fig.4.36:Removal efficiency as a function of time for pH varying PIE at 0.6g/l ssc

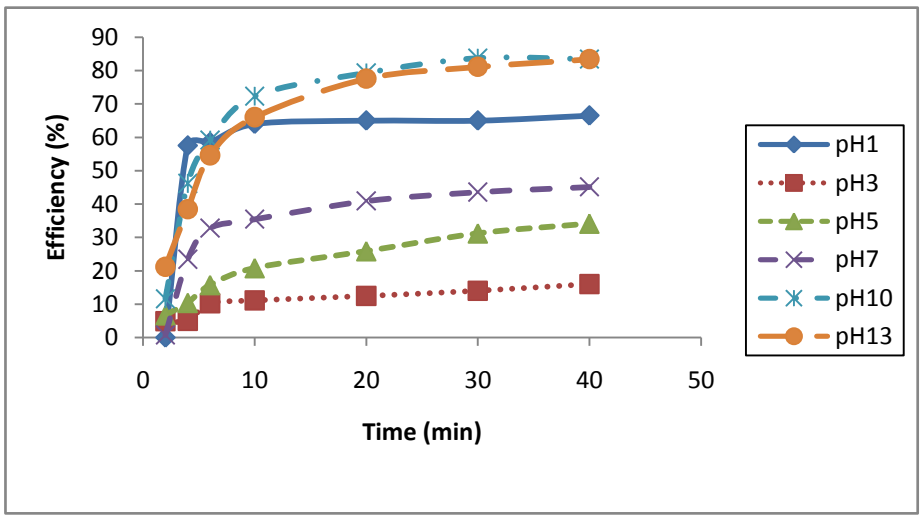

Fig.4.37:Removal efficiency as a function of time for pH varying PIE at 0.7g/l ssc

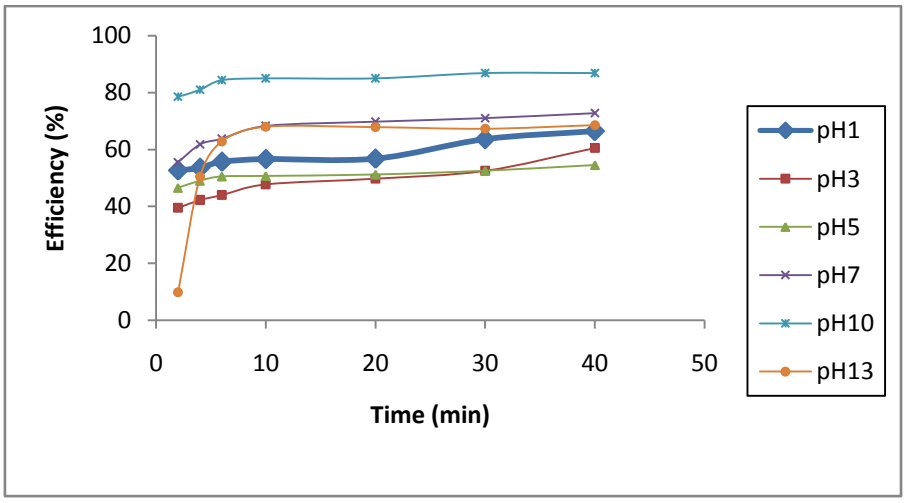

Fig.4.38:Removal efficiency as a function of time for pH varying PIE at 0.1g/l cosc

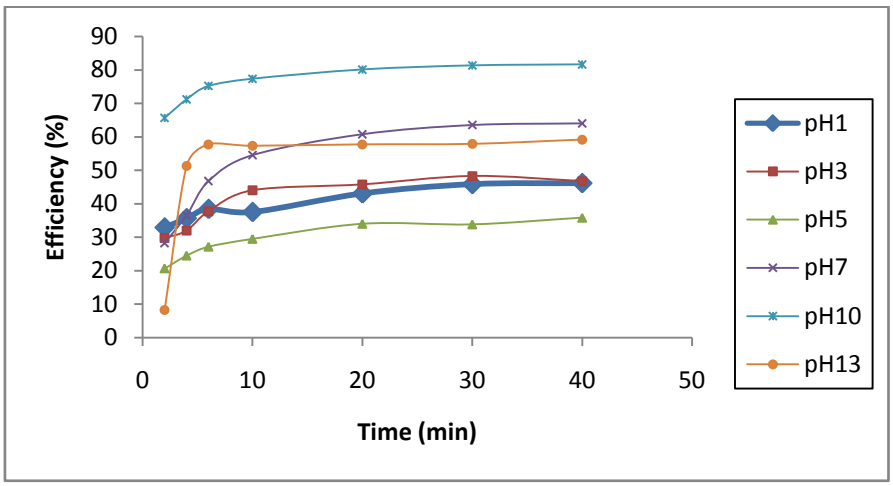

Fig.4.39:Removal efficiency as a function of time for pH varying PIE at 0.2g/l cosc

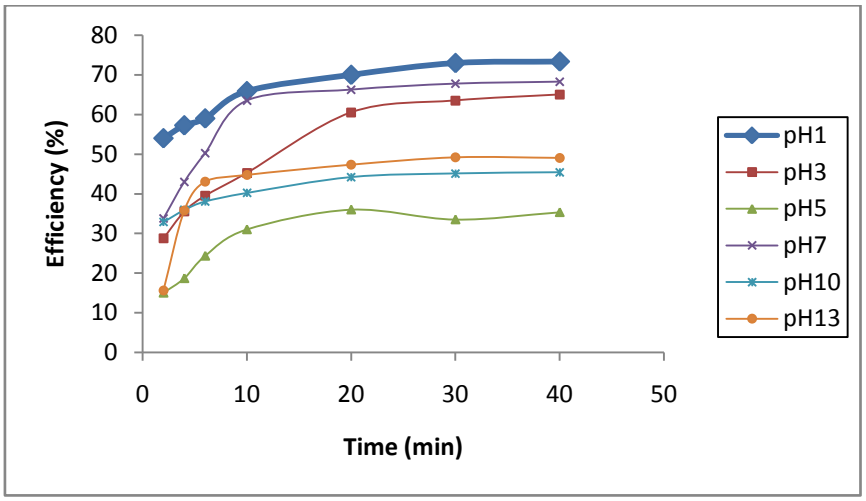

Fig.4.40:Removal efficiency as a function of time for pH varying PIE at 0.3g/l cosc

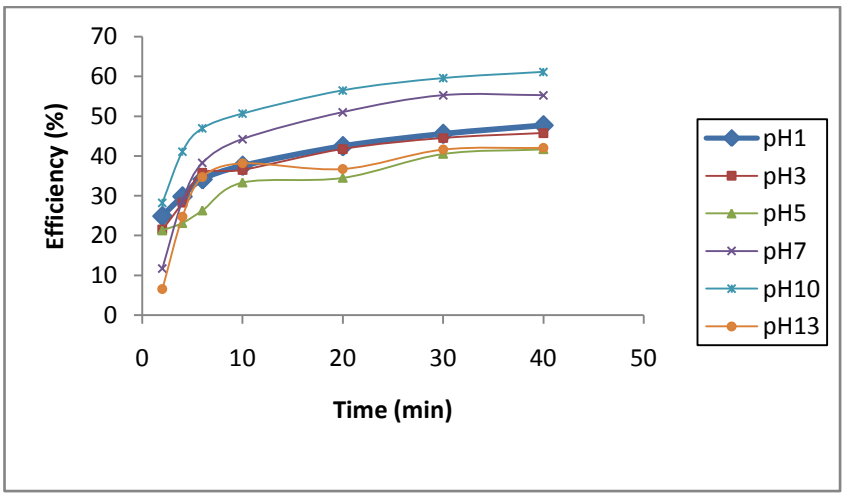

Fig.4.41:Removal efficiency as a function of time for pH varying PIE at 0.4g/l cosc

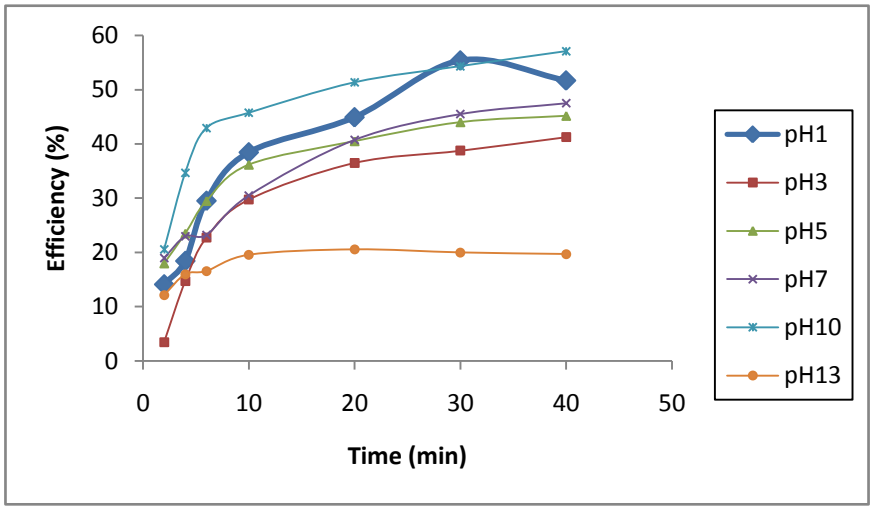

Fig.4.42:Removal efficiency as a function of time for pH varying PIE at 0.5g/l cosc

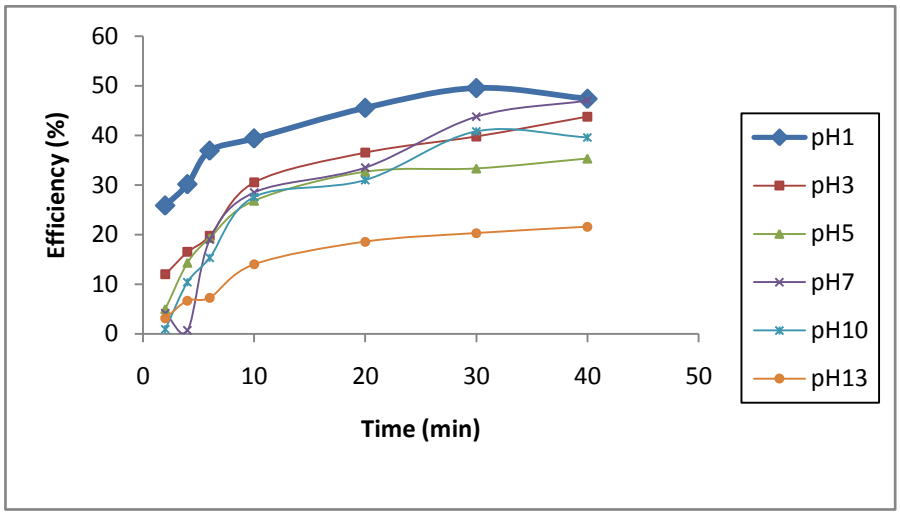

Fig.4.43:Removal efficiency as a function of time for pH varying PIE at 0.6g/l cosc

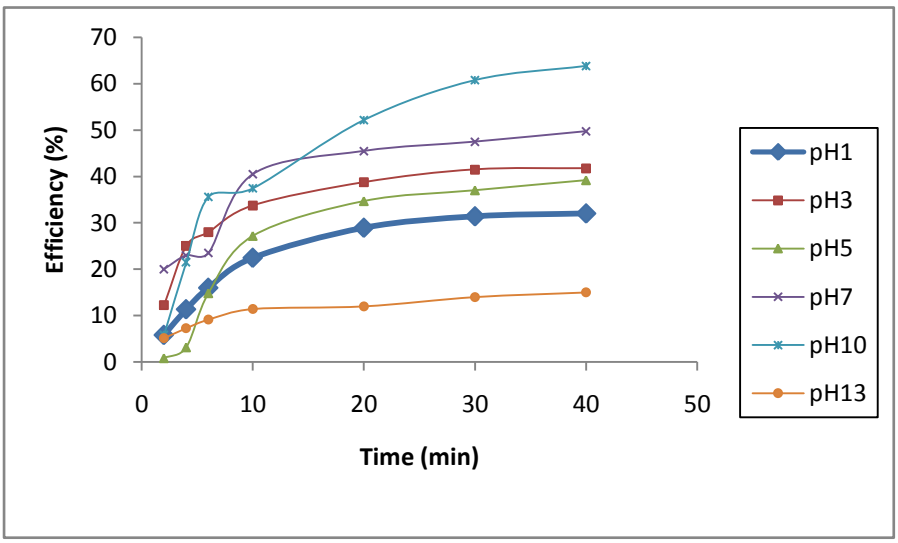

Fig.4.44:Removal efficiency as a function of time for pH varying PIE at 0.7g/l cosc

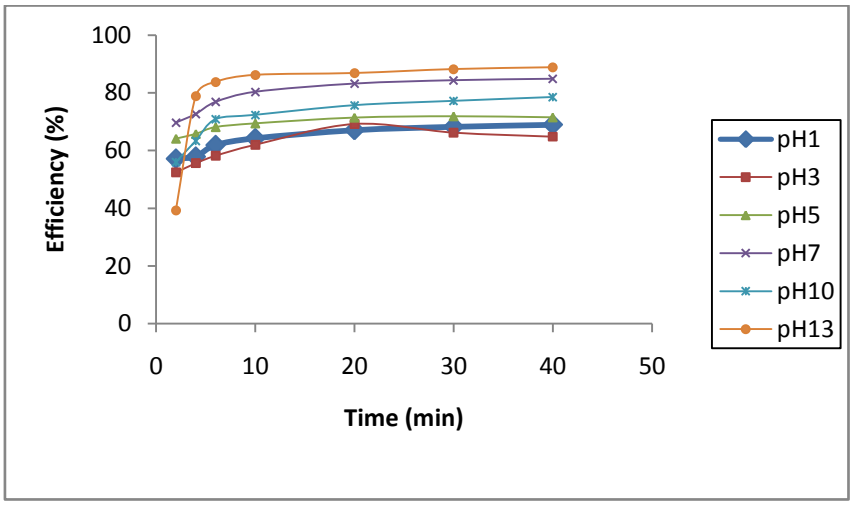

Fig.4.45: Removal efficiency as a function of time for pH varying PIE as 0.1g/l tosc

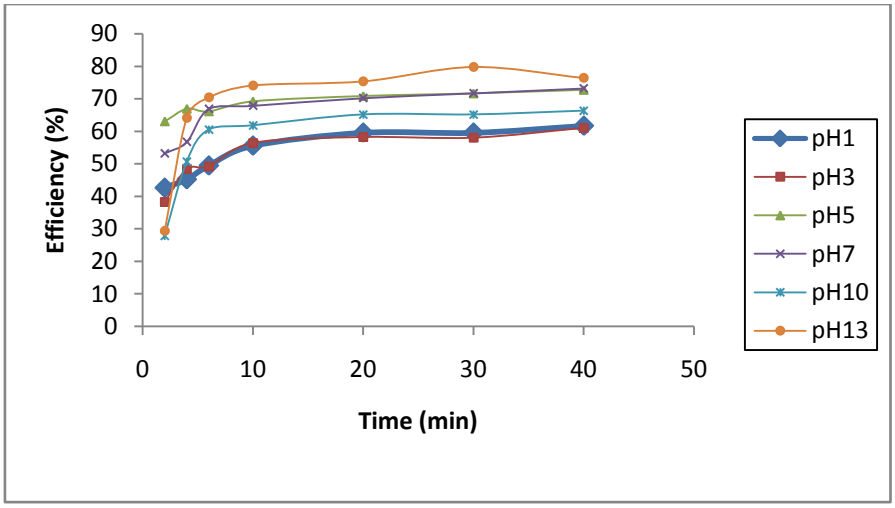

Fig.4.46: Removal efficiency as a function of time for pH varying PIE as 0.2g/l tosc

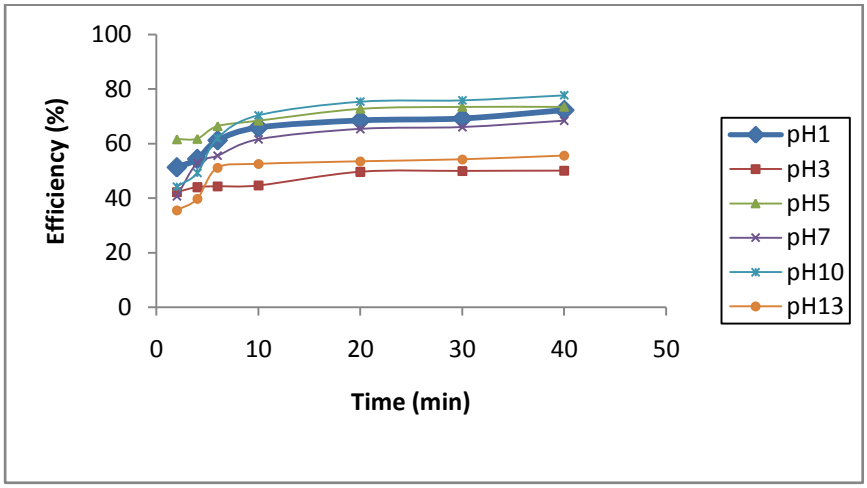

Fig.4.47: Removal efficiency as a function of time for pH varying PIE as 0.3g/l tosc

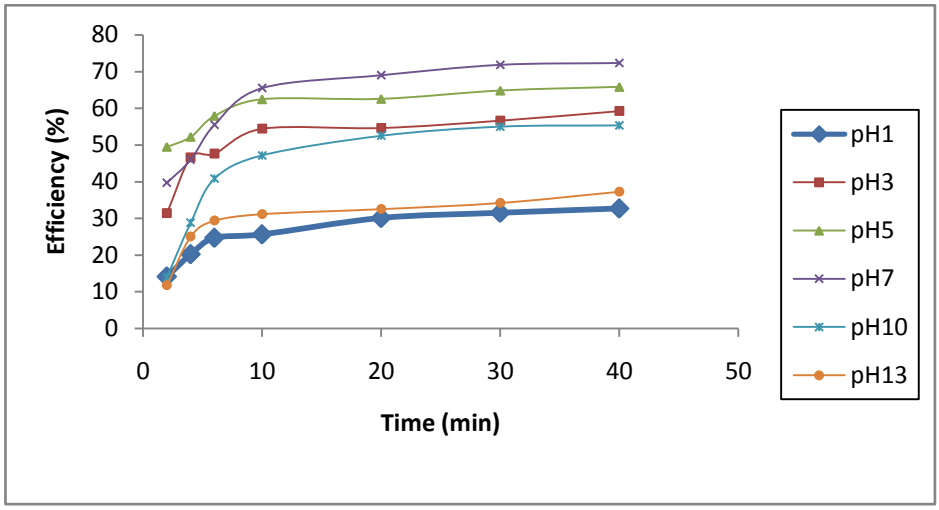

Fig.4.48: Removal efficiency as a function of time for pH varying PIE as 0.4g/l tosc

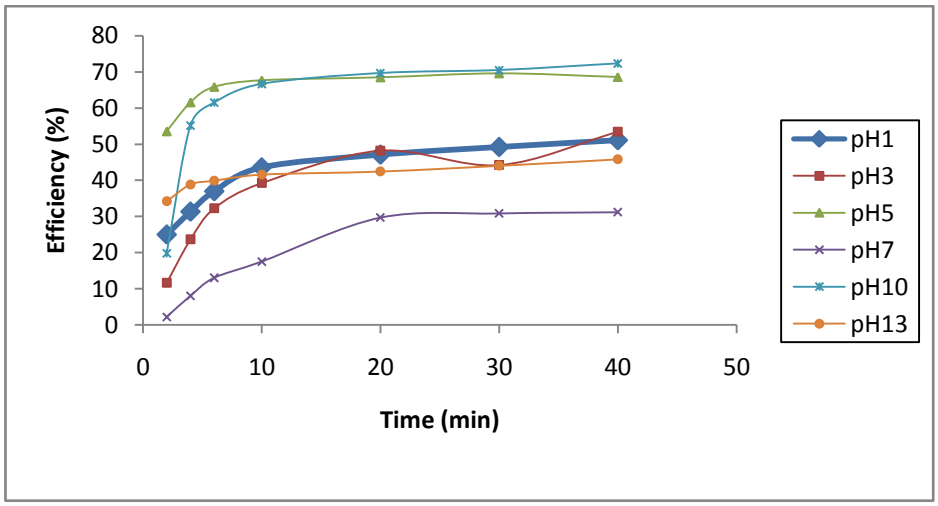

Fig.4.49: Removal efficiency as a function of time for pH varying PIE as 0.5g/l tosc

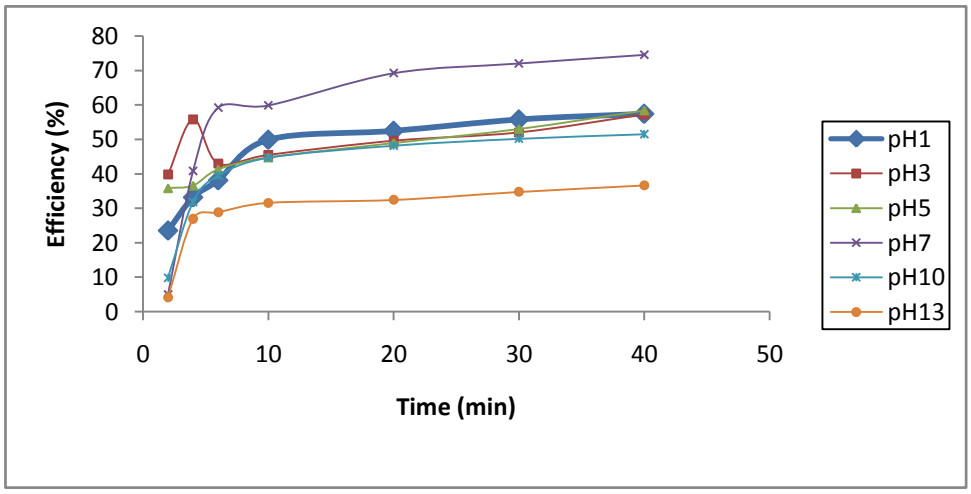

Fig.4.50: Removal efficiency as a function of time for pH varying PIE as 0.6g/l tosc

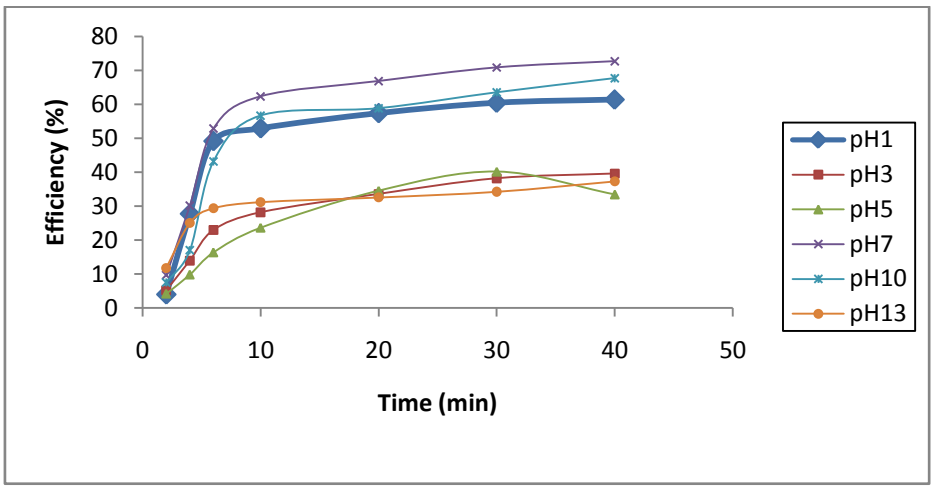

Fig.4.51: Removal efficiency as a function of time for pH varying PIE as 0.7g/l tosc

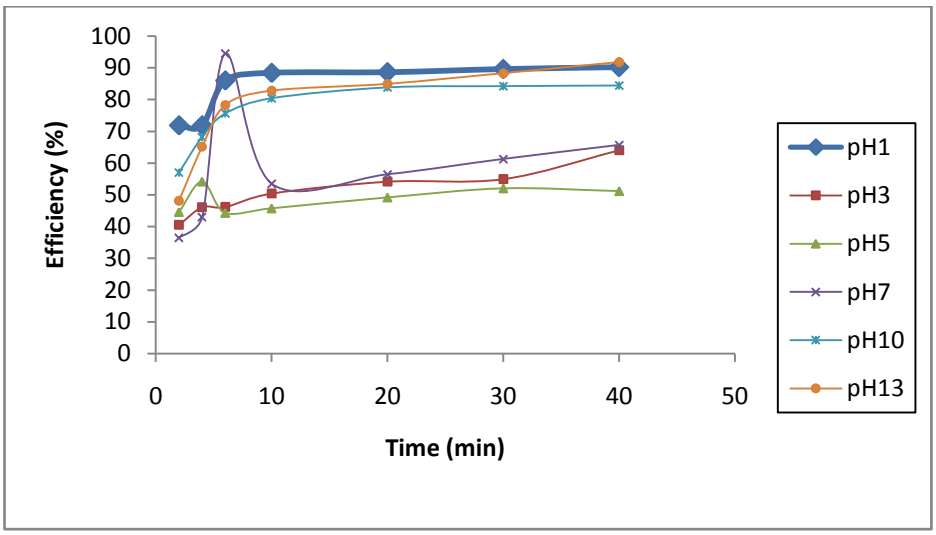

Fig.4.52:Removal efficiency as a function of time for pH varying PIE at 0.1g/l ptsc

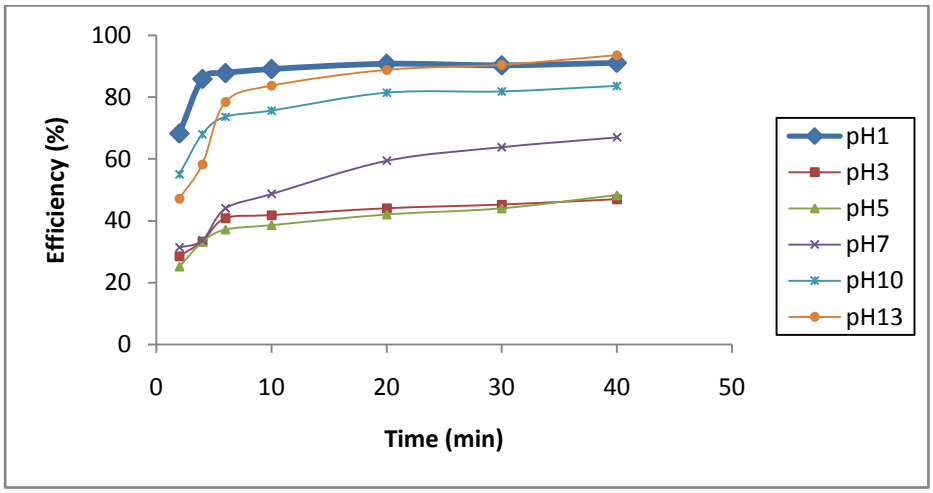

Fig.4.53:Removal efficiency as a function of time for pH varying PIE at 0.2g/l ptsc

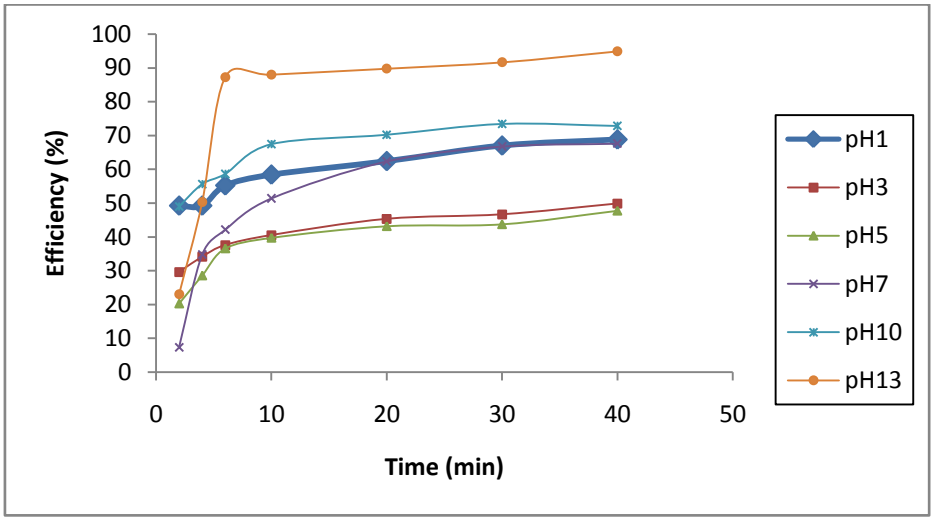

Fig.4.54:Removal efficiency as a function of time for pH varying PIE at 0.3g/l ptsc

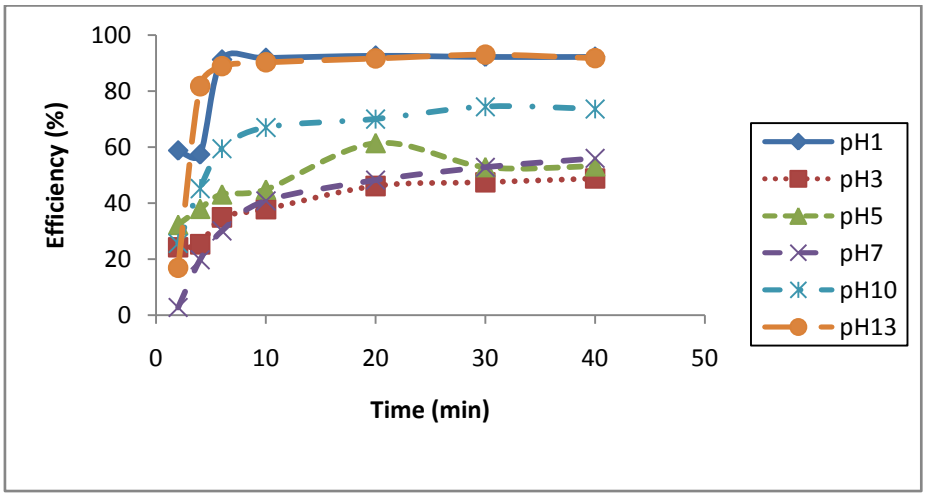

Fig.4.55:Removal efficiency as a function of time for pH varying PIE at 0.4g/l ptsc

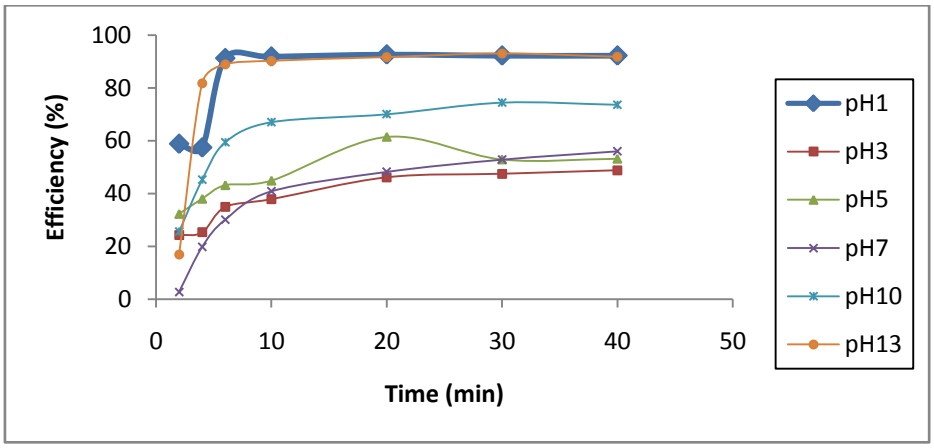

Fig.4.56:Removal efficiency as a function of time for pH varying PIE at 0.5g/l ptsc

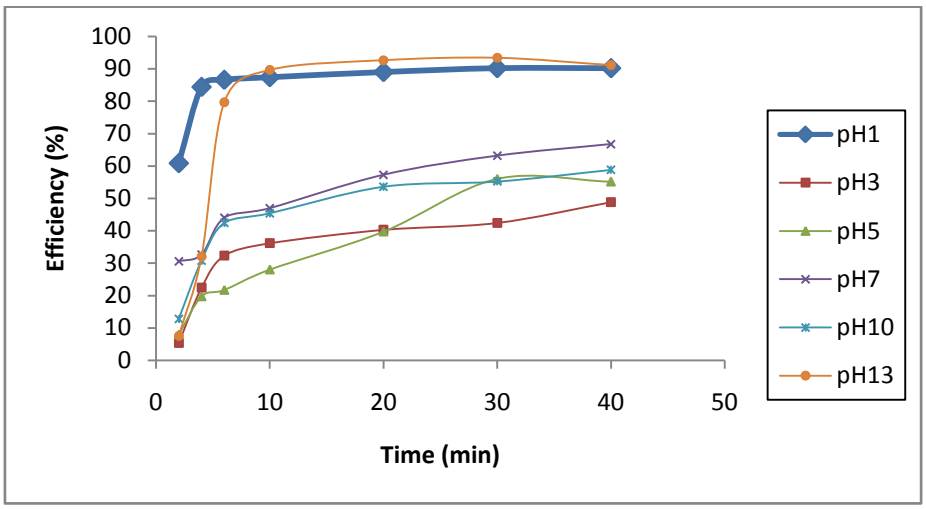

Fig.4.57:Removal efficiency as a function of time for pH varying PIE at 0.6g/l ptsc

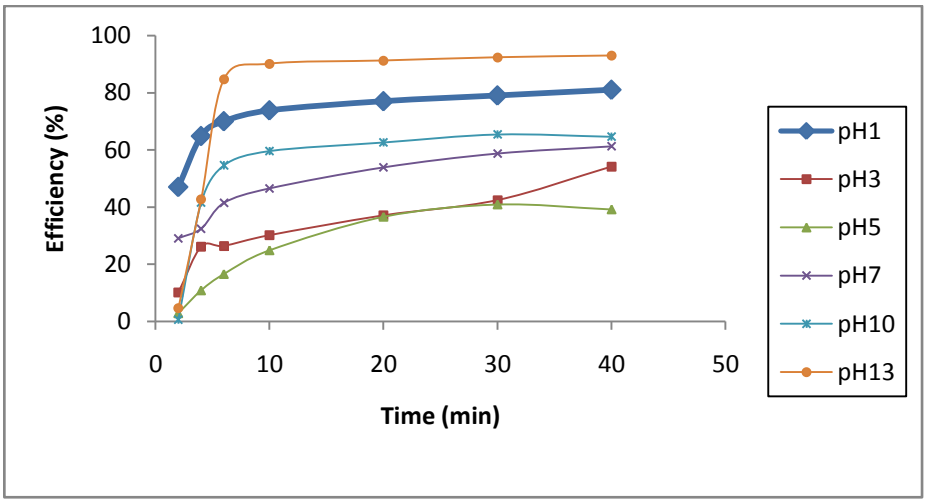

Fig.4.58:Removal efficiency as a function of time for pH varying PIE at 0.7g/l ptsc

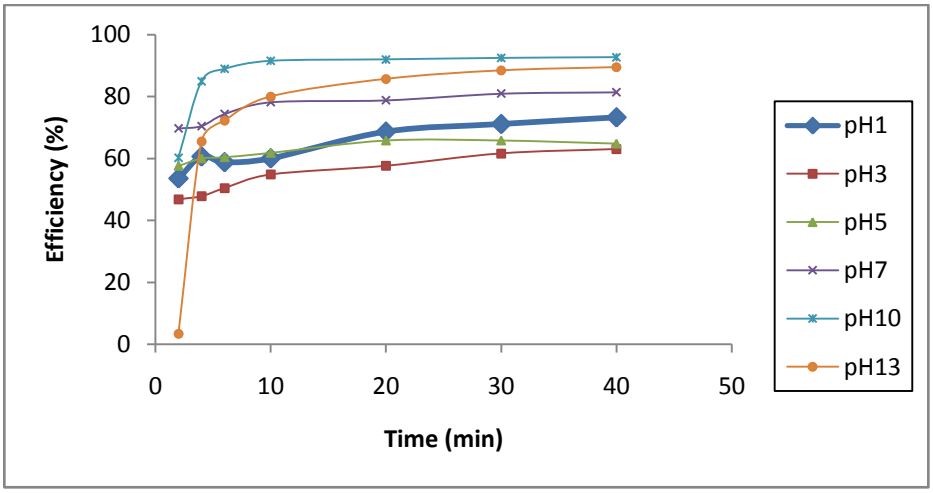

Fig.4.59:Removal eficiency as a function of time for pH varying PIE at 0.1g/l mpsc

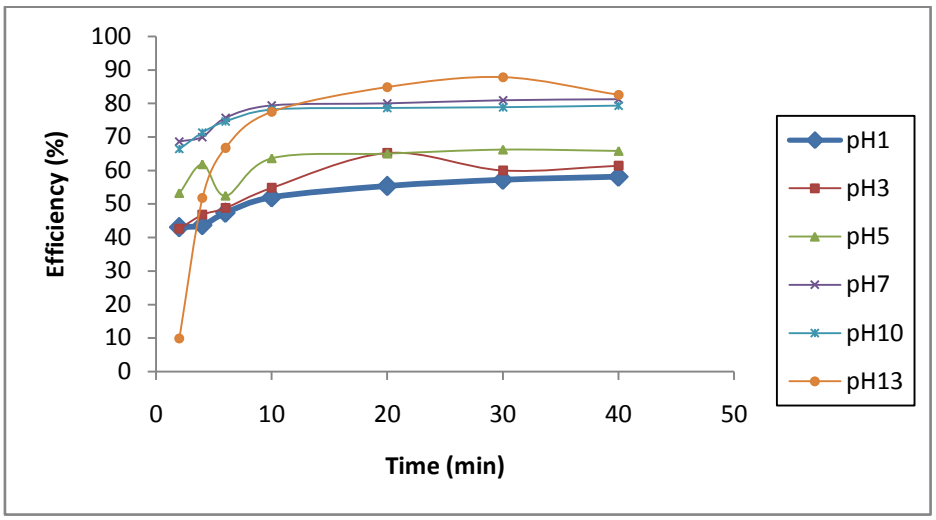

Fig.4.60:Removal eficiency as a function of time for pH varying PIE at 0.2g/l mpsc

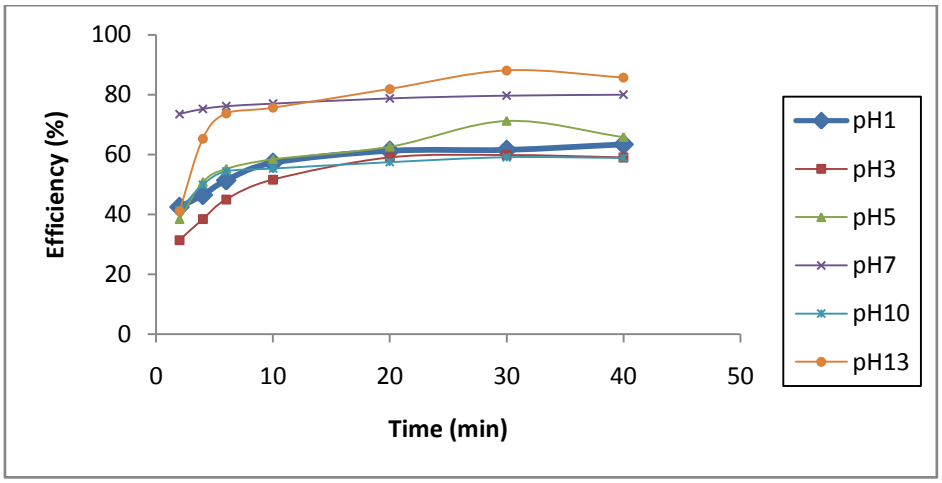

Fig.4.61:Removal eficiency as a function of time for pH varying PIE at 0.3g/l mpsc

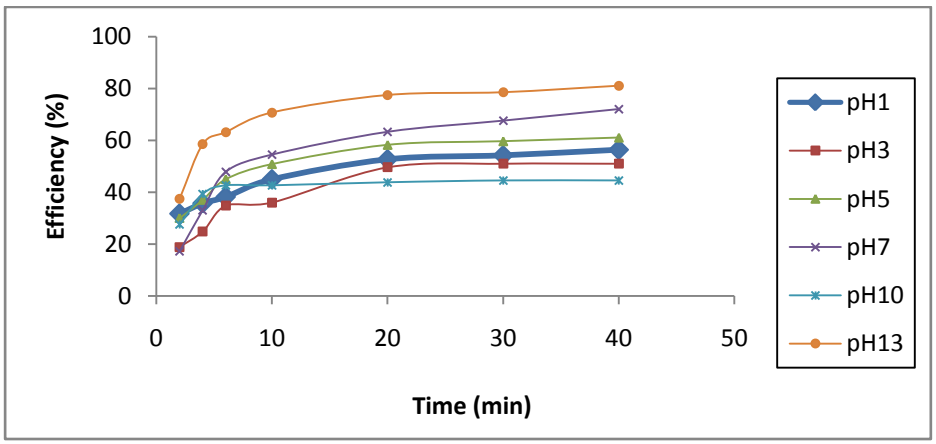

Fig.4.62:Removal eficiency as a function of time for pH varying PIE at 0.4g/l mpsc

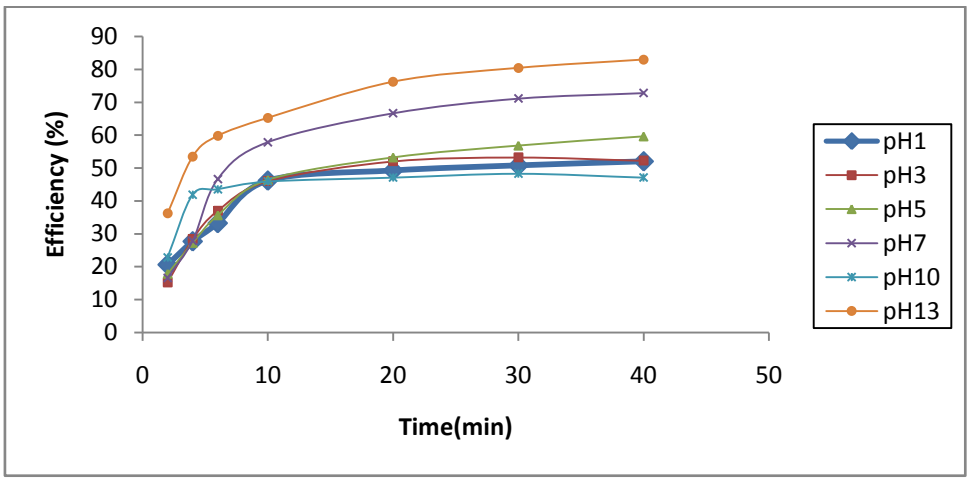

Fig.4.63:Removal eficiency as a function of time for pH varying PIE at 0.5g/l mpsc

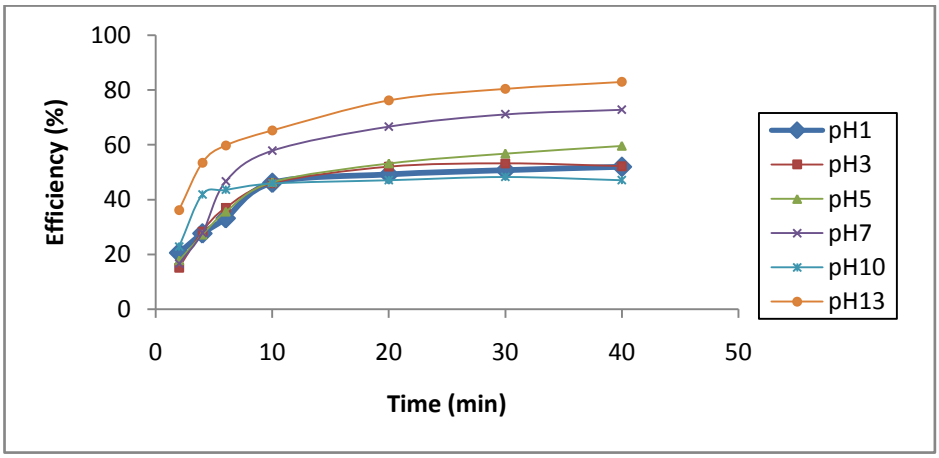

Fig.4.64:Removal eficiency as a function of time for pH varying PIE at 0.6g/l mpsc

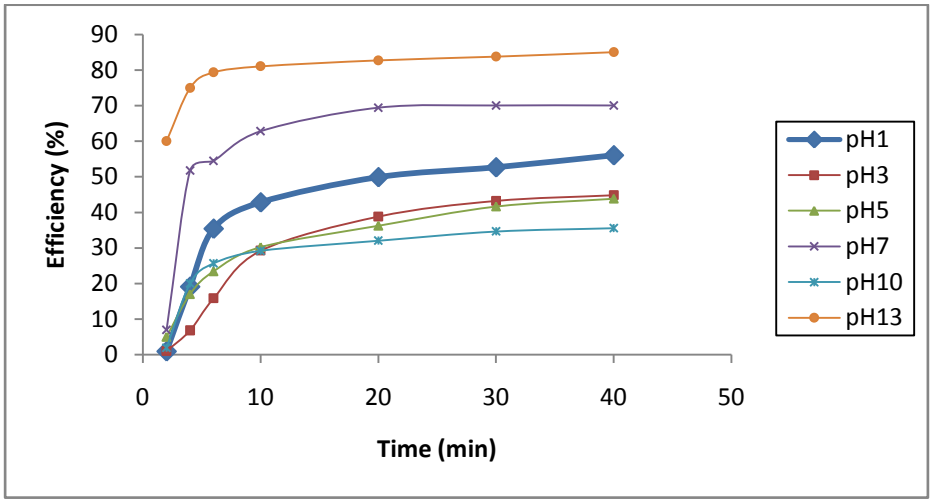

Fig.4.65:Removal eficiency as a function of time for pH varying PIE at 0.7g/l mpsc

4.1.2.3 Removal efficiency for varying coag-flocculants dosage at constant pH in VIE

The graphical results are presented in figs.4.66 to 4.95. These depicts time dependent turbidity precursors removal efficiency profile for evaluation of effectiveness of coag-flocculants at a particular VIE pH. The observed trend is similar to the plots of 4.1 to 4.30. On specific terms, the maximum optimum coag-flocculation activity for PTSC is achieved at 0.2g/l, 40minutes, though the rest of the dosages recorded impressive performance at pH10. For MPSC, the maximum performance is achieved at 0.7g/l, though beyond this dosage, good results were obtained from 0.1 to 0.6g/l at the time of 40minutes. It is worthy to note that at early stage of the coag-flocculation process with 0.7g/l achieved removal efficiency E%> 87.00% as shown in fig.4.95. This indicate that MPSC is a good organic coag-flocculants for water purification process which is most suitable in strong alkaline region. Consider, SSC, it could be observed that the optimal performance are recorded at 0.1g/l for all pH studied except pH 1, where maximum efficiency is recorded at 0.2g/l as shown in figs. 4.66,4.67,4.69,4.70,4.71 and 4.72 respectively. Also for COSC and TOSC, the maximum performances are achieved at 0.6g/l and 0.1g/l as shown in figs. 4.75 and 4.79, 40minutes and 30minutes respectively.

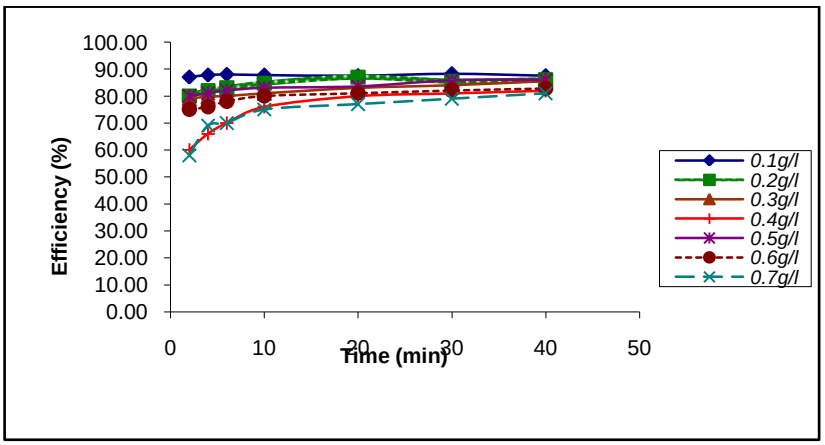

Fig.4.66:Removal efficiency as a function of time and ssc dosage for VIE at pH 1

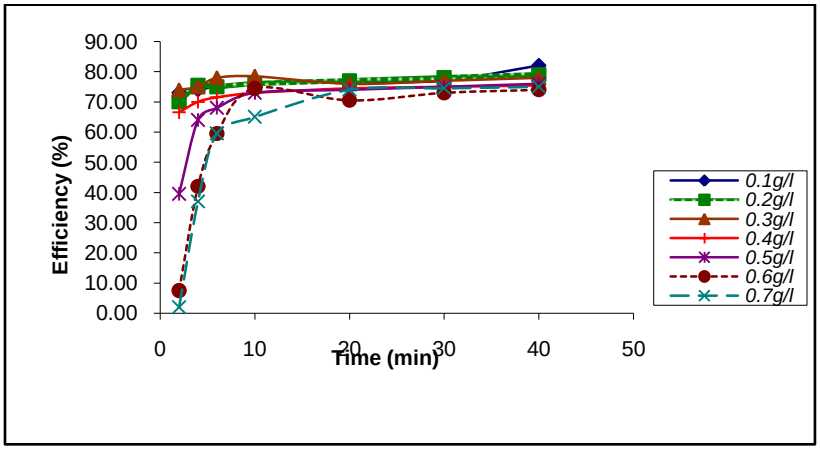

Fig.4.67:Removal efficiency as a function of time and ssc dosage for VIE at pH 3

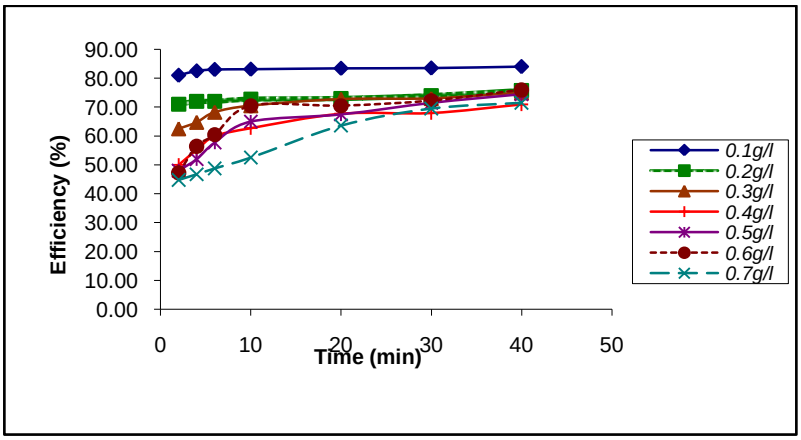

Fig.4.68:Removal efficiency as a function of time and ssc dosage for VIE at pH 5

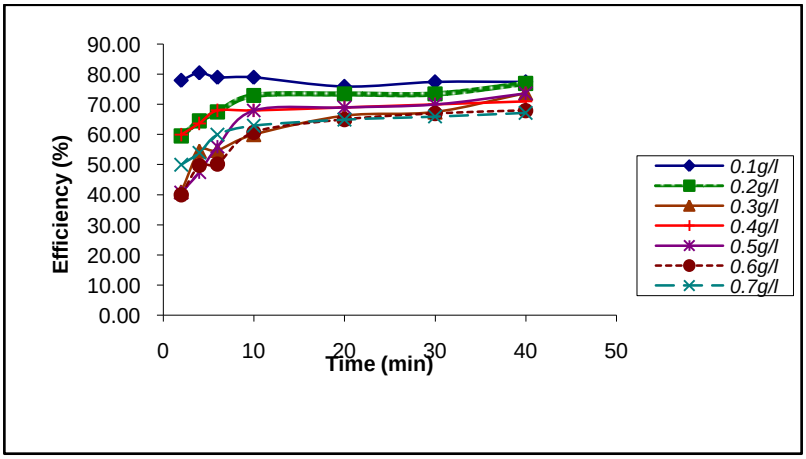

Fig.4.69:Removal efficiency as a function of time and ssc dosage for VIE at pH 7

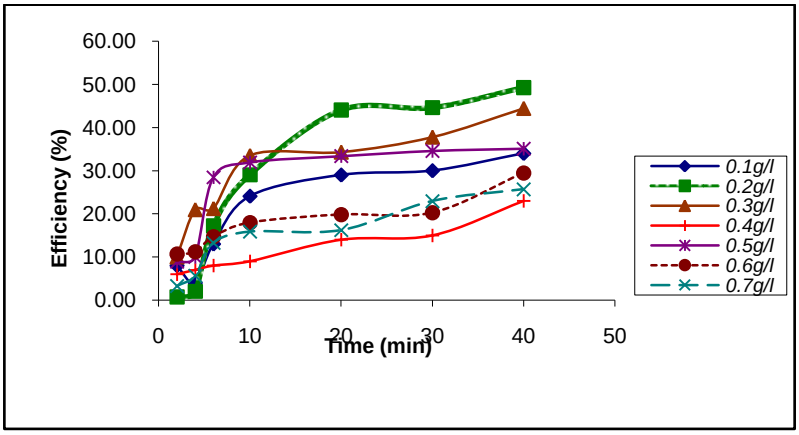

Fig.4.70:Removal efficiency as a function of time and ssc dosage for VIE at pH 10

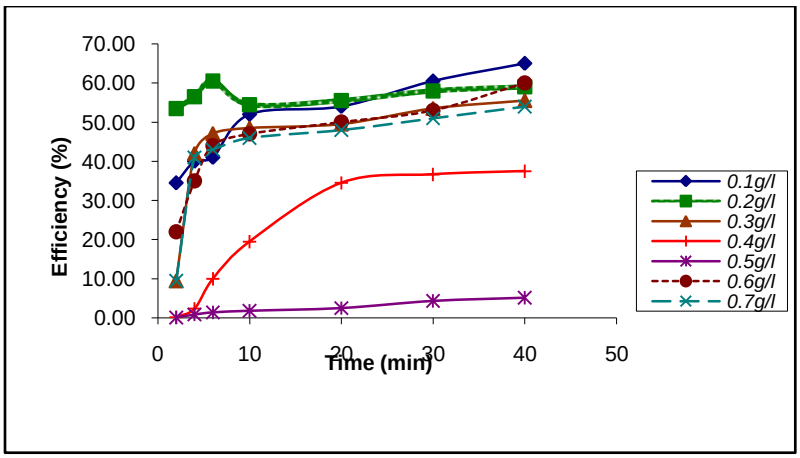

Fig.4.71:Removal efficiency as a function of time and ssc dosage for VIE at pH 13

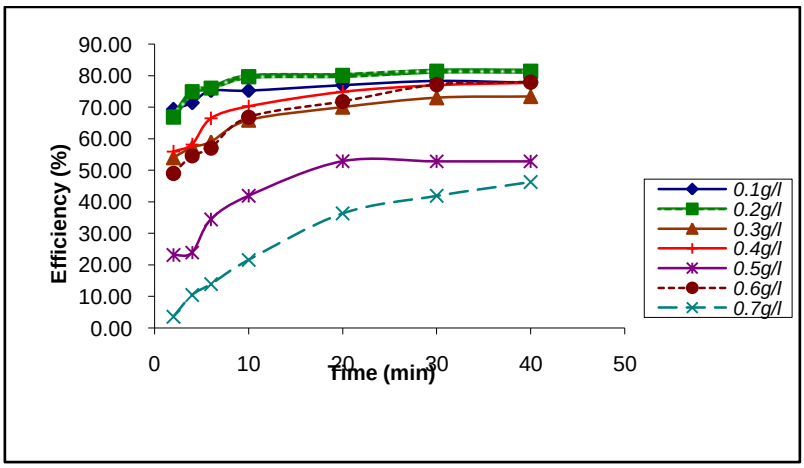

Fig.4.72:Removal efficiency as a function of time and cosc dosage for VIE at pH 1

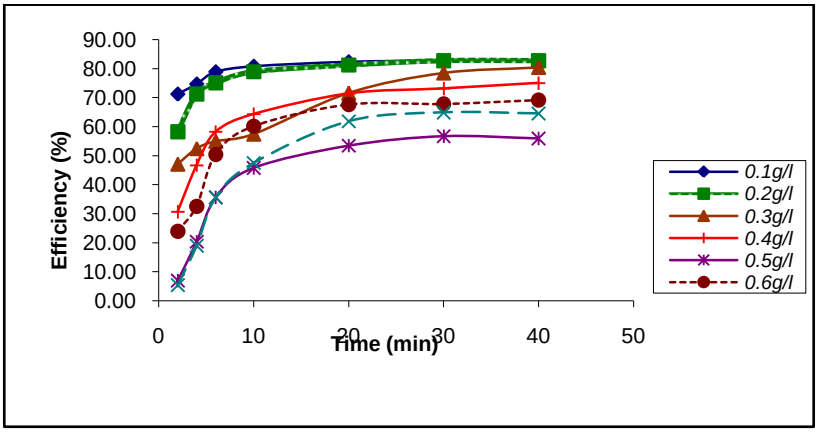

Fig.4.73:Removal efficiency as a function of time and cosc dosage for VIE at pH 3

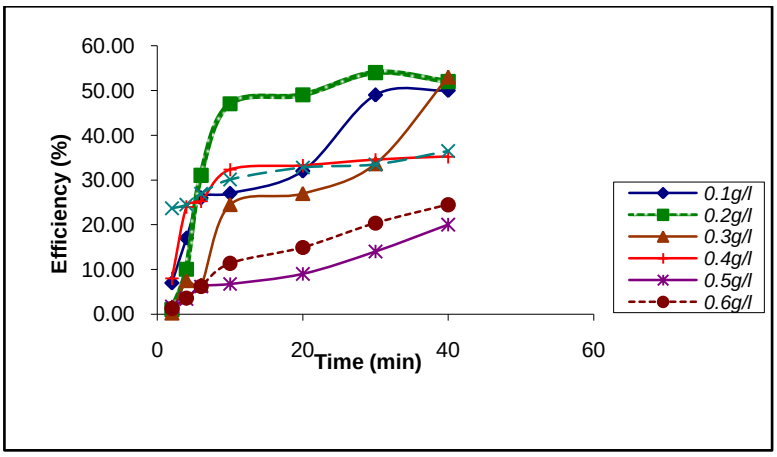

Fig.4.74:Removal efficiency as a function of time and cosc dosage for VIE at pH 5

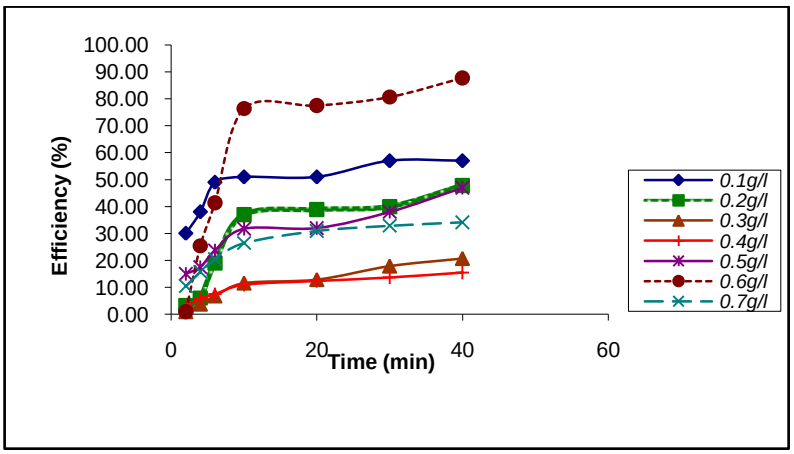

Fig.4.75:Removal efficiency as a function of time and cosc dosage for VIE at pH 7

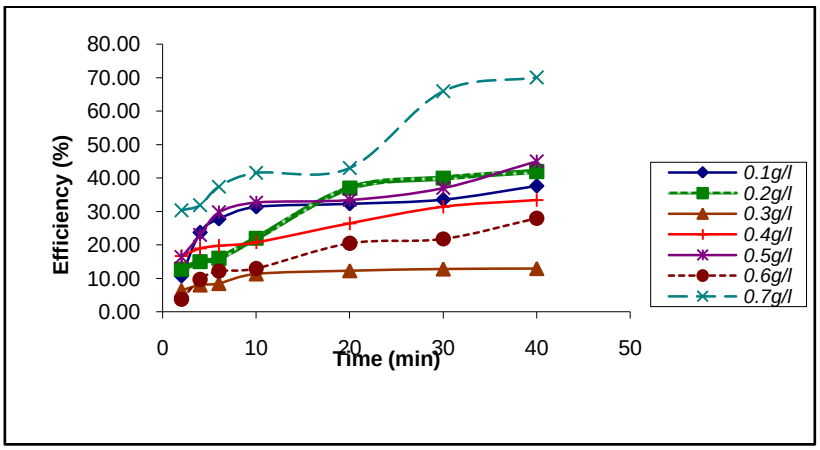

Fig.4.76:Removal efficiency as a function of time and cosc dosage for VIE at pH 10

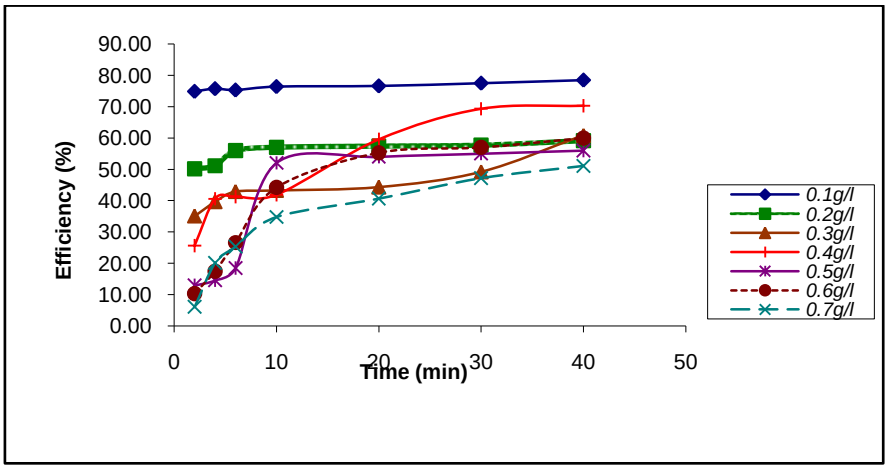

Fig.4.77:Removal efficiency as a function of time and cosc dosage for VIE at pH 13

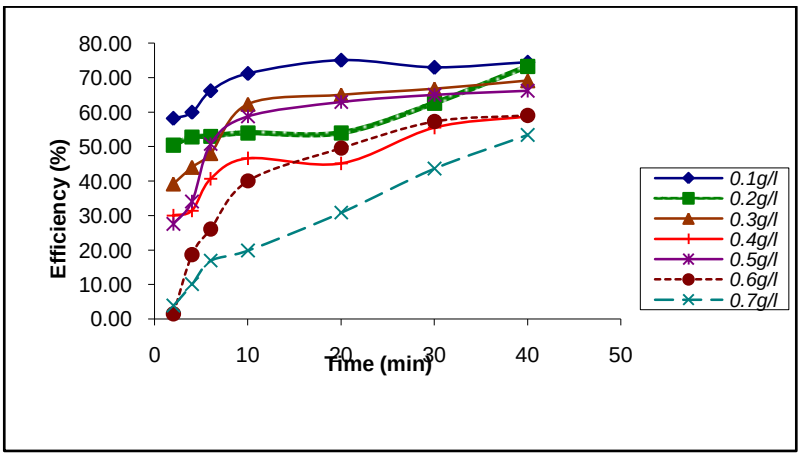

Fig.4.78:Removal efficiency as a function of time and tosc dosage for VIE at pH 1

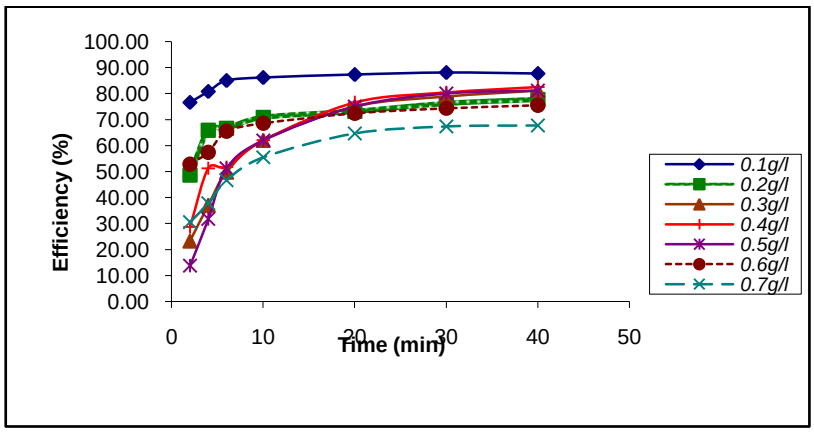

Fig.4.79:Removal efficiency as a function of time and tosc dosage for VIE at pH 3

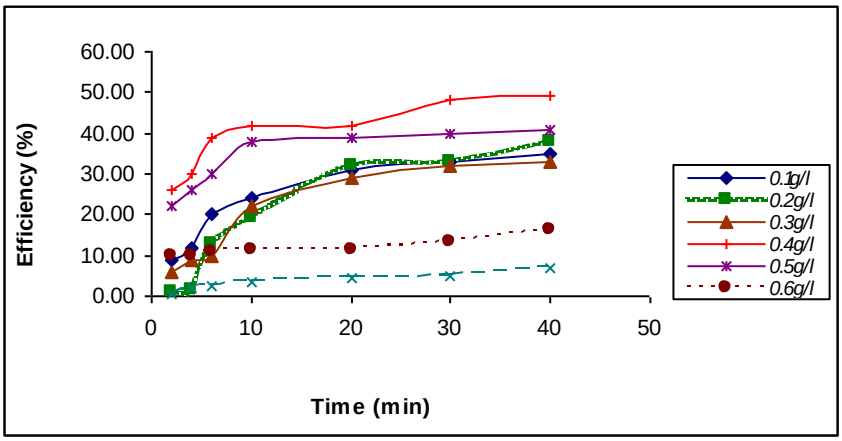

Fig.4.80: Removal efficiency as a function of time and tosc dosage for VIE at pH 5

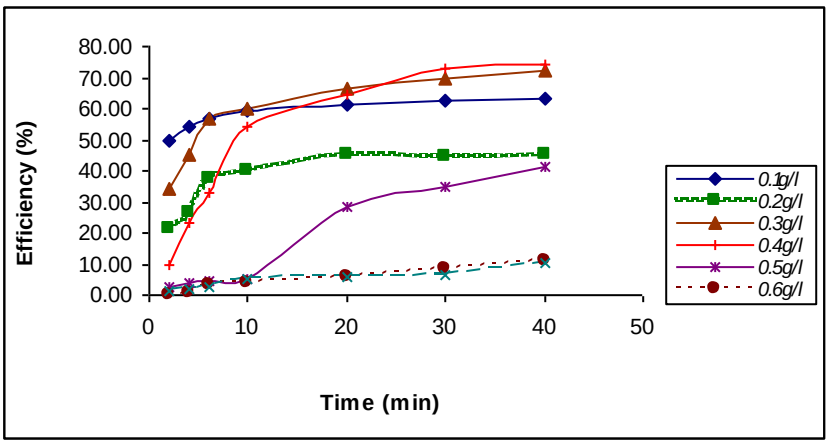

Fig.4.81: Removal efficiency as a function of time and tosc dosage for VIE at pH 7

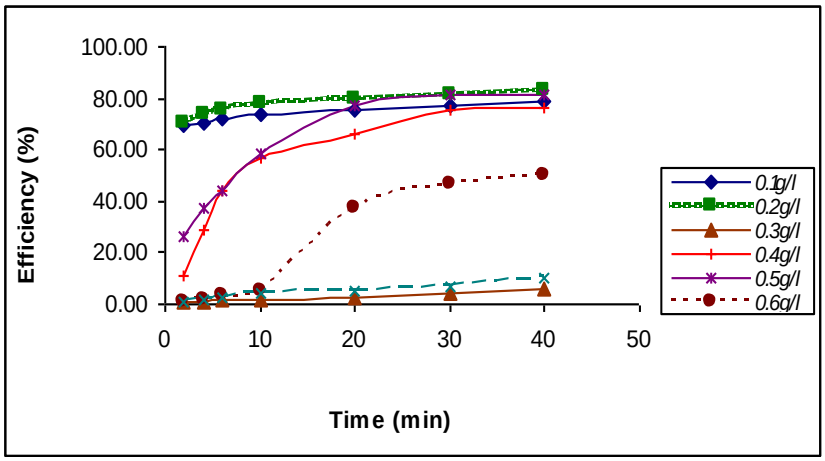

Fig.4.82: Removal efficiency as a function of time and tosc dosage for VIE at pH 10

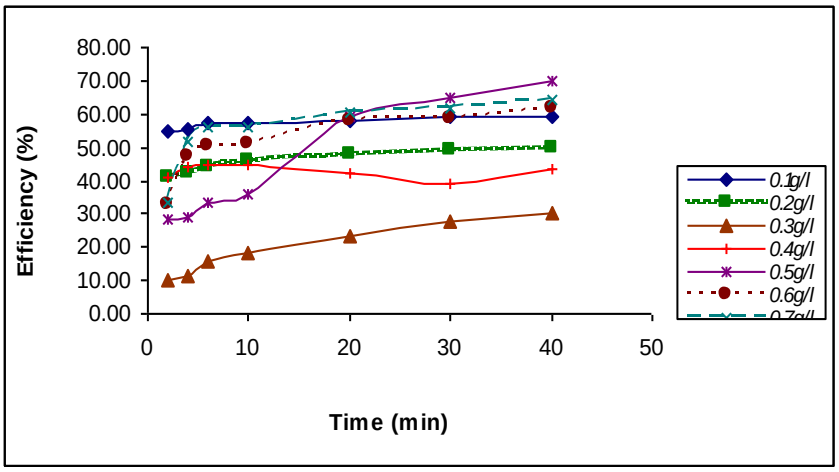

Fig.4.83: Removal efficiency as a function of time and tosc dosage for VIE at pH 13

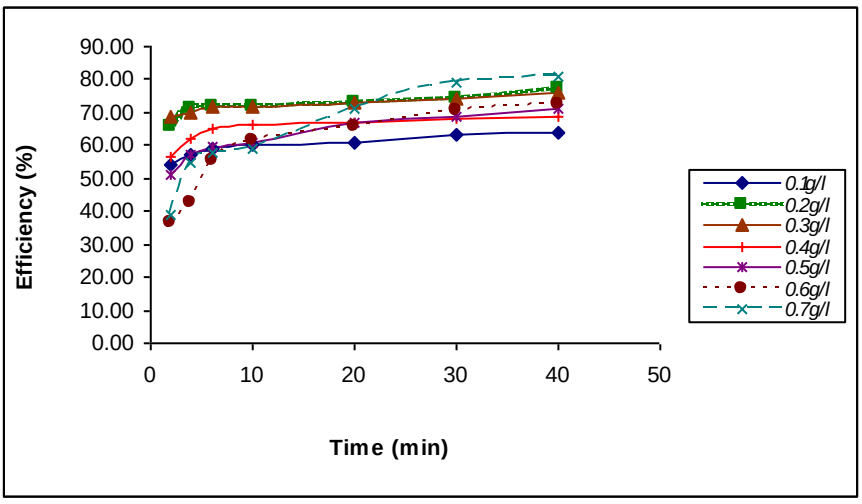

Fig.4.84: Removal efficiency as a function of time and ptsc dosage for VIE at pH 1

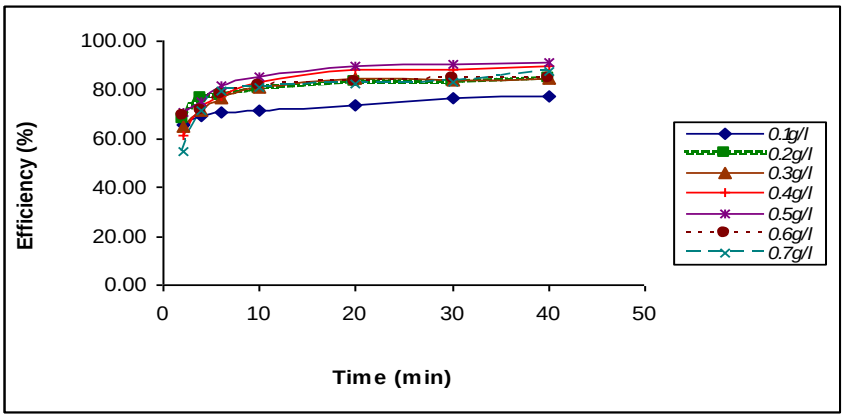

Fig.4.85: Removal efficiency as a function of time and ptsc dosage for VIE at pH 3

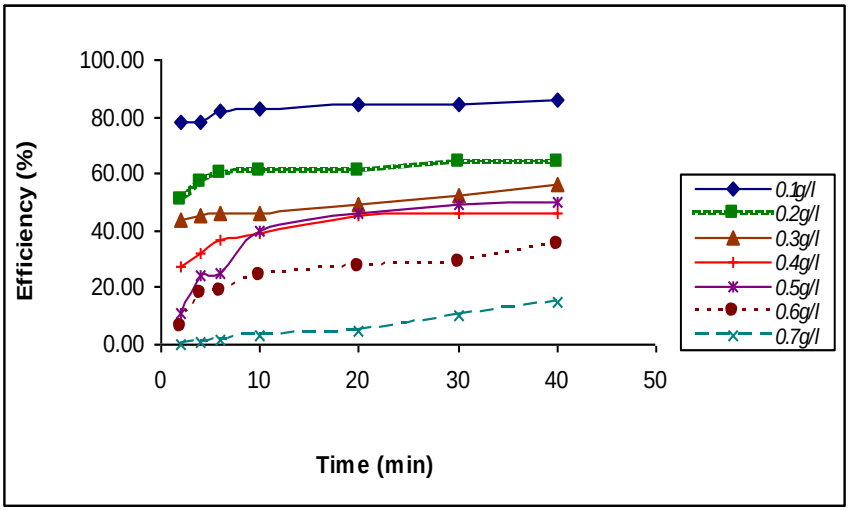

Fig.4.86: Removal efficiency as a function of time and ptsc dosage for VIE at pH 5

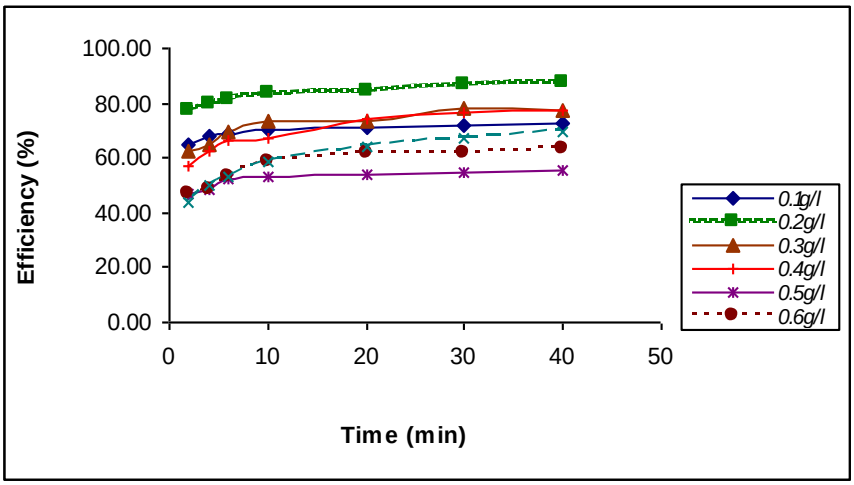

Fig.4.87: Removal efficiency as a function of time and ptsc dosage for VIE at pH 7

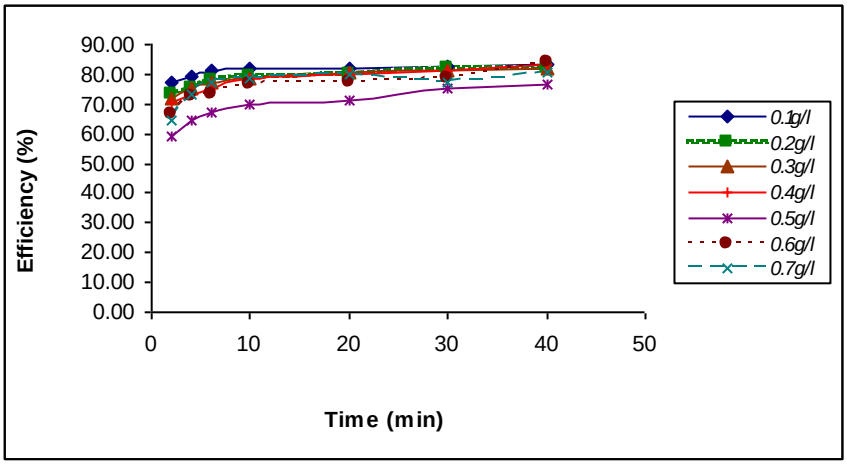

Fig.4.88: Removal efficiency as a function of time and ptsc dosage for VIE at pH 10

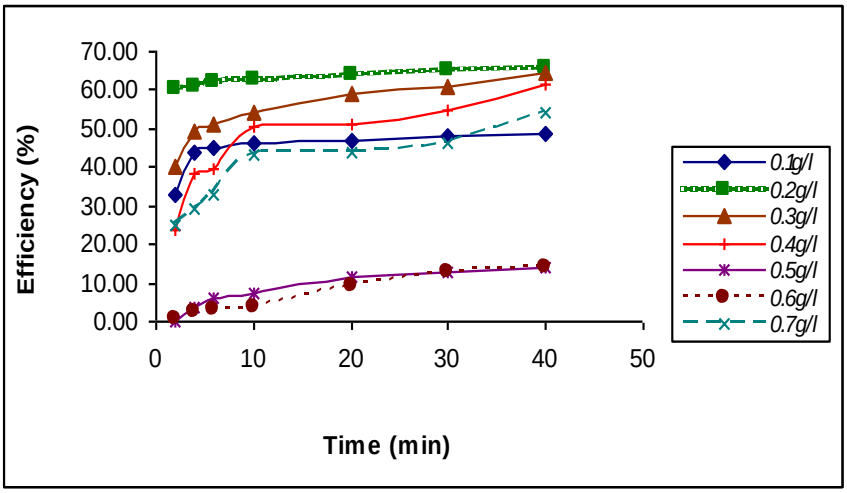

Fig.4.89: Removal efficiency as a function of time and ptsc dosage for VIE at pH 13

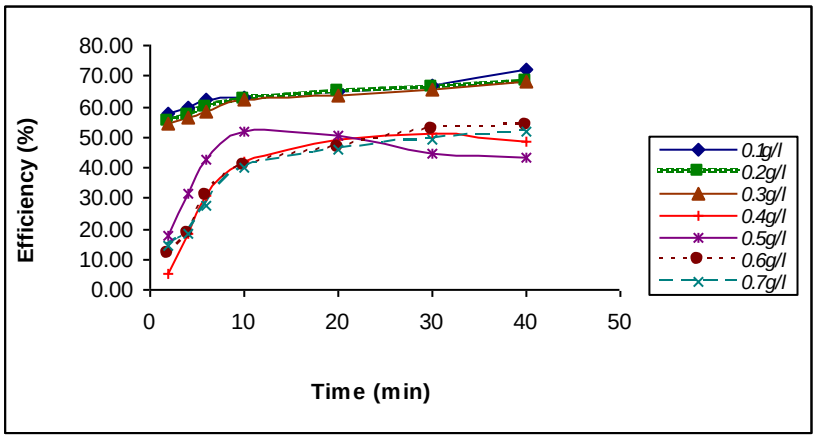

Fig.4.90: Removal efficiency as a function of time and mpsc dosage for VIE at pH 1

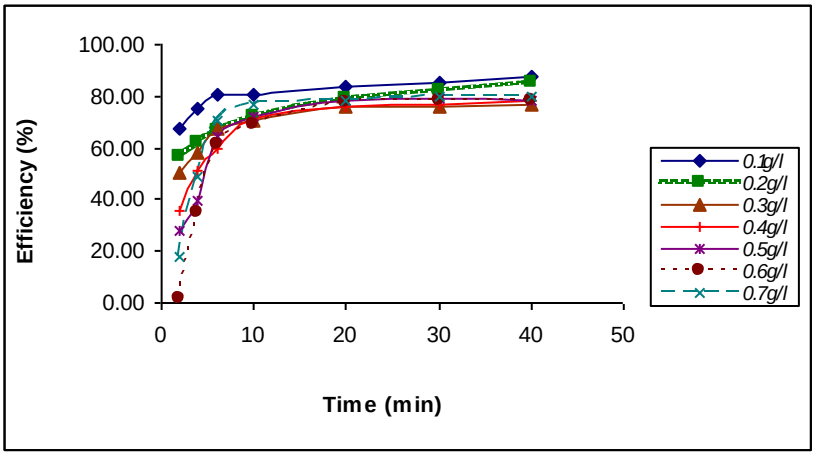

Fig.4.91: Removal efficiency as a function of time and mpsc dosage for VIE at pH 3

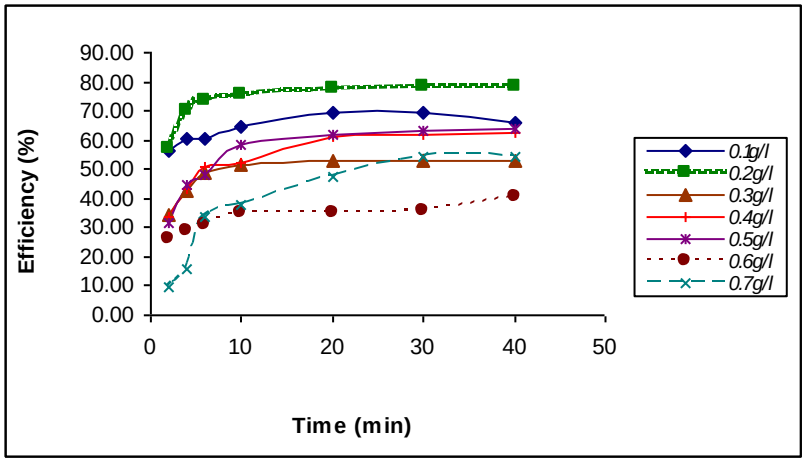

Fig.4.92: Removal efficiency as a function of time and mpsc dosage for VIE at pH 5

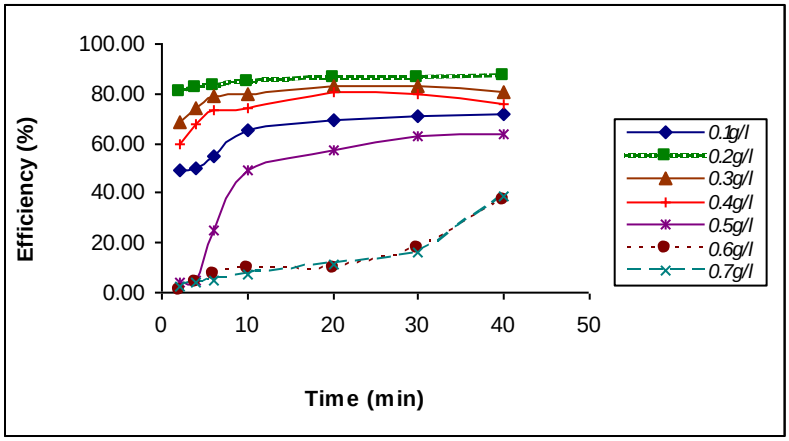

Fig.4.93: Removal efficiency as a function of time and mpsc dosage for VIE at pH 7

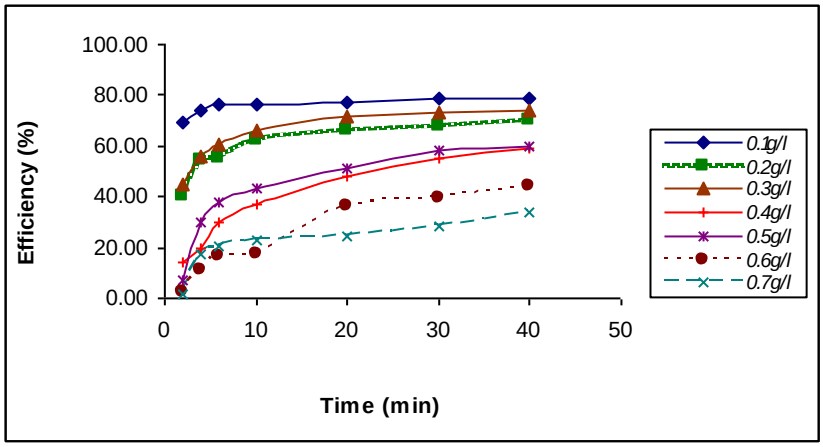

Fig.4.94: Removal efficiency as a function of time and mpsc dosage for VIE at pH 10

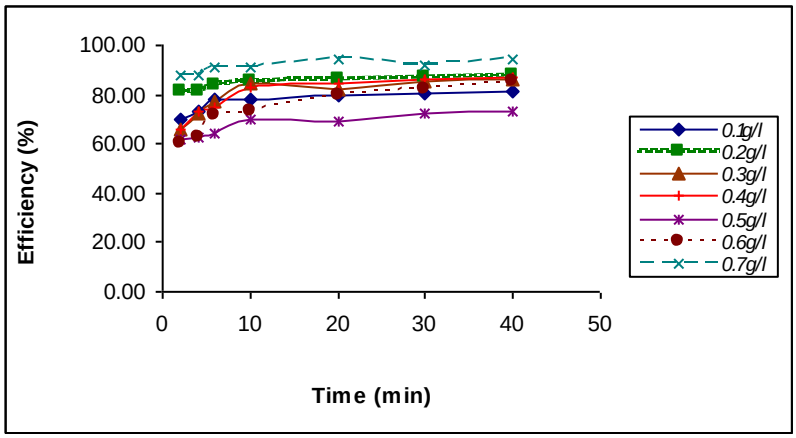

Fig.4.95: Removal efficiency as a function of time and mpsc dosage for VIE at pH 13

4.1.2.4 Removal efficiency for pH varying Wastewater at constant coag-flocculants dosage in VIE.

The results graphically presented in figures.4.96 to 4.130 depicts how coag-flocculant dosage affected the efficiency at varying effluent pH medium. The general features of the figures follow the same behavioral pattern witnessed in PIE. The remarkable difference is that the coag-flocculant performed better in PIE than VIE. This is justified by high efficiency value recorded for individual coag-flocculants in PIE following the presence of high TDSS prior to treatment.

Individual results show that the optimum pH for SSC is recorded at pH of 1 between 2-40mins for 0.1g/l dosage. Though the efficiency values recorded for other dosages are satisfactory. An indication that SSC has high degree of dissociation into complexes or radicals in acidic medium.

Whereas, in case of COSC, least optimal performance are recorded at the pH 5, 7 and 10 for the dosages considered. This an indication that COSC is sparingly hydrolysable at those pH, leading to low cationic radicals available for sorption of anionic radicals. However, the optimum efficiency of COSC is recorded at pH of 3 for 0.1 to 0.2g/l dosage and 30 – 40min settling time as shown in the figures. 4.104 to 4.110.

Considering, figures.4.111 to 4.116 for TOSC, an observation indicates that low performance is recorded at pH of 5 for all the dosages. The implication is that pH of 5 is not suitable for practical coag-flocculation process involving TOSC and PIE. Though optimum is recorded at pH of 3. In the case of PTSC, the coag-flocculation activity presented in figures.4.117 to 4.123, show that the efficiency values recorded at pH of 3 and 10 for all the dosages are satisfactory. Expectedly the optimal performance of PTSC lies between pH of 3 and 10, whereas the figures.4.124 to 4.130, illustrating the coag-flocculation behavior of MPSC, indicate that the performance recorded at pH of 13 for all the dosages are relatively high, supporting the fact that the pH media is optimal for coag-flocculation operation for MPSC – VIE system.

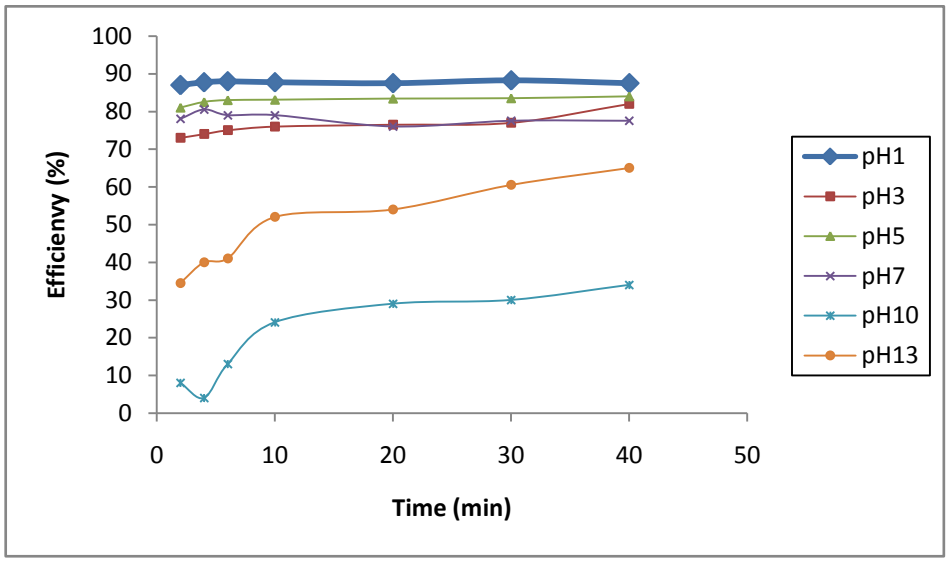

Fig.4.96: Removal efficiency as a function of time for pH varying VIE at 0.1g/l ssc

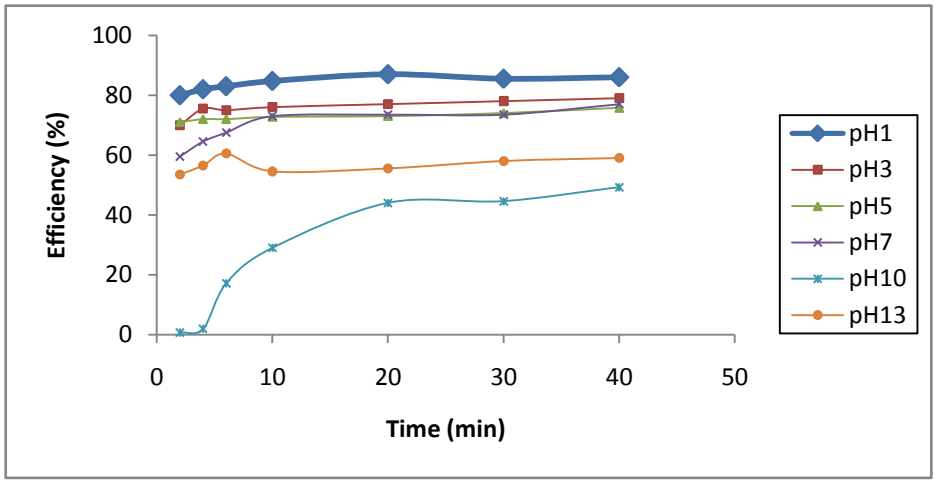

Fig.4.97:Removal efficiency as a function of time for pH varying VIE at 0.2g/l ssc

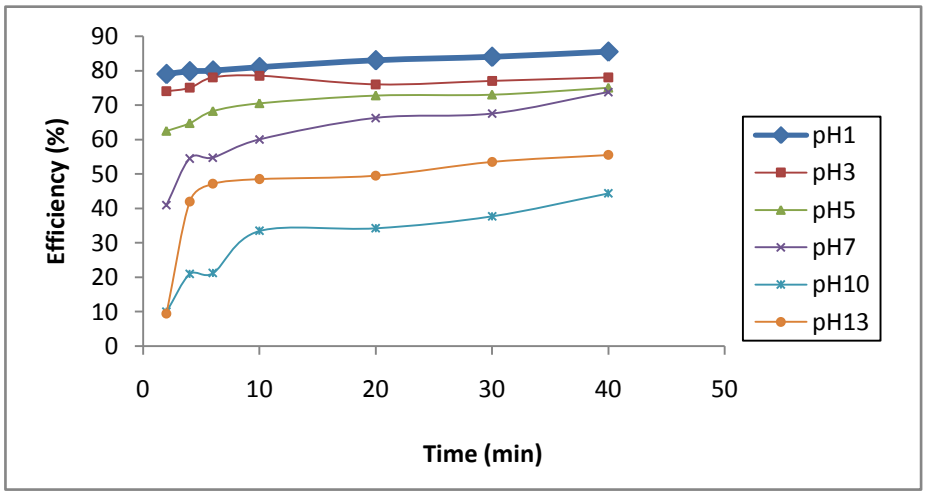

Fig.4.98:Removal efficiency as a function of time for pH varying VIE at 0.3g/l ssc

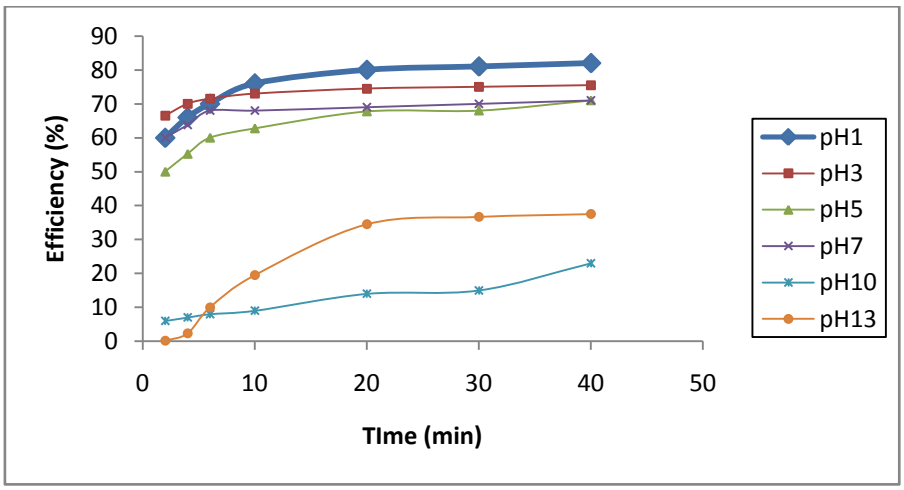

Fig.4.99:Removal efficiency as a function of time for pH varying VIE at 0.4g/l ssc

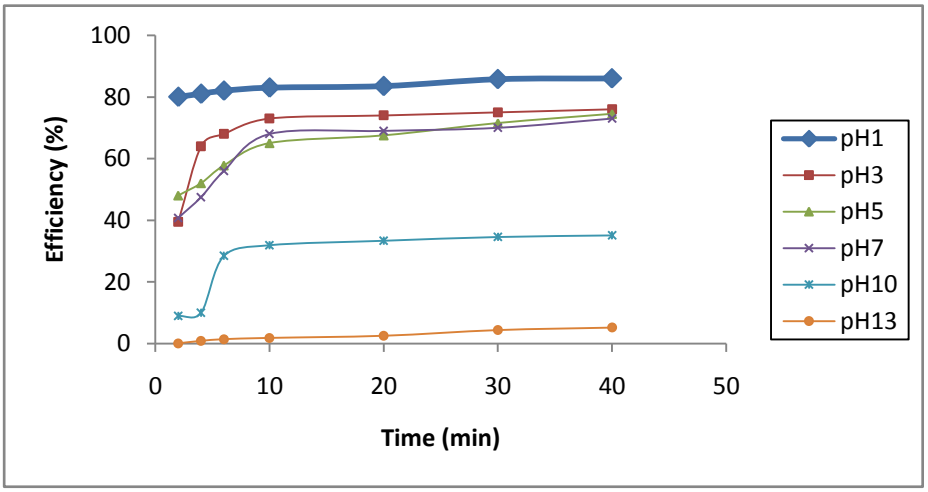

Fig.4.100:Removal efficiency as a function of time for pH varying VIE at 0.5g/l ssc

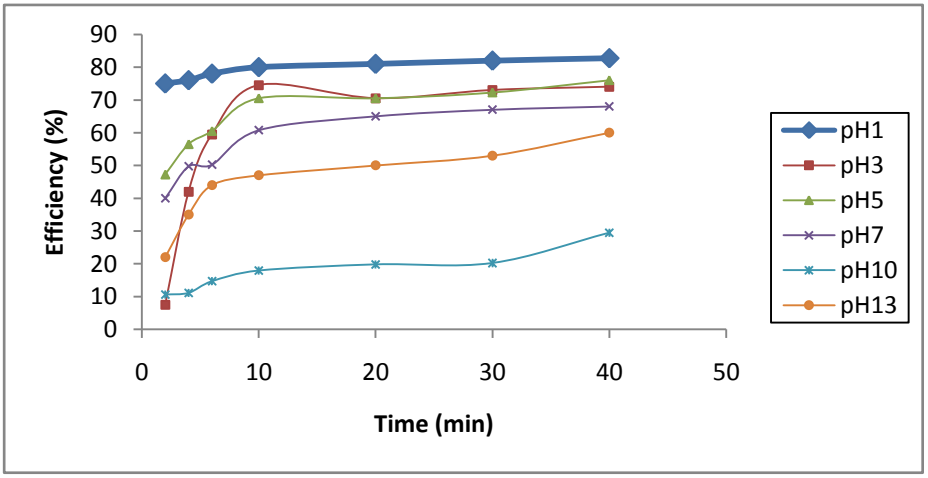

Fig.4.101:Removal efficiency as a function of time for pH varying VIE at 0.6g/l ssc

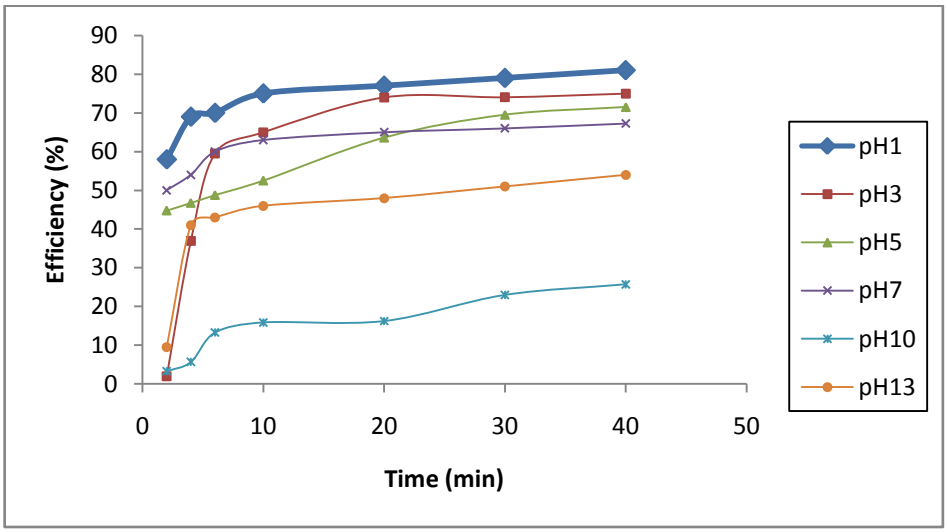

Fig.4.102: Removal efficiency as a function of time for pH varying VIE at 0.7g/l ssc

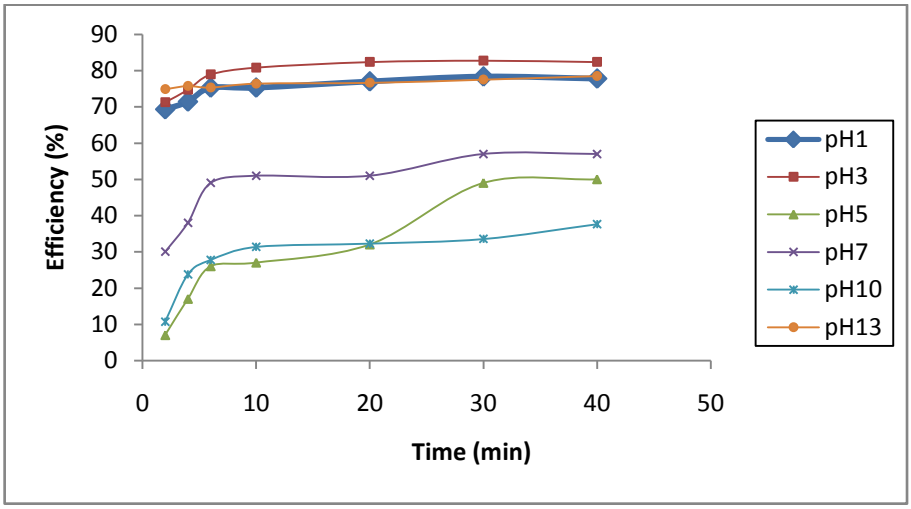

Fig.4.103: Removal efficiency as a function of time for pH varying VIE at 0.1g/l cosc

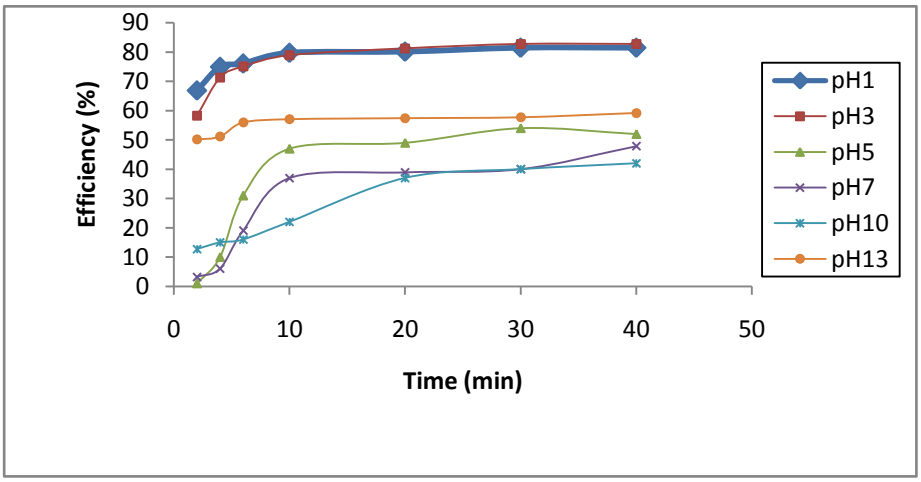

Fig.4.104: Removal efficiency as a function of time for pH varying VIE at 0.2g/l cosc

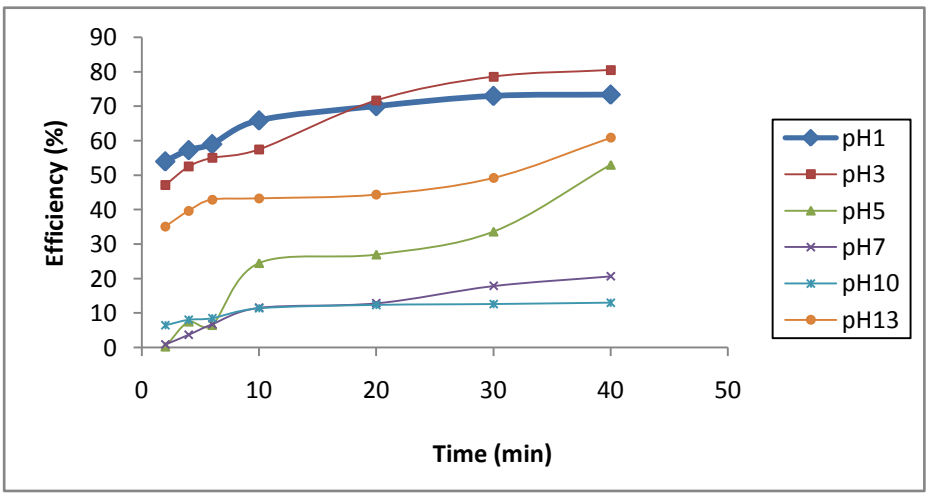

Fig.4.105: Removal efficiency as a function of time for pH varying VIE at 0.3g/l cosc

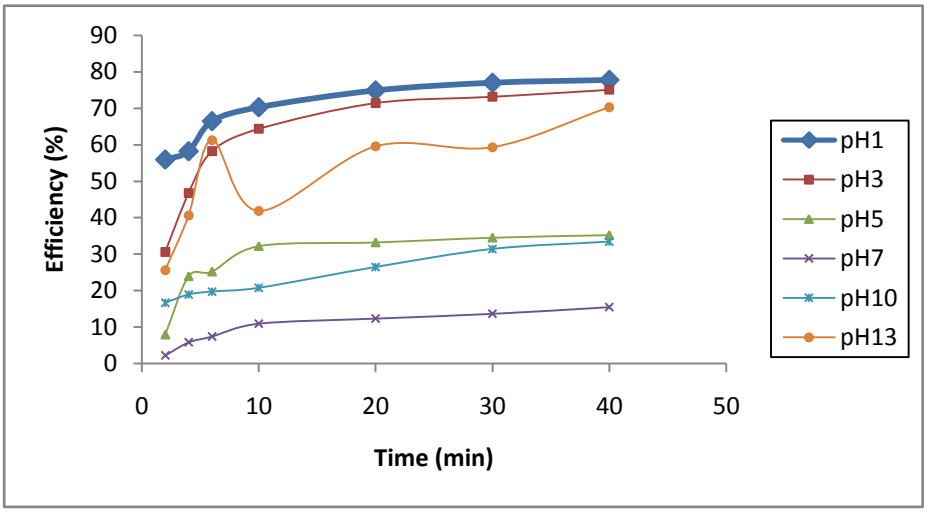

Fig.4.106: Removal efficiency as a function of time for pH varying VIE at 0.4g/l cosc

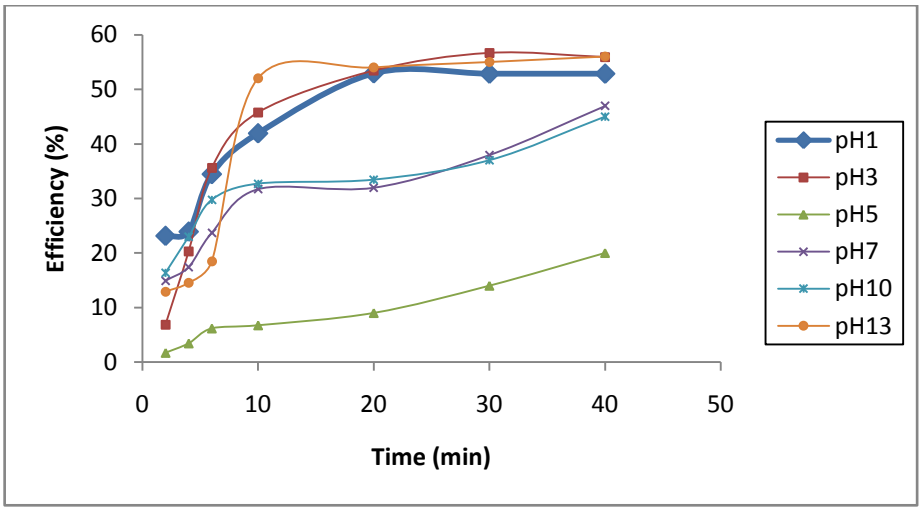

Fig.4.107: Removal efficiency as a function of time for pH varying VIE at 0.5g/l cosc

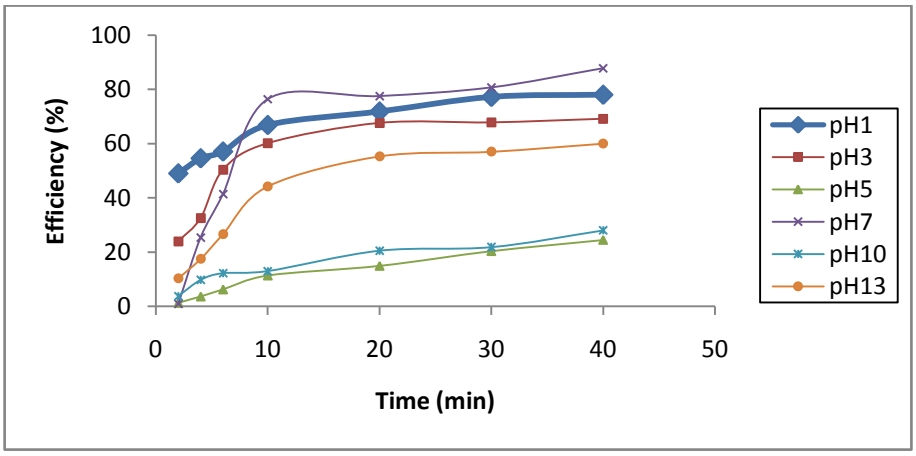

Fig.4.108: Removal efficiency as a function of time for pH varying VIE at 0.6g/l cosc

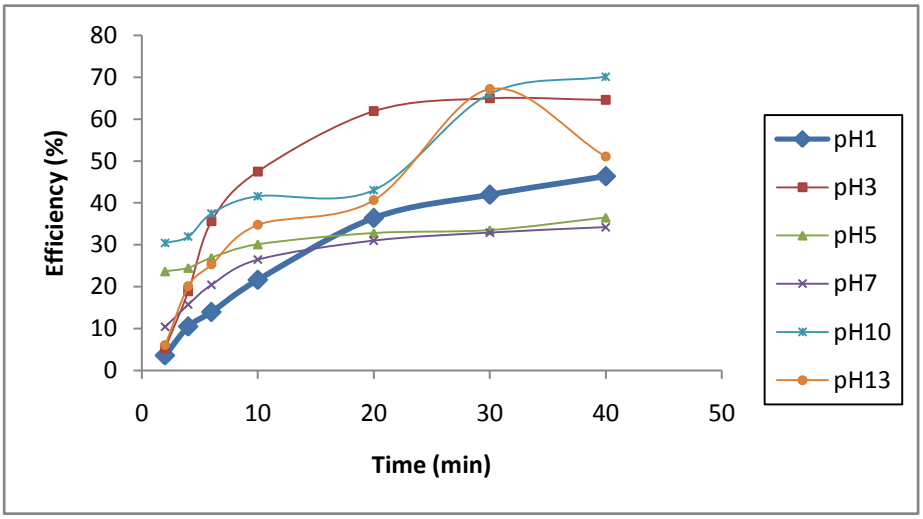

Fig.4.109: Removal efficiency as a function of time for pH varying VIE at 0.7g/l cosc

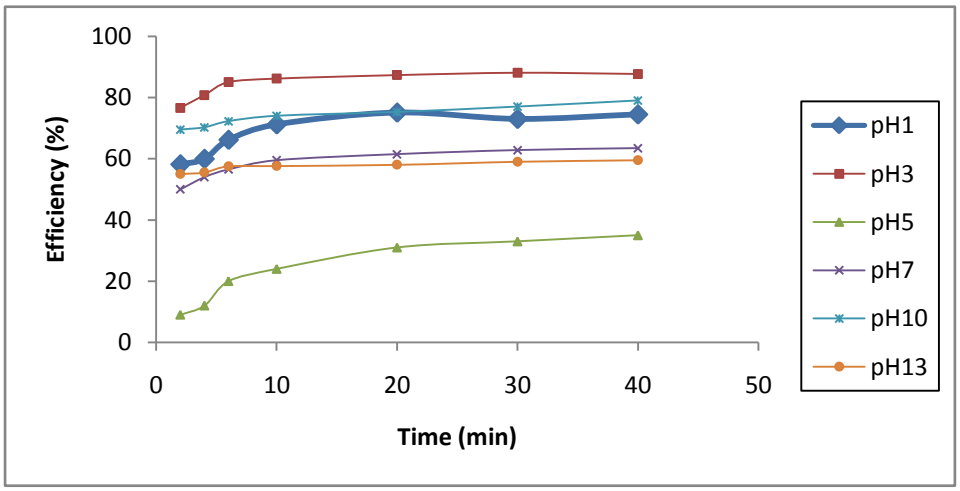

Fig.4.110: Removal efficiency as a function of time for pH varying VIE at 0.1g/l Tosc

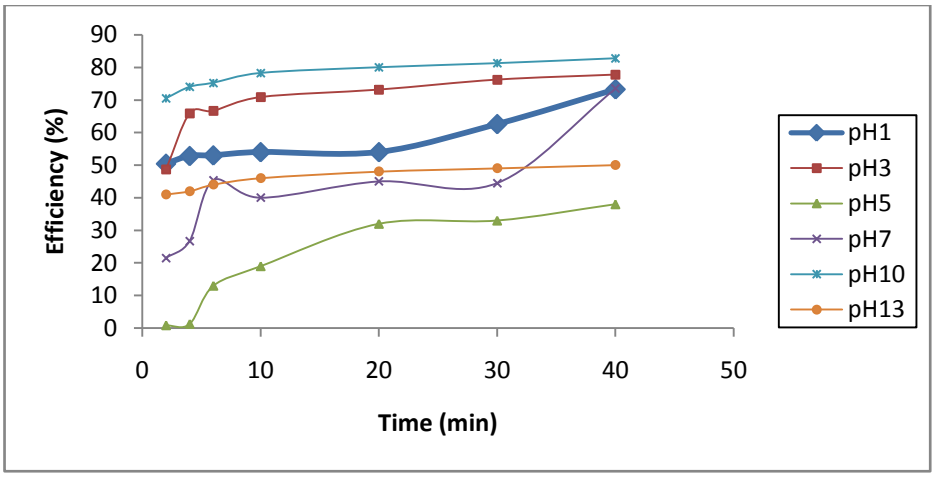

Fig.4.111: Removal efficiency as a function of time for pH varying VIE at 0.2g/l Tosc

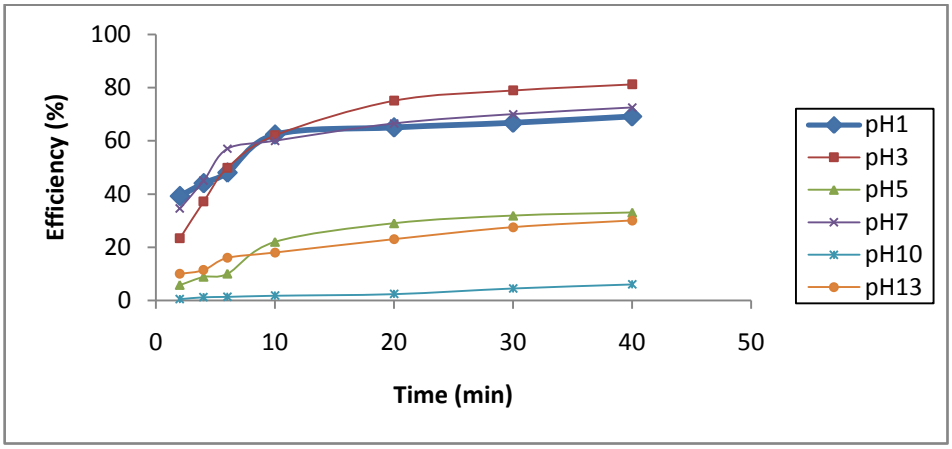

Fig.4.112: Removal efficiency as a function of time for pH varying VIE at 0.3g/l Tosc

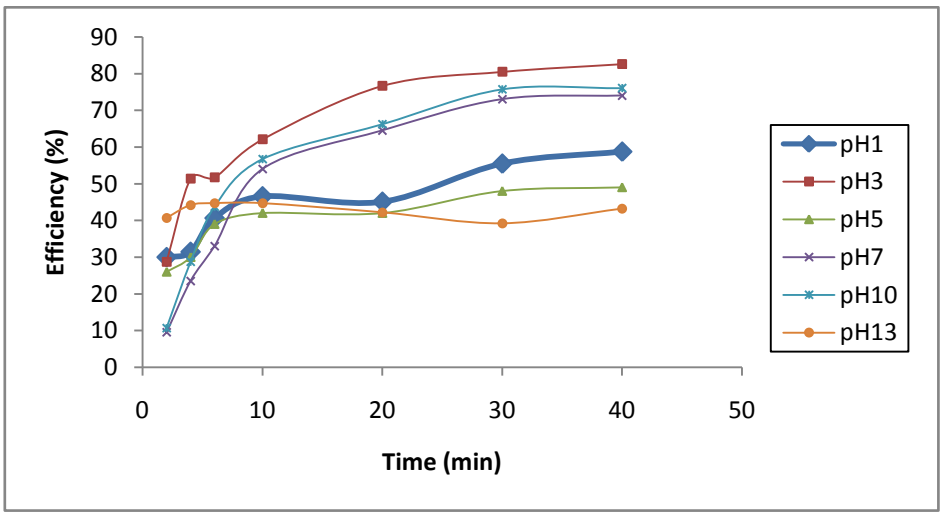

Fig.4.113: Removal efficiency as a function of time for pH varying VIE at 0.4g/l Tosc

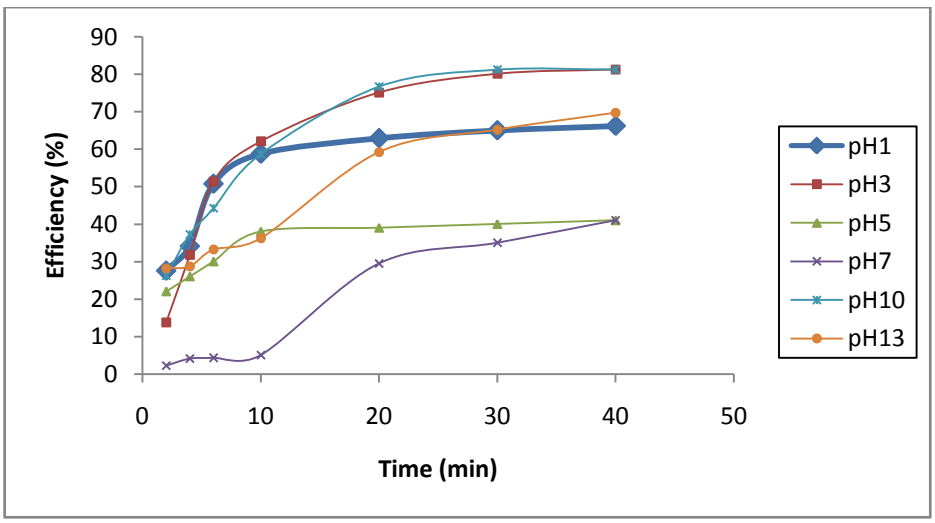

Fig.4.114: Removal efficiency as a function of time for pH varying VIE at 0.5g/l Tosc

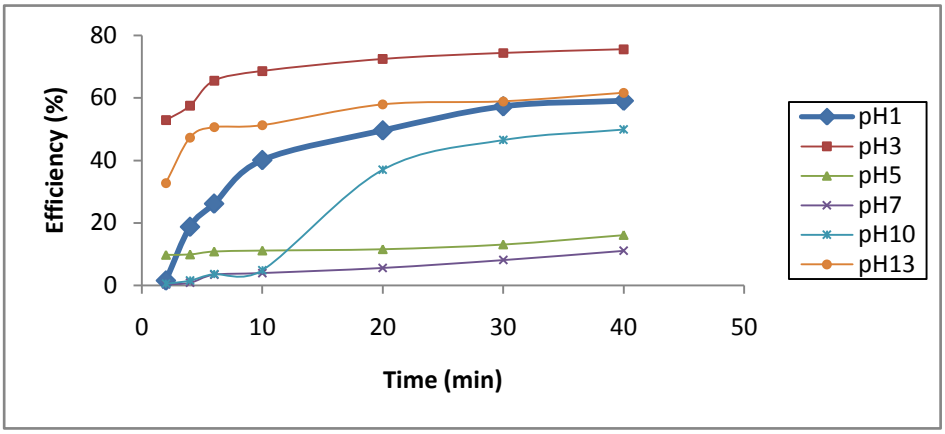

Fig.4.115: Removal efficiency as a function of time for pH varying VIE at 0.6g/l Tosc

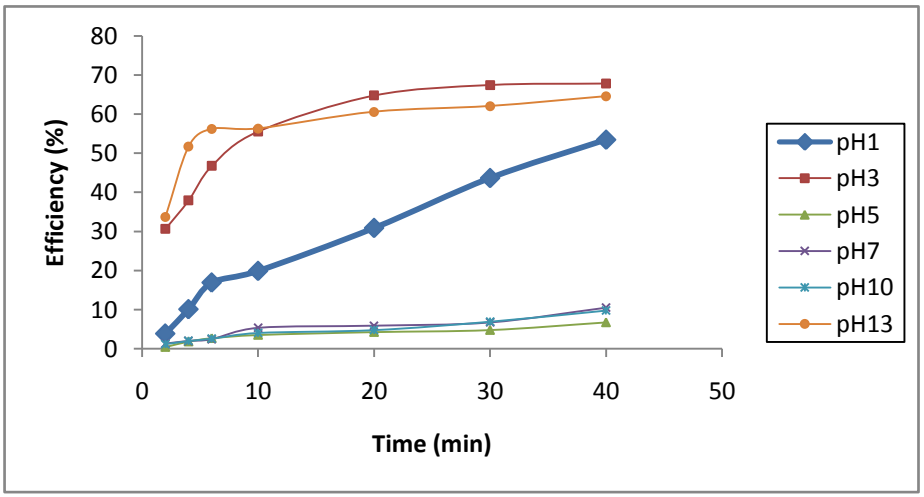

Fig.4.116: Removal efficiency as a function of time for pH varying VIE at 0.7g/l Tosc

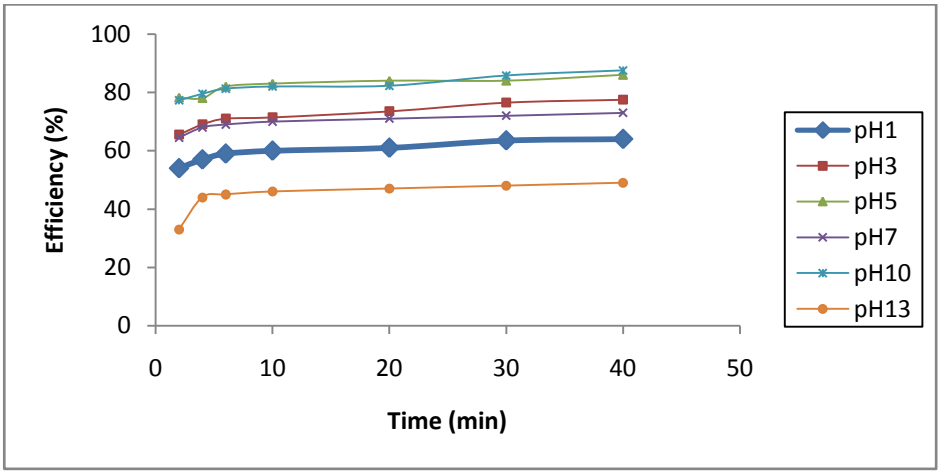

Fig.4.117: Removal efficiency as a function of time for pH varying VIE at 0.1g/l ptsc

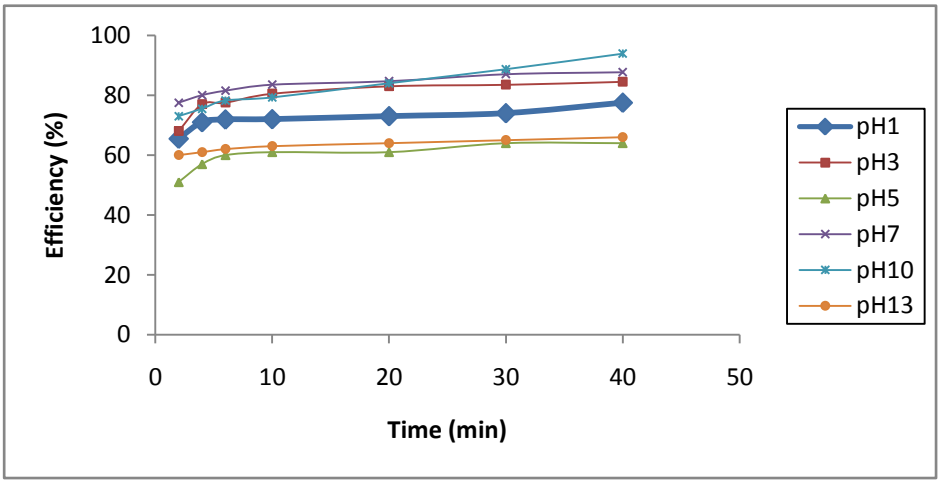

Fig.4.118: Removal efficiency as a function of time for pH varying VIE at 0.2g/l ptsc

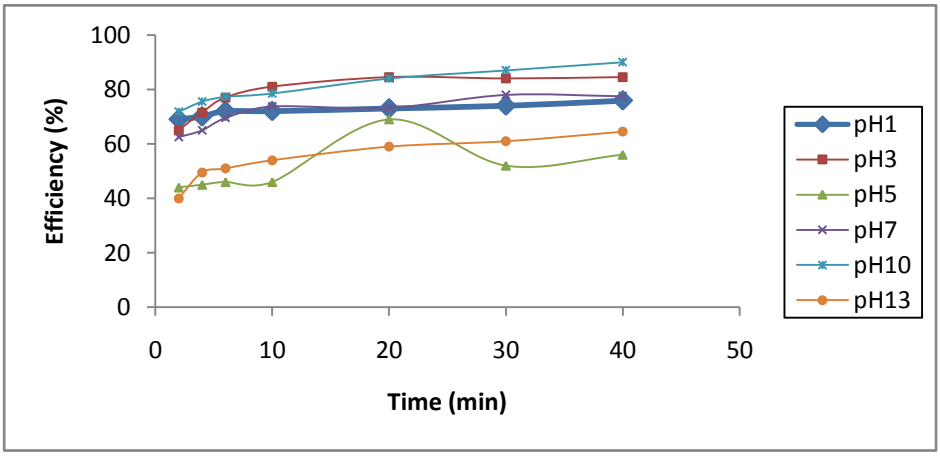

Fig.4.119:Removal efficiency as a function of time for pH varying VIE at 0.3g/l ptsc

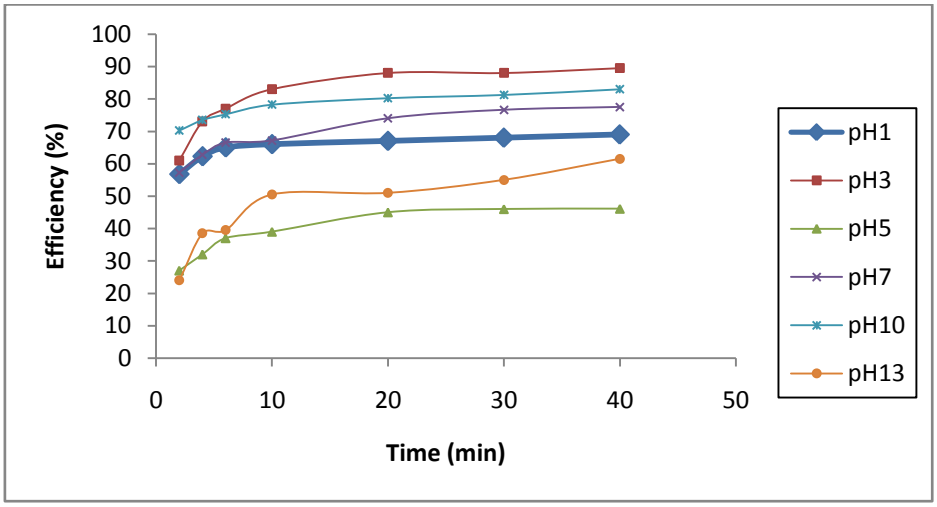

Fig.4.120: Removal efficiency as a function of time for pH varying VIE at 0.4g/l ptsc

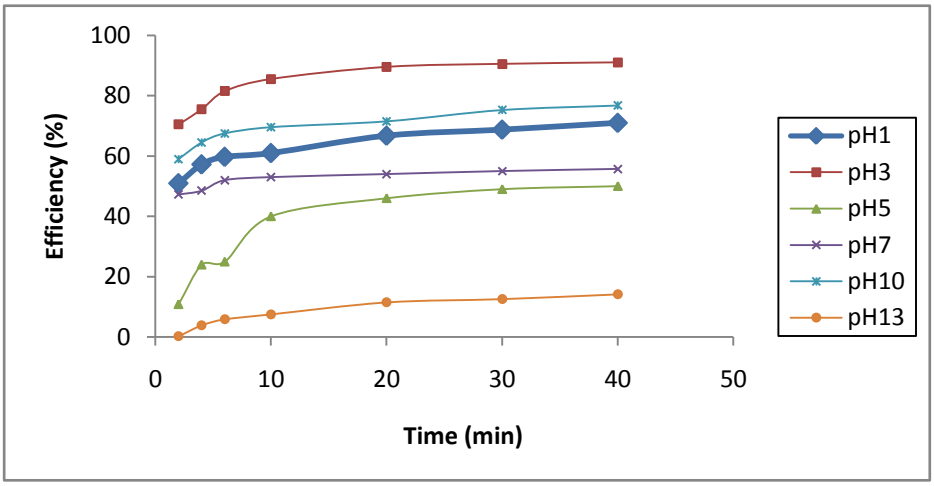

Fig.4.121: Removal efficiency as a function of time for pH varying VIE at 0.5g/l ptsc

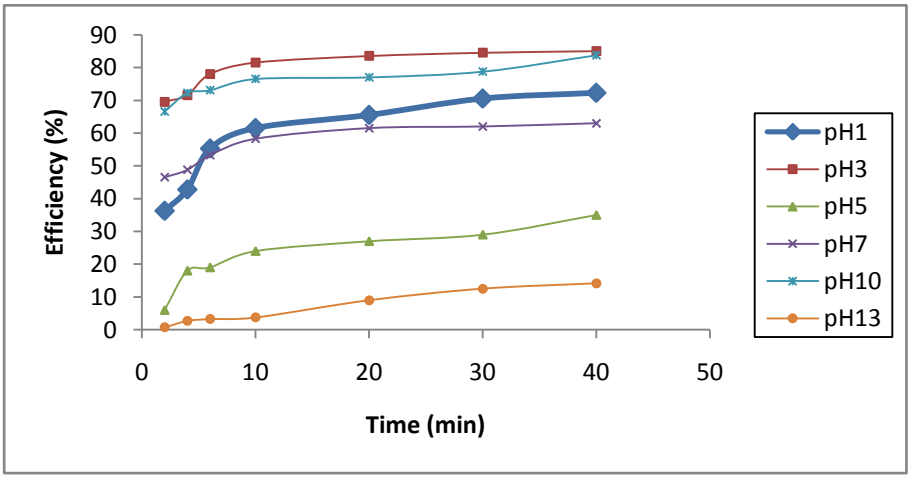

Fig.4.122: Removal efficiency as a function of time for pH varying VIE at 0.6g/l ptsc

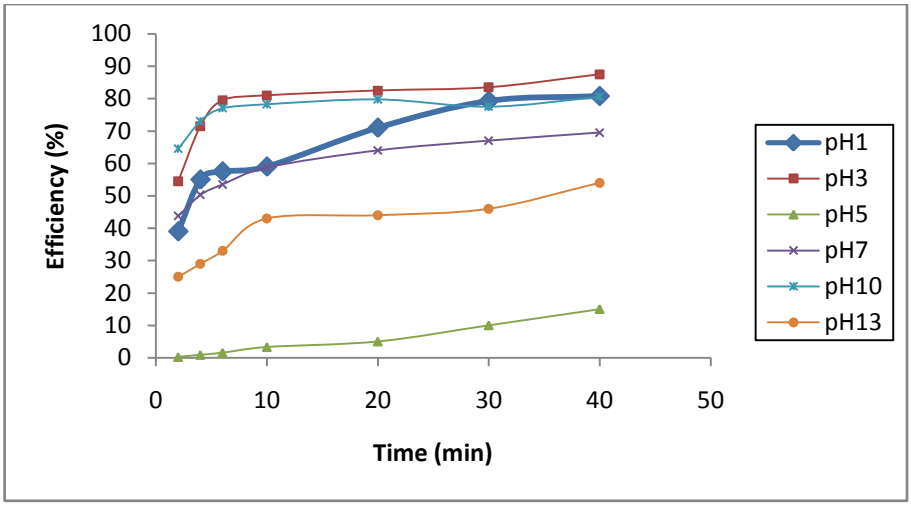

Fig.4.123: Removal efficiency as a function of time for pH varying VIE at 0.7g/l ptsc

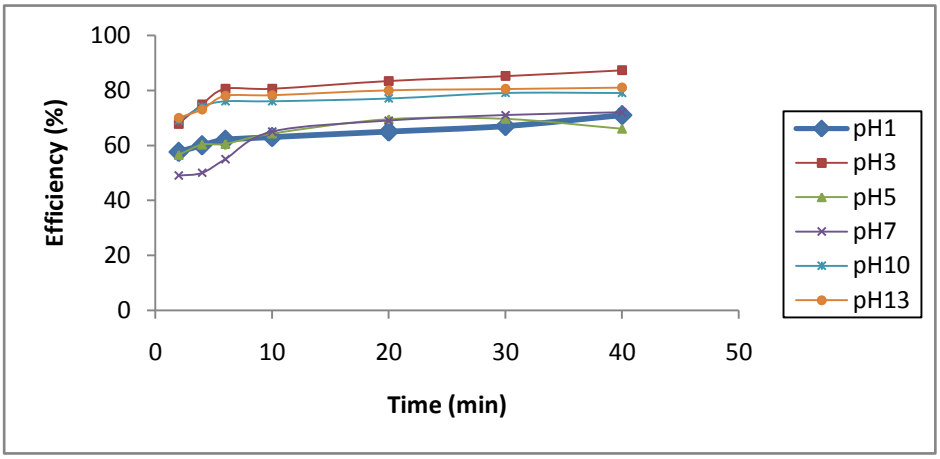

Fig.4.124: Removal efficiency as a function of time for pH varying VIE 0.1g/l mpsc

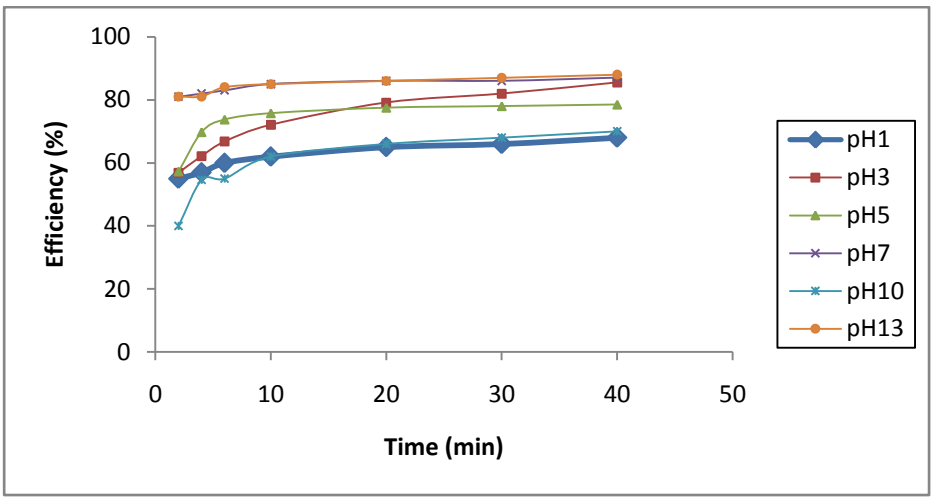

Fig.4.125: Removal efficiency as a function of time for pH varying VIE 0.2g/l mpsc

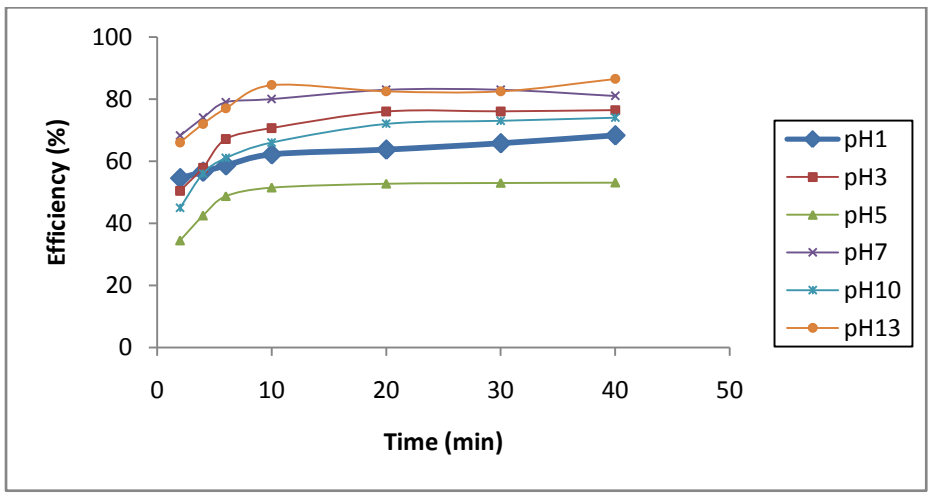

Fig.4.126: Removal efficiency as a function of time for pH varying VIE 0.3g/l mpsc

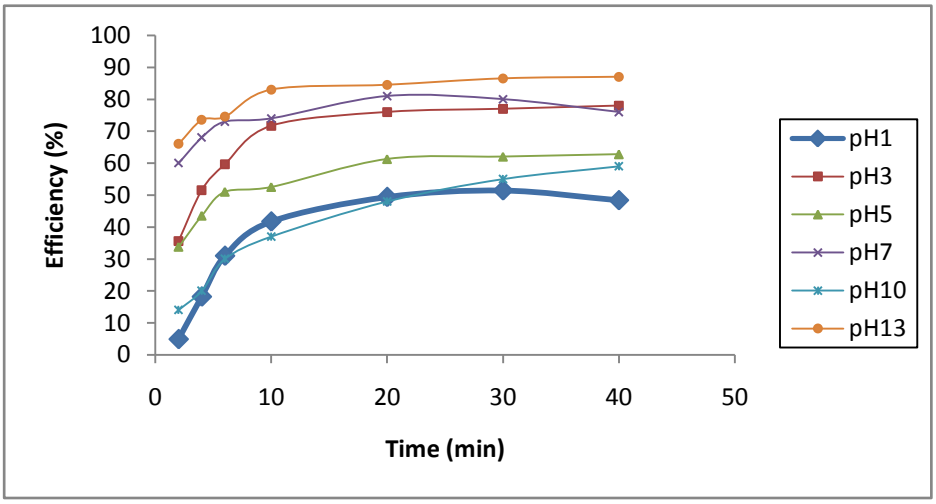

Fig.4.127: Removal efficiency as a function of time for pH varying VIE 0.4g/l mpsc

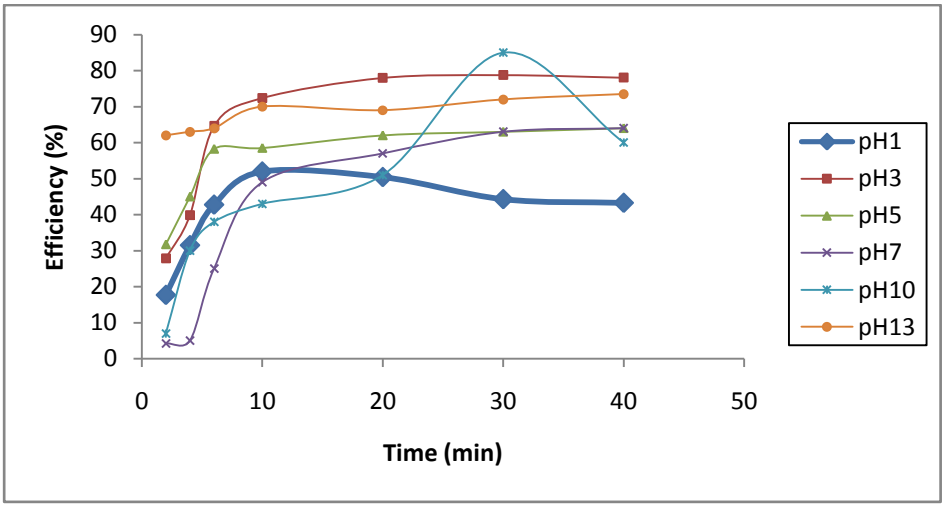

Fig.4.128: Removal efficiency as a function of time for pH varying VIE 0.5g/l mpsc

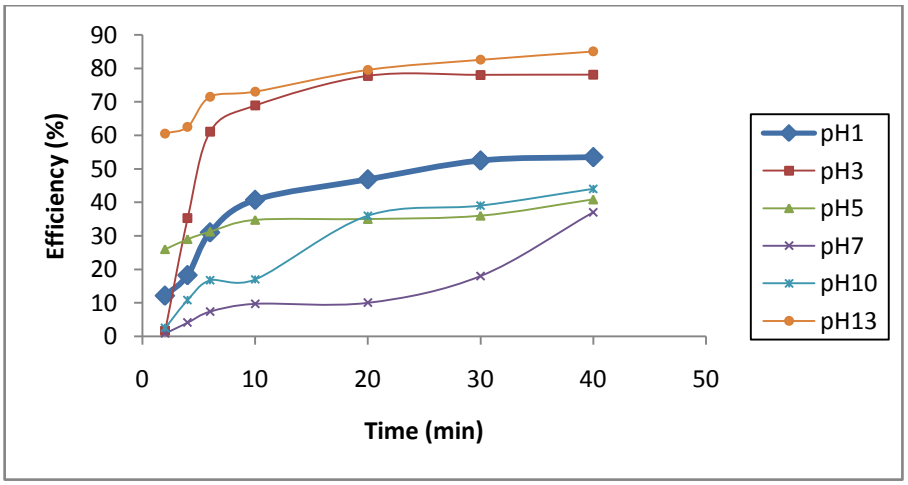

Fig.4.129: Removal efficiency as a function of time for pH varying VIE 0.6g/l mpsc

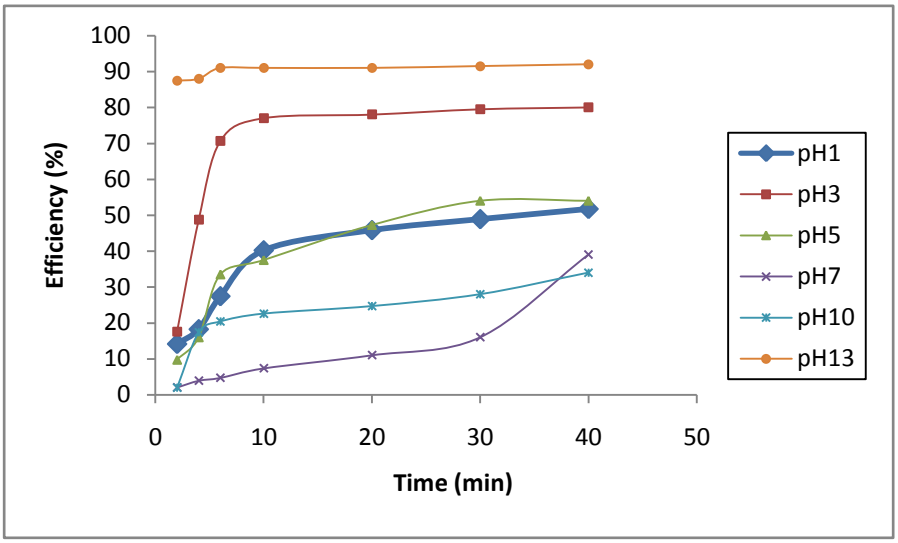

Fig.4.130:Removal efficiency as a function of time for pH varying VIE 0.7g/l mpsc

4.1.3. Coag-flocculation kinetic results, parameters and plots

Kinetic parametric results and plots of varying dosage and pH related with PIE and VIE coag-flocculation treatment are presented in this section in the following order.

4.1.3.1. General kinetic results / parameters

The general kinetic results / parameters both PIE and VIE are presented and elaborated in this section. The kinetic results of PIE for varying dosage and pH are presented in tables 4.3 to 4.32 and tables 4.33 to 4.67 respectively, while their corresponding graphs are figures. 4.131 to 4.160 and figures. 4.161 to 4.195, respectively, for the VIE, the kinetic results for the varying dosage and pH are presented in tables 4.68 to 4.97 and tables 4.98 to 4.132, respectively, and their corresponding graphs are figures. 4.196 to 4.225 and figures. 4.226 to 4.260. It is worthy of mentioning that the linear regression efficiency of determination and coag-flocculation rate constant values posted in the tables were determined from plots of ^{1}/TDSS Vs time as shown in the referred figures. Intuitively, k is the aggregation process, while R^2 was employed to determine the degree of accuracy of these aggregations in the system on addition of the coag-flocculants. The values of R^2 presented on the referred tables above, show that on general terms, most R^2 values are satisfactory (R^2>0.70), suggesting a monolayer and homogenous surface adsorption, controlled by electrostatic repulsion mechanism (Montgometry,1985). This further supports the theory of micro- kinetics as the controlling mechanism of coag-flocculation systems. Invariably, it is apparent, from equation (15) that α, order of

reaction relates inversely with coag-flocculation reaction constant K, (which equally implies rate per particle concentration) is associated with energy barrier (KT) and particle interaction potential hence it is expected that for higher K to be obtained, is a condition for lower α and high particle interaction (Fridkhsberg, 1984).

It is observed from the tables referred above , high K corresponds to the least $\tau_{1/2}$ obtained in this work, a phenomenon that amplified a strong relationship among K, $\tau_{1/2}$ and rate of aggregation. On the strength of that, the values of $\tau_{1/2}$, obtained are generally satisfactory, though millisecond has been reported (Von Smoluchowski, 1917). Overview, of K_R values in the tables, indicate minimal variations, due to insignificant changes in the values of temperature and viscosity of the effluent medium (i.e K_R=fn(Tη)). In the vicinity near a unit of $K_{R,}$ ε_p relates proportionally to 2k =β_{BR}. Apparently, high β_{BR} result in high kinetic energy to overcome electrostatic barrier translating to fast coag-flocculation, generally, obtainable in practical terms in coag-flocculation systems. It should be noted from the tables that high $\tau_{1/2}$ corresponds to low ε_p and K, indicating presence of repulsive force in the system. From theoretical considering, $\tau_{1/2}$ and K_R are understood to be the prerequisite factors for coagulation efficiency prior to flocculation.

In general, the discrepancies observed among the results posted in the tables are due to unattainable assumptions that there is perfect homogeneity of effluent particles and the coag-flocculants throughout the dispersion before particle aggregation (Menkiti, et al., 2012). These draw-backs may be caused by under-dosing or over-dosing of the coag-flocculant in the effluent sample, which creates an imbalance in the coag-flocculant/effluent sample ratio. This phenomenon will result in uneven distribution of the coag-flocculants in the effluent sample, leading to non-homogeneity of the solution followed by inadequate attraction of TDSS by coag-flocculants. Another limitation is the effect of interactions between van der waal's forces and repulsive forces which is capable of altering theoretical predicted values. Also low or high coagulant dosage could have effect on the results, because high coagulant dosage may cause particle dispersion leading to generation of outrageous values. On the other hand, low dosage may result in the provision of insufficient adsorption sites for TDSS attachment.

4.1.3.2. Kinetic results of dosage varying caog-flocculants in PIE.

These results are presented in tables 4.3 to 4.32, showing the coag-flocculation rate pararmeters for various coag-flocculant dosage in PIE at a particular pH. The results contained in the tables are for SSC, COSC, TOSC, PTSC and MPSC involving 10 different parameters. For the SSC, table 4.3, 4.6 and 4.7 posted good values for the $\tau_{1/2}$, giving credence to the high values of K obtained in this process for all the dosages considered. The best value of $\tau_{1/2}$ of 0.178min is recorded for 0.3g/l at pH of 1 in table 4.3. Thus high K value requires minimum coag-flocculation period to accomplish the treatment operation in the system. The highest values $\tau_{1/2}$ of 8.599min with the corresponding lowest values of K 9.54E- 06l/g.min were recorded for table 4.4 for 0.7g/l dosage. This occurrence is attributable to particle redispersion or returbidization of the system. It is pertinent to point out that there is minimal variation in ε_p values posted in tables 4.3 to 4.8. This is an indication that the variations in K values and the viscosity of the effluent medium were relatively minimal throughout the operation.

For COSC, the highest and least values of K recorded are 6.322E-06(l/g.min) and 1.10E-06 (l/g.min) for 0.6g/l of table 4.12 and 0.7g/l of table 4.14 respectively. It is worthy to mention that it is only in table 4.12 that had values of $\tau_{1/2}$ posted for all the dosages is under 1min(i.e $\tau_{1/2}$<1min). This implies that COSC bio-coagulant performed best in a neutral pH effluent media. It could be observed that with the exception of table 4.14, majority of the R^2 values posted in the tables 4.9 to 4.13 are greater than 0.70, indicating high agreement between the experimental results and the theoretical model equation. Also observe negligible variations in the values of β_{BR} posted in tables 4.9 to 4.13. This accounts for near stability in the values of these parameters; ε_p, K_B, operating temperature and viscosity of the effluent medium.

Considering TOSC, Tables 4.15 and 4.18, indicate that there is minimal variations in the values of K for all the dosages with exception of 0.1g/l(table 4.15) and 0.5g/l(table 4.18) respectively. This is evidence that at pH 1, 7 and 10 the rate of particle coag-flocculation is less sensitive to coag-flocculant dosage. Also observe that the values of K_R posted in the tables have insignificant variations, justifying minimal variations in the operating temperature and viscosity of the effluent

medium. It is worthy to note that with exception of 0.5g/l, all other $\tau_{1/2}$ posted in table 4.18 are less than 1. The implication is that TOSC performance is generally good at pH of 7 and this supports high K values obtained.

The parameters posted in tables 4.21 to 4.26 are for PTSC. Tables 4.21, 4.24, 4.25 and 4.26 presented high results, the $\tau_{1/2}$ values posted for all dosages are below 1min. this phenomenon reflected on the high values of K presented in these tables. The implication is that TOSC has wider applicability in waste water and water treatment because it is capable of achieving good performance in both acidic and alkaline effluent media. There is approximately negligible variation in values of K_R and ε_p presented in the tables.

Consider the rate parameters displayed in tables 4.27 to 4.32 for MPSC. The values of $\tau_{1/2}$ posted in table 4.30 for all the dosages studied is less than 1min, suggesting that MPSC has a high potency at pH of 7. Though optimum values of K(2.18E-04l/g.min) and $\tau_{1/2}$ (0.33min) for 0.1g/l dosage were posted in table 4.32, indicating best performance at pH of 13. The highest $\tau_{1/2}$ (2.16min) and least K (7.0E-06l/g min) for 0.1g/l dosage were posted in table 4.29, indicating lowest performance of MPSC at pH of 5.

Table 4.4: Coag-flocculation kinetic parameters and linear regression coefficient of SSC in PIE at varying dosage and pH of 1.

Parameters	0.1g/l	0.2g/l	0.3g/l	0.4g/l	0.5g/l	0.6g/	0.7g/l
Y	1.12E-03 X+4.719E-03	6.29E-05 X+2.702E-03	2. 033E -04 X+3.8366E-03	1.402E-04 X+4.2625E-03	2.84E-05 X+2.7449E-03	1.33E-04 X+5.0104E-03	2.44E-05 X+2.825E-03
α	2.000	2.000	2.000	2.000	2.000	2.000	2.000
R^2	0.469	0.749	0.960	0.633	0.816	0.953	0.956
K(l/g.min)	1.12E-04	6.29E-05	2.033E-04	1.402E-04	2.84E-05	1. 733E-05	2.44E-05
K_R(l/min)	1.5289E-19	1.5315E-19	1.52152E-19	1.5315E-19	1.5341E-19	1.5366E-19	1.5366E-19
β_{BR}(l/g.min)	2.24E-04	1.258-04	4.066E-04	2.804E-04	5.68E-05	3.466E-04	4.88E-05
$\varepsilon_p(g^{-1})$	1.4651 E+15	8. 2142E+15	2.6549E+15	1.8278E+15	3.7025E+14	2.2556E+15	3.1758E+14
$^{\tau}{}_{1/2}$ (min)	0.32	0.58	0.18	0.26	1.28	0.21	1.48
(-r)	$1.12E\text{-}04N_t^2$	$6.29E\text{-}05N_t^2$	$2.033E\text{-}04N_t^2$	$1.402E\text{-}04N_t^2$	$2.84E\text{-}05N_t^2$	$1.733E\text{-}04N_t^2$	$2.44E\text{-}05N_t^2$
N_o(g/l)	211.9093	370.0962	260.6474	234.6041	364.3120	199.5849	353.9823

Table 4.5:Coag-flocculation kinetic parameters and linear regression coefficient of SSC in PIE at varying dosage and pH of 3.

Parameters	0.1g/l	0.2g/l	0.3g/l	0.4g/l	0.5g/l	0.6g/l	0.7g/l
Y	6.0E-06 X+1.295E-03	5.23E-06 X+1.3382E-03	8. 338E -06 X+1.3635E-03	7.768E-06 X+1.3183E-03	2.16E-05 X+2.0628E-03	4.445E-06 X+1.2077E-03	9.54E-06 X+1.165E-03
α	2.000	2.000	2.000	2.000	2.000	2.000	2.000
R^2	0.843	0.748	0.850	0.948	0.972	0.722	0.806
K(l/g.min)	6.0E-06	5.23E-06	8.338E-06	7.768E-06	2.16E-05	4. 455E-06	9.54E-06
K_R(l/min)	1.5494E-19	1.5494E-19	1.5494E-19	1.5494E-19	1.5504E-19	1.5504E-19	1.5504E-19
β_{BR} (l/g.min)	1.2E-05	1.046E-05	1.6676E-05	1.5536E-05	4.32E-05	8.91E-06	1.908E-05

$\varepsilon_p(g^{-1})$	7.7449 E+13	6. 7510E+13	1.0763E+14	1.6027E+14	2.7864E+14	5.7469E+13	1.2307E+14
$\tau_{1/2}$ (min)	4.03	4.62	2.90	3.11	1.12	5.42	2.53
(-r)	$6.0E\text{-}06N_t^2$	$5.23E\text{-}06N_t^2$	$8.338E\text{-}06N_t^2$	$7.768E\text{-}06N_t^2$	$2.16E\text{-}05N_t^2$	$4.455E\text{-}06N_t^2$	$9.54E\text{-}06N_t^2$
N_o(g/l)	772.2008	747.3842	733.4067	758.5527	484.8955	828.0202	858.3691

Table 4.6: Coag-flocculation kinetic parameters and linear regression coefficient of SSC in PIE at varying dosage and pH of 5.

Parameters	0.1g/l	0.2g/l	0.3g/l	0.4g/l	0.5g/l	0.6g/l	0.7g/l
Y	6.0E-06 X+1.306E-03	2.76E-05 X+1.183E-03	3. 925E -06 X+1.2133E-03	1.266E-06 X+1.1552E-03	1.22E-05 X+9.234E-04	4.763E-06 X+9.223E-04	7.57E-06 X+7.32E-04
α	2.000	2.000	2.000	2.000	2.000	2.000	2.000
R^2	0.664	0.678	0.865	0.586	0.962	0.945	0.952
K(l/g.min)	6.0E-06	2.76E-05	3.925E-06	1.266E-05	1.22E-05	4. 763E-06	7.57E-06
K_R(l/min)	1.5862E-19	1.5862E-19	1.5867E-19	1.5867E-19	1.5867E-19	1.5872E-19	1.5872E-19
β_{BR}(l/g.min)	1.2E-05	5.55E-05	7.85E-06	2.532E-05	2.44E-05	9.526E-06	1.514E-05
ε_p (g^{-1})	7.5653 E+13	3.4800E+14	4.9474E+13	1.5958E+13	1.5378E+14	6.0018E+13	9.5388E+13
$\tau_{1/2}$ (min)	3.02	0.66	4.62	1.43	1.48	3.80	2.39
(-r)	$6.0E\text{-}06N_t^2$	$2.76E\text{-}05N_t^2$	$3.925E\text{-}06N_t^2$	$1.266E\text{-}05N_t^2$	$1.22E\text{-}05N_t^2$	$4.763E\text{-}06N_t^2$	$7.57E\text{-}06N_t^2$
N_o(g/l)	765.6968	845.3085	824.1985	865.6510	1082.9543	1084.2459	1366.1202

Table 4.7: Coag-flocculation kinetic parameters and linear regression coefficient of SSC in PIE at varying dosage and pH of 7.

Parameters	0.1g/l	0.2g/l	0.3g/l	0.4g/l	0.5g/l	0.6g/l	0.7g/l
Y	7.8E-05 X+2.741E-03	8.44E-05 X+1.985E-03	7. 978E -05 X+1.957E-03	6.172E-05 X+8.82E-04	7.15E-05 X+1.0454E-03	6.604E-05 X+1.0194E-04	9.61E-05 X+1.064E-03
α	2.000	2.000	2.000	2.000	2.000	2.000	2.000
R^2	0.970	0 .829	0.934	0.971	0.953	0.919	0.963
K(l/g.min)	7.8E-06	8.44E-05	7.978E-05	6.172E-05	7.15E-05	6.604E -06	9.61E -06
K_R(l/min)	1.5392E-19	1.5392E-19	1.5417E-19	1.5417E-19	1.5417E-19	1.5417E-19	1.5417E-19
β_{BR}(l/g.min)	1.56E-04	1.688E-04	1.5956E-04	1.2344E-04	1.59E-04	1.3208E-04	1.938E-04
$\varepsilon_p(g^{-1})$	1.0135E+15	1.0967E+15	1.0350E+15	8.0067E+14	1.0313E+15	8.5672E+14	1.2571E+15
$\tau_{1/2}$ (min)	0.31	0.29	0.30	0.39	0.30	0.37	0.25
(-r)	$7.8E\text{-}06N_t^2$	$8.44E\text{-}05N_t^2$	$7.978E\text{-}05N_t^2$	$6.172E\text{-}05N_t^2$	$7.95E\text{-}05N_t^2$	$6.604E\text{-}05N_t^2$	$9.69E\text{-}05N_t^2$
N_o(g/l)	364.8304	503.7783	510.8818	1133.7868	956.5716	914.0768	939.8496

Table 4.8: Coag-flocculation kinetic parameters and linear regression coefficient of SSC in PIE at varying dosage and pH of 10.

Parameters	0.1g/l	0.2g/l	0.3g/l	0.4g/l	0.5g/l	0.6g/l	0.7g/l
Y	9.1E-05 X+2.204E-03	7.07E-05 X+1.677E-03	4. 44E -05 X+1.7116E-03	4.599E-05 X+1.1886E-04	6. 59E-05 X+1.2385E-03	4.840E-05 X+1.0162E-04	9.43E-05 X+1.148E-03
α	2.000	2.000	2.000	2.000	2.000	2.000	2.000
R^2	0.830	0 .806	0.844	0.831	0.876	0.871	0.909
K(l/g.min)	9.1E-05	7.07E-05	4.443E-05	43.599E-05	6.59E-05	4.840E -05	9.43E -05
K_R(l/min)	1.5545E-19	1.5545E-19	1.5545E-19	1.5371E-19	1.5371E-19	1.5371E-19	1.5371E-19
β_{BR}(l/g.min)	1.82E-04	1.414E-04	8.886E-05	9.198E-05	1.318E-04	9.68E-05	1.886E-04
$\varepsilon_p(g^{-1})$	1.1708E+15	9.0962E+14	5.7163E+14	5.9071E+14	8.4644E+14	6.2167E+14	1.2112E+15
$\tau_{1/2}$ (min)	0.27	0.34	0.54	0.53	0.37	0.50	0.26
(-r)	$9.1E\text{-}05N_t^2$	$7.07E\text{-}05N_t^2$	$4.443E\text{-}05N_t^2$	$4.599E\text{-}05N_t^2$	$6.59E\text{-}05N_t^2$	$4.840E\text{-}05N_t^2$	$9.43E\text{-}05N_t^2$
N_o(g/l)	453.7205	596.3029	584.2487	841.3259	807.4283	984.0583	871.0801

Table 4.9: Coag-flocculation kinetic parameters and linear regression coefficient of SSC in PIE at varying dosage and pH of 13.

Parameters	0.1g/l	0.2g/l	0.3g/l	0.4g/l	0.5g/l	0.6g/l	0.7g/l
Y	7.1E-05	9.90E-05	5.073E -05	3.339E-05	3. 83E-05	1.7360E-05	9.38E-05
	X+2.523E-03	X+2.017E-03	X+1.6026E-03	X+1.0009E-04	X+1.2157E-03	X+8.612E-04	X+6.94E-03
α	2.000	2.000	2.000	2.000	2.000	2.000	2.000
R^2	0.517	0 .693	0.628	0.790	0.745	0.793	0.730
K(l/g.min)	7.1E-05	9.90E-05	5.073E -05	3.339E-05	3. 83E-05	1.7360E-05	9.38E-05
K_R(l/min)	1.5596E-19	1.5596E-19	1.5596E-19	1.5622E-19	1.5622E-19	1.5622E-19	1.56471E-19
β_{BR}(l/g.min)	1.42E-04	1.98E-04	1.0146E-04	6.678E-05	7.66E-05	3.472E-05	1.876E-05
$\varepsilon_p(g^{-1})$	9.1049E+15	1.2696E+15	6.5055E+14	4.2747E+14	4.9033E+14	2.2225E+14	1.1990E+15
$\tau_{1/2}$ (min)	0.56	0.18	0.36	0.54	0.47	1.04	1.93
(-r)	7.1E-05N_t^2	9.90E-05 N_t^2	5.073E -05N_t^2	3.339E-05N_t^2	3. 83E-05N_t^2	1.7360E-05N_t^2	9.38E-05N_t^2
N_o(g/l)	396.3535	495.7858	623.9860	999.1008	822.5714	1161.1605	1440.9222

Table 4.10: Coag-flocculation kinetic parameters and linear regression coefficient of COSC in PIE at varying dosage and pH of 1.

Parameters	0.1g/l	0.2g/l	0.3g/l	0.4g/l	0.5g/l	0.6g/l	0.7g/l
Y	1.0E-05	7.34E-06	8.837E -06	1.095E-05	2.03E-05	1.150E-05	8.08E-06
	X+1.1454E-03	X+1.172E-03	X+1.2224E-03	X+1.0735E-03	X+9.458E-04	X+1.1055E-03	X+8.6E-04
α	2.000	2.000	2.000	2.000	2.000	2.000	2.000
R^2	0.655	0 .917	0.703	0.924	0.861	0.817	0.859
K(l/g.min)	1.0E-05	7.34E-06	8.837E -06	1.095E-05	2.03E-05	1.150E-05	8.08E-06
K_R(l/min)	1.5468E-19	1.5468E-19	1.5468E-19	1.5479E-19	1.5479E-19	1.5484E-19	1.5484E-19
β_{BR}(l/g.min)	2.0E-05	1.468E-05	1.7674E-05	2.19E-05	4.06E-05	2.3E-05	1.616E-05
$\varepsilon_p(g^{-1})$	1.2930E+14	9.4906E+13	1.1426E+14	1.4148E+14	2.6229E+14	1.4854E+14	1.0437E+14
$\tau_{1/2}$ (min)	2.42	3.29	2.73	2.21	1.18	2.10	2.99
(-r)	1.0E-05N_t^2	7.34E -06N_t^2	8.837E -06N_t^2	1.095E -05N_t^2	2.03E -05N_t^2	1.150E -05N_t^2	8.08E -06N_t^2
N_o(g/l)	873.0574	853.2423	818.0628	931.5324	1057.3060	904.56807	1162.7907

Table 4.11 Coag-flocculation kinetic parameters and linear regression coefficient of COSC in PIE at varying dosage and pH of 3.

Parameters	0.1g/l	0.2g/l	0.3g/l	0.4g/l	0.5g/l	0.6g/l	0.7g/l
Y	1.2E-05	7.49E-06	2.145E -05	8.287E-06	9.86E-06	1.030E-05	8.29E-06
	X+1.027E-03	X+9.46E-04	X+8.787E-04	X+8.639E-04	X+7.206E-04	X+7.309E-04	X+7.99E-04
α	2.000	2.000	2.000	2.000	2.000	2.000	2.000
R^2	0.932	0 .722	0.976	0.839	0.847	0.931	0.800
K(l/g.min)	1.2E-05	7.49E-06	2.145E -05	8.287E-06	9.86E-06	1.03E-05	8.29E-06
K_R(l/min)	1.5443E-19	1.5443E-19	1.5443E-19	1.5448E-19	1.5448E-19	1.5448E-19	1.5448E-19
β_{BR}(l/g.min)	2.4E-05	1.498E-05	4.29E-05	1.6574E-05	1.972E-05	2.06E-05	1.658E-05
$\varepsilon_p(g^{-1})$	1.5541E+14	9.70002E+13	2.7780E+14	1.0729E+14	1.2765E+14	1.3335E+14	1.0733E+14
$\tau_{1/2}$ (min)	1.51	2.42	0.84	2.19	1.84	1.76	2.19
(-r)	1.2E-05N_t^2	7.49E -06N_t^2	2.145E -05N_t^2	8.287E -06N_t^2	9.86E -06N_t^2	1.030E -05N_t^2	8.29E -06N_t^2
N_o(g/l)	973.7098	1057.0825	1138.0448	1157.5414	1368.1762	1203.5143	1251.5645

Table 4.12: Coag-flocculation kinetic parameters and linear regression coefficient of COSC in PIE at varying dosage and pH of 5.

Parameters	0.1g/l	0.2g/l	0.3g/l	0.4g/l	0.5g/l	0.6g/l	0.7g/l
Y	6E-06	5.83E-06	7.437E -05	9.751E-06	1.26E-05	9.7E-06	1.4E-05
	X+1.606E-03	X+1.093E-03	X+1.0464E-03	X+1.0764E-03	X+1.0839E-03	X+9.588E-04	X+8.88E-04
α	2.000	2.000	2.000	2.000	2.000	2.000	2.000
R^2	0.851	0 .844	0.689	0.919	0.871	0.806	0.850

K(l/g.min)	6E-06	5.83E-06	7.437E -05	9.751E-06	1.26E-05	9.7E-06	1.4E-05
K_R(l/min)	1.5750E-19	1.5750E-19	1.5775E-19	1.5775E-19	1.5775E-19	1.5775E-19	1.5801E-19
β_{BR}(l/g.min)	1.2E-05	1.166E-05	1.4874E-05	1.9502E-05	2.52E-05	1.94E-05	2.80E-05
$\varepsilon_p(g^{-1})$	7.6190E+13	7.4032E+13	9.4288E+13	1.2363E+14	1.5975E+14	1.2298E+14	1.7720E+14
$\tau_{1/2}$ (min)	4.03	4.14	3.25	2.48	1.92	2.49	1.73
(-r)	6E-06N_t^2	5.83E -06N_t^2	7.437E -06N_t^2	9.751E -06N_t^2	1.26E -06N_t^2	9.7E -06N_t^2	1.4E -05N_t^2
N_o(g/l)	622.6650	914.9131	955.6575	929.0227	929.5943	1042.9704	1126.1261

Table 4.13: Coag-flocculation kinetic parameters and linear regression coefficient of COSC in PIE at varying dosage and pH of 7.

Parameters	0.1g/l	0.2g/l	0.3g/l	0.4g/l	0.5g/l	0.6g/l	0.7g/l
Y	4.0E-05	4.43E-05	5.155E -05	3.305E-05	3.38E-05	6.322E-05	3.39E-05
	X+3.148E-03	X+1.989E-03	X+2.2514E-03	X+1.6962E-03	X+1.2257 E-03	X+9.113E-04	X+1.352E-04
α	2.000	2.000	2.000	2.000	2.000	2.000	2.000
R^2	0.836	0 .847	0.762	0.828	0.823	0.860	0.757
K(l/g.min)	4.0E-05	4.43E-05	5.155E -05	3.305E-05	3.38E-05	6.322E-05	3.39E-05
K_R(l/min)	1.5417E-19	1.5417E-19	1.5417E-19	1.5417E-19	1.5443E-19	1.5443E-19	1.5443E-19
β_{BR}(l/g.min)	8.0E-05	8.86E-05	5.155E-05	6.61E-05	6.76E-05	1.2644E-05	6.78E-05
$\varepsilon_p(g^{-1})$	5.1891E+14	5.7469E+14	3.343E+14	4.2875E+14	4.3774E+14	8.1875E+14	4.3903E+14
$\tau_{1/2}$ (min)	0.60	0.55	0.47	0.73	0.71	0.38	0.71
(-r)	4.0E-05N_t^2	4.43E -05N_t^2	5.155E -05N_t^2	3.305E -05N_t^2	3.38E -05N_t^2	6.322E -05N_t^2	3.39E -05N_t^2
N_o(g/l)	317.6620	502.7652	444.1681	589.5531	815.8603	1097.3335	739.6450

Table 4.14: Coag-flocculation kinetic parameters and linear regression coefficient of COSC in PIE at varying dosage and pH of 10.

Parameters	0.1g/l	0.2g/l	0.3g/l	0.4g/l	0.5g/l	0.6g/l	0.7g/l
Y	4.4E-05	4.02E-05	5.741 E -06	1.822E-05	1.60E-05	1.163E-05	2.90E-05
	X+3.569E-03	X+2.272E-03	X+1.0302E-03	X+1.074E-03	X+9.823E-04	X+7.145E-04	X+7.63E-04
α	2.000	2.000	2.000	2.000	2.000	2.000	2.000
R^2	0.743	0 .827	0.848	0.866	0.840	0.922	0.967
K(l/g.min)	4.4E-05	4.02E-05	5.741 E -06	1.822E-05	1.60E-05	1.163E-05	2.90E-05
K_R(l/min)	1.5622E-19	1.5647E-19	1.5647E-19	1.5647E-19	1.5647E-19	1.5647E-19	1.5647E-19
β_{BR}(l/g.min)	8.8E-05	8.04E-05	1.1482E-05	3.644E-05	3.2E-05	2.326E-05	5.8E-05
$\varepsilon_p(g^{-1})$	5.6331E+14	5.1384E+14	7.3381E+13	2.3281E+13	2.0417E+14	1.4841E+14	3.7006E+14
$\tau_{1/2}$ (min)	0.60	0.55	0.47	0.73	0.71	0.38	0.71
(-r)	4.4E-05N_t^2	4.02E -05N_t^2	5.741E -05N_t^2	1.822E -05N_t^2	1.60E -05N_t^2	1.163E -05N_t^2	2.90E -05N_t^2
N_o(g/l)	280.1905	440.1408	970.6853	931.0987	1081.0189	1399.5801	1310.6160

Table 4.15: Coag-flocculation kinetic parameters and linear regression coefficient of COSC in PIE at varying dosage and pH of 13.

Parameters	0.1g/l	0.2g/l	0.3g/l	0.4g/l	0.5g/l	0.6g/l	0.7g/l
Y	2.7E-05	1.35E-05	1.050E -05	9.089E-06	1.71E-06	4.518E-05	1.10E-05
	X+1.437E-03	X+1.318E-03	X+1.0694E-03	X+9.324E-04	X+8.425E-04	X+7.546E-04	X+1.59E-04
α	2.000	2.000	2.000	2.000	2.000	2.000	2.000
R^2	0.490	0 .324	0.579	0.621	0.626	0.881	0.904
K(l/g.min)	2.7E-05	1.35E-05	1.050E -05	9.089E-06	1.71E-06	4.518E-05	1.10E-05
K_R(l/min)	1.5647E-19	1.5647E-19	1.5647E-19	1.5673E-19	1.5673E-19	1.5673E-19	1.5673E-19
β_{BR}(l/g.min)	5.4E-05	2.7E-05	2.1E-05	1.8178E-05	3.42E-06	9.036E-06	2.20E-06
$\varepsilon_p(g^{-1})$	3.4511E+14	1.7256E+14	1.3421E+14	1.1598E+14	2.1821E+13	5.7653E+13	1.4037E+13
$\tau_{1/2}$ (min)	0.67	1.34	1.73	1.99	10.61	4.01	1.65
(-r)	2.7E-05N_t^2	1.35E -05N_t^2	1.050E -05N_t^2	9.089E -06N_t^2	1.71E -06N_t^2	4.518E -06N_t^2	1.10E -06N_t^2
N_o(g/l)	695.8942	758.7253	935.1038	10721.5011	1186.0189	1325.2054	1317.5231

Table 4.16: Coag-flocculation kinetic parameters and linear regression coefficient of TOSC in PIE at varying dosage and pH of 1.

Parameters	0.1g/l	0.2g/l	0.3g/l	0.4g/l	0.5g/l	0.6g/l	0.7g/l
Y	1.4E-06	1.28E-05	1.149E -05	4.253E-05	1. 00E-05	1.490E-05	2.02E-05
	X+1.423E-03	X+1.084E-03	X+7.276E-04	X+8.517 E-04	X+8.648E-04	X+8.648E-04	X+8.52E-04
α	2.000	2.000	2.000	2.000	2.000	2.000	2.000
R^2	0.870	0 .837	0.856	0.813	0.833	0.835	0.721
K(l/g.min)	1.4E-06	1.28E-05	1.149E -05	4.253E-05	1. 00E-05	1.490E-05	2.02E-05
K_R(l/min)	1.5484E-19	1.5484E-19	1.5494E-19	1.5494E-19	1.5494E-19	1.5494E-19	1.5499E-19
β_{BR}(l/g.min)	2.8E-06	2.56E-05	4.298E-05	8.506E-05	2.00E-05	2.98E-05	4.04E-05
$\varepsilon_P(g^{-1})$	1.8083E+13	1.6533 E+14	2.7740E+14	5.4899E+14	1.2908E+14	1.9233E+14	2.6066E+14
$\tau_{1/2}$ (min)	12.94	1.42	0.84	0.43	1.81	2.24	0.90
(-r)	$1.4E-06N_t^2$	$1.28E-05N_t^2$	$1.149E -05N_t^2$	$4.253E-05N_t^2$	$1.00E-05N_t^2$	$1.490E-05N_t^2$	$2.02E-05N_t^2$
N_o(g/l)	702.7407	922.5092	374.3815	1174.1223	1156.3367	1156.3367	1173.7089

able 4.17: Coag-flocculation kinetic parameters and linear regression coefficient of TOSC in PIE at varying dosage and pH of 3.

Parameters	0.1g/l	0.2g/l	0.3g/l	0.4g/l	0.5g/l	0.6g/l	0.7g/l
Y	1.3E-05	9.92E-06	3.778E -06	9.959E-06	1. 11E-05	8.526E-06	7.26E-06
	X+1.091E-03	X+9.24E-04	X+8.259E-04	X+8.757E-04	X+6.381E-04	X+8.574E-04	X+5.76E-04
α	2.000	2.000	2.000	2.000	2.000	2.000	2.000
R^2	0.942	0 .750	0.663	0.706	0.826	0.938	0.864
K(l/g.min)	1.3E-05	9.92E-06	3.778E -06	9.959E-06	1.11E-05	8.526E-06	7.26E-06 K_R(l/min)
1.5474E-19	1.5474E-19	1.5474E-19	1.5474E-19	1.5484E-19	1.5484E-19	1.5484E-19	
β_{BR}(l/g.min)	2.6E-05	1.984E-05	7.556E-06	1.9918E-05	2.22E-05	1.7052E-05	1.452E-05
$\varepsilon_P(g^{-1})$	1.6802E+14	1.2822E+14	4.8830E+13	1.2872E+14	1.4337E+14	1.1013E+14	9.3774E+13
$\tau_{1/2}$ (min)	1.17	1.53	4.01	1.52	1.37	1.78	2.09
(-r)	$1.3E-05N_t^2$	$9.92E-06N_t^2$	$3.778E -06N_t^2$	$9.959E-06N_t^2$	$1.11E-06N_t^2$	$8.526E-06N_t^2$	$7.26E-06N_t^2$
N_o(g/l)	916.5903	1082.2511	1210.8003	1141.9436	1567.1525	1166.3168	1736.1111

Table 4.18: Coag-flocculation kinetic parameters and linear regression coefficient of TOSC in PIE at varying dosage and pH of 5.

Parameters	0.1g/l	0.2g/l	0.3g/l	0.4g/l	0.5g/l	0.6g/l	0.7g/l
Y	8E-06	1.01E-05	1.487E -05	1.012E-05	9. 281E-06	8.227E-06	6.42E-06
	X+1.339E-03	X+1.302E-03	X+1.2262E-03	X+9.774E-04	X+1.1762E-03	X+7.036E-04	X+5.05E-04
α	2.000	2.000	2.000	2.000	2.000	2.000	2.000
R^2	0.747	0.8660	0.838	0.776	0.537	0.830	0.753
K(l/g.min)	8E-06	1.01E-05	1.487E -05	1.012E-05	9. 281E-06	8.227E-06	6.42E-06
K_R(l/min)	1.5724E-19	1.5724E-19	1.5724E-19	1.5724E-19	1.5750E-19	1.5750E-19	1.5750E-19
β_{BR}(l/g.min)	1.6E-05	2.02E-05	2.974E-05	2.02E-05	1.856E-05	1.6454E-05	1.284E-05
$\varepsilon_p(g^{-1})$	1.0176E+14	1.2847E+14	1.8914E+13	1.2872E+14	1.1784E+14	1.0447E+14	8.1524E+13
$\tau_{1/2}$ (min)	1.74	1.38	0.93	1.37	1.50	1.69	2.16
(-r)	$8-06N_t^2$	$1.01E-05N_t^2$	$1.487E -05N_t^2$	$1.012E-05N_t^2$	$9.28E-06N_t^2$	$8.227E-06N_t^2$	$6.42E-06N_t^2$
N_o(g/l)	746.8260	768.04916	815.5276	1023.1226	850.1955	1421.2621	1980.1980

Table 4.19: Coag-flocculation kinetic parameters and linear regression coefficient of TOSC in PIE at varying dosage and pH of 7.

Parameter	0.1g/l	0.2g/l	0.3g/l	0.4g/l	0.5g/l	0.6g/l	0.7g/l
Y	7.1E-05	3.02E-05	8.033E -05	4.224E-05	9. 67E-06	5.5327E-05	5.15E-05
	X+3.064E-03	X+2.0372E-03	X+1.2237E-03	X+1.5915E-04	X+8.918E-04	X+1.2753E-03	X+1.25E-03
α	2.000	2.000	2.000	2.000	2.000	2.000	2.000
R^2	0.873	0 .768	0.798	0.836	0.857	0.882	0.843

K(l/g.min)	7.1E-05	3.02E-05	8.033E -05	4.224E-05	9. 67E-06	5.5327E-05	5.15E-05
K_R(l/min)	1.5468E-19	1.5468E-19	1.5468E-19	1.5494E-19	1.5494E-19	1.5494E-19	1.5520E-19
β_{BR}(l/g.min)	1.42E-04	6.04E-05	1.6066E-04	8.448E-05	1.934E-05	1.1064E-04	1.03E-04
$\varepsilon_p(g^{-1})$	9.1802E+14	3.9048E+14	1.0387E+15	5.4524E+14	1.2482E+14	7.1408E+14	6.6366E+14
$\tau_{1/2}$ (min)	0.34	0.83	0.30	0.57	2.50	0.44	0.47
(-r)	$7.1E\text{-}05N_t^2$	$3.02E\text{-}05N_t^2$	$8.033E\text{ -}05N_t^2$	$4.224E\text{-}05N_t^2$	$9.67E\text{-}06N_t^2$	$5.5327E\text{-}05N_t^2$	$5.1E\text{-}06N_t^2$
N_o(g/l)	326.3708	490.9180	817.1938	628.3380	1121.3277	784.1292	800.000

Table 4.20: Coag-flocculation kinetic parameters and linear regression coefficient of TOSC in PIE at varying dosage and pH of 10.

Parameters	0.1g/l	0.2g/l	0.3g/l	0.4g/l	0.5g/l	0.6g/l	0.7g/l
Y	4.5E-05	2.52E-05	5.695E -05	2.101E-05	3.90E-05	1.635E-05	4.04E-05
	X+2.272E-03	X+1.654E-03	X+1.759E-03	X+1.1778E-03	X+1.6824E-03	X+1.1711E-03	X+1.094E-03
α	2.000	2.000	2.000	2.000	2.000	2.000	2.000
R^2	0.829	0 .586	0.832	0.769	0.682	0.702	0.848
K(l/g.min)	4.5E-05	2.52E-05	5.695E -05	2.101E-05	3.90E-05	1.635E-05	4.04E-05
K_R(l/min)	1.5571E-19	1.5571E-19	1.5571E-19	1.5596E-19	1.5596E-19	1.5596E-19	1.5622E-19
β_{BR}(l/g.min)	9.0E-05	5.04E-05	1.139E-04	4.202E-05	7.8E-05	3.27E-05	8.08E-05
$\varepsilon_p(g^{-1})$	5.7800E+14	3.236 8E+14	7.3149E+14	2.6943E+14	5.0013E+14	2.101E+14	5.1722E+14
$\tau_{1/2}$ (min)	0.54	0.96	0.42	1.15	0.62	1.48	0.60
(-r)	$4.5E\text{-}05N_t^2$	$2.52E\text{ -}05N_t^2$	$5.695E\text{ -}05N_t^2$	$2.101E\text{ -}05N_t^2$	$3.90E\text{ -}06N_t^2$	$1.635E\text{ -}05N_t^2$	$4.04E\text{ -}06N_t^2$
N_o(g/l)	440.1408	604.5949	568.5048	849.0406	594.3890	853.8980	914.0768

Table 4.21: Coag-flocculation kinetic parameters and linear regression coefficient of TOSC in PIE at varying dosage and pH of 13.

Parameters	0.1g/l	0.2g/l	0.3g/l	0.4g/l	0.5g/l	0.6g/l	0.7g/l
Y	7.5E-05	3.21E-05	7.701E -06	1.012E-05	3.50E-06	4.764E-06	4.46E-06
	X+2.177E-03	X+1.343E-03	X+9.253E-04	X+7.481E-04	X+8.385E-04	X+6.654E-04	X+6.75E-04
α	2.000	2.000	2.000	2.000	2.000	2.000	2.000
R^2	0.660	0.591	0.599	0.752	0.827	0.555	0.674
K(l/g.min)	7.5E-05	3.21E-05	7.701E -06	1.012E-05	3.50E-06	4.764E-06	4. 46E-06
K_R(l/min)	1.5826E-19	1.5826E-19	1.5826E-19	1.5826E-19	1.5826E-19	1.5826E-19	1.5826E-19
β_{BR}(l/g.min)	1.5E-04	6.42E-05	1.54E-04	2.024E-05	7.0E-06	9.528E-06	8.92E-06
$\varepsilon_p(g^{-1})$	9.4781E+14	4.0566E+14	9.74359E+13	1.2789E+14	4.4158E+13	6.0106E+13	5.6271E+13
$\tau_{1/2}$ (min)	0.21	0.50	2.09	1.59	4.60	3.38	3.61
(-r)	$7.5E\text{-}05N_t^2$	$3.21E\text{ -}05N_t^2$	$7.701E\text{ -}06N_t^2$	$1.012E\text{ -}05N_t^2$	$3.50E\text{ -}06N_t^2$	$4.764E\text{ -}06N_t^2$	$4.46E\text{ -}06N_t^2$
N_o(g/l)	459.3477	744.6016	1080.7306	133.7197	1192.6058	1502.855	1481.4815

Table 4.22:Coag-flocculation kinetic parameters and linear regression coefficient of PTSC in PIE at varying dosage and pH of 1.

Parameters	0.1g/l	0.2g/l	0.3g/l	0.4g/l	0.5g/l	0.6g/l	0.7g/l
Y	7.9E-05	7.44E-05	1.664E -05	2.532E-05	9.84E-05	7.486E-05	3.70E-05
	X+2.414E-03	X+3.057E-03	X+9.815E-04	X+7.044E-04	X+3.694E-03	X+2.6494E-03	X+1.282E-03
α	2.000	2.000	2.000	2.000	2.000	2.000	2.000
R^2	0.754	0 .708	0.965	0.907	0.495	0.663	0.851
K(l/g.min)	7.9E-05	7.44E-05	1.664E -05	2.532E-05	9.84E-05	7.486E-05	3. 70E-05
K_R(l/min)	1.5468E-19	1.5468E-19	1.5468E-19	1.5468E-19	1.5468E-19	1.5520E-19	1.5520E-19
β_{BR}(l/g.min)	1.58E-04	1.488E-04	3.328E-05	5.064E-05	1.968E-04	1.4972E-04	7.4E-05
$\varepsilon_p(g^{-1})$	1.0215E+15	9.6199E+15	2.1479E+14	3.2684E+14	1.2702E+15	9.6469E+15	4.7680E+14
$\tau_{1/2}$ (min)	0.19	0.20	0.91	0.60	0.15	0.20	0.41
(-r)	$7.8E\text{-}05N_t^2$	$7.44E\text{ -}05N_t^2$	$1.664E\text{ -}05N_t^2$	$2.532E\text{ -}05N_t^2$	$9.84E\text{ -}05N_t^2$	$7.486E\text{ -}05N_t^2$	$3.70E\text{ -}05N_t^2$
N_o(g/l)	414.2502	327.1181	1018.8487	1419.6479	270.6506	377.4439	780.0312

Table 4.23: Coag-flocculation kinetic parameters and linear regression coefficient of PTSC in PIE at varying dosage and pH of 3.

Parameters	0.1g/l	0.2g/l	0.3g/l	0.4g/l	0.5g/l	0.6g/l	0.7g/l
Y	1.6E-05	9.94E-05	9.82E -06	9.834E-06	1.13E-05	1.238E-05	1.40E-05
	X+1.138E-03	X+2.27E-04	X+9.901E-04	X+1.0617E-03	X+9.258E-04	X+8.258E-04	X+1.19E-04
α	2.000	2.000	2.000	2.000	2.000	2.000	2.000
R^2	0.911	0.783	0.919	0.837	0.864	0.824	0.753
K(l/g.min)	1.6E-05	9.94E-05	9.-82E -06	9.834E-06	1.13E-05	1.238E-05	1.40E-05
K_R(l/min)	1.5443E-19	1.5443E-19	1.5443E-19	1.5468E-19	1.5468E-19	1.5468E-19	1.54680E-19
β_{BR}(l/g.min)	3.2E-05	1.988E-04	1.8164E-05	1.9668E-05	2.26E-05	2.476E-05	2.80E-05
$\varepsilon_p(g^{-1})$	2.0721E+14	1.2873E+15	1.1762E+14	1.2715E+14	1.4611E+14	1.6007E+14	1.8102E+14
$\tau_{1/2}$ (min)	1.13	0.18	19.95	1.84	1.60	1.46	1.29
(-r)	$1.6E-05N_t^2$	$9.94E-05N_t^2$	$9.082E-05N_t^2$	$9.834E-05N_t^2$	$1.13E-05N_t^2$	$1.238E-05N_t^2$	$1.40E-05N_t^2$
N_o(g/l)	878.7346	4405.2863	1009.9990	9418857	1090.8694	1210.9470	1221.0012

Table 4.24: Coag-flocculation kinetic parameters and linear regression coefficient of PTSC in PIE at varying dosage and pH of 5.

Parameters	0.1g/l	0.2g/l	0.3g/l	0.4g/l	0.5g/l	0.6g/l	0.7g/l
Y	6E-06	9.03E-06	1.002E -05	9.614E-06	1.26E-05	2.299E-05	1.22E-05
	X+1.273E-03	X+1.028E-03	X+9.966E-04	X+1.2027E-03	X+1.1358E-04	X+7.709E-04	X+7.84E-04
α	2.000	2.000	2.000	2.000	2.000	2.000	2.000
R^2	0.897	0 .877	0.790	0.869	0.842	0.943	0.859
K(l/g.min)	6E-06	9.03E-06	1.002E -05	9.614E-06	1.26E-05	2.299E-05	1.22E-05
K_R(l/min)	1.5801E-19	1.5801E-19	1.5801E-19	1.5801E-19	1.5826E-19	1.5826E-19	1.5852E-19
β_{BR}(l/g.min)	1.2E-05	1.806E-05	2.004E-05	1.9228E-05	2.52E-05	4.598E-05	2.44E-05
$\varepsilon_p(g^{-1})$	7.5945E+13	1.1430E+14	1.2683E+14	1.2169E+14	1.5923E+14	2.9053E+14	1.5392E+14
$\tau_{1/2}$ (min)	3.02	2.01	1.81	1.89	1.44	0.79	1.48
(-r)	$6E-06N_t^2$	$9.03E-05N_t^2$	$1.002E-05N_t^2$	$9.614E-06N_t^2$	$1.26E-05N_t^2$	$2.299E-05N_t^2$	$1.22E-05N_t^2$
N_o(g/l)	785.5460	972.7626	1003.4116	831.4625	880.4367	1297.1851	1275.5102

Table 4.25: Coag-flocculation kinetic parameters and linear regression coefficient of PTSC in PIE at varying dosage and pH of 7.

Parameters	0.1g/l	0.2g/l	0.3g/l	0.4g/l	0.5g/l	0.6g/l	0.7g/l
Y	3.3E-05	4.42E-05	5.298E -05	4.205E-06	3.18E-05	4.362E-05	3.23E-05
	X+1.766E-03	X+1.54E-03	X+1.429E-03	X+1.94567E-03	X+1.2541E-03	X+1.5058E-03	X+1.535E-03
α	2.000	2.000	2.000	2.000	2.000	2.000	2.000
R^2	0.946	0 .968	0.896	0.878	0.898	0.979	0.952
K(l/g.min)	3.3E-05	4.42E-05	5.298E -05	4.205E-06	3.18E-05	4.362E-05	3.23E-05
K_R(l/min)	1.5545E-19	1.5545E-19	1.5545E-19	1.5571E-19	1.5571E-19	1.5571E-19	1.5571E-19
β_{BR}(l/g.min)	6.6E-05	8.84E-05	1.0596E-05	8.41E-05	6.36E-05	8.724E-05	6.46E-05
$\varepsilon_p(g^{-1})$	4.2457E+14	5.6867E+14	6.8163E+14	5.4011E+14	4.0845E+14	5.6027E+14	4.1487E+14
$\tau_{1/2}$ (min)	0.73	0.55	0.46	0.57	0.76	0.55	0.75
(-r)	$3.3E-05N_t^2$	$4.42E-05N_t^2$	$5.298E-05N_t^2$	$4.205E-06N_t^2$	$3.18E-05N_t^2$	$4.362E-05N_t^2$	$3.23E-05N_t^2$
N_o(g/l)	566.2514	649.3506	699.7901	513.9803	797.3846	664.0988	651.4658

Table 4.26: Coag-flocculation kinetic parameters and linear regression coefficient of PTSC in PIE at varying dosage and pH of 10.

Parameters	0.1g/l	0.2g/l	0.3g/l	0.4g/l	0.5g/l	0.6g/l	0.7g/l
Y	9.9E-05	8.99E-05	4.595E -05	8.263E-06	6.06E-05	2.878E-05	3.75E-05
	X+3.212E-03	X+2.875E-03	X+2.1916E-03	X+2.175E-03	X+1.8434E-03	X+1.393E-03	X+1.654E-03
α	2.000	2.000	2.000	2.000	2.000	2.000	2.000
R^2	0.763	0 .865	0.859	0.824	0.811	0.842	0.634

K(l/g.min)	9.9E-05	8.99E-05	4.595E -05	8.263E-06	6.06E-05	2.878E-05	3.75E-05
K_R(l/min)	1.5622E-19	1.5647E-19	1.5647E-19	1.5647E-19	1.5673E-19	1.5673E-19	1.5673E-19
β_{BR}(l/g.min)	1.98E-04	1.798E-04	9.19E-05	1.6526E-04	1.212E-05	5.756E-05	7.5E-05
$\varepsilon_p(g^{-1})$	1.2674E+15	1.1491E+15	5.8733E+14	1.0562E+15	7.7330E+14	3.6726E+14	4.7853E+14
$\tau_{1/2}$ (min)	0.24	0.27	0.53	0.29	0.40	0.84	0.64
(-r)	$9.9E-05N_t^2$	$8.99E-05N_t^2$	$4.595E-05N_t^2$	$8.263E-06N_t^2$	$6.06E-05N_t^2$	$2.878E-05N_t^2$	$3.75E-05N_t^2$
N_o(g/l)	311.3325	347.8261	456.2876	459.7701	542.47591	717.8751	604.5949

Table 4.27: Coag-flocculation kinetic parameters and linear regression coefficient of PTSC in PIE at varying dosage and pH of 13.

Parameters	0.1g/l	0.2g/l	0.3g/l	0.4g/l	0.5g/l	0.6g/l	0.7g/l
Y	1.46E-04	2.04E-04	2.491E -04	2.005E-04	1.51E-04	1.959E-05	2.03E-04
	X+1.46E-03	X+1.175E-03	X+2.4337E-03	X+3.2039E-03	X+3.3286E-03	X+1.9558E-03	X+1.961E-03
α	2.000	2.000	2.000	2.000	2.000	2.000	2.000
R^2	0.945	0 .967	0.877	0.762	0.608	0.639	0.780
K(l/g.min)	1.46E-04	2.04E-04	2.491E -04	2.005E-04	1.51E-04	1.959E-05	2.03E-04
K_R(l/min)	1.5801E-19	1.5801E-19	1.5801E-19	1.5826E-19	1.5826E-19	1.5826E-19	1.5826E-19
β_{BR}(l/g.min)	2.92E-04	4.08E-04	4.982E-04	4.01E-04	3.02E-04	3.918E-04	4.06E-04
$\varepsilon_p(g^{-1})$	18480E+15	2.5821E+15	3.1530E+15	2.5378E+15	1.9083E+15	2.4757E+15	2.5654E+15
$\tau_{1/2}$ (min)	0.12	0.09	0.07	0.09	0.12	0.09	0.09
(-r)	$1.46E-04N_t^2$	$2.04E-4N_t^2$	$2.491E-04N_t^2$	$2.005E-04N_t^2$	$1.51E-04N_t^2$	$1.959E-04N_t^2$	$2.03E-04N_t^2$
N_o(g/l)	684.9315	851.0638	697.4960	32.1196	300.4266	511.2997	509.9439

Table 4.28:Coag-flocculation kinetic parameters and linear regression coefficient of MPSC in PIE at varying dosage and pH of 1.

Parameters	0.1g/l	0.2g/l	0.3g/l	0.4g/l	0.5g/l	0.6g/l	0.7g/l
Y	3.1E-05	1.320E-05	1.882E -05	1.685E-05	1. 58E-05	1.399E-05	2.261E-05
	X+1.701 E-03	X+1.381E-03	X+1.4474E-03	X+1.1625E-04	X+1.0748E-03	X+9.399E-04	X+9.48E-03
α	2.000	2.000	2.000	2.000	2.000	2.000	2.000
R^2	0.954	0 .889	0.829	0.918	0.779	0.881	0.839
K(l/g.min)	3.1E-05	1.320E-05	1.882E -05	1.685E-05	1. 58E-05	1.399E-05	2.261E-05
K_R(l/min)	1.5417E-19	1.5417E-19	1.4613E-19	1.4613E-19	1.4613E-19	1.4638E-19	1.4638E-19
β_{BR}(l/g.min)	6.2E-05	2.6E-05	3.764E-05	3.37E-05	3.16E-05	2.798E-05	4.52E-05
$\varepsilon_p(g^{-1})$	4.0215E+14	1.7124 E+14	2.5758E+14	2.302E+14	2.1625E+14	1.9115E+14	3.0879E+14
$\tau_{1/2}$ (min)	0.74	1.73	1.21	1.36	1.45	1.63	1.01
(-r)	$3.1E-05N_t^2$	$1.320E-05N_t^2$	$1.882E-05N_t^2$	$1.685E-05N_t^2$	$1. 58E-05N_t^2$	$1.399E-05N_t^2$	$2.261E-05N_t^2$
N_o(g/l)	587.8895	724.1130	690.8940	860.2151	930.4057	1063.9430	1054.8523

Table 4.29: Coag-flocculation kinetic parameters and linear regression coefficient of MPSC in PIE at varying dosage and pH of 3.

Parameters	0.1g/l	0.2g/l	0.3g/l	0.4g/l	0.5g/l	0.6g/l	0.7g/l
Y	1.1E-05	1. 05E-05	1.297E -05	1.104E-05	1. 12E-05	1.495E-05	1.08E-05
	X+9.43 E-04	X+9.15E-04	X+8.154E-04	X+6.567E-04	X+5.736E-04	X+5.736E-04	X+5.34E-04
α	2.000	2.000	2.000	2.000	2.000	2.000	2.000
R^2	0.960	0 .908	0.780	0.848	0.728	0.940	0.892
K(l/g.min)	1.1E-05	1. 05E-05	1.297E -05	1.104E-05	1. 12E-05	1.495E-05	1.08E-05
K_R(l/min)	1.5468E-19	1.5468E-19	1.5474E-19	1.5474E-19	1.5474E-19	1.5474E-19	1.5474E-19
β_{BR}(l/g.min)	2.2E-05	2.1E-05	2.594E-05	2.208E-05	2.24E-05	2.99E-05	2.16E-05
$\varepsilon_P(g^{-1})$	1.4223E+14	1.3576E+14	1.6764E+14	1.4269E+14	1.4476E+14	1.9323E+14	1.3959E+14
$\tau_{1/2}$ (min)	1.38	1.44	1.17	1.37	1.35	1.01	1.40
(-r)	$1.1E-05N_t^2$	$1. 05E-05N_t^2$	$1.297E-05N_t^2$	$1.104E-05N_t^2$	$1.12E-05N_t^2$	$1.495E-05N_t^2$	$1.08E-05N_t^2$
N_o(g/l)	1060.4454	1092.8962	1226.3920	1522.7653	1424.5014	1743.3752	1872.6592

Table 4.30: Coag-flocculation kinetic parameters and linear regression coefficient of MPSC in PIE at varying dosage and pH of 5.

Parameters	0.1g/l	0.2g/l	0.3g/l	0.4g/l	0.5g/l	0.6g/l	0.7g/l
Y	7E-06 X+1.228E-03	9.57E-06 X+1.157E-03	1.805E -05 X+9.154E-04	1.437E-05 X+7.913E-04	1.59E-05 X+6.7E-04	1.743E-05 X+7.216E-04	3.04E-05 X+4.174E-04
α	2.000	2.000	2.000	2.000	2.000	2.000	2.000
R^2	0.728	0 .592	0.742	0.859	0.906	0.838	0.754
K(l/g.min)	7E-06	9.57E-06	1.805E -05	1.437E-05	1. 59E-05	1.743E-05	3.04E-05
K_R(l/min)	1.5750E-19	1.5750E-19	1.5774E-19	1.5774E-19	1.5774E-19	1.5774E-19	1.5801E-19
β_{BR}(l/g.min)	1.4E-05	1.914E-05	3.61E-05	2.874E-05	3.18E-05	3.486E-05	6.08E-05
$\varepsilon_P(g^{-1})$	8.8889E+13	1.2152E+14	2.2884E+14	1.8219E+14	2.0158E+14	2.2098E+14	3.8479E+14
$\tau_{1/2}$ (min)	2.16	1.58	0.84	1.05	0.95	0.87	0.50
(-r)	$7E-06N_t^2$	$9.57E-06N_t^2$	$1.805E-05N_t^2$	$1.437E-05N_t^2$	$1.59E-05N_t^2$	$1.743E-05N_t^2$	$3.04E-05N_t^2$
N_o(g/l)	814.3322	864.3042	105.1083	1263.7432	1492.5373	1386.9626	2398.0815

Table 4.31: Coag-flocculation kinetic parameters and linear regression coefficient of MPSC in PIE at varying dosage and pH of 7.

Parameters	0.1g/l	0.2g/l	0.3g/l	0.4g/l	0.5g/l	0.6g/l	0.7g/l
Y	4.1E-06 X+2.688E-03	4. 04E-05 X+2.766E-03	2.726E -05 X+2.8525E-03	4.414E-05 X+1.0727E-03	5. 00E-05 X+1.0635E-03	5.957E-05 X+2.9E-03	3.76E-05 X+2.372E-03
α	2.000	2.000	2.000	2.000	2.000	2.000	2.000
R^2	0.856	0 .724	0.653	0.946	0.914	0.874	0.704
K(l/g.min)	4.1E-06	4. 04E-05	2.726E -05	4.414E-05	5. 00E-05	5.957E-05	3.76E-05
K_R(l/min)	1.5341E-19	1.5341E-19	1.5366E-19	1.5366E-19	1.5366E-19	1.5366E-19	1.5366E-19
β_{BR}(l/g.min)	8.2E-05	8.08E-05	5.452E-05	8.828E-05	1.0E-04	1.19146E-04	7.5366E-05
$\varepsilon_P(g^{-1})$	5.3452E+14	5.2669E+14	3.5481E+14	5.7452E+14	6.5079E+14	7.7535E+14	4.8939E+14
$\tau_{1/2}$ (min)	0.59	0.60	0.89	0.55	0.48	0.41	0.64
(-r)	$4.1E-06N_t^2$	$4. 04E-05N_t^2$	$2.726E -05N_t^2$	$4.414E-05N_t^2$	$5.00E-05N_t^2$	$5.957E-05N_t^2$	$3.76E-05N_t^2$
N_o(g/l)	372.0238	361.5390	350.5697	932.22711	940.2915	526.3158	728.863

Table 4.32: Coag-flocculation kinetic parameters and linear regression coefficient of MPSC in PIE at varying dosage and pH of 10.

Parameters	0.1g/l	0.2g/l	0.3g/l	0.4g/l	0.5g/l	0.6g/l	0.7g/l
Y	4.8E-05 X+1.978E-03	4. 46E-05 X+1.696E-03	2.910E -05 X+1.1365E-03	1. 493E-05 X+9.336E-04	1. 05E-05 X+9.571E-04	1.493E-05 X+9.36E-04	1.63E-05 X+9.96E-04
α	2.000	2.000	2.000	2.000	2.000	2.000	2.000
R^2	0.762	0 .853	0.874	0.890	0.873	0.826	0.740
K(l/g.min)	4.8E-05	4. 46E-05	2.910E -05	1. 493E-05	1. 05E-05	1.493E-05	1.63E-05
K_R(l/min)	1.5699E-19	1.5699E-19	1.5699E-19	1.5709E-19	1.5709E-19	1.5709E-19	1.5709E-19
β_{BR}(l/g.min)	9.6E-05	8.92E-05	3.82E-05	2.986E-05	4.1E-05	2.986E-04	3.26E-05
$\varepsilon_P(g^{-1})$	6.1150E+14	5.6819E+14	2.4333E+14	1.9008E+14	2.6100E+14	1.9008E+14	2.0752E+14
$\tau_{1/2}$ (min)	0.50	0.54	1.26	1.62	1.18	1.62	1.48
(-r)	$4.8E-05N_t^2$	$4. 46E-05N_t^2$	$2.910E -05N_t^2$	$1.493E-05N_t^2$	$1.05E-05N_t^2$	$1.493E-05N_t^2$	$1.63E-05N_t^2$
N_o(g/l)	505.5612	5891.6226	879.8944	1071.1225	1044.8229	1068. 3761	1004.0161

Table 4.33: Coag-flocculation kinetic parameters and linear regression coefficient of MPSC in PIE at varying dosage and pH of 13.

Parameters	0.1g/l	0.2g/l	0.3g/l	0.4g/l	0.5g/l	0.6g/l	0.7g/l
Y	2.18E-04 X+2.176E-03	1. 51E-04 X+2.267E-03	1.3540E -04 X+2.5965E-03	9. 215E-05 X+2.2123E-03	1. 20E-05 X+1.0726E-03	6.846E-05 X+2.2946E-03	8.92E-05 X+3.877E-03
α	2.000	2.000	2.000	2.000	2.000	2.000	2.000

R^2 `	0.925	0 .665	0.902	0.897	0.952	0.788	0.743
K(l/g.min)	2.18E-05	1. 51E-04	1.3540E -04	9. 215E-05	1.20E-05	6.846E-05	8.92E-05
K_R(l/min)	1.5724E-19	1.5724E-19	1.5724E-19	1.5734E-19	1.5734E-19	1.5734E-19	1.5734E-19
β_{BR}(l/g/.min)	4.36E-04	3.02E-04	2.708E-04	1.843E-04	2.4E-04	1.3692E-04	1.784E-04
$\varepsilon_P(g^{-1})$	2.7728E+15	1.9206E+15	1.7222E+15	1.1713E+15	1.5254E+15	8.7022E+14	1.1339E+14
$\tau_{1/2}$ (min)	0.33	0.48	0.54	0.79	0.60	1.06	0.81
(-r)	2.18E-05N_t^2	1.51E-04N_t^2	1.3540E -04N_t^2	9.215E-05N_t^2	1.20E-05N_t^2	6.846E-05N_t^2	8.92E-05N_t^2
N_o(g/l)	459.5588	441.1116	385.1338	452.0183	932.3140	435. 8058	257.9314

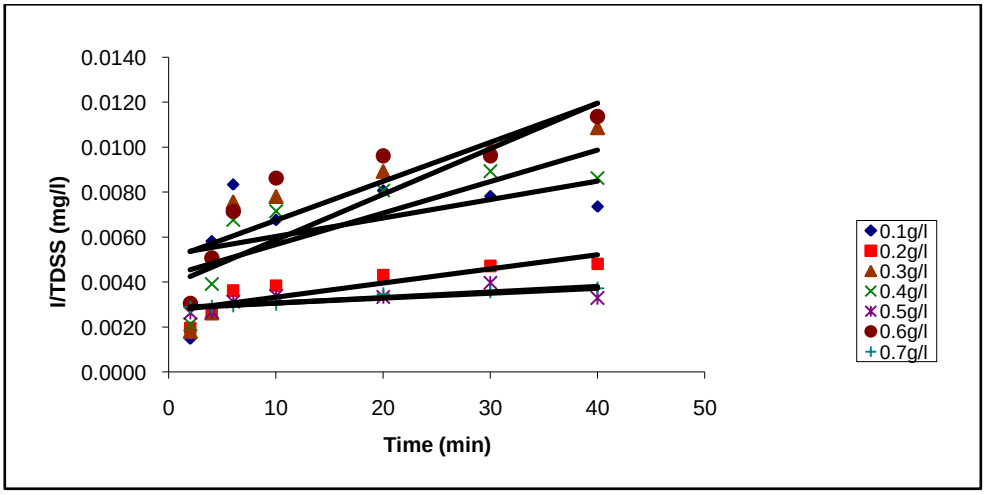

Fig.4.131: Kinetic plot of tdss removal using varying ssc dosages for PIE at pH 1

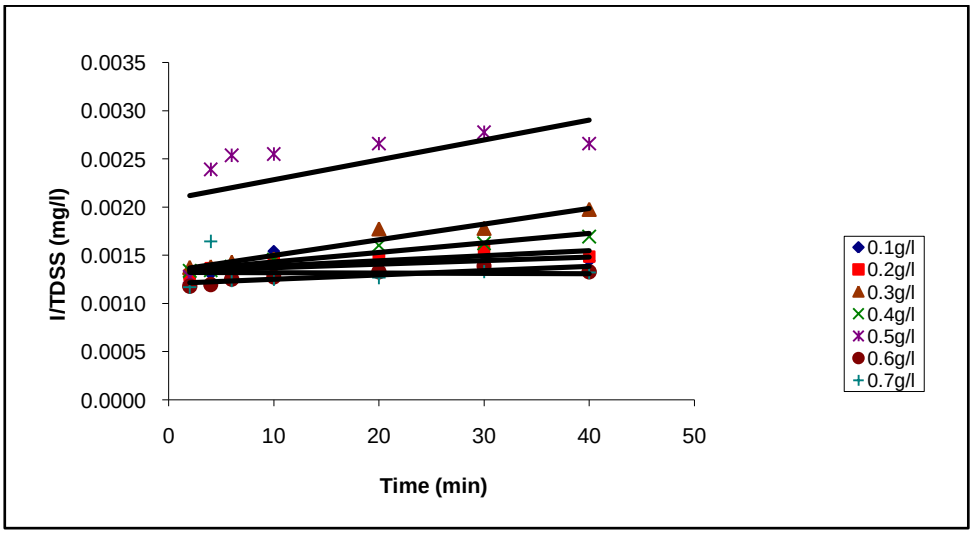

Fig.4.132: Kinetic plot of tdss removal using varying ssc dosages for PIE at pH 3

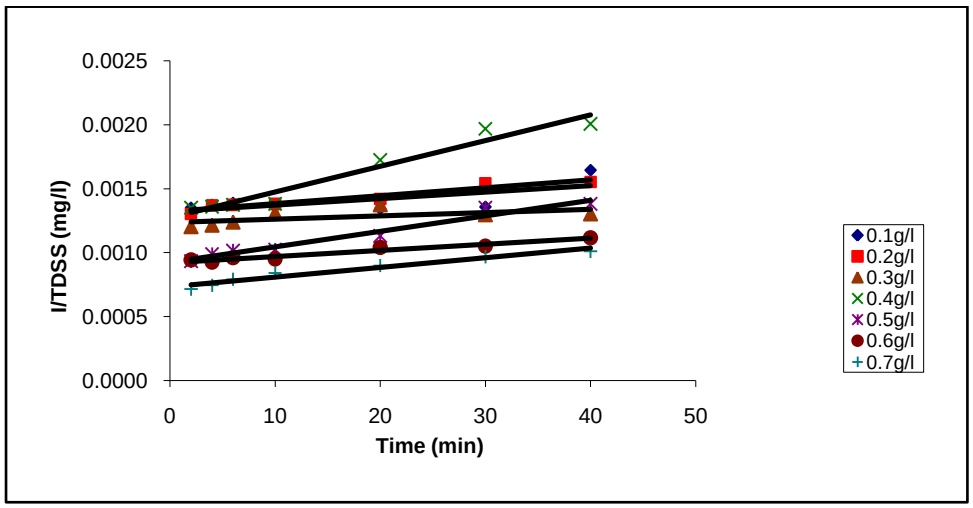

Fig.4.133: Kinetic plot of tdss removal using varying ssc dosages for PIE at pH 5

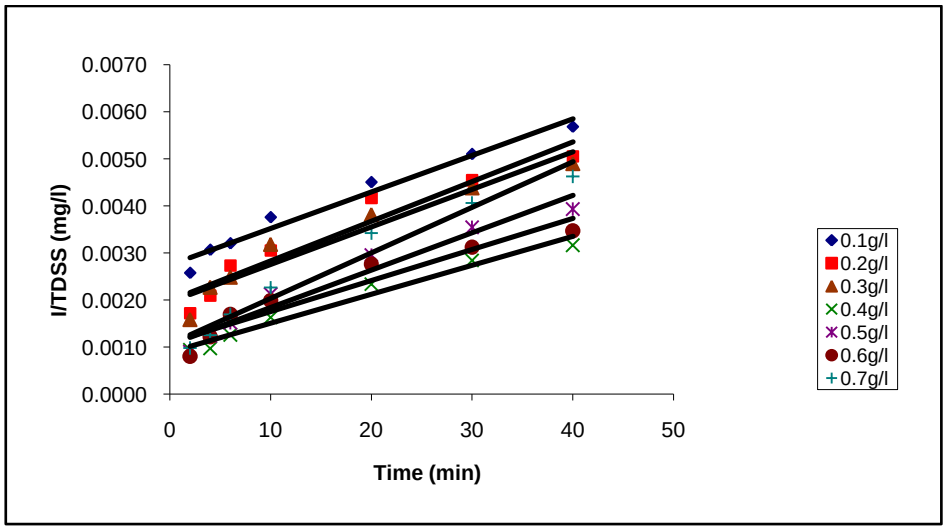

Fig.4.134: Kinetic plot of tdss removal using varying ssc dosages for PIE at pH 7

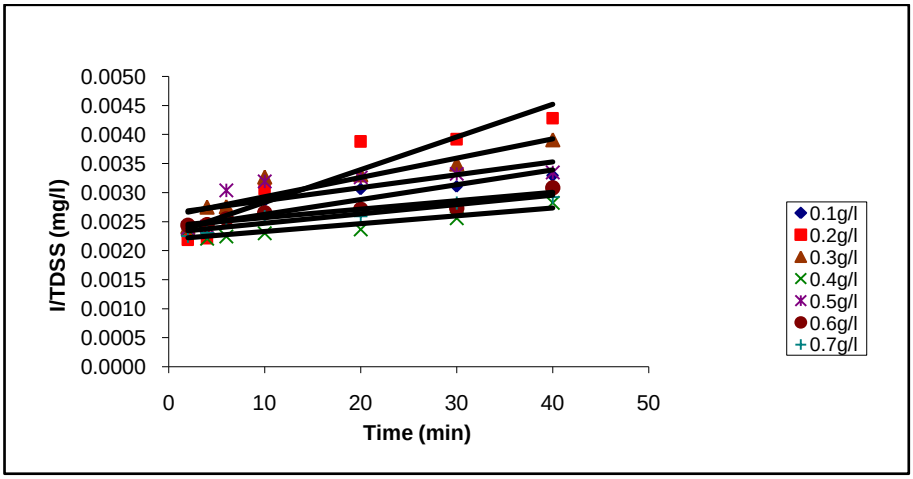

Fig.4.135: Kinetic plot of tdss removal using varying ssc dosages for PIE at pH 10

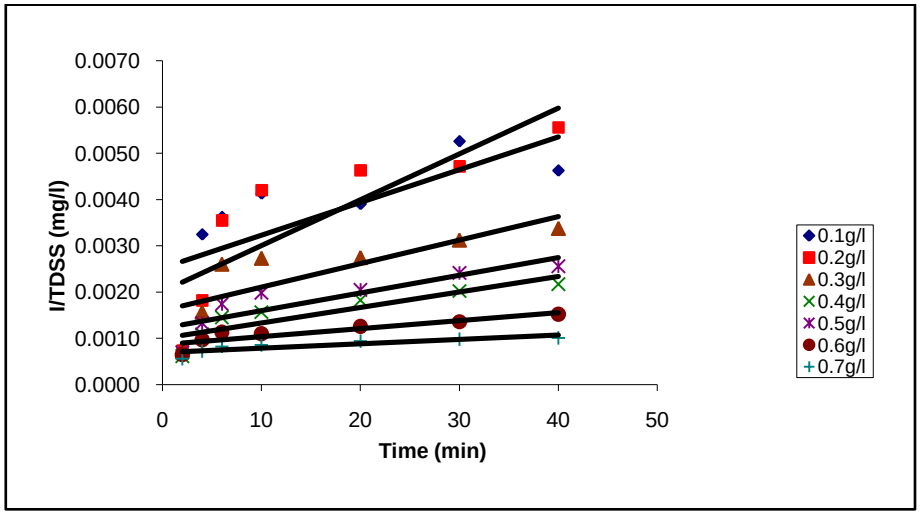

Fig.4.136: Kinetic plot of TDSS removal using varying SSC dosages for PIE at pH 13

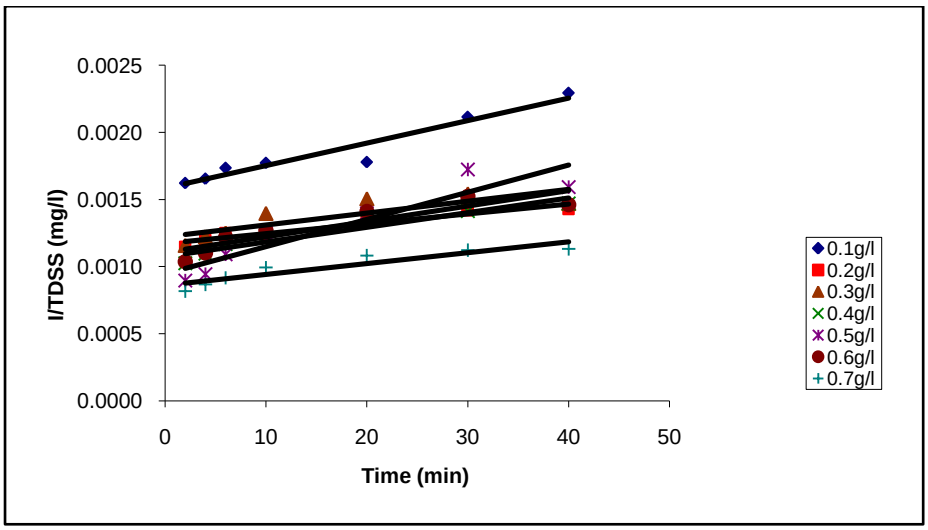

Fig.4.137: Kinetic plot TDSS removal using varying cosc dosages for PIE at pH 1

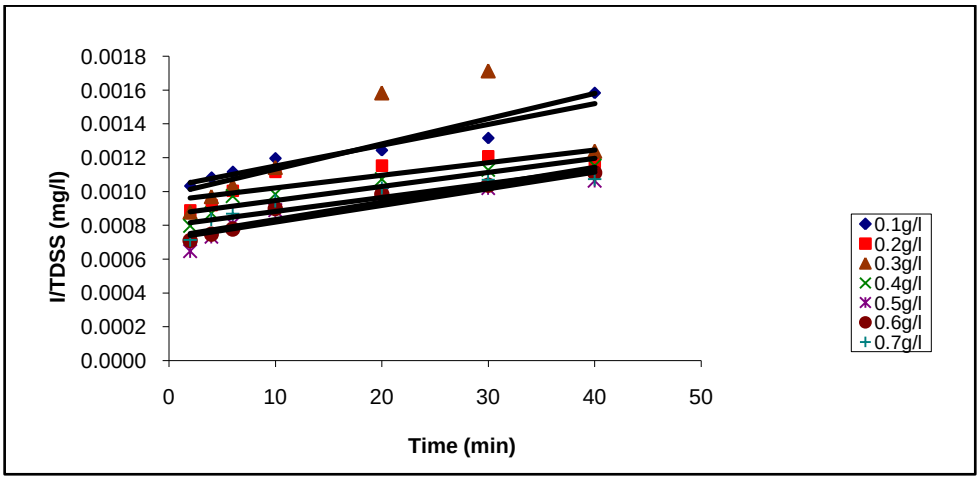

Fig.4.138: Kinetic plot TDSS removal using varying cosc dosages for PIE at pH 3

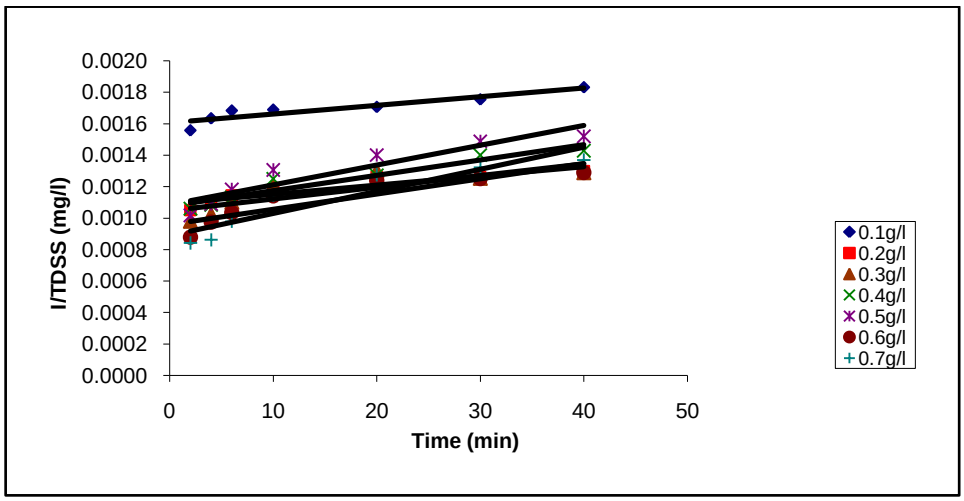

Fig.4.139: Kinetic plot TDSS removal using varying cosc dosages for PIE at pH 5

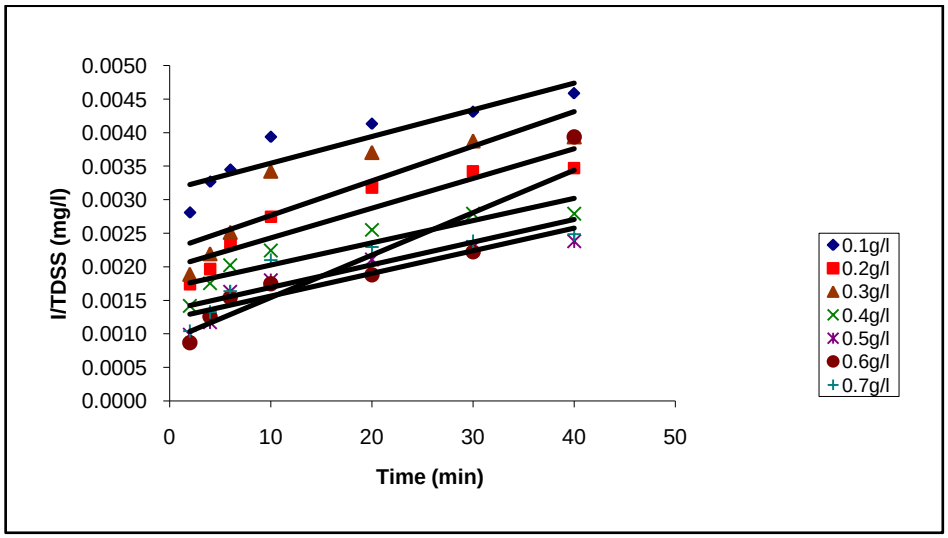

Fig.4.140: Kinetic plot TDSS removal using varying cosc dosages for PIE at pH 7

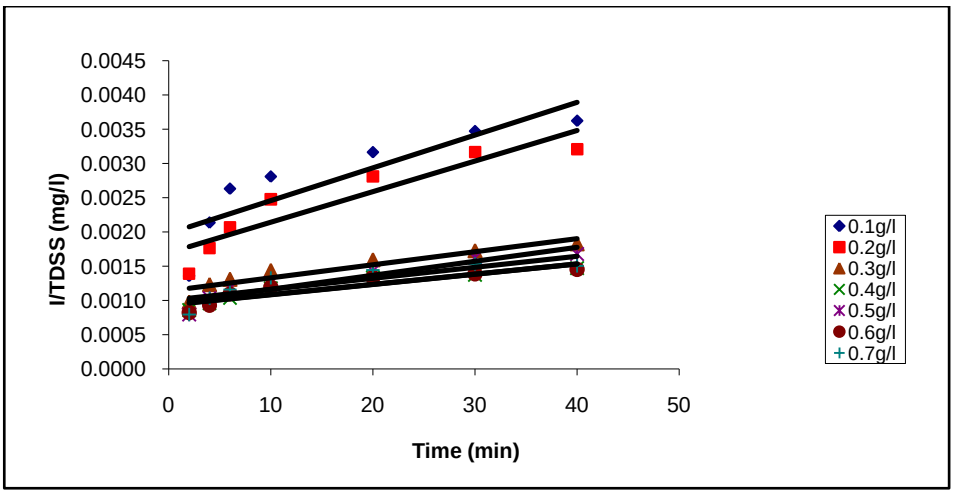

Fig.4.141: Kinetic plot TDSS removal using varying cosc dosages for PIE at pH 10

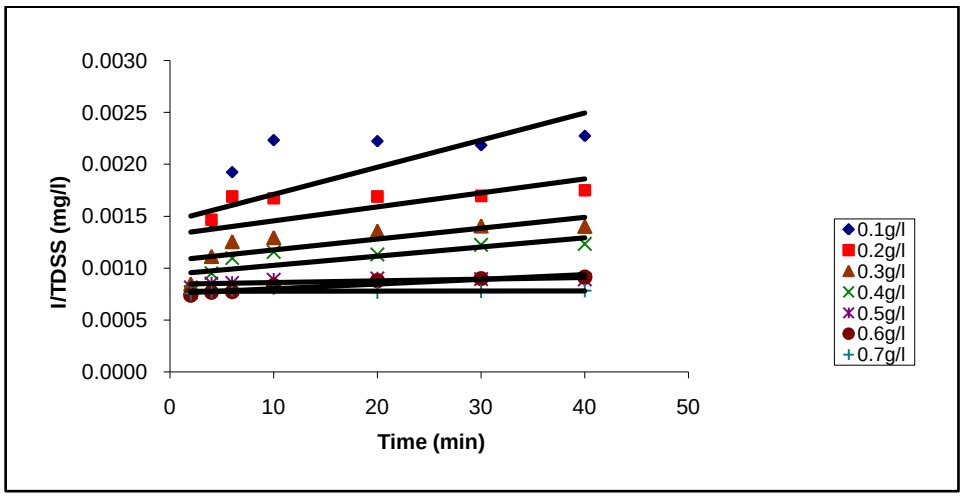

Fig.4.142: Kinetic plot TDSS removal using varying cosc dosages for PIE at pH 13

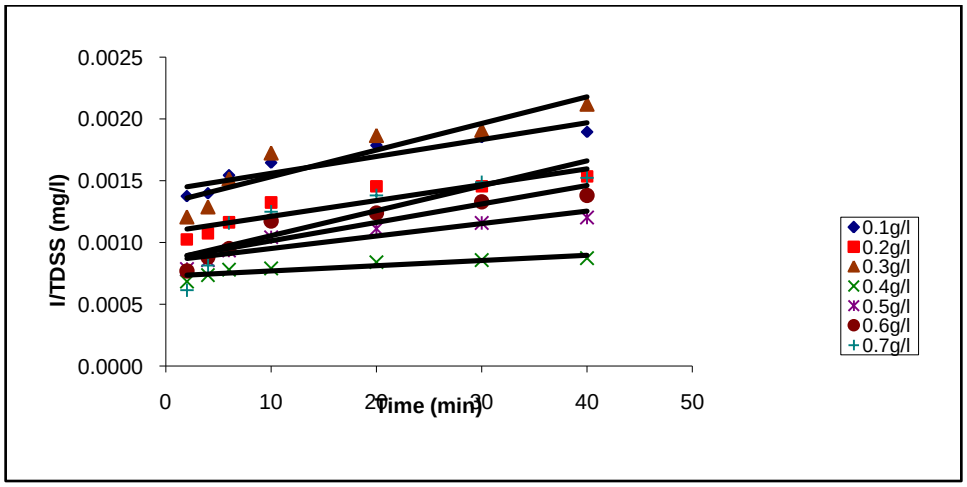

Fig.4.143: Kinetic plot TDSS removal using varying tosc dosages for PIE at pH 1

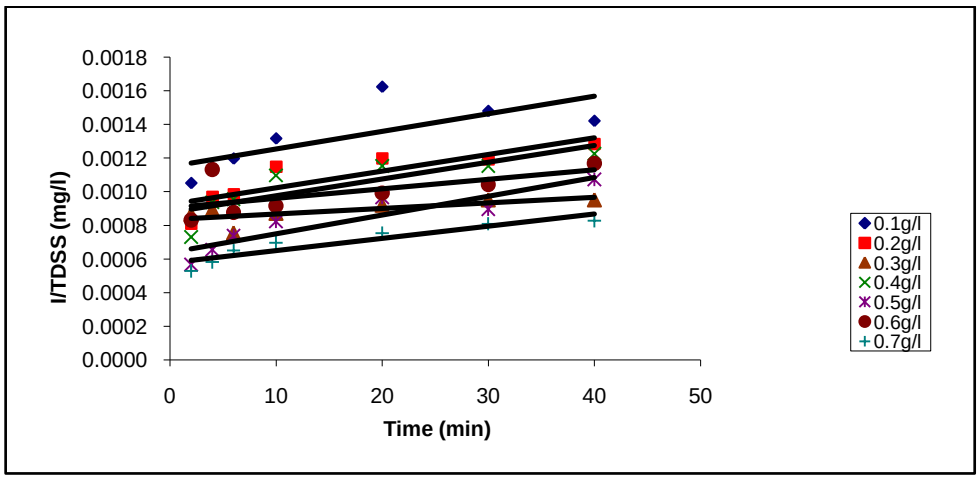

Fig.4.144: Kinetic plot TDSS removal using varying tosc dosages for PIE at pH 3

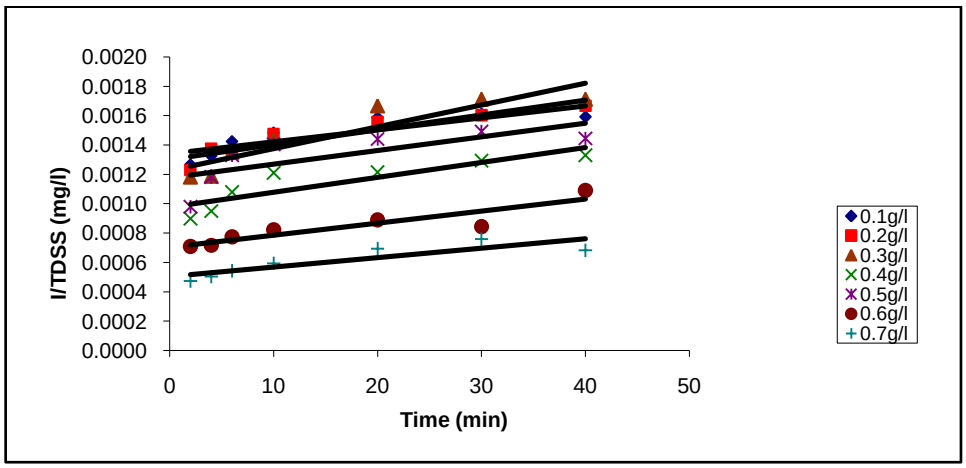

Fig.4.145: Kinetic plot TDSS removal using varying tosc dosages for PIE at pH 5

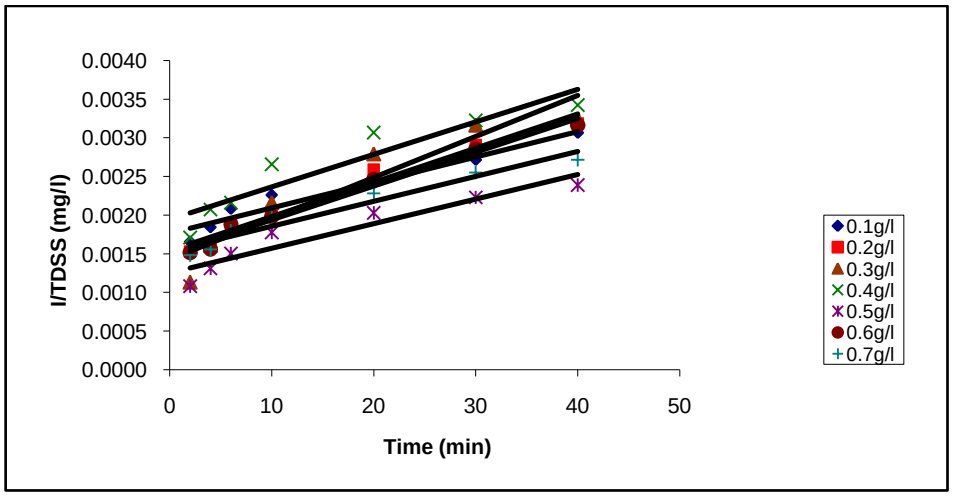

Fig.4.146: Kinetic plot TDSS removal using varying tosc dosages for PIE at pH 7

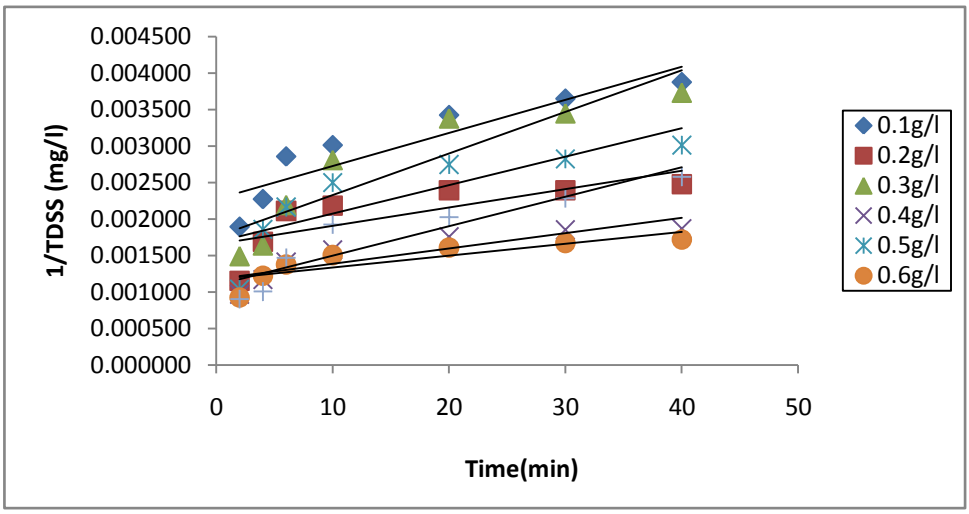

Fig.4.147: Kinetic plot TDSS removal using varying tosc dosages for PIE at pH 10

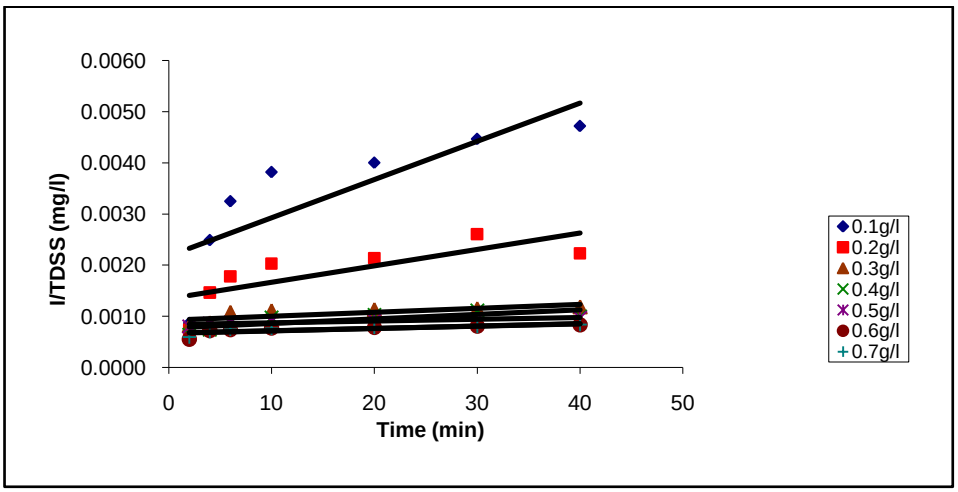

Fig.4.148: Kinetic plot TDSS removal using varying tosc dosages for PIE at pH 13

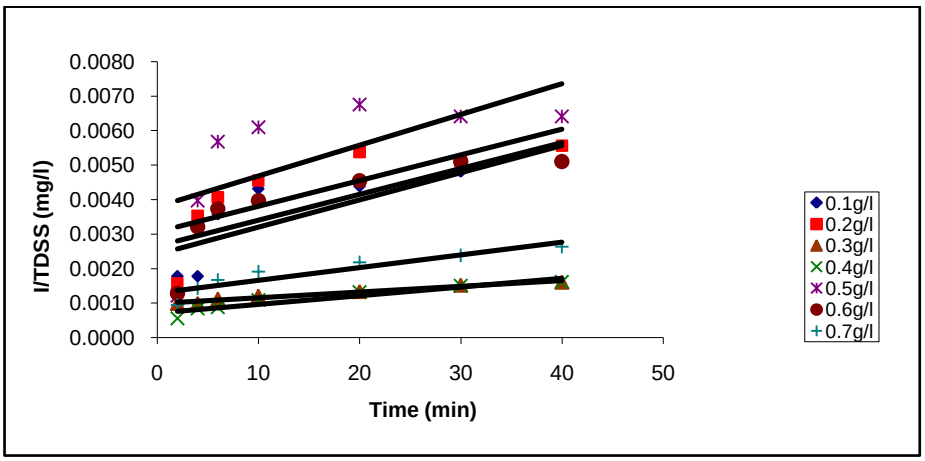

Fig. 4.149: Kinetic plot of TDSS removal using varying ptsc dosages for PIE at pH 1

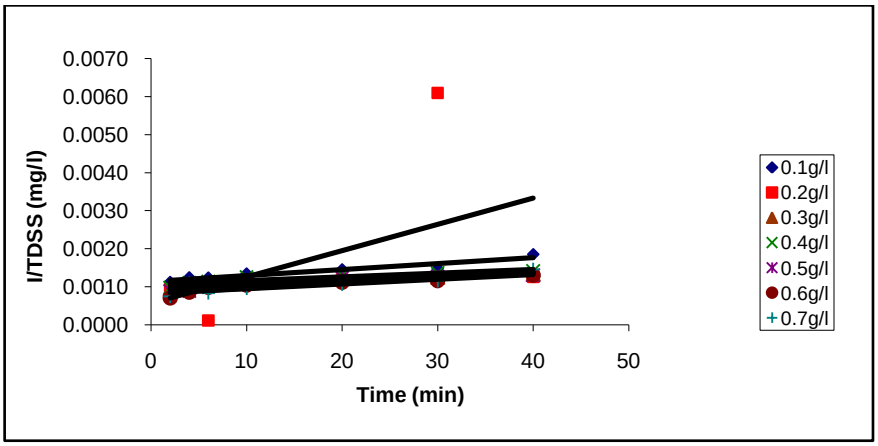

Fig. 4.150: Kinetic plot of TDSS removal using varying ptsc dosages for PIE at pH 3

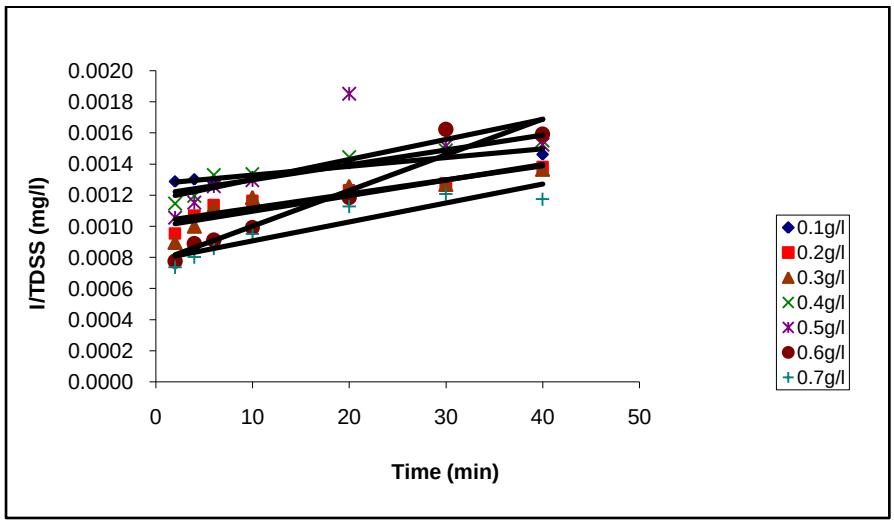

Fig. 4.151: Kinetic plot of TDSS removal using varying ptsc dosages for PIE at pH 5

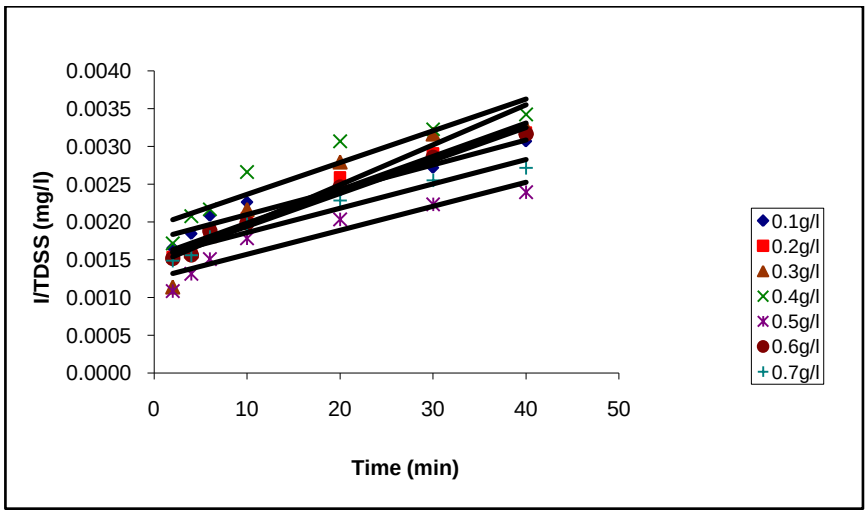

Fig. 4.152: Kinetic plot of TDSS removal using varying ptsc dosages for PIE at pH 7

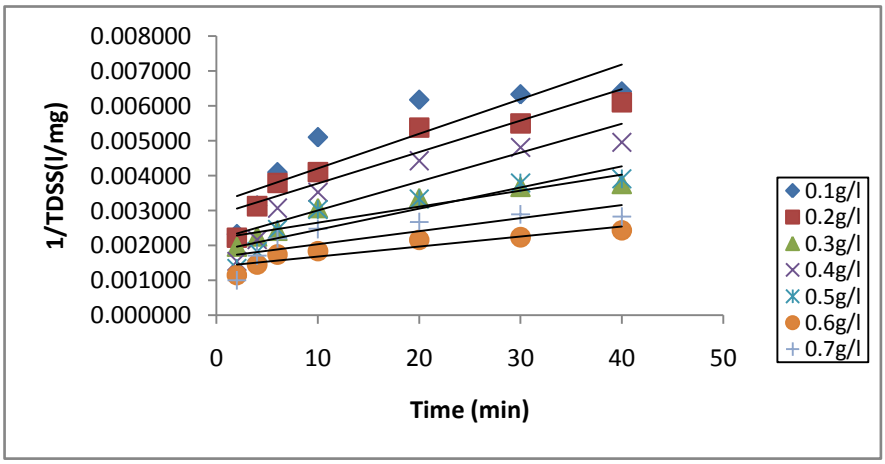

Fig. 4.153: Kinetic plot of TDSS removal using varying ptsc dosages for PIE at pH 10

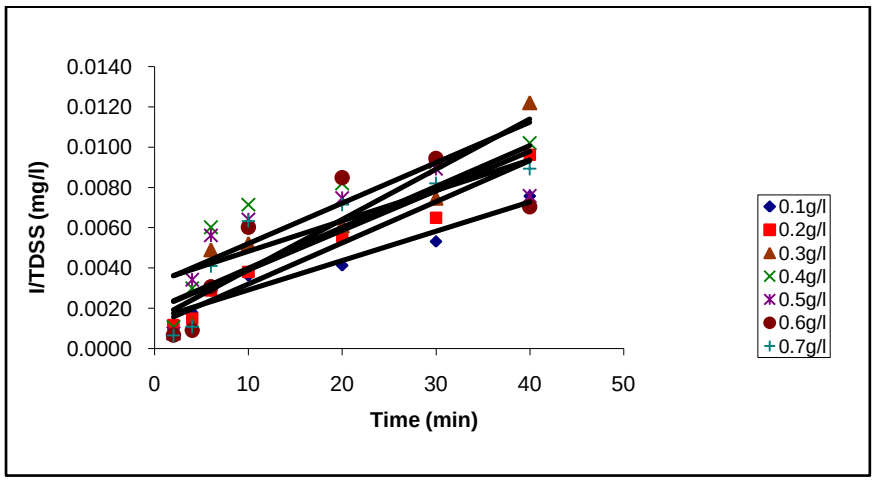

Fig. 4.154: Kinetic plot of TDSS removal using varying ptsc dosages for PIE at pH 13

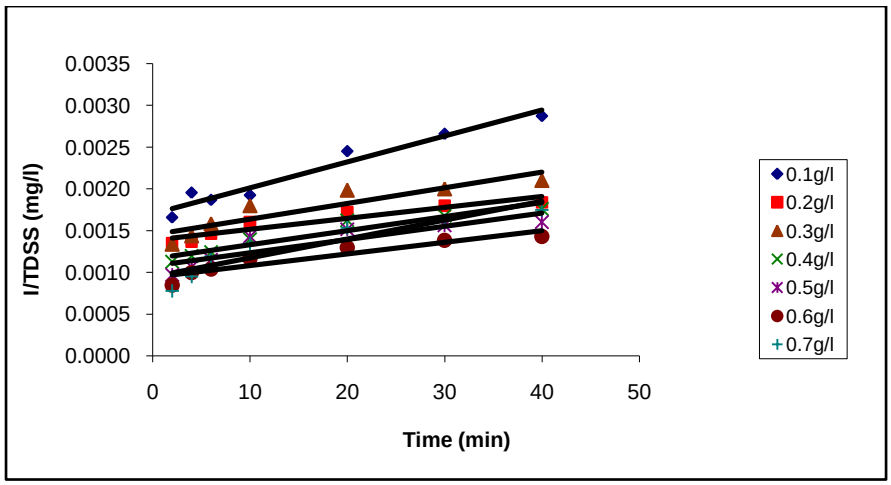

Fig. 4.155: Kinetic plot of TDSS removal using varying mpsc dosages for PIE at pH 1

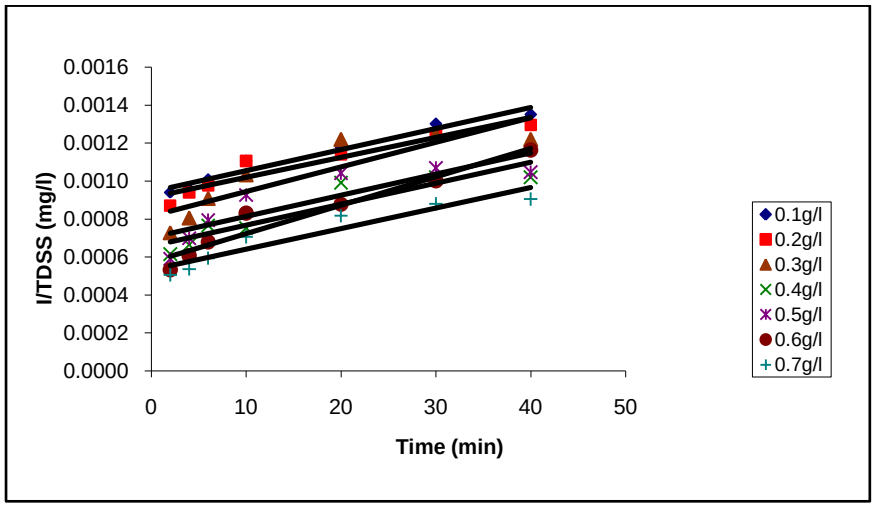

Fig. 4.156: Kinetic plot of TDSS removal using varying mpsc dosages for PIE at pH 3

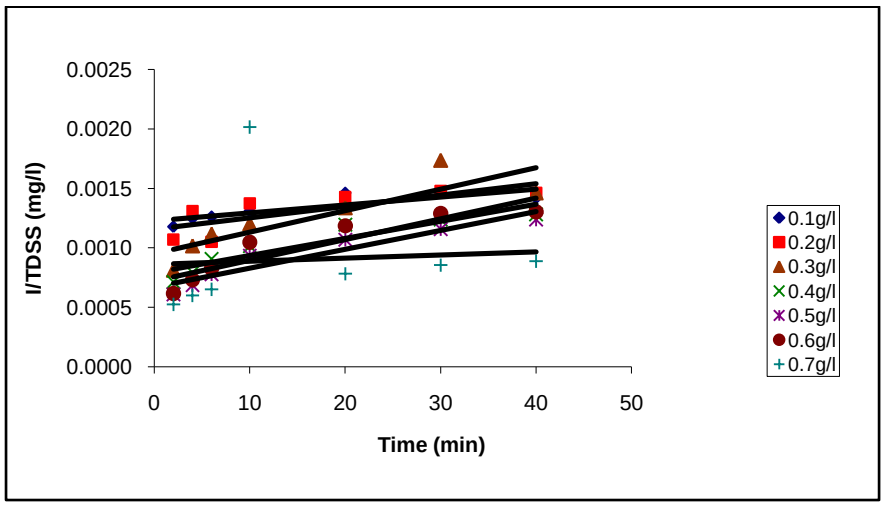

Fig. 4.157: Kinetic plot of TDSS removal using varying mpsc dosages for PIE at pH 5

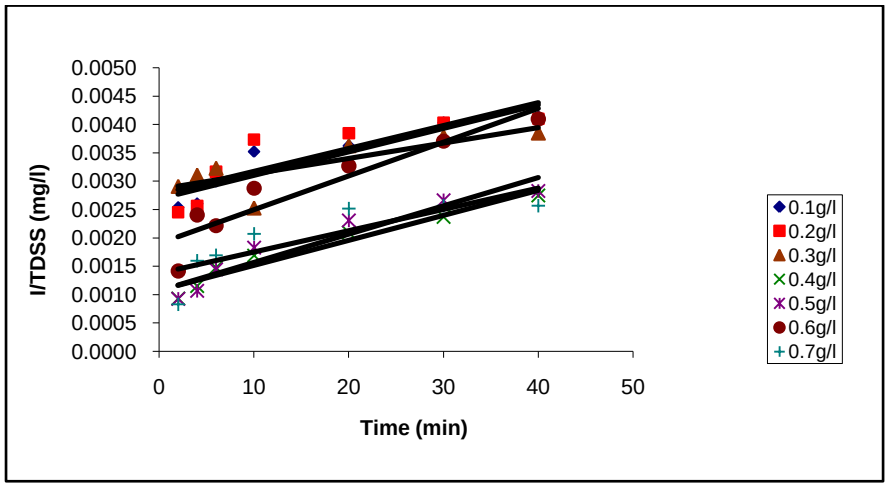

Fig.4.158: Kinetic plot of TDSS removal using varying mpsc dosages for PIE at pH 7

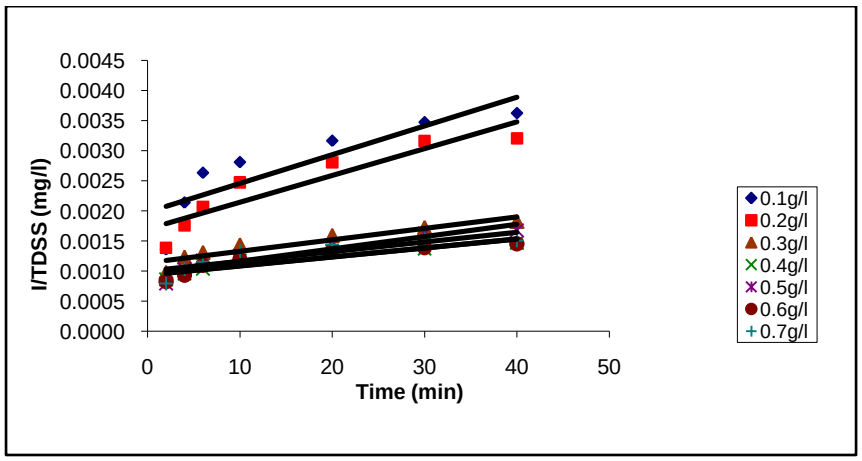

Fig. 4.159: Kinetic plot of TDSS removal using varying mpsc dosages for PIE at pH 10

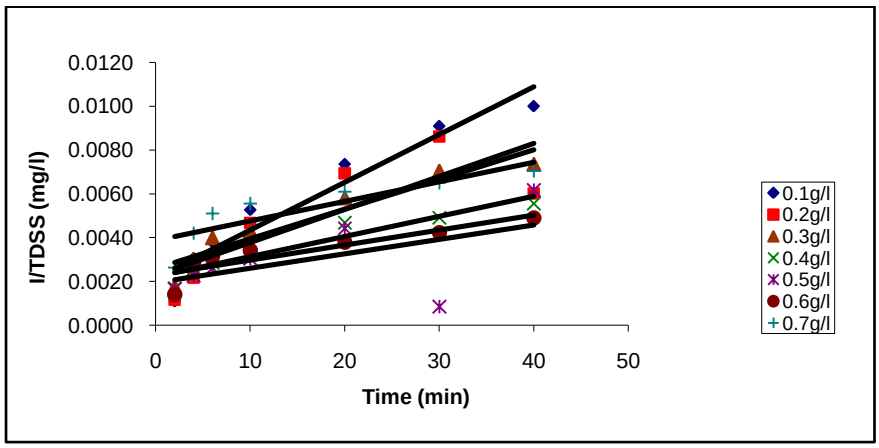

Fig. 4.160: Kinetic plot of TDSS removal using varying mpsc dosages for PIE at pH 13

4.1.3.3. Kinetic results of pH varying PIE at constant dosage

This section presents coag-flocculation kinetic results for SSC, COSC, TOSC, PTSC and MPSC for varying pH of the effluent at given coag-flocculant dosage. The results are presented in tables 4.33 to 4.67. Overview on the SSC results posted in tables 4.33 to 4.39, show that all the $\tau_{1/2}$ values recorded with corresponding relatively high K for different pH and dosages are capable of achieving maximum coag-flocculation. This is expected because majority of the $\tau_{1/2}$ values are within subminutes and also K having a link with the rate of particle aggregation and $\tau_{1/2}$. Consequent on this low $\tau_{1/2}$ values is a necessary condition for high K values for efficient operation. However, optimum performance is achieved for pH 1 and 0.3g/l dosage (K=2.033E-04l/g.min and $\tau_{1/2}$ =0.178min) followed by pH 13 and 0.2g/l dosage (k=9.90E-05l/g.min and $\tau_{1/2}$ =0.183min). The linear plots are displayed in fig 4.159 to 4.165. For COSC, it can be observed from tables 4.44 and 4.46 that $\tau_{1/2}$ of 10.594 min for pH of 13 and 0.5g/l dosage; $\tau_{1/2}$ of 16.469 min for pH of 13 and 0.7g/l dosage were obtained respectively. The implication is that strong alkaline media does not guarantee efficient performance of COSC at high dosage. Also at high $\tau_{1/2}$ values it cannot provide maximum condition for efficient operation in waste water treatment practice with the exception of these combinations: pH of 13 and 0.5g/l dosage ; pH of 13 and 0.7g/l dosage, optimum efficiency of COSC for the rest of the dosages and pH following also the fact that the highest $\tau_{1/2}$ of 4.207 min, is obtainable. In overall, there is insignificant variation in the values of K_R ε_p and β_{BR}, indicating minimal variation in the temperature.The linear plots are posted in figures 4.166 to 4.172.

Consider the functional parameters posted in tables 4.47 to 4.53 for TOSC. The least K is obtained at 0.1g/l dosage for pH of 1 with corresponding high $\tau_{1/2}$. The implication is that optimum condition for efficient performance of TOSC cannot be achieved. The TOSC performance could be optimum between pH of 7 and 13 for 0.1, 0.2 and 0.4g/l dosages. The majority of R^2 values are greater than 0.65, indicating that TOSC are relatively good as an aggregating agent in a coag-flocculation system for all pH and dosages considered. There is negligible variations in the values of K_R and $\varepsilon_{p,}$ indicating minimal fluctuation in temperature. Tables 4.54 to 4.60 present rate coag-flocculation parameters for PTSC. Observation from the tables show that pH of 13 for all dosages recorded least $\tau_{1/2}$ and high K values, implying that maximum performance can be achieved in pH of 13. The least value of K is recorded at 3.019min and 6.06E-06l/g.min at 0.1g/l dosage and pH of 5. The implication is that PTSC generally has high potency in water and waste water purifications, since the highest coag-flocculation period ($\tau_{1/2}$) obtained is within a single minute digit (3.019min). The linear plots are presented in figs.4.182 to 4.188.

In the case of MPSC, it should be observed that maximum coag-flocculation could be obtained at pH 7 for all the dosages considered, following the lowest $\tau_{1/2}$ value of less than 1min. though optimum performance of MPSC is recorded for pH 13 and 0.1g/l dosage. Looking on the kinetic tables for MPSC, it can be observed that the highest $\tau_{1/2}$ of 1.858min is still within good coag-flocculation operation limit, showing that the coag-flocculant is generally effective for all the pH and dosages studied. The corresponding linear rate plots are presented in figurese 4.189 to 4.195.

Table 4.34: Coag-flocculation kinetic parameters and linear regression coefficient of SSC in PIE at varying pH and 0.1g/l dosage.

Parameters	pH = 1	pH = 3	pH = 5	pH = 7	pH = 10	pH = 13
Y	1.12E-04X	6.0E-06X+	6.0E -06X+	7.8E-05X+	9.1E-05X+	7.1E-05X+
	+4.719E-03	1.295E-03	1.306E-03	2.741E-03	2.204E-03	2.523E-03
α	2.000	2.000	2.000	2.000	2.000	2.000
R^2	0.469	0.843	0.664	0.970	0.830	0.517
K(l/g.min)	1.12E-04	6.0E-0.6	6.0E-06	7.8E-05	9.1E-05	7.1E-05
K_R (l/min)	1.5289E-19	1.5494E-19	1.5862E-19	1.5392E-19	1.5545E-19	1.5596E-19
β_{BR}(l/g.min)	2.24E-04	1.2E-05	1.2E-05	1.56E-04	1.82E-04	1.42E-04
$\varepsilon_p(g^{-1})$	1.4651E+15	7.7449E+13	7.5653E+13	1.0135E+15	1.1708E+15	9.1049E+14
$\tau_{1/2}$ (min)	0.32	4.02	3.02	0.31	0.27	0.26
(-r)	$1.12E-04N_t^2$	$6.0E-06N_t^2$	$6.0E-06N_t^2$	$7.8E-05N_t^2$	$9.1E-05N_t^2$	$7.1E-05N_t^2$
N_o(g/l)	211.9093	772.2008	765.6968	364.8304	453.7205	396.3535

Table 4.35: Coag-flocculation kinetic parameters and linear regression coefficient of SSC in PIE at varying pH and 0.2g/l dosage.

Parameters	pH = 1	pH = 3	pH = 5	pH = 7	pH = 10	pH = 13
Y	6.29E-05X	5.23E-06X+	2.76E -05X+	8.44E-05X+	7.07E-05X+	9.90E-05X+
	+2.702E-03	1.338E-03	1.183E-03	1.957E-03	1.677E-03	2.017E-03
α	2.000	2.000	2.000	2.000	2.000	2.000
R^2	0.749	0.748	0.676	0.929	0.806	0.693
K(l/g.min)	6.29E-05	5.23E-06	2.76E-05	8.44E-05	7.07E-05	9.90E-05
K_R(l/min)	1.5315E-19	1.5494E-19	1.5862E-19	1.5392E-19	1.5545E-19	1.5596E-19
β_{BR}(l/g.min)	1.258E-04	1.046E-05	5.52E-05	1.688E-04	1.1414E-04	1.98E-04
$\varepsilon_p(g^{-1})$	8.2142E+1	6.7510E+13	3.4800E+13	1.0967E+15	9.0962E+14	1.2695E+15
$\tau_{1/2}$ (min)	0.58	4.62	0.66	0.29	0.34	0.18
(-r)	6.29E-05N_t^2	5.23E-06N_t^2	2.76E-06N_t^2	8.44E-05N_t^2	7.07E-05N_t^2	9.90E-05N_t^2
N_o(g/l)	370.0962	747.3842	845.3085	503.7783	596.3029	495.7858

Table 4.36: Coag-flocculation kinetic parameters and linear regression coefficient of SSC in PIE at varying pH and 0.3g/l dosage.

Parameters	pH = 1	pH = 3	pH = 5	pH = 7	pH = 10	pH = 13
Y	2.033E-04X	8.338E-06X+	3.925E -06X+	7.978E-05X+	4.443E-05X+	5.073E-05X+
	+3.8366E-03	1.3635E-03	+1.2133E-03	1.957E-03	1.7116E-03	1.6026E-03
α	2.000	2.000	2.000	2.000	2.000	2.000
R^2	0.940	0.850	0.865	0.931	0.844	0.628
K(l/g.min)	2.033E-04	8.338E-06	3.925E-06	7.978E-05	4.443E-05	5. 073E-05
K_R(l/min)	1.5315E-19	1.5494E-19	1.5867E-19	1.5417E-19	1.5545E-19	1.5596E-19
β_{BR}(l/g.min)	4.066E-04	1.6676E-05	7.85E-06	1.5956E-04	8.886E-04	1.0146E-04
$\varepsilon_p(g^{-1})$	2.6549E+15	1.0763E+14	4.9474E+13	1.0350E+15	5.7163E+14	6.5055E+14
$\tau_{1/2}$ (min)	0.18	2.90	4.62	0.30	0.54	0.36
(-r)	2.033E-04N_t^2	8.338E-06N_t^2	3.925E-06N_t^2	7.978E-05N_t^2	4.443E-05N_t^2	5.073E-05N_t^2
N_o(g/l)	260.6474	733.4067	824.1985	510.8818	584.2487	623.9860

Table 4.37: Coag-flocculation kinetic parameters and linear regression coefficient of SSC in PIE at varying pH and 0.4g/l dosage.

Parameters	pH = 1	pH = 3	pH = 5	pH = 7	pH = 10	pH = 13
Y	1.402E-04X	7.768E-06X+	1.266E -05X+	6.172E-05X+	4.599E-05X+	3.339E-05X+
	+4.2625E-03	1.3183E-03	1.1552E-03	8.82E-04	1.18866E-03	1.0009E-03
α	2.000	2.000	2.000	2.000	2.000	2.000
R^2	0.633	0.948	0.586	0.971	0.831	0.790
K(l/g.min)	1.402E-04	7.7688E-06	1.266E-05	6.172E-05	4.599E-05	3. 339E-05
K_R(l/min)	1.5341E-19	1.5494E-19	1.5867E-19	1.5417E-19	1.5571E-19	1.5622E-19
β_{BR}(l/g.min)	2.804E-04	1.5536E-05	2.532E-05	1.2344E-04	9.198E-05	6.678E-05
$\varepsilon_p(g^{-1})$	1.8278E+15	1.0027E+14	1.5958E+14	8.0067E+14	5.9071E+14	4.2747E+14
$\tau_{1/2}$ (min)	0.26	3.11	1.43	0.39	0.53	0.54
(-r)	1.402E-04N_t^2	7.768E-06N_t^2	1.266E-05N_t^2	6.172E-05N_t^2	4.599E-05N_t^2	3.339E-05N_t^2
N_o(g/l)	234.6041	758.5527	865.6510	1133.7868	841.3259	99.1008

Table 4.38: Coag-flocculation kinetic parameters and linear regression coefficient of SSC in PIE at varying pH and 0.5g/l dosage.

Parameters	pH = 1	pH = 3	pH = 5	pH = 7	pH = 10	pH = 13
Y	2.84E-05X	2.16E-05X+	1.22E -05X+	7.95E-05X+	6.59E-05X+	3.83E-05X+
	+2.7449E-03	2.0628E-03	9.234E-03	1.0454E-04	1.2385E-03	1.2157E-03
α	2.000	2.000	2.000	2.000	2.000	2.000
R^2	0.816	0.972	0.962	0.953	0.876	0.745
K(l/g.min)	2.84E-05	2.16E-05	1.22E-05	7.95E-05	6.59E-05	3. 83E-05
K_R(l/min)	1.5341E-19	1.5504E-19	1.5867E-19	1.5417E-19	1.5571E-19	1.5622E-19
β_{BR}(l/g.min)	5.68E-05	4.326E-05	2.44E-05	1.59E-04	1.318E-04	7.66E-05
$\varepsilon_p(g^{-1})$	3.7025E+14	2. 7864E+14	1.5378E+14	1.0313E+14	8.4644E+14	4.9033E+14
$\tau_{1/2}$ (min)	1.28	1.12	1.48	0.30	0.37	0.47
(-r)	2.84E-05N_t^2	2.16E-05N_t^2	1.22E-05N_t^2	7.95E-05N_t^2	6.59E-05N_t^2	3.83E-05N_t^2
N_o(g/l)	364.3120	484.8955	1082.9543	956.5716	807.4283	822.5714

Table 4.39: Coag-flocculation kinetic parameters and linear regression coefficient of SSC in PIE at varying pH and 0.6g/l dosage.

Parameters	pH = 1	pH = 3	pH = 5	pH = 7	pH = 10	pH = 13
Y	1.733E-04X	4.455E-06X+	4.763E -06X+	6.604E-05X+	4.840E-05X+	1.736E-05X+
	+5.0104E-03	1.20778E-03	9.223E-04	1.094E-03	1.0162E-03	8.612E-04
α	2.000	2.000	2.000	2.000	2.000	2.000
R^2	0.953	0.722	0.945	0.919	0.871	0.793
K(l/g.min)	1.733E-04	4.455E-06	4.763E-06	6.604E-05	4.840E-05	1. 735E-05
K_R(l/min)	1.5366E-19	1.5504E-19	1.5872E-19	1.5417E-19	1.5571E-19	1.5622E-19
β_{BR}(l/g.min)	3.466E-04	8.91E-06	9.526E-06	1.3208E-04	9.68E-05	3.472E-05
$\varepsilon_p(g^{-1})$	2.2556E+15	5. 7469E+13	6.0018E+13	8.5672E+14	6.2167E+14	2.2225E+14
$\tau_{1/2}$ (min)	0.209	5.42	3.80	0.37	0.50	1.04
(-r)	1.733E-04N_t^2	4.455E-06N_t^2	4.763E-06N_t^2	6.604E-05N_t^2	4.840E-05N_t^2	1.736E-05N_t^2
N_o(g/l)	199.5849	928.0202	1084.2459	914.0768	984.0583	1161.1705

Table 4.40: Coag-flocculation kinetic parameters and linear regression coefficient of SSC in PIE at varying pH and 0.7g/l dosage.

Parameters	pH = 1	pH = 3	pH = 5	pH = 7	pH = 10	pH = 13
Y	2.44E-05X	9.54E-06X+	7. 57E -06X+	9.69E-05X+	9.430E-05X+	9.38E-05X+
	+2.825E-03	1.165E-03	7.32E-04	1.064E-03	1.148E-03	6.94E-04
α	2.000	2.000	2.000	2.000	2.000	2.000
R^2	0.956	0.806	0.952	0.963	0.909	0.730
K(l/g.min)	2.44E-05	9.54E-06	7.57E-06	9.69E-05	9.43E-05	9. 38E-6
K_R(l/min)	1.5366E-19	1.5504E-19	1.5872E-19	1.5417E-19	1.5571E-19	1.5647E-19
β_{BR}(l/g.min)	4.88E-05	1.908-05	1.514E-05	1.938E-04	1.886E-04	1.876E-05
$\varepsilon_p(g^{-1})$	3.1758 E+14	1. 2307E+14	9.5388E+13	1.2571E+15	1.2112E+15	1.1990E+14
$\tau_{1/2}$ (min)	1.48	2.53	2.39	0.25	0.26	1.93
(-r)	2.44E-05N_t^2	9.54E-06N_t^2	7.57E-06N_t^2	9.69E-05N_t^2	9.43E-05N_t^2	9.38E-06N_t^2
N_o(g/l)	353.9823	858.3691	1366.1202	939.8496	8714.0801	1440.9222

Table 4.41: Coag-flocculation Kinetic parameters and linear regression coefficient of COSC in PIE at varying pH and 0.1g/l dosage.

Parameters	pH=1	pH=3	pH=5	pH=7	pH=10	pH=13
	1.0E-0.5x+	1.2E-0.5x+	6.0E-0.5x	4.0E-05x+	4.4E-05x+	2.7E-05x+
Y	1.1454E-03	1.027E-03	1.606E-03	3.148E-03	3.569E-03	1.437E-03
α	2.000	2.000	2.000	2.000	2.000	2.000
R^2	0.655	0 .932	0.851	0.836	0.743	0.490
K(l/g.min)	1.0E-05	1.2E-05	6.0E-05	4.0E-05	4.4E-05	2.7E-05
K_R(l/min)	1.5468E-19	1.5443E-19	1.5750E-19	1.5417E-19	1.5622E-19	1.5647E-19
β_{BR}(l/g.min)	2.0E-05	2.4E-05	1.2E-05	8.0E-05	8.8E-05	5.4E-05
$\varepsilon_p(g^{-1})$	1.2930E+14	1.5541E+14	7.6190E+13	5.1891E+15	5.6331E+14	3.4511E+14
$\tau_{1/2}$ (min)	2.42	1.51	4.03	0.60	0.55	0.67
(-r)	$1.0E-05N_t^2$	$1.2E-05N_t^2$	$6.0E-05N_t^2$	$4.0E-05N_t^2$	$4.4E-05N_t^2$	$2.7E-05N_t^2$
N_o(g/l)	873.0574	973.7098	622.6650	317.6620	208.1905	695.8942

Table 4.42: Coag-flocculation Kinetic parameters and linear regression coefficient of COSC in PIE at varying pH and 0.2g/l dosage.

Parameters	pH=1	pH=3	pH=5	pH=7	pH=10	pH=13
	7.34E-0.6x	7.49E-0.6x	5.83E-0.6x	4.43E-05x	4.02E-05x	1.35E-05x
Y	+1.172E-03+	9.46E-04	+1.093E-03	+1.989E-03	+2.272E-03	+1.318E-03
α	2.000	2.000	2.000	2.000	2.000	2.000
R^2	0.917	0 .722	0.844	0.847	0.827	0.324
K(l/g.min)	7.34E-06	7.49E-06	5.83E-06	4.43E-05	4.02E-05	1.35E-05
K_R(l/min)	1.5468E-19	1.5443E-19	1.5750E-19	1.5417E-19	1.5647E-19	1.5647E-19
β_{BR}(l/g.min)	1.468E-05	1.498E-05	1.166E-05	8.86E-05	8.04E-05	2.7E-05
$\varepsilon_p(g^{-1})$	9.4906E+13	9.7002E+13	7.4032E+13	5.7469E+14	5.1384E+14	1.7256E+14
$\tau_{1/2}$ (min)	3.29	2.42	4.14	0.55	0.60	1.34
(-r)	$7.34E-06N_t^2$	$7.49E-06N_t^2$	$5.83E-06N_t^2$	$4.43E-05N_t^2$	$4.02E-05N_t^2$	$1.35E-05_tE^2$
N_o(g/l)	853.2423	1057.0825	914.9131	502.7652	440.1408	758.7253

Table 4.43: Coag-flocculation Kinetic parameters and linear regression coefficient of COSC in PIE at varying pH and 0.3g/l dosage.

Parameters	pH=1	pH=3	pH=5	pH=7	pH=10	pH=13	
	8.837E-0.6x	2.145E-0.5x	7.437E-0.6x	5.155E-05x	5.741E-05x	1.050E-05x	
Y	+1.2224E-03	+8.787E-04+	1.0464E-03	+2.2514E-03	+1.0302E-03	+1.0694E-03	α
	2.000	2.000	2.000	2.000	2.000	2.000	
R^2	0.703	0 .976	0.689	0.762	0.848	0.579	
K(l/g.min)	8.837E-06	2.145E-05	7.437E-06	5.155E-05	5.741E-05	1.050E-05	
K_R(l/min)	1.5468E-19	1.5443E-19	1.5775E-19	1.5417E-19	1.5647E-19	1.5647E-19	
β_{BR}(l/g.min)	1.7674E-05	4.29E-05	1.4874E-05	5.155E-05	1.1482E-05	2.1E-05	
$\varepsilon_p(g^{-1})$	1.1426E+14	2.7780E+14	9.4288E+13	3.3437E+14	7.3381E+13	1.341E+14	
$\tau_{1/2}$ (min)	2.73	0.84	3.25	0.47	4.21	1.73	
(-r)	$8.837E-06N_t^2$	$2.145E-05N_t^2$	$7.437E-05N_t^2$	$5.155E-05N_t^2$	$5.741E-05N_t^2$	$7.050E-05N_t^2$	
N_o(g/l)	818.0628	1138.0448	955.6575	444.1681	970.6853	935.1038	

Table 4.44: Coag-flocculation Kinetic parameters and linear regression coefficient of COSC in PIE at varying pH and 0.4g/l dosage.

Parameters	pH=1	pH=3	pH=5	pH=7	pH=10	pH=13
	1.095E-0.5x	8.287E-0.6x	9.751E-0.6x	3.305E-05x	1.822E-05x	9.089E-06x
Y	+1.0735E-03	+8.639E-04+	1.0764E-03	+1.6962E-03	+1.074E-03	+9.324E-04
α	2.000	2.000	2.000	2.000	2.000	2.000
R^2	0.924	0 .839	0.919	0.828	0.866	0.621
K(l/g.min)	1.924E-05	8.287E-06	9.751E-06	3.305E-05	1.822E-05	9.089E-06
K_R(l/min)	1.5479E-19	1.5448E-19	1.5775E-19	1.5417E-19	1.5647E-19	1.5673E-19
β_{BR}(l/g.min)	2.19E-05	1.6574E-05	1.9502E-05	6.61E-05	3.644E-05	1.8178E-04
$\varepsilon_p(g^{-1})$	1.4148E+14	1.0729E+14	1.2363E+14	4.2875E+14	2.3289E+14	1.1598E+15
$\tau_{1/2}$ (min)	2.21	2.19	2.48	0.73	1.33	1.99
(-r)	$1.095E\text{-}05N_t^2$	$8.287E\text{ -}06N_t^2$	$9.751E\text{-}06N_t^2$	$3.305E\text{-}05N_t^2$	$1.822E\text{-}05N_t^2$	$9.089E\text{-}06N_t^2$
N_o(g/l)	931.5324	1157.5414	929.0227	589.5531	931.0987	1072.5011

Table 4.45 Coag-flocculation Kinetic parameters and linear regression coefficient of COSC in PIE at varying pH and 0.5g/l dosage.

Parameters	pH=1	pH=3	pH=5	pH=7	pH=10	pH=13
	2.03E-05x	9.86E-06x+	1.26E-05x	3.38E-05x	1.60E-05x	1.71E-06x
Y	+9.458E-04	7.206E-04	+1.0839E-03	+1.2257E-03	+9.823E-04	+8.425E-04
α	2.000	2.000	2.000	2.000	2.000	2.000
R^2	0.861	0 .847	0.871	0.823	0.840	0.626
K(l/g.min)	2.03E-05	9.86E-06	1.26E-05	3.38E-05	1.60E-05	1.71E-06
K_R(l/min)	1.5479E-19	1.5448E-19	1.5775E-19	1.5443E-19	1.5673E-19	1.5673E-19
β_{BR}(l/g.min)	4.06E-05	1.972E-05	2.52E-05	6.76E-05	3.2E-05	3.42E-06
$\varepsilon_p(g^{-1})$	2.6229E+14	1.2765E+14	1.5975E+14	4.3774E+14	2.0417E+14	2.1821E+13
$\tau_{1/2}$ (min)	1.19	1.84	1.92	0.71	1.51	10.59
(-r)	$2.03E\text{-}05N_t^2$	$9.86E\text{ -}06N_t^2$	$1.26E\text{-}05N_t^2$	$3.38E\text{-}05N_t^2$	$1.60E\text{-}05N_t^2$	$1.71E\text{-}05N_t^2$
N_o(g/l)	1057.3060	1368.1762	922.5943	815.8603	1018.0189	1186.9436

Table 4.46: Coag-flocculation Kinetic parameters and linear regression coefficient of COSC in PIE at varying pH and 0.6g/l dosage.

Parameters	pH=1	pH=3	pH=5	pH=7	pH=10	pH=13
	1.150E-05x	1.030E-05x+	9.7E-06x	6.322E-05x	1.163E-05x	4.518E-06x
Y	+1.1055E-03	7.309E-04	+9.588E-04	+9.113E-04	+7.145E-04+	7.546E-04
α	2.000	2.000	2.000	2.000	2.000	2.000
R^2	0.817	0 .931	0.806	0.860	0.922	0.881
K(l/g.min)	1.150E-05	1.030E-05	9.7E-06	6.322E-05	1.163E-05	4.518E-06
K_R(l/min)	1.5484E-19	1.5448E-19	1.5775E-19	1.5443E-19	1.5673E-19	1.5673E-19
B_{BR}(l/g.min)	2.3E-05	2.06E-05	1.94E-05	1.2644E-04	2.326E-05	9.036E-06
$\varepsilon_p(g^{-1})$	4.7680E+14	1.8102E+14	1.5392E+13	4.1487E+15	4.7853E+14	2.5654E+15
$\tau_{1/2}$ (min)	2.10	1.76	2.49	0.38	2.08	4.01
(-r)	$1.150E\text{-}05N_t^2$	$1.030E\text{ -}05N_t^2$	$9.7E\text{-}06N_t^2$	$6.322E\text{-}05N_t^2$	$1.163E\text{-}05N_t^2$	$4.518E\text{-}06N_t^2$
N_o(g/l)	904.56807	1203.5143	1042.9704	1097.3335	1399.5801	1325.2054

Table 4.47: Coag-flocculation Kinetic parameters and linear regression coefficient of COSC in PIE at varying pH and 0.7g/l dosage.

Parameters	pH=1	pH=3	pH=5	pH=7	pH=10	pH=13
	8.08E-06 x	8.29E-06x+	1.4E-05x	3.39E-05x	2.90E-05x	1.10E-06x
Y	+8.6E-04	7.99E-04	+8.88E-04	+1.352E-03	+7.63E-04	+7.59E-04
α	2.000	2.000	2.000	2.000	2.000	2.000
R^2	0.859	0 .800	0.850	0.757	0.967	0.904
K(l/g.min)	3.70E-05	1.40E-05	1.22E-05	3.23E-05	3.75E-05	2.03E-05
K_R(l/min)	1.5484E-19	1.5448E-19	1.5801E-19	1.5443E-19	1.5673E-19	1.5673E-19
β_{BR}(l/g.min)	1.616E-05	1.658E-05	2.80E-05	6.78E-05	5.8E-05	2.20E-06
$\varepsilon_p(g^{-1})$	1.0437E+14	1.0733E+14	1.7720E+14	4.3903E+14	3.7006E+14	1.4037E+13
$\tau_{1/2}$ (min)	2.99	2.19	1.73	0.71	0.83	16.47
(-r)	8. 08E-06N_t^2	8.29E -06N_t^2	1.4E-05N_t^2	3.39E-05N_t^2	2.90E-05N_t^2	1.10E-06N_t^2
N_o(g/l)	1162.7907	1251.5645	1126.1261	739.6450	1310.6160	1317.5231

Table 4.48: Coag-Flocculation kinetic parameters and linear regression coefficient of TOSC in PIE at varying pH and 0.1g/l dosage**.**

Parameters	pH=1	pH=3	pH=5	pH=7	pH=10	pH=13
	1.4E-0.6x+	1.3E-0.5x+	8.E-0.5x	7.1E-05x+	4.5E-05x+	7.5E-05x+
Y	1.423E-03	1.091E-03	1.339E-03	3.064E-03	2.272E-04	2.177E-03
α	2.000	2.000	2.000	2.000	2.000	2.000
R^2	0.870	0 .942	0.747	0.873	0.829	0.660
K(l/g.min)	1.4E-06	1.3E-05	8E -06	7.1E-05	4.5E-05	7.5E-05
K_R(l/min)	1.5484E-19	1.5474E-19	1.5724E-19	1.5468E-19	1.5571E-19	1.5826E-19
β_{BR}(l/g.min)	2.8E-05	2.6E-05	1.6E-05	1.42E-04	9.0E-05	1.5E-04
$\varepsilon_p(g^{-1})$	1.8083E+13	1.6802E+14	1.0176E+14	9.1802E+14	5.7800E+14	9.4781E+14
$\tau_{1/2}$ (min)	12.94	1.17	1.74	0.34	0.54	0.21
(-r)	1.4E-05N_t^2	1.3E -05N_t^2	8E-06N_t^2	7.1E-05N_t^2	4.5E-05N_t^2	7.5E-05N_t^2
N_o(g/l)	702.7407	916.5903	746.8260	326.3708	440.1408	459.3477

Table 4.49: Coag-Flocculation kinetic parameters and linear regression coefficient of TOSC in PIE at varying pH and 0.2g/l dosage**.**

Parameters	pH=1	pH=3	pH=5	pH=7	pH=10	pH=13
	1.28E-0.5x	9.92E-0.6x	1.01E-0.5x+	3.02E-05x	2.52E-05x+	3.21E-05x+
Y	+1.084E-03+	9.24E-04	1.302E-03	+2.037E-03	1.654E-03	1.343E-03
α	2.000	2.000	2.000	2.000	2.000	2.000
R^2	0.837	0 .750	0.866	0.768	0.586	0.591
K(l/g.min)	1.28E-05	9.92E-06	1.01E -05	3.02E-05	2.52E-05	3.21E-05
K_R(l/min)	1.5484E-19	1.5474E-19	1.5724E-19	1.5468E-19	1.5571E-19	1.5826E-19
β_{BR}(l/g.min)	2.56E-05	1.984E-05	2.02E-05	6.04E-05	5.04E-05	6.42E-05
$\varepsilon_p(g^{-1})$	1.6533E+14	1.2822E+14	1.2847E+14	3.9048E+14	3.2368E+14	4.0566E+14
$\tau_{1/2}$ (min	1.42	1.53	1.38	0.80	0.96	0.50
(-r)	1.28E-05N_t^2	9.92E -06N_t^2	1.01E-05N_t^2	3.02E-05N_t^2	2.52E-05N_t^2	3.21E-05N_t^2
N_o(g/l)	922.5092	1082.2511	768.04916	490.9180	604.5949	744.6016

Table 4.50: Coag-Flocculation kinetic parameters and linear regression coefficient of TOSC in PIE at varying pH and 0.3g/l dosage.

Parameters	pH=1	pH=3	pH=5	pH=7	pH=10	pH=13
	2.149E-0.5x	3.778E-0.6x+	1.487E-0.5x	8.033E-05x	5.695E-05x+	7.701E-05x+
Y	+7.276E-04	8.259E-04	+1.2262E-03	+1.2237E-03	+1.759E-03	9.253E-04
α	2.000	2.000	2.000	2.000	2.000	2.000
R^2	0.856	0 .663	0.838	0.798	0.832	0.599
K(l/g.min)	2.149E-05	3.778E-06	1.487E -05	8.033E-05	5.695E-05	7.701E-06
K_R(l/min)	1.5494E-19	1.5474E-19	1.5724E-19	1.5468E-19	1.5571E-19	1.5826E-19
β_{BR}(l/g.min)	4.298E-05	7.556E-06	2.974E-05	1.6066E-04	1.139E-05	1.542E-05
$\varepsilon_p(g^{-1})$	2.7740E+14	4.8830E+13	1.8914E+14	1.0387E+15	7.3149E+14	9.7435E+13
$\tau_{1/2}$ (min)	0.84	4.01	0.93	0.30	0.42	2.09
(-r)	$2.149E-05N_t^2$	$3.778E-06N_t^2$	$1.487E-05N_t^2$	$8.033E-05N_t^2$	$5.695E-05N_t^2$	$7.701E-06N_t^2$
N_o(g/l)	1374.3815	1210.8003	815.5276	817.1938	568.5048	1080.7306

Table 4.51: Coag-Flocculation kinetic parameters and linear regression coefficient of TOSC in PIE at varying pH and 0.4g/l dosage.

Parameters	pH=1	pH=3	pH=5	pH=7	pH=10	pH=13
	4.253E-0.5x	9.959E-0.6x	1.012E-0.5x	4.224E-05x	2.101E-05x	1.012E-05x
Y	+8.517E-04	8.757E-04	+9.774E-04	+1.5915E-03	+1.1778E-03	+7.481E-04
α	2.000	2.000	2.000	2.000	2.000	2.000
R^2	0.813	0 .706	0.776	0.836	0.769	0.752
K(l/g.min)	4.253E-05	9.959E-06	1.012E -05	4.224E-05	2.101E-05	1.012E-06
K_R(l/min)	1.5494E-19	1.5474E-19	1.5724E-19	1.5494E-19	1.5596E-19	1.5826E-19
β_{BR}(l/g.min)	8.506E-05	1.9918E-05	2.02E-05	8.448E-04	4.202E-05	2.024E-05
$\varepsilon_p(g^{-1})$	5.4899E+14	1.2872E+14	1.2872E+14	5.4524E+14	2.6943E+14	1.2789E+14
$\tau_{1/2}$ (min)	0.43	1.52	1.37	0.57	1.15	1.59
(-r)	$4.253E-05N_t^2$	$9.959E-06N_t^2$	$1.012E-05N_t^2$	$4.224E-05N_t^2$	$2.101E-05N_t^2$	$1.012E-06N_t^2$
N_o(g/l)	1174.1223	1141.9436	1023.1226	628.3380	849.0406	1336.9197

Table 4.52: Coag-Flocculation kinetic parameters and linear regression coefficient of TOSC in PIE at varying pH and 0.5g/l dosage.

Parameters	pH=1	pH=3	pH=5	pH=7	pH=10	pH=13
	1.00E-0.5x+	1.11E-0.5x+	9.28-0.6x+	9.67E-06x	3.90E-05x	3.50E-06x+
Y	8.648E-04	6.381E-04	1.1762E-03	+8.918E-04	+1.6824E-03	8.385E-04
α	2.000	2.000	2.000	2.000	2.000	2.000
R^2	0.833	0 .826	0.537	0.857	0.682	0.827
K(l^3/g.min)	1.00E-05	1.11E-05	9.28E -06	9.67E-06	3.90E-05	3.50E-06
K_R(l/min)	1.5494E-19	1.5484E-19	1.5750E-19	1.5494E-19	1.5596E-19	1.5852E-19
β_{BR}(l/g.min)	2.00E-05	2.22E-05	1.856E-05	1.934E-05	7.8E-05	7.0E-06
$\varepsilon_p(g^{-1})$	1.2908E+14	1.4337E+14	1.1784E+14	1.2482E+14	5.0013E+14	4.4158E+13
$\tau_{1/2}$ (min)	1.81	1.37	1.50	2.50	0.62	4.60
(-r)	$1.00E-05N_t^2$	$1.11E-05N_t^2$	$9.28E-06N_t^2$	$9.67E-06N_t^2$	$3.90E-05N_t^2$	$3.50E-06N_t^2$
N_o(g/l)	1156.3367	1567.1525	850.1955	1121.3277	594.3890	1192.6058

Table 4.53: Coag-Flocculation kinetic parameters and linear regression coefficient of TOSC in PIE at varying pH and 0.6g/l dosage.

Parameters	pH=1	pH=3	pH=5	pH=7	pH=10	pH=13
	1.490E-0.5x	8.526E-0.6x	8.227-0.6x	5.532E-05x	1.635E-05x	4.46E-06x
Y	+8.648E-04+	8.574E-04 +	7.036E-03	+1.2753E-03	+1.1711E-03	+6.75E-04
α	2.000	2.000	2.000	2.000	2.000	2.000
R^2	0.835	0 .938	0.830	0.882	0.702	0.674
K(l/g.min)	1.490E-05	8.526E-05	8.227E -06	5.532E-05	1.635E-05	4.46E-06
K_R(l/min)	1.5494E-19	1.5484E-19	1.5750E-19	1.5494E-19	1.5596E-19	1.5852E-19
β_{BR}(l/g.min)	2.98E-05	1.7052E-05	1.6454E-05	1.1064E-04	3.27E-05	8.92E-06
$\varepsilon_p(g^{-1})$	1.9233E+14	1.1013E+14	1.0447E+14	7.1408E+14	2.1001E+14	5.6271E+13
$\tau_{1/2}$ (min)	2.34	1.78	1.69	0.44	1.47	3.38
(-r)	$1.490E-05N_t^2$	$8.526E-06N_t^2$	$8.227E-06N_t^2$	$5.532E-05N_t^2$	$1.635E-05N_t^2$	$4.46E-06N_t^2$
N_o(g/l)	1156.3367	1166.3168	1421.2621	784.1292	853.8980	1481.4815

Table 4.54: Coag-Flocculation kinetic parameters and linear regression coefficient of TOSC in PIE at varying pH and 0.7g/l dosage.

Parameters	pH=1	pH=3	pH=5	pH=7	pH=10	pH=13
	2.02E-0.5x	7.26E-0.6x +	6.42-0.6x	5.15E-05x	4.04E-05x	4.46E-06x
Y	+8.524E-04	5.76E-04	+5.05E-04	+1.25E-03	+1.094E-03+	6.75E-04
α	2.000	2.000	2.000	2.000	2.000	2.000
R^2	0.721	0 .864	0.753	0.843	0.848	0.674
K(l/g.min)	2.02E-05	7.26E-06	6.42E -06	5.15E-05	4.04E-05	4.46E-06
K_R(l/min)	1.5499E-19	1.5484E-19	1.5750E-19	1.5520E-19	1.5622E-19	1.5852E-19
β_{BR}(l/g.min)	4.04E-05	1.452E-05	1.284E-05	1.03E-04	8.08E-05	8.92E-06
$\varepsilon_p(g^{-1})$	2.6066E+14	9.377E+14	8.152E+13	6.6366E+14	5.1722E+14	5.6271E+13
$\tau_{1/2}$ (min)	0.90	2.09	2.16	0.47	0.60	3.61
(-r)	$2.02E-05N_t^2$	$7.26E-06N_t^2$	$6.42E-06N_t^2$	$5.15E-05N_t^2$	$4.04E-05N_t^2$	$4.46E-06N_t^2$
N_o(g/l)	1173.7089	1736.1111	1980.1980	800.00	914.0768	1481.4815

Table 4.55: Coag-Flocculation Kinetic Parameters and linear regression coefficient of PTSC in PIE at varying pH and 0.1g/l dosage.

Parameters	pH=1	pH=3	pH=5	pH=7	pH=10	pH=13
	7.9E-0.5x	1.6E-0.5x	6.0E-0.6x	3.3E-05x	9.9E-05x+	1.46E-04x+
Y	2.414E-03	+1.138E-03+	1.273E-03	1.766E-03	3.212E-03	1.46E-03
α	2.000	2.000	2.000	2.000	2.000	2.000
R^2	0.784	0 .911	0.897	0.946	0.763	0.945
K(l/g.min)	7.9E-05	1.6E-05	6.0E -06	3.3E-05	9.9E-05	1.46E-04
K_R(l/l)	1.5468E-19	1.5443E-19	1.5801E-19	1.5545E-19	1.5622E-19	1.5801E-19
β_{BR}(l/g.l)	1.58E-04	3.2E-05	1.2E-05	6.6E-05	1.98E-04	2.92E-04
$\varepsilon_p(g^{-1})$	1.0215E+15	2.0721E+14	7.5945E+13	4.2457E+15	1.2674E+15	1.8480E+15
$\tau_{1/2}$ (min)	0.91	1.13	3.02	0.73	0.24	0.12
(-r)	$.9E-05N_t^2$	$1.6E-05N_t^2$	$6.0E-06N_t^2$	$3.3E-05N_t^2$	$9.9E-05N_t^2$	$1.46E-04N_t^2$
N_o(g/l)	414.2502	878.7346	785.5460	566.2514	311.3325	684.9315

Table 4.56: Coag-Flocculation Kinetic Parameters and linear regression coefficient of PTSC in PIE at varying pH and 0.2g/l dosage.

Parameters	pH=1	pH=3	pH=5	pH=7	pH=10	pH=13
	7.44E-0.5x	9.94E-0.5x	9.03E-0.6x	4.42E-05x	8.99E-05x	2.04E-04x
Y	+3.057E-03+	2.27E-04	+1.028E-03	+1.54E-03	+2.875E-03	+1.175E-03
α	2.000	2.000	2.000	2.000	2.000	2.000
R^2	0.708	0 .783	0.877	0.968	0.865	0.967
K(l/g.min)	7.44E-05	9.94E-05	9.03E -06	4.42E-05	8.99E-05	2.04E-04
K_R(l/min)	1.5468E-19	1.5443E-19	1.5801E-19	1.5545E-19	1.5647E-19	1.5801E-19
β_{BR}(l/g.min)	1.488E-04	1.988E-04	1.806E-05	8.84E-05	1.798E-04	4.08E-04
$\varepsilon_p(g^{-1})$	9.61991E+15	1.2873E+15	1.1430E+14	5.6867E+15	1.1491E+15	2.582E+15
$\tau^1/_2$ (min)	0.20	0.18	2.01	0.55	0.27	0.09
(-r)	$7.44E\text{-}05N_t^2$	$9.94E\text{ -}05N_t^2$	$9.03E\text{-}06N_t^2$	$4.42E\text{-}05N_t^2$	$8.99E\text{-}05N_t^2$	$2.04E\text{-}04N_t^2$
N_o(g/l)	327.1181	4405.2863	972.7626	649.3506	347.8261	851.0638

Table 4.57: Coag-Flocculation Kinetic Parameters and linear regression coefficient of PTSC in PIE at varying pH and 0.3g/l dosage.

Parameters	pH=1	pH=3	pH=5	pH=7	pH=10	pH=13
	2.532E-0.5x	9.082E-0.6x	1.002E-0.5x	5.298E-05x	4.595E-05x	2.491E-04x
Y	+7.044E-04+	9.90E-04	+9.966E-03	+1.429E-03	+2.1916E-03	+1.4337E-03
α	2.000	2.000	2.000	2.000	2.000	2.000
R^2	0.965	0 .919	0.790	0.896	0.859	0.877
K(l/g.min)	1.664E-05	9.082E-06	1.002E -05	5.298E-05	4.595E-05	2.491E-04
K_R(l/min)	1.5494E-19	1.5443E-19	1.5801E-19	1.5545E-19	1.5647E-19	1.5801E-19
β_{BR}(l/g.min)	3.328E-05	1.8164E-05	2.004E-05	1.0596E-04	9.19E-05	4.982E-04
$\varepsilon_p(g^{-1})$	2.147E+14	1.1762 E+14	1.2683E+14	6.8163E+14	5.8733E+14	3.1530E+15
$\tau_{1/2}$ (min)	0.91	1.99	1.81	0.46	0.53	0.07
(-r)	$1.664E\text{-}05N_t^2$	$9.082E\text{ -}06N_t^2$	$1.002E\text{-}05N_t^2$	$5.298E\text{-}05N_t^2$	$4.595E\text{-}05N_t^2$	$2.491E\text{-}04N_t^2$
N_o(g/l)	1018.8487	1009.9990	1003.4116	699.7901	456.2876	697.4960

Table 4.58: Coag-Flocculation Kinetic Parameters and linear regression coefficient of PTSC in PIE at varying pH and 0.4g/l dosage.

Parameters	pH=1	pH=3	pH=5	pH=7	pH=10	pH=13
	2.532E-0.5x	9.834E-0.6x	9.614E-0.6x	4.205E-05x	8.263E-05x	2.005E-04x
Y	+7.044E-04+	1.0617E-03+	1.2027E-03	+1.9456E-03	+2.175E-03+	3.2039E-03
α	2.000	2.000	2.000	2.000	2.000	2.000
R^2	0.907	0 .837	0.869	0.878	0.824	0.762
K(l/g.min)	2.532E-05	9.834E-06	9.614E -06	4.205E-05	8.263E-05	2.005E-04
K_R(l/min)	1.5494E-19	1.5468E-19	1.5801E-19	1.5571E-19	1.5647E-19	1.5826E-19
β_{BR}(l/g.min)	5.064E -05	1.9668E-05	1.9228E-05	8.41E-05	1.6526E-04	4.01E-04
$\varepsilon_p(g^{-1})$	3.2684E+14	1.2715E+14	1.2169E+14	5.4011E+15	1.0562E+15	2.5378E+15
$\tau_{1/2}$ (min)	0.60	1.84	1.88	0.57	0.29	0.09
(-r)	$1.12E\text{-}04N_t^2$	$6.0E\text{ -}06N_t^2$	$6.0E\text{-}06N_t^2$	$7.8E\text{-}05N_t^2$	$9.1E\text{-}05N_t^2$	$7.1E\text{-}05N_t^2$
N_o(g/l)	1419.6479	941.8857	831.4625	513.9803	459.7701	312.1196

Table 4.59: Coag-Flocculation Kinetic Parameters and linear regression coefficient of PTSC in PIE at varying pH and 0.5g/l dosage.

Parameters	pH=1	pH=3	pH=5	pH=7	pH=10	pH=13
	9.8E-0.5x+	1.13E-0.5x+	1.26E-0.5x	3.18E-05x	6.06E-05x+	1.51E-04x+
Y	3.6948E-03	9.167E-04	+1.1358E-03	+1.2541E-03	1.8434E-03	3.3286E-03
α	2.000	2.000	2.000	2.000	2.000	2.000
R^2	0.495	0 .864	0.842	0.898	0.811	0.608
K(l/g.min)	9.84E-05	1.13E-05	1.26E -05	3.18E-05	6.06E-05	1.51E-04
K_R(l/min)	1.5494E-19	1.5468E-19	1.5826E-19	1.5571E-19	1.5673E-19	1.5826E-19
β_{BR}(l/g.min)	1.968E-04	2.26E-05	2.52E-05	6.36E-05	1.212E-04	3.02E-04
$\varepsilon_p(g^{-1})$	1.2702E+15	1.4611E+14	1.5923E+14	4.0845E+15	7.7330E+14	1.9083E+15
$\tau_{1/2}$ (min)	0.15	1.60	1.44	0.76	0.40	0.12
(-r)	$9.84E\text{-}05N_t^2$	$1.13E\text{ -}05N_t^2$	$1.26E\text{-}05N_t^2$	$3.18E\text{-}05N_t^2$	$6.06E\text{-}05N_t^2$	$1.51E\text{-}04N_t^2$
N_o(g/l)	270.6506	1090.8694	880.4367	797.3846	542.4759	300.4266

Table 4.60: Coag-Flocculation Kinetic Parameters and linear regression coefficient of PTSC in PIE at varying pH and 0.6g/l dosage.

Parameters	pH=1	pH=3	pH=5	pH=7	pH=10	pH=13
	7.486E-0.5x	1.238E-0.5x	2.29E-0.5x	4.362E-05x	2.878E-05x	1.959E-04x
Y	+2.6494E-03	+8.25E-04	+7.709E-04	+1.5058E-03	+1.393E-03	+1.958E-03
α	2.000	2.000	2.000	2.000	2.000	2.000
R^2	0.663	0 .824	0.943	0.979	0.842	0.639
K(l/g.min)	7.486E-05	1.238E-05	2.299E -05	4.362E-05	2.878E-05	1.959E-04
K_R(l/min)	1.5520E-19	1.5468E-19	1.5826E-19	1.5571E-19	1.5673E-19	1.5826E-19
β_{BR}(l/g.min)	1.4972E-04	2.476E-05	4.598E-05	8.724E-05	5.756E-05	3.918E-04
$\varepsilon_p(g^{-1})$	9.6469E+15	1.6007E+14	2.9053E+14	5.6027E+14	3.6726E+14	2.4757E+15
$\tau_{1/2}$ (min)	0.20	1.46	0.79	0.55	0.84	0.09
(-r)	$7.486E\text{-}05N_t^2$	$1.238E\text{ -}06N_t^2$	$2.299E\text{-}05N_t^2$	$4.362E\text{-}05N_t^2$	$2.878E\text{-}05N_t^2$	$1.959E\text{-}04N_t^2$
N_o(g/l)	377.4439	1210.9470	1297.1851	664.0988	717.8751	511.2997

Table 4.61: Coag-Flocculation Kinetic Parameters and linear regression coefficient of PTSC in PIE at varying pH and 0.7g/l dosage.

Parameters	pH=1	pH=3	pH=5	pH=7	pH=10	pH=13
	3.70E-0.5x	1.40E-0.5x+	1.22E-0.5x	3.23E-05x	3.75E-05x	2.03E-04x
Y	+1.282E-03	8.19E-04	+7.84E-04	+1.535E-03	+1.654E-03	+1.961E-03
α	2.000	2.000	2.000	2.000	2.000	2.000
R^2	0.851	0 .753	0.859	0.952	0.634	0.780
K(l/g.min)	3.70E-05	1.40E-05	1.22E-05	3.23E-05	3.75E-05	2.03E-05
K_R(l/min)	1.5520E-19	1.5468E-19	1.5852E-19	1.5571E-19	1.5673E-19	1.5826E-19
B_{BR}(l/g.min)	7.4E-05	2.80E-05	2.44E-05	6.46E-04	7.5E-05	4.06E-04
$\varepsilon_p(g^{-1})$	4.7680E+14	1.8102E+14	1.5392E+13	4.1487E+15	4.7853E+14	2.5654E+15
$\tau_{1/2}$ (min)	0.41	1.30	1.48	0.75	0.64	0.09
(-r)	$3.70E\text{-}05N_t^2$	$1.40E\text{ -}05N_t^2$	$1.22E\text{-}05N_t^2$	$3.23E\text{-}05N_t^2$	$3.75E\text{-}05N_t^2$	$2.03E\text{-}05N_t^2$
N_o(g/l)	780.0312	1221.0012	1275.5102	651.4658	604.5949	509.9439

Table 4.62: Coag-flocculation kinetic parameters and linear regression coefficient of MPSC in PIE at varying pH and 0.1g/l dosage.

Parameters	pH=1	pH=3	pH=5	pH=7	pH=10	pH=13
Y	3.1E-0.5x+	1.1E-0.3x+	7.0E-0.6x+	4.1E-05x	4.8E-05x	2.18E-04x
	1.701E-03	9.43E-04	1.228E-03	+2.688E-03	+1.978E-03	+2.176E-03
α	2.000	2.000	2.000	2.000	2.000	2.000
R^2	0.954	0 .960	0.728	0.856	0.762	0.925
K(l/g.min)	1.3E-0.5	1.1E-05	7.0E -06	4.1E-05	4.8E-05	2.18E-04
K_R(l/min)	1.5417E-19	1.5468E-19	1.5750E-19	1.5341E-19	1.5699E-19	1.5724E-19
β_{BR}(l/g.min)	6.2E-05	2.2E-05	1.4E-05	8.2E-05	9.6E-05	4.36E-04
$\varepsilon_p(g^{-1})$	4.0215E+14	1.4223E+14	8.8889E+13	5.3452E+14	6.1150E+14	2.7728E+15
$\tau_{1/2}$ (min)	0.74	1.38	2.16	0.59	0.50	0.33
(-r)	$3.1E-05N_t^2$	$1.1E-05N_t^2$	$7.0E-06N_t^2$	$4.1E-05N_t^2$	$4.8E-05N_t^2$	$2.18E-04N_t^2$
N_o(g/l)	587.8895	1060.4454	814.3322	372.0238	505.5612	459.5588

Table 4.63 :Coag-flocculation kinetic parameters and linear regression coefficient of MPSC in PIE at varying pH and 0.2g/l dosage.

Parameters	pH=1	pH=3	pH=5	pH=7	pH=10	pH=13
	1.32E-0.5x+	1.05E-0.5x+	9.57E-0.6x+	4.04E-05x+	4.46E-05x	1.51E-04x+
Y	1.381E-03	9.15E-04	1.157E-03	2.766E-03	+1.696E-03	2.267E-03
α	2.000	2.000	2.000	2.000	2.000	2.000
R^2	0.889	0 .908	0.592	0.724	0.853	0.665
K(l/g.min)	1.32E-0.5	1.05E-05	9.57E -06	4.04E-05	4.46E-05	1.51E-04
K_R(l/min)	1.5417E-19	1.5468E-19	1.5750E-19	1.5341E-19	1.5699E-19	1.5724E-19
β_{BR}(l/g.min)	2.64E-05	2.1E-05	1.914E-05	8.08E-05	8.92E-05	3.02E-04
$\varepsilon_p(g^{-1})$	1.7124E+14	1.3576E+14	1.2152E+13	5.2669E+14	5.6819E+14	1.9206E+15
$\tau_{1/2}$ (min)	1.73	1.44	1.58	0.60	0.54	0.48
(-r)	$1.32E-05N_t^2$	$1.05E-05N_t^2$	$9.57E-06N_t^2$	$4.04E-05N_t^2$	$4.46E-05N_t^2$	$1.51E-04N_t^2$
N_o(g/l)	724.1130	1092.8962	864.3042	361.5390	589.6226	441.1116

Table 4.64 : Coag-flocculation kinetic parameters and linear regression coefficient of MPSC in PIE at varying pH and 0.3g/l dosage.

Parameters	pH=1	pH=3	pH=5	pH=7	pH=10	pH=13
	1.882E-0.5x+	1.297E-0.5x+	1.805E-0.5x+	2.726E-05x	1.1910E-05x	1.354E-04x
Y	1.4474E-03	8.154E-04	9.514E-04	+2.8525E-03	+1.1365E-03	+2.5965E-03
α	2.000	2.000	2.000	2.000	2.000	2.000
R^2	0.828	0 .780	0.742	0.653	0.874	0.902
K(l/g.min)	1.882E-0.5	1.297E-05	1.805E -05	2.726E-05	1.910E-05	1.354E-04
K_R(l/min)	1.4613E-19	1.5474E-19	1.5775E-19	1.5366E-19	1.5699E-19	1.5724E-19
β_{BR}(l/g.min)	3.764E-05	2.594E-05	3.61E-05	5.452E-05	3.82E-05	2.708E-04
$\varepsilon_p(g^{-1})$	2.5758E+14	1.6764E+14	2.2884E+14	5.5481E+14	2.4333E+14	1.7222E+15
$\tau_{1/2}$ (min)	1.21	1.17	0.84	0.89	1.26	0.54
(-r)	$1.882E-05N_t^2$	$1.297E-05N_t^2$	$1.805E-05N_t^2$	$2.726E-05N_t^2$	$1.910E-05N_t^2$	$1.354E-04N_t^2$
N_o(g/l)	690.8940	1226.3920	105.1083	350.5697	879.8944	385.1338

Table 4.65: Coag-flocculation kinetic parameters and linear regression coefficient of MPSC in PIE at varying pH and 0.4g/l dosage.

Parameters	pH=1	pH=3	pH=5	pH=7	pH=10	pH=13
	1.685E-0.5x+	1.104E-0.5x+	1.437E-0.5x	4.414E-05x	1.493E-05x+	9.215E-04x
Y	1.1625E-05	6.567E-04	+7.913E-04	+1.0727E-03	9.336E-04	+2.2123E-03
α	2.000	2.000	2.000	2.000	2.000	2.000
R^2	0.918	0 .848	0.859	0.946	0.890	0.897
K(l/g.min)	1.6858E-0.5	1.104E-05	1.437E-05	4.414E-05	1.493E-05	9.215E-05
K_R(l/min)	1.4613E-19	1.5474E-19	1.5775E-19	1.5366E-19	1.5709E-19	1.5734E-19
β_{BR}(l/g.min)	3.37E-05	2.208E-05	2.874E-05	8.828E-05	2.986E-05	1.043E-04
$\varepsilon_p(g^{-1})$	2.3062E+14	1.4269E+14	1.8219E+14	5.7452E+14	1.9008E+14	1.1713E+15
$\tau_{1/2}$ (min)	1.36	1.37	1.05	0.55	1.62	0.79
(-r)	$1.685E-05N_t^2$	$1.104E-05N_t^2$	$1.437E-05N_t^2$	$4.414E-05N_t^2$	$1.493E-05N_t^2$	$9.215E-05N_t^2$
N_o(g/l)	890.2151	1522.7653	1263.7432	932.2271	1071.1225	452.0183

Table 4.66: Coag-flocculation kinetic parameters and linear regression coefficient of MPSC in PIE at varying pH and 0.5g/l dosage.

Parameters	pH=1	pH=3	pH=5	pH=7	pH=10	pH=13
	1.58E-0.5x+	1.12E-0.5x	1.59E-0.5x+	5.00E-05x	2.05E-05x	1.20E-04x+
Y	1.0748E-03	+5.736E-04	6.7E-04	+1.0635E-03	+9.571E-04x	1.0726E-03
α	2.000	2.000	2.000	2.000	2.000	2.000
R^2	0.779	0 .728	0.906	0.914	0.873	0.952
K(l/g.min)	1.58E-0.5	1.12E-05	1.59E-05	5.00E-05	2.05E-05	1.20E-04
K_R(l/min)	1.4613E-19	1.5474E-19	1.5775E-19	1.5366E-19	1.5709E-19	1.5734E-19
β_{BR}(l/g.min)	3.16E-05	2.24E-05	3.18E-05	1.0E-04	4.1E-05	2.4E-04
$\varepsilon_p(g^{-1})$	2.1625E+14	1.4476E+14	2.0158E+14	6.5079E+14	2.6100E+14	1.5254E+15
$\tau_{1/2}$ (min)	1.45	1.35	0.95	0.48	1.18	0.60
(-r)	$1.58E-05N_t^2$	$1.12E-05N_t^2$	$1.59E-05N_t^2$	$5.00E-05N_t^2$	$2.05E-05N_t^2$	$1.20E-05N_t^2$
N_o(g/l)	930.4057	1424.5014	1492.5373	940.2915	1044.8229	932.3140

Table 4.67: Coag-flocculation kinetic parameters and linear regression coefficient of MPSC in PIE at varying pH and 0.6g/l dosage.

Parameters	pH=1	pH=3	pH=5	pH=7	pH=10	pH=13
	1.399E-0.5x	1.495E-0.5x	1.743E-0.5x	5.957E-05x	1.493E-05x	6.846E-05x
Y	+9.399E-04	+5.736E-04	+7.21E-04	+1.9E-03	+9.36E-04	+2.946E-03
α	2.000	2.000	2.000	2.000	2.000	2.000
R^2	0.881	0 .940	0.838	0.874	0.826	0.788
K(l/g.min)	1.399E-0.5	1.495E-05	1.743E -05	5.957E-05	1.493E-05	6.846E-04
K_R(l/min)	1.4638E-19	1.5474E-19	1.5775E-19	1.5366E-19	1.5709E-19	1.5734E-19
β_{BR}(l/g.min)	2.798E-05	2.99E-05	3.486E-05	1.1914E-04	2.986E-05	1.3692E-04
$\varepsilon_p(g^{-1})$	1.9115E+14	1.9323E+14	2.2098E+14	7.753E+14	1.9008E+14	8.7022E+14
$\tau_{1/2}$ (min)	1.63	1.01	0.87	0.41	1.62	1.06
(-r)	$1.399E-05N_t^2$	$1.495E-05N_t^2$	$1.743E-05N_t^2$	$5.957E-05N_t^2$	$1.493E-05N_t^2$	$6.846E-04N_t^2$
N_o(g/l)	1063.9430	1743.3752	1386.9626	526.3158	1068.3761	435.8058

Table 4.68: Coag-flocculation kinetic parameters and linear regression coefficient of MPSC in PIE at varying pH and 0.7g/l dosage.

Parameters	pH=1	pH=3	pH=5	pH=7	pH=10	pH=13
	2.261E-0.5x	1.08E-0.5x+	3.04E-0.5x+	3.76E-05x+	1.63E-05x+	8.92E-05x+
Y	+9.48E-04	5.34E-04	4.17E-04	1.372E-03	9.96E-04	3.877E-03
α	2.000	2.000	2.000	2.000	2.000	2.000
R^2	0.839	0 .897	0.754	0.704	0.740	0.743
K(l/g.min)	2.261E-05	1.08E-05	3.04E-05	3.76E-05	1.63E-05	8.92E-05
K_R(l/min)	1.4638E-19	1.5474E-19	1.5801E-19	1.5366E-19	1.5709E-19	1.5734E-19
β_{BR}(l/g.min)	4.52E-05	2.16E-05	6.08E-05	7.52E-05	3.26E-05	1.784E-04
$\varepsilon_p(g^{-1})$	3.08979E+14	1.3959E+14	3.8479E+14	4.8939E+14	2.0752E+14	1.1339E+15
$\tau_{1/2}$ (min)	1.01	1.40	0.50	0.64	1.48	0.81
(-r)	$2.261E\text{-}05N_t^2$	$1.08E\text{-}05N_t^2$	$3.04E\text{-}05N_t^2$	$3.76E\text{-}05N_t^2$	$1.63E\text{-}05N_t^2$	$8.92E\text{-}05N_t^2$
N_o(g/l)	1054.8523	1872.6592	2398.0815	728.863	1004.0161	257.9314

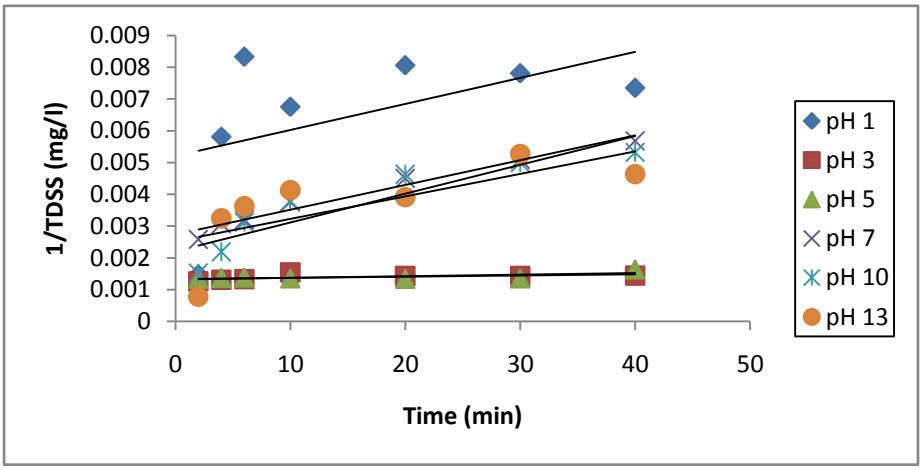

Fig.4.161: kinetic plot of TDSS removal for pH varying PIE medium at 0.1g/l ssc dossage

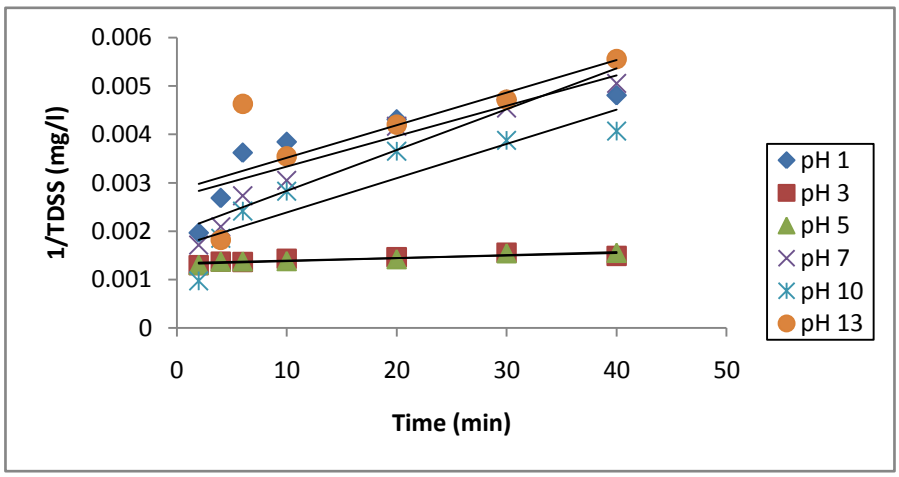

Fig.4.162: kinetic plot of TDSS removal for pH varying PIE medium at 0.2g/l ssc dossage

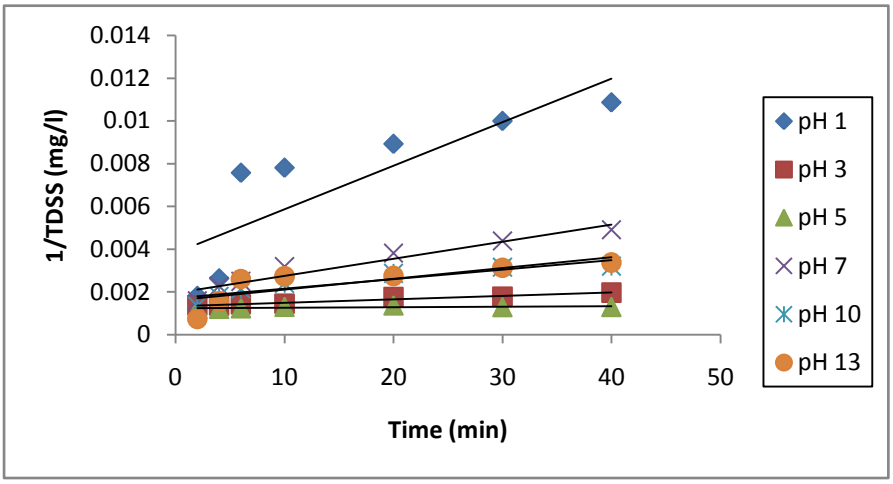

Fig.4.163: kinetic plot of TDSS removal for pH varying PIE medium at 0.3g/l ssc dossage

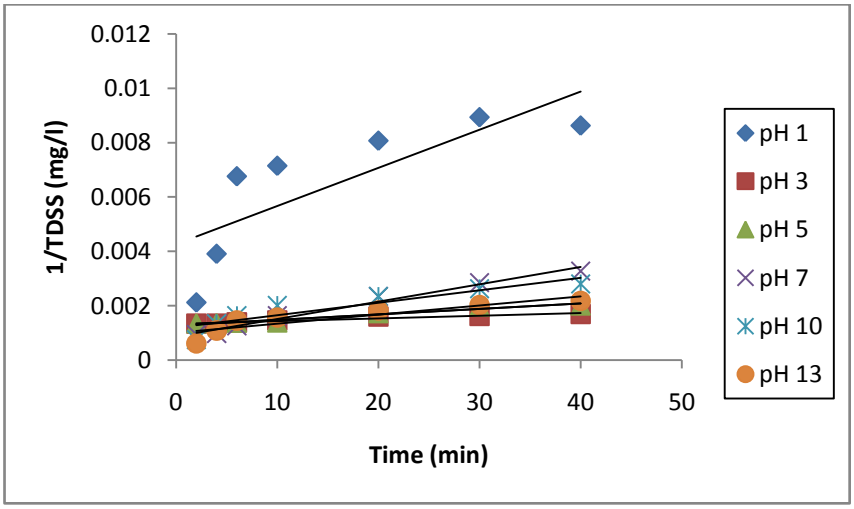

Fig.4.164: kinetic plot of TDSS removal for pH varying PIE medium at 0.4g/l ssc dossage

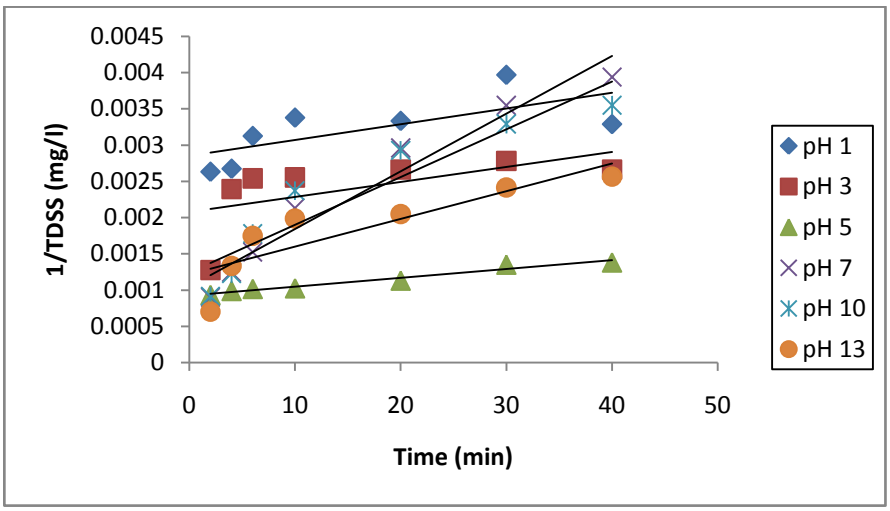

Fig.4.165: kinetic plot of TDSS removal for pH varying PIE medium at 0.5g/l ssc dossage

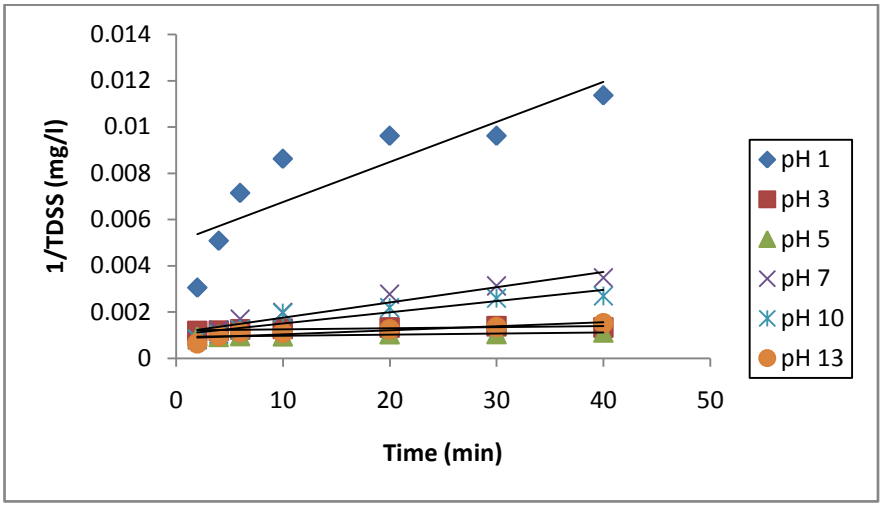

Fig.4.166: kinetic plot of TDSS removal for pH varying PIE medium at 0.6g/l ssc dossage

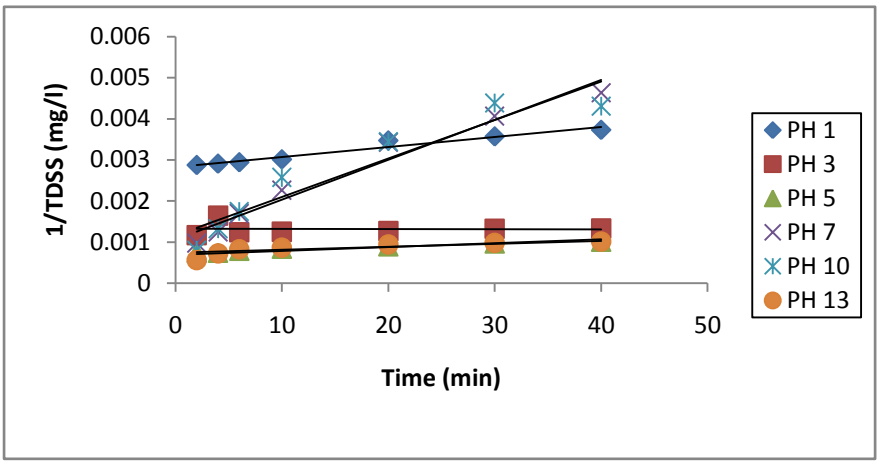

Fig.4.167: kinetic plot of TDSS removal for pH varying PIE medium at 0.7g/l ssc dossage

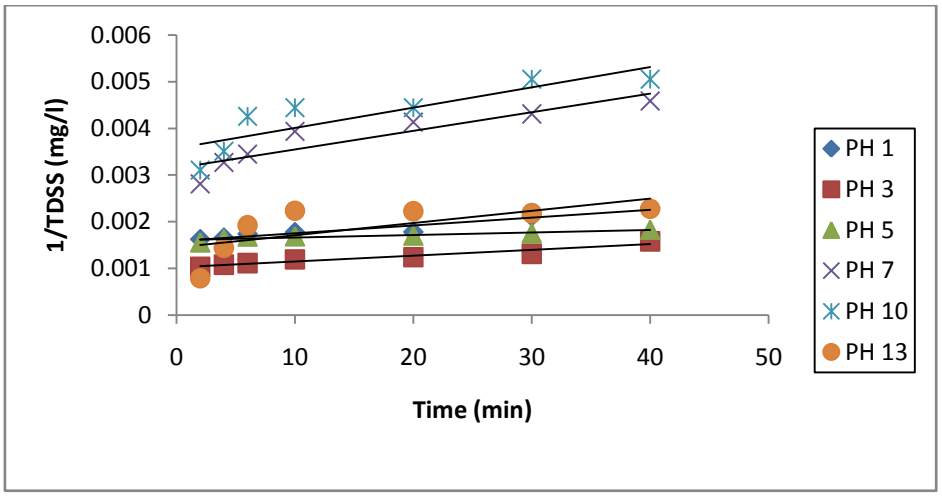

Fig.4.168: kinetic plot of TDSS removal for pH varying PIE medium at 0.1g/l cosc dossage

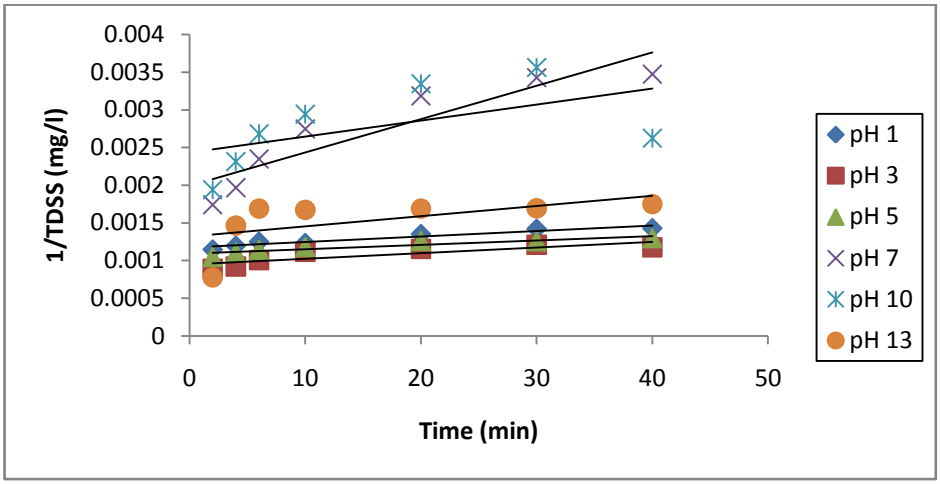

Fig.4.169: kinetic plot of TDSS removal for pH varying PIE medium at 0.2g/l cosc dossage

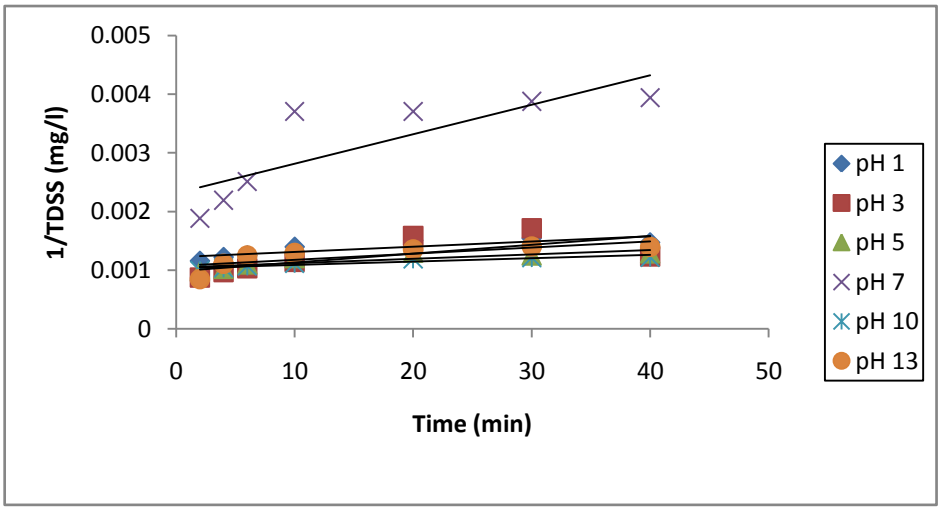

Fig.4.170: kinetic plot of TDSS removal for pH varying PIE medium at 0.3g/l cosc dossage

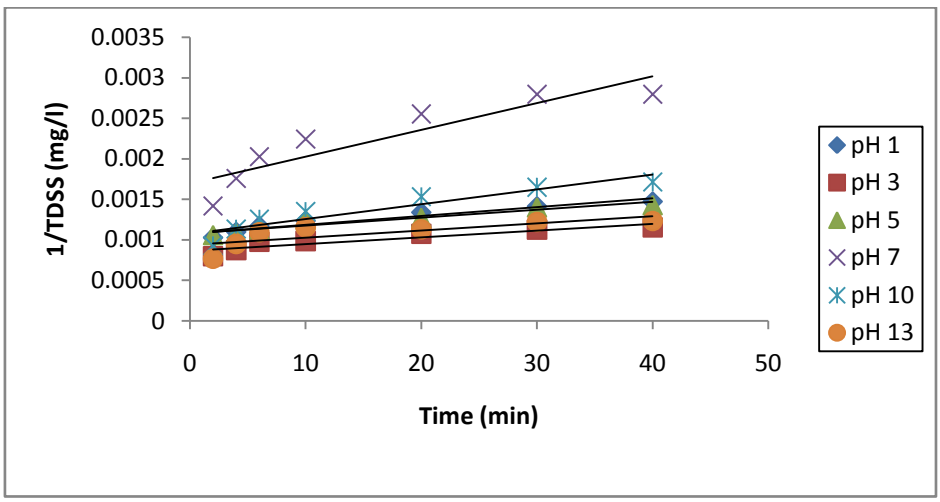

Fig.4.171: kinetic plot of TDSS removal for pH varying PIE medium at 0.4g/l cosc dossage

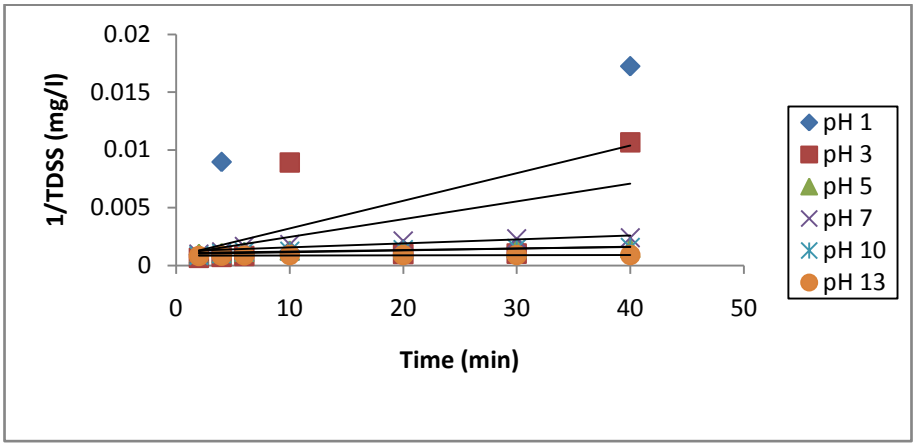

Fig.4.172: kinetic plot of TDSS removal for pH varying PIE medium at 0.5g/l cosc dossage

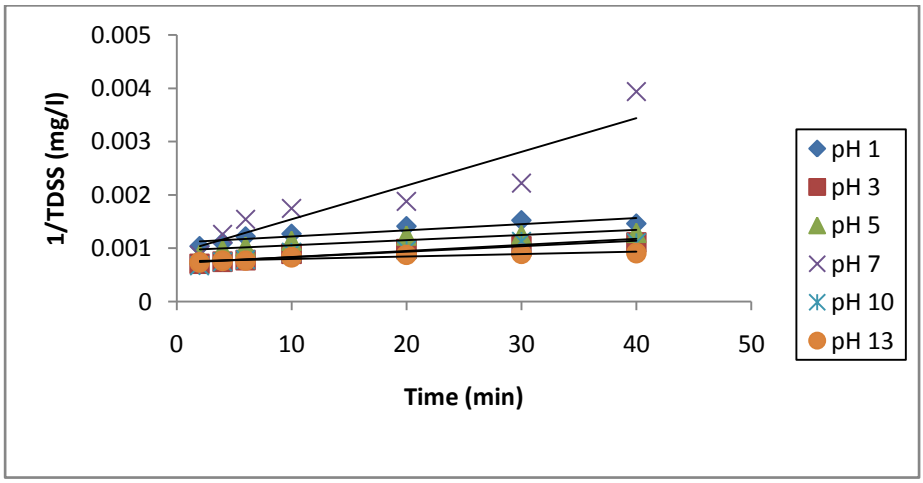

Fig.4.173: kinetic plot of TDSS removal for pH varying PIE medium at 0.6g/l cosc dossage

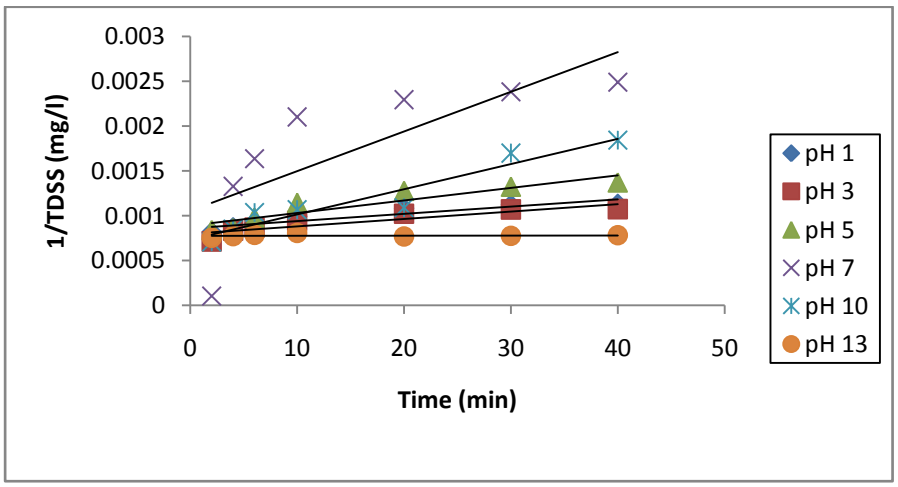

Fig.4.174: kinetic plot of TDSS removal for pH varying PIE medium at 0.7g/l cosc dossage

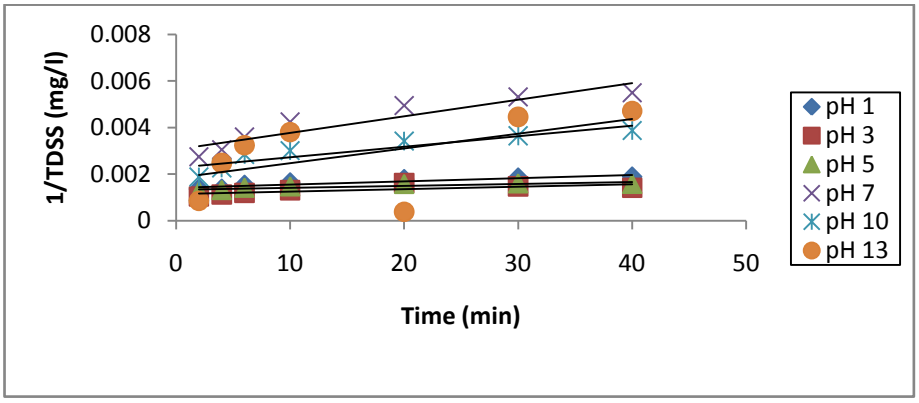

Fig.4.175: kinetic plot of TDSS removal for pH varying PIE medium at 0.1g/l tosc dossage

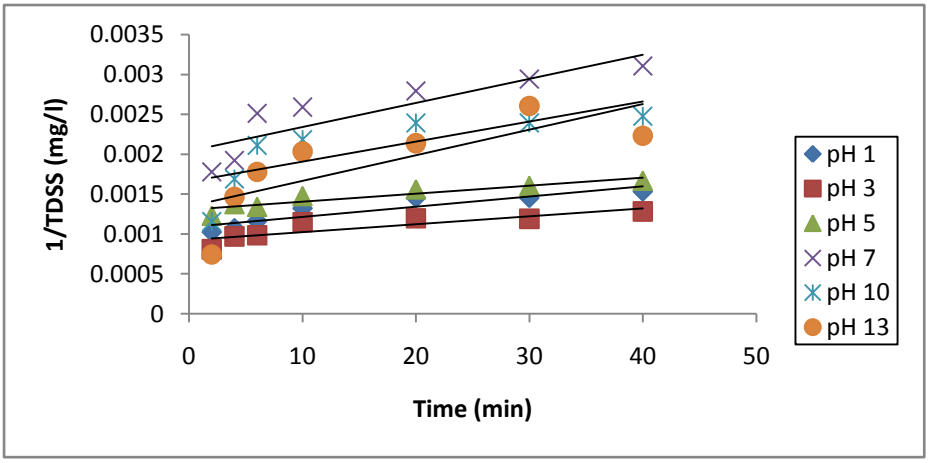

Fig.4.176: kinetic plot of TDSS removal for pH varying PIE medium at 0.2g/l tosc dossage

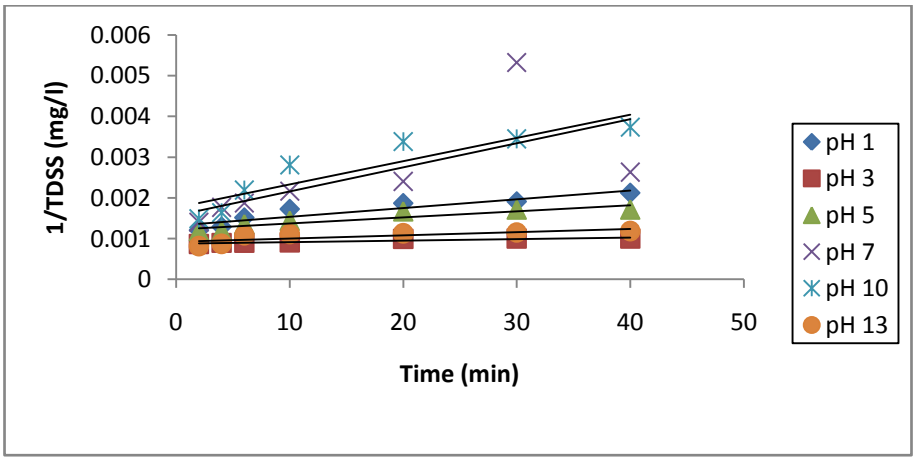

Fig.4.177: kinetic plot of TDSS removal for pH varying PIE medium at 0.3g/l tosc dossage

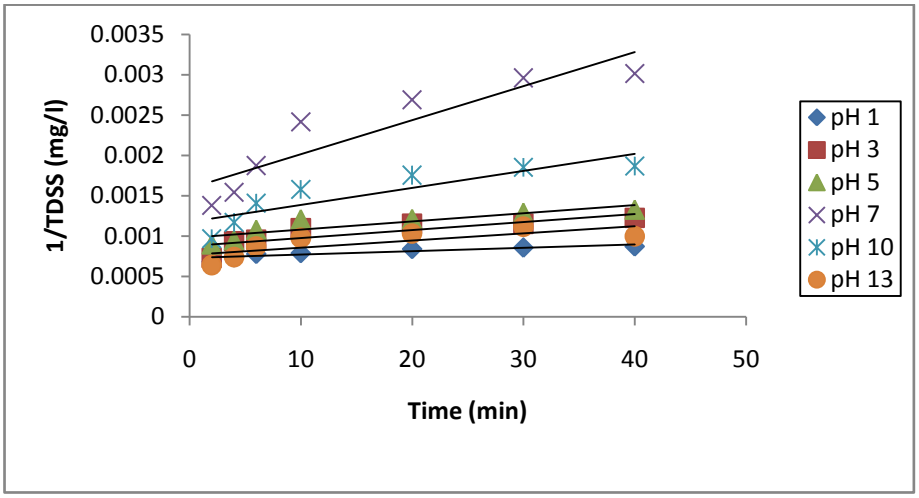

Fig.4.178: kinetic plot of TDSS removal for pH varying PIE medium at 0.4g/l tosc dossage

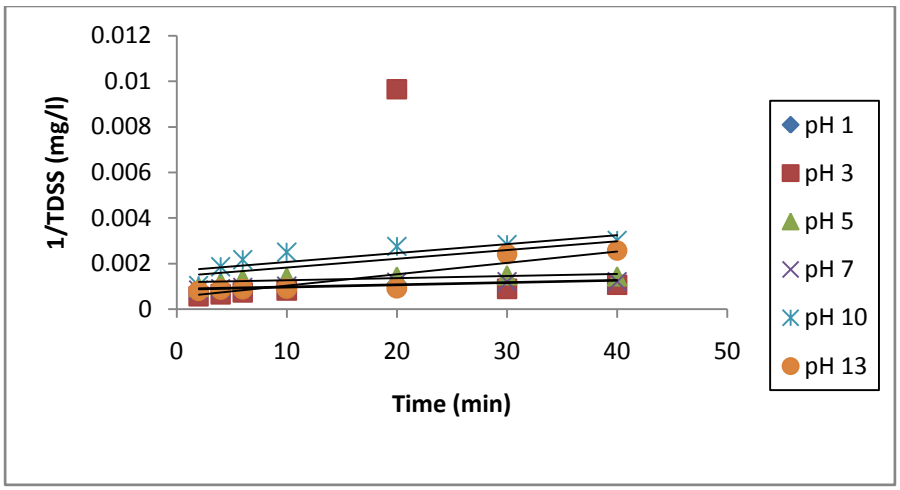

Fig.4.179: kinetic plot of TDSS removal for pH varying PIE medium at 0.5g/l tosc dossage

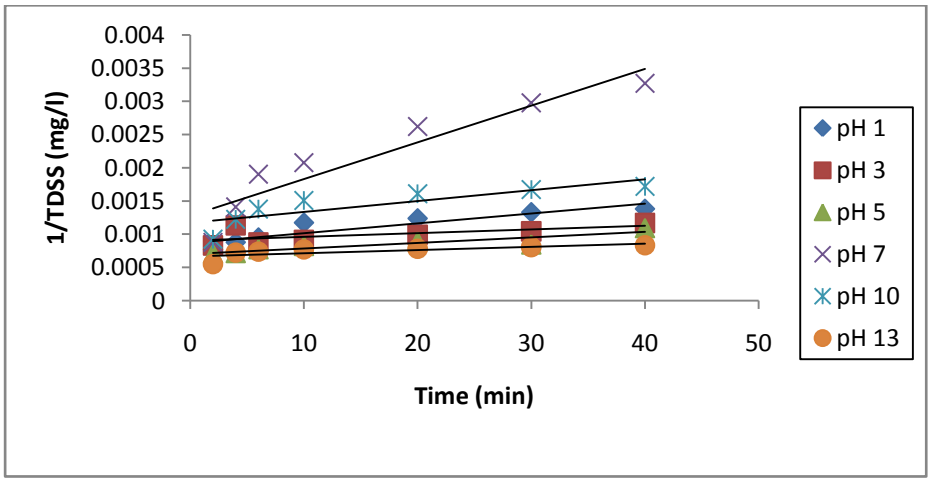

Fig.4.180: kinetic plot of TDSS removal for pH varying PIE medium at 0.6g/l tosc dossage

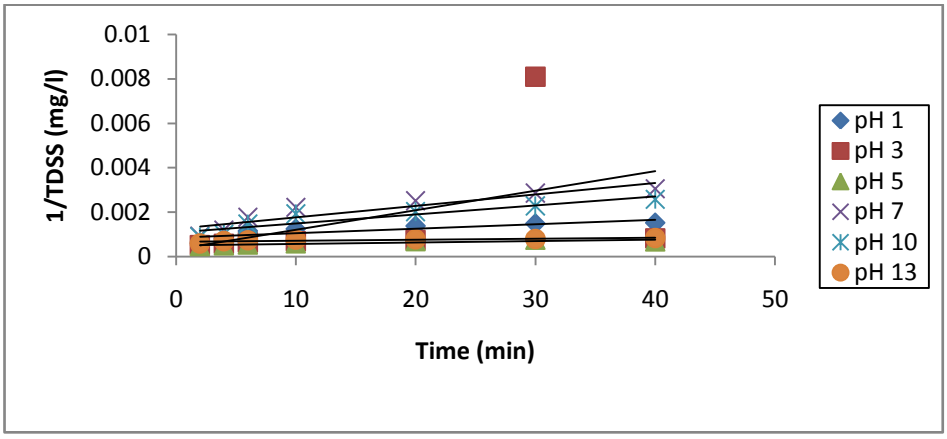

Fig.4.181: kinetic plot of TDSS removal for pH varying PIE medium at 0.7g/l tosc dossage

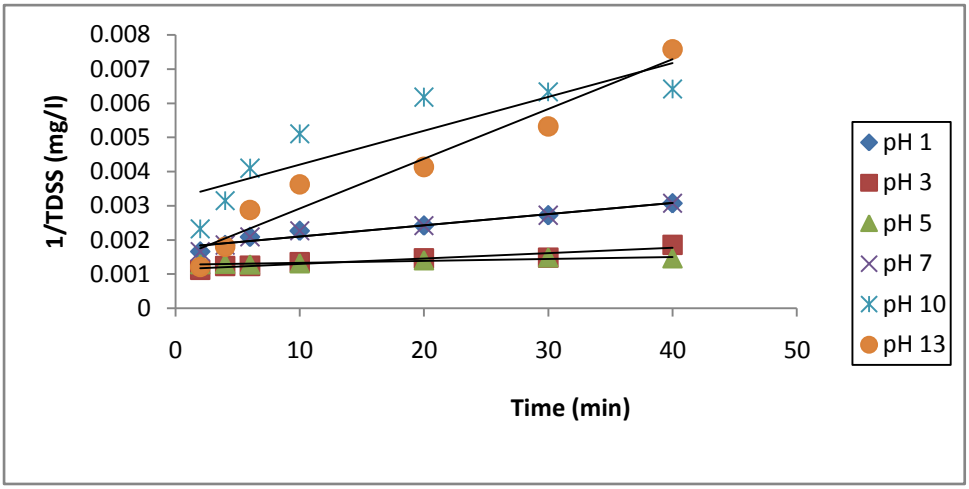

Fig.4.182: kinetic plot of TDSS removal for pH varying PIE medium at 0.1g/l ptsc dossage

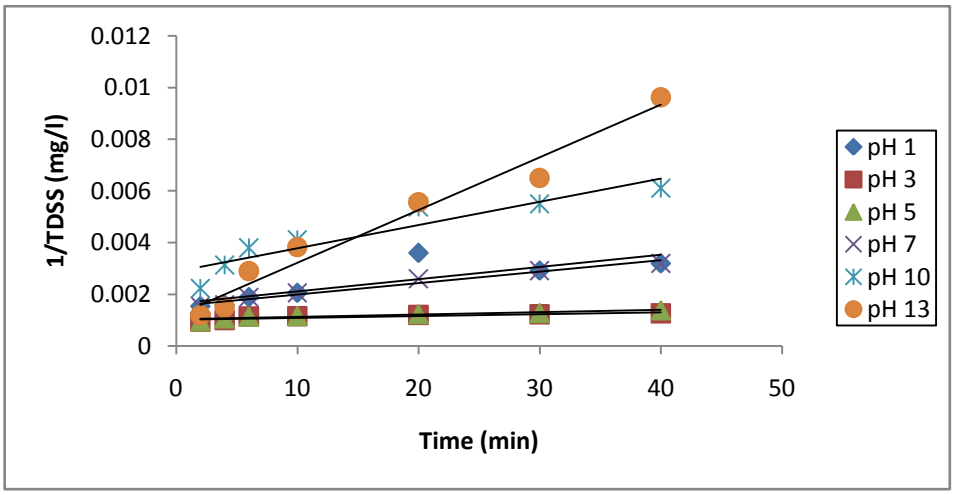

Fig.4.183: kinetic plot of TDSS removal for pH varying PIE medium at 0.2g/l ptsc dossage

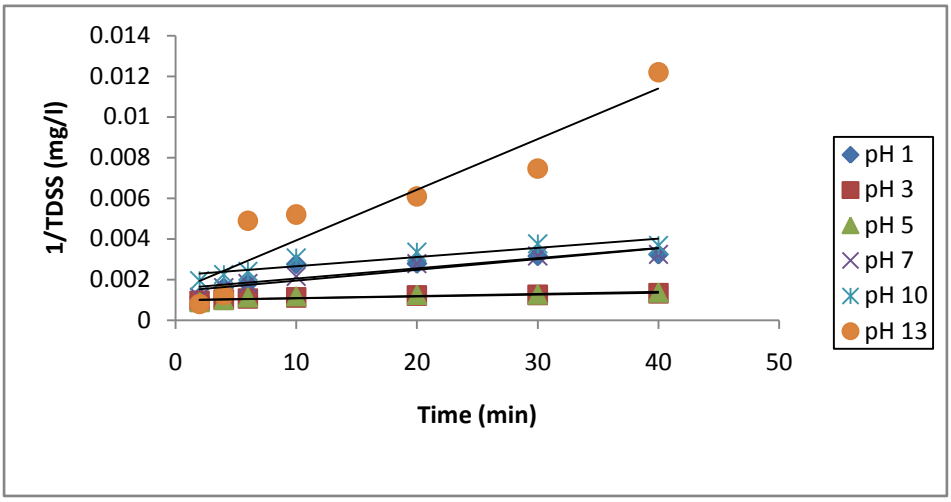

Fig.4.184: kinetic plot of TDSS removal for pH varying PIE medium at 0.3g/l ptsc dossage

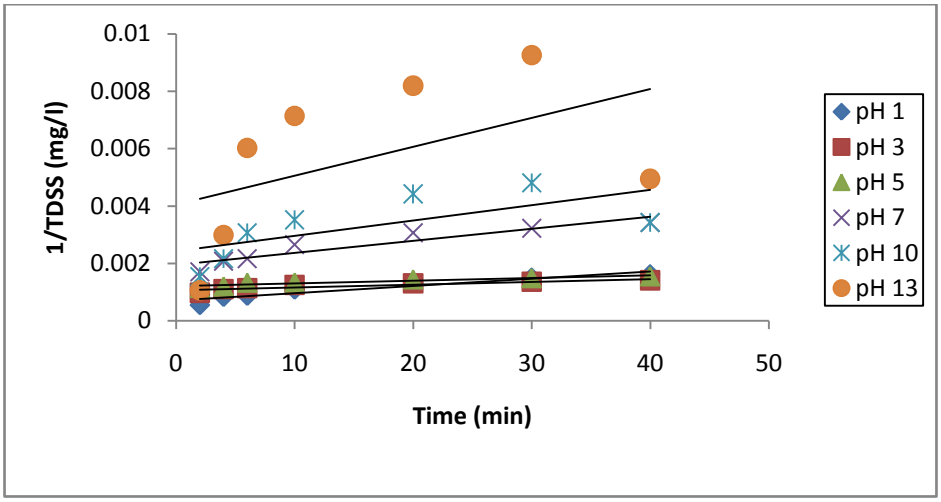

Fig.4.185: kinetic plot of TDSS removal for pH varying PIE medium at 0.4g/l ptsc dossage

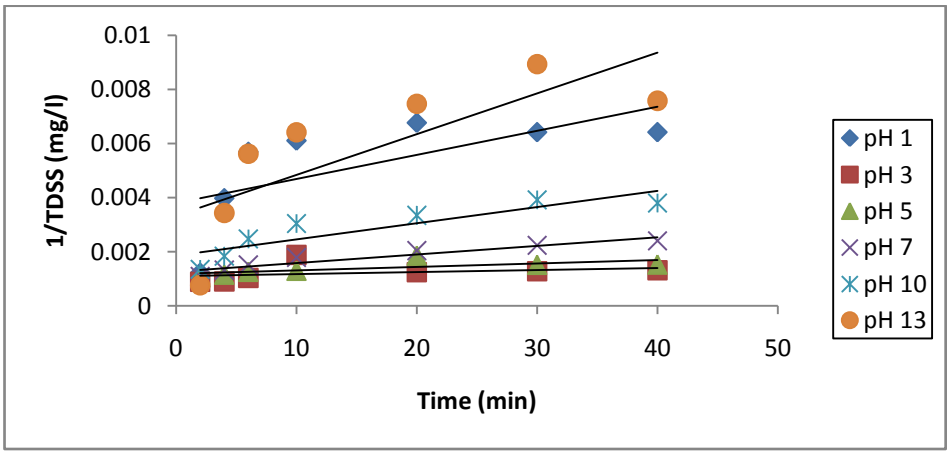

Fig.4.186: kinetic plot of TDSS removal for pH varying PIE medium at 0.5g/l ptsc dossage

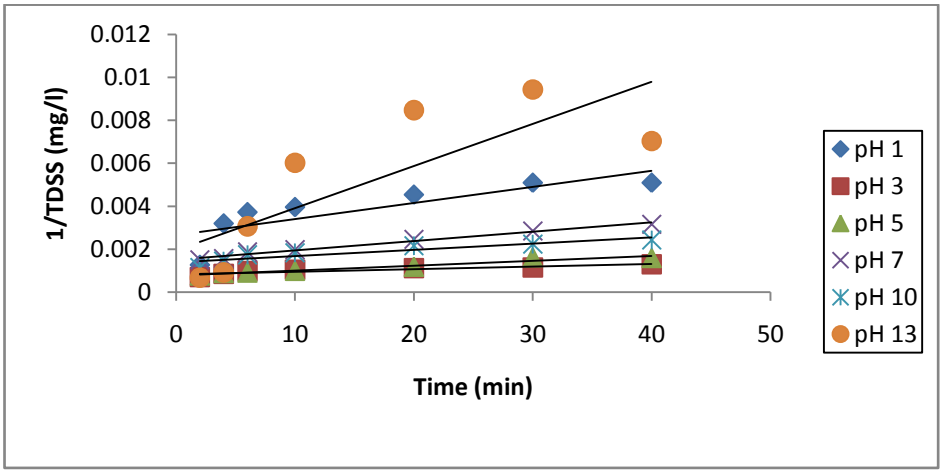

Fig.4.187: kinetic plot of TDSS removal for pH varying PIE medium at 0.6g/l ptsc dossage

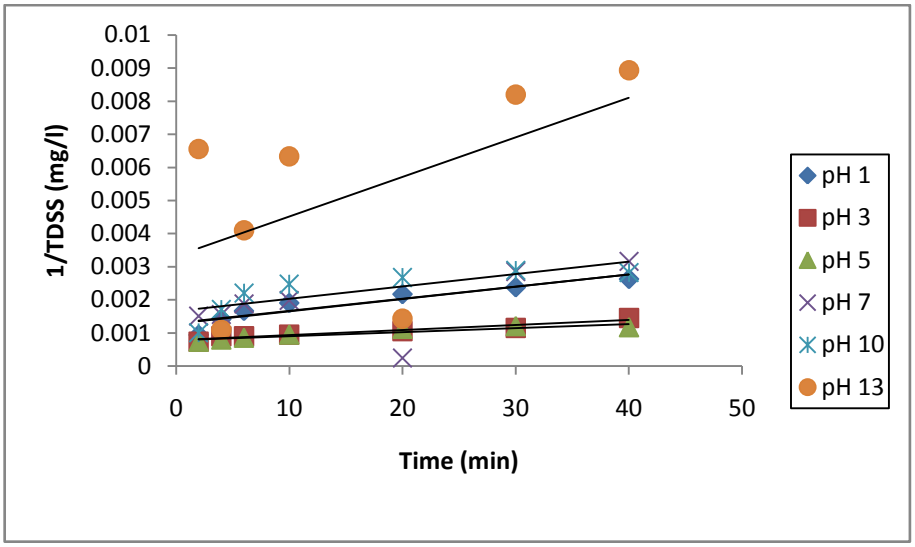

Fig.4.188: kinetic plot of TDSS removal for pH varying PIE medium at 0.7g/l ptsc dossage

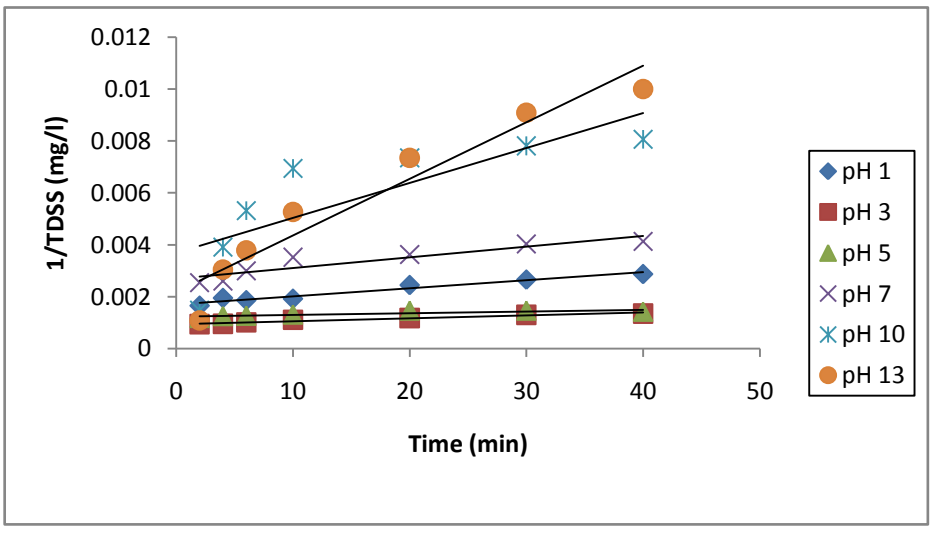

Fig.4.189: kinetic plot of TDSS removal for pH varying PIE medium at 0.1g/l mpsc dossage

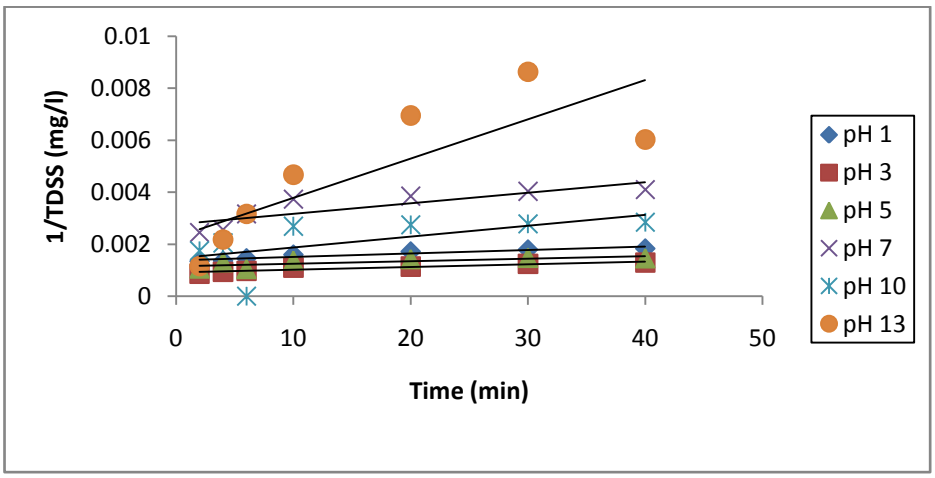

Fig.4.190: kinetic plot of TDSS removal for pH varying PIE medium at 0.2g/l mpsc dossage

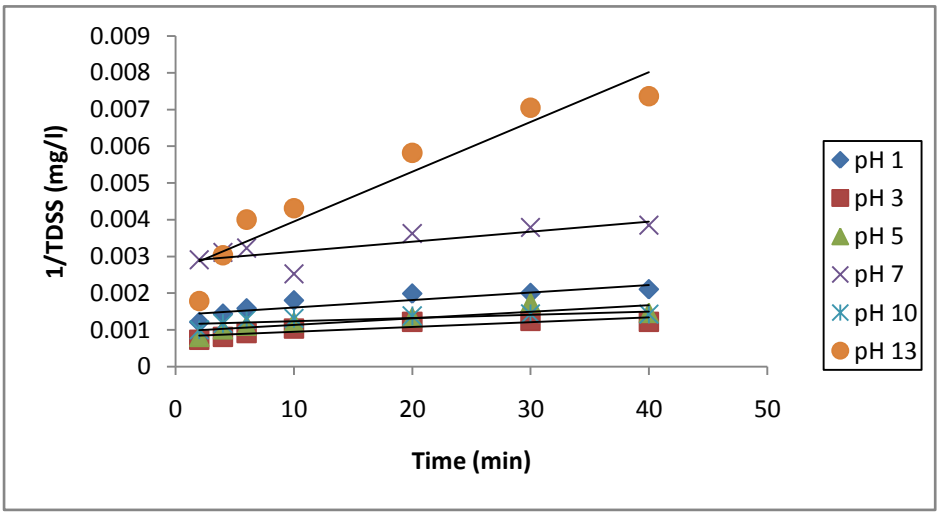

Fig.4.191: kinetic plot of TDSS removal for pH varying PIE medium at 0.3g/l mpsc dossage

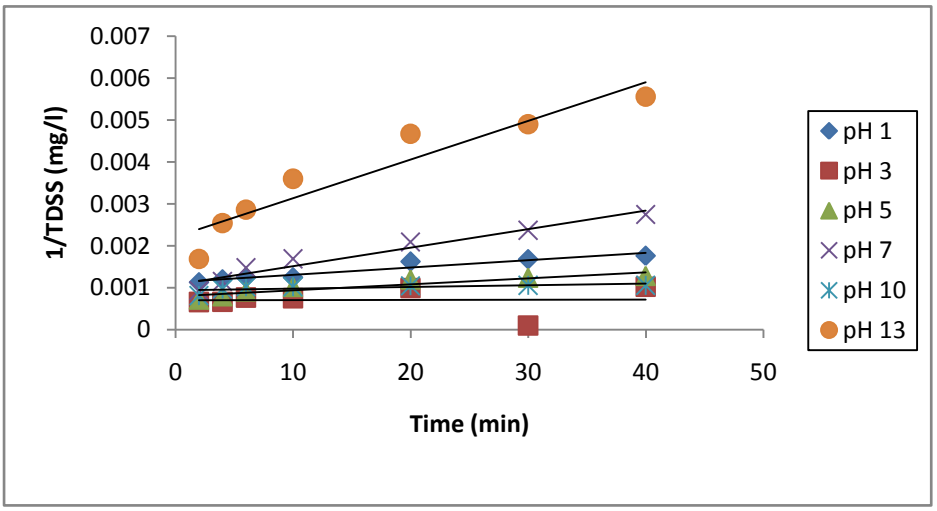

Fig.4.192: kinetic plot of TDSS removal for pH varying PIE medium at 0.4g/l mpsc dossage

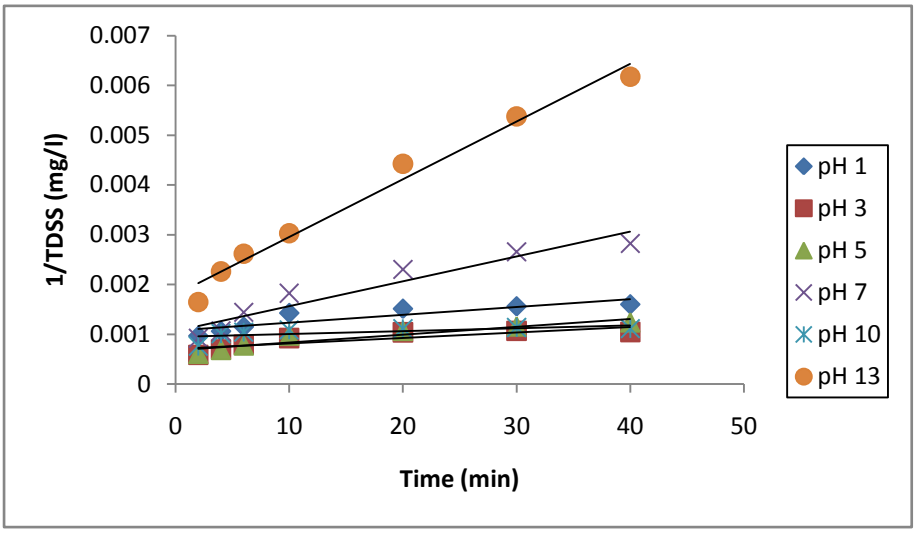

Fig.4.193: kinetic plot of TDSS removal for pH varying PIE medium at 0.5g/l mpsc dossage

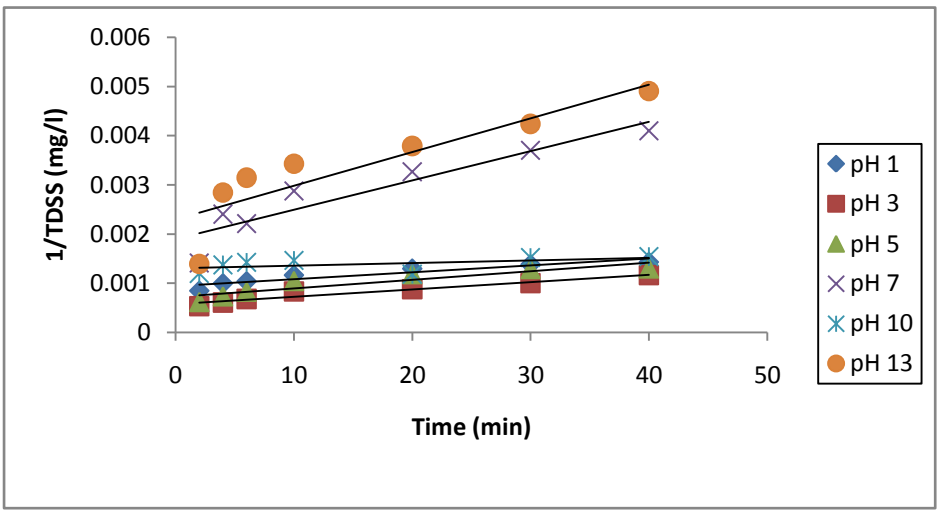

Fig.4.194: kinetic plot of TDSS removal for pH varying PIE medium at 0.6g/l mpsc dossage

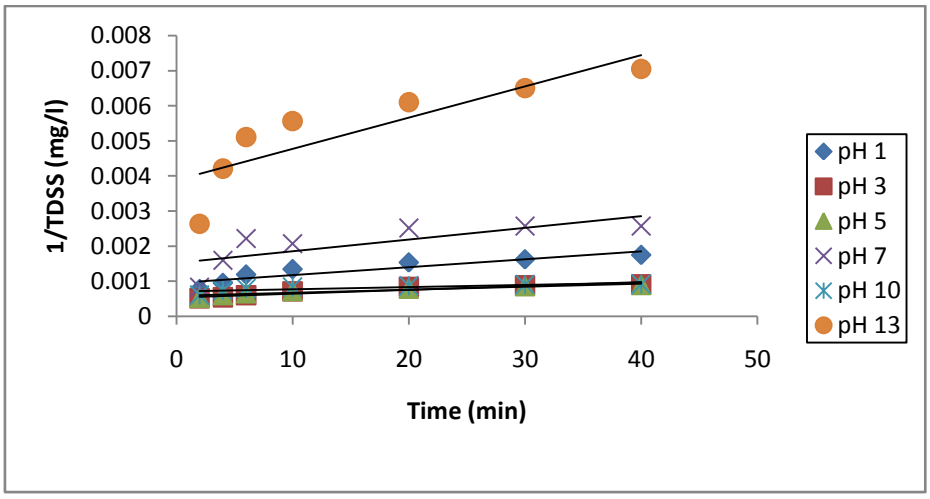

Fig.4.195: kinetic plot of TDSS removal for pH varying PIE medium at 0.7g/l mpsc dosage

4.1.3.4: Kinetic results of dosage varying coag-flocculant in VIE

The results under consideration are presented in tables 4.68 to 4.97. For SSC, a critical observation on tables 4.69 and 4.72, show that all the values of $\tau_{1/2}$ recorded are under subminutes with the exception $\tau_{1/2}$ for pH 3 and 0.4g/l. However, the $\tau_{1/2}$ recorded for pH of 3 and 0.4g/l is 1.10min which is far below the coag-flocculation operation limit. The above phenomenon provide the best efficiency status for the coag-flocculation treatment for SSC. General efficiency status of SSC is satisfactory following low $\tau_{1/2}$ obtained, though, milliseconds has been reported (Von smoluchowski, 1917). The corresponding linear kinetic plots are presented in figs.4.196 to 4.201

Considering, COSC functional parameters posted in tables 4.75 to 4.80. It should be observed that majority of $\tau_{1/2}$ values recorded for all dosages and pH 1, 3, 5, 7 and 10 lies within 1 min. Though the highest $\tau_{1/2}$ of 3.15min $<$ 5 min, justifying the effectiveness of COSC in the treatment of wastewater in practical terms. It is also pertinent to note that the highest efficiency level recorded for (pH of 10 and 0.5g/l), following K = 6.23E – 05l/g.min and $\tau_{1/2}$ = 0.29min, indicate that best performance of COSC is achieved at alkaline region.

The rate parameters for TOSC are posted in tables 4.81 to 4.86. An observation of the tables indicate that, apart from $\tau_{1/2}$ of 16.32min recorded for (pH of 13 and 0.4g/l), all other $\tau_{1/2}$ are in the range of 0 to 5.05min, showing that TOSC can be considered efficient for wastewater and water treatment purposes. The high $\tau_{1/2}$ of 16.32min may be attributed to the fact that TOSC could not utilize its full potentials at that combination, owing to non homogeneity between TDSS and the Coag-flocculants particles in VIE (Menkiti, et al, 2012). The implication will result in less adsorption of TDSS on the coag-flocculant complex or cations. From the foregoing, the higher TDSS attachment, on the coag-flocculants radicals, the lower the $\tau_{1/2}$. The corresponding kinetic linear plots are presented in figs. 4.208 to 4.213

For PTSC, the results are presented in tables 4.87 to 4.92. Generally, the performance of PTSC can be said to be efficient for all pH and dosages considered, because the highest $\tau_{1/2}$ of 3.07min is within coag-flocculation operation limit. Specifically, the best performance of PTSC is recorded for pH of 10 and 0.2g/l dosage, supported by $\tau_{1/2}$ of 0.19min and K of 1.91E – 04 l/g.min. This is an indication that there is relatively perfect

mixing between the TDSS and coag-flocculants particles throughout the dispersion period. The corresponding linear plots are presented in figures. 4.214 to 4.219

Considering MPSC, the results are presented in tables 4.93 to 4.97. Generally, the functional parameters have similar behavior as the ones of PTSC. Hence the discussion on PTSC is still applicable to this case. But it should be noted that MPSC optimum coag-flocculation is achieved at pH of 13 and 0.4g/l .The implication of these results from theoretical background, is that, it is favorable to operate coag-flocculation process with, the pH and dosage range considered. The corresponding linear kinetic plots are presented in figures.4.220 to 4.225

Table 4.69: Coag-Flocculation Kinetic Parameters and Linear Regression Coefficient of SSC in VIE at varying dosage and pH of 1.

Parameters	0.1g/l	0.2g/l	0.3g/l	0.4g/l	0.5g/l	0.6g/l	0.7g/l
Y	1.8E-05x + 2.094E-03	2.57E-05x + 1.371E-03	1.602E-05x + 6.8991E-03	1.785E-05x + 5.34E-03	3.26E-05x + 6.2114E-03	9.664E-06x + 6.0344E-03	8.44E-06x + 5.444E-03
α	2.000	2.000	2.000	2.000	2.000	2.000	2.000
R^2	0.843	0.798	0.873	0.959	0.856	0.872	0.776
K(l/g.min)	1.8E-05	2.57E-05	1.602-05	1.785E-05	3.26E-05	9.664E-06	8.44E-06
K_R(l/min)	1.1829E-19	1.1829E-19	1.1848E-19	1.1848E-19	1.1848E-19	1.1848E-19	1.1868E-19
β_{BR}(l/g.min)	3.6E-05	5.14E-05	3.204E-05	3.57E-05	6.52E-05	1.9328E-05	1.688E-05
$\varepsilon_p(g^{-1})$	3.0434E+14	4.3453E+14	2.7061E+14	3.0132E+14	5.5030E+14	1.6286E+14	1.4223E+14
$\tau_{½}$ (min)	2.01	1.41	2.26	2.03	1.11	3.75	4.29
(-r)	$1.8E\text{-}05N_t^2$	$2.57E\text{-}05N_t^2$	$1.602\text{-}05\ N_t^2$	$1.785E\text{-}05N_t^2$	$3.26E\text{-}05N_t^2$	$9.664E\text{-}06\ N_t^2$	$8.44E\text{-}06N_t^2$
N_o (g/l)	117.0823	141.4827	144.9464	187.2659	160.9943	165.716	183.6885

Table 4.70: Coag-Flocculation Kinetic Parameters and Linear Regression Coefficient of SSC in VIE at varying dosage and pH of 3.

Parameters	0.1g/l	0.2g/l	0.3g/l	0.4g/l	0.5g/l	0.6g/l	0.7g/l
Y	3.6E-05x + 4.438E-03	2.84E-05x + 3.906E-03	3.786E-05x + 3.4615E-03	2.190E-05x + 3.715E-03	5.57E-05x + 2.5454E-03	6.828E-05x + 1.9915E-03	7.93E-05x + 1.809E-03
α	2.000	2.000	2.000	2.000	2.000	2.000	2.000
R^2	0.855	0.818	0.974	0.775	0.775	0.670	0.747
K(l/g.min)	3.6E-05	2.84E-05	3.786E-05	2.190E-05	5.57E-05	6.828E-05	7.93E-05
K_R(l/min)	1.1809E-19	1.1809E-19	1.1829E-19	1.1829E-19	1.1829E-19	1.1868E-19	1.1868E-19
β_{BR}(l/g.min)	7.2E-05	5.65E-05	7.572E-05	4.38E-05	1.114E-04	1.3656E-04	1.586E-04
$\varepsilon_p(g^{-1})$	6.097E+14	4.8099E+14	6.4012E+14	3.7028E+14	9.4175E+14	1.1507E+15	1.3364E+15
$\tau_{½}$ (min)	0.67	0.85	0.64	1.10	0.43	0.35	0.30
(-r)	$3.6E\text{-}05N_t^2$	$2.84E\text{-}05N_t^2$	$3.786E\text{-}05N_t^2$	$2.190E\text{-}05N_t^2$	$5.57E\text{-}05N_t^2$	$6.828E\text{-}05N_t^2$	$7.93E\text{-}05N_t^2$
N_o (g/l)	225.3267	256.0164	288.8921	268.9401	392.8656	502.1341	552.7916

Table 4.71: Coag-Flocculation Kinetic Parameters and Linear Regression Coefficient of SSC in VIE at varying dosage and pH of 5.

Parameters	0.1g/l	0.2g/l	0.3g/l	0.4g/l	0.5g/l	0.6g/l	0.7g/l
Y	2.4E-05x + 5.882E-03	1.53E-05x + 3.962E-03	3.30E-05x + 3.0976E-03	3.114E-05x + 2.3914E-03	5.40E-05x + 2.2006E-03	5.523E-05x + 2.42E-03	5.25E-05x + 1.842E-03
α	2.000	2.000	2.000	2.000	2.000	2.000	2.000
R^2	0.664	0.676	0.865	0.686	0.962	0.945	0.952
K(l/g.min)	2.4E-05	1.53E-05	3.30E-05	3.114E-05	5.40E-05	5.523E-05	5.25E-05
K_R(l/min)	1.1691E-19	1.1691E-19	1.1691E-19	1.1711E-19	1.1711E-19	1.1711E-19	1.1731E-19
β_{BR}(l/g.min)	4.8E-05	3.06E-05	6.6E-05	6.228E-05	1.08E-04	1.1046E-04	1.05E-04
$\varepsilon_p(g^{-1})$	4.1057E+14	2.6174E+14	5.6454E+14	5.3181E+14	9.2221E+14	9.4322E+14	8.9506E+14
$\tau_{½}$ (min)	1.51	2.37	1.10	1.16	0.67	0.65	0.69
(-r)	$2.4E\text{-}05N_t^2$	$1.53E\text{-}05N_t^2$	$3.30E\text{-}05N_t^2$	$3.114E\text{-}05N_t^2$	$5.40E\text{-}05N_t^2$	$5.523E\text{-}05N_t^2$	$5.25E\text{-}05N_t^2$
N_o (g/l)	170.0102	252.3978	322.8306	418.1651	454.4215	413.2231	542.8882

Table 4.72 Coag-Flocculation Kinetic Parameters and Linear Regression Coefficient of SSC in VIE at varying dosage and pH of 7.

Parameters	0.1g/l	0.2g/l	0.3g/l	0.4g/l	0.5g/l	0.6g/l	0.7g/l
Y	2.2E-05x + 4.659E-03	4.38E-05x + 3.02E-03	5.087E-05x +2.0513E-03	+2.843E-05x + 2.7637E-03	4.47E-05x + 2.0219E-03	2.709E-05x + 2.2255E-03	3.46E-05x + 1.971E-03
α	2.000	2.000	2.000	2.000	2.000	2.000	2.000
R^2	0.896	0.780	0.937	0.760	0.723	0.850	0.938
K(l/g.min)	2.2E-05	4.38E-05	5.087E-05	2.843E-05	4.47E-05	2.709E-05	3.46E-05
K_R(l/min)	1.1770E-19	1.1770E-19	1.1770E-19	1.1770E-19	1.1789E-19	1.1789E-19	1.1789E-19
β_{BR}(l/g.min)	4.4E-05	8.76E-05	1.0174E-05	5.686E-05	8.94E-05	5.418E-05	6.92E-05
$\varepsilon_p(g^{-1})$	3.7383E+14	7.4427E+14	8.6440E+14	4.8309E+14	7.5833E+14	4.5958E+14	5.8699E+14
$\tau_{½}$ (min)	1.65	0.83	0.71	1.27	0.81	1.34	1.05
(-r)	$2.2E\text{-}05N_t^2$	$4.38E\text{-}05N_t^2$	$5.087E\text{-}05N_t^2$	$2.843E\text{-}05N_t^2$	$4.47E\text{-}05N_t^2$	$2.709E\text{-}05N_t^2$	$3.46E\text{-}05N_t^2$
N_o (g/l)	214.6383	331.1258	482.4952	361.8338	494.5843	449.3372	507.3567

Table 4.73: Coag-Flocculation Kinetic Parameters and Linear Regression Coefficient of SSC in VIE at varying dosage and pH of 10.

Parameters	0.1g/l	0.2g/l	0.3g/l	0.4g/l	0.5g/l	0.6g/l	0.7g/l
Y	2.6E-05x + 2.369E-03	4.70E-05x + 2.225E-03	4.516E-05x + 1.2635E-03	4.867E-05x + 9.985E-04	4.80E-05x + 7.737E-04	3.247E-05x + 8.512E-04	2.36E-05x + 5.95E-04
α	2.000	2.000	2.000	2.000	2.000	2.000	2.000
R^2	0.849	0.886	0.951	0.982	0.997	0.877	0.961
K(l/g.min)	2.6E-05	4.70E-05	4.516E-05	4.867E-05	4.80E-05	3.247E-05	2.36E-05
K_R(l/min)	1.1711E-19	1.1711E-19	1.1711E-19	1.1731E-19	1.1731E-19	1.1750E-19	1.1750E-19
β_{BR}(l/g.min)	5.2E-05	9.4E-05	9.032E-05	9.734E-05	9.6E-05	6.494E-05	4.72E-05
$\varepsilon_p(g^{-1})$	4.4403E+14	8.0266E+14	7.7124E+14	8.2977E+14	8.1834E+14	5.5268E+14	4.0170E+14
$\tau_{½}$ (min)	0.62	0.34	0.36	0.33	0.34	0.50	0.68
(-r)	$2.6E\text{-}05N_t^2$	$4.70E\text{-}05N_t^2$	$4.516E\text{-}05N_t^2$	$4.867E\text{-}05N_t^2$	$4.80E\text{-}05N_t^2$	$3.247E\text{-}05N_t^2$	$2.36E\text{-}05N_t^2$
N_o (g/l)	422.1190	449.4382	791.4523	1001.5023	1292.4906	1174.8120	1680.6723

Table 4.74: Coag-Flocculation Kinetic Parameters and Linear Regression Coefficient of SSC in VIE at varying dosage and pH of 13.

Parameters	0.1g/l	0.2g/l	0.3g/l	0.4g/l	0.5g/l	0.6g/l	0.7g/l
Y	3.6E-05x + 1.681E-03	1.0E-05x + 2.362E-03	3.455E-05x + 1.6151E-03	2.058E-05x + 1.0398E-03	1.10E-05x + 7.251E-04	1.431E-05x + 7.793E-04	2.06E-05x + 1.618E-04
α	2.000	2.000	2.000	2.000	2.000	2.000	2.000
R^2	0.963	0.964	0.785	0.834	0.715	0.847	0.639
K(l/g.min)	3.6E-05	1.0E-05	3.455E-05	2.058E-05	1.10E-05	1.431E-05	2.06E-05
K_R(l/min)	1.1770E-19	1.1779E-19	1.1789E-19	1.1789E-19	1.1809E-19	1.1809E-19	1.1809E-19
β_{BR}(l/g.min)	7.2E-05	2.0E-05	6.91E-05	4.116E-05	2.20E-05	2.862E-05	4.12E-05
$\varepsilon_p(g^{-1})$	6.1172E+14	1.6992E+14	5.8614E+14	3.4914E+14	1.8630E+14	2.4236E+14	3.4889E+14
$\tau_{½}$ (min)	0.50	1.81	0.52	4.21	1.65	1.27	0.88
(-r)	$3.6E\text{-}05N_t^2$	$1.0E\text{-}05\ N_t^2$	$3.455E\text{-}05N_t^2$	$2.058E\text{-}05\ N_t^2$	$1.10E\text{-}05N_t^2$	$1.431E\text{-}05N_t^2$	$2.06E\text{-}05N_t^2$
N_o (g/l)	594.8840	423.3700	619.1567	961.7234	1379.1201	1283.2029	618.0470

Table 4.75: Coag-Flocculation Kinetic Parameters and Linear Regression Coefficient of COSC inVIE at varying dosage and pH of 1.

Parameters	0.1g/l	0.2g/l	0.3g/l	0.4g/l	0.5g/l	0.6g/l	0.7g/l
Y	2.6E-05x + 2.962E-03	4.16E-05x + 3.128E-03	4.286E-05x + 1.9978E-03	4.896E-05x + 2.0545E-03	1.95E-05x + 1.1437E-03	4.84E-05x + 1.6271E-03	1.84E-05x + 8.66E-04
α	2.000	2.000	2.000	2.000	2.000	2.000	2.000
R^2	0.776	0.694	0.877	0.888	0.807	0.978	0.977
K(l/g.min)	2.6E-05	4.16E-05	4.286E-05	4.896E-05	1.95E-05	4.84E-05	1.84E-05
K_R(l/min)	1.1848E-19	1.1848E-19	1.1868E-19	1.1868E-19	1.1868E-19	1.1887E-19	1.1887E-19
β_{BR}(l/g.min)	5.2E-05	8.32E-05	8.572E-05	9.792E-05	3.9E-05	9.68E-05	3.68E-05
$\varepsilon_p(g^{-1})$	4.3889E+14	7.0223E+14	2.6997E+14	8.2508E+14	3.2861E+14	8.1433E+14	3.0958E+14
$\tau_{½}$ (min)	0.93	0.58	0.56	0.49	1.24	0.50	1.31
(-r)	$2.6E\text{-}05N_t^2$	$4.16E\text{-}05N_t^2$	$4.286E\text{-}05N_t^2$	$4.896E\text{-}05N_t^2$	$1.95E\text{-}05N_t^2$	$4.84E\text{-}05N_t^2$	$1.84E\text{-}05N_t^2$
N_o (g/l)	337.6097	319.6931	500.5506	486.7364	874.3552	614.5904	1154.7344

Table 4.76: Coag-Flocculation Kinetic Parameters and Linear Regression Coefficient of COSC in VIE at varying dosage and pH of 3**.**

Parameters	0.1g/l	0.2g/l	0.3g/l	0.4g/l	0.5g/l	0.6g/l	0.7g/l
Y	4.4E-05x + 3.411E-03	6.45E-05x + 2.725E-03	7.115E-05x + 1.5377E-03	5.211E-05x + 1.5184-03	2.55E-05x + 1.0739E-03	4.102E-05x + 1.338E-03	4.06E-05x + 1.022E-03
α	2.000	2.000	2.000	2.000	2.000	2.000	2.000
R^2	0.692	0.769	0.953	0.870	0.798	0.794	0.863
K(l/g.min)	4.4E-05	6.45E-05	7.115E-05	5.211E-05	2.55E-05	4.102E-05	4.06E-05
K_R(l/min)	1.1868E-19	1.1868E-19	1.1868E-19	1.1887E-19	1.1887E-19	1.1907E-19	1.1907E-19
β_{BR}(l/g.min)	8.8E-05	1.29E-04	1.423E-04	1.0422E-04	5.1E-05	8.204E-05	8.12E-05
$\varepsilon_p(g^{-1})$	7.4149E+14	1.0870E+15	1.1990E+15	8.7676E+14	4.2904E+14	6.8901E+14	6.8195E+14
$\tau_{½}$ (min)	0.55	0.37	0.34	0.46	0.95	0.59	0.60
(-r)	$4.4E\text{-}05N_t^2$	$6.45E\text{-}05N_t^2$	$7.115E\text{-}05N_t^2$	$5.211E\text{-}05N_t^2$	$2.55E\text{-}05N_t^2$	$4.102E\text{-}05N_t^2$	$4.06E\text{-}05N_t^2$
N_o (g/l)	293.1692	366.9725	650.3219	658.5880	931.1854	747.3816	978.4736

Table 4.77: Coag-Flocculation Kinetic Parameters and Linear Regression Coefficient of COSC inVIE at varying dosage and pH of 5.

Parameters	0.1g/l	0.2g/l	0.3g/l	0.4g/l	0.5g/l	0.6g/l	0.7g/l
Y	4.2E-05x + 2.452E-03	6.02E-05x + 2.663E-03	2.494E-05x + 1.4425E-03	4.444E-05x + 1.3095E-03	4.30E-05x + 1.2127E-03	2.713E-05x + 7.869E-04	3.16E-05x + 9.57E-04
α	2.000	2.000	2.000	2.000	2.000	2.000	2.000
R^2	0.927	0.716	0.934	0.912	0.890	0.987	0.874
K(l/g.min)	4.2E-05	6.02E-05	2.494E-05	4.444E-05	4.30E-05	2.713E-05	3.16E-05
K_R(l/min)	1.1731E-19	1.1731E-19	1.1731E-19	1.1731E-19	1.1750E-19	1.1750E-19	1.1750E-19
β_{BR}(l/g.min)	8.84E-05	1.204E-04	4.988E-05	8.888E-05	8.6E-05	5.426E-05	6.32E-05
$\varepsilon_p(g^{-1})$	7.1605E+14	1.0263E+15	4.2520E+14	7.5765E+14	7.3191E+14	4.6179E+14	5.3787E+14
$\tau_{½}$ (min)	0.58	0.40	0.97	0.54	0.56	0.89	0.76
(-r)	$4.2E\text{-}05N_t^2$	$6.02E\text{-}05N_t^2$	$2.494E\text{-}05N_t^2$	$4.444E\text{-}05N_t^2$	$4.30E\text{-}05N_t^2$	$2.713E\text{-}05N_t^2$	$3.16E\text{-}05N_t^2$
N_o (g/l)	407.8303	375.5163	693.2409	763.6502	824.6063	1270.8095	1044.9321

Table 4.78: Coag-Flocculation Kinetic Parameters and Linear Regression Coefficient of COSC inVIE at varying dosage and pH of 7.

Parameters	0.1g/l	0.2g/l	0.3g/l	0.4g/l	0.5g/l	0.6g/l	0.7g/l
Y	4.4E-05x + 3.569E-03	4.98E-05x + 2.293E-03	5.745E-06x + 1.0301E-03	1.794E-05x + 1.0764E-03	1.60E-05x + 9.841E-03	1.145E-05x + 7.173E-04	2.90E-05x + 7.63E-04
α	2.000	2.000	2.000	2.000	2.000	2.000	2.000
R^2	0.743	0.824	0.847	0.858	0.837	0.894	0.967
K(l/g.min)	4.4E-05	4.98E-05	5.745E-06	1.794E-05	1.60E-05	1.145E-05	2.90E-05
K_R(l/min)	1.1789E-19	1.1789E-19	1.1789E-19	1.1809E-19	1.1809E-19	1.1829E-19	1.1829E-19
β_{BR}(l/g.min)	8.8E-05	9.96E-05	1.149E-05	3.588E-05	3.2E-05	2.29E-05	5.8E-05
$\varepsilon_p(g^{-1})$	7.4646E+14	8.4486E+14	9.7464E+14	3.038E+14	2.7098E+14	1.9359E+14	4.9032E+14
$\tau_{½}$ (min)	0.41	0.36	3.15	1.01	1.13	1.58	0.62
(-r)	$4.4E\text{-}05N_t^2$	$4.98E\text{-}05N_t^2$	$5.745E\text{-}06N_t^2$	$1.794E\text{-}05N_t^2$	$1.60E\text{-}05N_t^2$	$1.145E\text{-}05N_t^2$	$2.90E\text{-}05N_t^2$
N_o (g/l)	280.1905	436.1099	970.7795	929.0227	1016.1569	1394.1168	1310.6160

Table 4.79: Coag-Flocculation Kinetic Parameters and Linear Regression Coefficient of COSC inVIE at varying dosage and pH of 10.

Parameters	0.1g/l	0.2g/l	0.3g/l	0.4g/l	0.5g/l	0.6g/l	0.7g/l
Y	6.0E-06x + 2.106E-03	4.21E-05x + 2.29E-03	1.967E-05x + 1.8413E-03	2.909E-05x + 1.2093E-03	6.23E-05x + 1.4855E-03	2.140E-05x + 1.5599E-03	3.11E-05x + 8.89E-04
α	2.000	2.000	2.000	2.000	2.000	2.000	2.000
R^2	0.614	0.875	0.709	0.946	0.776	0.968	0.896
K(l/g.min)	6.0E-06	4.21E-05	1.967E-05	2.909E-05	6.23E-05	2.140E-05	3.11E-05
K_R(l/min)	1.1750E-19	1.1750E-19	1.1750E-19	1.1789E-19	1.1789E-19	1.1789E-19	1.1809E-19
β_{BR}(l/g.min)	1.2E-05	8.42E-05	3.934E-05	5.818E-05	1.246E-04	4.280E-05	6.22E-05
$\varepsilon_p(g^{-1})$	1.0213E+14	7.1660E+14	3.3481E+14	4.9351E+14	1.0569E+15	3.6305E+14	5.2672E+14
$\tau_{½}$ (min)	3.12	0.43	0.92	0.62	0.29	0.85	0.58
(-r)	$6.0E\text{-}05N_t^2$	$4.21E\text{-}05N_t^2$	$1.967E\text{-}05N_t^2$	$2.909E\text{-}05N_t^2$	$6.23E\text{-}05N_t^2$	$2.140E\text{-}05N_t^2$	$3.11E\text{-}05N_t^2$
N_o (g/l)	474.8338	436.6812	543.0946	826.9247	673.1743	641.0667	1124.8594

Table 4.80: Coag-Flocculation Kinetic Parameters and Linear Regression Coefficient of COSC in VIE at varying dosage and pH of 13.

Parameters	0.1g/l	0.2g/l	0.3g/l	0.4g/l	0.5g/l	0.6g/l	0.7g/l
Y	1.4E-05x + 2.518E-03	5.91E-06x + 1.483E-03	1. 764E-05x + 1.0551E-03	1.534E-05x + 1.0315E-03	2.15E-05x + 7.593E-04	2.111E-05x + 6.641E-04	1.67E-05x + 8.28E-04
α	2.000	2.000	2.000	2.000	2.000	2.000	2.000
R^2	0.815	0.732	0.900	0.818	0.946	0.956	0.937
K(l/g.min)	1.4E-05	5.91E-06	1. 764E-05	1.534E-05	2.15E-05	2.111E-05	1.67E-05
K_R(l/min)	1.1868E-19	1.1868E-19	1.1887E-19	1.1887E-19	1.1907E-19	1.1907E-19	1.1926E-19

β_{BR}(l/g.min)	2.8E-05	1.182E-05	3.528E-05	3.068E-05	4.3E-05	4.222E-05	3.34E-05
$\varepsilon_p(g^{-1})$	2.3593E+14	9.9596E+13	2.9679E+14	2.5810E+14	3.6113E+14	3.5458E+14	2.8006E+15
τ½ (min)	1.29	3.07	1.03	1.18	0.84	0.86	1.08
(-r)	1.4E-05N_t^2	5.91E-06N_t^2	1. 764E-05N_t^2	1.534E-05N_t^2	2.15E-05N_t^2	2.111E-05 N_t^2	1.67E-05N_t^2
N_o (g/l)	3970.1406	674.3088	947.7775	969.4619	1317.0025	1505.7973	1207.7295

Table 4.81: Coag-Flocculation Kinetic Parameters and Linear Regression Coefficient of TOSC in VIE at varying dosage and pH of 1.

Parameters	0.1g/l	0.2g/l	0.3g/l	0.4g/l	0.5g/l	0.6g/l	0.7g/l
Y	2.7E-05x + 1.689E-03	2.69E-05x + 1.107E-03	2.515E-05x + 1.136E-03	1.420E-05x + 9.968E-04	2.52E-05x + 1.0591E-03	2.388E-05x + 7.267E-04	1.77E-05x + 6.35E-04
α	2.000	2.000	2.000	2.000	2.000	2.000	2.000
R^2	0.805	0.846	0.841	0.929	0.791	0.937	0.983
K(l/g.min)	2.7E-05	2.69E-05	2.515E-05	1.420E-05	2.52E-05	2.388E-05	1.77E-05
K_R(l/min)	1.1750E-19	1.1750E-19	1.1750E-19	1.1770E-19	1.1770E-19	1.1789E-19	1.1789E-19
β_{BR}(l/g.min)	5.4E-05	5.38E-05	5.05E-05	2.84E-05	5.04E-05	4.776E-05	3.54E-05
$\varepsilon_p(g^{-1})$	4.5957E+14	4.5787E+14	4.2809E+14	2.4129E+14	4.2821E+14	4.0512E+14	3.0028E+14
$\tau_{½}$ (min)	0.67	0.67	0.72	1.28	0.72	0.76	1.02
(-r)	2.7E-05N_t^2	52.69E-05N_t^2	2.515E-05N_t^2	1.420E-05N_t^2	2.52E-05N_t^2	2.388E-05N_t^2	1.77E-05N_t^2
N_o (g/l)	592.0663	903.3424	880.2817	1003.2103	944.1979	1376.0837	1574.8032

Table 4.82: Coag-Flocculation Kinetic Parameters and Linear Regression Coefficient of TOSC in VIE at varying dosage and pH of 3.

Parameters	0.1g/l	0.2g/l	0.3g/l	0.4g/l	0.5g/l	0.6g/l	0.7g/l
Y	7.6E-05x + 4.491E-03	4.53E-05x + 2.102E-03	9.041E-05x + 1.1253E-03	9.594E-05x + 1.2372-03	9.49E-05x + 1.0617E-03	4.021E-05x + 1.9934E-04	3.76E-05x + 1.325E-03
α	2.000	2.000	2.000	2.000	2.000	2.000	2.000
R^2	0.709	0.839	0.965	0.970	0.952	0.864	0.882
K(l/g.min)	7.6E-05	4.53E-05	9.041E-05	9.594E-05	9.49E-05	4.021E-05	3.76E-05
K_R(l/min)	1.1868E-19	1.1887E-19	1.1887E-19	1.1887E-19	1.1907E-19	1.1907E-19	1.1926E-19
β_{BR}(l/g.min)	1.52E-04	9.06E-05	1.8082E-04	1.9188E-04	1.898E-04	8.042E-05	7.52E-05
$\varepsilon_p(g^{-1})$	1.2808E+15	7.6218E+14	1.5212E+15	1.6142E+15	1.5940E+15	6.7540E+14	6.3056E+14
$\tau_{½}$ (min)	0.32	0.53	0.27	0.25	0.25	0.60	0.64
(-r)	7.6E-05N_t^2	4.53E-05N_t^2	9.041E-05N_t^2	9.594E-05N_t^2	9.49E-05N_t^2	4.021E-05N_t^2	3.76E-05N_t^2
N_o (g/l)	222.6676	475.9638	888.6519	808.2768	S941.8857	501.6555	754.7170

Table 4.83: Coag-Flocculation Kinetic Parameters and Linear Regression Coefficient of TOSC in VIE at varying dosage and pH of 5.

Parameters	0.1g/l	0.2g/l	0.3g/l	0.4g/l	0.5g/l	0.6g/l	0.7g/l
Y	2.4E-05x + 2.492E-03	3.72E-05x + 2.164E-03	2.502-05x + 2.1276E-03	3.109E05x + 3.152E-03	1.97E-05x + 2.9649E-03	1.927E-05x + 1.1292E-03	2.13E-05x + 1.197E-03
α	2.000	2.000	2.000	2.000	2.000	2.000	2.000
R^2	0.879	0.893	0.742	0.882	0.738	0.941	0.742
K(l/g.min)	2.4E-05	3.72E-05	2.502-05	3.109-05	1.97E-05	1.927E-05	2.13E-05
K_R(l/min)	1.1711E-19	1.1711E-19	1.1711E-19	1.1711E-19	1.1731E-19	1.1731E-19	1.1731E-19
β_{BR}(l/g.min)	4.8E-05	7.44E-05	5.004E-05	6.218E-05	3.94E-05	3.854E-05	4.26E-05
$\varepsilon_p(g^{-1})$	4.1987E+14	6.3530+14	4.2729E+14	5.3095E+14	3.3586+14	3.854E+14	3.631E+14
τ½ (min)	1.01	0.65	0.97	0.78	1.23	1.25	1.13
(-r)	2.4E-05N_t^2	3.72E-05N_t^2	2.502-05N_t^2	3.109-05N_t^2	1.97E-05N_t^2	1.927E-05N_t^2	2.13E-05N_t^2
N_o (g/l)	401.2841	462.1072	470.0132	317.2589	337.2795	885.5827	835.4219

Table 4.84: Coag-Flocculation Kinetic Parameters and Linear Regression Coefficient of TOSC in VIE at varying dosage and pH of 7.

Parameters	0.1g/l	0.2g/l	0.3g/l	0.4g/l	0.5g/l	0.6g/l	0.7g/l
Y	2.5E-05x + 1.835E-03	1.41E-05x + 1.49E-03	5.541E-05x + 1.928E-03	6.895E-05x + 1.3461E-03	2.70E-05x + 8.485E-04	2.691E-06x + 4.311E-04	2.39E-06x + 4.27E-04
α	2.000	2.000	2.000	2.000	2.000	2.000	2.000
R^2	0.622	0.833	0.910	0.838	0.934	0.870	0.964
K(l/g.min)	2.5E-05	1.41E-05	5.541E-05	6.895E-05	2.70E-05	2.691E-06	2.39E-06
K_R(l/min)	1.1711E-19	1.1711E-19	1.1711E-19	1.1731E-19	1.1731E-19	1.1731E-19	1.1750E-19
β_{BR}(l/g.min)	5.0E-05	2.82E-05	1.1082E-04	1.379E-04	5.4E-05	5.382E-06	4.78E-06
$\varepsilon_p(g^{-1})$	4.2695E+14	2.4080E+14	9.4629E+14	1.379E+14	4.6032E+14	4.5878E+13	4.0546E+13
$\tau_{½}$ (min)	0.48	0.86	0.22	0.18	0.45	4.49	5.05
(-r)	$2.4E-05N_t^2$	$3.72E-05N_t^2$	$2.502-05N_t^2$	$3.109-05N_t^2$	$1.97E-05N_t^2$	$1.927E-05N_t^2$	$2.13E-05N_t^2$
N_o (g/l)	544.9591	671.1409	518.6722	742.8869	1178.5504	2319.6474	2341.9204

Table 4.85: Coag-Flocculation Kinetic Parameters and Linear Regression Coefficient of TOSC in VIE at varying dosage and pH of 10.

Parameters	0.1g/l	0.2g/l	0.3g/l	0.4g/l	0.5g/l	0.6g/l	0.7g/l
Y	4.0E-05x + 3.597E-03	6.21E-05x + 3.976E-03	3.785E-06x + 6.665E-04	6.477E-06x + 5.991E-04	6.89E-06x + 6.24E-04	2.784E-05x + 9.747E-04	1.04E-05x + 6.27E-04
α	2.000	2.000	2.000	2.000	2.000	2.000	2.000
R^2	0.966	0.922	0.687	0.824	0.858	0.729	0.773
K(l/g.min)	4.0E-05	6.21E-05	3.785E-06	6.477E-06	6.89E-06	2.784E-05	1.04E-05
K_R(l/min)	1.1731E-19	1.1731E-19	1.1750E-19	1.1750E-19	1.1750E-19	1.1770E-19	1.1770E-19
β_{BR}(l/g.min)	8.0E-05	1.242E-04	7.57E-06	1.2954E-05	1.378E-05	5.56E-05	2.08E-05
$\varepsilon_p(g^{-1})$	6.8195E+14	1.0587E+15	6.4426E+13	1.1025E+14	1.1728E+14	4.7239E+14	1.7672E+14
$\tau_{½}$ (min)	0.36	0.23	3.83	2.24	2.10	0.52	1.39
(-r)	$4.0E-05N_t^2$	$6.21E-05N_t^2$	$3.785E-06N_t^2$	$6.477E-06N_t^2$	$6.89E-06N_t^2$	$2.784E-05N_t^2$	$1.04E-05N_t^2$
N_o (g/l)	278.0095	251.5091	1500.3751	1669.1704	1602.5561	1025.9567	1594.8963

Table 4.86: Coag-Flocculation Kinetic Parameters and Linear Regression Coefficient of TOSC in VIE at varying dosage and pH of 13.

Parameters	0.1g/l	0.2g/l	0.3g/l	0.4g/l	0.5g/l	0.6g/l	0.7g/l
Y	1.3E-05x + 2.094E-03	1.01E-05x + 1.371E-03	6.159E-06x + 1.264E-03	4.881E-07x + 6.47E-04	5.24E-06x + 5.907E-04	3.326E-06x + 5.81E-04	4.04E-06x + 5.75E-04
α	2.000	2.000	2.000	2.000	2.000	2.000	2.000
R^2	0.730	0.885	0.833	0.731	0.954	0.780	0.682
K(l/g.min)	1.3E-05	1.01E-05	6.159E-06	4.881E-07	5.24E-06	3.326E-06	4.04E-06
K_R(l/min)	1.1731E-19	1.1731E-19	1.1750E-19	1.1750E-19	1.1750E-19	1.1770E-19	1.1770E-19
β_{BR}(l/g.min)	2.6E-05	2.02E-05	1.1750E-05	9.762E-07	1.048E-05	6.652-06	8.08E-06
$\varepsilon_p(g^{-1})$	2.2163E+14	1.7219E+14	1.0483+14	8.3081E+14	8.9191E+14	5.6517E+13	6.8649E+13
$\tau_{½}$ (min)	1.24	1.59	2.61	3.30	3.07	4.94	2.99
(-r)	$1.3E-05N_t^2$	$61.01E-05N_t^2$	$6.159E-06N_t^2$	$4.881E-07N_t^2$	$5.24E-06N_t^2$	$3.326E-06N_t^2$	$4.04E-06N_t^2$
N_o (g/l)	477.5549	25729.3946	790.5763	1545.5763	1692.9067	1721.1704	1739.1304

Table 4.87: Coag-Flocculation Kinetic Parameters and Linear Regression Coefficient of PTSC in VIE at varying dosage and pH of 1.

Parameters	0.1g/l	0.2g/l	0.3g/l	0.4g/l	0.5g/l	0.6g/l	0.7g/l
Y	1.6E-05x + 2.351E-03	3.22E-05x + 3.476E-03	1.243E-05x + 3.931E-03	2.066E-05x + 2.6956E-03	3.67E-05x + 2.3757E-03	5.56E-05x + 1.9111E-03	1.0E-04x + 1.831E-03
α	2.000	2.000	2.000	2.000	2.000	2.000	2.000
R^2	0.939	0.818	0.906	0.859	0.944	0.909	0.952
K(l/g.min)	1.6E-05	3.22E-05	1.243E-05	2.066E-05	3.67E-05	5.56E-05	1.0E-04
K_R(l/min)	1.1809E-19	1.1809E-19	1.1809E-19	1.1829E-19	1.1829E-19	1.1829E-19	1.1829E-19
β_{BR}(l/g.min)	3.2E-05	6.44E-05	2.486E-05	4.132E-05	7.34E-05	1.112E-05	2.0E-05
$\varepsilon_p(g^{-1})$	2.7098E+14	5.4535E+14	2.1052E+14	3.4931E+14	6.2051E+14	9.4006E+14	1.6908E+14
$\tau_{½}$ (min)	2.26	1.13	2.91	1.75	0.99	0.65	0.36
(-r)	$1.6E-05N_t^2$	$3.22E-05N_t^2$	$1.243E-05N_t^2$	$2.066E-05N_t^2$	$3.67E-05N_t^2$	$5.56E-05N_t^2$	$1.0E-04N_t^2$
N_o (g/l)	425.3509	287.6870	254.3882	370.9749	420.9286	546.1496	546.1496

Table 4.88: Coag-Flocculation Kinetic Parameters and Linear Regression Coefficient of PTSC in VIE at varying dosage and pH of 3.

Parameters	0.1g/l	0.2g/l	0.3g/l	0.4g/l	0.5g/l	0.6g/l	0.7g/l
Y	4.0E-05x + 3.326E-03	7.92E-05x + 4.236E-03	1.041E-04x + 3.3103E-03	1.802E-04x + 3.6614E-03	1.91E-04x + 4.6059E-03	9.345E-05x + 4.082E-03	1.26E-04x + 3.516E-03
α	2.000	2.000	2.000	2.000	2.000	2.000	2.000
R^2	0.942	0.813	0.946	0.863	0.793	0.816	0.818
K(l/g.min)	4.0E-05	7.92E-05	1.041E-04	1.802E-04	4.15E-05	9.345E-05	1.26E-04
K_R(l/min)	1.1750E-19	1.1750E-19	1.1770E-19	1.1770E-19	1.1789E-19	1.1789E-19	1.1809E-19
β_{BR}(l/g.min)	8.0E-05	1.584E-04	2.082E-04	3.604E-04	3.82E-04	1.869E-04	2.52E-04
$\varepsilon_p(g^{-1})$	6.8085E+14	1.3481E+15	1.7689E+15	3.0620E+15	3.2403E+15	1.5854E+15	2.1340E+15
$\tau_{½}$ (min)	0.91	0.46	0.35	0.20	0.87	0.39	0.29
(-r)	$4.0E-05N_t^2$	$7.92E-05\ N_t^2$	$1.041E-04\ N_t^2$	$1.802E-04N_t^2$	$1.91E-04N_t^2$	$9.345E-05N_t^2$	$1.26E-04N_t^2$
N_o (g/l)	300.6615	236.0718	302.0874	273.1196	217.1128	244.9780	284.4141

Table 4.89: Coag-Flocculation Kinetic Parameters and Linear Regression Coefficient of PTSC in VIE at varying dosage and pH of 5.

Parameters	0.1g/l	0.2g/l	0.3g/l	0.4g/l	0.5g/l	0.6g/l	0.7g/l
Y	1.28E-04x + 1.0439E-02	3.26E-05x + 4.929E-03	2.371E-05x + 3.9268E-03	1.918E-05x + 3.1605E-03	4.29E-05x + 2.6946E-03	2.124E-05x + 2.5018-03	1.70E-05x + 1.908E-03
α	2.000	2.000	2.000	2.000	2.000	2.000	2.000
R^2	0.824	0.704	0.963	0.797	0.873	0.863	0.966
K(l/g.min)	1.28E-04	3.26E-05	2.371E-05	1.918E-05	4.29E-05	2.124E-05	1.70E-05
K_R(l/min)	1.1672E-19	1.1672E-19	1.1672E-19	1.1691E-19	1.1691E-19	1.1691E-19	1.1711E-19
β_{BR}(l/g.min)	2.56E-04	6.52E-05	4.742E-05	3.836E-05	8.58E-05	4.24E-05	3.4E-05
$\varepsilon_p(^{g-1})$	2.1933E+15	5.5860E+14	4.0627E+14	3.2812E+14	7.3390E+14	3.6267E+14	2.9033E+14
$\tau_{½}$ (min)	0.28	1.11	1.53	1.89	0.84	1.71	2.13
(-r)	$1.28E-05N_t^2$	$3.26E-05N_t^2$	$2.371E-05N_t^2$	$1.918E-05N_t^2$	$4.29E-05N_t^2$	$2.124E-05N_t^2$	$1.70E-05N_t^2$
N_o (g/l)	957.9461	202.8809	254.6603	316.4056	371.1126	399.7122	524.1090

Table 4.90: Coag-Flocculation Kinetic Parameters and Linear Regression Coefficient of PTSC in VIE at varying dosage and pH of 7.

Parameters	0.1g/l	0.2g/l	0.3g/l	0.4g/l	0.5g/l	0.6g/l	0.7g/l
Y	2.7E-05x + 3.094E-03	8.16E-05x + 5.095E-03	4.886E-05x + 3.1454E-03	3.805E-05x + 2.456E-03	1.43E-05x + 1.7876E-03	1.904E-05x + 2.0493E-03	4.06E-05x + 2.061E-03
α	2.000	2.000	2.000	2.000	2.000	2.000	2.000
R^2	0.931	0.957	0.820	0.858	0.926	0.972	0.949
K(l/g.min)	2.7E-05	8.16E-05	4.886E-05	3.805E-05	1.43E-05	1.904E-05	4.06E-05
K_R(l/min)	1.1750E-19	1.1750E-19	1.1750E-19	1.1770E-19	1.1770E-19	1.1789E-19	1.1789E-19

β_{BR}(l/g.min)	5.4E-05	1.632E-04	9.772E-05	7.61E-05	2.86E-05	3.808E-05	8.12E-05
$\varepsilon_p(g^{-1})$	4.5957E+14	1.3889E+15	8.3166E+14	6.4656E+14	2.4299E+14	3.2301E+14	6.8878E+14
$\tau_{½}$ (min)	1.34	0.44	0.74	0.95	2.53	0.90	0.89
(-r)	2.7E-05N_t^2	8.16E-05N_t^2	4.886E-05N_t^2	3.805E-05N_t^2	1.43E-05N_t^2	1.904E-05 N_t^2	4.06E-05N_t^2
N_o (g/l)	323.2062	196.2709	317.9246	407.1661	559.4093	487.9715	485.2014

Table 4.91: Coag-Flocculation Kinetic Parameters and Linear Regression Coefficient of PTSC in VIE at varying dosage and pH of 10.

Parameters	0.1g/l	0.2g/l	0.3g/l	0.4g/l	0.5g/l	0.6g/l	0.7g/l
Y	3.3E-05x + 5.295E-03	4.15E-05x + 4.431E-03	4.484E-05x + 4.3117E-03	6.515E-05x + 3.9346E-03	4.76E-05x + 2.8821E-03	7.161E-05x + 3.4758E-03	4.74E-05x + 3.897E-03
α	2.000	2.000	2.000	2.000	2.000	2.000	2.000
R^2	0.661	0.799	0.807	0.922	0.934	0.893	0.639
K(l/g.min)	3.3E-05	1.91E-04	4.484E-05	6.515E-05	4.76E-05	7.161E-05	4.74E-05
K_R(l/min)	1.1672E-19	1.1672E-19	1.1672E-19	1.1711E-19	1.1711E-19	1.1731E-19	1.1731E-19
β_{BR}(l/g.min)	6.6E-05	8.3E-04	8.968E-05	1.303E-05	9.52E-05	1.2209E-05	8.0812E-05
$\varepsilon_p(g^{-1})$	5.6546E+14	7.1110E+14	7.6833E+14	1.1126E+15	8.1291E+14	1.2209E+15	8.0812E+14
$\tau_{½}$ (min)	1.10	0.19	0.81	0.56	0.76	0.51	0.76
(-r)	3.3E-05N_t^2	4.15E-05N_t^2	4.484E-05N_t^2	6.515E-05N_t^2	4.76E-05N_t^2	7.161E-05N_t^2	4.74E-05N_t^2
N_o (g/l)	188.8574	225.6827	231.9271	4254.1554	346.9692	287.7036	256.6076

Table 4.92: Coag-Flocculation Kinetic Parameters and Linear Regression Coefficient of PTSC in VIE at varying dosage and pH of 13.

Parameters	0.1g/l	0.2g/l	0.3g/l	0.4g/l	0.5g/l	0.6g/l	0.7g/l
Y	2.1E-05x + 3.201E-03	4.28E-05x + 5.014E-03	5.626E-05x + 3.9699E-03	6.024E-05x + 3.221E-03	7.30E-05x + 1.4663E-03	1.463E-05x + 1.8948E-03	4.17E-05x + 2.998E-03
α	2.000	2.000	2.000	2.000	2.000	2.000	2.000
R^2	0.709	0.699	0.922	0884	0.649	0.783	0.894
K(l/g.min)	2.1E-05	4.28E-05	5.626E-05	6.024E-05	7.30E-05	1.463E-05	4.17E-05
K_R(l/min)	1.1848E-19	1.1848E-19	1.1868E-19	1.1868E-19	1.1868E-19	1.1887E-19	1.1887E-19
β_{BR}(l/g.min)	4.2E-05	8.56E-05	1.1252E-04	1.2048E-04	4.60E-05	2.926E-05	8.34E-05
$\varepsilon_p(g^{-1})$	3.5449E+14	7.2248E+14	9.4810E+14	1.0152E+15	3.8760E+14	2.4615E+14	7.0161E+14
$\tau_{½}$ (min)	1.29	3.07	1.03	1.18	0.84	0.86	1.08
(-r)	2.1E-05N_t^2	4.28E-05N_t^2	5.626E-05N_t^2	6.024E-05N_t^2	7.30E-05N_t^2	1.463E-05N_t^2	4.17E-05N_t^2
N_o (g/l)	312.4024	199.4416	251.8955	310.4626	681.9887	527.7602	333.5557

Table 4.93: Coag-Flocculation Kinetic Parameters and Linear Regression Coefficient of MPSC in VIE at varying dosage and pH of 1.

Parameters	0.1g/l	0.2g/l	0.3g/l	0.4g/l	0.5g/l	0.6g/l	0.7g/l
Y	3.4E-05x + 2.619E-03	2.02E-05 x + 2.483E-03	2.569E-05x + 2.5082 E-03	2.695E-05x + 1.3805 E-03	2.01E-05x + 1.596 E-03	2.933E-05x + 1.377 E-03	2.61E-05x + 1.378 E-03
α	2.000	2.000	2.000	2.000	2.000	2.000	2.000
R^2	0.990	0.815	0.943	0.792	0.751	0.885	0.879
K(l/g.min)	3.4E-05	2.02E-05	2.569E-05	2.695E-05	2.01E-05	2.933E-05	2.61E-05
K_R(l/min)	1.1750E-19	1.1750E-19	1.1750E-19	1.1770E-19	1.1770 E-19	1.1789 E-19	1.1789 E-19
β_{BR}(l/g.min)	6.8E-05	4.04E-05	5.138 E-05	5.39 E-05	4.02 E-05	5.866 E-05	5.22 E-05
$\varepsilon_p(g^{-1})$	5.7872E+14	3.4383 E+14	4.3728 E+14	4.5794 E+14	3.4155 E+14	4.9758 E+14	4.4279 E+14
$\tau_{½}$ (min)	0.71	1.20	0.91	0.90	1.20	0.82	0.93
(-r)	3.4E-05N_t^2	2.02E-05 N_t^2	2.569E095N_t^2	2.695E-05 N_t^2	2.01E-05 N_t^2	2.933E-05N_t^2	2.61E-05 N_t^2
N_o (g/l)	381.8251	402.7386	398.6923	724.3752	626.5664	726.2164	725.6894

Table 4.94: Coag-Flocculation Kinetic Parameters and Linear Regression Coefficient of MPSC in VIE at varying dosage and pH of 3.

Parameters	0.1g/l	0.2g/l	0.3g/l	0.4g/l	0.5g/l	0.6g/l	0.7g/l
Y	8.1E-05x + 2.874E-03	8.92E-05x + 1.734E-03	3.726E-05x + 1.871E-03	5.590E-05x + 1.6371E-03	6.36E-05x + 1.5535E-03	6.560E-05x + 1.3175E-03	6.86E-05x + 1.704E-03
α	2.000	2.000	2.000	2.000	2.000	2.000	2.000
R^2	0.920	0.991	0.803	0.702	0.720	0.753	0.700
K(l/g.min)	8.1E-05	8.92E-05	3.726E-05	5.590E-05	6.36E-05	6.560E-05	6.86E-05
K_R(l/min)	1.1926E-19	1.1926E-19	1.1957E-19	1.1957E-19	1.1887E-19	1.1887E-19	1.1868E-19
β_{BR}(l/g.min)	1.62E-04	1.784E-04	7.452E-05	1.118E-04	1.272E-05	1.312E-04	1.372E-04
$\varepsilon_p(g^{-1})$	1.3584E+15	1.4959E+15	6.2323 E+14	9.350E+14	1.0701E+15	1.1037E+15	1.1560E+15
$\tau_{½}$ (min)	0.30	0.27	0.65	0.43	0.38	0.37	0.35
(-r)	$8.1E\text{-}05N_t^2$	$8.92E\text{-}05N_t^2$	$3.726E\text{-}05N_t^2$	$5.590E\text{-}05N_t^2$	$6.36E\text{-}05N_t^2$	$6.560E\text{-}05N_t^2$	$6.86E\text{-}05N_t^2$
N_o (g/l)	347.9471	576.7013	534.4735	610.8362	643.7078	759.0133	586.8545

Table 4.95: Coag-Flocculation Kinetic Parameters and Linear Regression Coefficient of MPSC in VIE at varying dosage and pH of 5.

Parameters	0.1g/l	0.2g/l	0.3g/l	0.4g/l	0.5g/l	0.6g/l	0.7g/l
Y	2.3E-05x + 2.597E-03	3.95E-05 x + 3.409E-03	1.296E-05x + 1.8445E-03	2.634E-05x + 1.8962E-03	3.17E-05x + 1.8953E-03	7.668E-06x + 1.5092E-03	3.07E-05x + 1.316E-03
α	2.000	2.000	2.000	2.000	2.000	2.000	2.000
R^2	0.915	0.668	0.729	0.710	0.786	0.853	0.890
K(l/g.min)	2.3-05	3.95E-05	1.296-05	2.634E-05	3.17E-05	7.668E-06	3.07E-05
K_R(l/min)	1.1672E-19	1.1672E-19	1.1672E-19	1.1672E-19	1.1691E-19	1.1691E-19	1.1691E-19
β_{BR}(l/g.min)	4.6E-05	7.9E-05	2.592E-05	5.268E-05	6.34E-05	1.5336E-05	6.14E-05
$\varepsilon_p(g^{-1})$	3.9411E+14	6.7683E+14	2.2207E+14	4.5134E+14	5.4230E+14	1.3118E+14	5.251E+14
$\tau_{½}$ (min)	1.58	0.92	2.80	1.38	1.14	4.73	1.18
(-r)	$2.3E\text{-}05N_t^2$	$3.95E\text{-}05N_t^2$	$1.296\text{-}05N_t^2$	$2.634E\text{-}05N_t^2$	$3.17E\text{-}05N_t^2$	$7.668E\text{-}06N_t^2$	$3.07E\text{-}05N_t^2$
N_o (g/l)	385.0597	293.3412	542.1523	527.3705	527.6210	662.6027	759.8784

Table 4.96: Coag-Flocculation Kinetic Parameters and Linear Regression Coefficient of MPSC in VIE at varying dosage and pH of 7.

Parameters	0.1g/l	0.2g/l	0.3g/l	0.4g/l	0.5g/l	0.6g/l	0.7g/l
Y	7.1E-05x + 4.442E-03	7.49E-05 x + 1.0963E-02	9.155E-05x + 8.642E-03	1.382E-04x + 6.3613E-03	9.63E-05x + 2.3403E-03	4.247E-05x + 1.608E-03	4.40E-05x + 1.606E-0
α	2.000	2.000	2.000	2.000	2.000	2.000	2.000
R^2	0.743	0.896	0.638	0.892	0.861	0.943	0.868
K(l/g.min)	7.1-05	7.49E-05	9.155E-05	1.382E-04	9.63E-05	4.247E-06	4.40E-05
K_R(l/min)	1.1789E-19	1.1789E-19	1.1789E-19	1.1770E-19	1.1770E-19	1.1789E-19	1.1789E-19
β_{BR}(l/g.min)	1.42E-04	1.4998E-04	1.831E-04	2.764E-04	1.926E-04	8.494E-05	8.8E-05
$\varepsilon_p(g^{-1})$	1.2045E+15	1.2707E+15	1.5531E+15	2.3483E+15	1.6364E+15	7.2050+14	7.4646E+14
τ½ (min)	0.51	0.48	0.40	0.26	0.38	0.85	0.82
(-r)	$7.1E\text{-}05N_t^2$	$7.49E\text{-}05N_t^2$	$9.155E\text{-}05N_t^2$	$1.382E\text{-}04N_t^2$	$9.63E\text{-}05N_t^2$	$4.247E\text{-}06N_t^2$	$4.40E\text{-}05N_t^2$
N_o (g/l)	225.1238	91.2159	115.7140	157.2006	427.2956	621.8905	622.6650

Table 4.97: Coag-Flocculation Kinetic Parameters and Linear Regression Coefficient of MPSC in VIE at varying dosage and pH of 10.

Parameters	0.1g/l	0.2g/l	0.3g/l	0.4g/l	0.5g/l	0.6g/l	0.7g/l
Y	6.9E-05x + 7.982E-03	8.04E-05 x + 4.373E-03	1.074E-04x + 4.7161E-03	7.267E-05x + 2.5681E-03	7.33E-05x + 2.7996E-03	5.335E-05x + 1.944E-03	5.22E-05x + 1.379E-03
α	2.000	2.000	2.000	2.000	2.000	2.000	2.000
R^2	0.746	0.849	0.846	0.978	0.910	0.927	0.930
K(l/g.min)	6.9E-05	8.04E-05	1.074E-04	7.267E-05	7.33E-05	5.335E-06	5.22E-05
K_R(l/min)	1.1770E-19	1.1770E-19	1.1750E-19	1.1750E-19	1.1750E-19	1.1731E-19	1.1731E-19
β_{BR}(l/g.min)	1.38E-04	1.608E-04	2.148E-04	1.4534E-04	1.466E-04	1.067E-04	1.044E-05
$\varepsilon_p(g^{-1})$	1.1725E+15	1.3662E+15	1.8281E+15	1.2369E+15	1.2477E+15	9.0956E+14	8.8995E+14
$\tau_{½}$ (min)	0.53	0.45	0.34	0.50	0.49	0.68	0.69
(-r)	$6.9E\text{-}05N_t^2$	$8.04E\text{-}05N_t^2$	$1.074E\text{-}04N_t^2$	$7.267E\text{-}05N_t^2$	$7.33E\text{-}05N_t^2$	$5.335E\text{-}06N_t^2$	$5.22E\text{-}05N_t^2$
N_o (kg/m^3)	125.2819	228.6770	212.0396	389.3929	357.2066	514.4033	725.1632

Table 4.98: Coag-Flocculation Kinetic Parameters and Linear Regression Coefficient of MPSC in VIE at varying dosage and pH of 13.

Parameters	0.1g/l	0.2g/l	0.3g/l	0.4g/l	0.5g/l	0.6g/l	0.7g/l
Y	1.04E-04x + 8.263E-03	1.67E-04 x + 1.1809E-03	2.252E-04x + 7.9894E-03	2.634E-04x + 7.6084E-03	6.35E-06x + 5.8533E-03	2.31E-05x + 5.5059E-03	5.22E-05x + 1.732E-02
α	2.000	2.000	2.000	2.000	2.000	2.000	2.000
R^2	0.733	0.910	0.756	0.864	0.868	0.978	0.918
K(l/g.min)	1.04E-04	1.67E-04	2.252E-04	2.634E-04	6.35E-06	2.31E-05	5.22E-05
K_R(l/min)	1.1809E-19	1.1809E-19	1.1829E-19	1.1829E-19	1.1848E-19	1.1848E-19	1.1848E-19
β_{BR}(l/g.min)	2.08E-04	3.34E-04	4.504E-04	5.268E-04	1.27E-04	4.636E-04	1.2E-05
$\varepsilon_p(g^{-1})$	1.7614E+15	2.8284E+15	3.8076E+15	4.4535E+15	1.0719E+15	3.9129E+14	1.0128E+16
τ½ (min)	0.70	0.43	0.32	0.28	1.14	0.31	0.12
(-r)	$1.04E\text{-}04N_t^2$	$1.67E\text{-}04N_t^2$	$2.252E\text{-}04N_t^2$	$2.634E\text{-}04N_t^2$	$6.35E\text{-}06N_t^2$	$2.31E\text{-}05N_t^2$	$5.22E\text{-}05N_t^2$
N_o (g/l)	121.0214	84.6812	125.1658	131.4337	170.8438	181.6233	57.7367

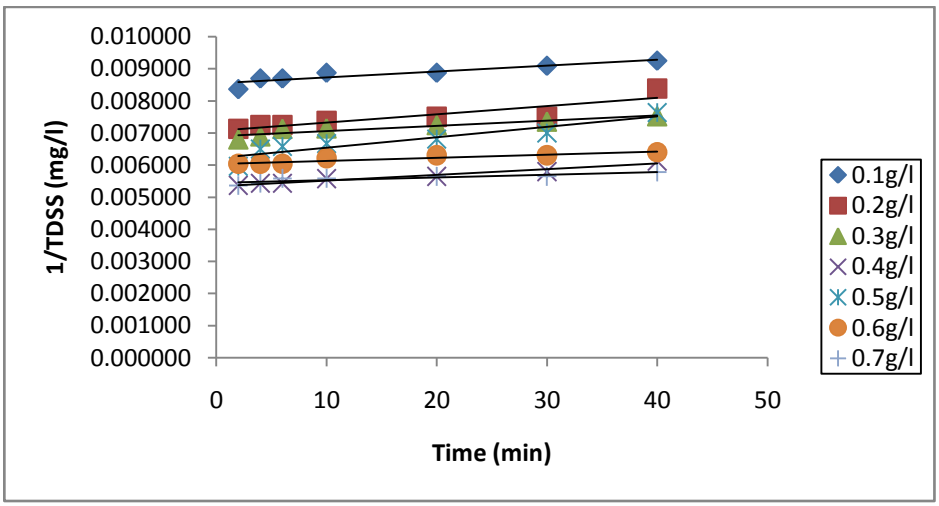

Fig.4.196: Kinetic plot of TDSS removal using varying ssc dosages for VIE at pH 1

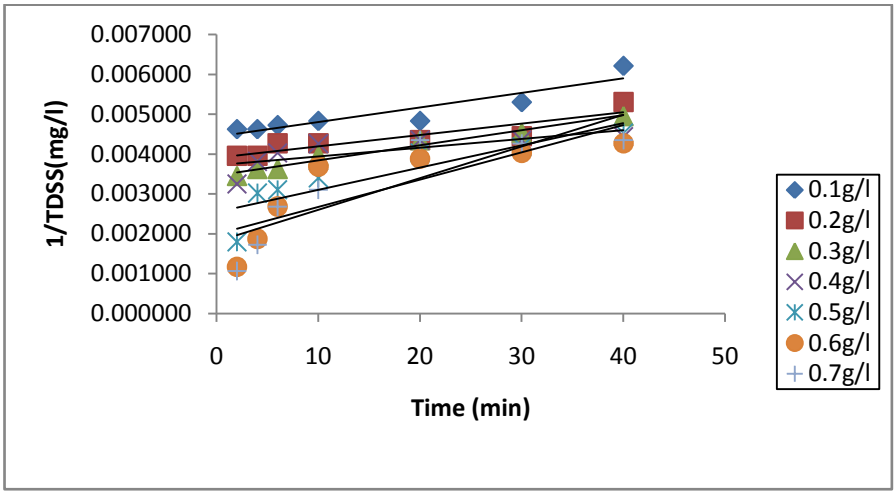

Fig.4.197: Kinetic plot of TDSS removal using varying ssc dosages for VIE at pH 3

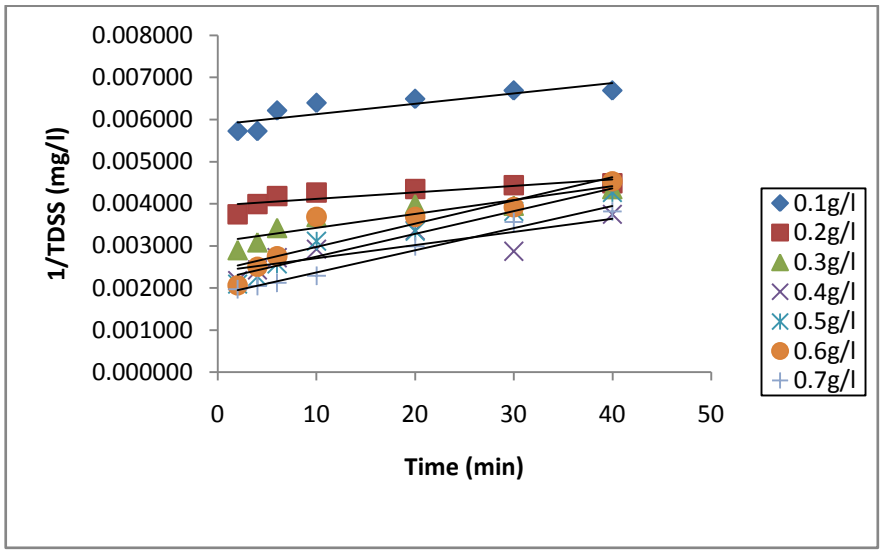

Fig.4.198:Kinetic plot of TDSS removal using varying ssc dosages for VIE at pH

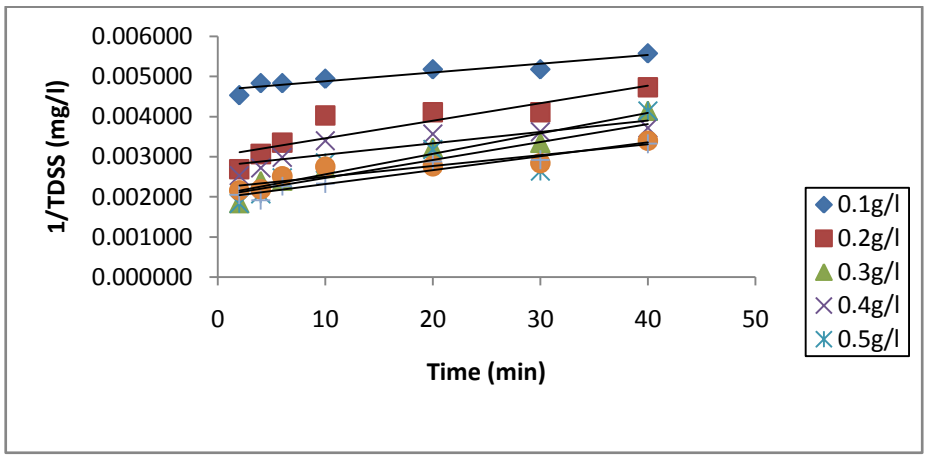

Fig.4.199:Kinetic plot of TDSS removal using varying ssc dosages for VIE at pH 7

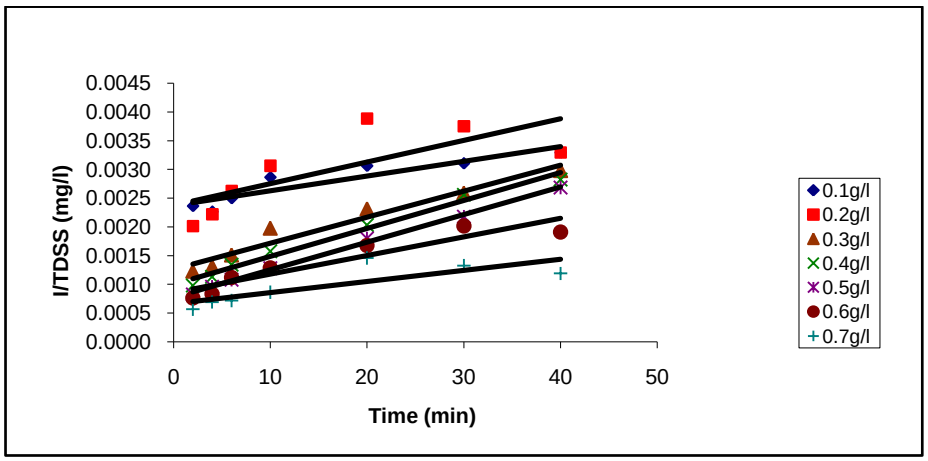

Fig.4.200:Kinetic plot of TDSS removal using varying ssc dosages for VIE at pH 10

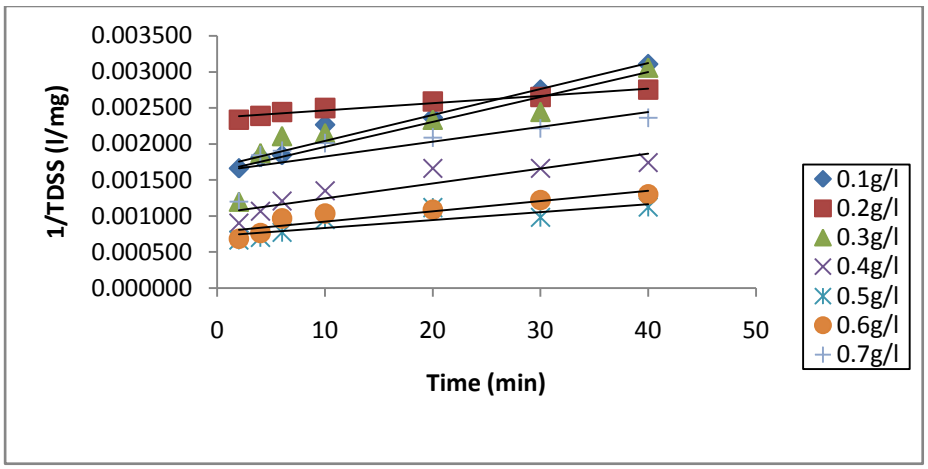

Fig.4.201:Kinetic plot of TDSS removal using varying ssc dosages for VIE at pH 13

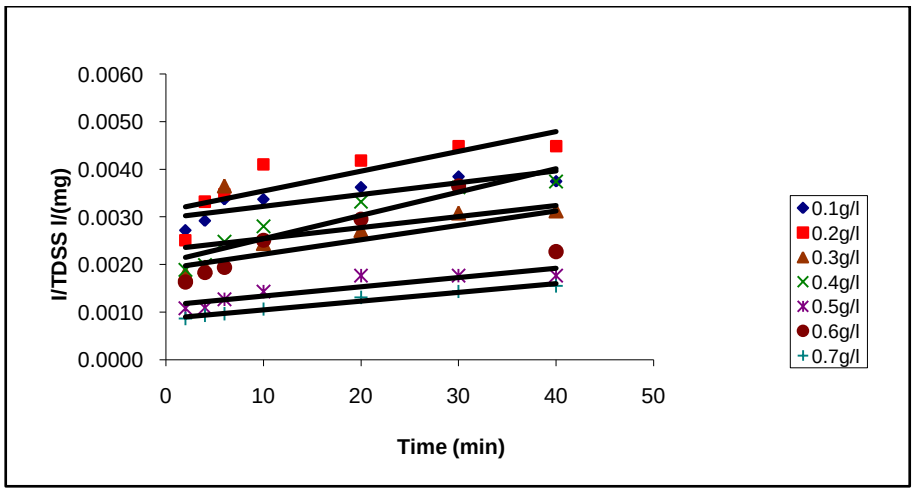

Fig.4.202:Kinetic plot of TDSS removal using varying cosc dosages for VIE at pH 1

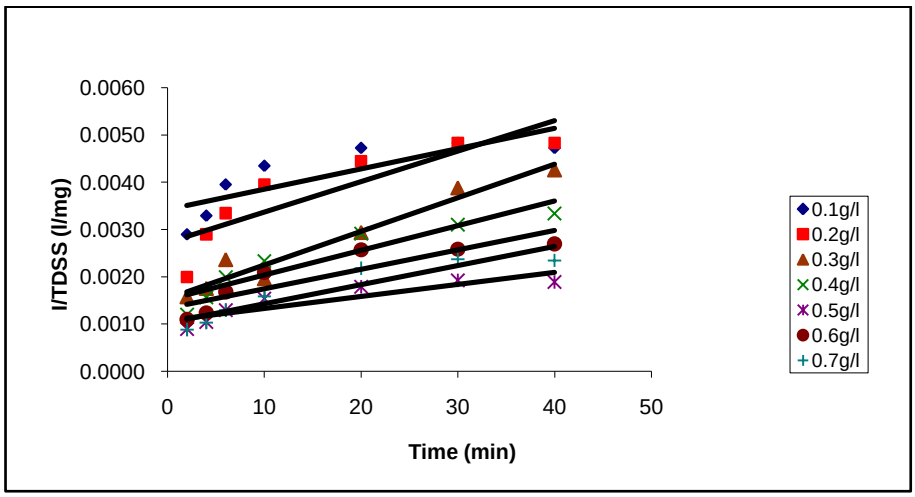

Fig.4.203: Kinetic plot of TDSS removal using varying cosc dosages for VIE at pH 3

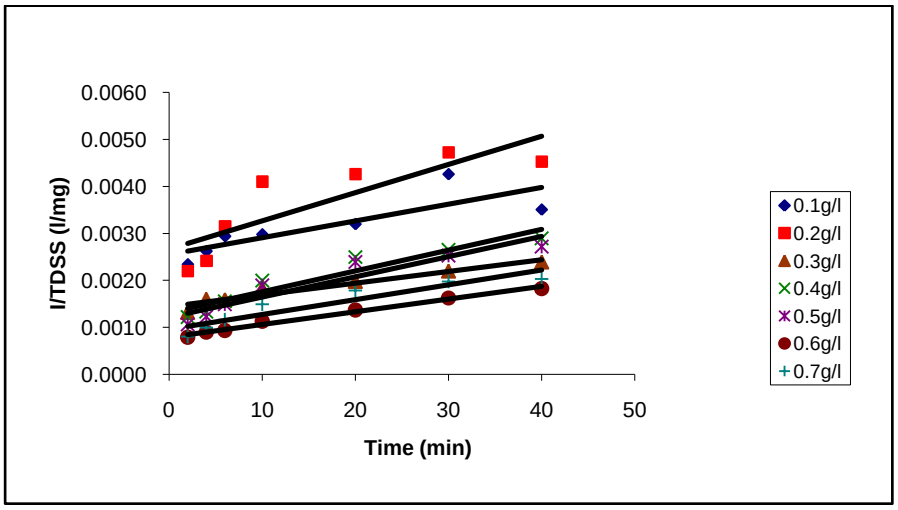

Fig.4.204: Kinetic plot of TDSS removal using varying cosc dosages for VIE at pH 5

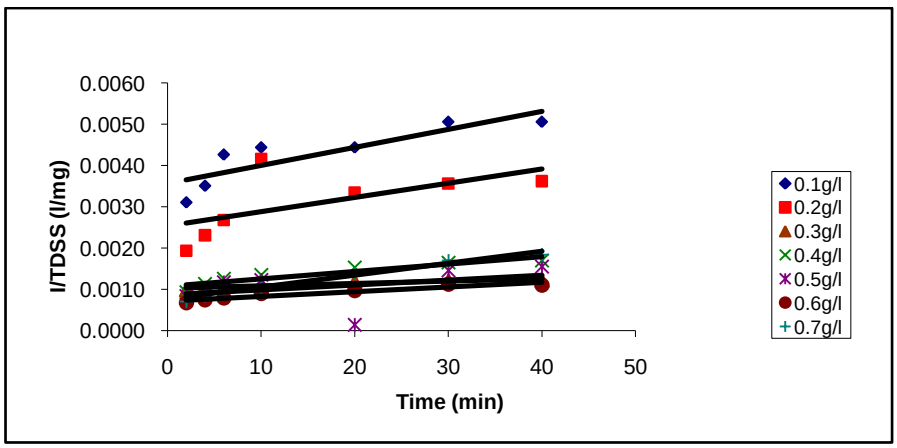

Fig.4.205: Kinetic plot of TDSS removal using varying cosc dosages for VIE at pH 7

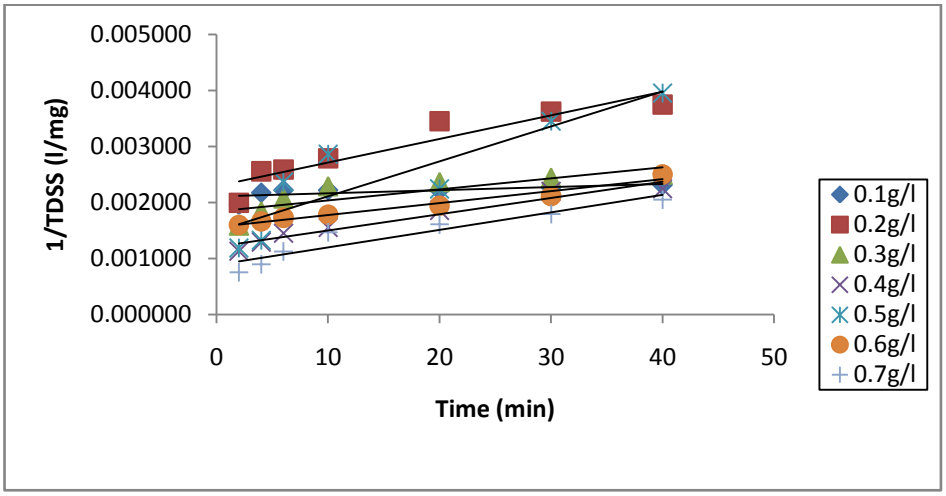

Fig.4.206: Kinetic plot of TDSS removal using varying cosc dosages for VIE at pH 10

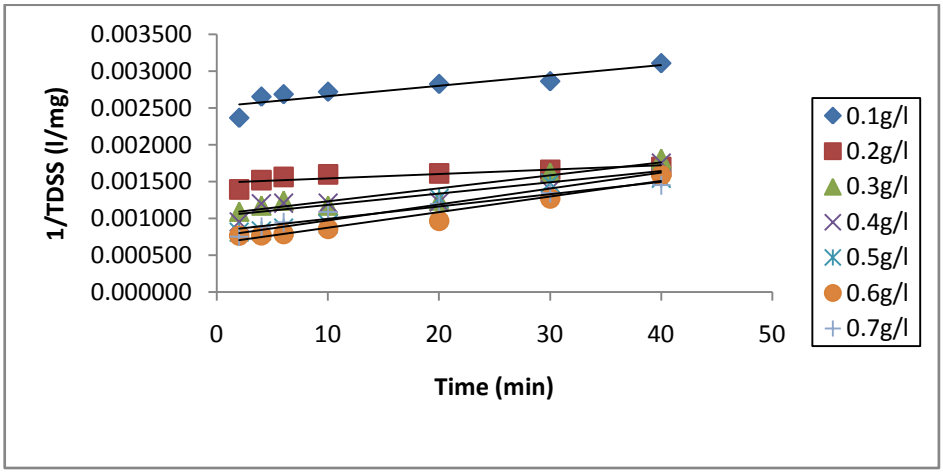

Fig.4.207: Kinetic plot of TDSS removal using varying cosc dosages for VIE at pH 13

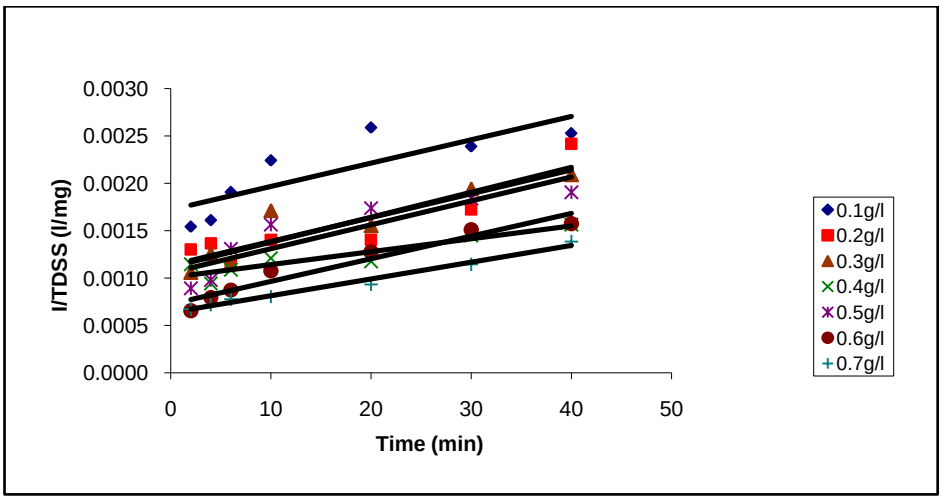

Fig.4.208: Kinetic plot of TDSS removal using varying tosc dosages for VIE at pH 1

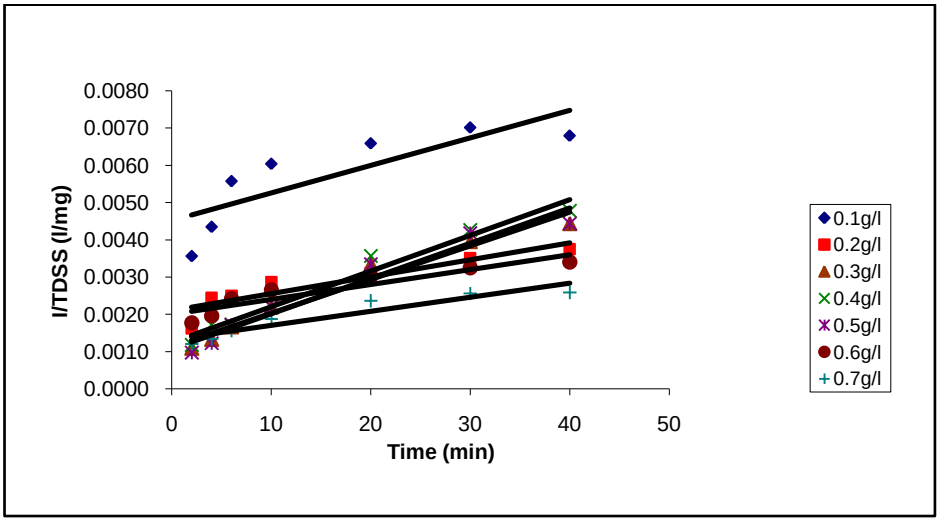

Fig.4.209: Kinetic plot of TDSS removal using varying tosc dosages for VIE at pH 3

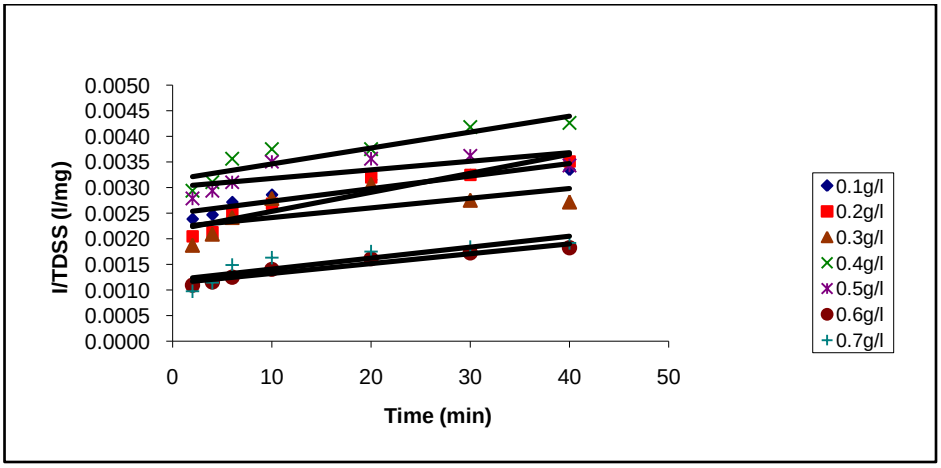

Fig.4.210: Kinetic plot of TDSS removal using varying tosc dosages for VIE at pH 5

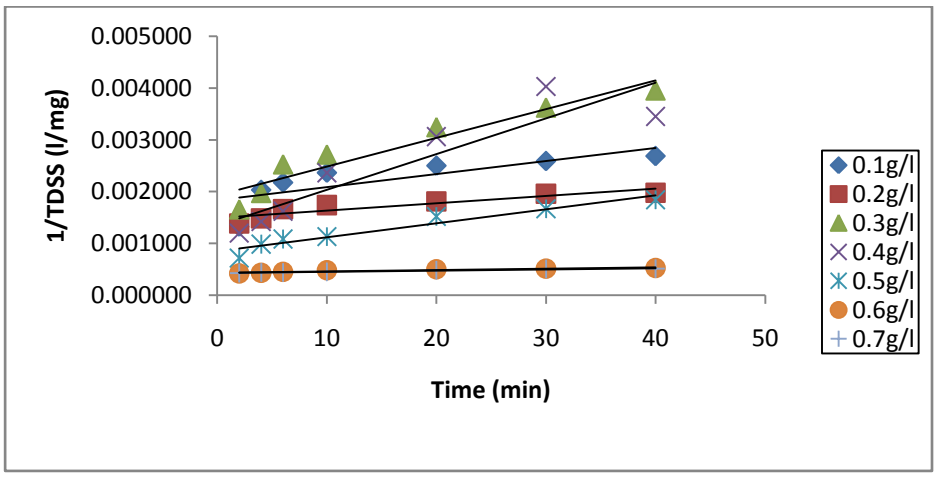

Fig.4.211: Kinetic plot of TDSS removal using varying tosc dosages for VIE at pH 7

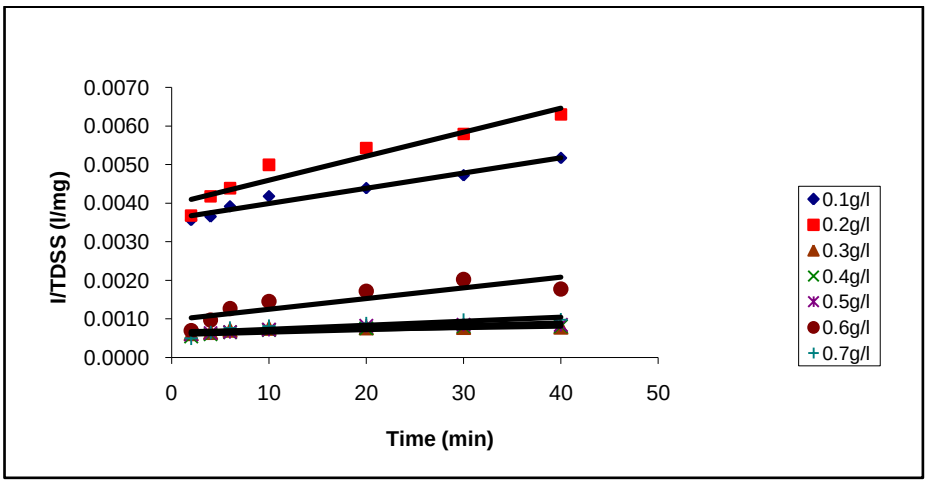

Fig.4.212: Kinetic plot of TDSS removal using varying tosc dosages for VIE at pH 10

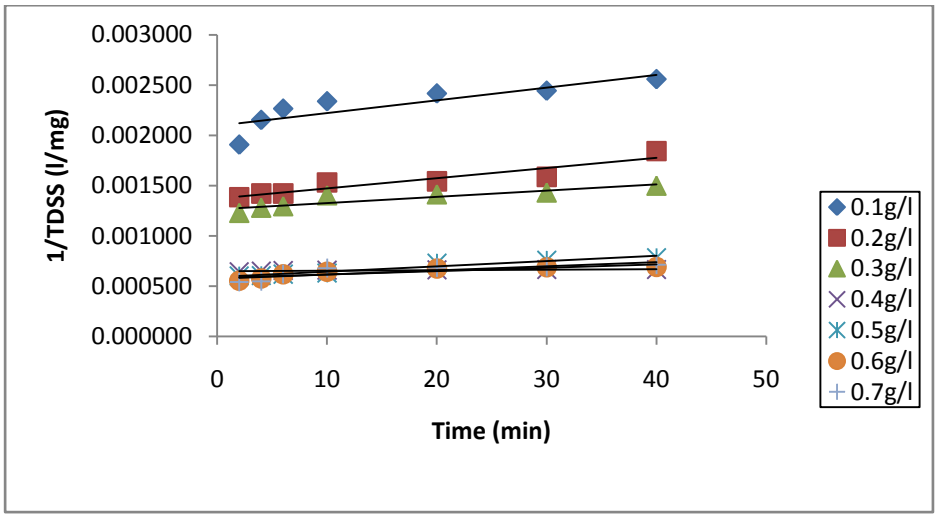

Fig.4.213: Kinetic plot of TDSS removal using varying tosc dosages for VIE at pH 13

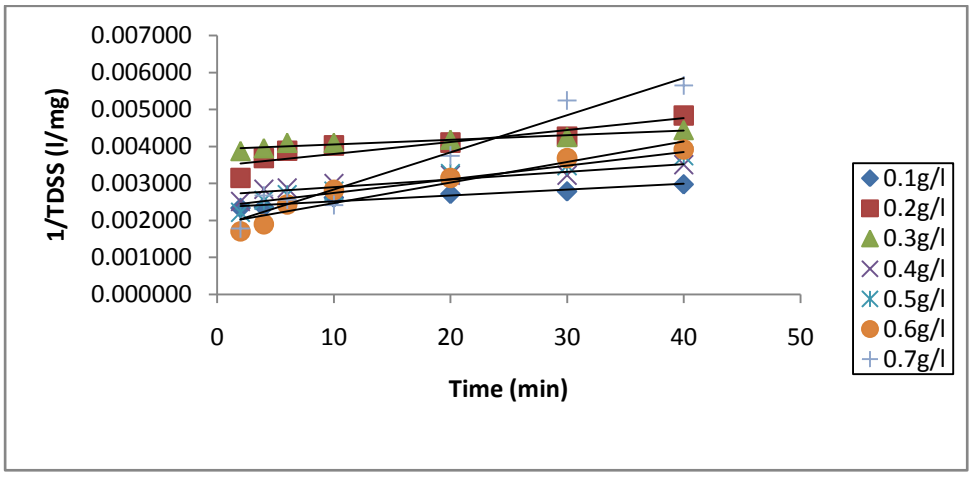

Fig.4.214: Kinetic plot of TDSS removal using varying ptsc dosages for VIE at pH 1

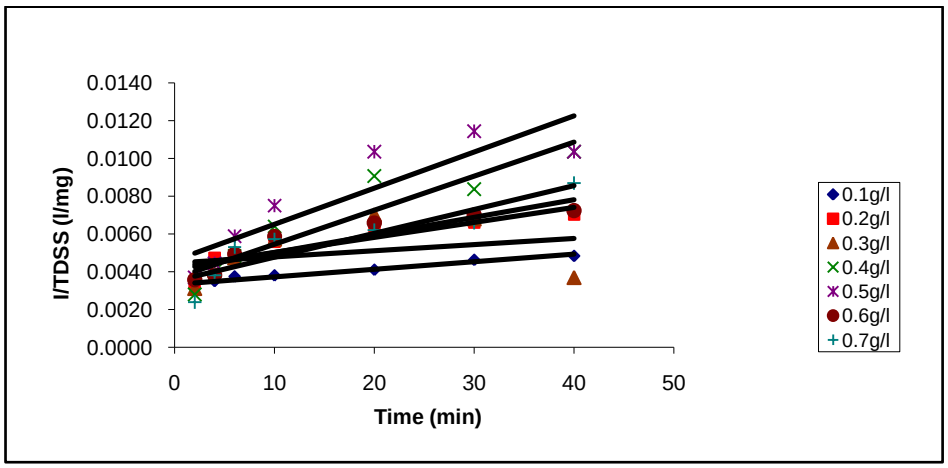

Fig.4.215: Kinetic plot of TDSS removal using varying ptsc dosages for VIE at pH 3

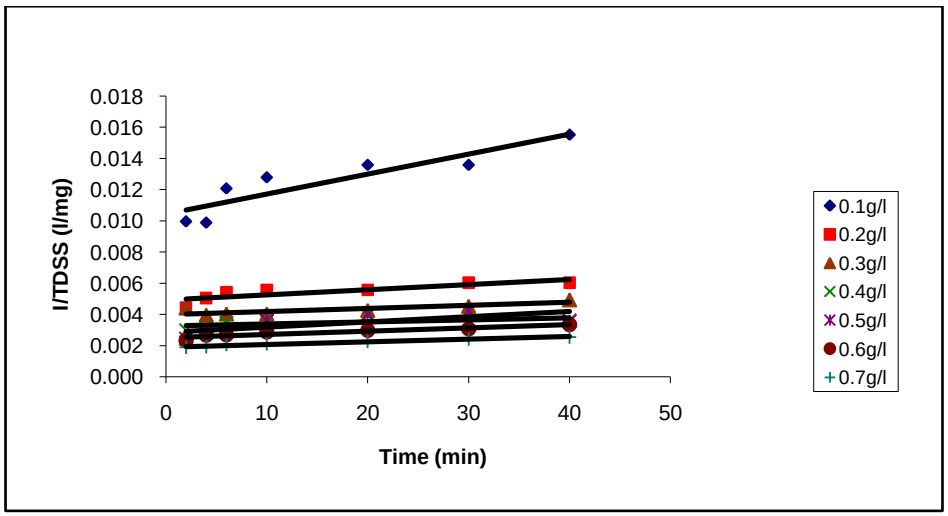

Fig.4.216: Kinetic plot of TDSS removal using varying ptsc dosages for VIE at pH 5

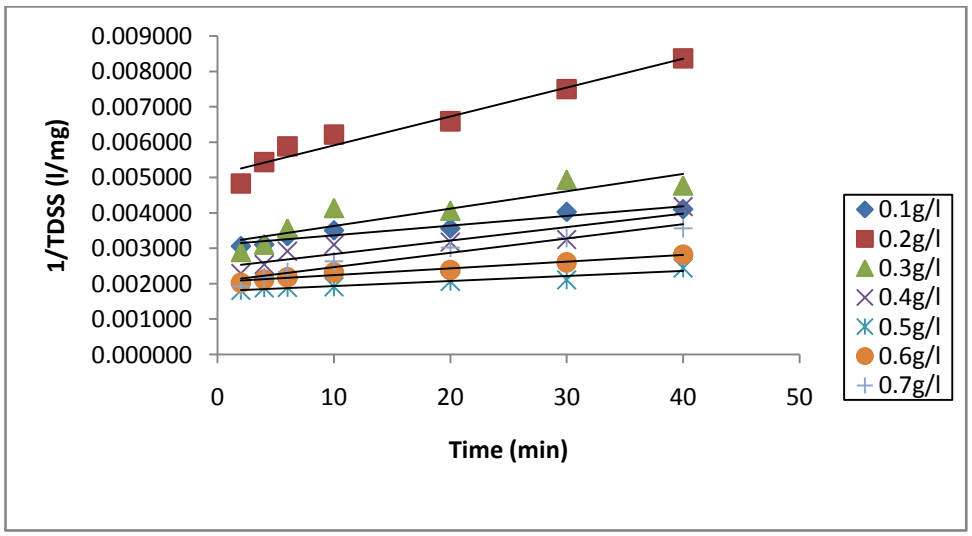

Fig.4.217: Kinetic plot of TDSS removal using varying ptsc dosages for VIE at pH 7

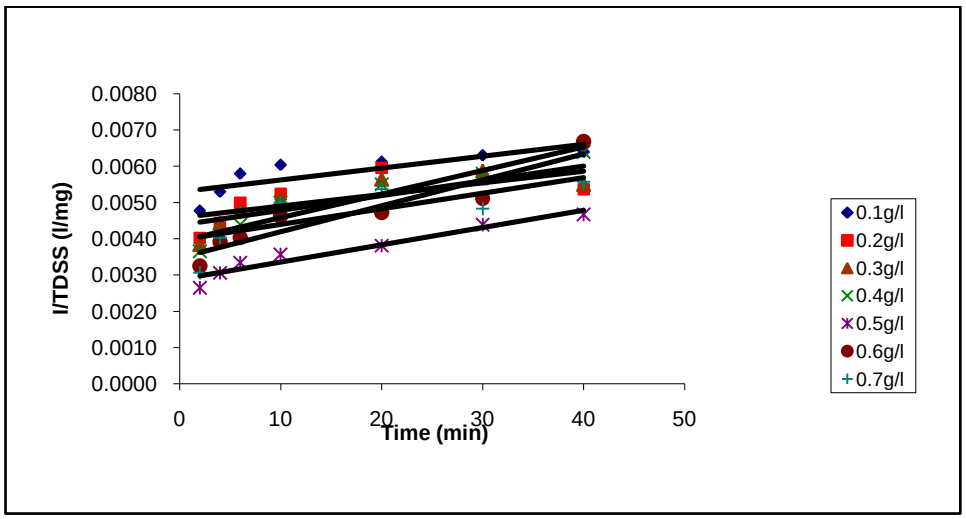

Fig.4.218: Kinetic plot of TDSS removal using varying ptsc dosages for VIE at pH 10

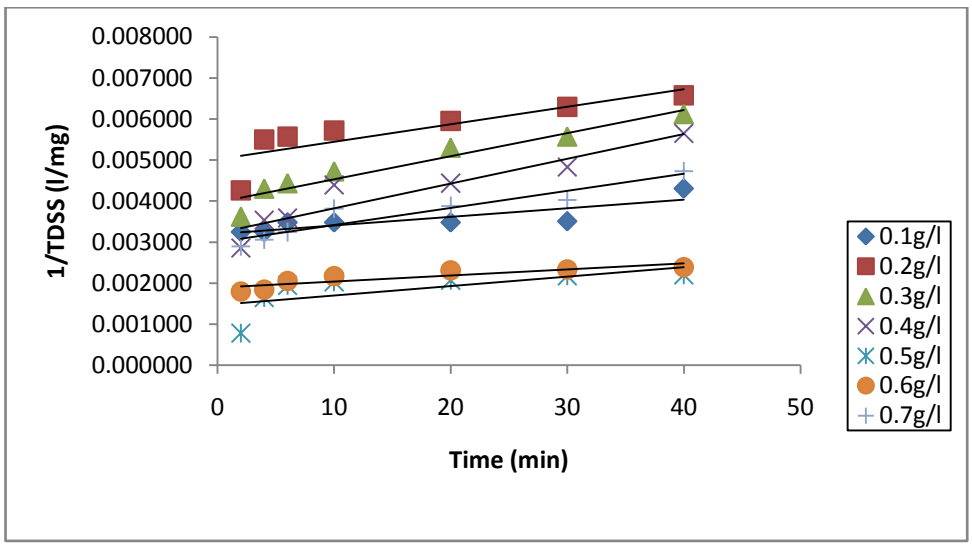

Fig.4.219: Kinetic plot of TDSS removal using varying ptsc dosages for VIE at pH 13

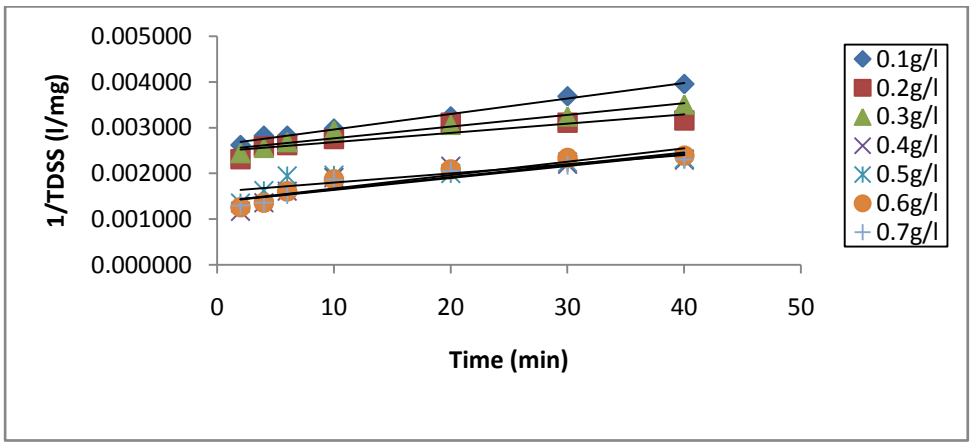

Fig.4.220: Kinetic plot of TDSS removal using varying mpsc dosages for VIE at pH 1

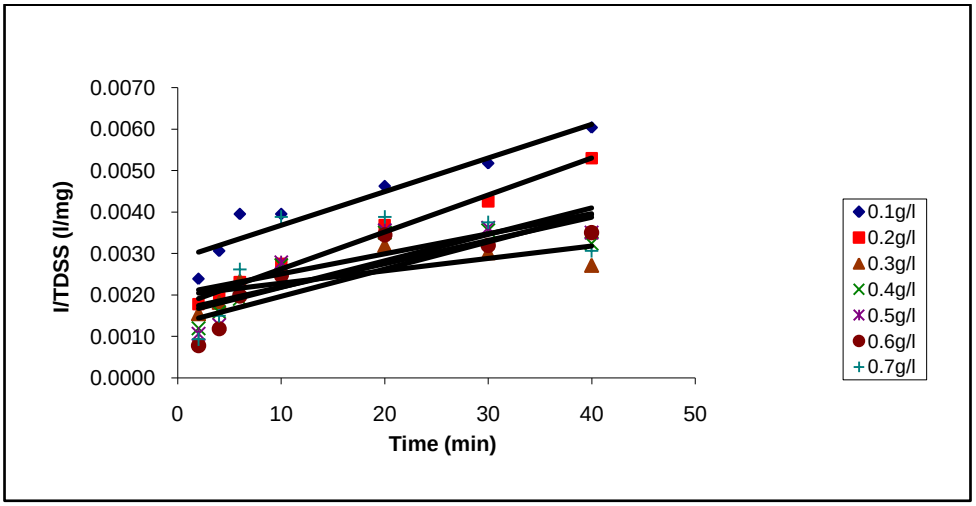

Fig.4.221: Kinetic plot of TDSS removal using varying mpsc dosages for VIE at pH 3

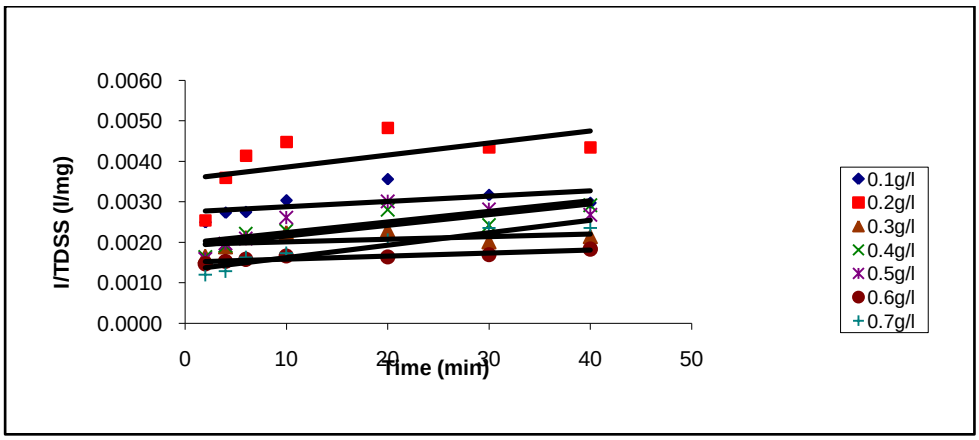

Fig.4.222: Kinetic plot of TDSS removal using varying mpsc dosages for VIE at pH 5

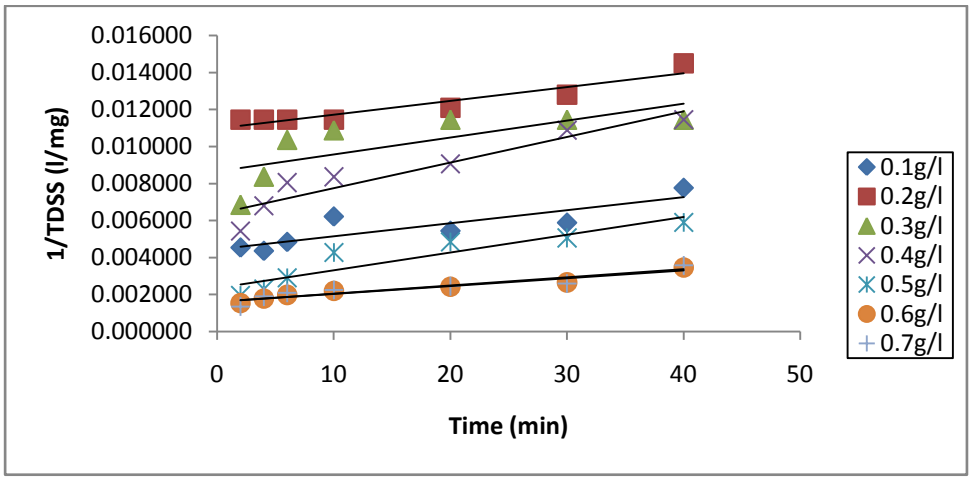

Fig.4.223: Kinetic plot of TDSS removal using varying mpsc dosages for VIE at pH 7

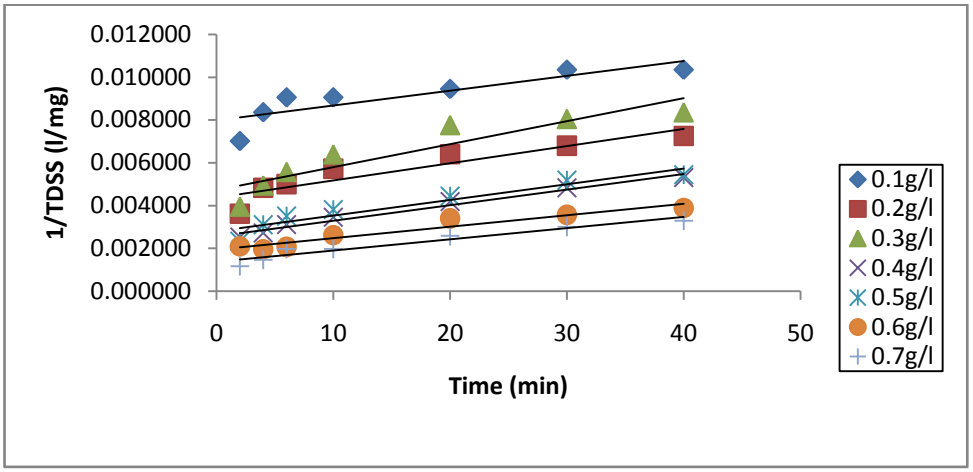

Fig.4.224: Kinetic plot of TDSS removal using varying mpsc dosages for VIE at pH 10

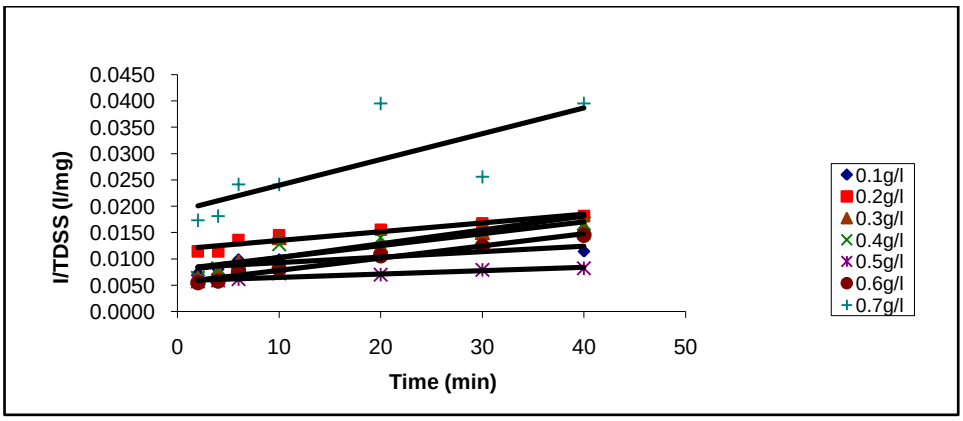

Fig.4.225: Kinetic plot of TDSS removal using varying mpsc dosages for VIE at pH 10

4.1.3.5 Kinetic results of pH varying VIE at constant dosage

The general results for pH varying VIE at constant dosage are presented in tables 4.98 to 4.132. For the SSC, the results are presented in tables 4.99 to 4.105. The best results for SSC is found in table 4.105 where the highest and lowest $\tau_{1/2}$ are recorded at 4.29min and 0.30min. The overall results indicate that satisfactory performance of SSC is expected at any given combination of pH and dosage within the ambits of this work as shown in tables 4.98 to 4.105. However, the optimum performance is recorded at the combination of pH 3 and 0.7 g/l dosage. The corresponding linear plots are presented in figures.4.226 to 4.232.

In case of COSC, the results are presented in tables 4.106 to 4.112. The optimum performance is achieved at $\tau_{1/2}$ of 0.34min for the combination of pH of 3 and 0.3g/l dosage. Though, the general results provided good performance for any combination

of pH and dosage as shown in tables 4.106 to 4.112. This is an indication that coag-flocculant dispersion in VIE is relatively satisfactory throughout the operation. The corresponding plots are presented in figures.4.233 to 4.238

Considering TOSC, the kinetic parameters are presented in tables 4.113 to 4.119. A critical observation of the tables, show that the best and worst pH for the coag-flocculation activity using TOSC are pH of 3 and pH of 13 at constant dosage of 0.4g/l. At the pH of 3 the best coag-flocculation period of 0.25min was obtained, while the maximum coag-flocculation period was 16.32min, showing that the system performance is least at pH of 13 and 0.4g/l dosage.

Presented in the tables 4.120 to 4.126 are the functional parameters of PTSC. The general results posted in the tables indicate that they were satisfactory for all the pH and dosages considered. For the single fact that the highest $\tau_{1/2}$ of 3.07 min is less than 5min which is the maximum coag-flocculation period (Von Smoluchowski, 1917), indicate that practical coag-flocculation process can be carried out at those conditions. The corresponding linear kinetic plots are presented in figs. 4.247 to 4.253.

In case of Table 4.127 to 4.133 presenting kinetic results associated with MPSC. Looking at tables 4.127 to 4.130, show that best coag-flocculation period is achieved at the pH of 13. However, it is pertinent to note that generally, all the coag-flocculation period obtained in the operation are satisfactory following maximum $\tau_{1/2} < 5$min.

Specifically, the performance in respect of K and $\tau_{1/2}$ values for pH of 7, 10,13 and 0.4g/l dosage respectively provide best conditions for coag-flocculation activity of MPSC. Note that minimal variation in the values of K_R and ε_p indicates near stability in operating temperature and effluent viscosity. The corresponding linear kinetic plots are presented in figures.4.254 and 4.260.

Table 4.99: Coag-Flocculation Kinetic Parameters and Linear Regression coefficient of SSC in VIE at varying pH and 0.1g/l dosage.

Parameters	pH=1	pH=3	pH=5	pH=7	pH=10	pH=13
Y	1.8E-05x + 8.541E-04	3.6E-05x + 4.438E-03	2.4E-05x + 5.882E-03	2.2E-05x + 4.659E-03	2.6E-05x + 2.369E-03	3.6E-05x + 1.681E-04
α	2.000	2.000	2.000	2.000	2.000	2.000
R^2	0.843	0.855	0.664	0.896	0.849	0.963
K(l/g.min)	1.8E-05	3.6E-05	2.4E-05	2.2E-05	2.6E-05	3.6E-05
K_R(l/min)	1.1829E-19	1.1809E-19	1.1691E-19	1.1770E-19	1.1711E-19	1.1770E-19
β_{BR}(l/g.min)	3.6E-05	7.2E-05	4.8E-05	4.4E-05	5.2E-05	7.2E-05
$\varepsilon_p(g^{-1})$	3.0434E+14	6.097E+14	4.1057E+14	3.7383E+14	4.4403E+14	6.1172E+14
$\tau_{½}$ (min)	2.01	0.67	1.51	1.65	0.61	0.50
(-r)	1.8E-05N_t^2	3.6E-05N_t^2	2.4E-05N_t^2	2.2E-056N_t^2	2.6E-05N_t^2	3.6E-06N_t^2
N_o (g/l)	117.0823	225.3267	170.0102	214.6383	422.1190	594.884

Table 4.100: Coag-Flocculation Kinetic Parameters and Linear Regression coefficient of SSC in VIE at varying pH and 0.2g/l dosage.

Parameters	pH=1	pH=3	pH=5	pH=7	pH=10	pH=13
Y	2.57E-05x + 7.068E-03	2.84E-05x + 3.906E-03	1.53E-05x + 3.962E-03	4.38E-05x + 3.02E-03	4.70E-05x + 2.225E-03	1.0E-05x + 2.362E-03
α	2.000	2.000	2.000	2.000	2.000	2.000
R^2	0.798	0.818	0.676	0.780	0.886	0.964
K(l/g.min)	2.57E-05	2.84E-05	1.53E-05	4.38E-05	4.70E-05	1.0E-05
K_R(l/min)	1.1829E-19	1.1809E-19	1.1691E-19	1.1770E-19	1.1711E-19	1.1770E-19
β_{BR}(l/g.min)	5.14E-05	5.68E-05	3.06E-05	8.76E-05	9.4E-05	2.0E-05
$\varepsilon_p(g^{-1})$	4.3453E+14	4.8099E+14	2.6174E+14	7.4427E+14	8.0266E+14	1.6992E+14
$\tau_{½}$ (min)	1.41	0.85	2.37	0.83	0.34	1.81
(-r)	2.57E-05N_t^2	2.84E-05N_t^2	1.53E-05N_t^2	4.38E-05N_t^2	4.70E-05N_t^2	1.0E-05N_t^2
N_o (g/l)	141.4827	256.0164	252.3978	331.1258	449.4382	423.3700

Table 4.101: Coag-Flocculation Kinetic Parameters and Linear Regression coefficient of SSC in VIE at varying pH and 0.3g/l dosage**.**

Parameters	pH=1	pH=3	pH=5	pH=7	pH=10	pH=13
Y	1.602E-05x + 6.8991E-03	3.786E-05x + 3.4615E-03	3.30E-05x + 3.0976E-03	5.087E-05x + 2.0513E-03	4.516E-05x + 1.2635E-03	3.455E-05x + 1.6151E-03
α	2.000	2.000	2.000	2.000	2.000	2.000
R^2	0.873	0.974	0.865	0.937	0.951	0.785
K(l/g.min)	1.602E-05	3.786E-05	3.30E-05	5.087E-05	4.516E-05	3.455E-05
K_R(l/min)	1.1848E-19	1.1829E-19	1.1691E-19	1.1770E-19	1.1711E-19	1.1789E-19
β_{BR}(l/g.min)	3.204E-05	7.572E-05	6.6E-05	1.0174E-05	9.032E-05	6.91E-05
$\varepsilon_p(g^{-1})$	2.7061E+14	6.4012E+14	5.6454E+14	8.6440E+14	7.7124E+14	5.8614E+14
$\tau_{½}$ (min)	2.26	0.64	1.10	0.71	0.36	0.52
(-r)	1.602E-05N_t^2	3.786E-05N_t^2	3.30E-05N_t^2	5.087E-05N_t^2	4.516E-05N_t^2	3.455E-05N_t^2
N_o (g/min)	144.9464	288.8921	322.8306	482.4952	791.4523	619.1567

Table 4.102: Coag-Flocculation Kinetic Parameters and Linear Regression coefficient of SSC in VIE at varying pH and 0.4g/l dosage.

Parameters	pH=1	pH=3	pH=5	pH=7	pH=10	pH=13
Y	1.785E-05x + 5.34E-03	2.190E-05x + 3.7183E-03	3.114E-05x + 2.3914E-03	2.843E-05x + 2.7637E-03	4.867E-05x + 9.985E-04	2.058E-05x + 1.0398E-03
α	2.000	2.000	2.000	2.000	2.000	2.000
R^2	0.959	0.775	0.586	0.760	0.982	0.834
K(l/g.min)	1.785E-05	2.190E-05	3.114E-05	2.843E-05	4.867E-05	2.058E-05
K_R(l/min)	1.1848E-19	1.1829E-19	1.1711E-19	1.1770E-19	1.1731E-19	1.1789E-19
β_{BR}(l/g.min)	3.57E-05	4.38E-05	6.228E-05	5.686E-05	9.734E-05	4.116E-05
$\varepsilon_p(g^{-1})$	3.0132E+14	3.7028E+14	5.3181E+14	4.8309E+14	8.2977E+14	3.4914E+14
$\tau_{½}$ (min)	2.03	1.10	1.16	1.27	0.33	0.88
(-r)	1.785E-05N_t^2	2.190E-05N_t^2	3.114E-05N_t^2	2.843E-05N_t^2	4.867E-05 N_t^2	2.058E-05N_t^2
N_o (g/l)	187.2659	268.9401	418.1651	361.8338	1001.5023	961.7234

Table 4.103: Coag-Flocculation Kinetic Parameters and Linear Regression Efficient of SSC in VIE at varying pH and 0.5g/l dosage.

Parameters	pH=1	pH=3	pH=5	pH=7	pH=10	pH=13
Y	3.26E-05x + 6.2114E-03	5.57E-05x + 32.5454E-03	5.40E-05x + 2.2006E-03	4.47E-05x + 2.0219E-03	4.80E-05x + 7.737E-04	1.10E-05x + 7.251E-04
α	2.000	2.000	2.000	2.000	2.000	2.000
R^2	0.856	0.775	0.962	0.723	0.997	0.715
K(l/g.min)	3.26E-05	5.57E-05	5.40E-05	4.47E-05	4.80E-05	1.10E-05
K_R(l/min)	1.1848E-19	1.1829E-19	1.1711E-19	1.1789E-19	1.1731E-19	1.1809E-19
β_{BR}(l/g.min)	6.52E-05	1.114E-04	1.08E-04	8.94E-05	9.6E-05	2.20E-05
$\varepsilon_p(g^{-1})$	5.5030E+14	9.4175E+14	9.2221E+14	7.5833E+14	8.1834E+14	1.8630E+14
$\tau_{½}$ (min)	1.11	0.43	0.67	0.81	0.34	1.65
(-r)	$3.26E\text{-}05N_t^2$	$5.57E\text{-}05N_t^2$	$5.40E\text{-}05N_t^2$	$4.47E\text{-}05N_t^2$	$4.80E\text{-}05N_t^2$	$1.10E\text{-}05N_t^2$
N_o (g/l)	160.9943	392.8656	454.4215	494.5843	1292.4906	1379.1201

Table 4.104: Coag-Flocculation Kinetic Parameters and Linear Regression coefficient of SSC in VIE at varying pH and 0.6g/l dosage.

Parameters	pH=1	pH=3	pH=5	pH=7	pH=10	pH=13
Y	9.664E-06x + 6.0344E-03	6.828E-05x + 1.9915E-03	5.523E-05x + 2.42E-03	2.709E-05x + 2.22255E-03	3.247E-05x + 8.512E-04	1.431E-05x + 7.793E-04
α	2.000	2.000	2.000	2.000	2.000	2.000
R^2	0.872	0.690	0.945	0.850	0.877	0.847
K(l/g.min)	9.664E-06	6.828E-05	5.523E-05	2.709E-05	3.247E-05	1.431E-05
K_R(l/min)	1.1848E-19	1.1868E-19	1.1711E-19	1.1789E-19	1.1750E-19	1.1809E-19
β_{BR}(l/g.min)	1.9328E-05	1.3656E-04	1.1046E-04	5.418E-05	6.494E-05	2.20862E-05
$\varepsilon_p(g^{-1})$	1.6286E+14	1.1507E+15	9.4322E+14	4.5958E+14	5.6268E+14	2.4236E+14
$\tau_{½}$ (min)	3.75	0.35	0.65	1.34	0.50	1.25
(-r)	$9.664E\text{-}06N_t^2$	$6.828E\text{-}05N_t^2$	$5.523E\text{-}05N_t^2$	$2.709E\text{-}05N_t^2$	$3.247E\text{-}05N_t^2$	$1.431E\text{-}05N_t^2$
N_o (g/l)	165.7166	502.1341	413.2231	449.3372	117.8120	1283.2029

Table 4.105: Coag-Flocculation Kinetic Parameters and Linear Regression coefficient of SSC in VIE at varying pH and 0.7g/l dosage.

Parameters	pH=1	pH=3	pH=5	pH=7	pH=10	pH=13
Y	8.44E-06x + 5.444E-03	7.93E-05x + 1.809E-03	5.25E-05x + 1.842E-03	3.46E-05x + 1.971E-03	3.247E-05x + 5.95E-04	2.06E-05x + 1.618E-03
α	2.000	2.000	2.000	2.000	2.000	2.000
R^2	0.776	0.747	0.952	0.938	0.961	0.639
K(l/g.min)	8.44E-06	7.93E-05	5.25E-05	3.46E-05	3.247E-05	2.06E-05
K_R(l/min)	1.1868E-19	1.1868E-19	1.1731E-19	1.1789E-19	1.1750E-19	1.1809E-19
β_{BR}(l/g.min)	1.688E-05	1.586E-04	1.05E-04	6.92E-05	4.72E-05	4.12E-05
$\varepsilon_p(g^{-1})$	1.4223E+14	1.3364E+15	8.9506E+14	5.8699E+14	4.0170E+14	3.4889E+14
$\tau_{½}$ (min)	4.29	0.30	0.69	1.05	0.68	0.88
(-r)	$8.44E\text{-}06N_t^2$	$7.93E\text{-}05N_t^2$	$5.25E\text{-}05N_t^2$	$3.46E\text{-}05N_t^2$	$3.247E\text{-}05N_t^2$	$2.06E\text{-}05N_t^2$
N_o (g/l)	183.6885	552.7916	542.8882	507.3567	1680.6723	618.0470

Table 4.106: Coag-Flocculation Kinetic Parameters and Linear Regression coefficient of COSC in VIE at varying pH and 0.1g/l dosage.

Parameters	pH=1	pH=3	pH=5	pH=7	pH=10	pH=13
Y	2.6E-05x + 2.962E-03	4.4E-05x + 3.411E-03	4.2E-05x + 2.452E-03	4.4E-05x + 3.569E-03	6.0E-06x + 2.106E-03	1.4E-05x + 2.518E-03
α	2.000	2.000	2.000	2.000	2.000	2.000
R^2	0.776	0.692	0.927	0.743	0.614	0.815
K(l/g.min)	2.6E-05	4.4E-05	4.2E-05	4.4E-05	6.0E-06	1.4E-05
K_R(l/min)	1.1848E-19	1.1868E-19	1.1731E-19	1.1789E-19	1.1750E-19	1.1868E-19
β_{BR}(l/g.min)	5.2E-05	8.8E-05	8.4E-05	8.8E-05	1.2E-05	2.8E-05
$\varepsilon_p(g^{-1})$	4.3889E+14	7.4149E+14	7.1605E+14	7.4646E+14	1.0213E+14	2.3593E+14
$\tau_{½}$ (min)	0.93	0.55	0.58	0.41	3.02	1.30
(-r)	$2.6E\text{-}05N_t^2$	$4.4E\text{-}05N_t^2$	$4.2E\text{-}05N_t^2$	$4.4E\text{-}05N_t^2$	$6.0E\text{-}06\ N_t^2$	$1.4E\text{-}05N_t^2$
N_o (g/l)	337.6097	293.1692	407.8303	280.1905	474.8338	397.1406

Table 4.107: Coag-Flocculation Kinetic Parameters and Linear Regression coefficient of COSC in VIE at varying pH and 0.2g/l dosage.

Parameters	pH=1	pH=3	pH=5	pH=7	pH=10	pH=13
Y	4.16E-05x + 3.18E-03	6.45E-05x + 2.725E-03	6.02E-05x + 2.663E-03	4.98E-05x + 2.293E-03	4.21E-05x + 2.29E-03	5.91E-06x + 1.483E-03
α	2.000	2.000	2.000	2.000	2.000	2.000
R^2	0.694	0.769	0.716	0.824	0.875	0.732
K(l/g.min)	4.16E-05	6.45E-05	6.02E-05	4.98E-05	4.21E-05	5.91E-06
K_R(l/min)	1.1848E-19	1.1868E-19	1.1731E-19	1.1789E-19	1.1750E-19	1.1868E-19
β_{BR}(l/g.min)	8.32E-05	1.29E-04	1.204E-04	9.96E-05	8.42E-05	1.1868E-05
$\varepsilon_p(g^{-1})$	7.0223E+14	1.0870E+15	1.0263E+15	8.4486E+14	7.1660E+14	9.9596E+13
$\tau_{½}$ (min)	34.84	22.47	24.07	21.83	25.82	183.92
(-r)	$4.16E\text{-}05N_t^2$	$6.45E\text{-}05N_t^2$	$6.02E\text{-}05N_t^2$	$4.98E\text{-}05N_t^2$	$4.21E\text{-}05N_t^2$	$5.91E\text{-}06N_t^2$
N_o (g/l)	319.6931	366.9725	375.5163	436.1099	436.6812	674.3088

Table 4.108: Coag-Flocculation Kinetic Parameters and Linear Regression coefficient of COSC in VIE at varying pH and 0.3g/l dosage.

Parameters	pH=1	pH=3	pH=5	pH=7	pH=10	pH=13
Y	4.286E-05x + 1.9978E-03	7.115E-05x + 1.5377E-03	2.494E-05x + 1.4425E-03	5.745E-06x + 1.0301E-03	1.967E-05x + 1.8413E-03	1.764E-05x + 1.0551E-03
α	2.000	2.000	2.000	2.000	2.000	2.000
R^2	0.877	0.953	0.934	0.847	0.709	0.900
K(l/g.min)	4.286E-05	7.115E-05	2.494E-05	5.745E-06	1.967E-05	1.764E-05
K_R(l/min)	1.18648E-19	1.1868E-19	1.1731E-19	1.1789E-19	1.1750E-19	1.1887E-19
β_{BR}(l/g.min)	8.572E-05	1.423E-04	4.988E-05	1.149E-05	3.934E-05	3.528E-05
$\varepsilon_p(g^{-1})$	2.6997E+14	1.1990E+15	4.2520E+14	9.7464E+13	3.3481E+14	2.9679E+14
$\tau_{½}$ (min)	0.56	0.34	0.97	3.15	0.92	1.03
(-r)	$4.286E\text{-}05N_t^2$	$7.115E\text{-}05N_t^2$	$2.494E\text{-}05N_t^2$	$5.745E\text{-}06N_t^2$	$1.967E\text{-}05N_t^2$	$1.764E\text{-}05N_t^2$
N_o (g/l)	500.5506	650.3219	3693.2409	970.7795	543.0946	947.7775

Table 4.109: Coag-Flocculation Kinetic Parameters and Linear Regression coefficient of COSC in VIE at varying pH and 0.4g/l dosage.

Parameters	pH=1	pH=3	pH=5	pH=7	pH=10	pH=13
Y	4.896E-05x + 2.0545E-03	5.211E-05x + 1.5184E-03	4.444E-05x + 1.3095E-03	1.794E-05x + 1.0764E-03	2.909E-05x + 1.2093E-03	1.534E-05x + 1.0315E-03
α	2.000	2.000	2.000	2.000	2.000	2.000
R^2	0.888	0.870	0.912	0.858	0.946	0.818
K(l/g.min)	4.896E-05	5.211E-05	4.444E-05	1.794E-05	2.909E-05	1.534E-05
K_R(l/min)	1.1868E-19	1.1887E-19	1.1731E-19	1.1809E-19	1.1789E-19	1.1887E-19
β_{BR}(l/g.min)	9.792E-05	1.0422E-04	8.888E-05	3.588E-05	5.818E-05	3.068E-05
$\varepsilon_p(g^{-1})$	8.2508E+14	8.7676E+15	7.5765E+14	3.0384E+14	4.9351E+14	2.5810E+14
$\tau_{½}$ (min)	0.49	0.46	0.54	1.01	0.62	1.18
(-r)	$4.896E\text{-}05N_t^2$	$5.211E\text{-}05N_t^2$	$4.444E\text{-}05N_t^2$	$1.794E\text{-}05N_t^2$	$2.909E\text{-}05N_t^2$	$1.534E\text{-}05N_t^2$
N_o (g/l)	486.7364	658.5880	763.6502	929.0227	826.9247	969.4619

Table 4.110: Coag-Flocculation Kinetic Parameters and Linear Regression coefficient of COSC in VIE at varying pH and 0.5g/l dosage**.**

Parameters	pH=1	pH=3	pH=5	pH=7	pH=10	pH=13
Y	1.95E-05x + 1.1437E-03	2.55E-05x + 1.0739E-03	4.30E-05x + 1.2127E-03	1.60E-05x + 9.841E-04	6.23E-05x + 1.4855E-03	2.15E-05x + 1.593E-04
α	2.000	2.000	2.000	2.000	2.000	2.000
R^2	0.807	0.798	0.890	0.837	0.776	0.964
K(l/g.min)	1.95E-05	2.55E-05	4.30E-05	1.60E-05	6.23E-05	2.15E-05
K_R(l/min)	1.1868E-19	1.1887E-19	1.1750E-19	1.1809E-19	1.1789E-19	1.1907E-19
β_{BR}(l/g.min)	3.9E-05	5.1E-05	8.6E-05	3.2E-05	1.246E-04	4.3E-05
$\varepsilon_p(g^{-1})$	3.2861E+14	4.2904E+14	7.3191E+14	2.7098E+14	1.0569E+15	3.6113E+14
$\tau_{½}$ (min)	1.24	0.95	33.70	0.56	0.29	0.84
(-r)	$1.95E\text{-}05N_t^2$	$2.55E\text{-}05N_t^2$	$4.30E\text{-}05N_t^2$	$1.60E\text{-}05N_t^2$	$6.23E\text{-}05N_t^2$	$2.15E\text{-}05N_t^2$
N_o (g/l)	874.3552	931.1854	824.6063	673.1740	673.1740	1317.0025

Table 4.111: Coag-Flocculation Kinetic Parameters and Linear Regression coefficient of COSC in VIE at varying pH and 0.6g/l dosage.

Parameters	pH=1	pH=3	pH=5	pH=7	pH=10	pH=13
Y	4.84E-05x + 1.6271E-03	4.102E-05x + 1.338E-03	2.713E-05x + 7.869E-04	1.145E-05x + 7.173E-04	2.140E-05x + 1.5599E-03	2.111E-05x + 6.641E-04
α	2.000	2.000	2.000	2.000	2.000	2.000
R^2	0.978	0.794	0.987	0.894	0.968	0.956
K(l/g.min)	4.84E-05	4.102E-05	2.713E-05	1.145E-05	2.140E-05	2.111E-05
K_R(l/min)	1.1887E-19	1.1907E-19	1.1750E-19	1.1829E-19	1.1789E-19	1.1907E-19
β_{BR}(l/g.min)	9.68E-05	8.204E-05	5.426E-05	2.29E-05	4.280E-05	4.222E-05
$\varepsilon_p(g^{-1})$	8.1433E+14	6.8901E+14	4.6179E+14	1.9359E+14	3.6305E+14	3.5458E+14
$\tau_{½}$ (min)	0.50	0.59	0.89	1.58	0.85	0.86
(-r)	$4.84E\text{-}05N_t^2$	$4.102E\text{-}05N^t{}_2$	$2.713E\text{-}05N_t^2$	$1.145E\text{-}05N_t^2$	$2.140E\text{-}05N_t^2$	$2.111E\text{-}05N_t^2$
N_o (g/l)	614.5904	747.3816	1270.8095	1394.1168	641.0667	1505.7973

Table 4.112: Coag-Flocculation Kinetic Parameters and Linear Regression coefficient of COSC in VIE at varying pH and 0.7g/l dosage.

Parameters	pH=1	pH=3	pH=5	pH=7	pH=10	pH=13
Y	1.84E-05x + 8.66E-04	4.06E-05x + 1.022E-03	3.16E-05x + 9.57E-04	2.90E-05x + 7.63173E-04	3.11E-05x + 8.89E-04	1.67E-05x + 8.28E-04
α	2.000	2.000	2.000	2.000	2.000	2.000
R^2	0.977	0.863	0.874	0.967	0.896	0.937
K(l/g.min)	1.84E-05	4.06E-05	3.16E-05	2.90E-05	3.11E-05	1.67E-05
K_R(l/min)	1.1887E-19	1.1907E-19	1.1750E-19	1.1829E-19	1.1809E-19	1.1926E-19
β_{BR}(l/g.min)	3.68E-05	8.12E-05	6.32E-05	5.8E-05	6.220E-05	3.34E-05
$\varepsilon_p(g^{-1})$	3.0958E+14	6.8195E+14	5.3787E+14	4.9032E+14	5.2672E+14	2.8006E+15
$\tau_{½}$ (min)	1.31	0.60	0.76	0.62	0.58	1.08
(-r)	$1.84E\text{-}05N_t^2$	$4.06E\text{-}05N_t^2$	$3.16E\text{-}05N_t^2$	$2.90E\text{-}05N_t^2$	$3.11E\text{-}05N_t^2$	$1.67E\text{-}05N_t^2$
N_o (g/l)	1154.7344	978.4736	1044.9321	1310.6160	1124.8594	1207.7295

Table 4.113: Coag-Flocculation Kinetic Parameters and Linear Regression Efficient of TOSC in VIE at varying pH and 0.1g/l dosage.

Parameters	pH=1	pH=3	pH=5	pH=7	pH=10	pH=13
Y	2.7E-05x + 1.689E-03	7.6E-05x + 4.491E-03	2.4E-05x + 2.492E-03	2.5E-05x + 1.835E-03	4.0E-05x + 3.597E-03	1.3E-05x + 2.094E-03
α	2.000	2.000	2.000	2.000	2.000	2.000
R^2	0.805	0.709	0.879	0.622	0.966	0.730
K(l/g.min)	2.7E-05	7.6E-05	2.4E-05	2.5E-05	4.0E-05	1.3E-05
K_R(l/min)	1.1750E-19	1.1868E-19	1.1711E-19	1.1711E-19	1.1731E-19	1.1731E-19
β_{BR}(l/g.min)	5.4E-05	1.52E-04	4.8E-05	5.0E-05	8.0E-05	2.6E-05
$\varepsilon_p(g^{-1})$	4.5957E+14	1.2808E+15	4.0987E+14	4.2695E+14	6.8195E+14	2.2163E+14
$\tau_{½}$ (min)	0.67	0.32	1.01	0.48	0.36	1.24
(-r)	$2.7E\text{-}05N_t^2$	$7.6E\text{-}05N_t^2$	$2.4E\text{-}05N_t^2$	$2.5E\text{-}05N_t^2$	$4.0E\text{-}05N_t^2$	$1.3E\text{-}05N_t^2$
N_o (g/l)	592.0663	222.6676	401.2841	544.9591	278.0095	477.5549

Table 4.114: Coag-Flocculation Kinetic Parameters and Linear Regression coefficient of TOSC in VIE at varying pH and 0.2g/l dosage.

Parameters	pH=1	pH=3	pH=5	pH=7	pH=10	pH=13
Y	2.69E-05x + 1.107E-03	4.53E-05x + 2.101E-03	3.72E-05x + 2.164E-03	1.41E-05x + 1.49E-03	6.21E-05x + 3.976E-03	1.01E-05x + 1.371E-03
α	2.000	2.000	2.000	2.000	2.000	2.000
R^2	0.846	0.839	0.893	0.833	0.922	0.885
K(l/g.min)	2.69E-05	4.53E-05	3.72E-05	1.41E-05	6.21E-05	1.01E-05
K_R(l/min)	1.1750E-19	1.1887E-19	1.1711E-19	1.1711E-19	1.1731E-19	1.1731E-19
β_{BR}(l/g.min)	5.38E-05	9.06E-04	7.44E-05	2.82E-05	1.242E-04	2.02E-05
$\varepsilon_p(g^{-1})$	4.5787E+14	7.6218E+15	6.3530E+14	2.4080E+14	1.0587E+15	1.7219E+14
$\tau_{½}$ (min)	0.67	0.53	0.65	0.86	0.23	1.59
(-r)	$2.69E\text{-}05N_t^2$	$4.53E\text{-}05N_t^2$	$3.72E\text{-}05N_t^2$	$1.41E\text{-}05N_t^2$	$6.21E\text{-}05N_t^2$	$1.01E\text{-}05N_t^2$
N_o (g/l)	903.3424	475.9638	462.1072	671.1409	251.5091	729.3946

Table 4.115: Coag-Flocculation Kinetic Parameters and Linear Regression coefficient of TOSC in VIE at varying pH and 0.3g/l dosage**.**

Parameters	pH=1	pH=3	pH=5	pH=7	pH=10	pH=13
Y	2.515E-05x + 1.136E-03	9.041E-05x + 1.1253E-03	2.502E-05x + 2.1276E-03	5.541E-05x + 1.928E-03	3.785E-05x + 6.665E-03	6159E-06x + 1.264E-03
α	2.000	2.000	2.000	2.000	2.000	2.000
R^2	0.841	0.965	0.742	0.910	0.678	0.833
K(l/g.min)	2.515E-05	9.041E-05	2.502E-05	5.541E-05	3.785E-05	6159E-06
K_R(l/min)	1.1750E-19	1.1887E-19	1.1711E-19	1.1711E-19	1.1750E-19	1.1750E-19
β_{BR}(l/g.min)	5.03E-05	1.8082E-04	5.004E-05	1.1082E-04	7.57E-06	1.2318E-05
$\varepsilon_p(g^{-1})$	4.2809E+14	1.5212E+15	4.2729E+14	9.4629E+14	6.4426E+13	1.0483E+14
$\tau_{½}$ (min)	0.72	0.27	0.97	0.22	3.83	2.61
(-r)	$2.515E\text{-}05N_t^2$	$9.041E\text{-}05N_t^2$	$2.502E\text{-}05N_t^2$	$5.541E\text{-}05N_t^2$	$3.785E\text{-}05N_t^2$	$6159E\text{-}06N_t^2$
N_o (g/l)	880.2817	888.6519	470.0132	518.6722	1500.3751	790.5763

Table 4.116: Coag-Flocculation Kinetic Parameters and Linear Regression coefficient of TOSC in VIE at varying pH and 0.4g/l dosage.

Parameters	pH=1	pH=3	pH=5	pH=7	pH=10	pH=13
Y	1.420E-05x + 9.968E-04	9.594E-05x + 1.2372E-03	3.109E-05x + 3.152E-03	6.895E-05x + 1.3461E-03	6.477E-06x + 5.991E-04	4.881E-07x + 6.47E-04
α	2.000	2.000	2.000	2.000	2.000	2.000
R^2	0.929	0.970	0.822	0.838	0.824	0.731
K(l/g.min)	1.420E-05	9.594E-05	3.109E-05	6.895E-05	6.477E-06	4.881E-07
K_R(l/min)	1.1770E-19	1.1887E-19	1.1711E-19	1.1731E-19	1.1750E-19	1.1750E-19
β_{BR}(l/g.min)	2.84E-05	1.9188E-04	6.218E-05	1.379E-04	1.2954E-05	9.762E-07
$\varepsilon_p(g^{-1})$	2.4129E+14	1.6142E+15	5.3095E+14	1.1755E+15	1.1025E+14	8.3081E+14
$\tau_{½}$ (min)	1.28	0.25	0.78	0.18	2.24	3.30
(-r)	$1.420E\text{-}05N_t^2$	$9.594E\text{-}05N_t^2$	$3.109E\text{-}05N_t^2$	$6.895E\text{-}05N_t^2$	$6.477E\text{-}06N_t^2$	$4.881E\text{-}07N_t^2$
N_o (g/l)	1003.2103	808.2768	4317.2589	742.8869	1669.1704	1545.5763

Table 4.117: Coag-Flocculation Kinetic Parameters and Linear Regression coefficient of TOSC in VIE at varying pH and 0.5g/l dosage.

Parameters	pH=1	pH=3	pH=5	pH=7	pH=10	pH=13
Y	2.52E-05x + 1.0591E-03	9.49E-05x + 1.0617E-03	1.97E-05x + 2.9649E-03	2.70E-05x + 8.485E-04	6.89E-06x + 6.24E-04	5.24E-06x + 5.907E-04
α	2.000	2.000	2.000	2.000	2.000	2.000
R^2	0.791	0.952	0.738	0.934	0.858	0.954
K(l/g.min)	2.52E-05	9.49E-05	1.97E-05	2.70E-05	6.89E-06	5.24E-06
K_R(l/min)	1.1770E-19	1.1907E-19	1.1731E-19	1.1731E-19	1.1750E-19	1.1750E-19
β_{BR}(l/g.min)	5.04E-05	1.898E-04	3.94E-05	5.4E-05	1.378E-05	1.048E-05
$\varepsilon_p(g^{-1})$	4.2821E+14	1.5940E+15	3.3586E+14	4.6032E+14	1.1728E+14	8.9191E+14
$\tau_{½}$ (min)	0.71	0.25	1.23	0.45	2.10	3.07
(-r)	$2.52E\text{-}05N_t^2$	$9.49E\text{-}05N_t^2$	$1.97E\text{-}05N_t^2$	$2.70E\text{-}05N_t^2$	$6.89E\text{-}06N_t^2$	$5.24E\text{-}06N_t^2$
N_o (g/l)	944.1979	941.8857	337.2795	1178.5504	1602.5561	1692.9067

Table 4.118: Coag-Flocculation Kinetic Parameters and Linear Regression coefficient of TOSC in VIE at varying pH and 0.6g/l dosage.

Parameters	pH=1	pH=3	pH=5	pH=7	pH=10	pH=13
Y	2.388E-05x + 7.267E-04	4.021E-05x + 1.9934E-03	1.927E-05x + 1.1292E-03	2.691E-06x + 4.311E-04	2.784E-05x + 9.747E-04	3.326E-06x + 5.81E-04
α	2.000	2.000	2.000	2.000	2.000	2.000
R^2	0.937	0.864	0.941	0.870	0.729	0.780
K(l/g.min)	2.388E-05	4.021E-05	1.927E-05	2.691E-06	2.784E-05	3.326E-06
K_R(l/min)	1.1789E-19	1.1907E-19	1.1731E-19	1.1731E-19	1.1770E-19	1.1770E-19
β_{BR}(l/g.min)	4.776E-05	8.042E-05	3.854E-05	5.382E-06	5.56E-05	6.652E-06
$\varepsilon_p(g^{-1})$	4.0512E+14	6.7540E+14	3.2853E+14	4.5878E+13	4.7239E+14	5.6517E+13
$\tau_{½}$ (min)	0.76	0.60	1.25	4.49	0.52	4.94.38
(-r)	$2.388E-05N_t^2$	$4.021E-05\ N_t^2$	$1.927E-05N_t^2$	$2.691E-06\ N_t^2$	$2.784E-05\ N_t^2$	$3.326E-06N_t^2$
N_o (g/l)	1376.0837	501.6555	885.5827	2319.6474	1025.9567	1721.1704

Table 4.119: Coag-Flocculation Kinetic Parameters and Linear Regression coefficient of TOSC in VIE at varying pH and 07g/l dosage**.**

Parameters	pH=1	pH=3	pH=5	pH=7	pH=10	pH=13
Y	1.77E-05x + 6.35E-04	3.76E-05x + 1.325E-03	2.13E-05x + 1.197E-03	2.39E-06x + 4.27E-04	1.04E-05x + 6.27E-04	4.04E-06x + 5.75E-04
α	2.000	2.000	2.000	2.000	2.000	2.000
R^2	0.983	0.882	0.742	0.964	0.773	0.682
K(l/g.min)	1.77E-05	3.76E-05	2.13E-05	2.39E-06	1.04E-05	4.04E-06
K_R(l/min)	1.1789E-19	1.1926E-19	1.1731E-19	1.1750E-19	1.1770E-19	1.1770E-19
β_{BR}(l/g.min)	3.54E-05	7.52E-05	4.26E-05	4.78E-06	2.08E-05	8.08E-06
$\varepsilon_p(g^{-1})$	3.0028E+14	6.3056E+14	3.6314E+14	4.0546E+13	1.7672E+14	6.8649E+13
$\tau_{½}$ (min)	1.02	0.64	1.13	5.04	1.40	3.99
(-r)	$1.77E-05N_t^2$	$3.76E-05N_t^2$	$2.13E-05N_t^2$	$2.39E-06N_t^2$	$1.04E-05N_t^2$	$4.04E-06N_t^2$
N_o (g/l)	1574.8032	754.7170	835.4219	2341.9204	1594.8963	1739.1304

Table 4.120: Coag-Flocculation Kinetic Parameters and Linear Regression coefficient of PTSC in VIE at varying pH and 0.1g/l dosage.

Parameters	pH=1	pH=3	pH=5	pH=7	pH=10	pH=13
Y	1.0E-05x + 2.351E-03	4.0E-05x + 3.326E-03	1.28E-04x + 1.0439E-02	2.7E-04x + 3.094E-03	3.3E-05x + 5.295E-04	2.1E-05x + 3.201E-03
α	2.000	2.000	2.000	2.000	2.000	2.000
R^2	0.939	0.942	0.824	0.931	0.661	0.709
K(l/g.min)	1.0E-05	4.0E-05	1.28E-04	2.7E-04	3.3E-05	2.1E-05
K_R(l/min)	1.1809E-19	1.1750E-19	1.1672E-19	1.1750E-19	1.1672E-19	1.1848E-19
β_{BR}(l/g.min)	3.2E-05	8.0E-05	2.56E-04	5.4E-05	6.6E-05	4.2E-05
$\varepsilon_p(g^{-1})$	2.7098E+14	6.8085E+15	2.1933E+15	4.5957E+14	5.6546E+14	3.5449E+14
$\tau_{½}$ (min)	2.26	0.91	0.28	1.34	1.11	1.29
(-r)	$1.0E-05N_t^2$	$4.0E-05N_t^2$	$1.28E-04N_t^2$	$2.7E-04N_t^2$	$3.3E-05N_t^2$	$2.1E-05N_t^2$
N_o (g/l)	425.3509	300.6615	957.9461	323.2062	188.8574	312.4024

Table 4.121: Coag-Flocculation Kinetic Parameters and Linear Regression coefficient of PTSC in VIE at varying pH and 0.2g/l dosage.

Parameters	pH=1	pH=3	pH=5	pH=7	pH=10	pH=13
Y	3.22E-05x + 3.476E-03	7.92E-05x + 4.236E-03	3.26E-05x + 4.929E-03	8.16E-05x + 5.095E-03	4.15E-05x + 4.431E-03	4.28E-05x + 5.014E-03
α	2.000	2.000	2.000	2.000	2.000	2.000
R^2	0.818	0.813	0.704	0.957	0.799	0.699
K(l/g.min)	3.22E-05	7.92E-05	3.26E-05	8.16E-05	1.91E-04	4.28E-05
K_R(l/min)	1.1809E-19	1.1750E-19	1.1672E-19	1.1750E-19	1.1672E-19	1.1848E-19
β_{BR}(l/g.min)	6.44E-05	1.584E-04	6.52E-05	1.632E-04	8.3E-05	8.562E-05
$\varepsilon_p(g^{-1})$	5.4535E+14	1.3481E+15	5.5860E+14	1.3889E+15	7.1110E+14	7.2248E+14
$\tau_{½}$ (min)	1.13	0.46	1.11	0.44	0.19	3.07
(-r)	$3.22E\text{-}05N_t^2$	$7.92E\text{-}05N_t^2$	$3.26E\text{-}05N_t^2$	$8.16E\text{-}05N_t^2$	$4.15E\text{-}05N_t^2$	$4.28E\text{-}05N_t^2$
N_o (g/l)	287.6870	236.0718	202.8809	196.2709	225.6827	199.4416

Table 4.122: Coag-Flocculation Kinetic Parameters and Linear Regression coefficient of PTSC in VIE at varying pH and 0.3g/l dosage.

Parameters	pH=1	pH=3	pH=5	pH=7	pH=10	pH=13
Y	1.243E-05x + 3.931E-03	1.041E-04x + 3.3103E-03	2.371E-05x + 3.9268E-03	4.886E-05x + 3.1454E-03	4.484E-05x + 4.3117E-03	5.626E-05x + 3.9699E-03
α	2.000	2.000	2.000	2.000	2.000	2.000
R^2	0.906	0.946	0.963	0.820	0.807	0.922
K(l/g.min)	1.243E-05	1.041E-04	2.371E-05	4.886E-05	4.484E-05	5.626E-05
K_R(l/min)	1.1809E-19	1.1770E-19	1.1672E-19	1.1750E-19	1.1672E-19	1.1868E-19
β_{BR}(l/g.min)	2.486E-05	2.082E-04	4.742E-05	9.772E-05	8.968E-05	1.1252E-04
$\varepsilon_p(g^{-1})$	2.1052E+14	1.7689E+15	4.0627E+14	8.3166E+14	7.6833E+14	9.4810E+14
$\tau_{½}$ (min)	2.91	0.35	1.53	0.74	0.81	1.03
(-r)	$1.243E\text{-}05N_t^2$	$1.041E\text{-}04N_t^2$	$2.371E\text{-}05N_t^2$	$4.886E\text{-}05N_t^2$	$4.484E\text{-}05N_t^2$	$5.626E\text{-}05N_t^2$
N_o (g/l)	254.3882	302.0874	254.6603	317.9246	231.9271	251.8955

Table 4.123: Coag-Flocculation Kinetic Parameters and Linear Regression coefficient of PTSC in VIE at varying pH and 0.4g/l dosage.

Parameters	pH=1	pH=3	pH=5	pH=7	pH=10	PH13
Y	2.066E-05x + 2.6956E-03	1.802E-04x + 3.6614E-03	1.918E-05x + 3.1605E-03	3.805E-05x + 2.456E-03	6.515E-05x + 3.9346E-03	6.024E-05x + 3.221E-03
α	2.000	2.000	2.000	2.000	2.000	2.000
R^2	0.859	0.863	0.797	0.858	0.922	0.884
K(l/g.min)	2.066E-05	1.802E-04	1.918E-05	3.805E-05	6.515E-05	6.024E-05
K_R(l/min)	1.1829E-19	1.1770E-19	1.1691E-19	1.1770E-19	1.1711E-19	1.1868E-19
β_{BR}(l/g.min)	4.1326E-05	3.604E-04	3.836E-05	7.61E-05	1.303E-04	1.2048E-04
$\varepsilon_p(g^{-1})$	3.4931E+14	3.0620E+15	3.2812E+14	6.4656E+14	1.1126E+15	1.0152E+15
$\tau_{½}$ (min)	1.75	0.20	1.89	0.95	0.56	1.18
(-r)	$2.066E\text{-}05N_t^2$	$1.802E\text{-}04N_t^2$	$1.918E\text{-}05N_t^2$	$3.805E\text{-}05N_t^2$	$6.515E\text{-}05N_t^2$	$6.024E\text{-}05N_t^2$
N_o (g/l)	370.9749	273.1196	316.4056	407.1661	254.1554	310.4626

Table 4.124: Coag-Flocculation Kinetic Parameters and Linear Regression coefficient of PTSC in VIE at varying pH and 0.5g/l dosage.

Parameters	pH=1	pH=3	pH=5	pH=7	pH=10	pH=13
Y	3.67E-05x + 2.3757E-03	1.91E-04x + 4.6059E-03	4.29E-05x + 2.6946E-03	1.43E-05x + 1.7876E-03	4.76E-05x + 2.8821E-03	2.30E-05x + 1.4663E-03
α	2.000	2.000	2.000	2.000	2.000	2.000
R^2	0.944	0.793	0.873	0.926	0.934	0.449
K(l/g.min)	3.67E-05	4.15E-05	4.29E-05	1.43E-05	4.76E-05	2.30E-05
K_R(l/min)	1.1829E-19	1.1789E-19	1.1691E-19	1.1770E-19	1.1711E-19	1.1868E-19
β_{BR}(l/g.min)	7.34E-05	3.82E-04	8.58E-05	2.86E-05	9.52E-04	4.60E-04
$\varepsilon_p(g^{-1})$	6.2051E+14	3.2403E+15	7.3390E+14	2.4299E+14	8.1291E+14	3.8760E+14
$\tau_{½}$ (min)	0.99	0.87	0.84	2.53	0.76	0.84
(-r)	$3.67E\text{-}05N_t^2$	$1.91E\text{-}04N_t^2$	$4.29E\text{-}05N_t^2$	$1.43E\text{-}05N_t^2$	$4.76E\text{-}05N_t^2$	$2.30E\text{-}05N_t^2$
N_o (g/l)	420.9286	217.1128	371.1126	559.4093	346.9692	681.9887

Table 4.125: Coag-Flocculation Kinetic Parameters and Linear Regression coefficient of PTSC in VIE at varying pH and 0.6g/l dosage.

Parameters	pH=1	pH=3	pH=5	pH=7	pH=10	pH=13
Y	5.56E-05x + 1.9111E-03	9.345E-05x + 4.082E-03	2.124E-05x + 2.5018E-03	1.904E-05x + 2.0493E-03	7.161E-05x + 3.4758E-03	1.463E-05x + 1.8948E-03
α	2.000	2.000	2.000	2.000	2.000	2.000
R^2	0.909	0.816	0.863	0.972	0.893	0.783
K(l/g.min)	5.56E-05	9.345E-05	2.124E-05	1.904E-05	7.161E-05	1.463E-05
K_R(l/min)	1.1829E-19	1.1789E-19	1.1691E-19	1.1789E-19	1.1731E-19	1.1887E-19
β_{BR}(l/g.min)	1.112E-04	1.869E-04	4.24E-05	3.808E-05	1.4322E-04	2.926E-05
$\varepsilon_p(g^{-1})$	9.4006E+14	1.5854E+15	3.6267E+14	3.2301E+14	1.2209E+15	2.4615E+14
$\tau_{½}$ (min)	0.65	0.39	1.71	1.90	0.51	0.86
(-r)	$5.56E\text{-}05N_t^2$	$9.345E\text{-}05N_t^2$	$2.124E\text{-}05N_t^2$	$1.904E\text{-}05N_t^2$	$7.161E\text{-}05N_t^2$	$1.463E\text{-}05N_t^2$
N_o (g/l)	523.2589	244.9780	399.7122	487.9715	287.7036	527.760

Table 4.126: Coag-Flocculation Kinetic Parameters and Linear Regression coefficient of PTSC in VIE at varying pH and 0.7g/l dosage.

Parameters	pH=1	pH=3	pH=5	pH=7	pH=10	pH=13
Y	1.0E-04x + 1.831E-03	1. 26E-04x + 3.516E-03	1.70E-05x + 1.908E-03	4.06E-05x + 2.061E-03	4.74E-05x + 3.897E-03	4.17E-05x + 2.998E-03
α	2.000	2.000	2.000	2.000	2.000	2.000
R^2	0.952	0.818	0.966	0.949	0.639	0.894
K(l/g.min)	1.0E-04	1. 26E-04	1.70E-05	4.06E-05	4.74E-05	4.17E-05
K_R(l/min)	1.1829E-19	1.1809E-19	1.1711E-19	1.1789E-19	1.1731E-19	1.1887E-19
β_{BR}(l/g.min)	2.0E-04	2.52E-04	3.4E-05	8.12E-05	9.48E-05	8.34E-05
$\varepsilon_p(g^{-1})$	1.6908E+15	2.1340E+15	2.9033E+14	6.8878E+14	8.0812E+14	7.0161E+14
$\tau_{½}$ (min)	0.36	0.29	2.13	0.89	0.76	1.08
(-r)	$1.0E\text{-}04N_t^2$	$1. 26E\text{-}04N_t^2$	$1.70E\text{-}05N_t^2$	$4.06E\text{-}05N_t^2$	$4.74E\text{-}05N_t^2$	$4.17E\text{-}05N_t^2$
N_o (g/l)	546.1496	284.4141	524.1090	485.2014	256.6076	333.557

Table 4127: Coag-Flocculation Kinetic Parameters and Linear Regression coefficient of MPSC in VIE at varying pH and 0.1g/l dosage.

Parameters	pH=1	pH=3	pH=5	pH=7	pH=10	pH=13
Y	3.4E-05x + 2.619E-03	8.1E-05x + 2.874E-03	2.3E-05x + 2.597E-03	7.9E-05x + 4.442E-03	6.9E-05x + 7.982E-03	1.04E-04x + 8.263E-03
α	2.000	2.000	2.000	2.000	2.000	2.000
R^2	0.990	0.902	0.915	0743	0.746	0.733
K(l/g.min)	3.4E-05	8.1E-05	2.3E-05	7.9E-05	6.9E-05	1.04E-04
K_R(l/min)	1.1750E-19	1.1926E-19	1.1672E-19	1.1789E-19	1.1770E-19	1.1809E-19
β_{BR}(l/g.min)	6.8E-05	1.62E-04	4.6E-05	1.42E-04	1.38E-04	2.08E-04
$\varepsilon_p(g^{-1})$	5.7872E+14	1.3584E+15	3.9411E+14	1.2045E+15	1.1725E+15	1.7614E+15
$\tau_{½}$ (min)	0.71	0.30	1.58	0.51	0.53	0.70
(-r)	3.4E-05N_t^2	8.1E-05N_t^2	2.3E-05N_t^2	7.9E-05N_t^2	6.9E-05N_t^2	1.04E-04N_t^2
N_o (g/l)	381.8251	347.9471	385.0597	225.1238	125.2819	121.0214

Table 4.128: Coag-Flocculation Kinetic Parameters and Linear Regression coefficient of MPSC in VIE at varying pH and 0.2g/l dosage.

Parameters	pH=1	pH=3	pH=5	pH=7	pH=10	pH=13
Y	2.02E-05x + 2.483E-03	8.92E-05x + 1.734E-03	3.95E-05x + 3.409E-03	7.49E-05x + 1.0963E-02	8.04E-05x + 4.373E-03	1.67E-04x + 1.1809E-03
α	2.000	2.000	2.000	2.000	2.000	2.000
R^2	0.815	0.991	0.668	0.896	0.849	0.910
K(l/g.min)	2.02E-05	8.92E-05	3.95E-05	7.49E-05	8.04E-05	1.67E-04
K_R(l/min)	1.1750E-19	1.1926E-19	1.1672E-19	1.1789E-19	1.1770E-19	1.1809E-19
β_{BR}(l/g.min)	4.04E-05	1.784E-04	7.9E-05	1.4998E-04	1.608E-04	3.34E-04
$\varepsilon_p(g^{-1})$	3.4383E+14	1.4959E+15	6.7683E+14	1.2707E+15	1.3662E+15	2.8284+15
$\tau_{½}$ (min)	1.20	0.27	0.92	0.48	0.45	0.43
(-r)	2.02E-05N_t^2	8.92E-05N_t^2	3.95E-05N_t^2	7.49E-05N_t^2	8.04E-05N_t^2	1.67E-04N_t^2
N_o (g/l)	402.7386	576.7013	293.3412	91.2159	228.6770	84.6812

Table 4.129: Coag-Flocculation Kinetic Parameters and Linear Regression coefficient of MPSC in VIE at varying pH and 0.3g/l dosage.

Parameters	pH=1	pH=3	pH=5	pH=7	pH=10	pH=13
Y	2.569E-05x + 2.5082E-03	3.726E-05x + 1.871E-03	1.296E-05x + 1.8445E-03	9.155E-05x + 8.642E-03	1.074E-04x + 4.7161E-03	2.252E-04x + 7.9894E-03
α	2.000	2.000	2.000	2.000	2.000	2.000
R^2	0.943	0.803	0.729	0.638	0.846	0.756
K(l/g.min)	2.569E-05	3.726E-05	1.296E-05	9.155E-05	1.074E-04	2.252E-04
K_R(l/min)	1.1750E-19	1.1957E-19	1.1672E-19	1.1789E-19	1.1750E-19	1.1829E-19
β_{BR}(l/g.min)	4.138E-05	7.452E-05	2.592E-05	1.831E-04	2.148E-04	4.504E-04
$\varepsilon_p(g^{-1})$	4.3728E+14	6.2323E+14	2.2207E+14	1.5531E+15	1.8281E+15	3.8076E+15
$\tau_{½}$ (min)	0.91	0.65	2.80	0.40	0.34	0.32
(-r)	2.569E-05N_t^2	3.726E-05N_t^2	1.296E-05N_t^2	9.155E-05N_t^2	1.074E-04N_t^2	2.252E-04N_t^2
N_o (g/l)	398.6923	534.4735	543.153	115.7140	212.0396	125.1658

Table 4.130: Coag-Flocculation Kinetic Parameters and Linear Regression coefficient of MPSC in VIE at varying pH and 0.4g/l dosage.

Parameters	pH=1	pH=3	pH=5	pH=7	pH=10	pH=13
Y	2.695E-05x + 1.3805E-03	5.590E-05x + 1.6371E-03	2.634E-05x + 1.8962E-03	1.382E-04x + 6.3613E-03	7.267E-05x + 2.5681-03	2.634E-04x + 7.6084E-03
α	2.000	2.000	2.000	2.000	2.000	2.000
R^2	0.792	0.702	0.710	0.892	0.978	0.864
K(l/g.min)	2.569E-05	3.726E-05	1.296E-05	9.155E-05	1.074E-04	2.252E-04
K_R(l/min)	1.1770E-19	1.1957E-19	1.1672E-19	1.1770E-19	1.1750E-19	1.1829E-19
β_{BR}(l/g.min)	5.39E-05	1.1181E-04	5.268E-05	2.764E-04	1.4534E-04	5.268E-04
$\varepsilon_p(g^{-1})$	4.5794E+14	9.350E+14	4.5134E+14	2.3483E+15	1.2369E+15	4.4535E+15
$\tau_{½}$ (min)	0.90	0.43	1.38	0.26	0.50	0.28
(-r)	$2.695E\text{-}05N_t^2$	$3.726E\text{-}05N_t^2$	$1.296E\text{-}05N_t^2$	$9.155E\text{-}05N_t^2$	$1.074E\text{-}04N_t^2$	$2.252E\text{-}04N_t^2$
N_o (g/l)	724.3752	610.8362	527.3705	157.2006	389.3929	131.4337

Table 4.131: Coag-Flocculation Kinetic Parameters and Linear Regression coefficient of MPSC in VIE at varying pH and 0.5g/l dosage.

Parameters	pH=1	pH=3	pH=5	pH=7	pH=10	pH=13
Y	2.01E-05x + 1.596E-03	6.36E-05x + 1.5535E-03	3.17E-05x + 1.8953E-03	9.63E-05x + 2.3403E-03	7.33E-05x + 2.7995E-03	6.35E-05x + 5.8533E-03
α	2.000	2.000	2.000	2.000	2.000	2.000
R^2	0.751	0.720	0.786	0.861	0.910	0.868
K(l/g.min)	2.01E-05	6.36E-05	3.17E-05	9.63E-05	7.33E-05	6.35E-05
K_R(l/min)	1.1770E-19	1.1887E-19	1.1691E-19	1.1770E-19	1.1750E-19	1.1848E-19
β_{BR}(l/g.min)	4.02E-05	1.272E-04	6.34E-05	1.926E-04	1.466E-04	1.27E-04
$\varepsilon_p(g^{-1})$	3.4155E+14	1.0701E+15	5.4230E+14	1.6364E+15	1.2477E+14	1.0719E+15
$\tau_{½}$ (min)	1.20	0.38	1.14	0.38	0.49	1.14
(-r)	$2.01E\text{-}05N_t^2$	$6.36E\text{-}05\ N_t^2$	$3.17E\text{-}05N_t^2$	$9.63E\text{-}05N_t^2$	$7.33E\text{-}05N_t^2$	$6.35E\text{-}05N_t^2$
N_o (g/l)	626.5664	643.7078	527.6210	427.2956	357.2066	170.8438

Table 4.132: Coag-Flocculation Kinetic Parameters and Linear Regression coefficient of MPSC in VIE at varying pH and 0.6 g/l dosage.

Parameters	pH=1	pH=3	pH=5	pH=7	pH=10	pH=13
Y	2.933E-05x + 1.377E-03	6.560E-05x + 1.3175E-03	7.668E-06x + 1.5092E-03	4.247E-05x + 1.608E-03	5.335E-05x + 1.944E-03	2.318E-05x + 5.5059E-03
α	2.000	2.000	2.000	2.000	2.000	2.000
R^2	0.885	0.753	0.853	0.943	0.927	0.978
K(l/g.min)	2.933E-05	6.560E-05	7.668E-06	4.247E-05	5.335E-05	2.318E-05
K_R(l/min)	1.1789E-19	1.1887E-19	1.1691E-19	1.1789E-19	1.1731E-19	1.1848E-19
β_{BR}(l/g.min)	5.866E-05	1.312E-04	1.5336E-05	8.494E-05	1.067E-04	4.636E-04
$\varepsilon_p(g^{-1})$	4.9758E+14	1.1037E+15	1.3118E+14	7.2050E+14	9.0956E+14	3.9129E+15
$\tau_{½}$ (min)	0.82	0.37	4.73	0.85	0.68	0.31
(-r)	$2.933E\text{-}05N_t^2$	$6.560E\text{-}05N_t^2$	$7.668E\text{-}06N_t^2$	$4.247E\text{-}05N_t^2$	$5.335E\text{-}05N_t^2$	$2.318E\text{-}05N_t^2$
N_o (g/l)	726.2164	759.0133	662.6027	621.8905	514.4033	181.6233

Table 4.133: Coag-Flocculation Kinetic Parameters and Linear Regression coefficient of MPSC in VIE at varying pH and 0.7g/l dosage.

Parameters	pH=1	pH=3	pH=5	pH=7	pH=10	pH=13
Y	2.61E-05x + 1.378E-03	6.86E-05x + 1.704E-03	3.07E-05x + 1.316E-03	4.40E-05x + 1.606E-03	5.22E-05x + 1.379E-03	2.318E-05x + 1.732E-02
α	2.000	2.000	2.000	2.000	2.000	2.000
R^2	0.879	0.700	0.890	0.868	0.930	0.918
K(l/g.min)	2.61E-05	6.86E-05	3.07E-05	4.40E-05	5.22E-05	2.318E-05
K_R(l/min)	1.1789E-19	1.1868E-19	1.1691E-19	1.1789E-19	1.1731E-19	1.1848E-19
β_{BR}(l/g.min)	5.22E-05	1.372E-04	6.14E-05	8.8E-05	1.044E-04	1.2E-03
$\varepsilon_p(g^{-1})$	4.4279E+14	1.1560E+15	5.2519E+14	7.4646E+14	8.8995E+14	1.0128E+16
$\tau_{½}$ (min)	0.93	0.35	1.18	0.82	0.69	0.12
(-r)	$2.61E\text{-}05N_t^2$	$6.86E\text{-}05N_t^2$	$3.07E\text{-}05N_t^2$	$4.40E\text{-}05N_t^2$	$5.22E\text{-}05N_t^2$	$2.318E\text{-}05N_t^2$
N_o (g/l)	725.6894	+586.8545	759.8784	622.6650	725.1632	57.7367

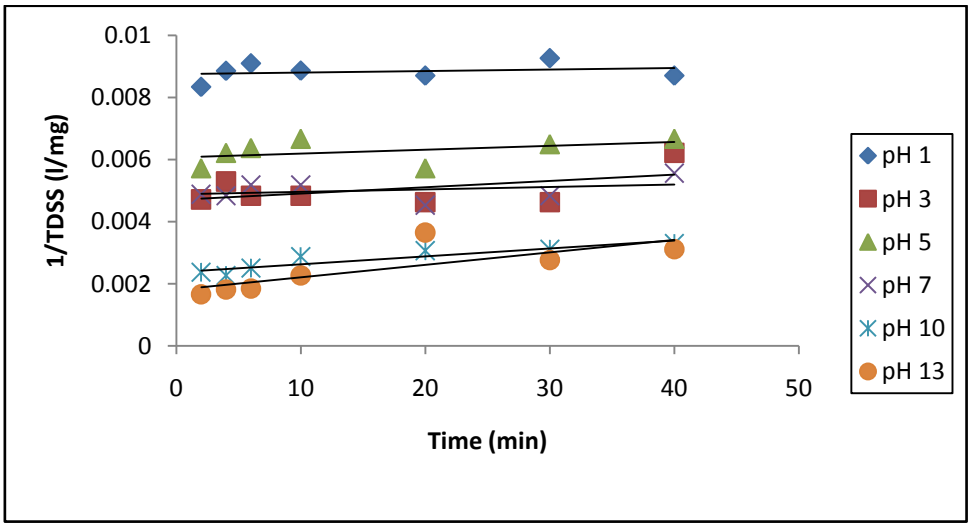

Fig.4.226: Kinetic plot of TDSS removal for pH varying VIE medium at 0.1g/l ssc dosage

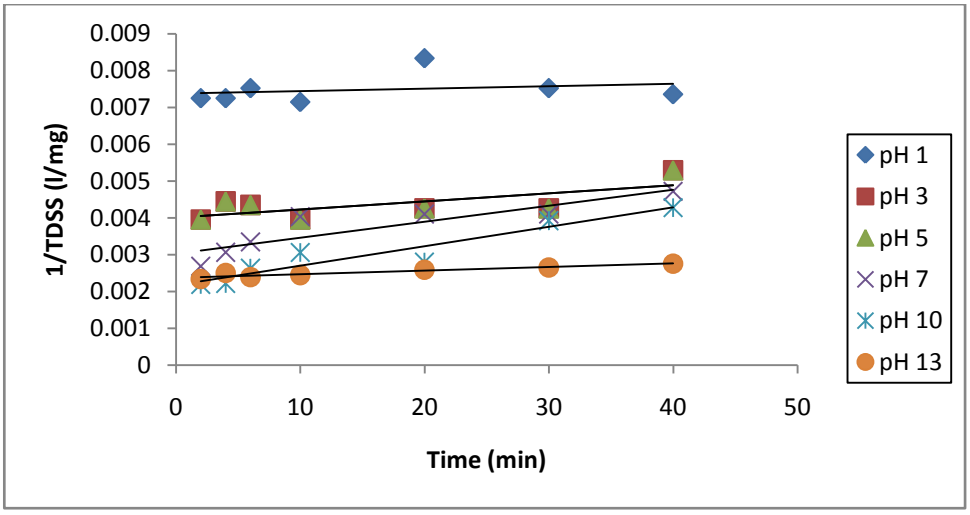

Fig.4.227: Kinetic plot of TDSS removal for pH varying VIE medium at 0.2g/l ssc dosage

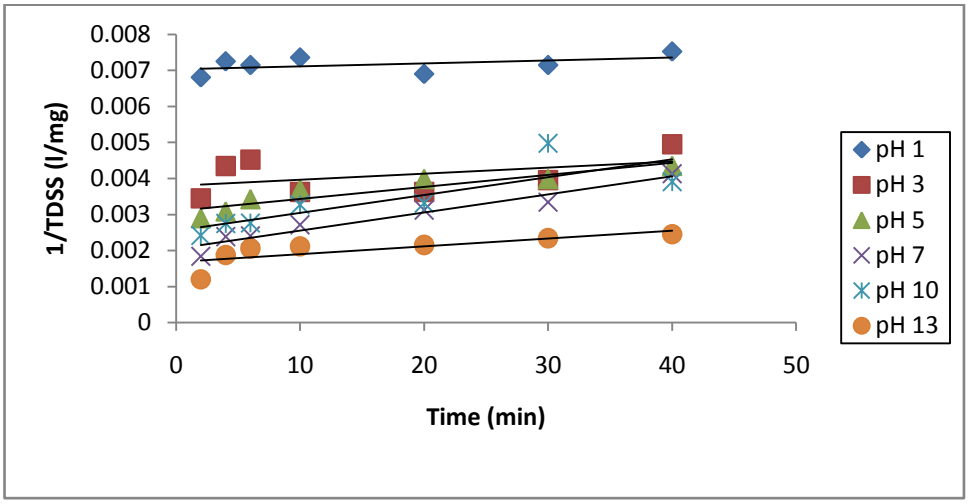

Fig.4.228: Kinetic plot of TDSS removal for pH varying VIE medium at 0.3g/l ssc dosage

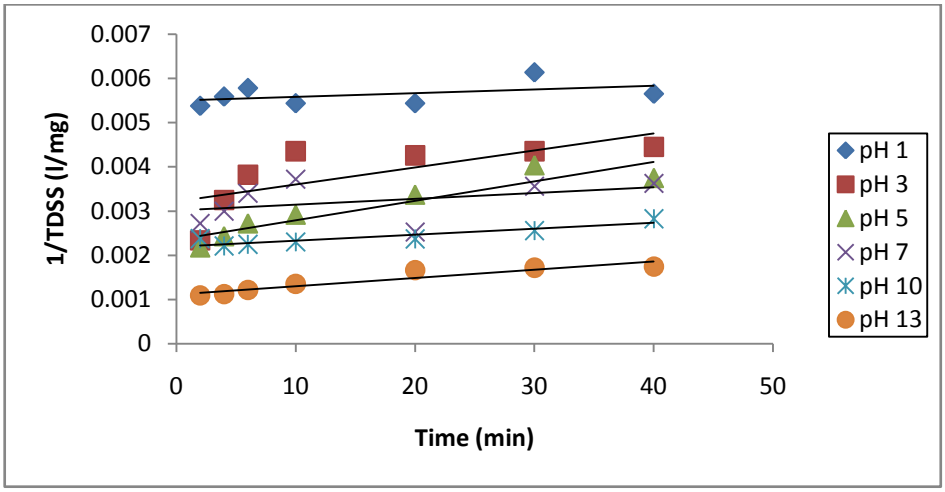

Fig.4.229: Kinetic plot of TDSS removal for pH varying VIE medium at 0.4g/l ssc dosage

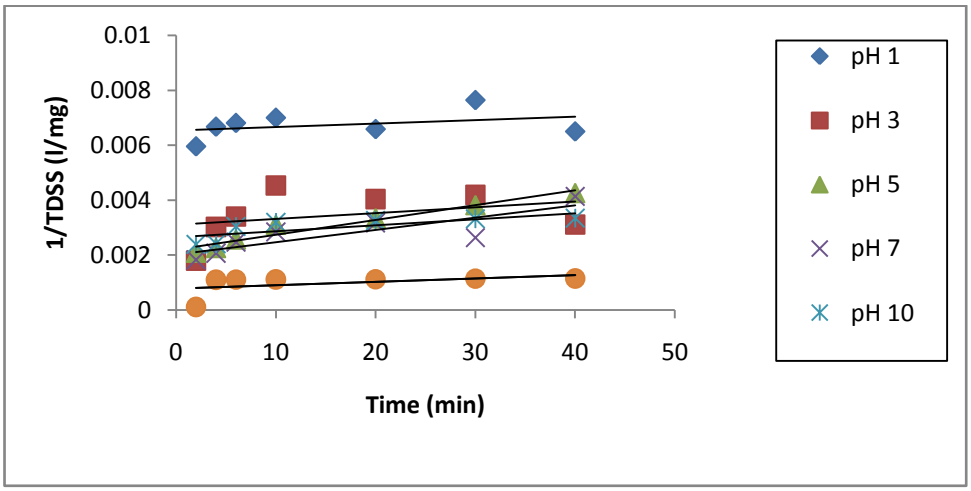

Fig.4.230: Kinetic plot of TDSS removal for pH varying VIE medium at 0.5g/l ssc dosage

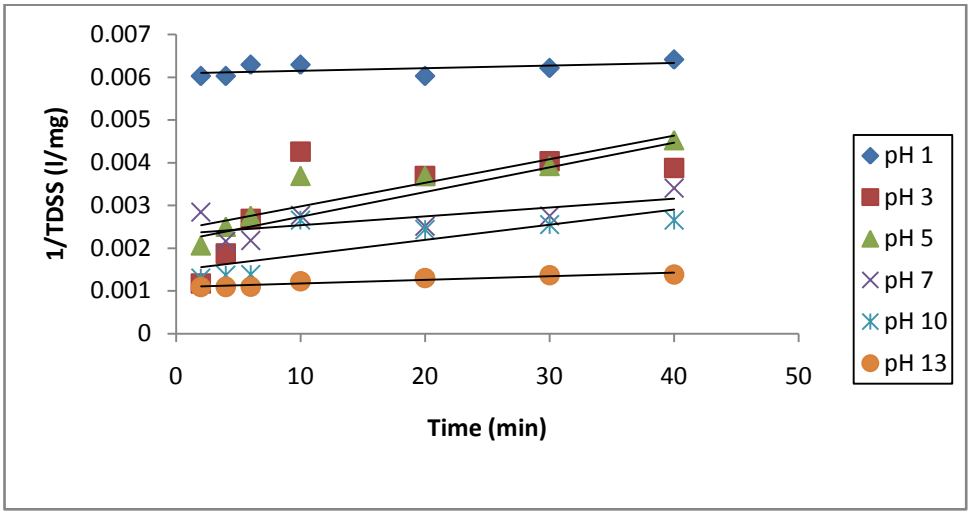

Fig.4.231: Kinetic plot of TDSS removal for pH varying VIE medium at 0.6g/l ssc dosage

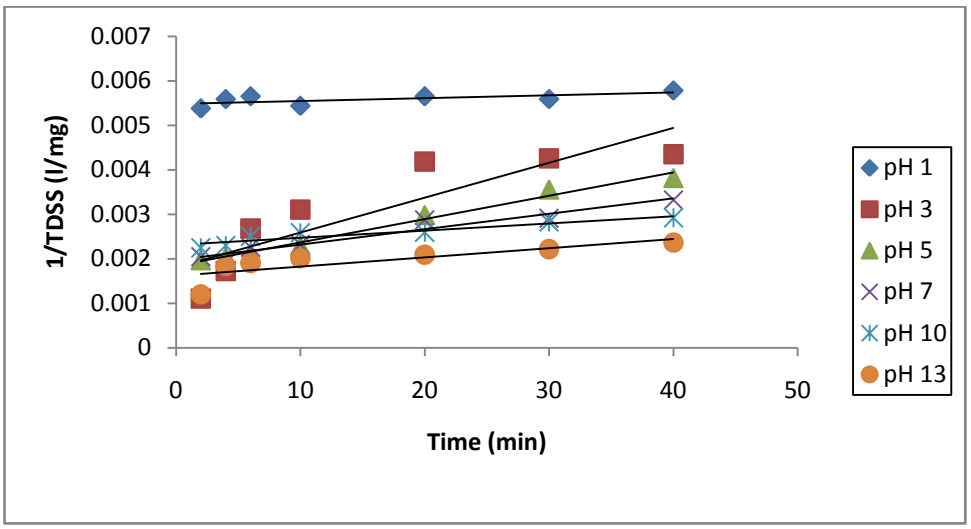

Fig.4.232: Kinetic plot of TDSS removal for pH varying VIE medium at 0.7g/l ssc dosage

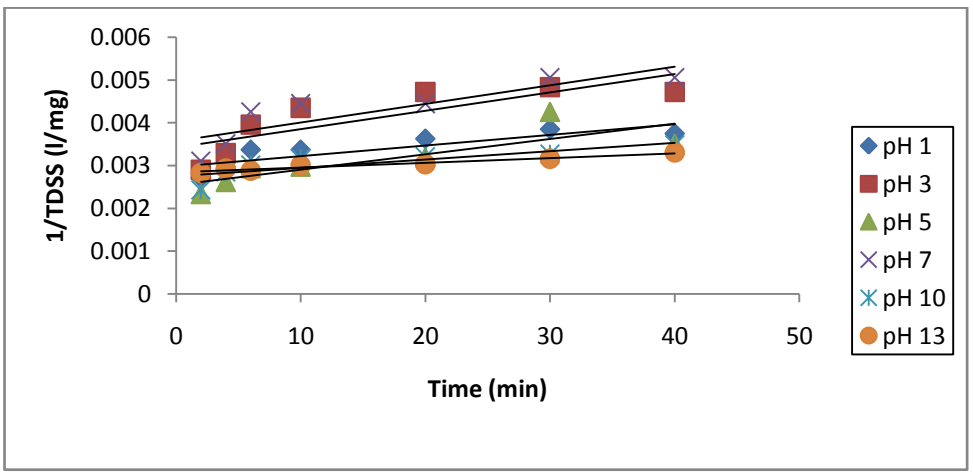

Fig.4.233: Kinetic plot TDSS removal for pH varying VIE medium at 0.1g/l cosc dosage

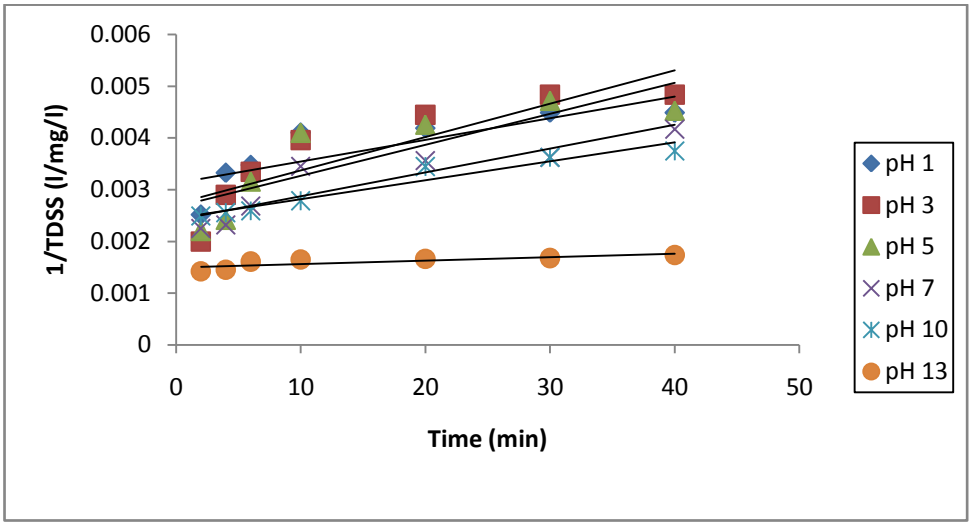

Fig.4.234: Kinetic plot TDSS removal for pH varying VIE medium at 0.2g/l cosc dosage

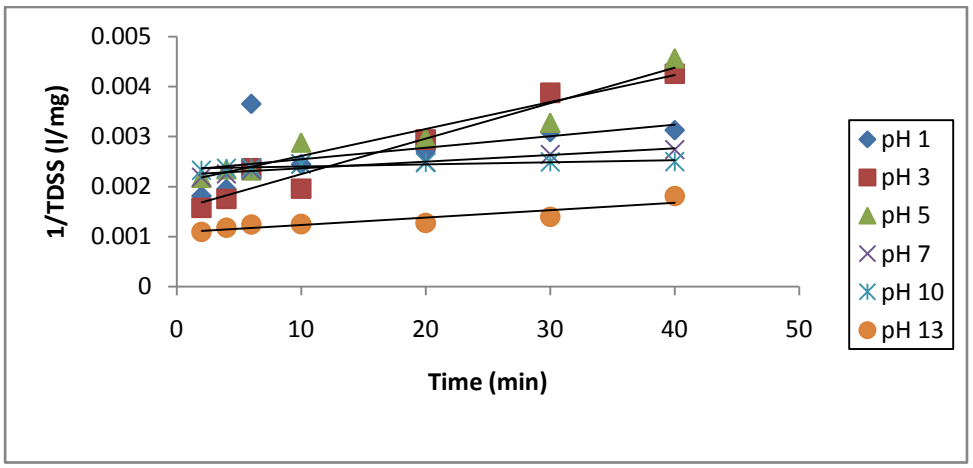

Fig.4.235: Kinetic plot TDSS removal for pH varying VIE medium at 0.3g/l cosc dosage

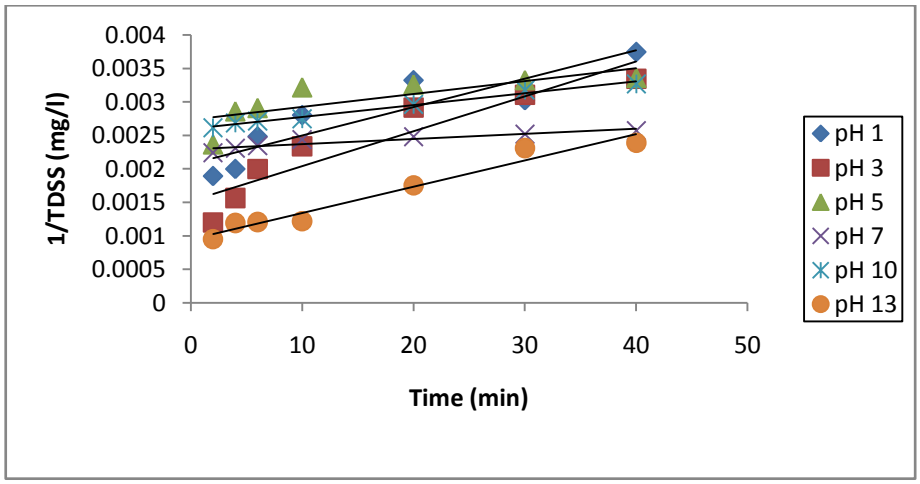

Fig.4.236: Kinetic plot TDSS removal for pH varying VIE medium at 0.4g/l cosc dosage

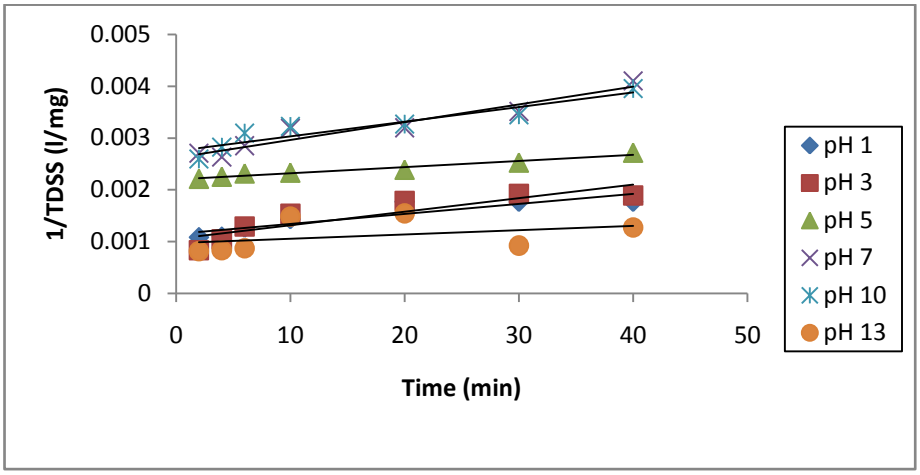

Fig.4.237: Kinetic plot TDSS removal for pH varying VIE medium at 0.5g/l cosc dosage

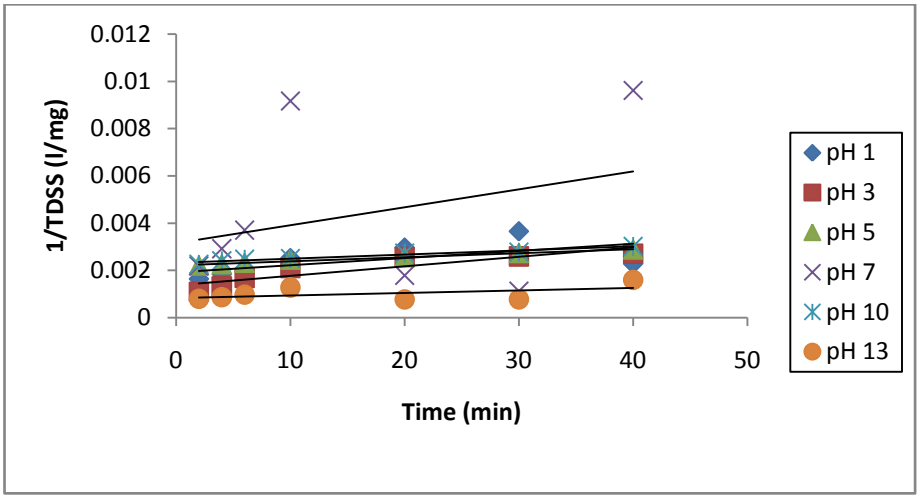

Fig.4.238: Kinetic plot TDSS removal for pH varying VIE medium at 0.6g/l cosc dosage

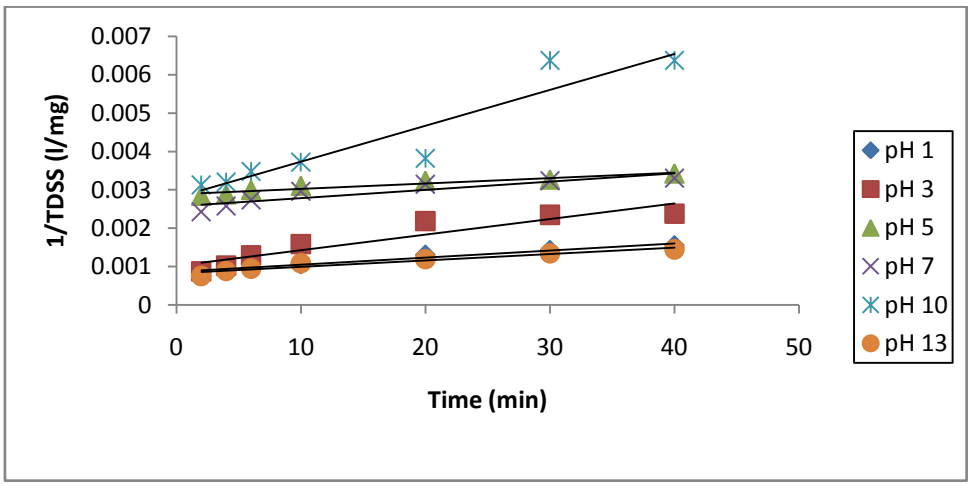

Fig.4.239: Kinetic plot TDSS removal for pH varying VIE medium at 0.7g/l cosc dosage

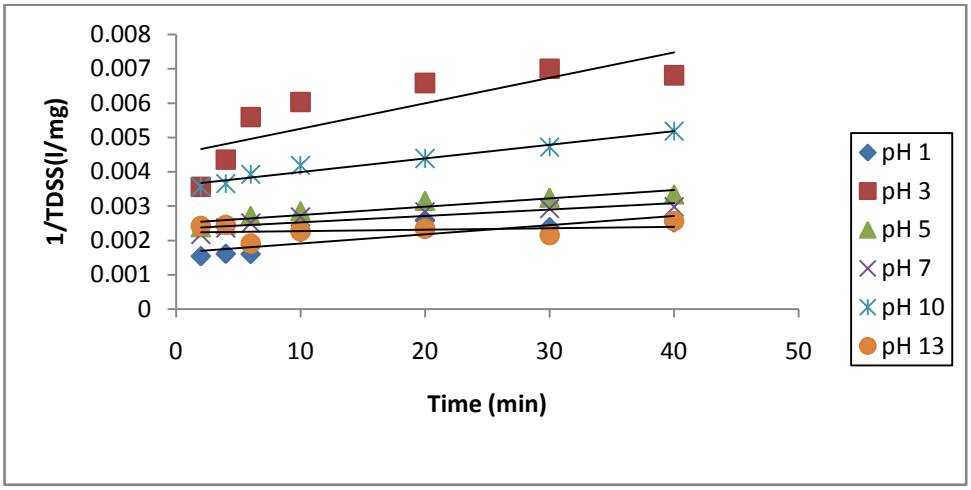

Fig.4.240: Kinetic plot TDSS removal for pH varying VIE medium at 0.1g/l tosc dosage

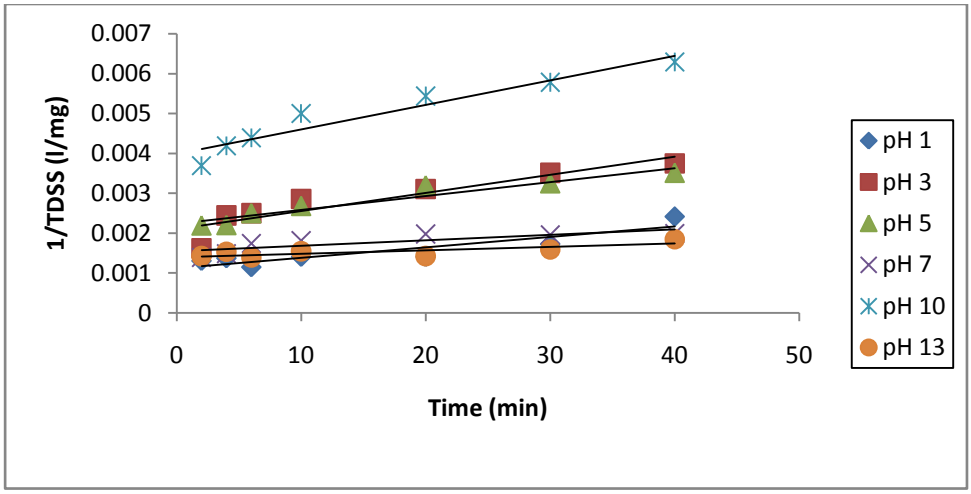

Fig.4.241: Kinetic plot TDSS removal for pH varying VIE medium at 0.2g/l tosc dosage

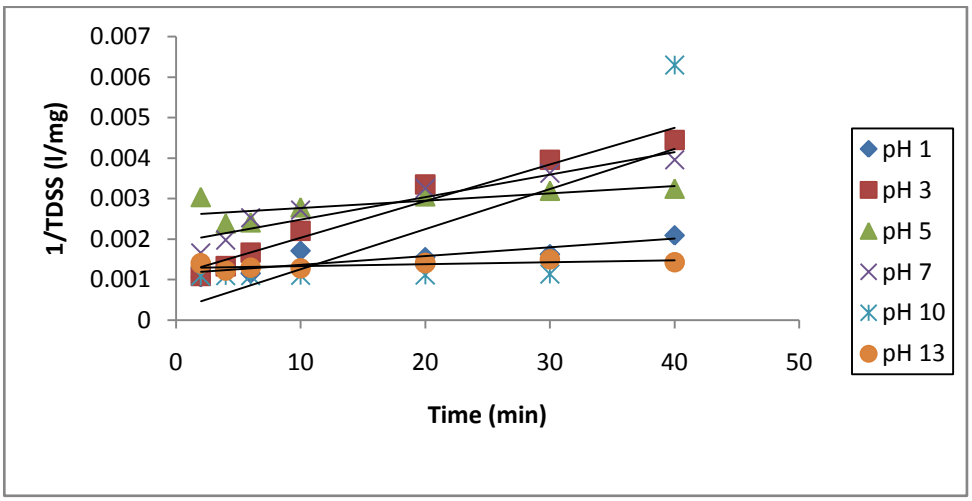

Fig.4.242: Kinetic plot TDSS removal for pH varying VIE medium at 0.3g/l tosc dosage

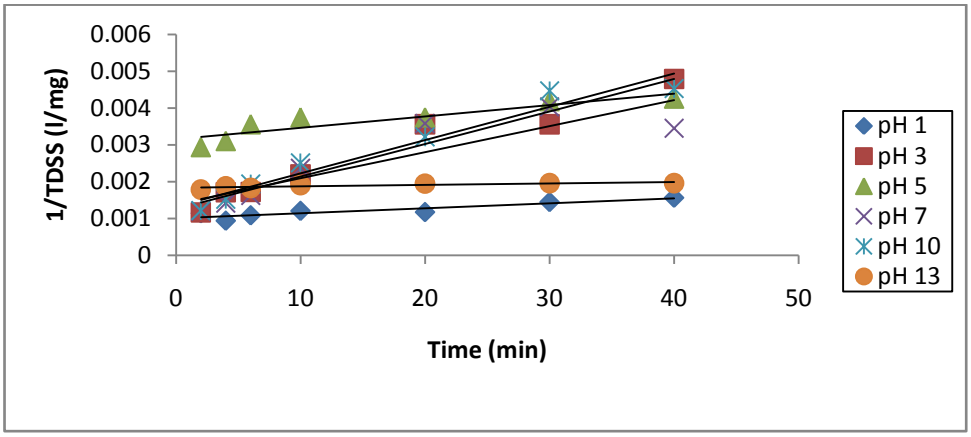

Fig.4.243: Kinetic plot TDSS removal for pH varying VIE medium at 0.4g/l tosc dosage

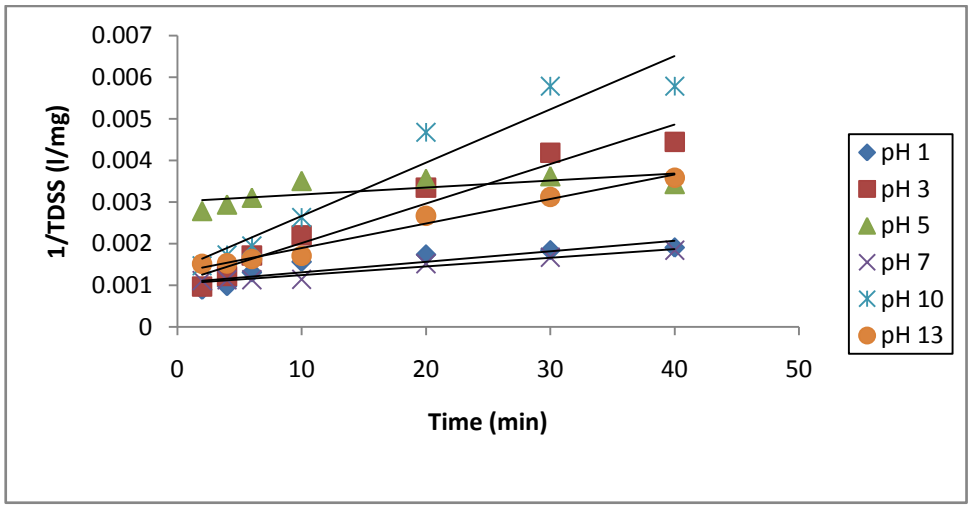

Fig.4.244: Kinetic plot TDSS removal for pH varying VIE medium at 0.5g/l tosc dosage

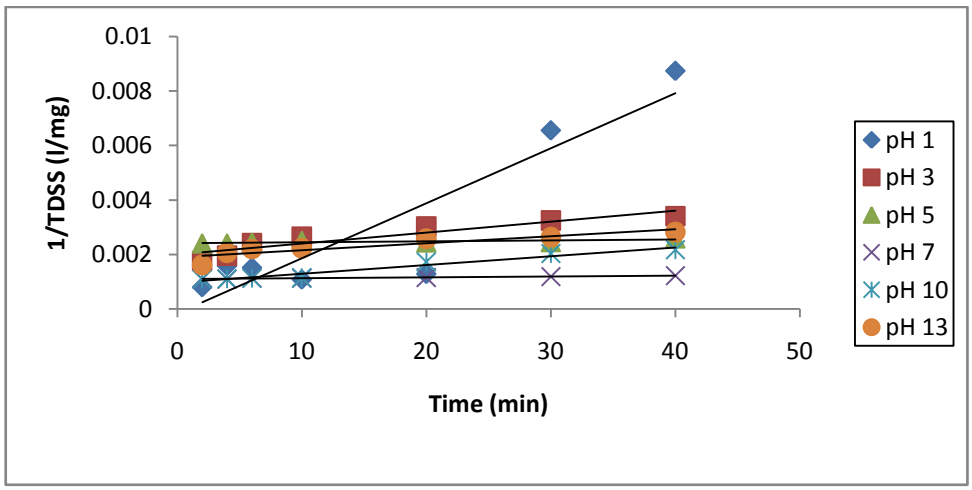

Fig.4.245: Kinetic plot TDSS removal for pH varying VIE medium at 0.6g/l tosc dosage

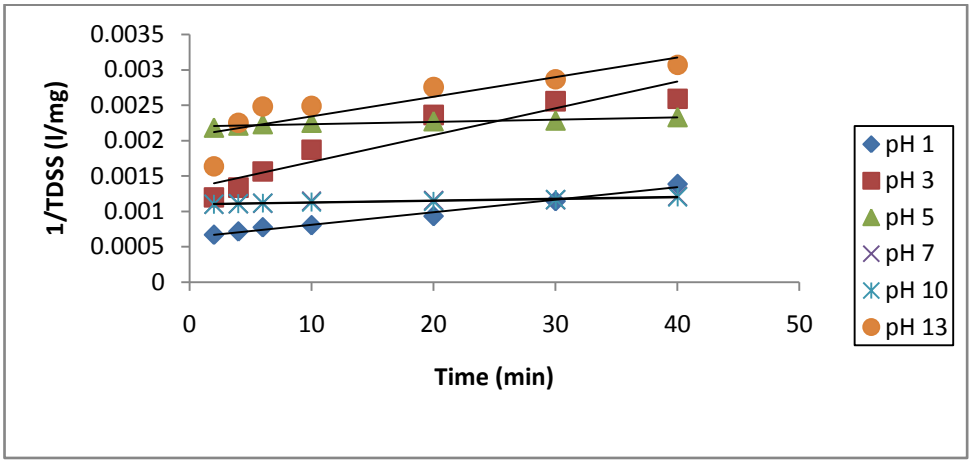

Fig.4.246: Kinetic plot TDSS removal for pH varying VIE medium at 0.7g/l tosc dosage

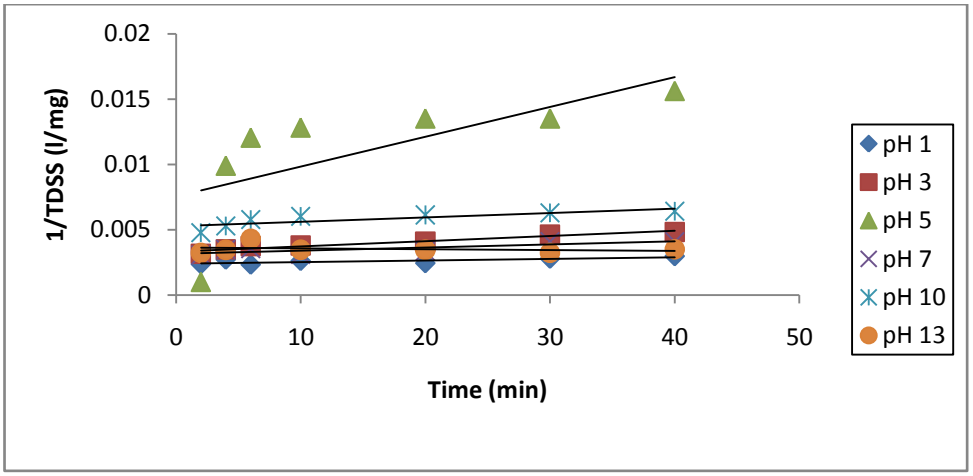

Fig.4.247: Kinetic plot TDSS removal for pH varying VIE medium at 0.1g/l ptsc dosage

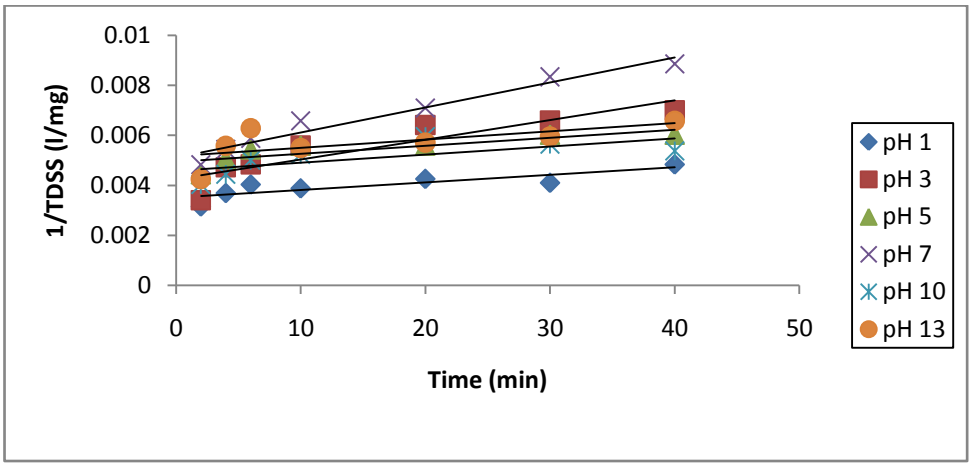

Fig.4.248: Kinetic plot TDSS removal for pH varying VIE medium at 0.2g/l ptsc dosage

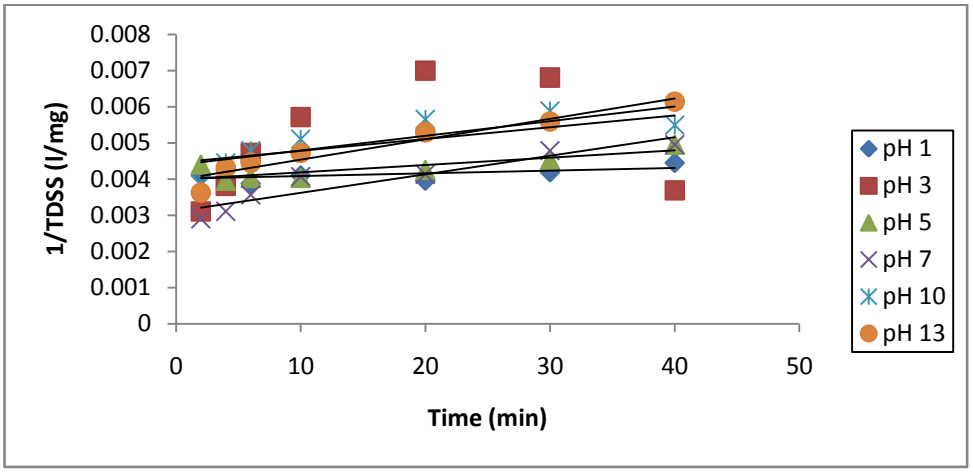

Fig.4.249: Kinetic plot TDSS removal for pH varying VIE medium at 0.3g/l ptsc dosage

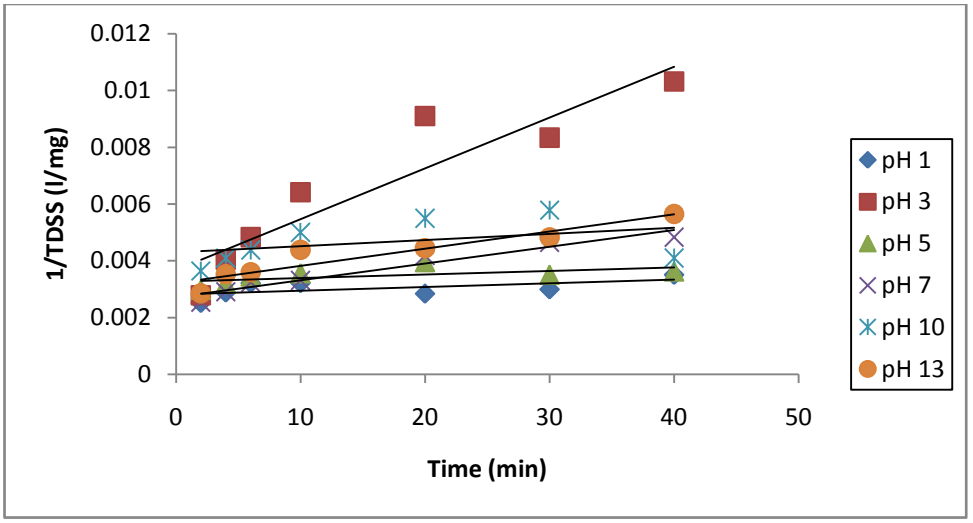

Fig.4.250: Kinetic plot TDSS removal for pH varying VIE medium at 0.4g/l ptsc dosage

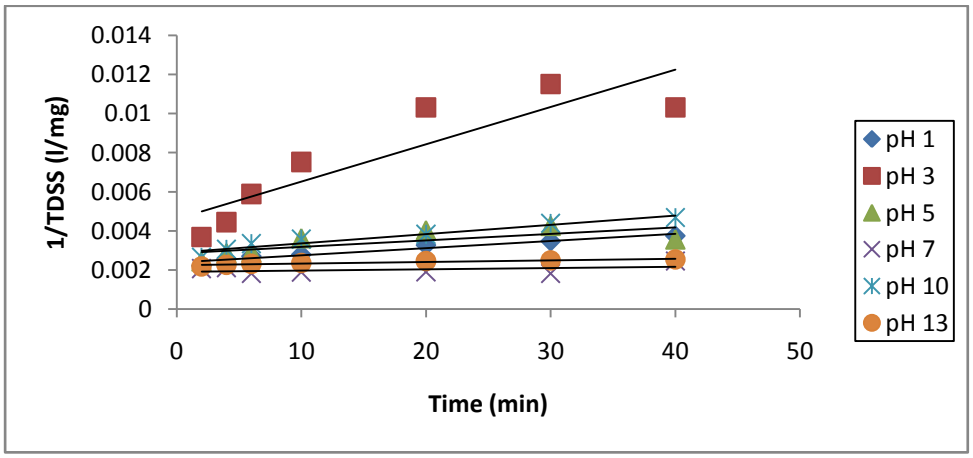

Fig.4.251: Kinetic plot TDSS removal for pH varying VIE medium at 0.5g/l ptsc dosage

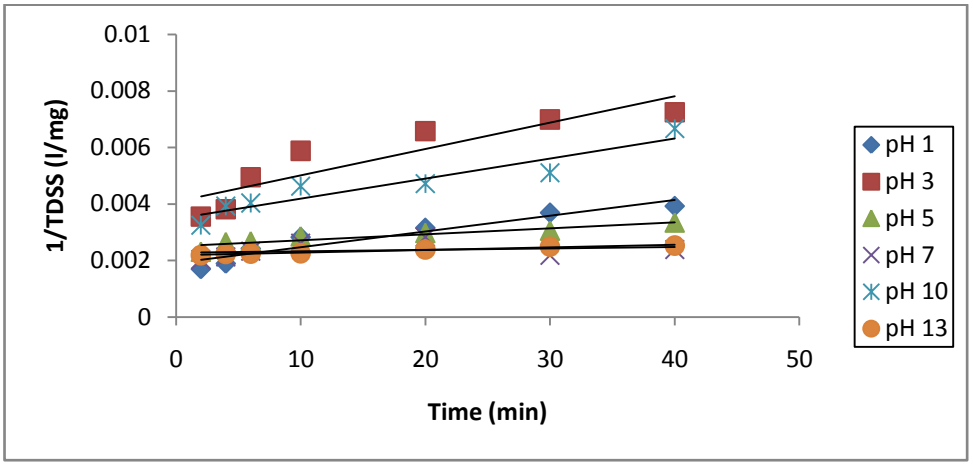

Fig.4.252: Kinetic plot TDSS removal for pH varying VIE medium at 0.6g/l ptsc dosage

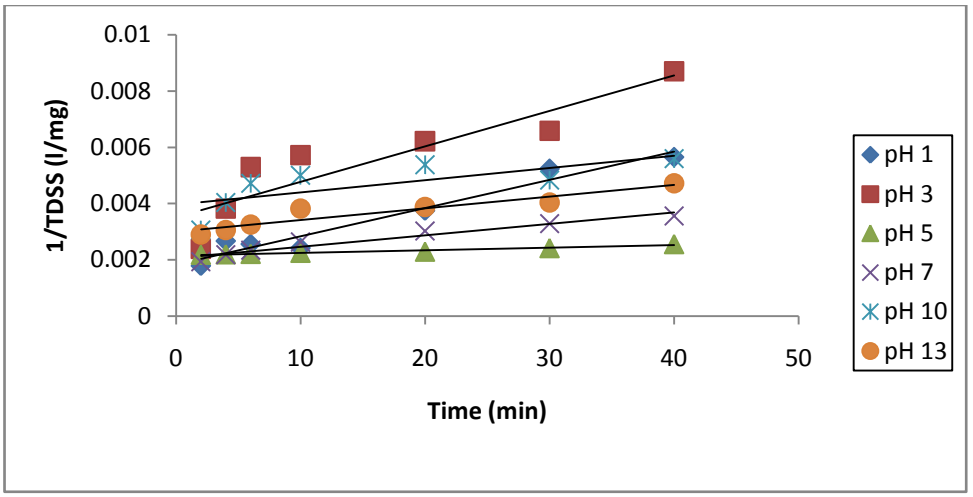

Fig.4.253: Kinetic plot TDSS removal for pH varying VIE medium at 0.7g/l ptsc dosage

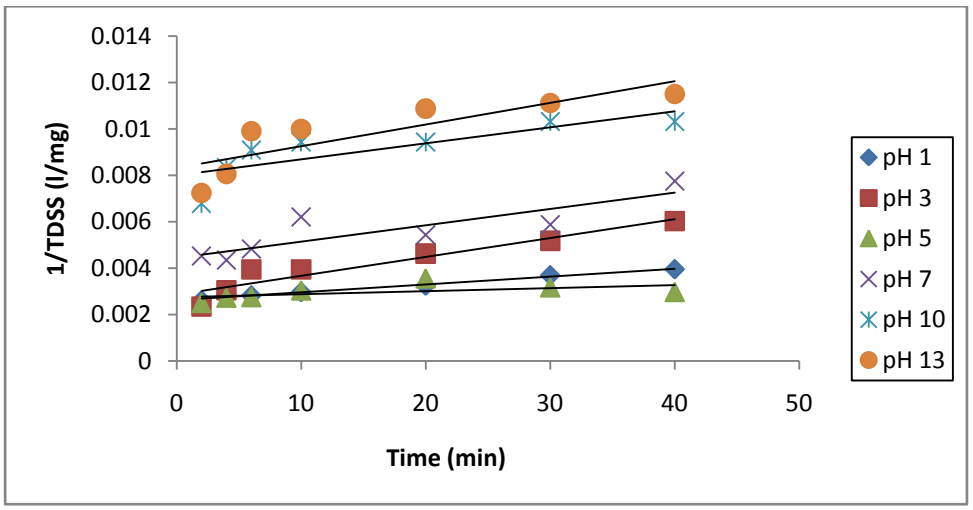

Fig.4.254: Kinetic plot TDSS removal for pH varying VIE medium at 0.1g/l mpsc dosage

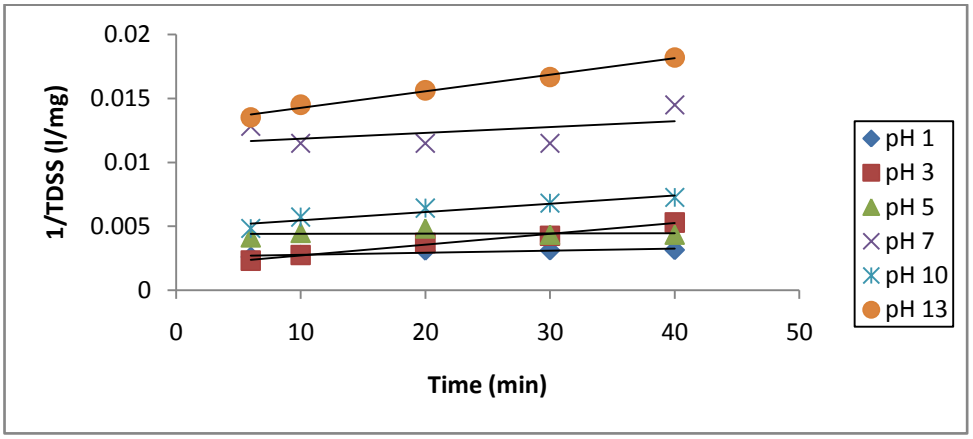

Fig.4.255: Kinetic plot TDSS removal for pH varying VIE medium at 0.2g/l mpsc dosage

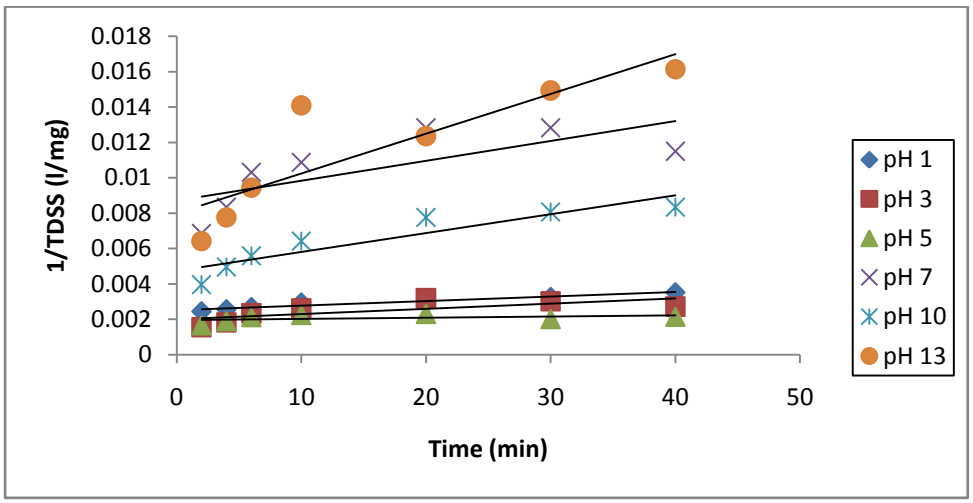

Fig.4.256: Kinetic plot TDSS removal for pH varying VIE medium at 0.3g/l mpsc dosage

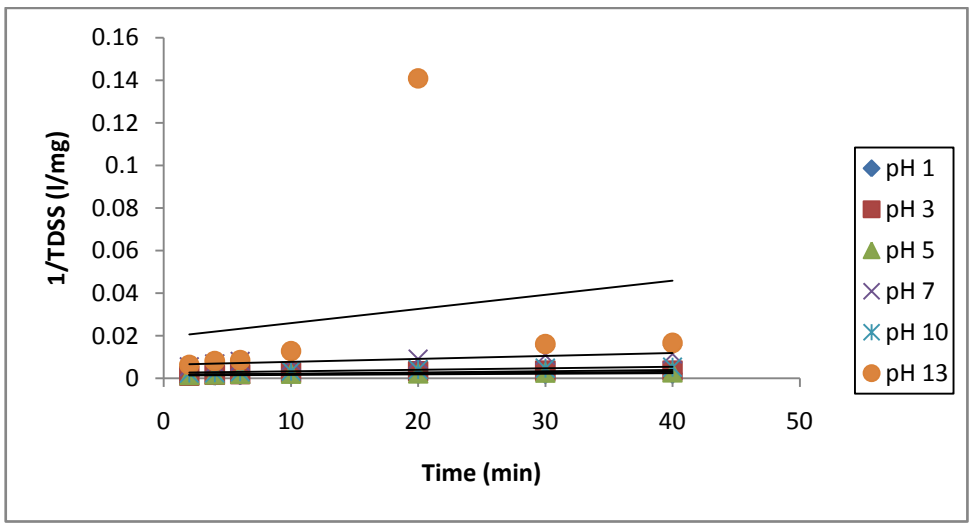

Fig.4.257: Kinetic plot TDSS removal for pH varying VIE medium at 0.4g/l mpsc dosage

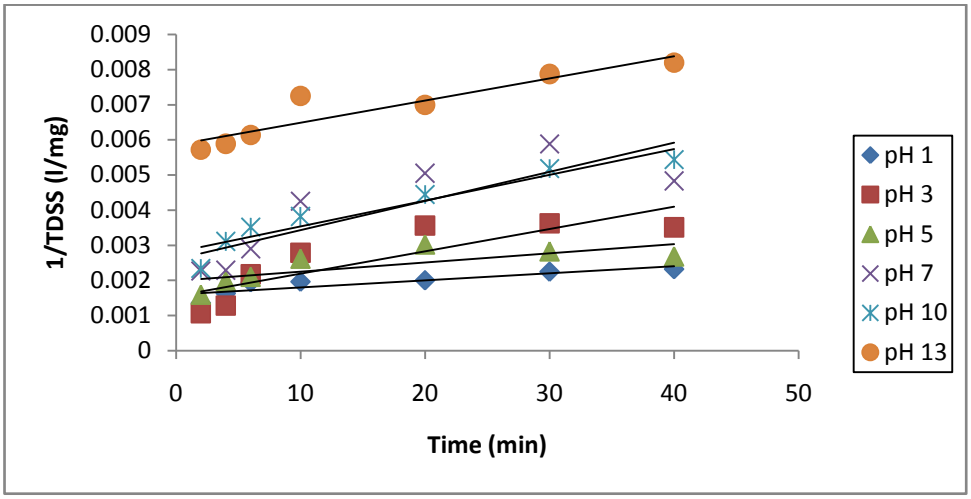

Fig.4.258: Kinetic plot TDSS removal for pH varying VIE medium at 0.5g/l mpsc dosage

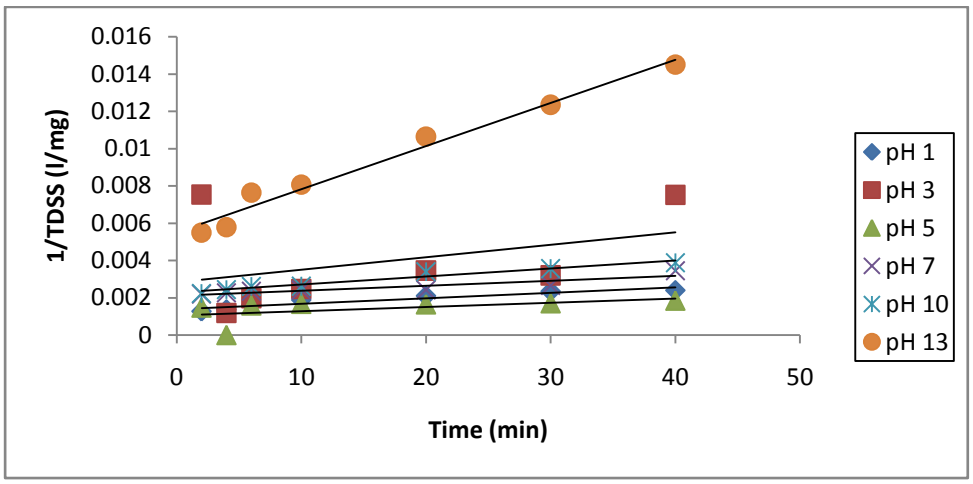

Fig.4.259: Kinetic plot TDSS removal for pH varying VIE medium at 0.6g/l mpsc dosage

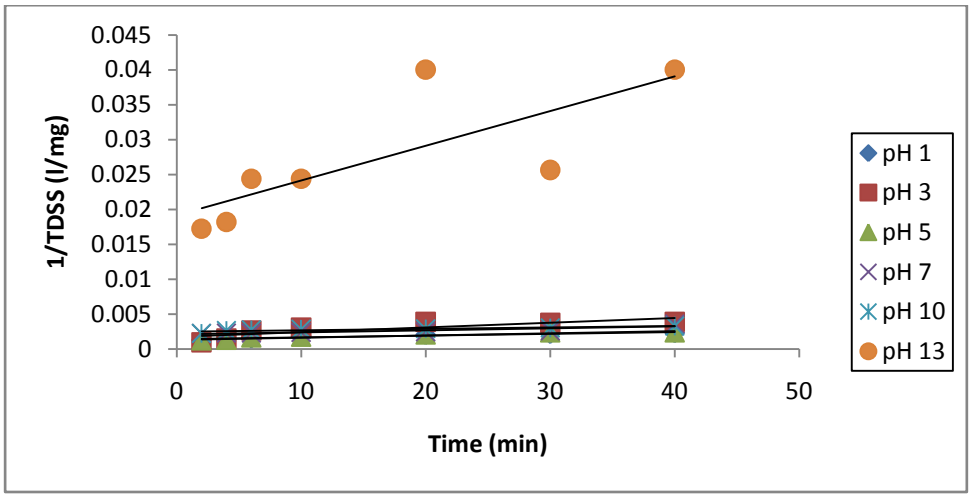

Fig.4.260: Kinetic plot TDSS removal for pH varying VIE medium at 0.7g/l mpsc dosage

4.1.4 Time Evolution of Cluster Size Distribution

The time evolution of particles cluster size distribution of the Coag-flocculation activity is presented in this section. The particle distribution behaviors are presented in the graphical illustrations of number of particles versus time.

The particle distribution in coag-flocculation can be denoted as monomers (singlets), dimmers (doublets), trimers (triplets); for m = 1,2,3, respectively. For monomer or primary (singlets) particles, m = 1, for dimmer or secondary (doublets), m = 2 and for trimer or tertiary (triplets) particles, m = 3. From the definition above, the singlets consists of single monomers; doublets consists of double monomers while the triplets consists of three monomers. The particle distribution plots clearly show the pattern and distribution of aggregation of ions/particles/ colloids as different particle classes floc into visible blobs.

In this section, the discussion is held at the same time for both PIE and VIE with respect to maximum and minimum coagulation period of the coag-flocculants under study. The representative curves are presented in figures.4.261 to 4.280 and the discussion presented in three steps as shown follows:

Step 1:

Consider figures. 4.265 (TOSC PIE mini.), figures. 4.279 (MPSC VIE mini), figures. 4.264 (COSC PIE maxi.), figures. 4.276 (TOSC VIE maxi.), and figures. 4.272 (SSC VIE maxi.). Observation on the curves show that they follow similar trends. The curves indicate that the singlets and the sum passes through maximum at different N_1, $\sum N_i$ values at t=0 because they are absent at $N_1=0$, $\sum N_i = 0$ and at the end of coag-flocculation process ($t = \infty$; $N_i = 0$). The mono-particles (singlets) decreases more rapidly than the sum of the particles.

The behaviors observed from the curves are expected in coag-flocculation where there is moderate colloidal entrapment and high potential hump.

This is supported by relatively low rate of coag-flocculation demonstrated at mainly high $\tau_{1/2}$ values. The predominant mechanism in these curves are charge neutralization with low bridging caused by presence of moderate repulsive forces between the sum of particles and the rest. The implication is to ensure moderate speed of coag-flocculation as demonstrated in the above referred figures. The unique nature of the formation of singlets, doublets and triplets in the figures, indicate presence of negligible Zeta

potential among the particles. The consequent upon this results in the coag-flocculants sweeps away the TDSS inherent in the effluents.

Step II:

This involves figure.4.264 (TOSC PIE max). The curves show that the singlets are at its peak (t = 0; N_1 = 2200/l), whereas the sum of particles are at maximum (t = 2mins; sum ($\sum N_i$) = 2247/l and at maximum coag-flocculation period t = ∞, N = 0. Also the singlets and sum of particles can be seen to decrease more rapidly throughout at different degrees. Supposedly, this is evidence of high rate of coag-flocculation supported by low $\tau_{1/2}$, but in this case it is relatively high $\tau_{1/2}$ value. This phenomenon is one of the discrepancies encountered in this work. It could be attributed to inaccurate measurement of the initial TDSS of the effluent which invariably is low. The overall behavior of the particles indicate immediate destabilization of the anionic complexes/ radicals in action. The dominant mechanism in these curves are minimal shear resistance and relatively high electrostatic attraction facilitating easy sweeping away of anionic complexes in form of TDSS from the system at the end of coag-flocculation process.

Step III:

This involves figure. 4.269 (MPSC PIE min), figure.4.270 (MPSC PIE maxi), figure. 4.267 (PTSC PIE min), figure. 4.268 (PTSC PIE maxi), figure. 4.261 (SSC PIE min), figure. 4.262 (SSC PIE maxi), figure. 4.280 (MPSC VIE maxi), figure. 4.263 (COSC PIE mini), figure. 4.275 (TOSC VIE mini), figure. 4.273 (COSC VIE min), figure. 4.274 (COSC VIE maxi), figure. 4.277 (PTSC VIE mini), figure. 4.278 (PTSC VIE maxi), figure. 4.271 (SSC VIE mini) and figure. 4.272 (SSC VIE maxi). The behavior of the curves in this case is similar to what is obtained in step II. The only difference is that the curve representing the sum of particles is optimum at t = 0. The behavior of the curves suggest that the cationic complexes and their various species formed instantly neutralizes the TDSS charges and thereby lowering repulsive forces or removal of the energy barrier. With minimal repulsive force existing, all class of particles are seen to fuse into one particle kernel at varying time mainly from 6 – 20min to infinity. This is evidence that either particle colloidal entrapment predominants or the cationic charges of the coag-flocculants overwhelms the anionic charges of the colloidal particles in the effluents.

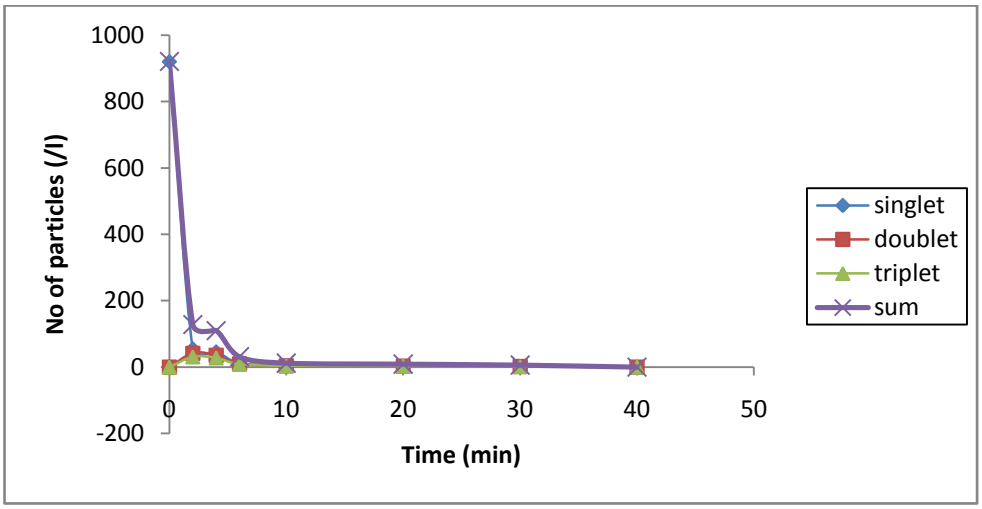

Fig.4.261:Particle distribution plot for ssc in PIE at minimum half life 0.18min

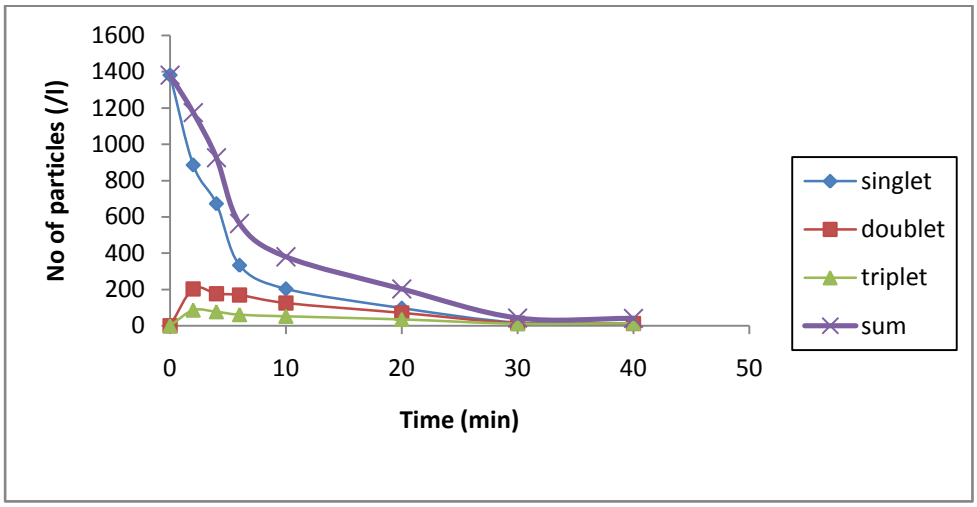

Fig.4.262:Particle distribution plot for ssc in PIE at maximum half life 5.42min

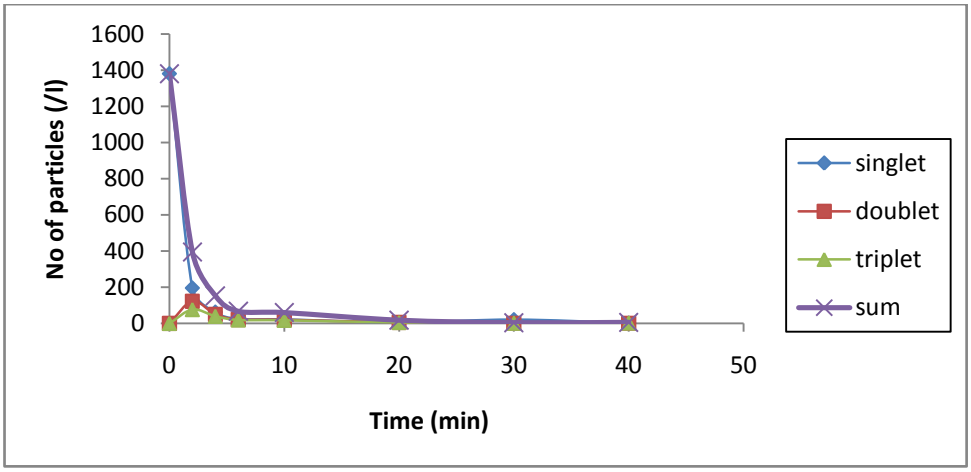

Fig.4.263:Particle distribution plot for cosc in PIE at minimum half life 0.38min

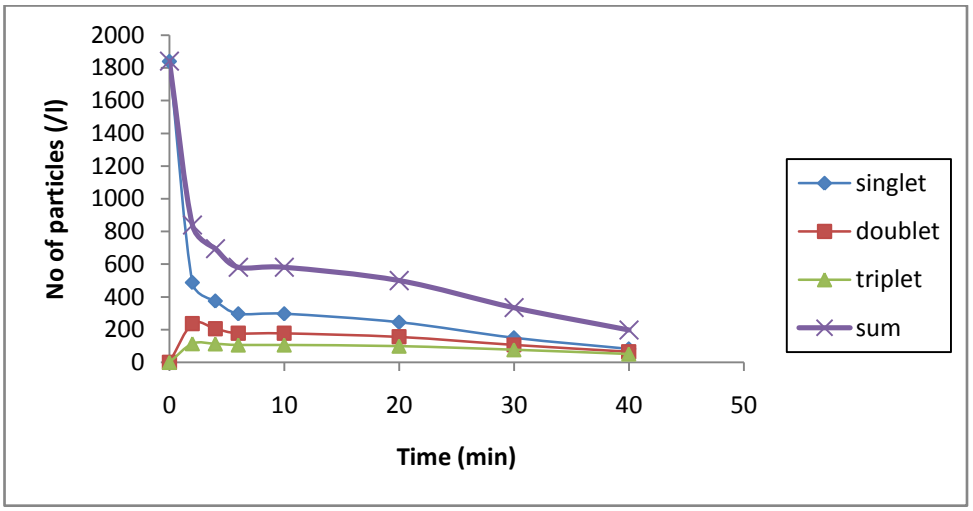

Fig.4.264:Particle distribution plot for cosc in PIE at maximum half life 16.47min

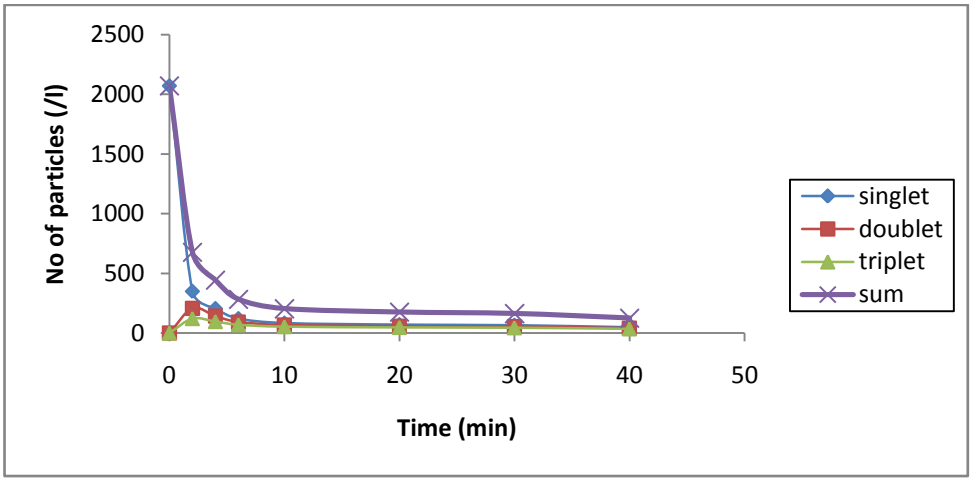

Fig.4.265:Particle distribution plot for tosc in PIE at minimum half life 0.21min

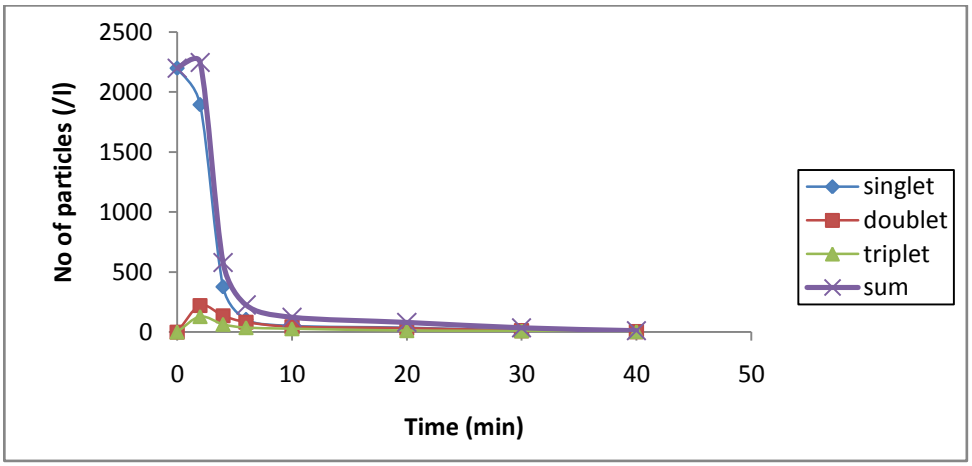

Fig.4.266:Particle distribution plot for tosc in PIE at maximum half life 12.94min

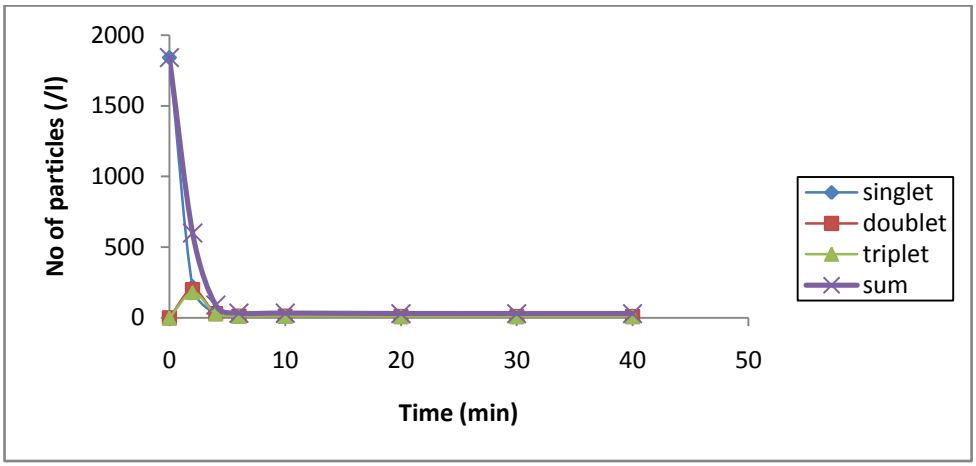

Fig.4.267:Particle distribution plot for ptsc in PIE at minimum half life 0.07min

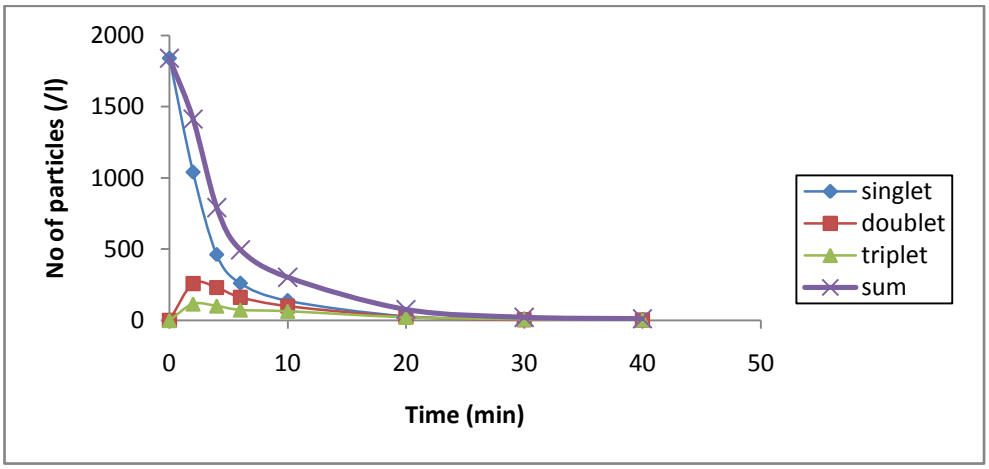

Fig.4.268:Particle distribution plot for ptsc in PIE at maximum half life 3.02min

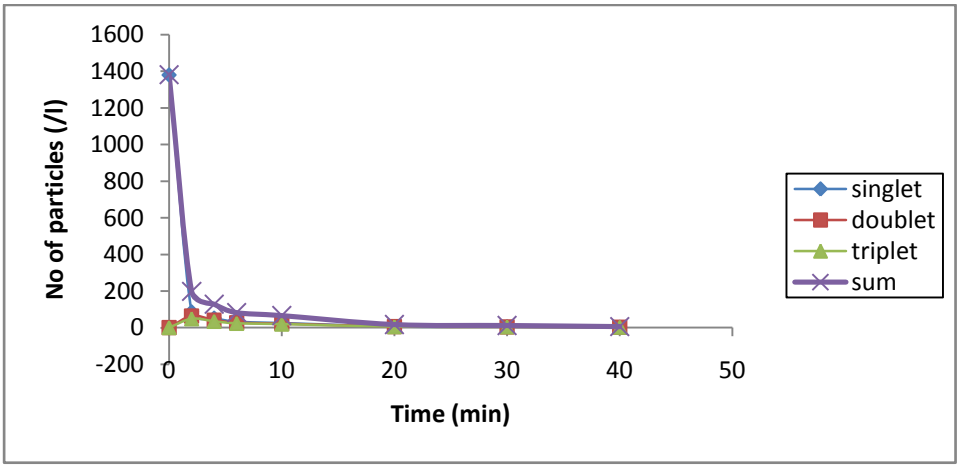

Fig.4.269:Particle distribution plot for mpsc in PIE at minimum half life 0.33min

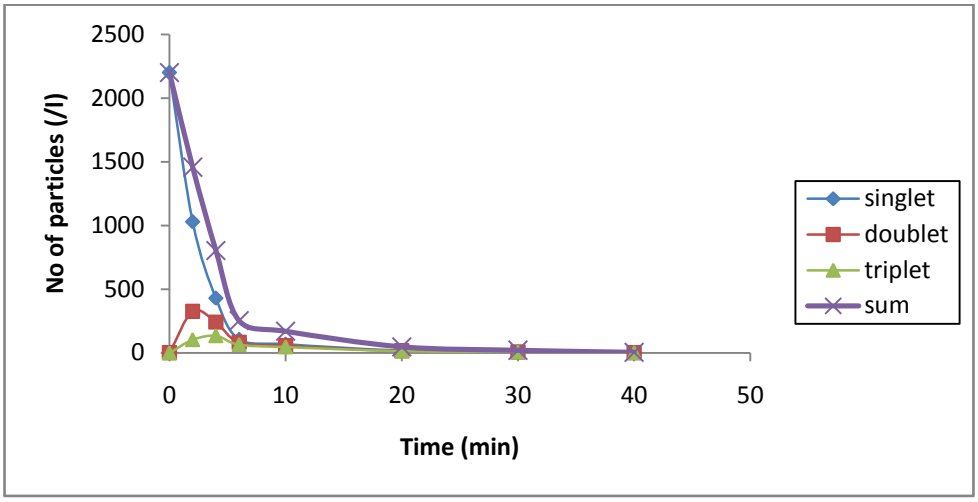

Fig.4.270:Particle distribution plot for mpsc in PIE at maximum half life 2.16min

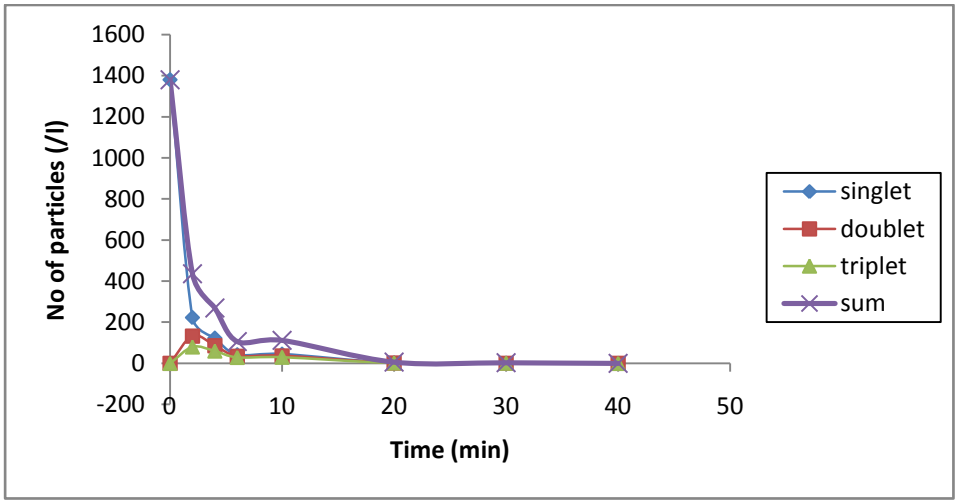

Fig.4.271:Particle distribution plot for ssc in VIE at minimum half life 0.30min

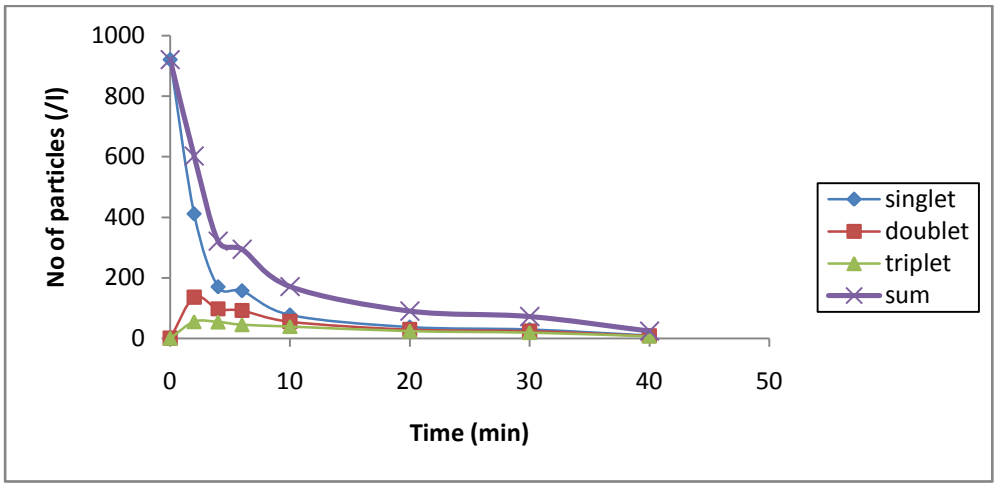

Fig.4.272:Particle distribution plot for ssc in VIE at maximum half life 4.29min

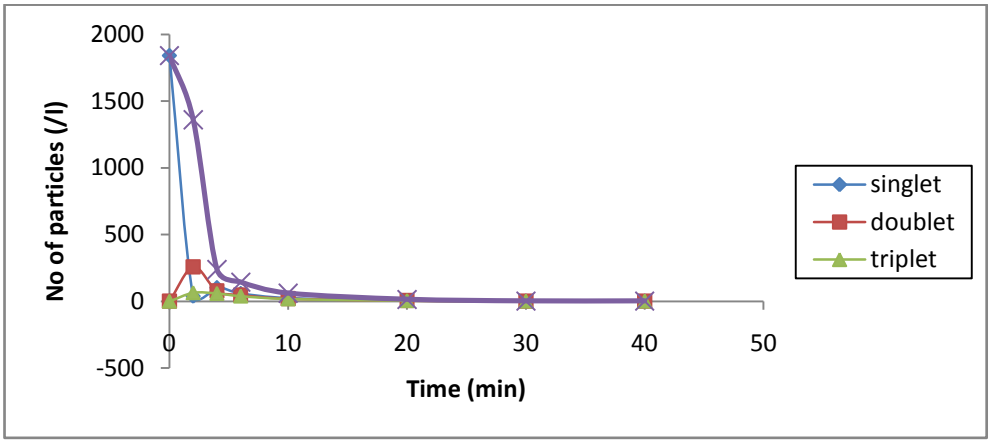

Fig.4.273:Particle distribution plot for cosc in VIE at minimum half life 0.29min

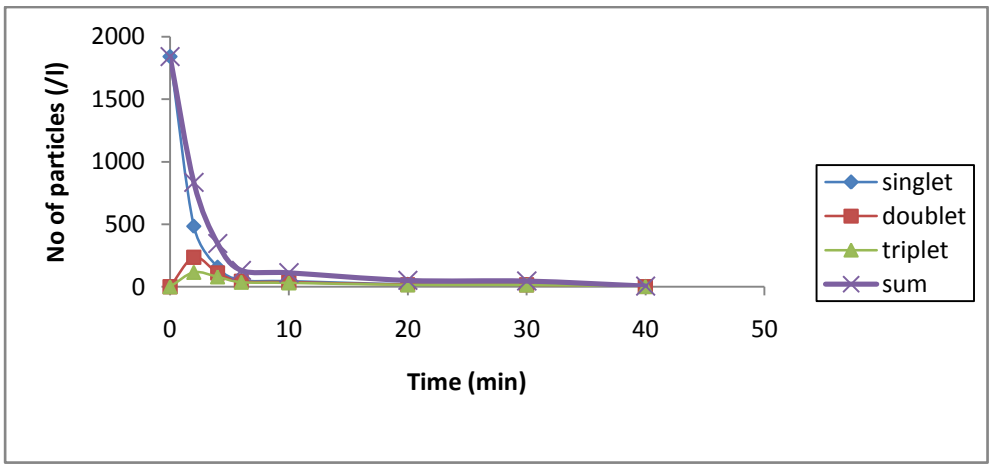

Fig.4.274:Particle distribution plot for cosc in VIE at maximum half life 3.15min

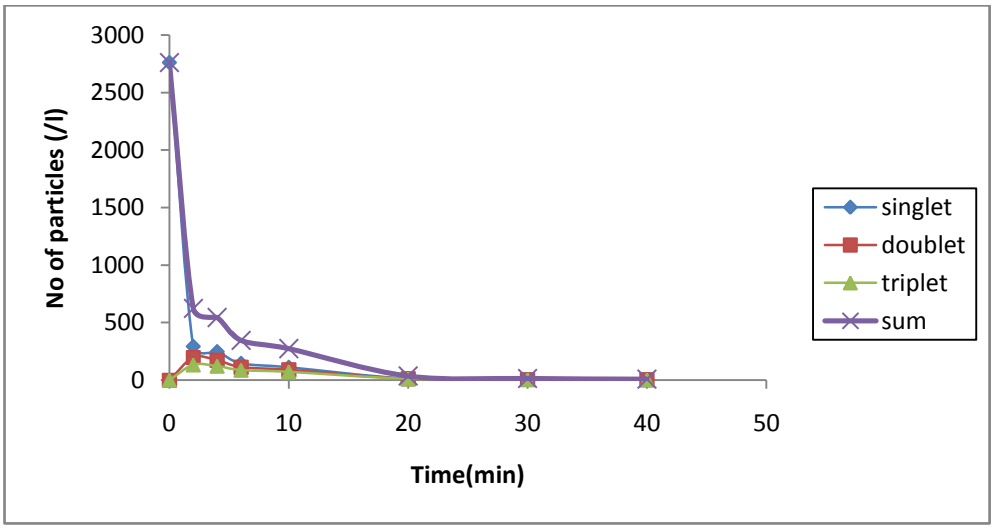

Fig.4.275:Particle distribution plot for tosc in VIE at mimimum half life 0.18min

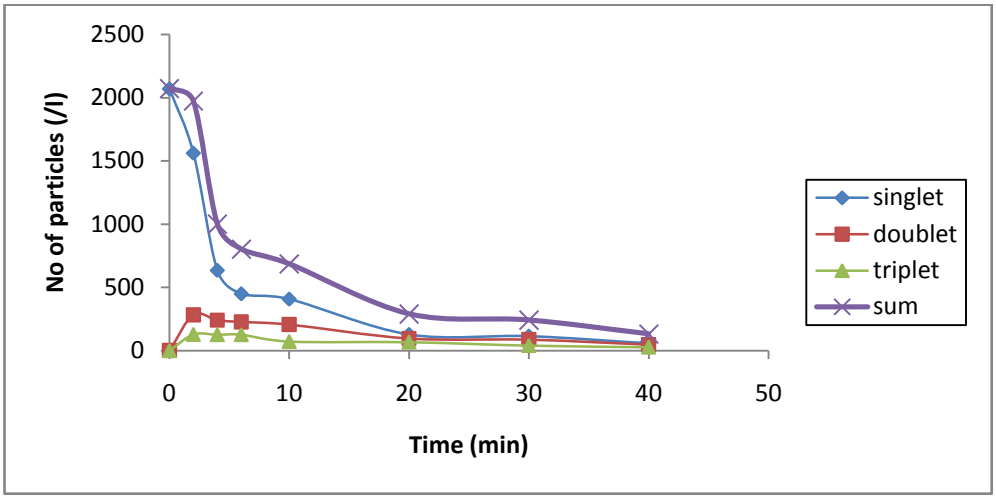

Fig.4.276:Particle distribution plot for tosc in VIE at maximum half life 32.98min

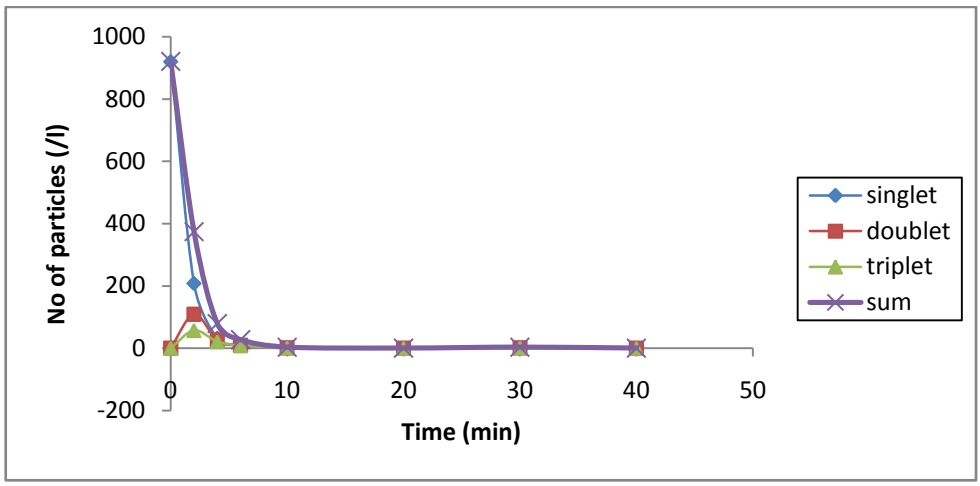

Fig.4.277:Particle distribution plot for ptsc in VIE at minimum half life 0.19min

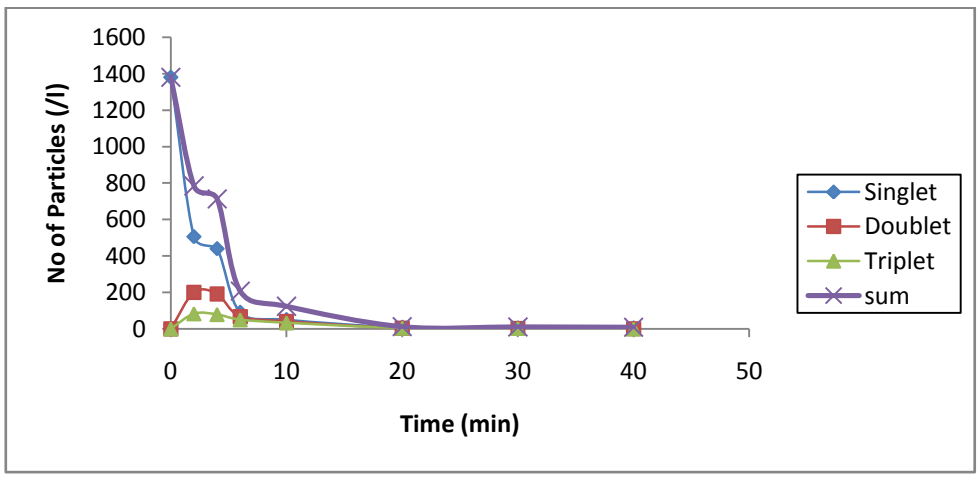

Fig.4.278:Particle distribution plot for ptsc in VIE at maximum half life 3.07min

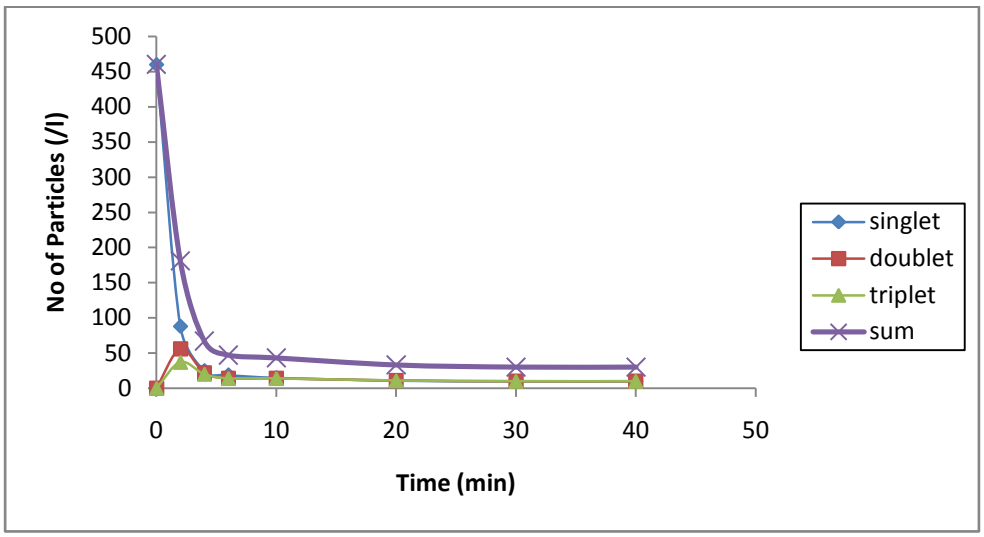

Fig.4.279:Particle distribution plot for mpsc in VIE at minimum half life 0.12min

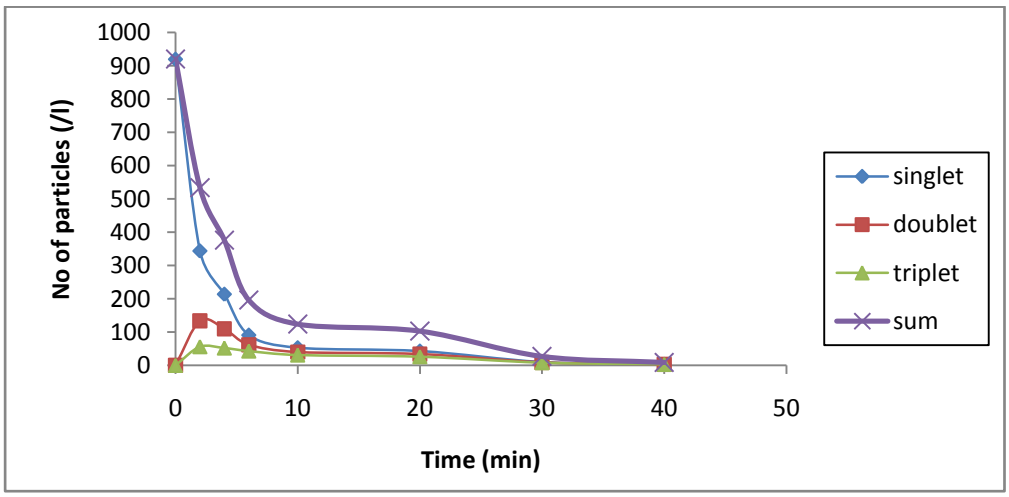

Fig.4.280:Particle distribution plot for mpsc in VIE at maximum half life 4.73min

4.1.5 Coag-flocculation optimization results of statistically Designed Experiment.

This section presents coag-flocculation optimization results and the corresponding surface plots obtained from Central Composite Design (CCD) of the experiment. For each of the design matrix, three variables, 17 experiments, 3 centre points and 6 star points were involved.

The tables of model coefficients and equations are presented in tables E1 to E2 of Appendix E and F1 to F2 of Appendix F, respectively.

The optimization results of the coag-flocculation process are presented in tables 4.133 and 4.134 for both PIE and VIE. With the objective of minimizing the quantity of TDSS in both PIE and VIE.

This section tends to analyse the interactive effects between the three variables (pH, dosage and settling time) and the single process response (TDSS removal) for the coag-flocculation process. For each table, the variations of factors for the various coag-flocculant are the same.

Observations from tables 4.133 and 4.134 indicate that maximum TDSS of 1.73173e+003 PTSC and 2.3083e+003 PTSC were recorded for both PIE and VIE respectively. In addition, the optimal values of the coded values generated were converted to real values. Based on the results posted in the tables, PTSC can successfully be employed as a good alternative aggregating agent to Alum.

The corresponding surface plot for most efficient coag-flocculants were presented in figures 4.281 to 4.286. These plots illustrate in three dimensions the interactive effects of two independent factors with the single process response which is the observed variable. It show areas of optimal performance on the plot surface for easy determination of the optimal TDSS values at two factors interactions in each case

A critical observation on the plots of PTSC in PIE, indicate that the optimal TDSS values were 300.00 mg/l, 100.00 mg/l and 100.00 mg/l for figures 4.281, 4.282 and 4.283 respectively. In each case, the optimal coag-flocculation is achieved at [dosage (-1, -0.5) and pH (0.13, 0.84)]; [Settling time (-1, -0.75) and pH (-0.75, 0.75)]; [settling time (1, 0.25) and dosage (-0.38, 0.7) for figures. 4.281 , 4.282, and 4.283 respectively.

Presented in figures 4.284 to 4.286 are the surface plots of PTSC in VIE. The optimal TDSS for the three figures are 160.00 mg/l, 250.00 mg/l and 250.00 mg/l for the referred figures above. From the figures, observe that the optimal area were obtained at [dosage (-1, -0.2) and pH (0.8, 1)]; [Settling time (0.5, 0.8) and pH (0.5, 1)]; [Settling time (-0.9, 0.6) and (-1, -0.8)] for figures 4.284, 4.285 and 4.286, respectively.

The general overview of the figures show that the darkest portion which depicts the optimal area are prevalent on a small segment of the surface plots This is indication that limited ranges of the factors are available for optimal coag-flocculation performance.

Analysis of variance (ANOVA) was applied for estimating the significance of the model at 5% significance level as shown in tables 4.135 to 4.144 for PIE and VIE respectively. Tables 4.135 to 4.144, describes the quantitative effect of the factors (X_1, X_2 and X_3) upon the response (Y). Coefficients with one factor represent the effect of that particular factor while the coefficients with more than one factor and those with second order terms

represent the interaction between those factors and the quadratic nature of the phenomena, respectively. The significance of the model equation using different coagulants in PIE and VIE media is discussed in the subsequent sections.

Table4.134: Optimum data of process model and various coag-flocculant in PIE

Sample	X_1(pH)		X_2(Dosage)		X_3(Settling time)		Y(TDSS	Y_{CV}(mg/l)
	CV*	RV** (g/l)	CV*	RV**(g/l)	CV*	RV**(g/l)	Removal mg/l)	
SSC	1.0000	0.7000	1.0000	0.7000	-1.0000	0.1000	1.4582e+003	1.4511e +003±1
COSC	1.0000	0.7000	1.0000	0.7000	-1.0000	0.1000	1.2066e+003	1.2054e+003±3
TOSC	1.0000	0.7000	1.0000	0.7000	-1.0000	0.1000	1.1071e+003	1.1010e+003
PTSC	-1.0000	0.1000	1.0000	0.7000	-1.0000	0.1000	1.73173+003	1.7300e +003±2
MPSC	-1.0000	0.1000	1.0000	0.7000	-1.0000	0.1000	1.6847e+003	1.6852e+003±2
ALUM	0.0075	0.4023	1.0000	0.7000	-1.0000	0.1000	1.1448e + 003	1.1430e+ 003±2

Table 4.135: Optimum data of process model and various coag-flocculant in VIE

Sample	X_1(pH)		X_2(Dosage)		X_3(Settling time)		Y(TDSS	Y_{CV}(mg/l)
	CV*	RV** (g/l)	CV*	RV**(g/l)	CV*	RV**(g/l)	Removal mg/l)	
SSC	1.0000	0.7000	1.0000	0.7000	-1.0000	0.1000	818.6182	818.6161
COSC	0.2568	0.4770	1.0000	0.7000	-1.0000	0.1000	780.3162	780.3141
TOSC	1.0000	0.7000	1.0000	0.7000	-1.0071	0.4021	551.1600	551.1612
PTSC	-1.0000	0.1000	0.6172	0.5852	-1.0000	0.1000	2.3083e+003	2.3053e+003±2
MPSC	-1.0000	0.1000	1.0000	0.7000	-1.0000	0.1000	1.3780e+003	1.3780e+003±3
ALUM	-1.0000	0.1000	-1.0000	0.1000	-1.0000	0.1000	281.7399	281.7379

4.1.5.1 ANOVA discussion on SSC in PIE

The most significant effect for performance of SSC is the pH while dosage is the least as presented in table 4.136. The implication is that changes in pH will have a major impact on coagulant efficiency. Although, changes in the settling time and dosage had a satisfactory influence in the coagulant effectiveness too. From the P-values presented in the table, it can be stated that the linear terms x_1, x_2, x_3, their interaction effects and the quadratic term of settling time (x_3^2) were significant to the model. Thus the quadratic term of pH(x_1^2) and dosage (x_2^2) have no major effects on the accuracy of the model. Hence they may be excluded from the model equation. The model accuracy is validated by the value of R^2 and Adjusted R^2. Testing for fitness of the model for coagulation using SSC is given as:

$Y=355.9577+297.0000x_1+145.7000x_2-292.1500x_3+148.5625x_1x_2-191.9375x_1x_3$
$+127.3125x_2x_3+34.8239x_1^2-42.6761x_2^2+388.5739x_3^2$ (4.1)

Deleting variables that were not significant, we have.

$Y=355.9577+297.000x_1+145.7000x_2-292.1500x_3+148.5625x_1x_2$
$191.9375x_1x_3+127.3125x_2x_3 +388.5739x_3^2$ (4.2)

Where Y is the turbidity (TDSS)

Table 4.136: Analysis of variance of statistically Designed Experiment for SSC in PIE

Variable	Coefficients	Se	Tstat	Pval	Remarks
Constant	355.9577	58.933	6.04	0.00052108	
X_1	297.0000	43.553	6.8193	0.00024881	Significant
X_2	145.7000	43.553	3.3454	0.012329	Significant
X_3	-292.1500	43.553	-6.7079	0.00027542	Significant
X_1X_2	148.5625	48.694	3.051	0.018558	Significant
X_1X_3	-191.9375	48.694	-3.9417	0.0055908	Significant
X_2X_3	127.3125	48.694	2.6146	0.034682	Significant
X_1^2	34.8239	84.141	0.41387	0.69135	Not Significant
X_2^2	-42.6761	84.141	-0.50719	0.6276	Not Significant
X_3^2	388.5739	84.141	4.6181	0.0024316	Significant

$R^2 = 0.9597$ Adj $R^2 = 0.9079$ MSE = 1.8968×10^4

4.1.5.2 ANOVA discussion on COSC in PIE

The main significant factor is the dosage (x_2) while pH (x_1) is the least as posted in table 4.137. Thus, a change in dosage has the greatest effect in the effectiveness of this coagulant, while a change in pH has the least effect. All their interaction and the quadratic terms with the exception of pH(x_1^2) were not significant. Checking the model fitness for coagulant using COSC in PIE is given as:

$Y=377.3732+98.3000x_1+185.3500x_2-143.9000x_3+19.6250x_1x_2-$
$80.3750x_1x_3+38.3750x_2x_3+450.9718X_1^2-25.2782X_2^2+165.9718X_3^2$ (4.3)

Deleting variables that were not significant we have:

$Y=377.3732+185.3500x_2-143.9000x_3+450.9718x_1^2$ (4.4)

Table 4.137: Analysis of variance of statistically Designed Experiment for COSC in PIE

Variable	Coefficients	Se	Tstal	Pval	Remarks
Constant	377.3732	75.217	5.0171	0.0015355	
X_1	98.3000	55.587	1.7684	0.12032	Not Significant
X_2	185.3500	55.587	3.3344	0.012516	Significant
X_3	-143.9000	55.587	-2.5887	0.036012	Significant
X_1X_2	19.6250	62.149	0.31578	0.76138	Not Significant
X_1X_3	-80.3750	62.149	-1.2933	0.23696	Not Significant
X_2X_3	38.3750	62.149	0.61747	0.55647	Not Significant
X_1^2	450.9718	107.39	4.1993	0.0040389	Significant
X_2^2	-25.2782	107.39	-0.23538	0.82065	Not Significant
X_3^2	165.9718	107.39	1.5455	0.16615	Not Significant

$R^2 = 0.8987$ Adj $R^2 = 0.7684$ MSE = 3.0900×10^4

4.1.5.3 ANOVA discussion on TOSC in PIE

In this case, the most linear significant factor is setting time (x_3), while pH (x_1) is the least as can be seen in table 4.138. Their interaction and the quadratic effects were not significant except the quadratic effect of settling time (x_3^2). Testing for the model fitness for coagulation using TOSC in PIE is given as:

$$Y=415.3239+48.0500x_1+273.000x_2-298.8000x_3+59.2500x_1x_2-31.6250x_1x_3-40.1250x_2x_3+631.9331x_1^2-146.5669x_2^2+80.1831x_3^2 \quad (4.5)$$

Deleting variables that were not significant, we have:

$$Y=415.3239+273.000x_2-298.8000x_3+631.9331x_1^2 \quad (4.6)$$

Table 4.138: Analysis of variance of statistically Designed Experiment for TOSC in PIE

Variable	Coefficients	Se	Tstal	Pval	Remarks
Constant	415.3239	98.22	4.2285	0.0038954	
X_1	48.0500	72.587	0.66196	0.52918	Not Significant
X_2	273.000	72.587	3.7617	0.0070592	Significant
X_3	-298.8000	72.587	4.1164	0.0044795	Significant
X_1X_2	59.2500	81.155	0.73009	0.48904	Not Significant
X_1X_3	-31.6250	81.155	-0.38969	0.70835	Not Significant

X_2X_3	-40.1250	81.155	-0.49443	0.63614	Not Significant
X_1^2	631.9331	140.23	4.5063	0.0027773	Significant
X_2^2	-146.5669	140.23	-1.0452	0.33069	Not Significant
X_3^2	80.1831	140.23	0.57178	0.58535	Not Significant

$R^2 = 0.8979$ Adj $R^2 = 0.7665$ MSE 5.2689×10^4

4.1.5.4 ANOVA discussion on PTSC in PIE.

Table 4.139, show that settling time (x_3) is the only main significant factor here. All other factors, their interaction and their quadratic effects were not significant. Hence they are excluded in the model equation of fitness for the coagulant.

$$Y=338.1338-345.0000x_3 \quad (4.7)$$

Table 4.139: Analysis of variance of statistically Designed Experiment for PTSC in PIE

Variable	Coefficients	Se	Tstal	Pval	Remarks
Constant	338.1338	99.611	3.3945	0.011528	
X_1	-23.6500	73.615	-0.32127	0.75739	Not Significant
X_2	138.3500	73.615	1.8794	0.10226	Not Significant
X_3	-345.0000	73.615	-4.6866	0.0022435	Significant
X_1X_2	-0.6250	82.304	-0.0075938	0.99415	Not Significant
X_1X_3	-132.3750	82.304	-1.6084	0.15179	Not Significant
X_2X_3	-128.7500	82.304	-1.5643	0.16172	Not Significant
X_1^2	94.8908	142.22	0.66721	0.52601	Not Significant
X_2^2	78.3908	142.22	0.5512	0.59864	Not Significant
X_3^2	91.6408	142.22	0.64436	0.53987	Not Significant

$R^2 = 0.8303$ Adj $R^2 = 0.6121$ MSE 5.4191×10^4

4.1.5.5 ANOVA discussion on MPSC in PIE

Table 4.140, show that settling time(x_3) is the most significant main factor with the dosage (x_2) being the least. Only the interaction effect of pH (x_1) is significant. All other interaction effects are not significant. The quadratic effects of settling time is significant while the rest were not.

The model fitnesss for coagulation using MPSC is given as.

$$Y=341.6690-166.5500x_1+53.400x_2-273.6000x_3-175.4375x_1x_2-11.1875x_1x_3+15.0625x_2x_3-3.0458x_1^2-78.5458x_2^2+303.7042x_3^2 \quad (4.8)$$

Deleting variable that were not significant, we have;

$$Y=3441.6690-166.5500x_1-273.6000x_3-175.4375x_1x_2+303.7042x_3^2 \quad (4.9)$$

Table 4.140: Analysis of variance of statistically Designed Experiment for MPSC in PIE

Variable	Coefficients	Se	Tstal	Pval	Remarks
Constant	341.6690	76.656	4.4572	0.0029461	
X_1	-166.5500	55.65	-2.94	0.021715	Significant
X_2	53.4500	56.65	0.9435	0.37684	Not Significant
X_3	-273.6000	56.65	-4.8296	0.0019003	Significant
X_1X_2	-175.4375	63.337	-2.7699	0.027698	Significant
X_1X_3	-11.1875	63.337	-0.17663	0.8648	Not Significant
X_2X_3	15.0625	63.337	0.23781	0.81884	Not Significant
X_1^2	-3.0458	109.45	-0.027829	0.97858	Not Significant
X_2^2	-78.5458	109.45	-0.71767	0.49621	Not Significant
X_3^2	303.7042	109.45	2.7749	0.027498	Significant

$R^2 = 0.8772$ Adj $R^2 = 0.7193$

4.1.5.6: ANOVA discussion on SSC in VIE

Table 4.141, show that all the linear terms (x_1x_2 and x_3), interaction of dosage(x_2^2) and settling time(x_3^2) were significant. However, the most main significant factor is pH(x_1). The insignificant parameter is excluded in the final model fitness equation.

The model fits for coagulation using SSC in VIE is given as;

$$Y=319.7937+207+207.2300x_1+58.4100x_2-79.7450x_3+25.7938x_1x_2-84.7312x_1x_3-16.1437x_2x_3+45.8986x_1^2-27.9014x_2^2+8.7736x32 \quad (4.10)$$

Deleting variable that were not significant, we have;

$$Y= 319.7937+207.2300x_1+58.4100x_2-79.7450x_3-16.1437x^2x^3 \quad (4.11)$$

Table 4.141: Analysis of variance of statistically Designed Experiment for SSC in VIE

Variable	Coefficients	Se	Tstal	Pval	Remarks
Constant	319.7937	30.578	10.458	1.591×10^{-5}	
X_1	207.2300	22.598	9.1704	$3.7753\ 10^{-5}$	Significant
X_2	58.4100	22.598	2.5848	0.03622	Significant
X_3	-79.7450	22.598	-3.5289	0.0096123	Significant
X_1X_2	25.7938	25.265	1.0209	0.34127	Not Significant
X_1X_3	-84.7312	25.265	-3.3537	0.012189	Significant
X_2X_3	-16.1437	25.265	-0.63897	0.54317	Not Significant

X_1^2	45.8986	43.658	1.0513	0.32804	Not Significant
X_2^2	-27.9014	43.658	-0.6391	0.5431	Not Significant
X_3^2	8.7736	43.658	0.20096	0.84644	Not Significant

$R^2 = 0.9437$ Adj $R^2 = 0.8714$ MSE 5.1066×10^3

4.1.5.7 ANOVA discussion on COSC in VIE

The linear most significant factor is dosage (x_2), while pH(x_1) is the least as presented in table 4.142. The interaction of dosage and settling time(x_2x_3) is significant and as well the quadratic term of settling time.

The model fits for coagulation using COSC in VIE is given as:

$$Y= 603.8208+62.9060x_1+289.4390x_2-167.0160x_3+9.1613x_1x_2+5.9988x_1x_3-139.3488x_2x_3-128.6365-94.7115x_2^2+264.5635x_3^2 \quad (4.12)$$

Deleting variable that were not significant:

$$Y=603.8208+289.4390x_2-167.0160x_3-139.3488-128.6365x_1^2+264.5635x_3^2 \quad (4.13)$$

Table 4.142: Analysis of variance of statistically Designed Experiment for COSC in VIE

Variable	Coefficients	Se	Tstal	Pval	Remarks
Constant	603.8208	39.8	15.172	1.3004×10^{-6}	
X_1	62.9060	29.413	2.1387	0.069765	Not Significant
X_2	289.4390	29.413	9.8406	2.3783×10^{-5}	Significant
X_3	-167.0160	29.413	-5.6784	0.00075201	Significant
X_1X_2	9.1613	32.884	0.27859	0.78861	Not Significant
X_1X_3	5.9988	32.884	0.18242	0.86042	Not Significant
X_2X_3	-139.3488	32.884	-4.2375	0.0038521	Significant
X_1^2	-128.6365	56.824	-2.2638	0.058007	Significant
X_2^2	-94.7115	56.824	-1.6668	0.1395	Not Significant
X_3^2	264.5635	56.824	4.6559	0.0023258	Significant

$R^2 = 0.9614$ Adj $R^2 = 0.9117$ MSE 8.6511×10^3

4.1.5.8 ANOVA discussion on TOSC in VIE

Table 4.143, show that only the dosage (x_2) is significant among the linear terms.

Thus the model equation is given as follows.

$$Y=676.46831+520.08001x_2 \quad (4.14)$$

Table 4.143: Analysis of variance of statistically Designed Experiment for TOSC in VIE

Variable	Coefficients	Se	Tstal	Pval	Remarks
Constant	676.4683 1	90.95	3.5426	0.0094369	
X_1	179.5100 1	41.12	1.2721	0.24398	Not Significant
X_2	520.0800 1	41.12	3.6854	0.0078036	Significant
X_3	-123.4150	141.12	-0.87455	0.41082	Not Significant
X_1X_2	166.0937 1	57.77	1.0527	0.32744	Not Significant
X_1X_3	168.5938 1	57.77	1.0686	0.32072	Not Significant
X_2X_3	-51.0438 1	57.77	-0.32352	0.75575	Not Significant
X_1^2	217.1430 2	72.63	0.79647	0.45192	Not Significant
X_2^2	548.9930 2	72.63	2.0137	0.083909	Not Significant
X_3^2	-412.98202	72.63	-1.5148	0.1736	Not Significant

$R^2 = 0.7803$ Adj R^2 0.4978 MSE 1.9914×10^5

4.1.5.9 ANOVA discussion on PTSC in VIE

Table 4.144, show that all linear and quadratic terms were not significant with the exception of the quadratic effect of settling times(x_3^2). Thus the model equation of fitness is given as:

$$Y=269.2197+125.5655x_3^2 \quad (4.15)$$

Table 4.144: Analysis of variance of statistically Designed Experiment for PTSC in VIE

Variable	Coefficients	Se	Tstal	Pval	Remarks
Constant	269.2197	33.946	7.9308	9.6341×10^{-5}	
X_1	-51.9950	25.087	-2.0726	0.07692	Not Significant
X_2	8.0750	25.087	0.32188	0.75694	Not Significant
X_3	-53.9500	25.087	-2.1505	0.06856	Not Significant
X_1X_2	3.4312	28.048	0.12234	0.90607	Not Significant
X_1X_3	33.9438	28.048	1.2102	0.26547	Not Significant
X_2X_3	-56.9063	28.048	-2.0289	0.082046	Not Significant

X_1^2	-2.5095	48.466	-0.051778	0.96015	Not Significant
X_2^2	-49.8595	48.466	-1.0287	0.33783	Not Significant
X_3^2	125.5655	48.466	2.5908	0.035904	Significant

$R^2 = 0.7605$ Adj $R^2 = 0.4525$ MSE 6.2935×10^3

4.1.5.10 ANOVA discussion on MPSC in VIE

All effects of linear and interaction terms of pH and settling time(x_1x_2) were significant. Thus, the interaction effects of x_1x_3 and x_2x_3 including all the quadratic effects were insignificant. The model equation is given as;

$$Y=158.8113-191.1800x_1+61.3150x_2-83.3250x_3-89.2062x_1x_2+47.8438x_1x_3$$
$$24.6438x_2x_3+53.2803x_1^2+29.5053x_2^2+41.2053x_3^2 \quad (4.16)$$

Deleting variable that were not significant we have:

$$Y=158.8113-191.1800x_1+61.3150x_2-83.3250x_3-89.2062x_1x_2 \quad (4.17)$$

Table 4.145: Analysis of variance of statistically Designed Experiment for MPSC in VIE

Variable	Coefficients	Se	Tstal	Pval	Remarks
Constant	158.8113	36.371	4.3665	0.0032882	
X_1	-191.1800	26.879	-7.1127	0.0019152	Significant
X_2	61.3150	26.879	2.2812	0.056538	Significant
X_3	-83.3250	26.879	-3.6	0.017321	Significant
X_1X_2	-89.2062	30.051	-2.9685	0.020853	Significant
X_1X_3	47.8438	30.051	1.5921	0.1554	Not Significant
X_2X_3	-24.6438	30.051	0.82006	0.43921	Not Significant
X_1^2	53.2803	51.928	1.026	0.33902	Not Significant
X_2^2	29.5053	51.928	0.5682	0.58766	Not Significant
X_3^2	41.2053	51.928	0.79351	0.45354	Not Significant

$R^2 = 0.9226$ Adj $R^2 = 0.8231$ MSE 7.2246×10^3

X_1 = pH -

X_2 = Dosage – (g)

X_3 = Settling time – (mins)

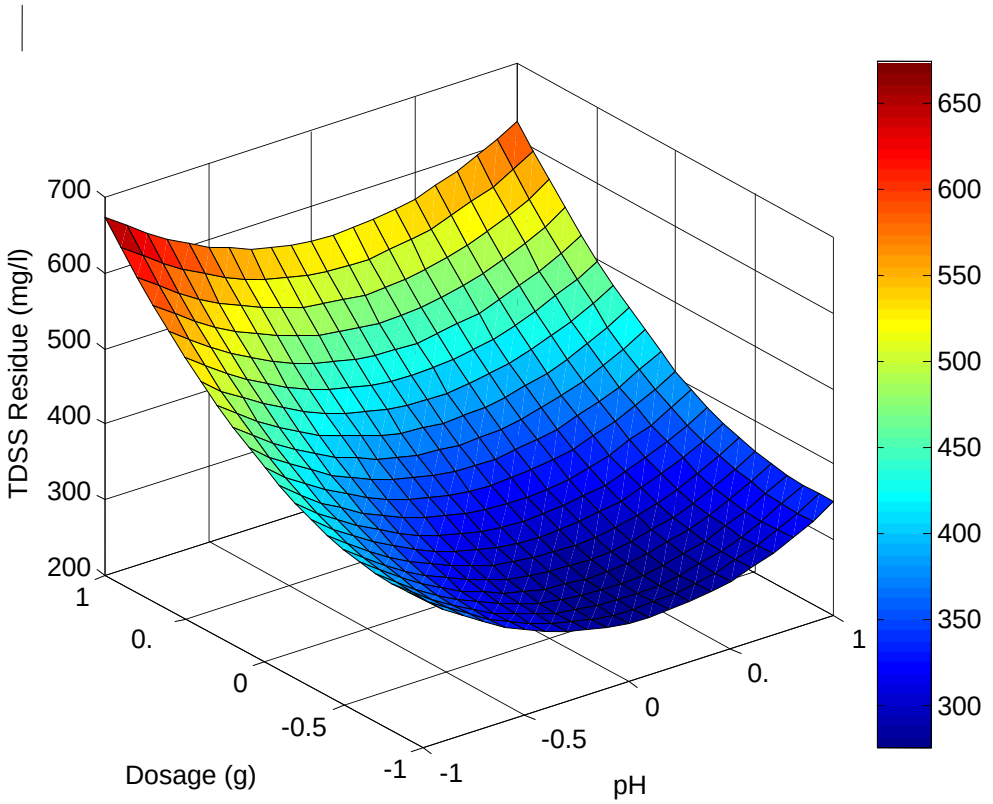

Fig.4.281:Coag.flocculation surface plots of ptsc in PIE showing interaction of dosage and pH

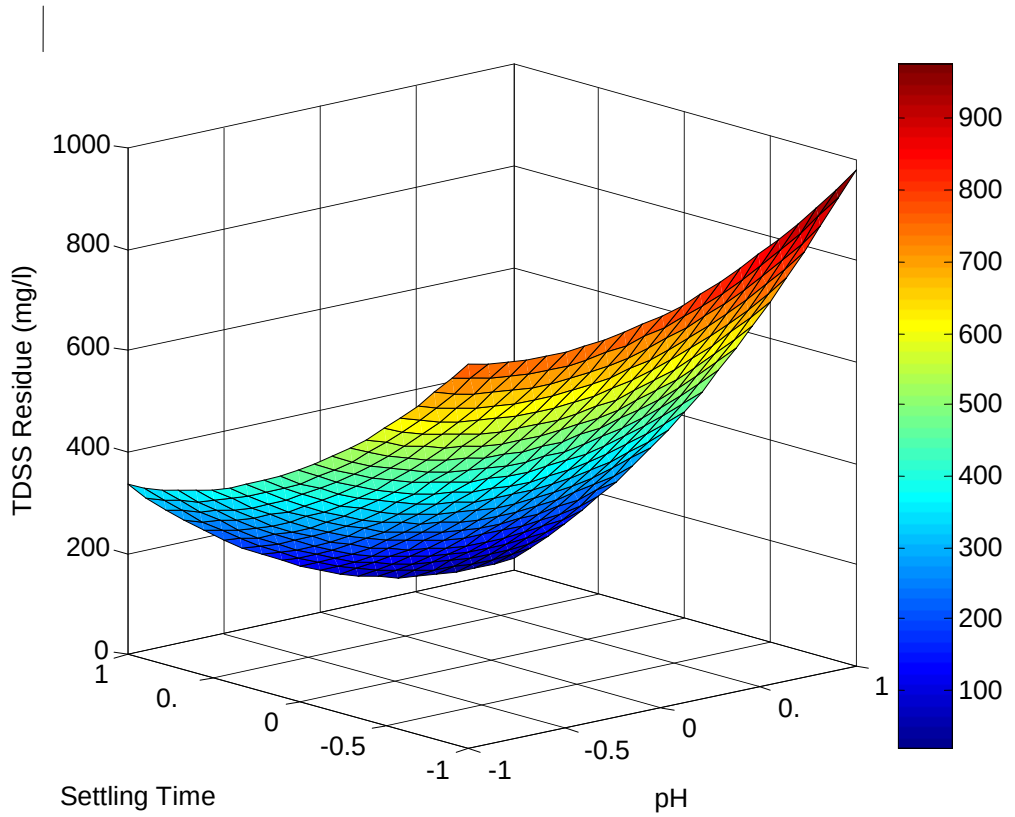

Fig.4.282:Coag.flocculation surface plots of ptsc in PIE showing interaction of settling time and pH

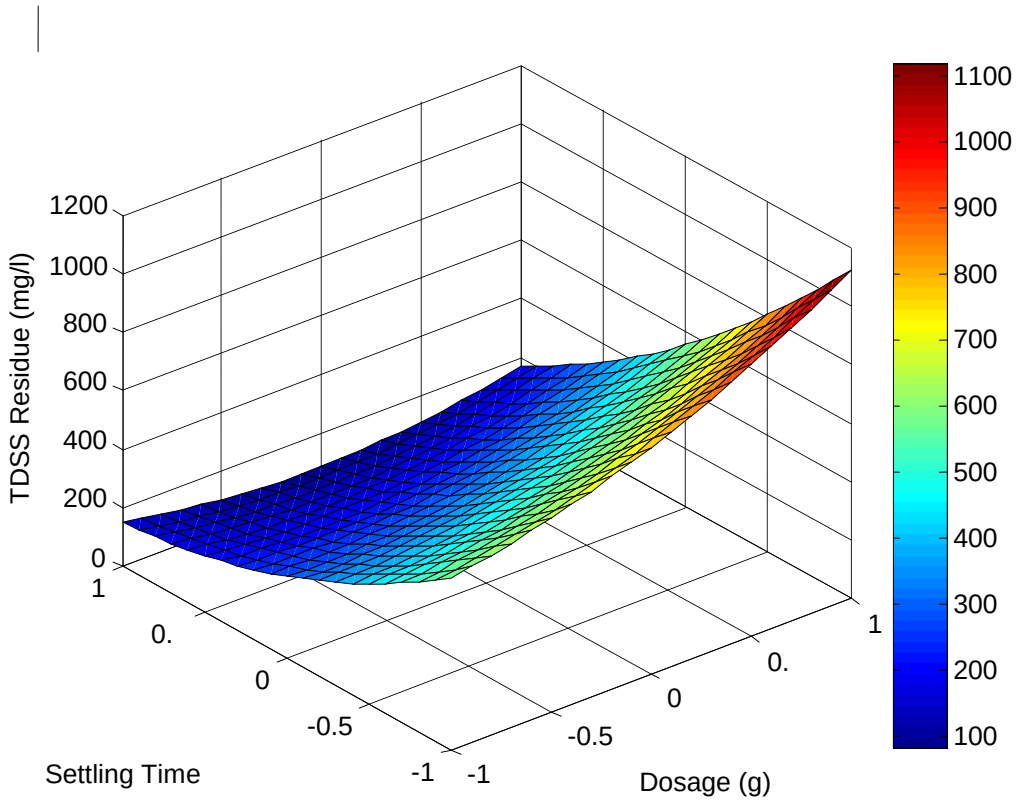

Fig.4.283:Coag.flocculation surface plots of ptsc in PIE showing interaction of settling time and dosage

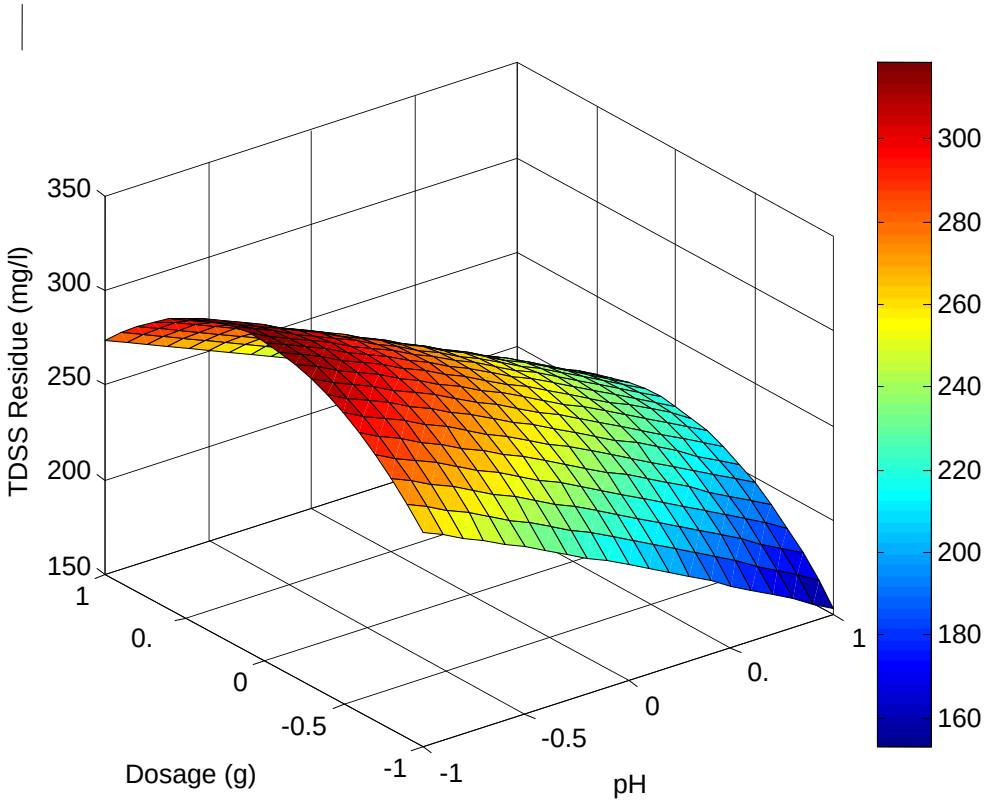

Fig.4.284:Coag.flocculation surface plots of ptsc in VIE showing interaction of dosage and pH

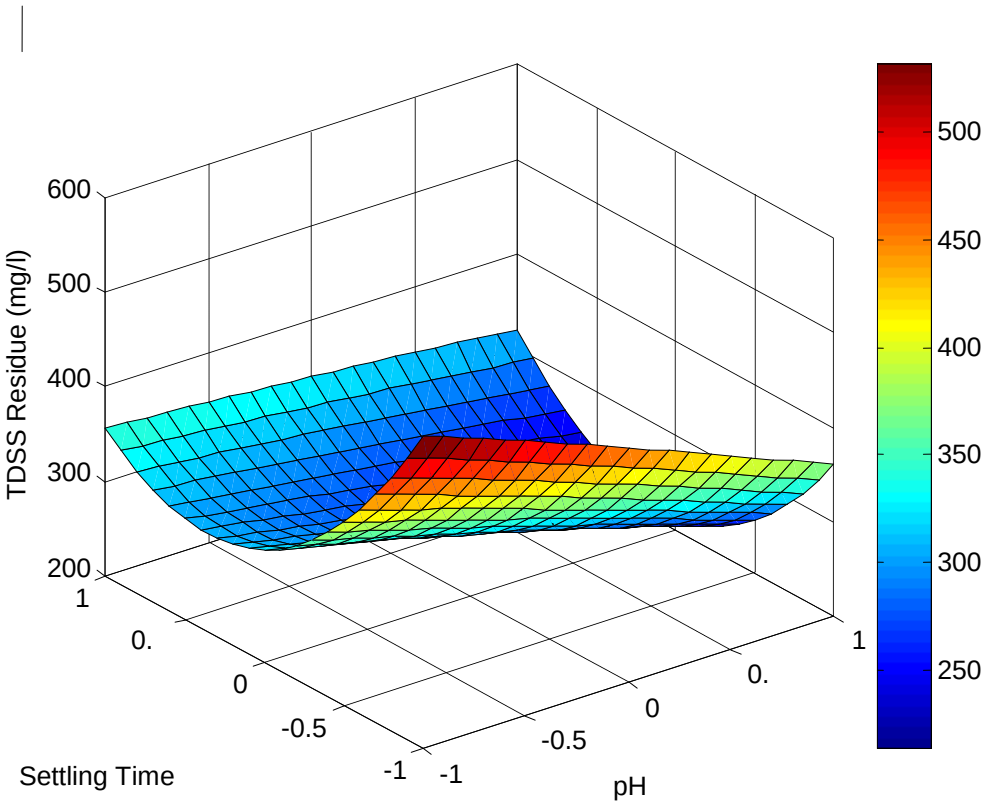

Fig.4.285:Coag.flocculation surface plots of ptsc in VIE showing interaction of settling time and pH

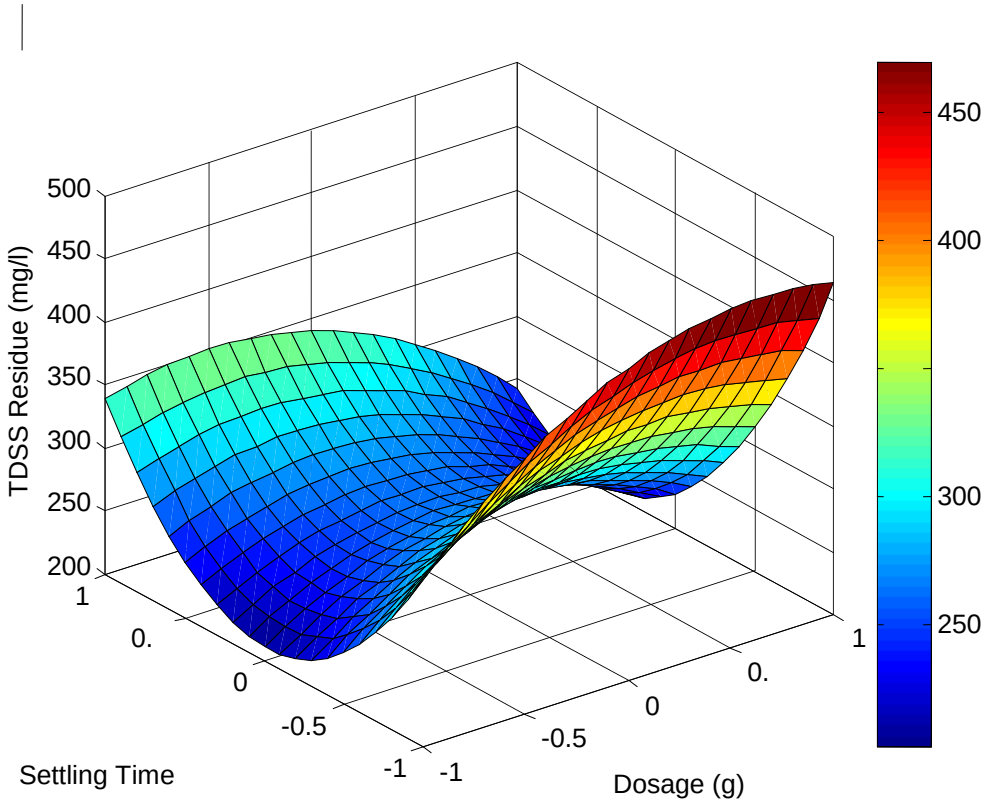

Fig.4.286:Coag.flocculation surface plots of ptsc in VIE showing interaction of settling time and dosage

4.1.6 Comparative Coag-flocculation Performance between Alum and Various Organic Coag-flocculants

This section presents coag-flocculation activity performance evaluation of the various aggregation agents by comparing the removal efficiency of the various organic coag-flocculant with that of alum which served as a control. The results are discussed as presented below.

4.1.6.1 Comparative coag-flocculation removal efficiency for varying dosages and constant pH of PIE medium

The results presented in figures. 4.287 to 4.316, showing the comparative removal efficiency between alum and various organic coag-flocculants. In each case alum being the control is compared individually with SSC, COSC, TOSC, PTSC and

MPSC. In this section, the pH of the PIE medium is constant as the dosage of the various coag-flocculants varies.

In the case of SSC, the results were presented in figures. 4.287 to 4.292, indicating that dosage of 0.2g/l provided the best performance at pH of 13 as shown in figure. 4.292 though the results obtained at the pH of 1, 7 and 10 for all the dosages are satisfactory. It should be observed that alum performed better than SSC at the pH of 7, for 0.1g/l dosage which is the optimum performance for the process. In general, as can be observed from figures. 4.287 to 4.292, SSC provided better performance than alum. Also it should be observed in figure. 4.290, that the difference between the efficiency values recorded for ALUM and SSC are near same, indicating that their performance activity can be favorably be compared at pH of 7. For COSC, the removal efficiency profile are presented in figures.4.293 to 4.298, show that the performance of COSC are better for the pH of 1 and 3 for all the dosages studied, whereas figures.4.293 to 4.295, displays the best performance for the alum, showing high level of performance over COSC for all the dosages considered with the exception of 0.3g/l and 0.6g/l as can be observed in figure. 4.295. Though the percentage efficiency recorded for COSC at 0.1 to 0.3g/l dosages are satisfactory as can be seen in the referred figures. Overall performance for the process show that alum is better than COSC.

Consider figures. 4.299 to 4.304 posted for the comparative analysis between TOSC and alum. The best performance is achieved by alum in figure. 4.302 for pH of 7, while TOSC showed high level of performance over alum in figs.4.299 to 4.301 and figures. 4.303 and 4.304 for all the dosages studied with the exception of 0.7g/l in fig.4.299, 0.6 to 0.7g/l in figure.4.301, 0.1 to 0.2g/l and 0.4g/l in figure 4.303, 0.6g/l in figure.4.304. In the case of PTSC, the results presented in figures 4.305 to 4.310 the maximum percentage efficiency was recorded in figure 4.310 at pH of 13 for all the dosages, whereas it is only in figure.4.308, that alum outperformed PTSC in all the dosages. In general the results emphasize the effectiveness of PTSC as an organic aggregating agent, when compared to other coag-flocculants studied in this work for the coag-flocculation in PIE systems. Consider figures 4.311 to 4.316, representing the comparative performance

involving MPSC and alum. MPSC generally performed better than alum. Alum has its best comparative result in figure 4.312 for all the dosages.

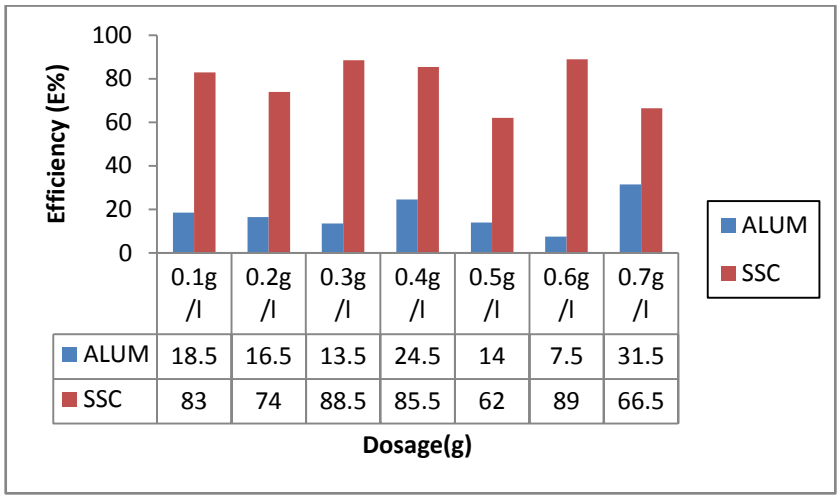

Fig.4.287: Comparative coag-flocculation performance at 40mins for varying ssc and alum dosages in PIE at pH of 1

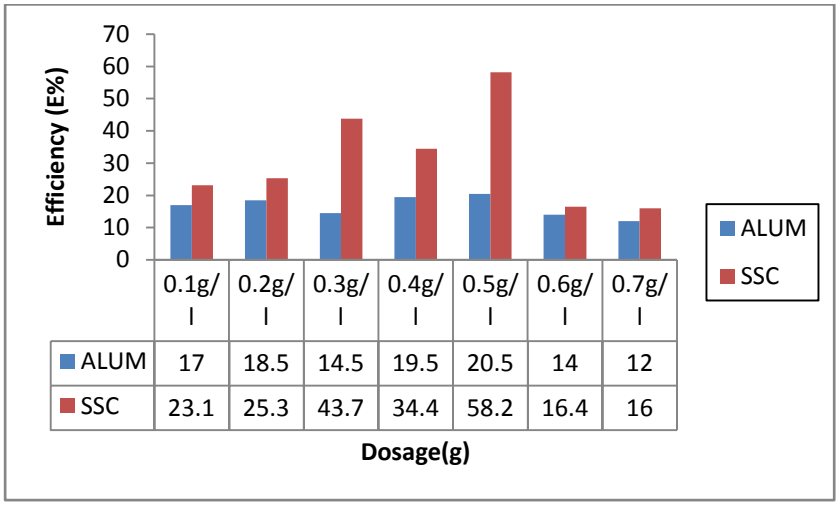

Fig.4.288: Comparative coag-flocculation performance at 40mins for varying ssc and alum dosages in PIE at pH of 3

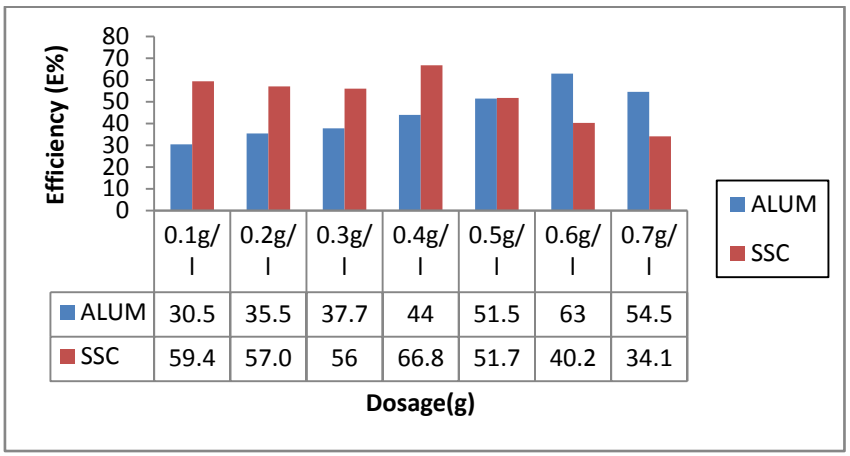

Fig.4.289: Comparative coag-flocculation performance at 40mins for varying ssc and alum dosages in PIE at pH of 5

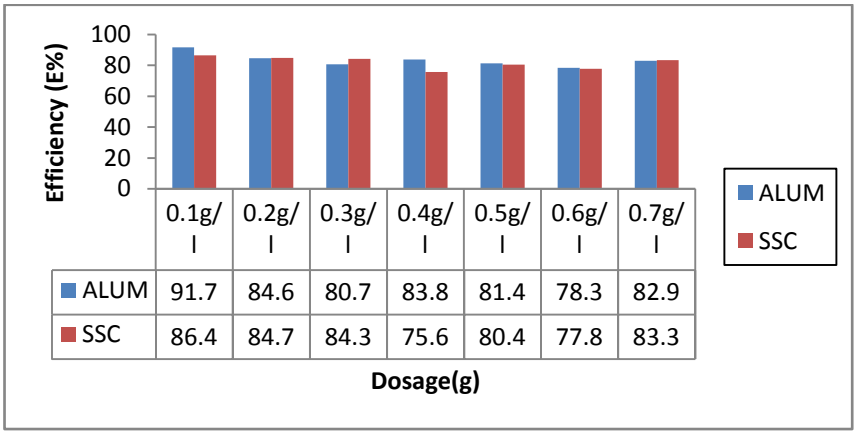

Fig.4.290: Comparative coag-flocculation performance at 40mins for varying ssc and alum dosages in PIE at pH of 7

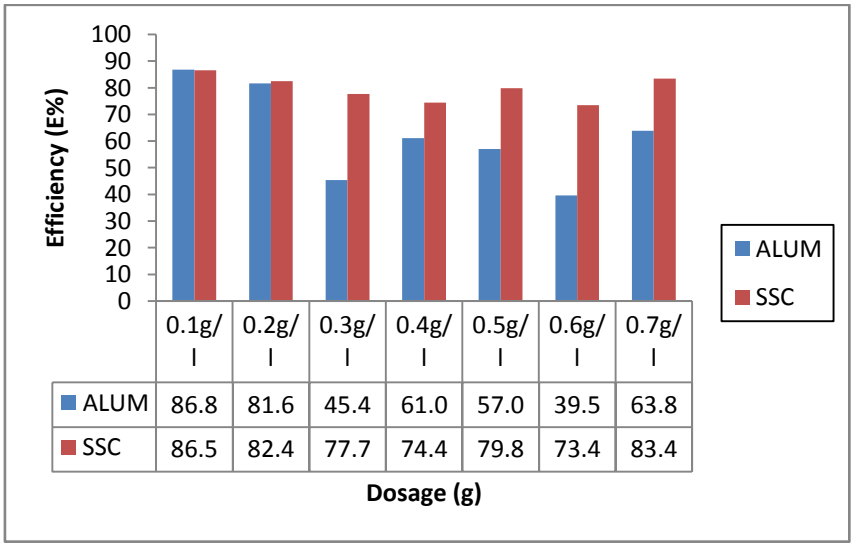

Fig.4.291: Comparative coag-flocculation performance at 40mins for varying ssc and alum dosages in PIE at pH of 10

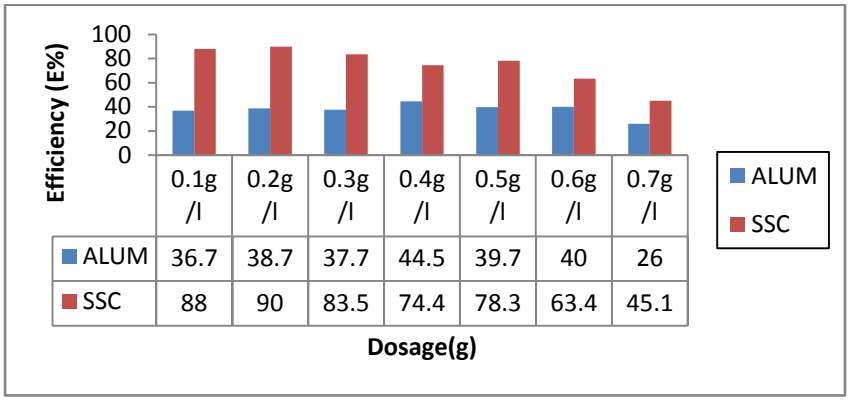

Fig.4.292: Comparative coag-flocculation performance at 40mins for varying ssc and alum dosages in PIE at pH of 13

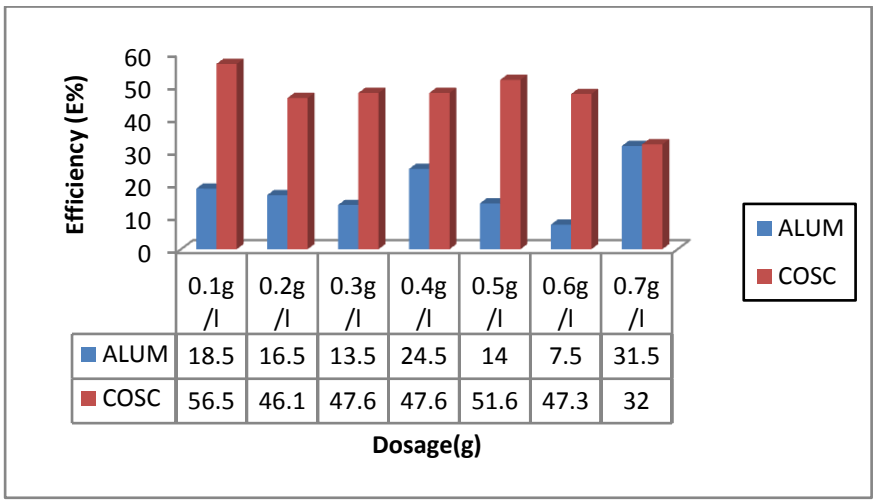

Fig.4.293: Comparative coag-flocculation performance at 40mins for varying cosc and alum dosages in PIE at pH of 1

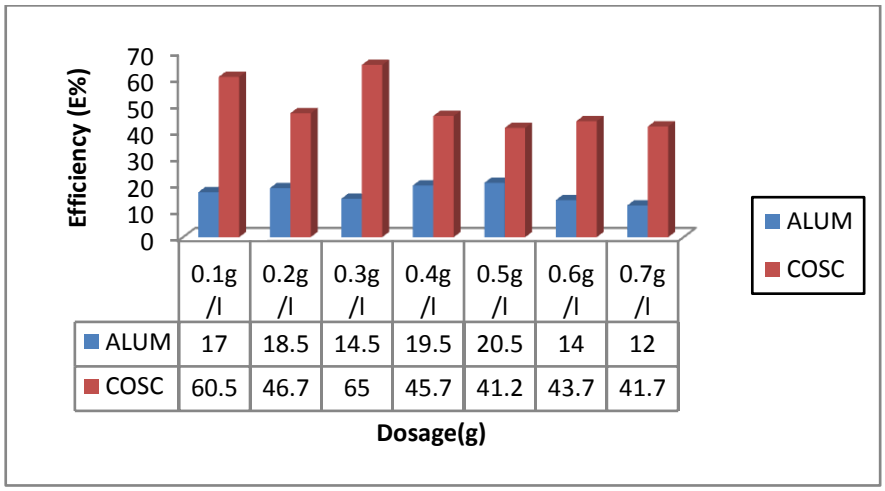

Fig.4.294: Comparative coag-flocculation performance at 40mins for varying cosc and alum dosages in PIE at pH of 3

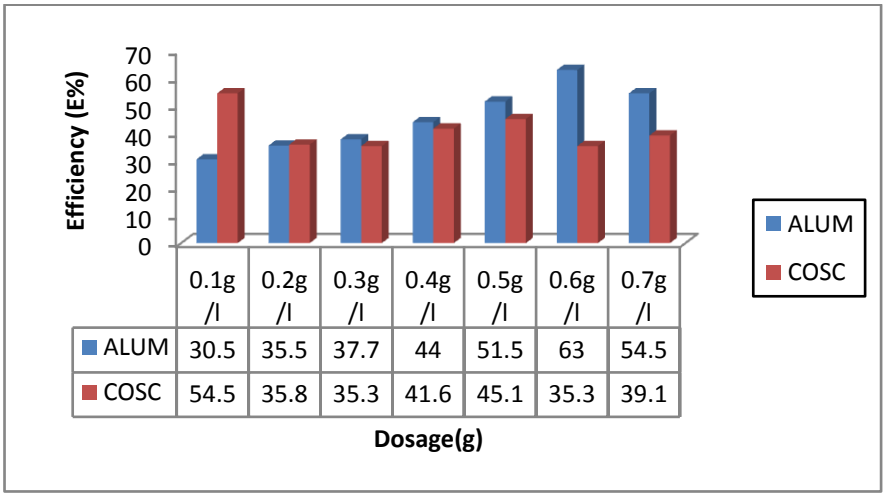

	0.1g /l	0.2g /l	0.3g /l	0.4g /l	0.5g /l	0.6g /l	0.7g /l
ALUM	30.5	35.5	37.7	44	51.5	63	54.5
COSC	54.5	35.8	35.3	41.6	45.1	35.3	39.1

Fig.4.295: Comparative coag-flocculation performance at 40mins for varying cosc and alum dosages in PIE at pH of 5

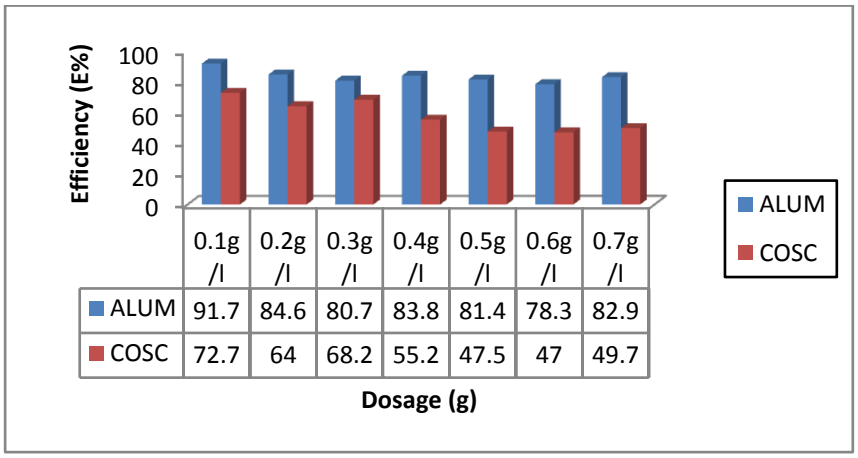

	0.1g /l	0.2g /l	0.3g /l	0.4g /l	0.5g /l	0.6g /l	0.7g /l
ALUM	91.7	84.6	80.7	83.8	81.4	78.3	82.9
COSC	72.7	64	68.2	55.2	47.5	47	49.7

Fig.4.296: Comparative coag-flocculation performance at 40mins for varying cosc and alum dosages in PIE at pH of 7

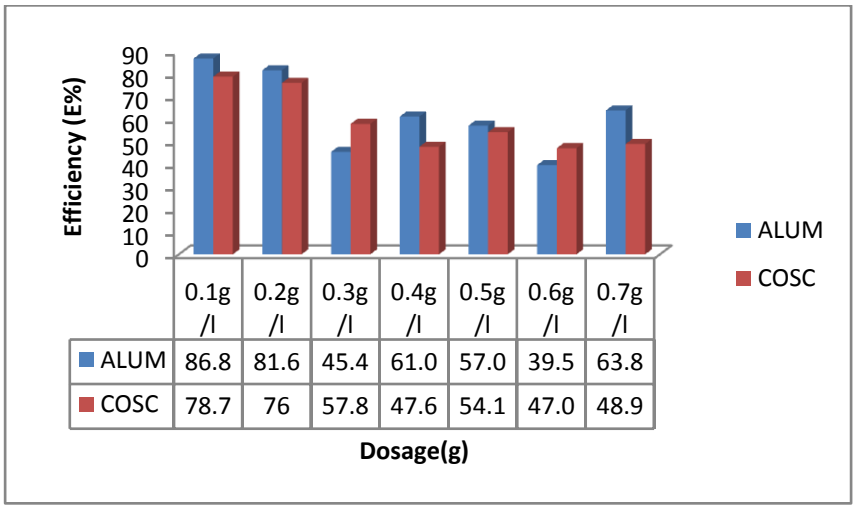

	0.1g /l	0.2g /l	0.3g /l	0.4g /l	0.5g /l	0.6g /l	0.7g /l
ALUM	86.8	81.6	45.4	61.0	57.0	39.5	63.8
COSC	78.7	76	57.8	47.6	54.1	47.0	48.9

Fig.4.297: Comparative coag-flocculation performance at 40mins for varying cosc and alum dosages in PIE at pH of 10

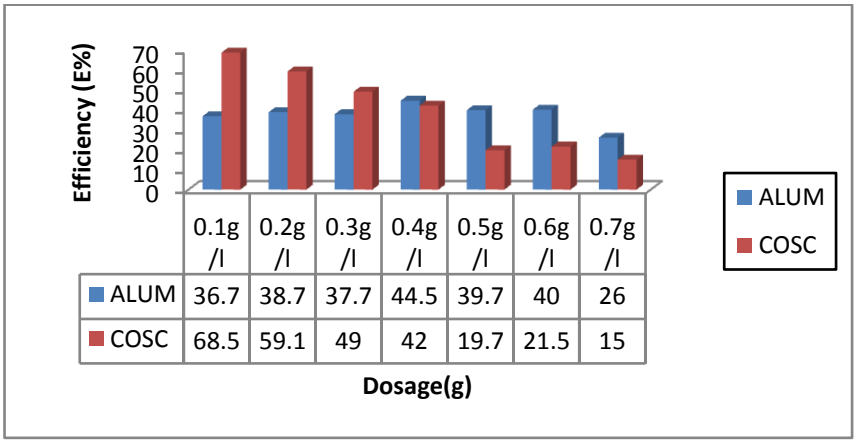

Fig.4.298: Comparative coag-flocculation performance at 40mins for varying cosc and alum dosages in PIE at pH of 13

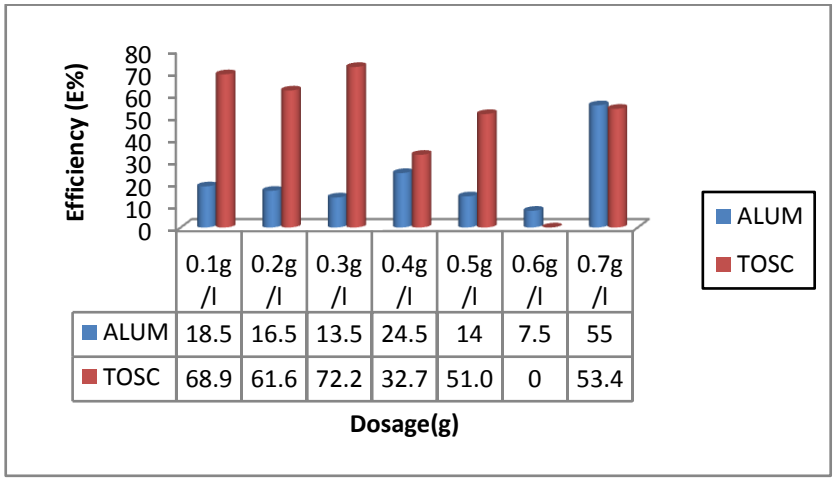

Fig.4.299: Comparative coag-flocculation performance at 40mins for varying tosc and alum dosages in PIE at pH of 1

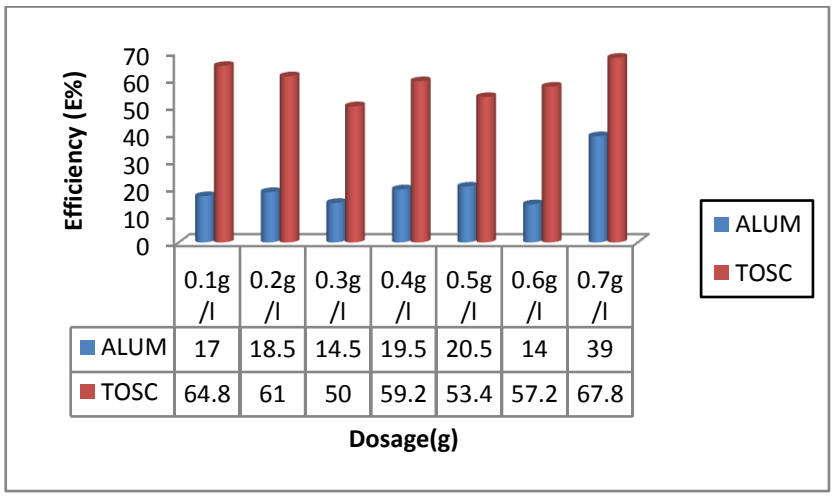

Fig.4.300: Comparative coag-flocculation performance at 40mins for varying tosc and alum dosages in PIE at pH of 3

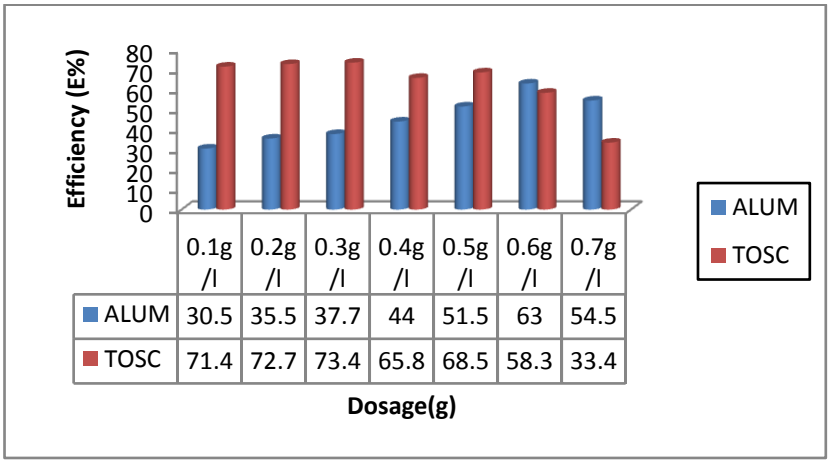

Fig.4.301: Comparative coag-flocculation performance at 40mins for varying tosc and alum dosages in PIE at pH of 5

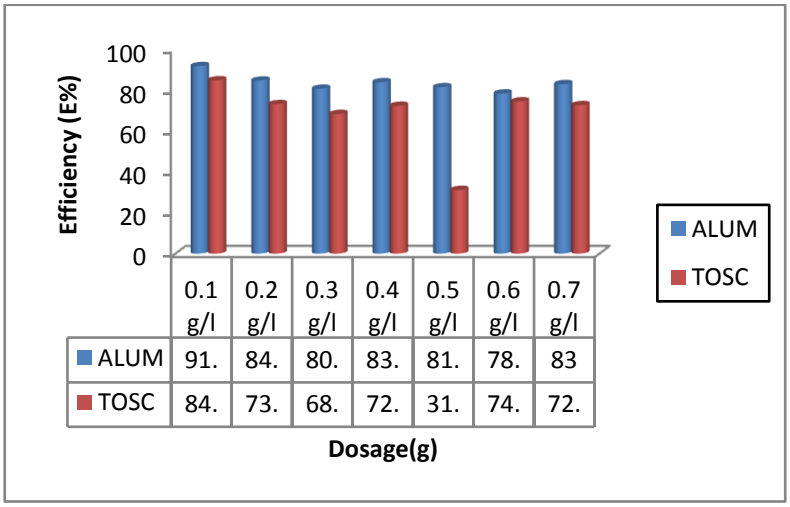

Fig.4.302: Comparative coag-flocculation performance at 40mins for varying tosc and alum dosages in PIE at pH of 7

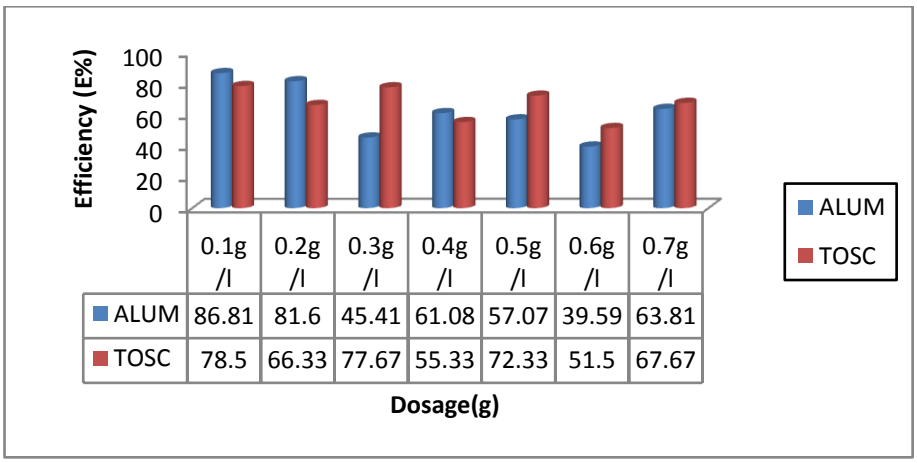

Fig.4.303: Comparative coag-flocculation performance at 40mins for varying tosc and alum dosages in PIE at pH of 10

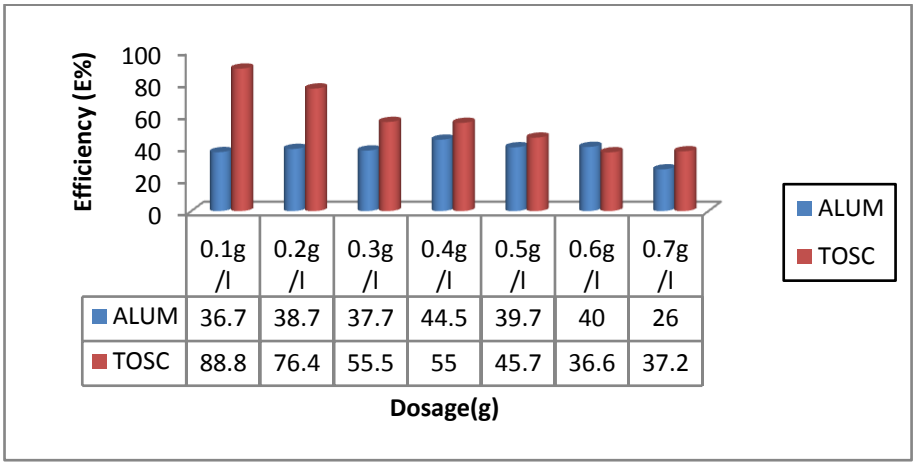

Fig.4.304: Comparative coag-flocculation performance at 40mins for varying tosc and alum dosages in PIE at pH of 13

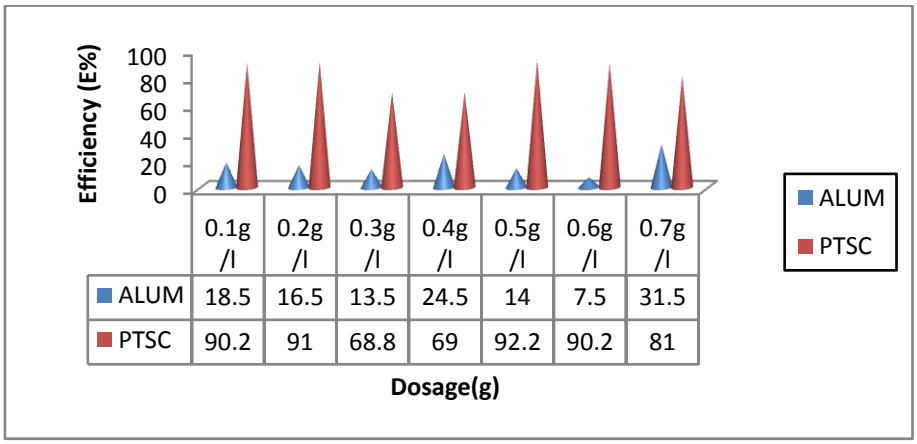

Fig.4.305: Comparative coag-flocculation performance at 40mins for varying ptsc and alum dosages in PIE at pH of 1

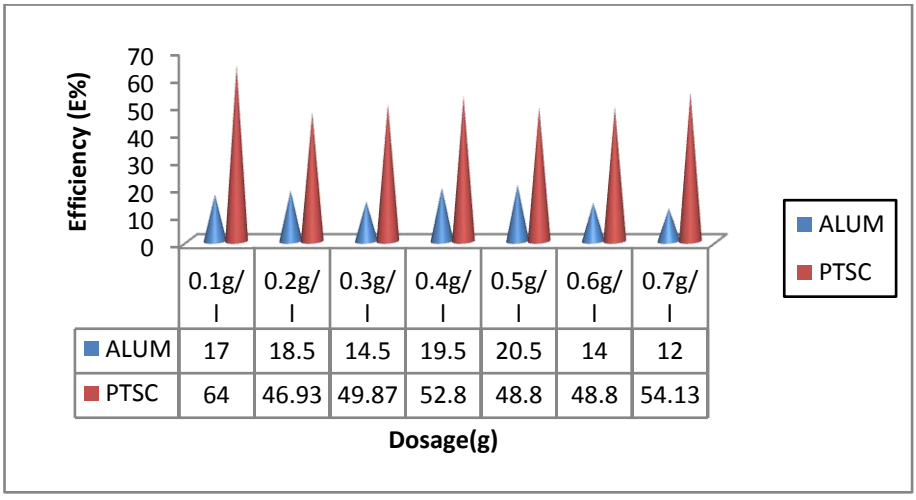

Fig.4.306: Comparative coag-flocculation performance at 40mins for varying ptsc and alum dosages in PIE at pH of 3

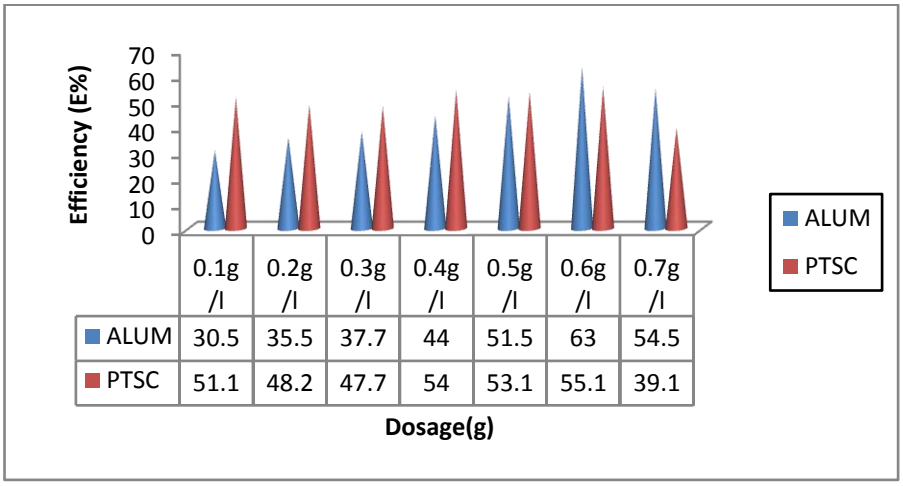

Fig.4.307: Comparative coag-flocculation performance at 40mins for varying ptsc and alum dosages in PIE at pH of 5

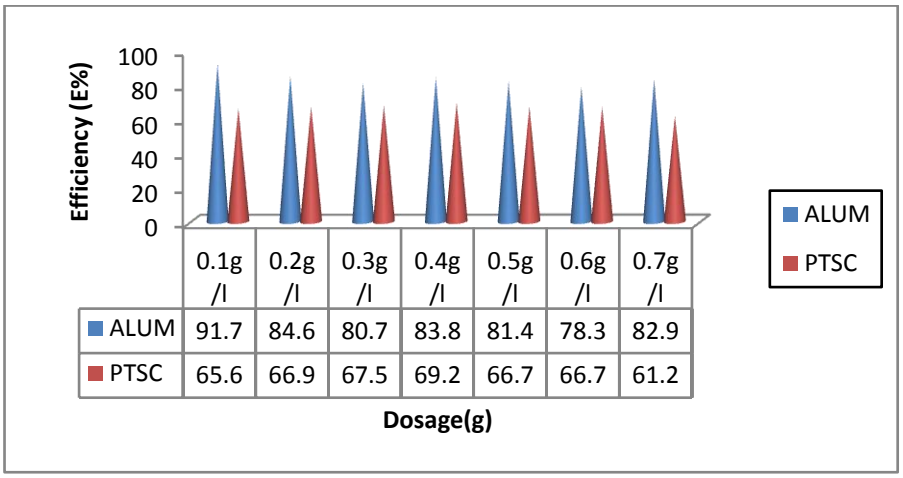

Fig.4.308: Comparative coag-flocculation performance at 40mins for varying ptsc and alum dosages in PIE at pH of 7

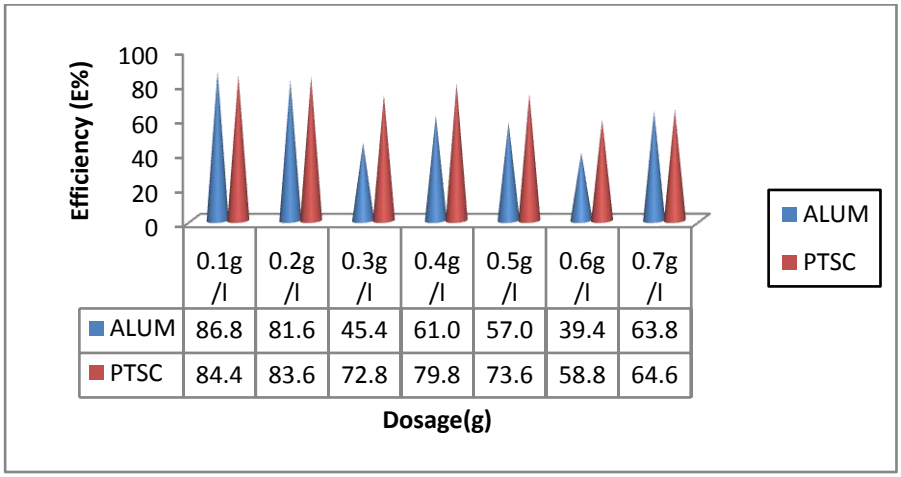

Fig.4.309: Comparative coag-flocculation performance at 40mins for varying ptsc and alum dosages in PIE at pH of 10

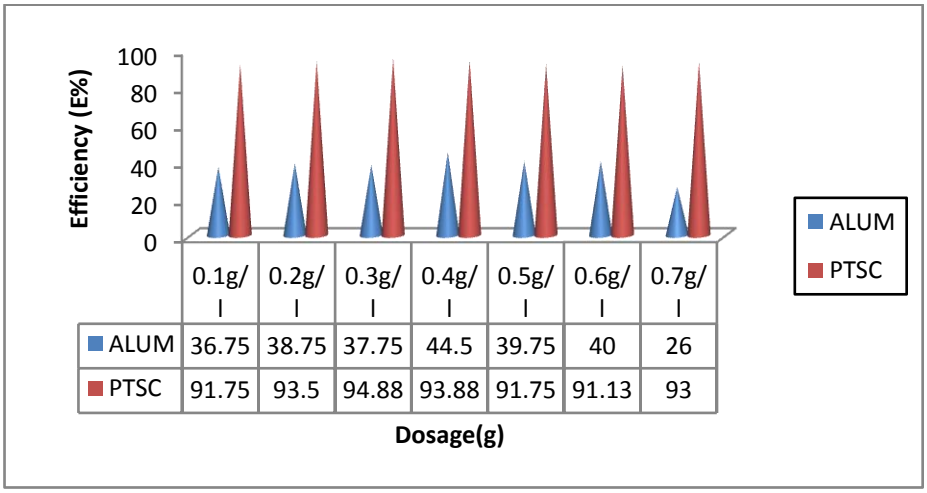

Fig.4.310: Comparative coag-flocculation performance at 40mins for varying ptsc and alum dosages in PIE at pH of 13

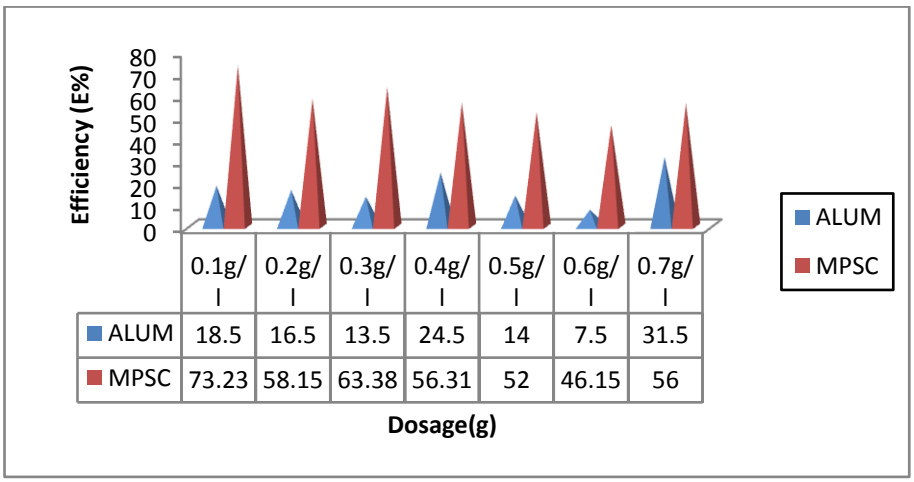

Fig.4.311: Comparative coag-flocculation performance at 40mins for varying mpsc and alum dosages in PIE at pH of 1

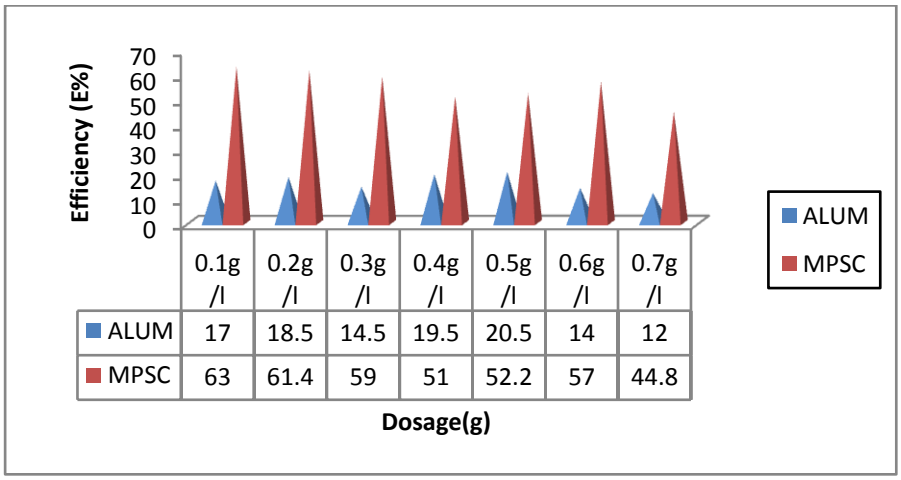

Fig.4.312: Comparative coag-flocculation performance at 40mins for varying mpsc and alum dosages in PIE at pH of 3

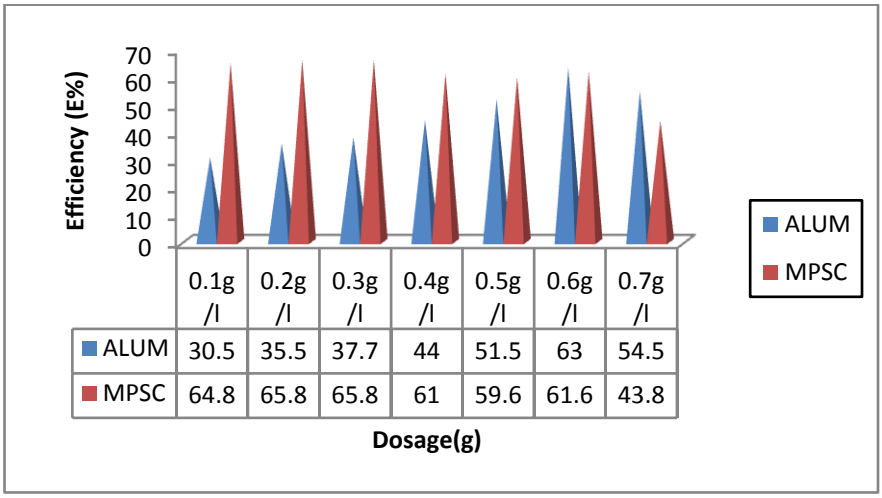

Fig.4.313: Comparative coag-flocculation performance at 40mins for varying mpsc and alum dosages in PIE at pH of 5

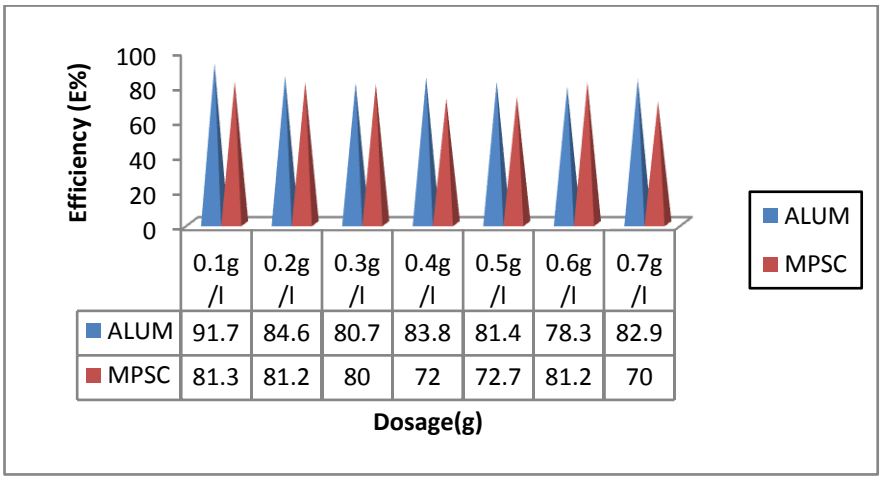

Fig.4.314: Comparative coag-flocculation performance at 40mins for varying mpsc and alum dosages in PIE at pH of 7

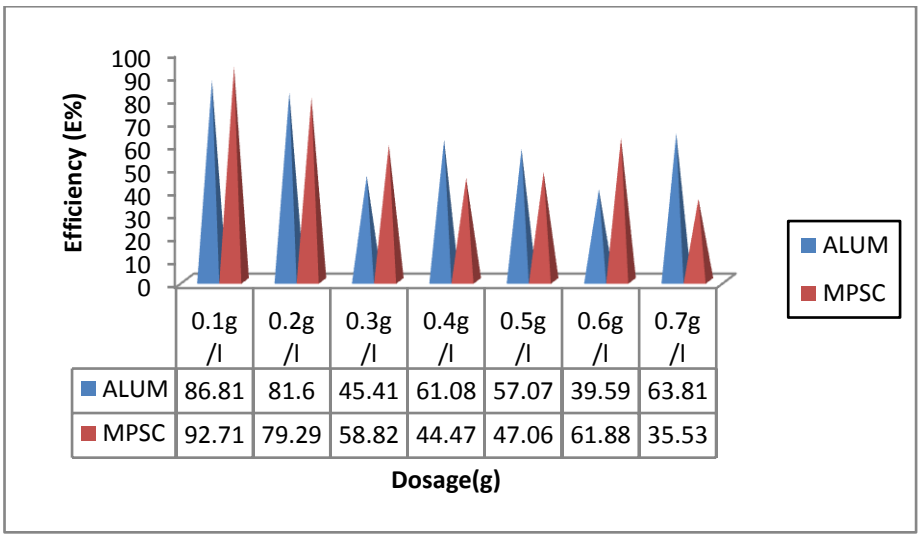

Fig.4.315: Comparative coag-flocculation performance at 40mins for varying mpsc and alum dosages in PIE at pH of 10

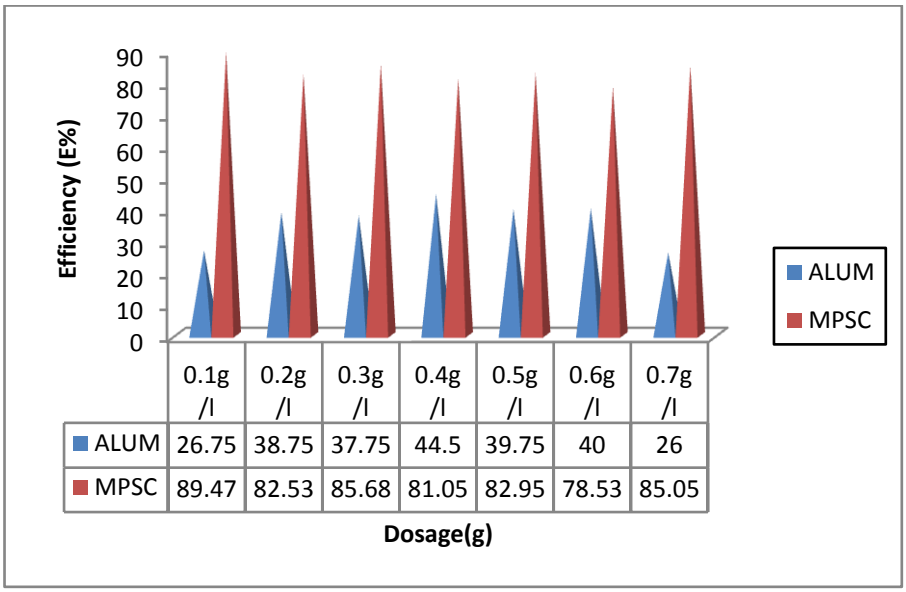

	0.1g /l	0.2g /l	0.3g /l	0.4g /l	0.5g /l	0.6g /l	0.7g /l
ALUM	26.75	38.75	37.75	44.5	39.75	40	26
MPSC	89.47	82.53	85.68	81.05	82.95	78.53	85.05

Fig.4.316: Comparative coag-flocculation performance at 40mins for varying mpsc and alum dosages in PIE at pH of 13

4.1.6.2 Comparative coag-flocculation removal efficiency for pH varying PIE medium at constant dosage

The results are presented in figures 4.317 to 4.351 for SSC, COSC, TOSC, PTSC and MPSC in pH varying PIE. In figures 4.317 to 4.351, the dosage of coag-flocculant is constant in each case.

For SSC comparison with alum, the results is displayed in figures 4.317 to 4.323. It is observed that alum performed better than SSC more at pH 7 for 0.1g/l, 0.4g/l, 0.5 g/l and 0.6g/l in figures 4.315, 4.318, 4.319, and figure 4.320 respectively. This is supported by the maximum percentage efficiency recorded by alum for the respective dosages at pH 7. Though the performance achieved by SSC at that condition is very much comparable. However, SSC outperformed alum at pH 1, 3, 5, 10 and 13 for 0.2 to 0.7g/l dosages as illustrated in figures 4.317 to 4.321.

The results of COSC and alum presented in figures 4.322 to 4.328, show that alum performed better than COSC at pH of 7 – 10 for 0.1, 0.2, 0.4, 0.5 and 0.7g/l dosages.This phenomenon amplified the fact that alum performed best under alkaline conditions. TOSC and alum presented in figures 4.329 to 4.335, indicate that alum is better than TOSC at the pH 7 for all the dosages. General performance outlook show that TOSC was better at wide pH range and dosages.

Considering figures. 4.336 to 4.342, presented for PTSC and alum. It can be observed that PTSC performed satisfactorily at the pH of 1, 10 and 13. The only exception is the result obtained for 0.6g/l and pH of 10. This is supported by the highest removal efficiency value recorded at pH of 13 and 0.3g/l dosage. The comparative results for MPSC presented in figures. 4.343 to 4.349, show that MPSC performed better than alum for all the dosages and pH of 1, 3, 5, and 13. The only exception are 0.1g/l and pH of 7., 0.2g/l and pH of 7, 10; 0.4g/l and pH of 7, 10; 0.5g/l and pH of 7, 10 and 0.7g/l and pH of 7, 10. The implication is that alum operates better in alkaline conditions.

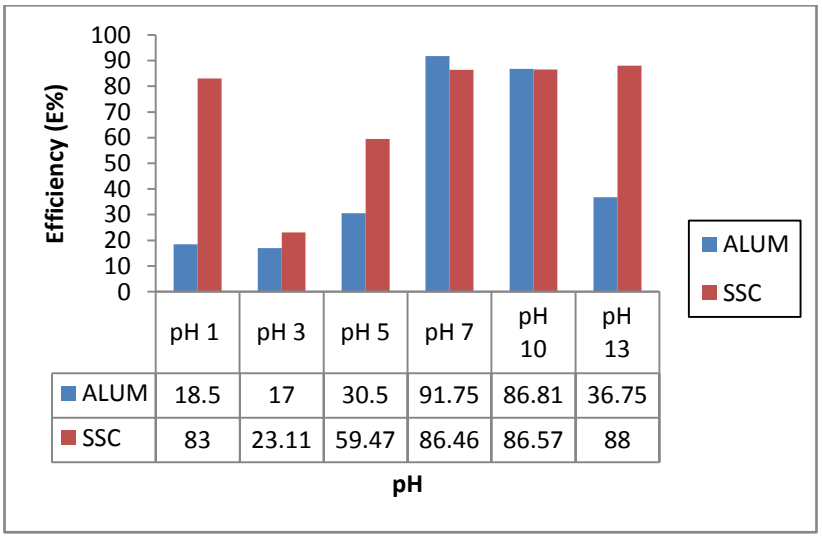

Fig.4.317: Comparative coag-flocculation performance at 40mins for 0.1g/l ssc and alum dosages in pH varying PIE

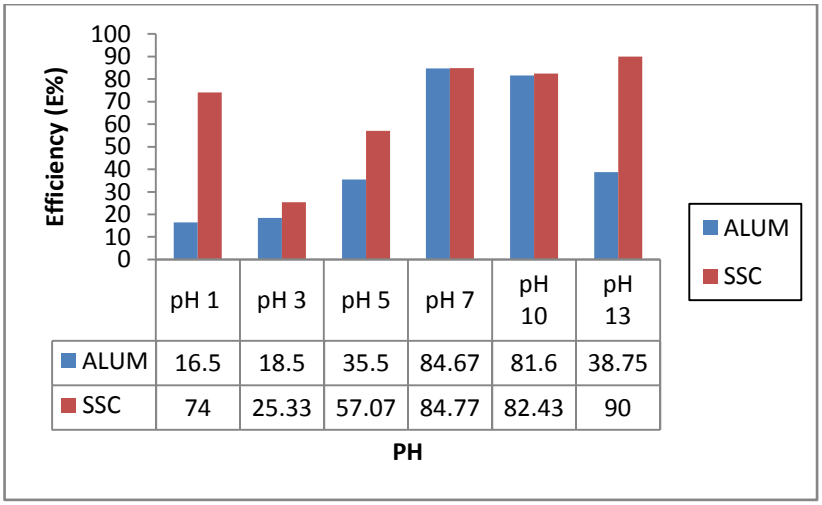

Fig.4.318: Comparative coag-flocculation performance at 40mins for 0.2g/l ssc and alum dosages in pH varying PIE

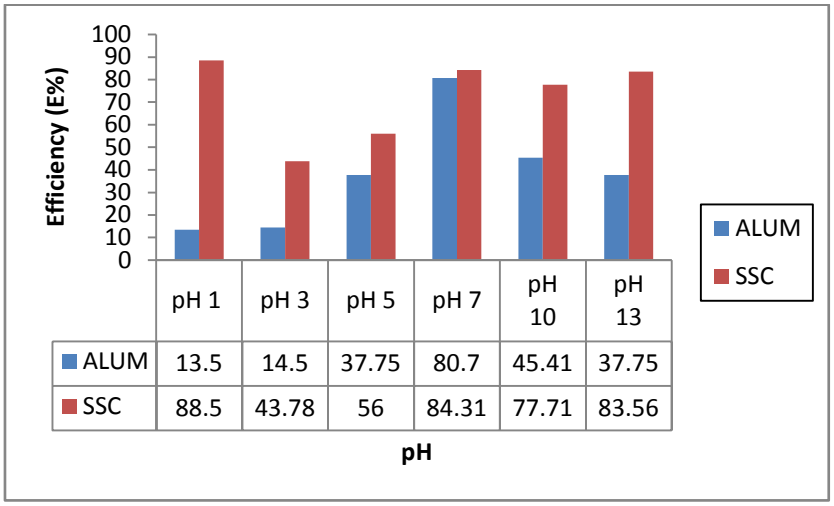

Fig.4.319: Comparative coag-flocculation performance at 40mins for 0.3g/l ssc and alum dosages in pH varying PIE

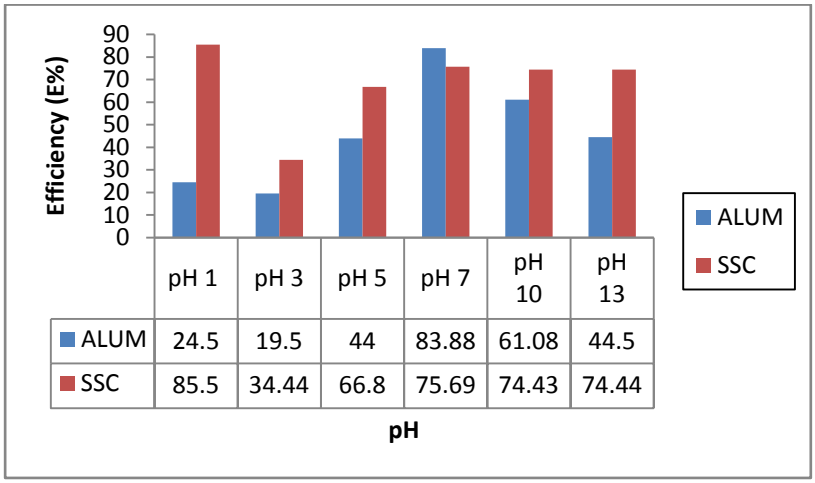

Fig.4.320: Comparative coag-flocculation performance at 40mins for 0.4g/l ssc and alum dosages in pH varying PIE

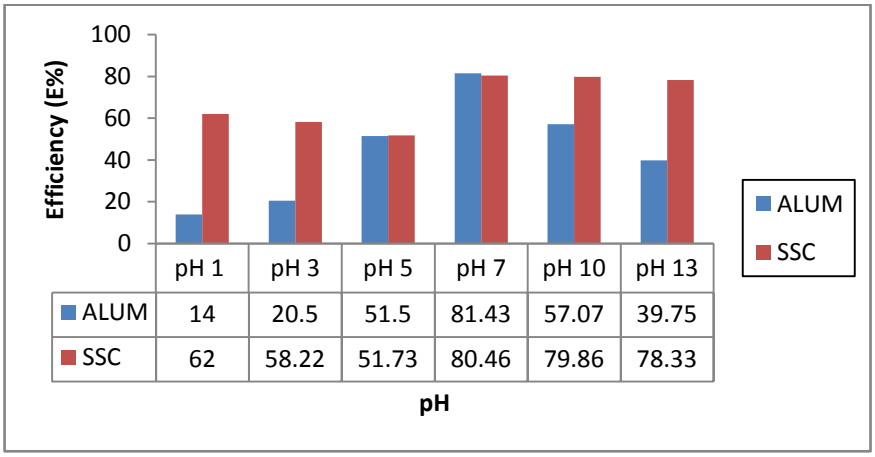

Fig.4.321: Comparative coag-flocculation performance at 40mins for 0.5g/l ssc and alum dosages in pH varying PIE

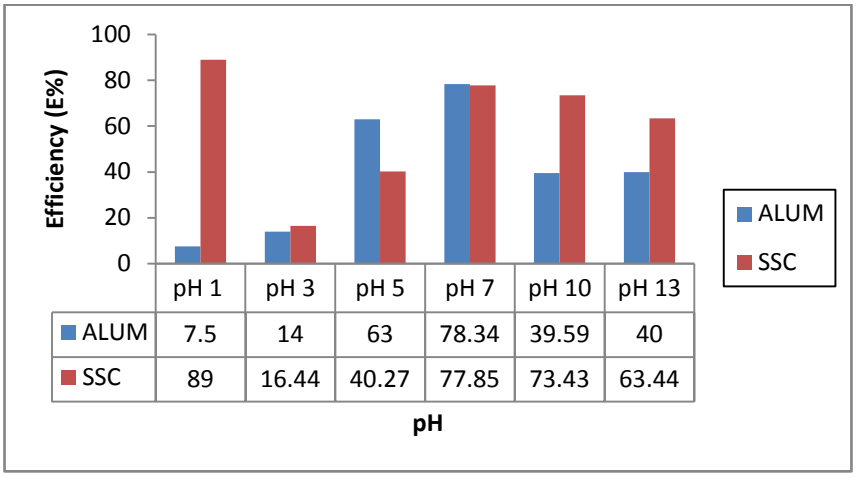

Fig.4.322: Comparative coag-flocculation performance at 40mins for 0.6g/l ssc and alum dosages in pH varying PIE

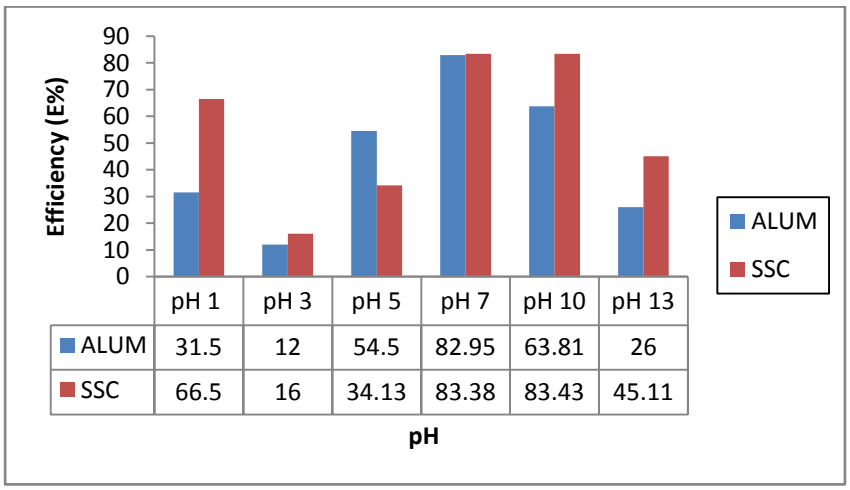

Fig.4.323: Comparative coag-flocculation performance at 40mins for 0.7g/l ssc and alum dosages in pH varying PIE

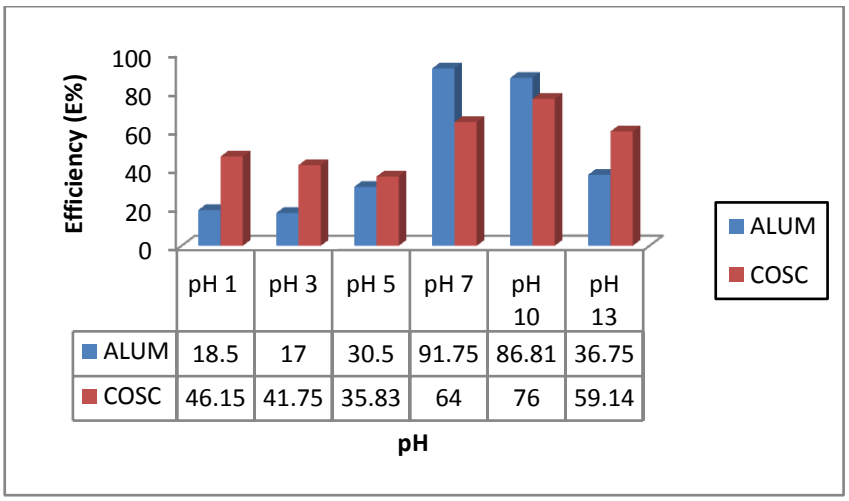

Fig.4.324: Comparative coag-flocculation performance at 40mins for 0.1g/l cosc and alum dosages in pH varying PIE

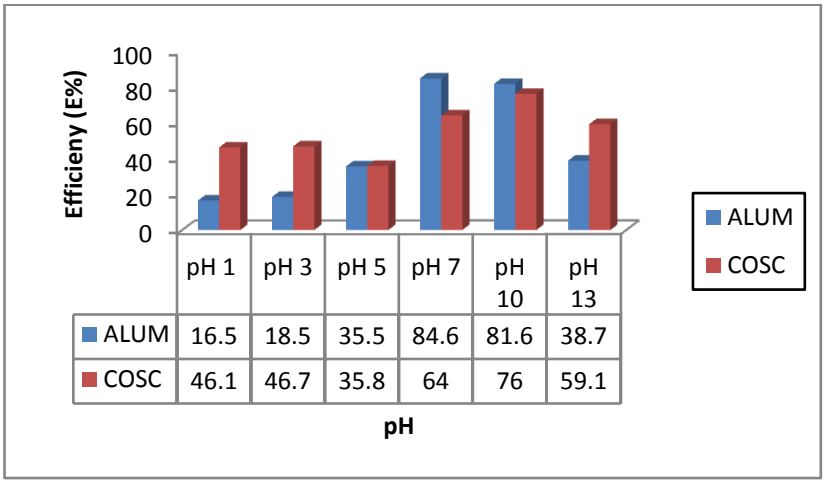

Fig.4.325: Comparative coag-flocculation performance at 40mins for 0.2g/l cosc and alum dosages in pH varying PIE

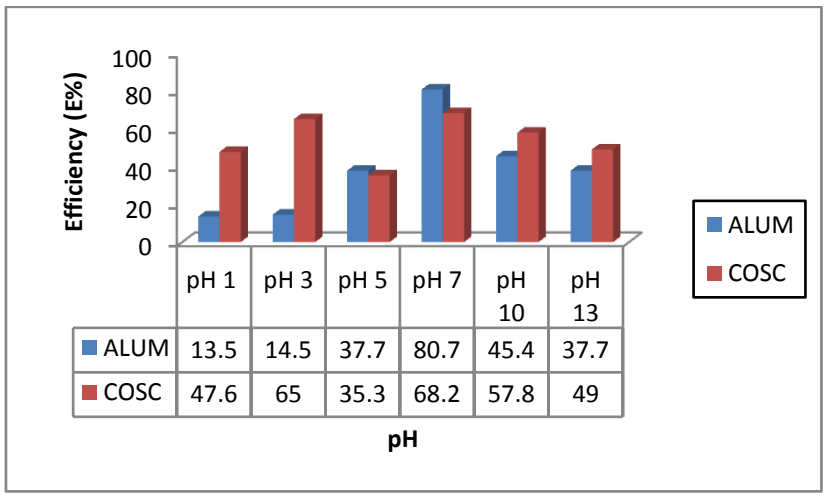

Fig.4.326: Comparative coag-flocculation performance at 40mins for 0.3g/l cosc and alum dosages in pH varying PIE

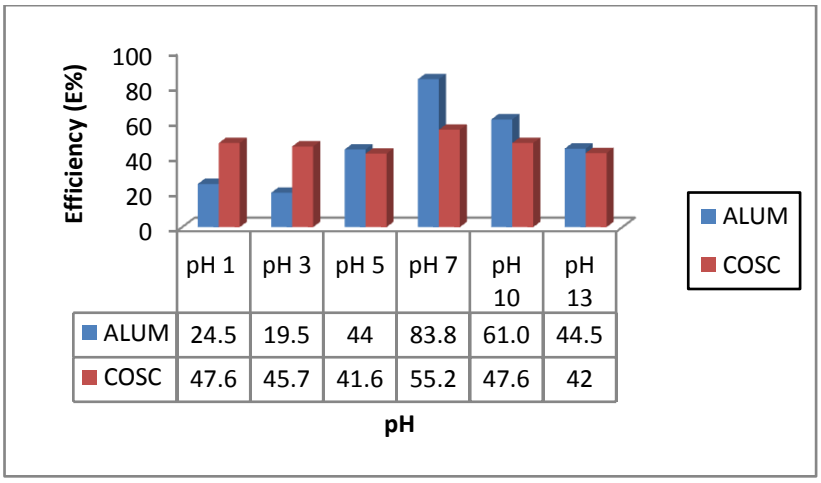

Fig.4.327: Comparative coag-flocculation performance at 40mins for 0.4g/l cosc and alum dosages in pH varying PIE

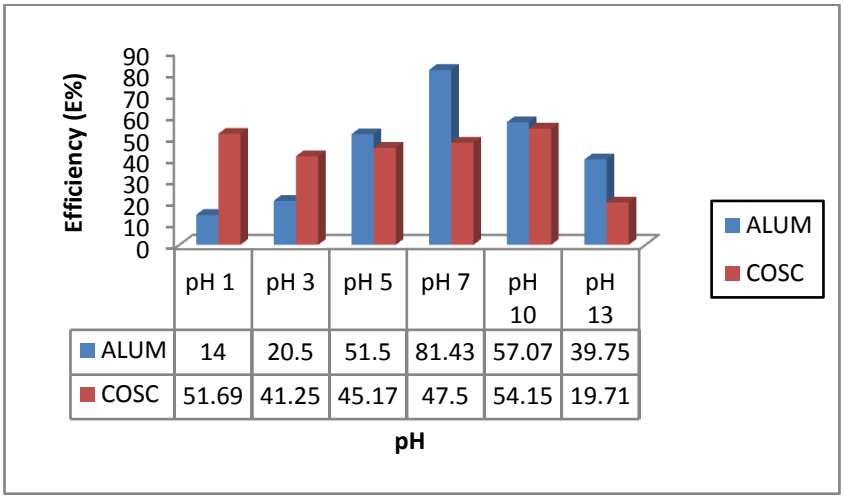

Fig.4.328: Comparative coag-flocculation performance at 40mins for 0.5g/l cosc and alum dosages in pH varying PIE

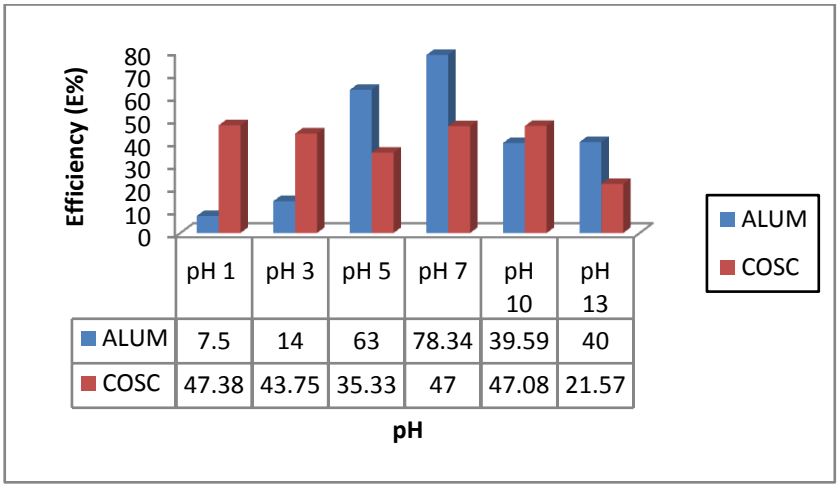

Fig.4.329: Comparative coag-flocculation performance at 40mins for 0.6g/l cosc and alum dosages in pH varying PIE

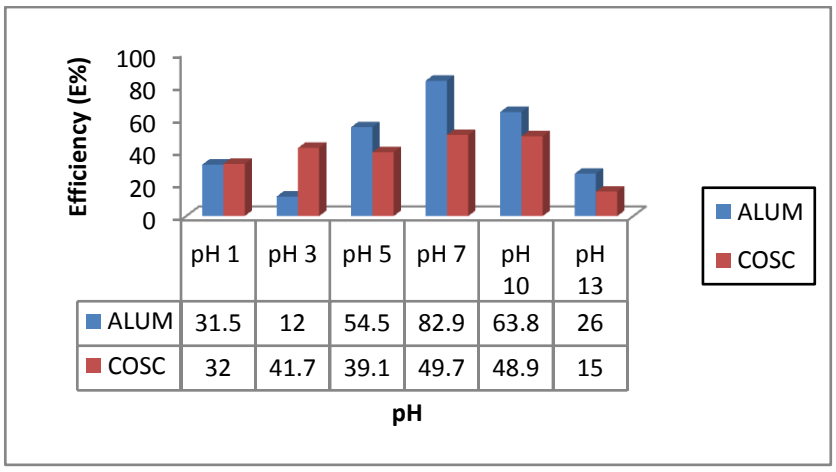

Fig.4.330: Comparative coag-flocculation performance at 40mins for 0.7g/l cosc and alum dosages in pH varying PIE

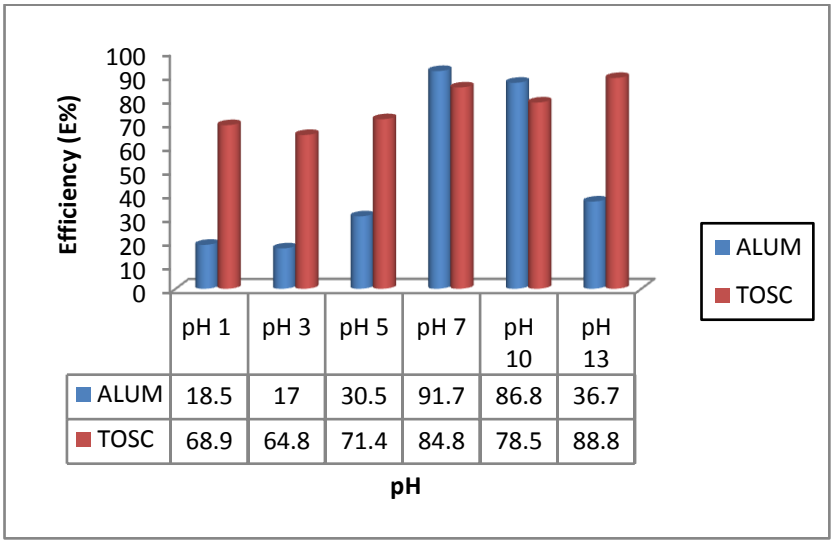

Fig.4.331: Comparative coag-flocculation performance at 40mins for 0.1g/l tosc and alum dosages in pH varying PIE

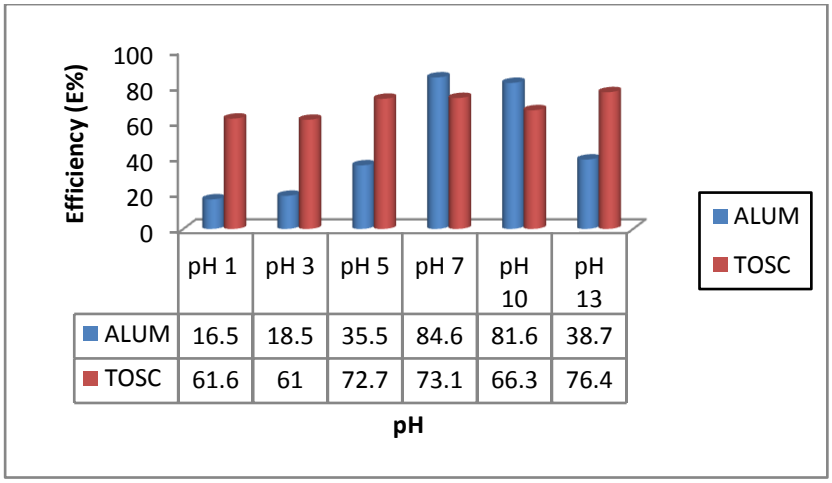

Fig.4.332: Comparative coag-flocculation performance at 40mins for 0.2g/l tosc and alum dosages in pH varying PIE

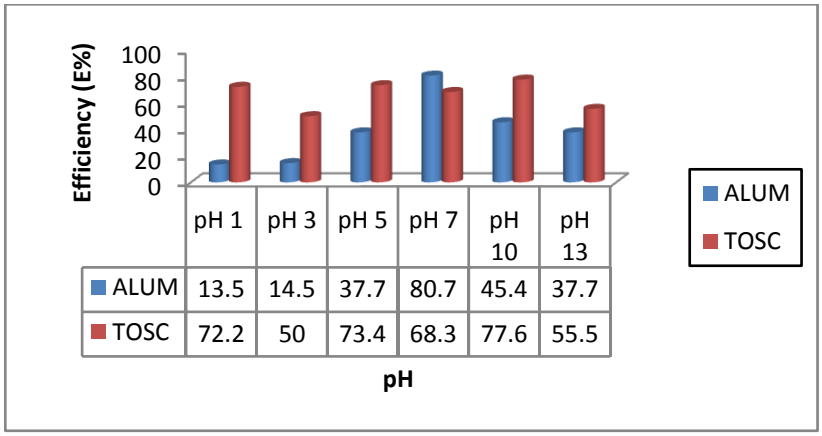

Fig.4.333: Comparative coag-flocculation performance at 40mins for 0.3g/l tosc and alum dosages in pH varying PIE

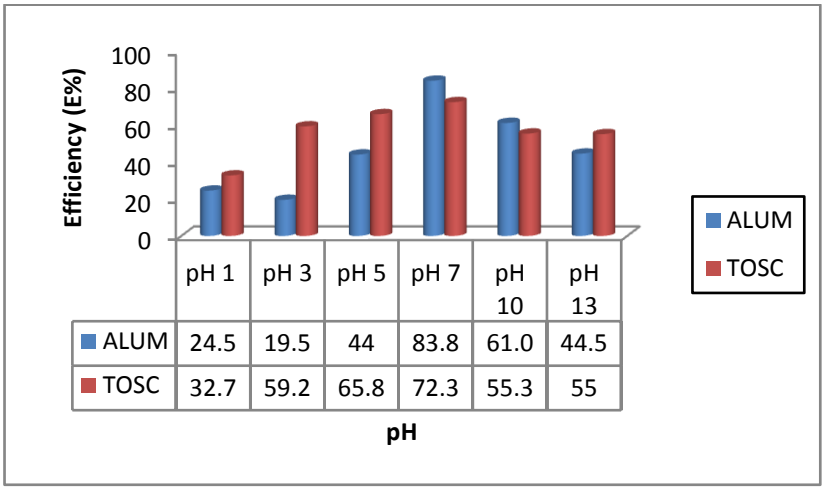

Fig.4.334: Comparative coag-flocculation performance at 40mins for 0.4g/l tosc and alum dosages in pH varying PIE

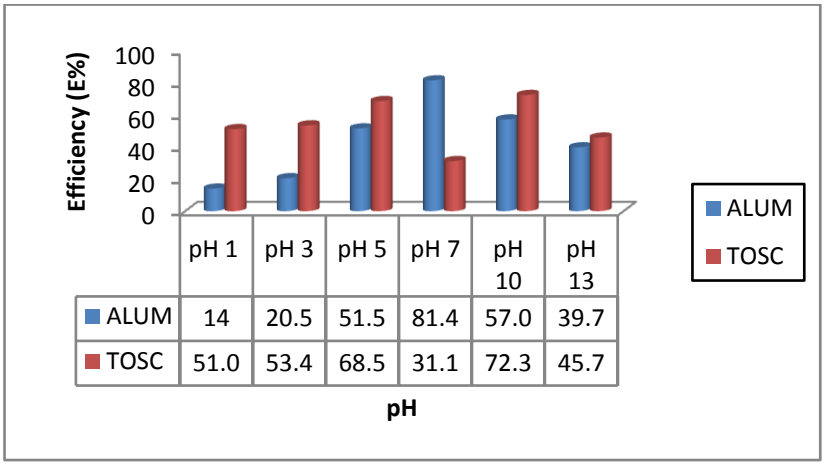

Fig.4.335: Comparative coag-flocculation performance at 40mins for 0.5g/l tosc and alum dosages in pH varying PIE

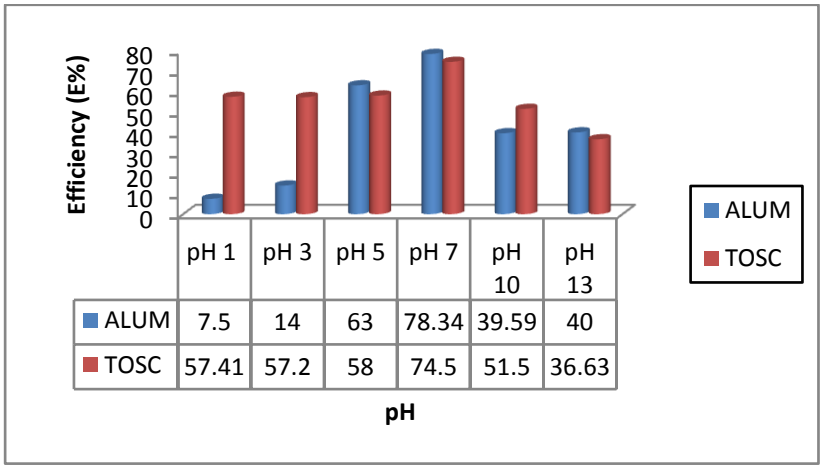

Fig.4.336: Comparative coag-flocculation performance at 40mins for 0.6 g/l tosc and alum dosages in pH varying PIE

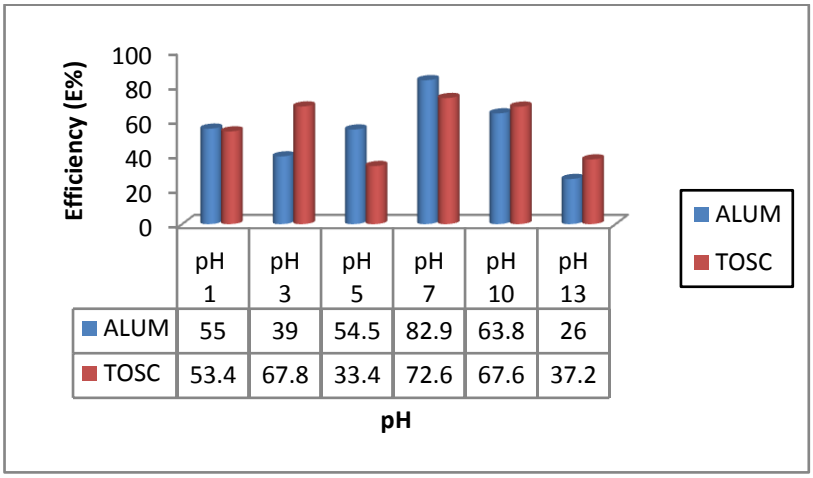

	pH 1	pH 3	pH 5	pH 7	pH 10	pH 13
ALUM	55	39	54.5	82.9	63.8	26
TOSC	53.4	67.8	33.4	72.6	67.6	37.2

Fig.4.337: Comparative coag-flocculation performance at 40mins for 0.7 g/l tosc and alum dosages in pH varying PIE

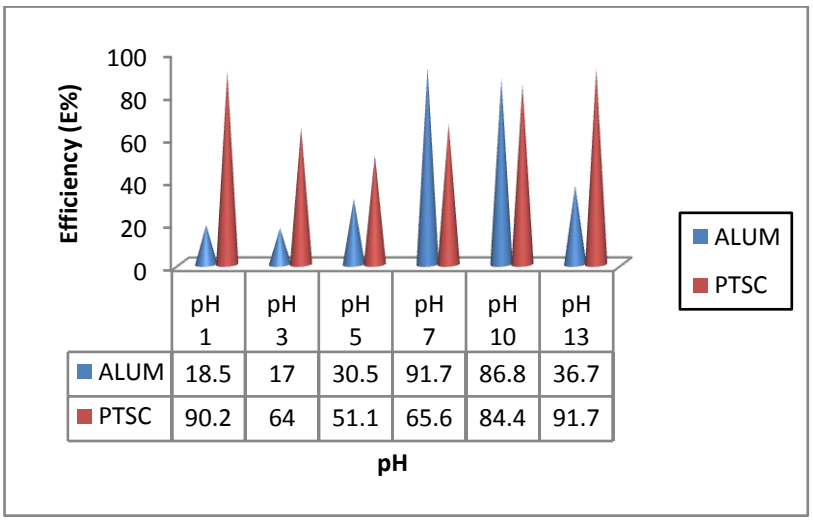

	pH 1	pH 3	pH 5	pH 7	pH 10	pH 13
ALUM	18.5	17	30.5	91.7	86.8	36.7
PTSC	90.2	64	51.1	65.6	84.4	91.7

Fig.4.338: Comparative coag-flocculation performance at 40mins for 0.1g/l ptsc and alum dosages in pH varying PIE

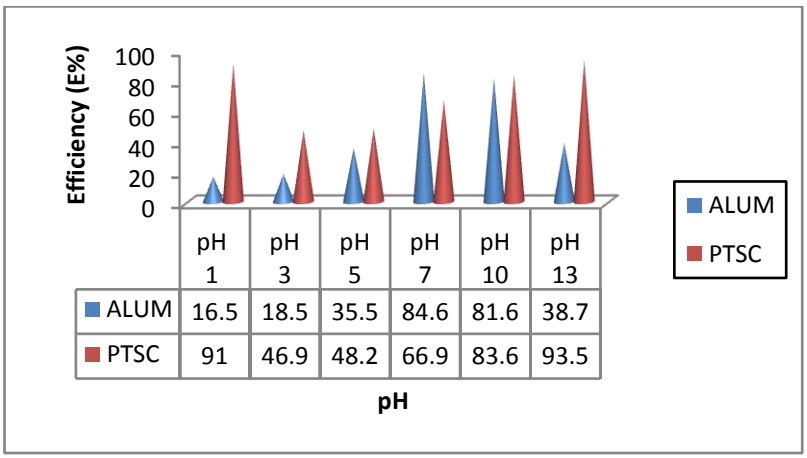

	pH 1	pH 3	pH 5	pH 7	pH 10	pH 13
ALUM	16.5	18.5	35.5	84.6	81.6	38.7
PTSC	91	46.9	48.2	66.9	83.6	93.5

Fig.4.339: Comparative coag-flocculation performance at 40mins for 0.2g/l ptsc and alum dosages in pH varying PIE

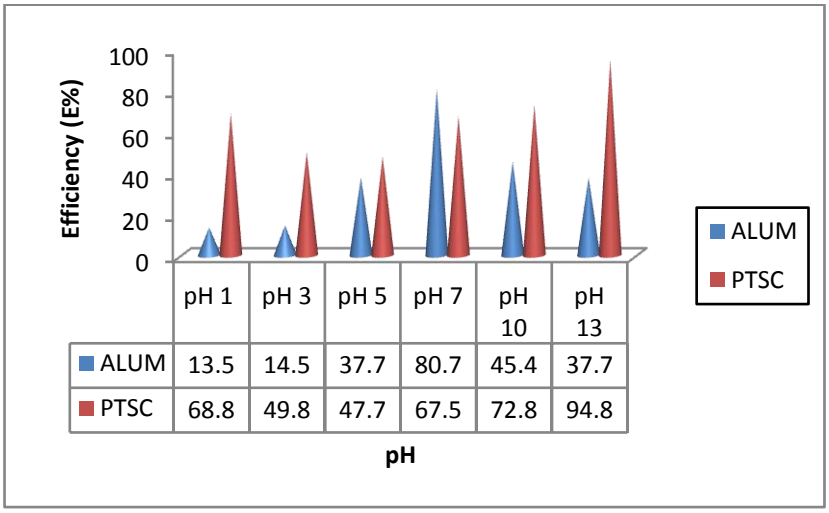

Fig.4.340: Comparative coag-flocculation performance at 40mins for 0.3 g/l ptsc and alum dosages in pH varying PIE

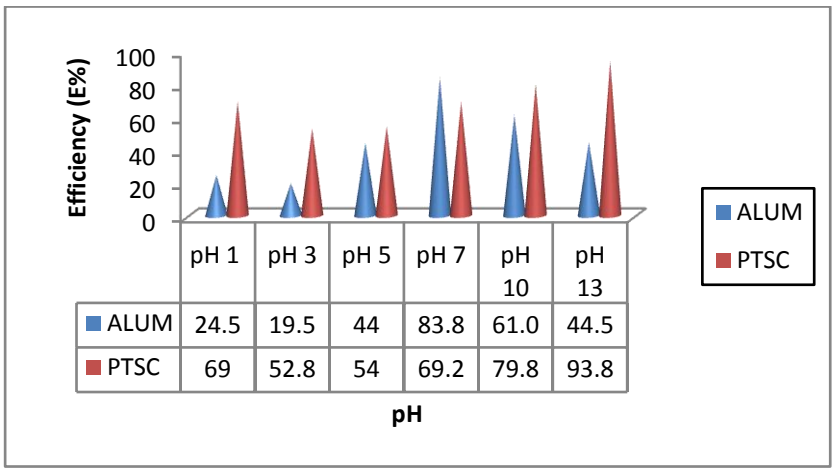

Fig.4.341: Comparative coag-flocculation performance at 40mins for 0.4 g/l ptsc and alum dosages in pH varying PIE

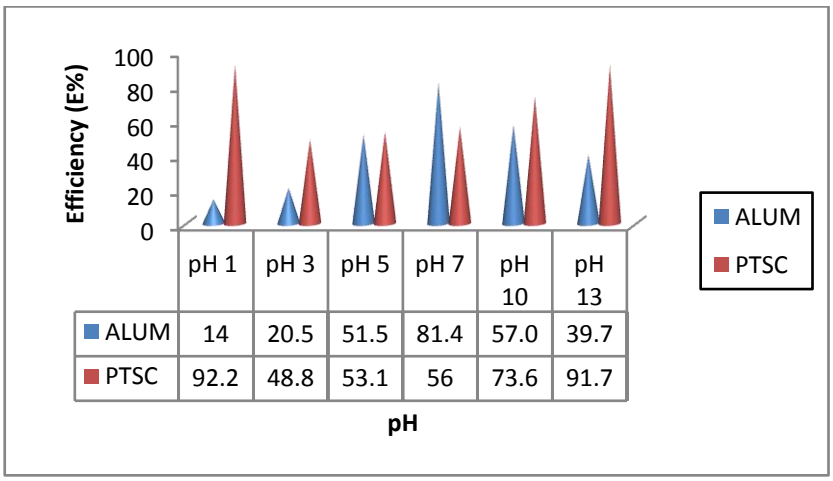

Fig.4.342: Comparative coag-flocculation performance at 40mins for 0.5g/l ptsc and alum dosages in pH varying PIE

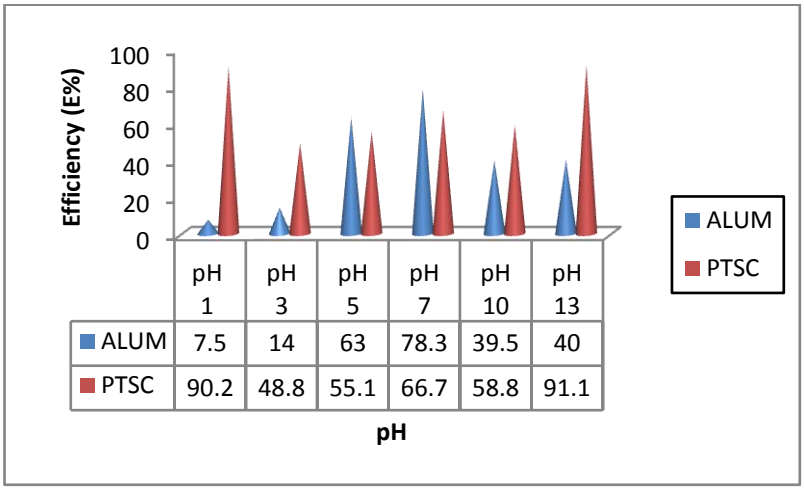

Fig.4.343: Comparative coag-flocculation performance at 40mins for 0.6g/l ptsc and alum dosages in pH varying PIE

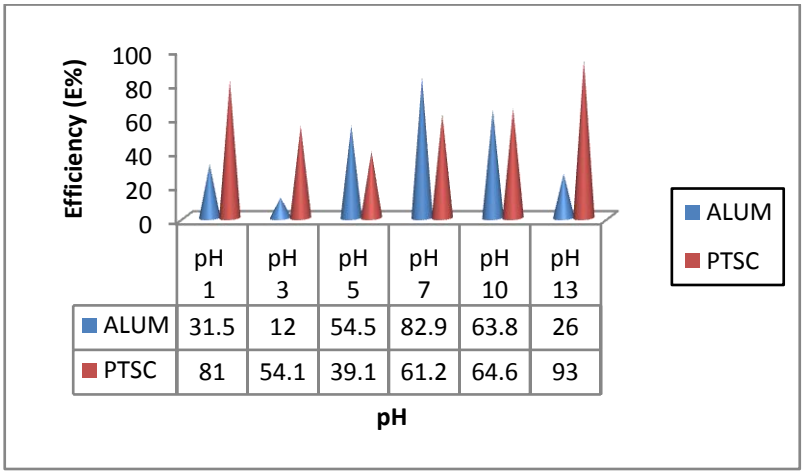

Fig.4.344: Comparative coag-flocculation performance at 40mins for 0.7g/l ptsc and alum dosages in pH varying PIE

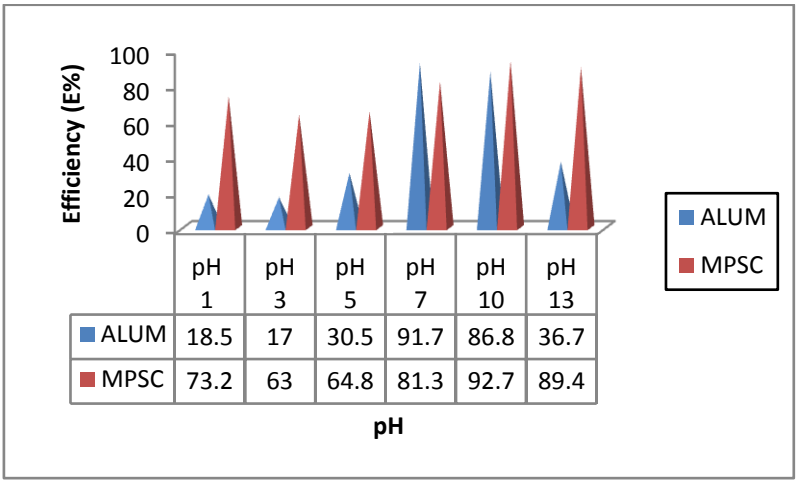

Fig.4.345: Comparative coag-flocculation performance at 40mins for 0.1g/l mpsc and alum dosages in pH varying PIE

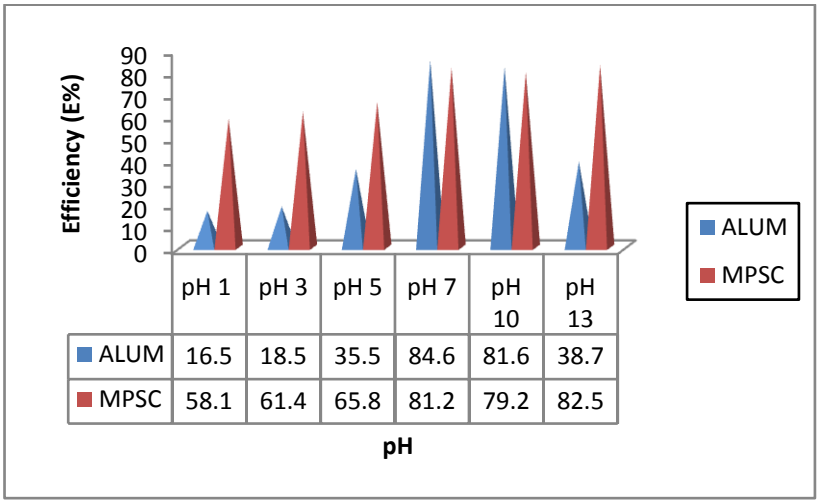

Fig.4.346: Comparative coag-flocculation performance at 40mins for 0.2g/l mpsc and alum dosages in pH varying PIE

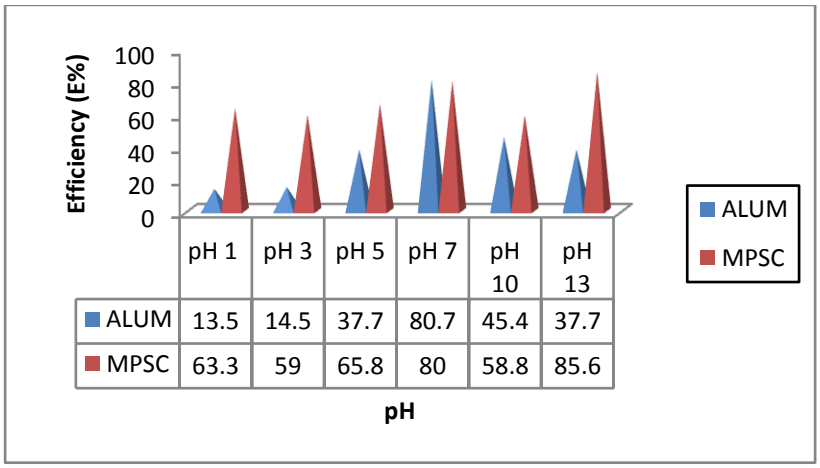

Fig.4.347: Comparative coag-flocculation performance at 40mins for 0.3g/l mpsc and alum dosages in pH varying PIE

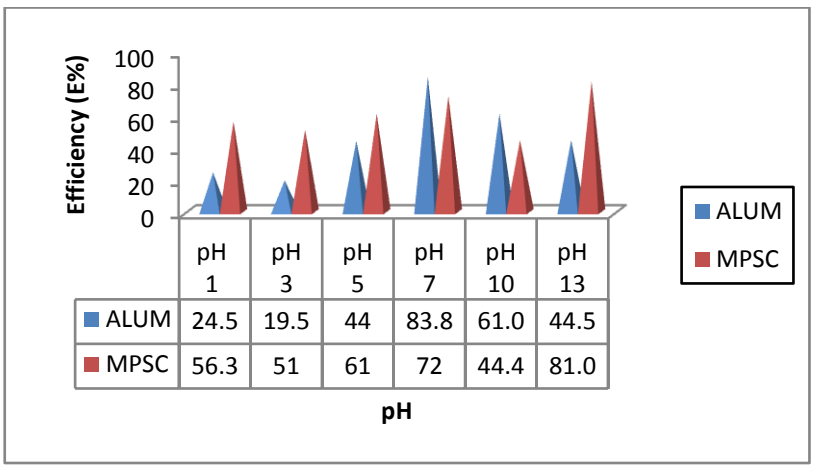

Fig.4.348: Comparative coag-flocculation performance at 40mins for 0.4g/l mpsc and alum dosages in pH varying PIE

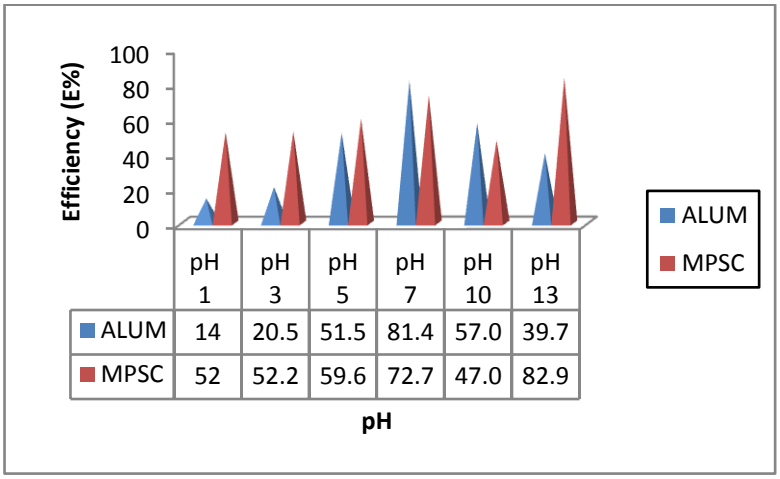

Fig.4.349: Comparative coag-flocculation performance at 40mins for 0.5g/l mpsc and alum dosages in pH varying PIE

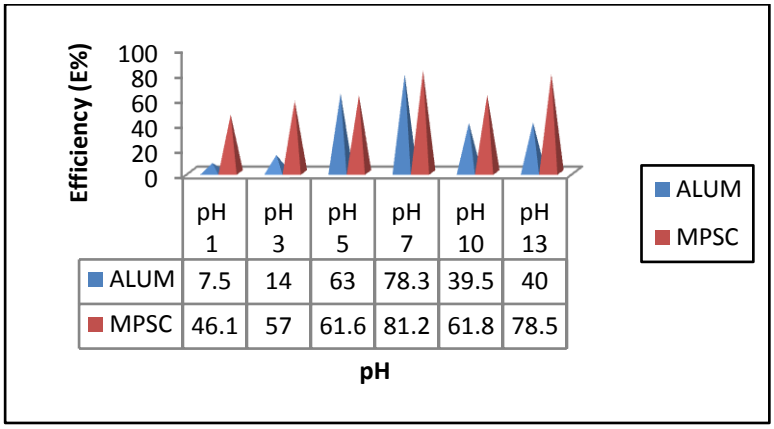

Fig.4.350: Comparative coag-flocculation performance at 40mins for 0.6g/l mpsc and alum dosages in pH varying PIE

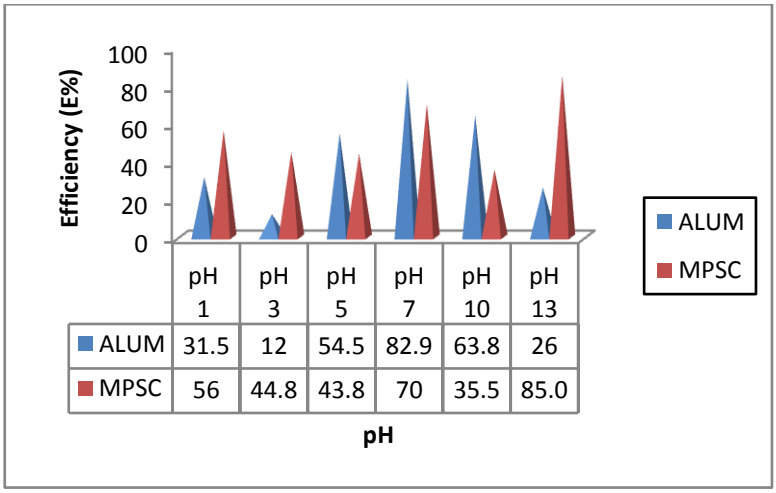

Fig.4.351: Comparative coag-flocculation performance at 40mins for 0.7g/l mpsc and alum dosages in pH varying PIE

4.1.6.3 Comparative removal efficiency for varying dosage and constant pH of VIE medium

The associated results are presented in figures. 4.352 to 4.381. They show the comparative removal efficiency between alum and different organic coag-flocculants. Alum performance is compared with each SSC, COSC, TOSC, PTSC and MPSC. Here, the dosages of different coag-flocculants are varying while pH of VIE medium is constant.

Displayed in figures. 4.352 to 4.357 are graphical demonstration of comparative removal efficiency between alum and SSC. Critical observation show that SSC performed better than alum only in figures. 4.352 and 4.353, while alum showed its effectiveness in figures. 4.352, 4.353, 4.354, 4.355 and 4.356. This is supported by the highest percentage efficiency value recorded for alum at pH 5 and 0.6g/l dosage as shown in figure. 4.352.

Consider the graphical illustration presented in figures. 4.358 to 4.363 for alum and COSC.The general outlook of the process show that alum performed better than COSC for pH 5 to 13. This supported by the highest value of percentage efficiency recorded for pH 5 and 0.6g/l dosage as shown in the figure. 4.360. The implication is that the coag-flocculation behavior of alum is optimum in weak acidic VIE medium. However, in figs. 4.358 and 4.359 the COSC removal potentials is better than ALUM. However, COSC compared favorably with alum in figure. 4.363

Consider figures. 4.364 to 4.369. They presented graphical comparison of coag-flocculation removal efficiency between alum and TOSC. Observations of the results show that TOSC outperformed alum in figures. 4.364 and 4.365. However, overall process observation indicate that alum is better than TOSC for a wide range of pH of VIE medium. For alum and PTSC comparison presented in figures. 4.370 to 4.375, indicate that PTSC performed better than alum in figures. 4.370, 4.371, 4.373, 4.374, while best performance of alum is recorded in figures. 4.370 and 4.373. This results emphasizes the potentials of PTSC as a good coag-flocculant.

For MPSC, the results are presented in figures. 4.376, 4.377, 4.378, 4.379, 4.380, 4.381. The performance of MPSC in the VIE pH medium of 1,3, 7, 10 and 13 are interesting results when compared with alum as shown in figures. 4.376, 4.377, 4.378, 4.379 and 4.380 with very negligible exceptions. One striking observation is that the organic coag-flocculants performed better with PIE when compared to VIE. This phenomenon may be

connected with high initial concentration of TDSS and colloidal particles associated with PIE.

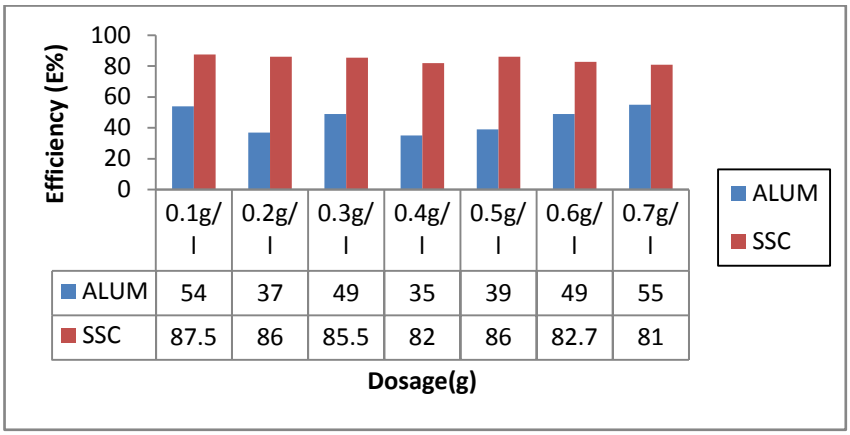

Fig.4.352: Comparative coag-flocculation performance at 40mins for varying ssc and alum dosages in VIE at pH of 1

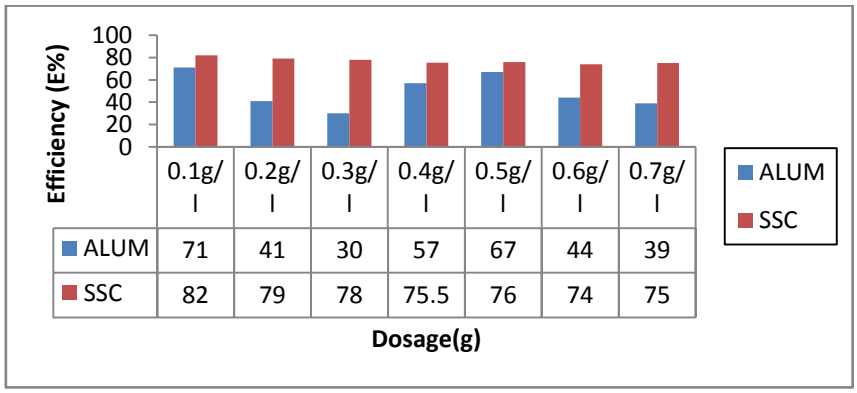

Fig.4.353: Comparative coag-flocculation performance at 40mins for varying ssc and alum dosages in VIE at pH of 3

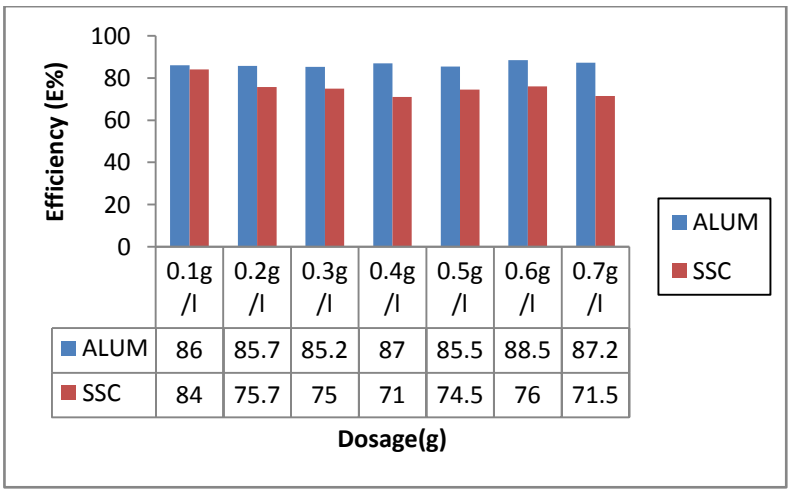

Fig.4.354: Comparative coag-flocculation performance at 40mins for varying ssc and alum dosages in VIE at pH of 5

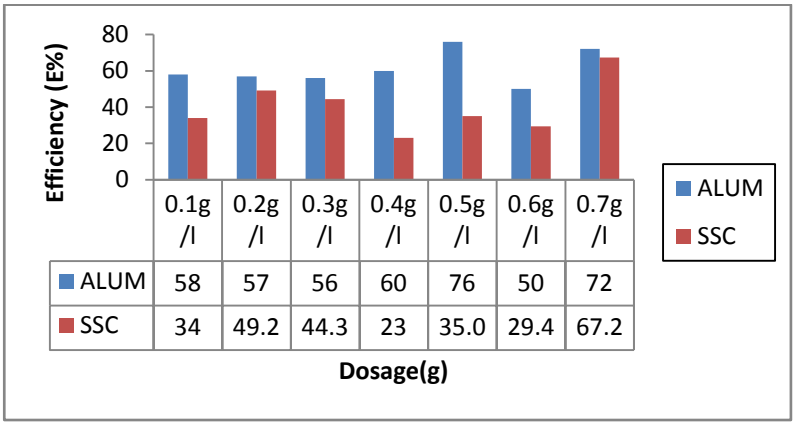

Fig.4.355: Comparative coag-flocculation performance at 40mins for varying ssc and alum dosages in VIE at pH of 7

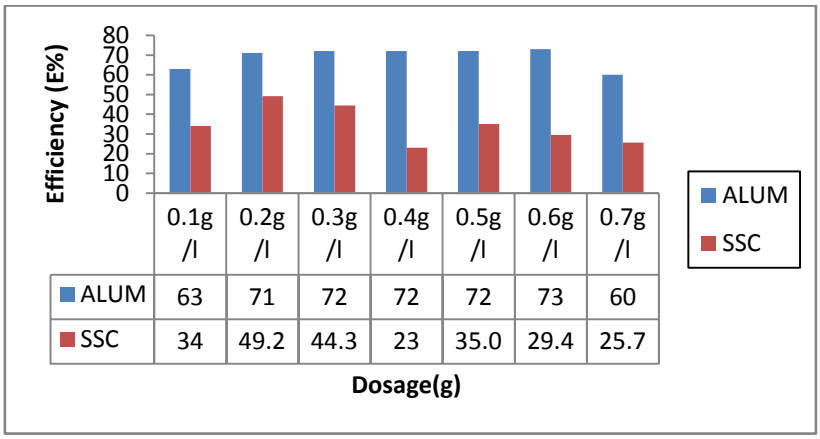

Fig.4.356: Comparative coag-flocculation performance at 40mins for varying ssc and alum dosages in VIE at pH of 10

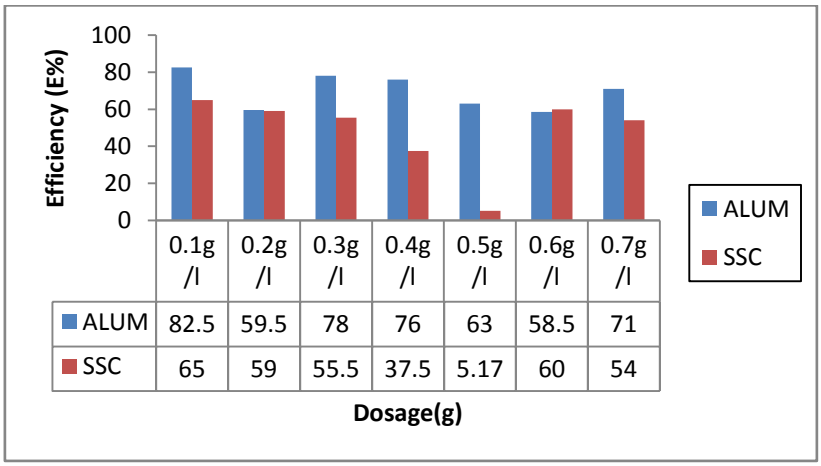

Fig.4.357: Comparative coag-flocculation performance at 40mins for varying ssc and alum dosages in VIE at pH of 13

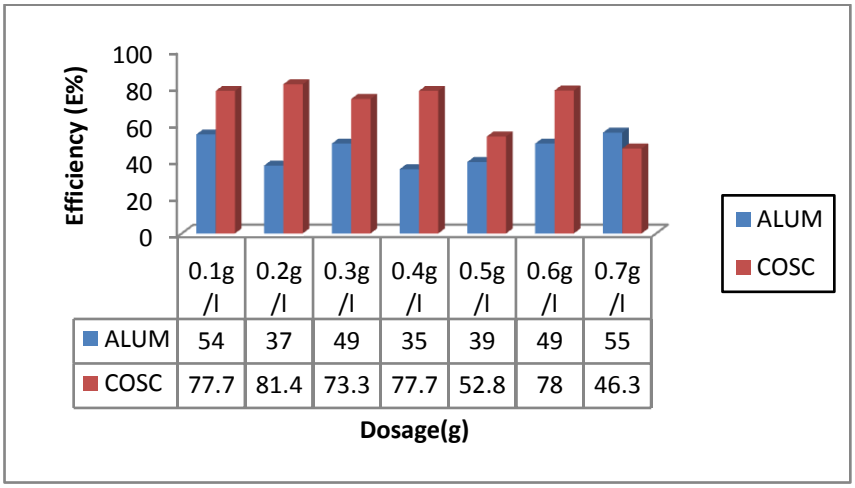

Fig.4.358: Comparative coag-flocculation performance at 40mins for varying cosc and alum dosages in VIE at pH of 1

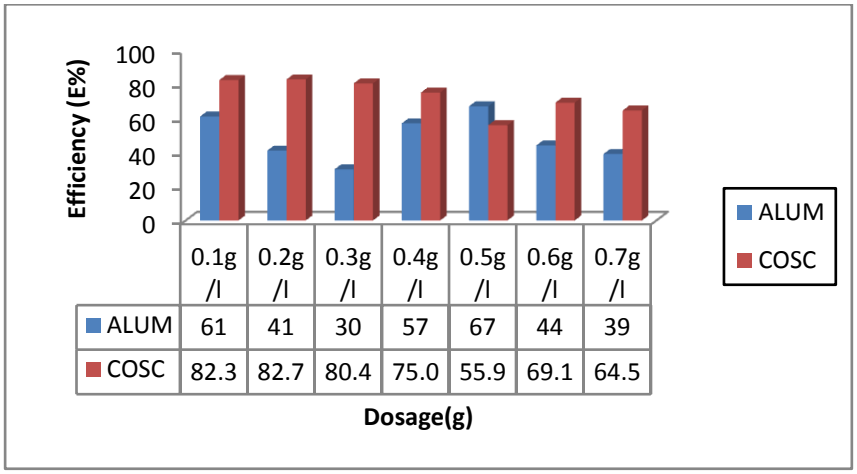

Fig.4.359: Comparative coag-flocculation performance at 40mins for varying cosc and alum dosages in VIE at pH of 3

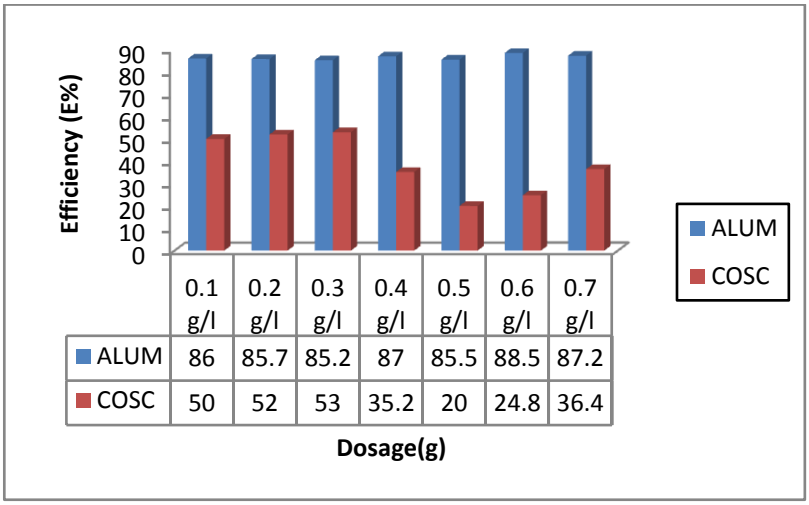

Fig.4.360: Comparative coag-flocculation performance at 40mins for varying cosc and alum dosages in VIE at pH of 5

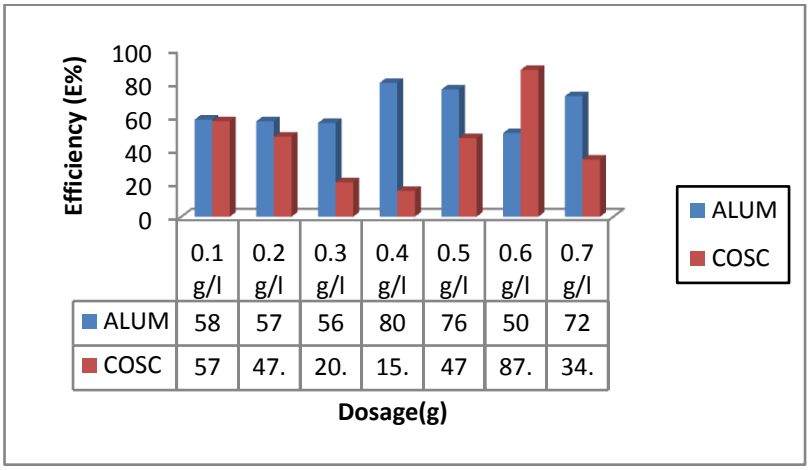

Fig.4.361: Comparative coag-flocculation performance at 40mins for varying cosc and alum dosages in VIE at pH of 7

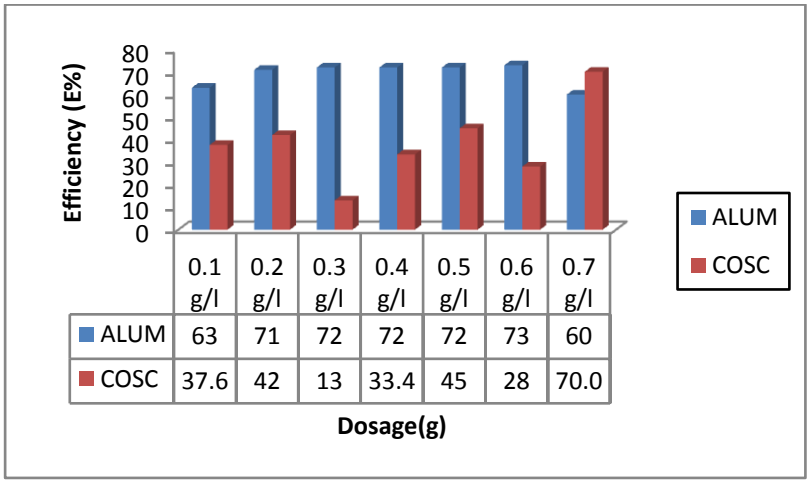

Fig.4.362: Comparative coag-flocculation performance at 40mins for varying cosc and alum dosages in VIE at pH of 10

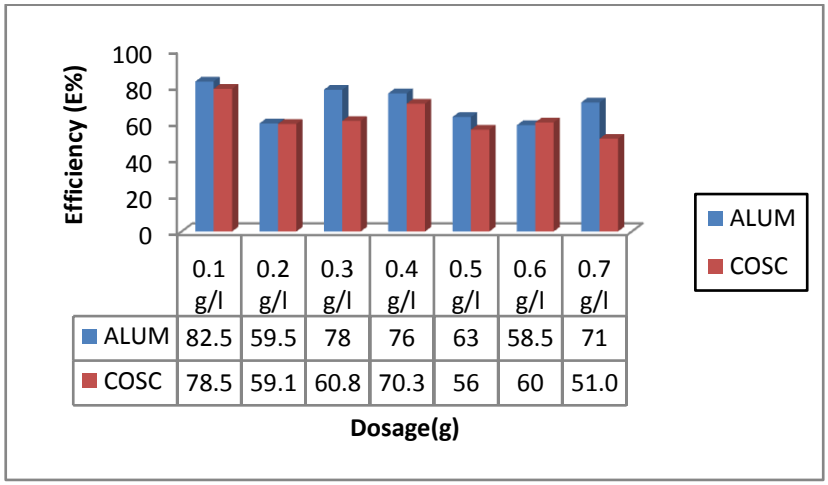

Fig.4.363: Comparative coag-flocculation performance at 40mins for varying cosc and alum dosages in VIE at pH of 13

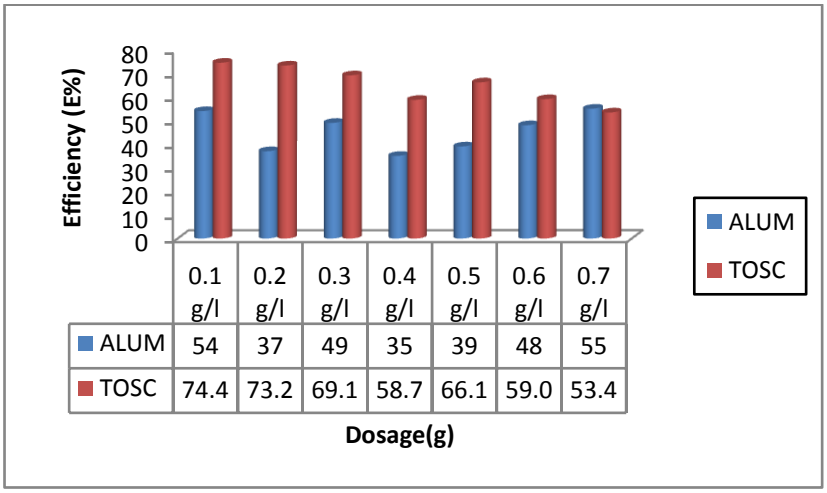

Fig.4.364: Comparative coag-flocculation performance at 40mins for varying tosc and alum dosages in VIE at pH of 1

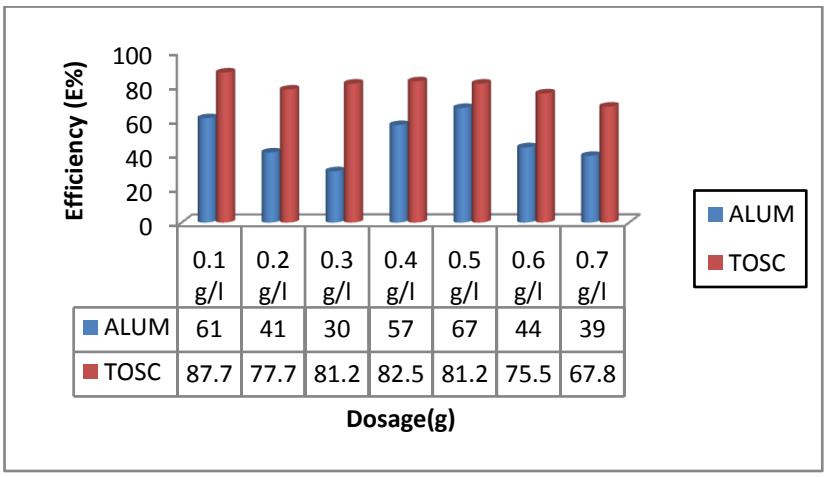

Fig.4.365: Comparative coag-flocculation performance at 40mins for varying tosc and alum dosages in VIE at pH of 3

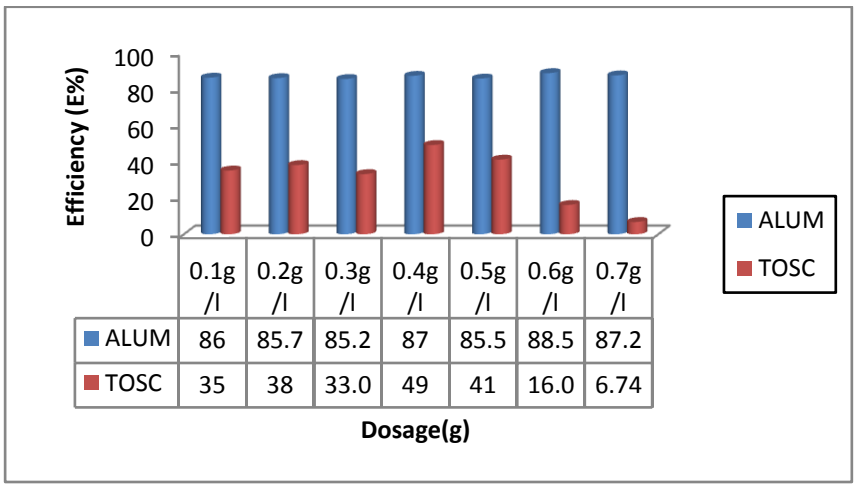

Fig.4.366: Comparative coag-flocculation performance at 40mins for varying tosc and alum dosages in VIE at pH of 5

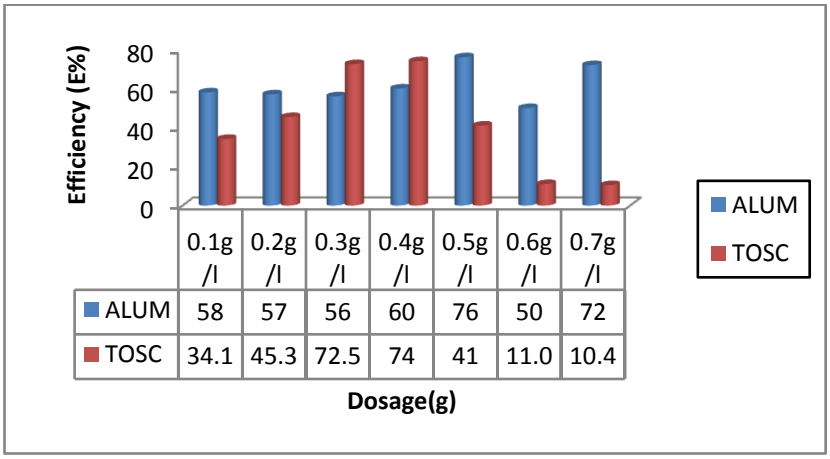

Fig.4.367: Comparative coag-flocculation performance at 40mins for varying tosc and alum dosages in VIE at pH of 7

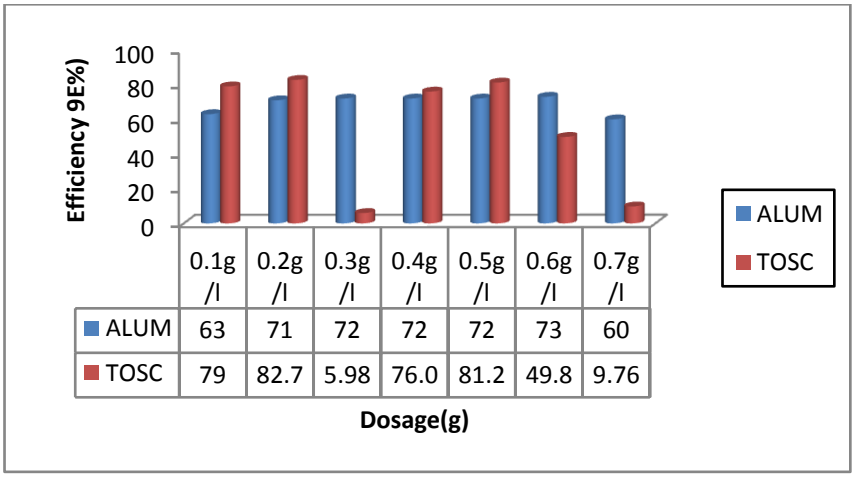

Fig.4.368: Comparative coag-flocculation performance at 40mins for varying tosc and alum dosages in VIE at pH of 10

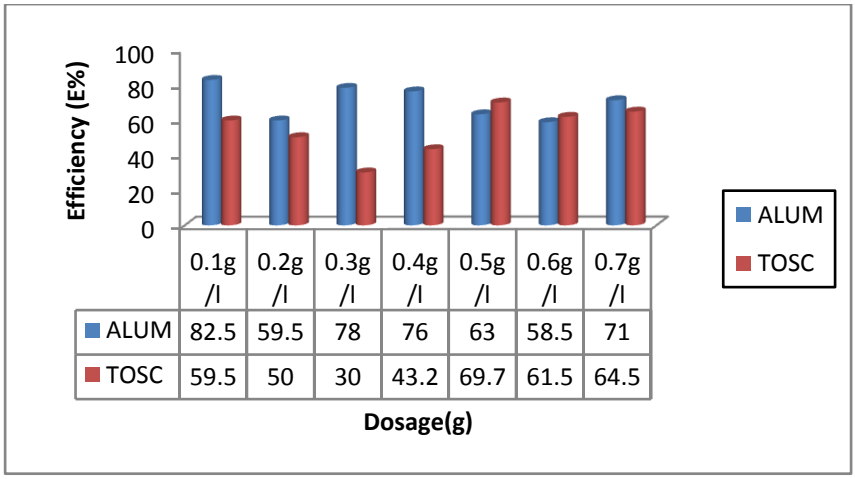

Fig.4.369: Comparative coag-flocculation performance at 40mins for varying tosc and alum dosages in VIE at pH of 13

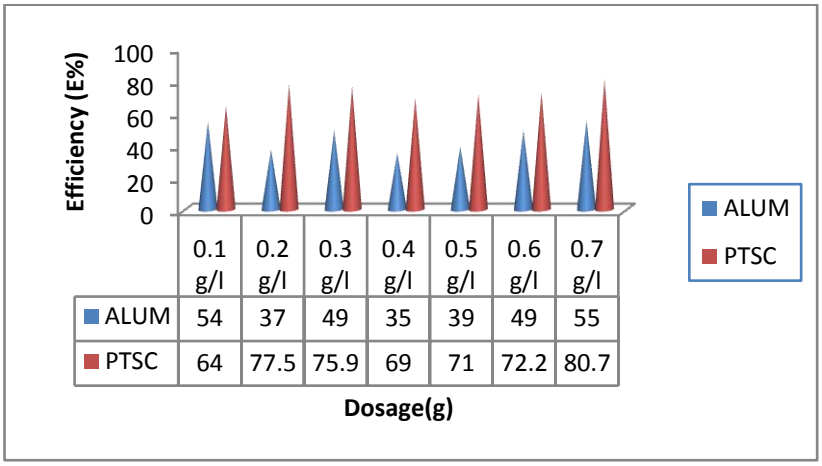

Fig.4.370: Comparative coag-flocculation performance at 40mins for varying ptsc and alum dosages in VIE at pH of 1

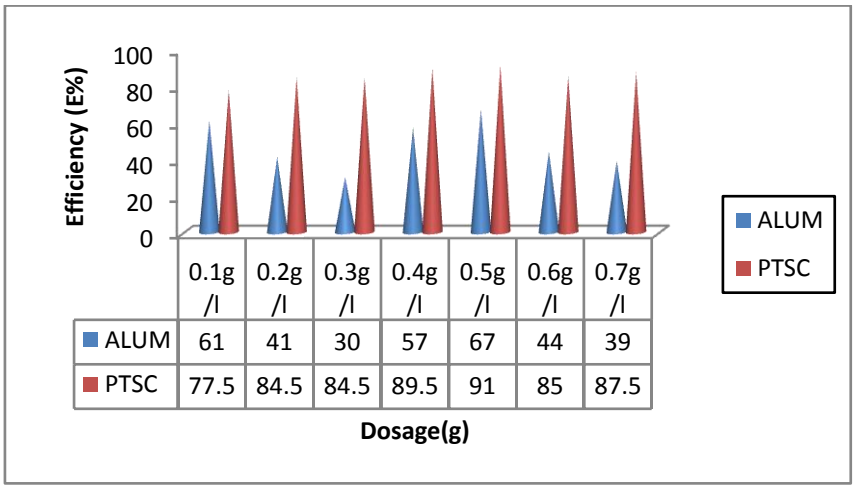

Fig.4.371: Comparative coag-flocculation performance at 40mins for varying ptsc and alum dosages in VIE at pH of 3

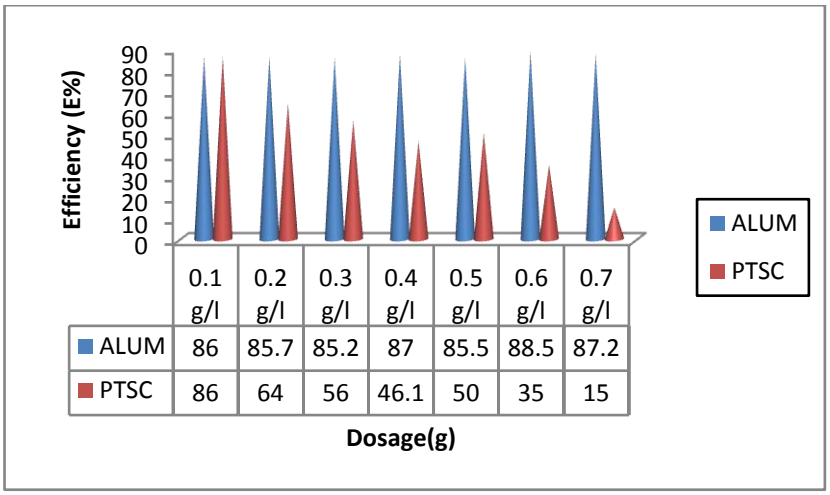

Fig.4.372: Comparative coag-flocculation performance at 40mins for varying ptsc and alum dosages in VIE at pH of 5

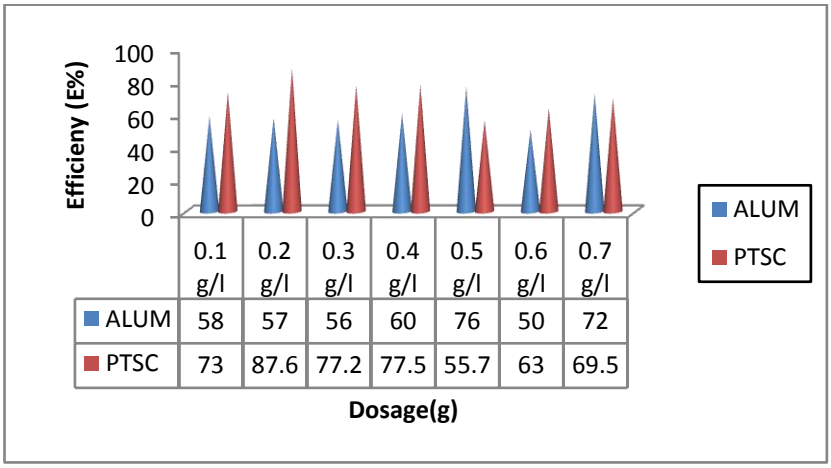

Fig.4.373: Comparative coag-flocculation performance at 40mins for varying ptsc and alum dosages in VIE at pH of 7

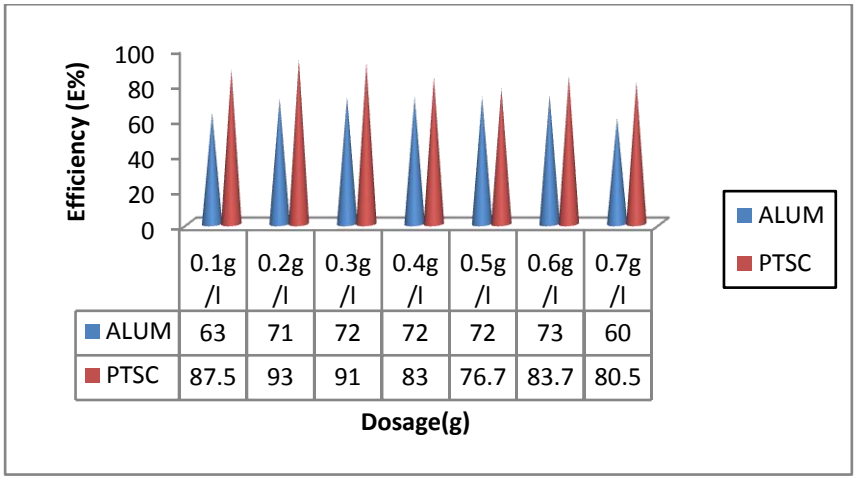

Fig.4.374: Comparative coag-flocculation performance at 40mins for varying ptsc and alum dosages in VIE at pH of 10

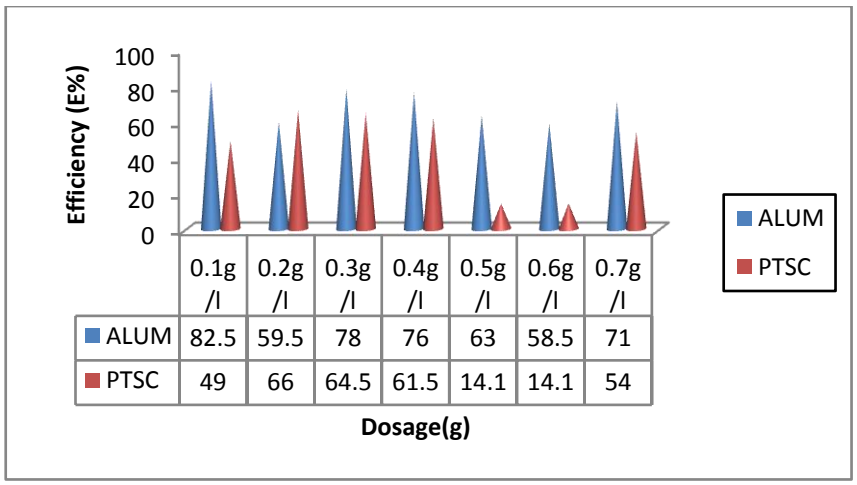

Fig.4.375: Comparative coag-flocculation performance at 40mins for varying ptsc and alum dosages in VIE at pH of 13

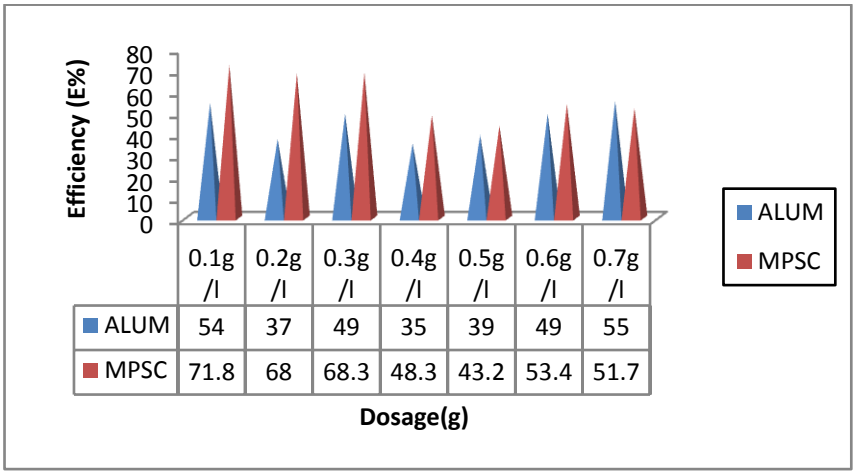

	0.1g /l	0.2g /l	0.3g /l	0.4g /l	0.5g /l	0.6g /l	0.7g /l
ALUM	54	37	49	35	39	49	55
MPSC	71.8	68	68.3	48.3	43.2	53.4	51.7

Fig.4.376: Comparative coag-flocculation performance at 40mins for varying mpsc and alum dosages in VIE at pH of 1

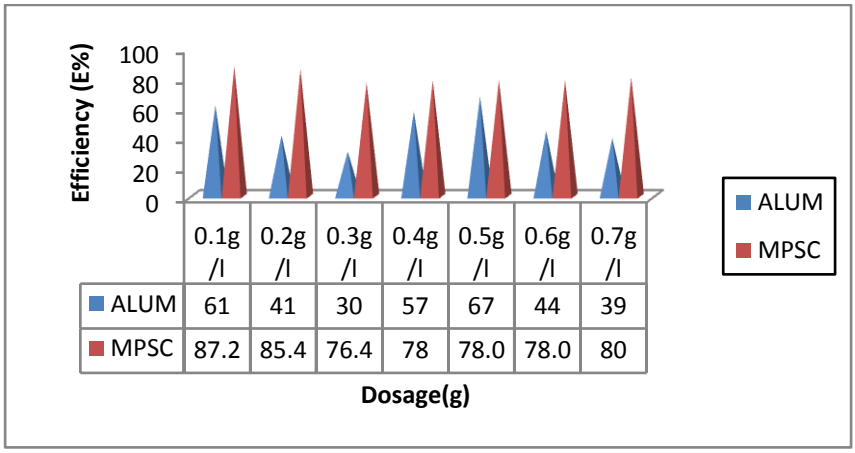

	0.1g /l	0.2g /l	0.3g /l	0.4g /l	0.5g /l	0.6g /l	0.7g /l
ALUM	61	41	30	57	67	44	39
MPSC	87.2	85.4	76.4	78	78.0	78.0	80

Fig.4.377: Comparative coag-flocculation performance at 40mins for varying mpsc and alum dosages in VIE at pH of 3

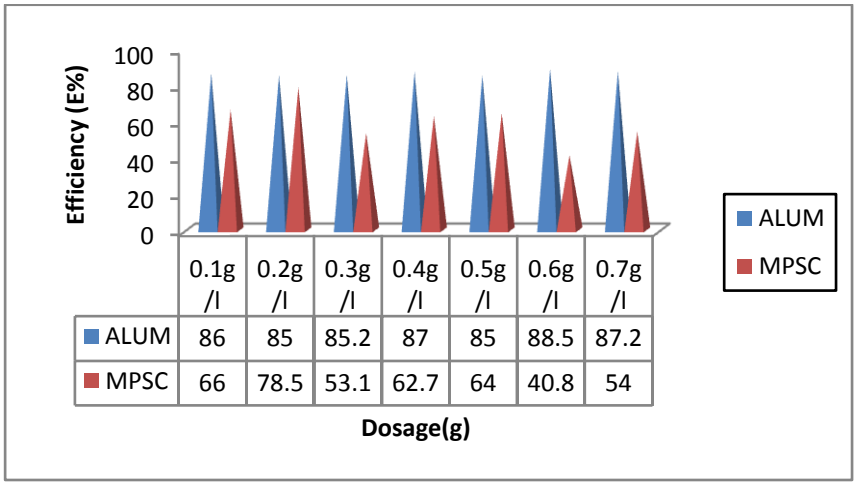

	0.1g /l	0.2g /l	0.3g /l	0.4g /l	0.5g /l	0.6g /l	0.7g /l
ALUM	86	85	85.2	87	85	88.5	87.2
MPSC	66	78.5	53.1	62.7	64	40.8	54

Fig.4.378: Comparative coag-flocculation performance at 40mins for varying mpsc and alum dosages in VIE at pH of 5

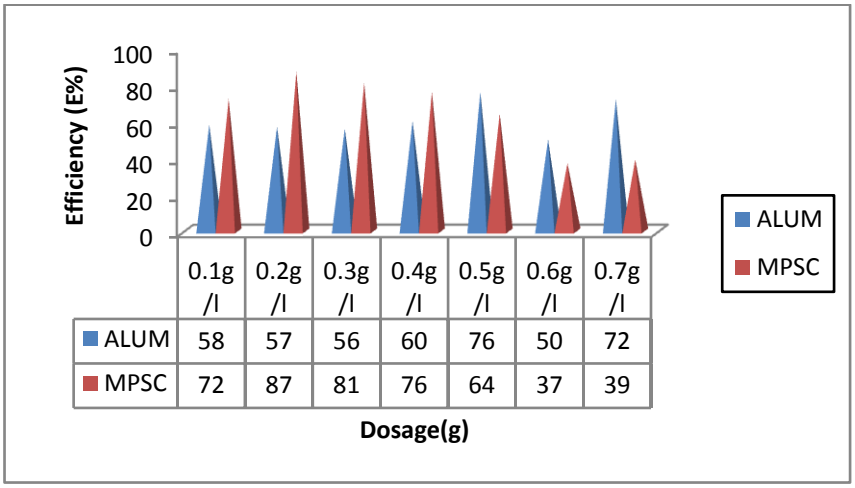

Fig.4.379: Comparative coag-flocculation performance at 40mins for varying mpsc and alum dosages in VIE at pH of 7

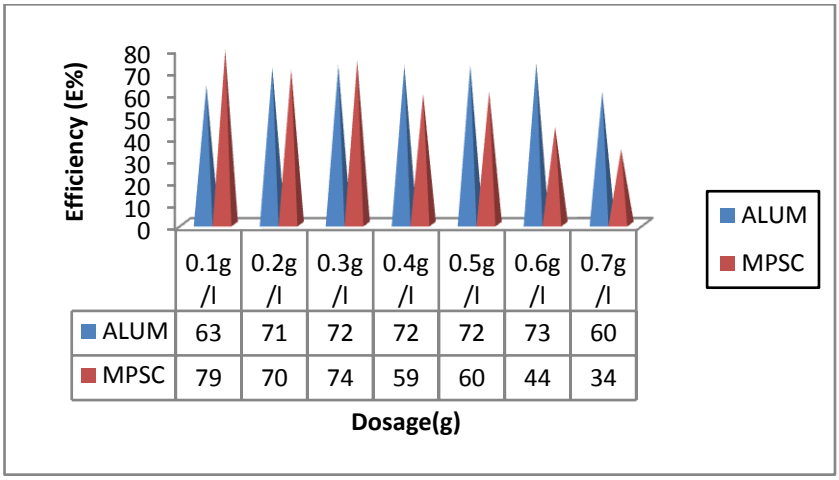

Fig.4.380: Comparative coag-flocculation performance at 40mins for varying mpsc and alum dosages in VIE at pH of 10

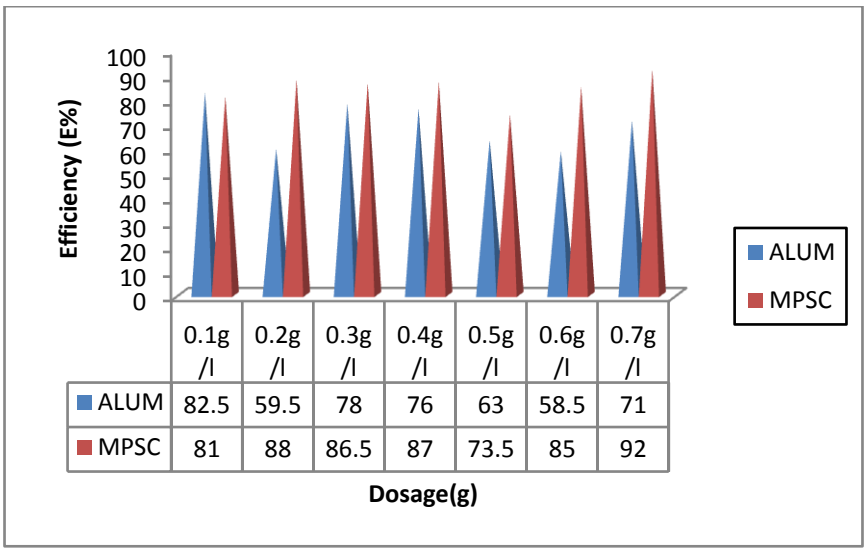

Fig.4.381: Comparative coag-flocculation performance at 40mins for varying mpsc and alum dosages in VIE at pH of 13

4.1.6.4. Comparative removal efficiency for pH varying VIE medium and constant dosage

The results are presented in figures 4382 to 4.413, showing the comparative performance between alum and various organic coag-flocculants. As usual alum performance is compared with the following SSC, COSC, TOSC, PTSC and MPSC separately in pH varying VIE. In this section, the dosage of coag-flocculant in each is constant.

For SSC comparison with alum, the results are presented in figures 4.382 to 4.386. It can be observed that SSC performed better than alum for virtually all the dosages and pH considered with only exceptions of pH of 5 and 10 as shown in the referred figures above. This result is expected because alum has been reported in this work (Lentech, 2008) to perform satisfactorily under alkaline conditions.

The results illustrated in figures 4.387 to 5.393 for alum and COSC, show that alum outperformed COSC for all dosages at the pH of 5, 7,10 and 13 as can be observed in the referred figures above with the exception of 0.6g/l dosage at pH of 7 and 13 as shown in figure. 4.392

Consider figures 4.394 to 4.400 for alum and TOSC. It can be observed that TOSC recorded high percentage removal efficiency more than alum for all dosages at only pH of 1 and 3 as shown in figures 4.394 to 4.400. Meanwhile the optimum percentage efficiency is recorded for alum at pH of 5 and 0.6g/l dosage. Thus confirming alum to have high level of performance than TOSC in the overal process.

For alum and PTSC comparison presented in figures 4.401 to 4.408, show that PTSC performed better than alum for all the dosages and pH with exception of pH of 5 and 13 as shown in figures 4.404, 4.405, 4.406, 4.407 and 4.408. This is expected because in the PIE results PTSC has done well. For MPSC, the results are similar to those of PTSC. In most of the figures, MPSC performed better than alum. The only difference in this case is that at the pH of 5 for all the dosages, alum recorded impressive results as can be observed in the figures4.409 to 4.413. MPSC in previous analysis in this report had displayed some level of high performance next to PTSC when compared wit h other coag-flocculants.

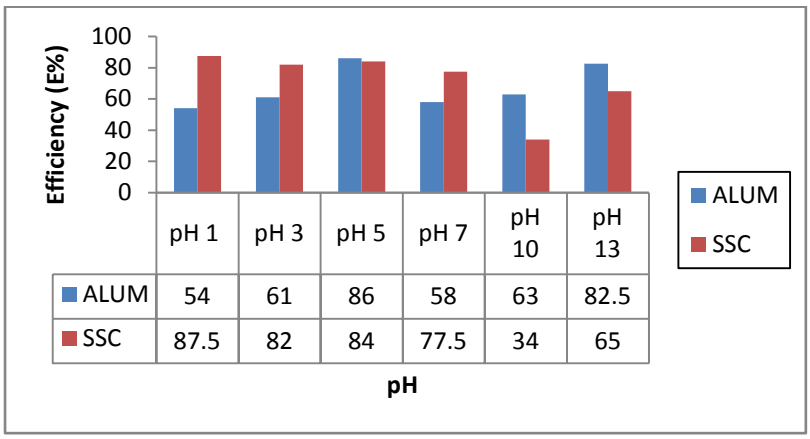

Fig.4.382: Comparative coag-flocculation performance at 40mins for 0.1g/l ssc andalum dosages in pH varying VIE

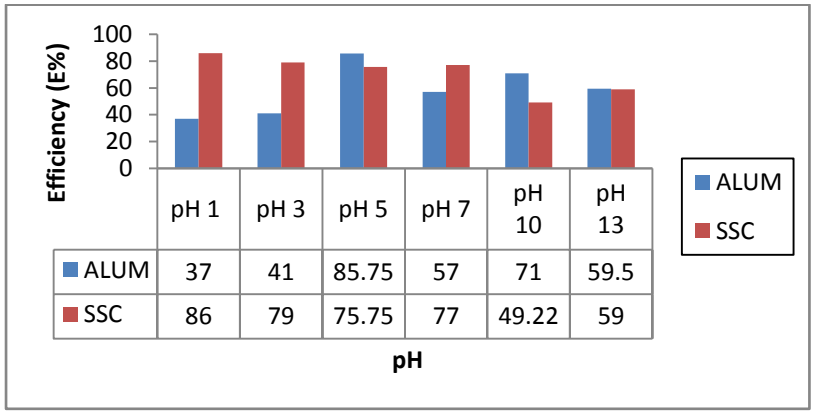

Fig.4.383: Comparative coag-flocculation performance at 40mins for 0.2g/l ssc andalum dosages in pH varying VIE

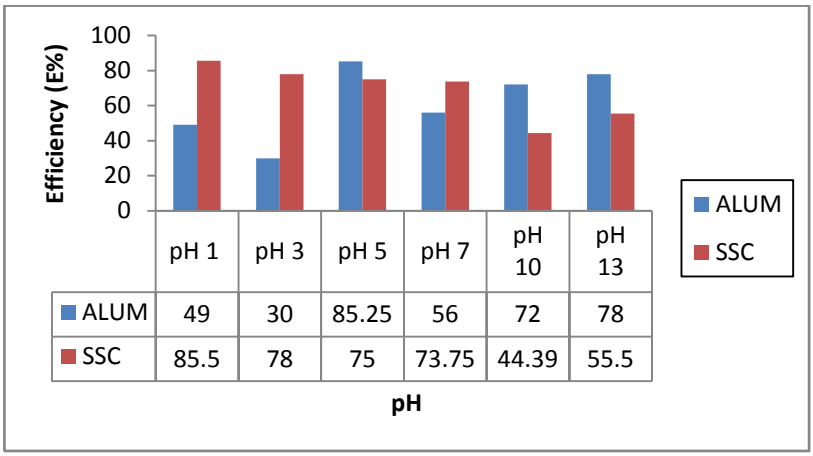

Fig.4.384: Comparative coag-flocculation performance at 40mins for 0.3g/l ssc andalum dosages in pH varying VIE

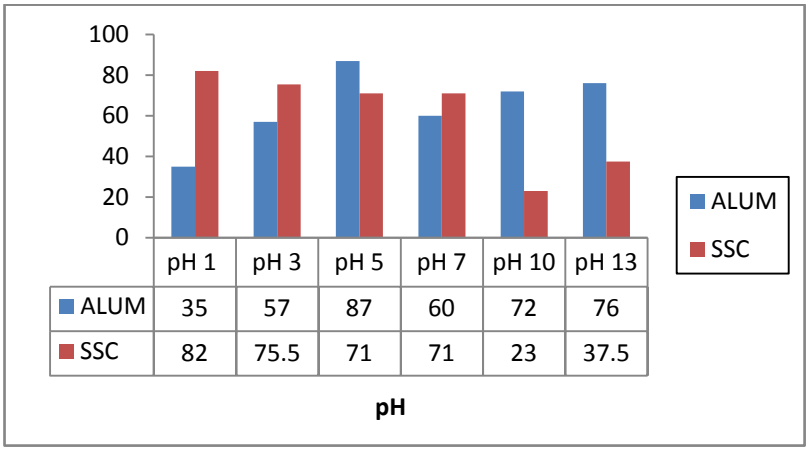

Fig.4.385: Comparative coag-flocculation performance at 40mins for 0.4g/l ssc and alum dosages in pH varying VIE

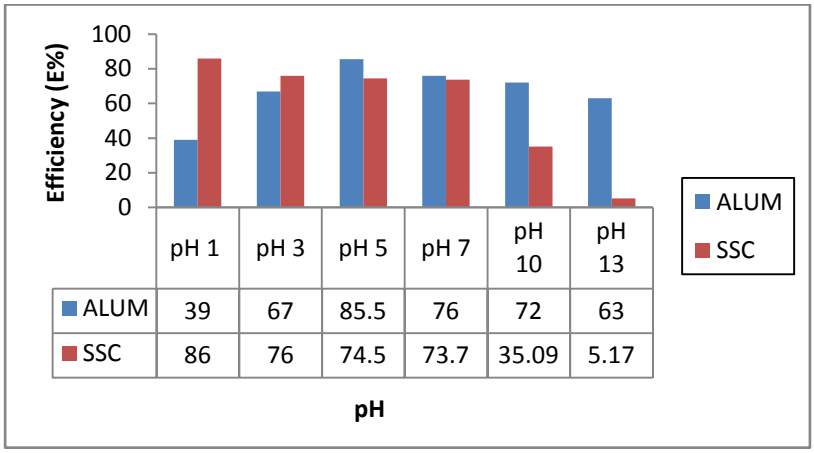

Fig.4.386: Comparative coag-flocculation performance at 40mins for 0.5g/l ssc and alum dosages in pH varying VIE

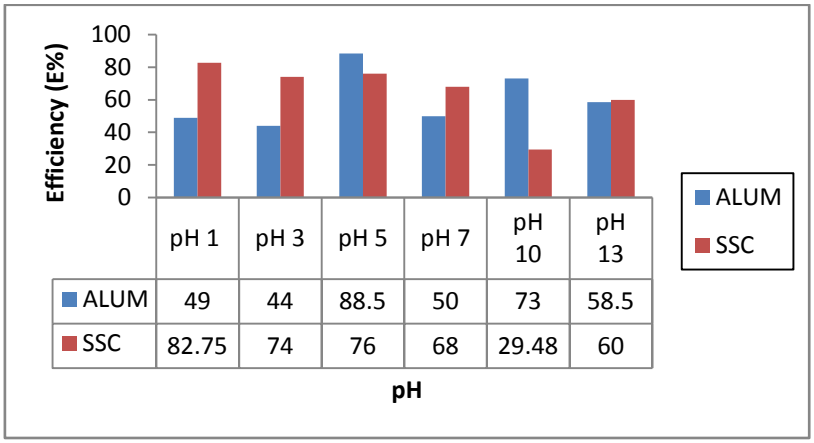

Fig.4.387: Comparative coag-flocculation performance at 40mins for 0.6g/l ssc and alum dosages in pH varying VIE

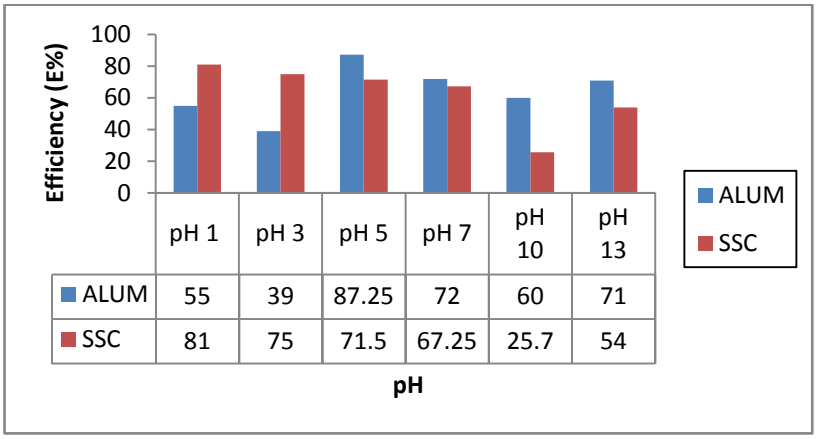

Fig.4.388: Comparative coag-flocculation performance at 40mins for 0.7g/l ssc and alum dosages in pH varying VIE

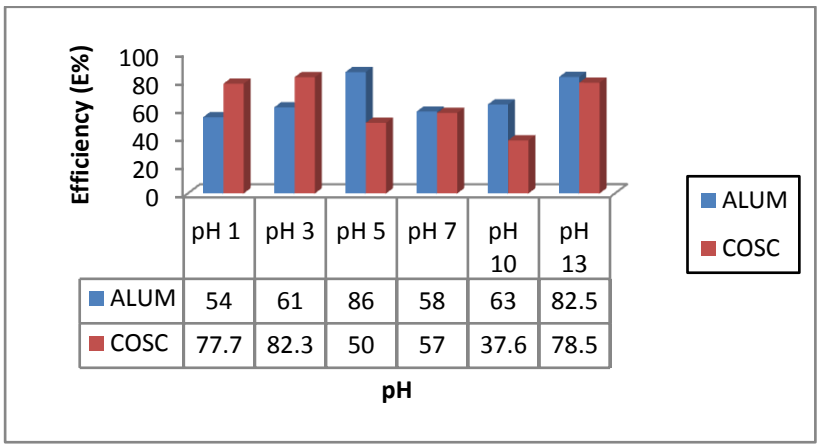

Fig.4.389: Comparative coag-flocculation performance at 40mins for 0.1g/l cosc and alum dosages in pH varying VIE

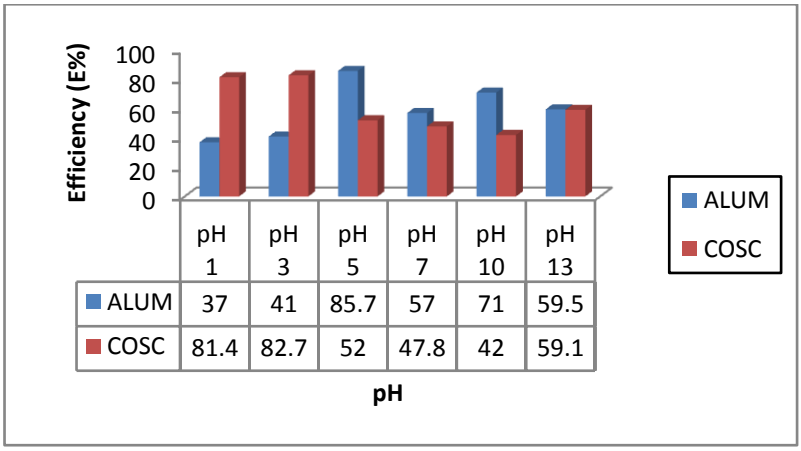

Fig.4.390: Comparative coag-flocculation performance at 40mins for 0.2g/l cosc and alum dosages in pH varying VIE

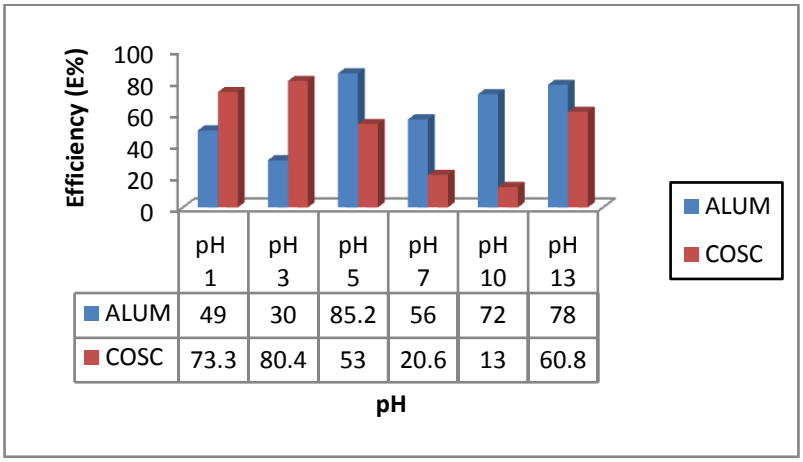

Fig.4.391: Comparative coag-flocculation performance at 40mins for 0.3g/l cosc and alum dosages in pH varying VIE

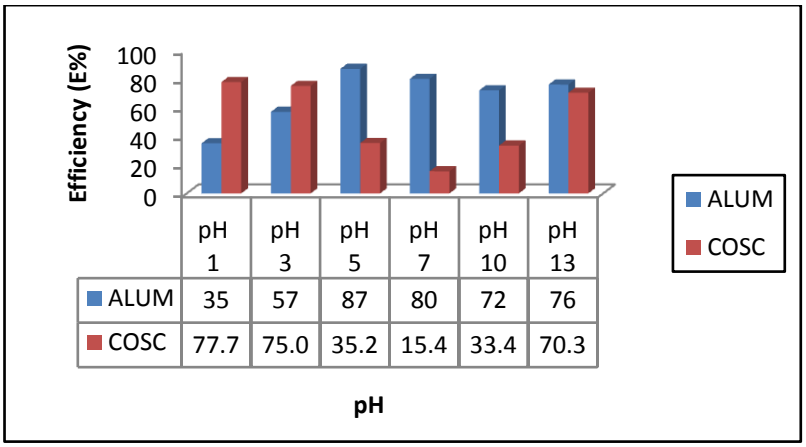

Fig.4.392: Comparative coag-flocculation performance at 40mins for 0.4g/l cosc and alum dosages in pH varying VIE

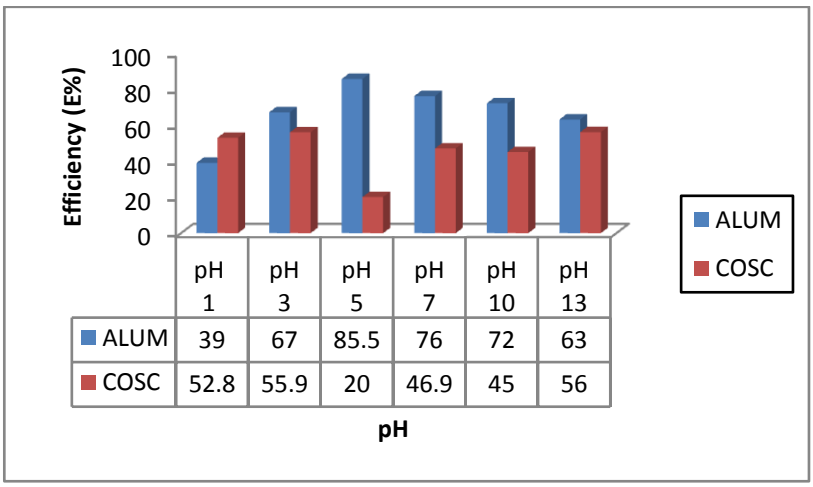

Fig.4.393: Comparative coag-flocculation performance at 40mins for 0.5g/l cosc and alum dosages in pH varying VIE

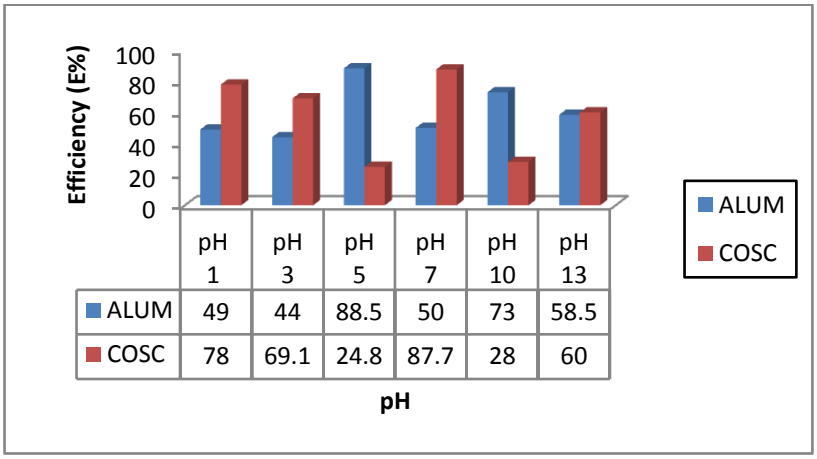

Fig.4.394: Comparative coag-flocculation performance at 40mins for 0.6g/l cosc and alum dosages in pH varying VIE

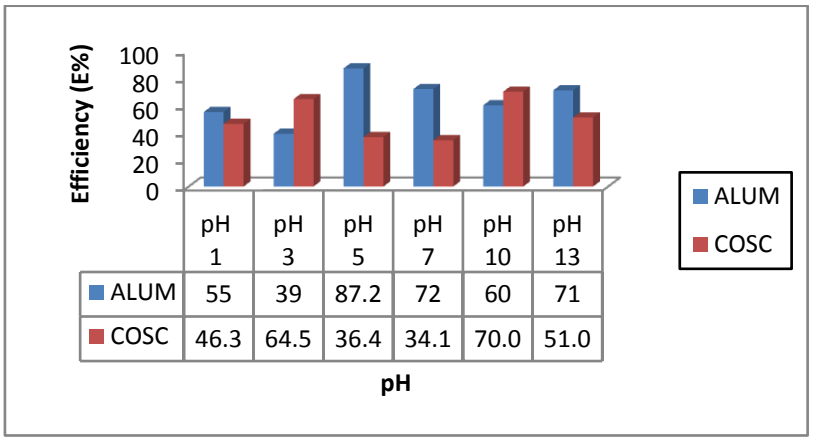

Fig.4.395: Comparative coag-flocculation performance at 40mins for 0.7g/l cosc and alum dosages in pH varying VIE

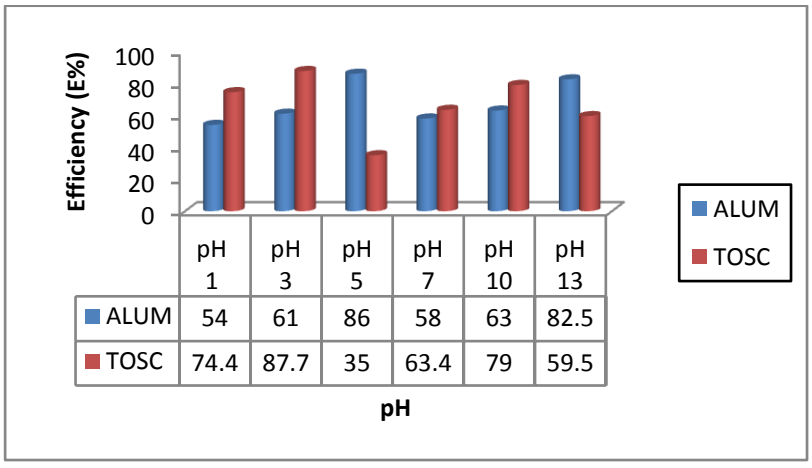

Fig.4.396: Comparative coag-flocculation performance at 40mins for 0.1g/l tosc and alum dosages in pH varying VIE

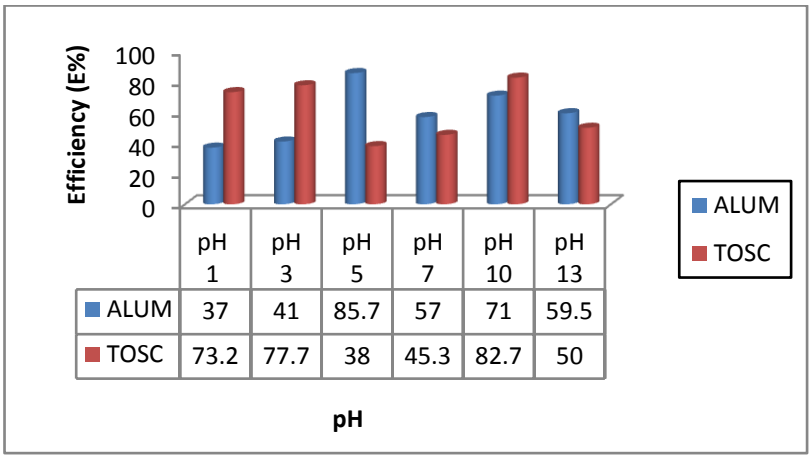

Fig.4.397:Comparative coag-flocculation performance at 40mins for 0.2g/l tosc and alum dosages in pH varying VIE

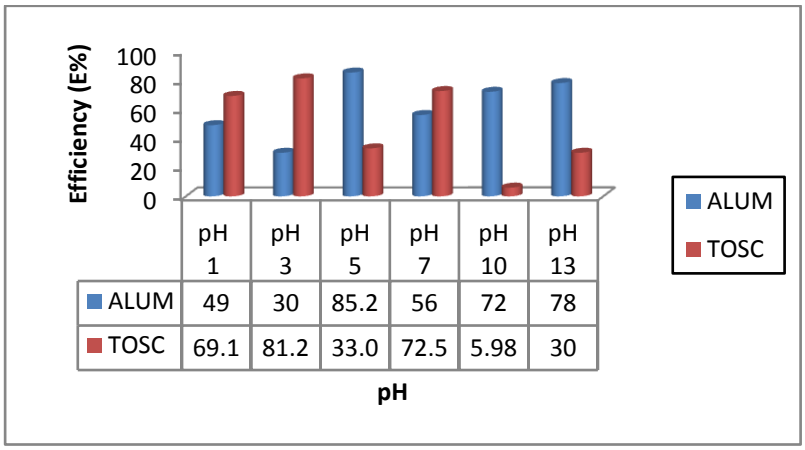

Fig.4.398:Comparative coag-flocculation performance at 40mins for 0.3g/l tosc and alum dosages in pH varying VIE

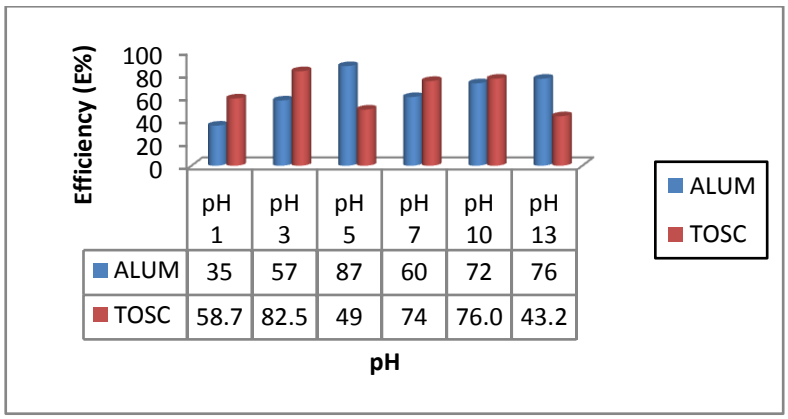

Fig.4.399:Comparative coag-flocculation performance at 40mins for 0.4g/l tosc and alum dosages in pH varying VIE

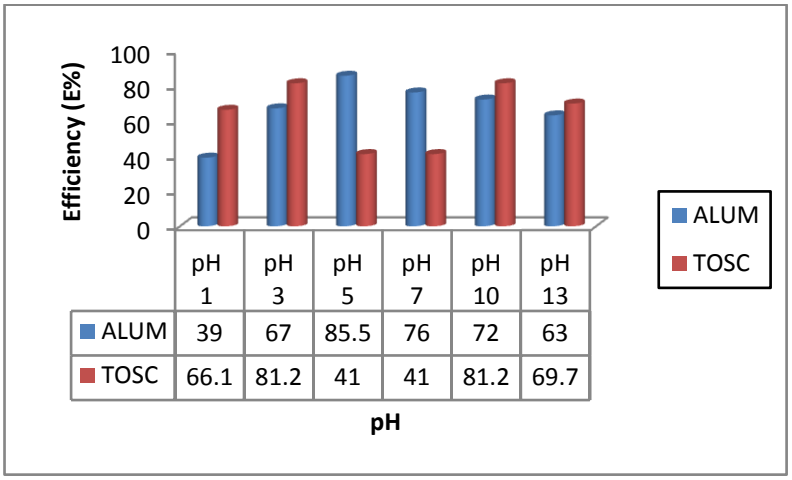

Fig.4.400:Comparative coag-flocculation performance at 40mins for 0.5g/l tosc and alum dosages in pH varying VIE

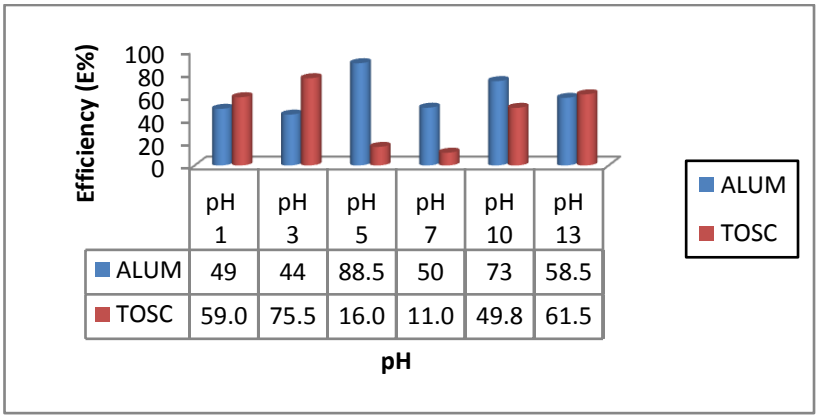

Fig.4.401:Comparative coag-flocculation performance at 40mins for 0.6g/l tosc and alum dosages in pH varying VIE

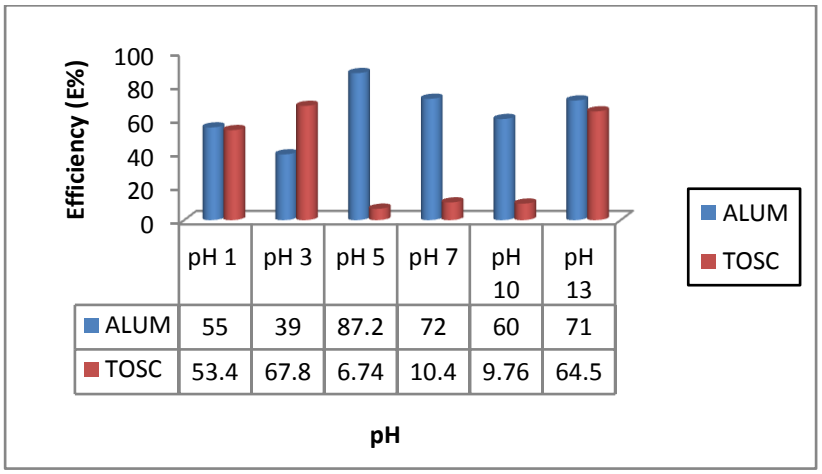

Fig.4.402:Comparative coag-flocculation performance at 40mins for 0.7g/l tosc and alum dosages in pH varying VIE

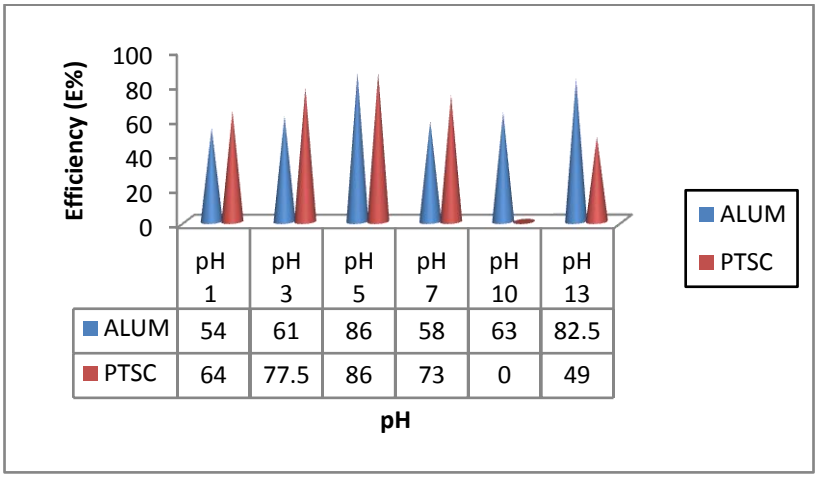

Fig.4.403: Comparative coag-flocculation performance at 40mins for 0.1g/l ptsc and alum dosages in pH varying VIE

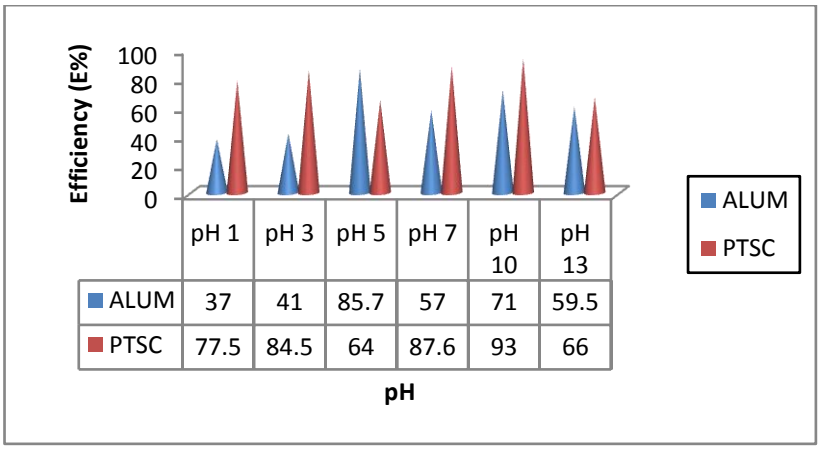

Fig.4.404:Comparative coag-flocculation performance at 40mins for 0.2g/l ptsc and alum dosages in pH varying VIE

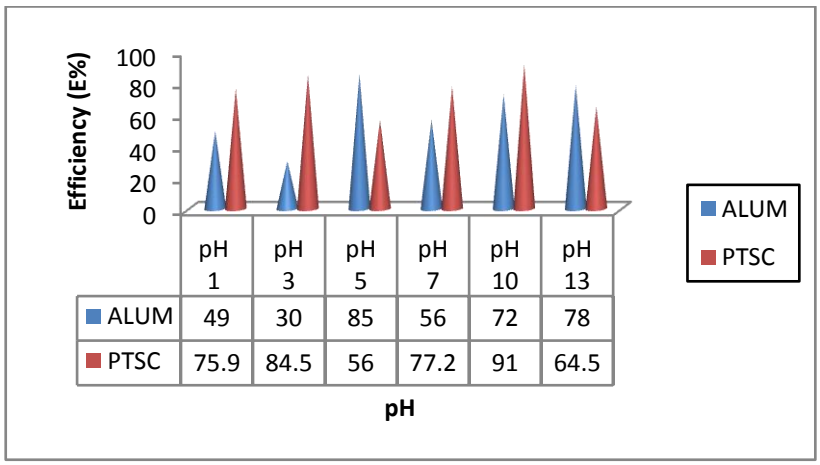

Fig.4.405:Comparative coag-flocculation performance at 40mins for 0.3g/l ptsc and alum dosages in pH varying VIE

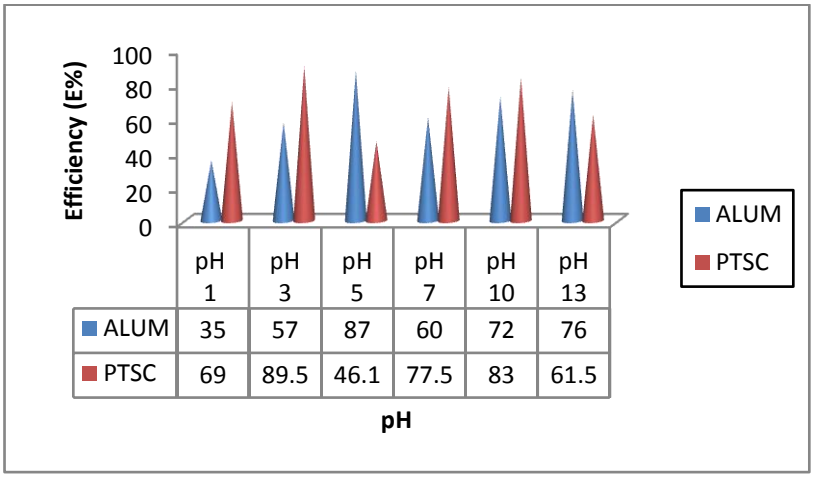

Fig.4.406:Comparative coag-flocculation performance at 40mins for 0.4g/l ptsc and alum dosages in pH varying VIE

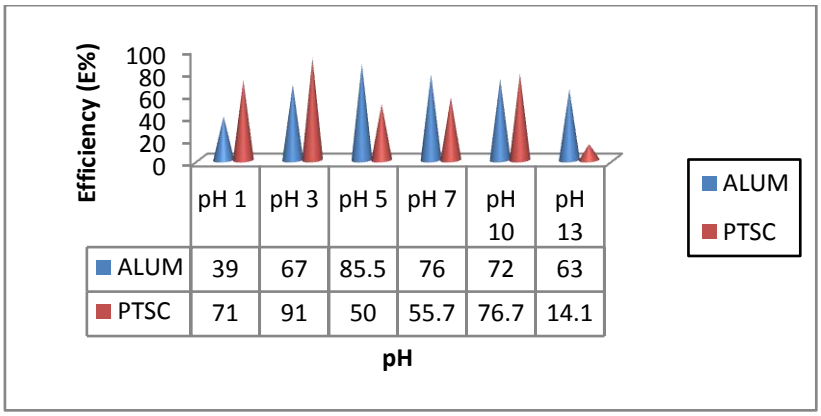

Fig.4.407:Comparative coag-flocculation performance at 40mins for 0.5g/l ptsc and alum dosages in pH varying VIE

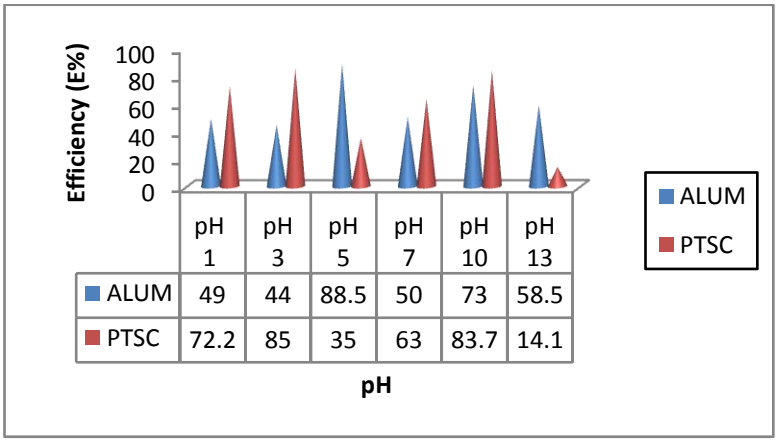

Fig.4.408:Comparative coag-flocculation performance at 40mins for 0.6g/l ptsc and alum dosages in pH varying VIE

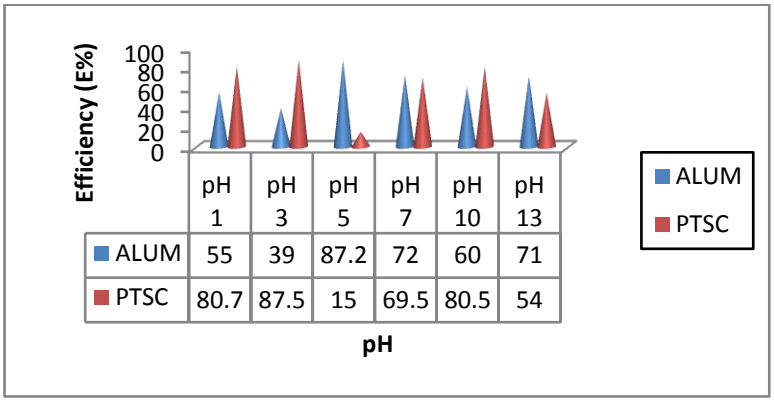

Fig.4.409:Comparative coag-flocculation performance at 40mins for 0.7g/l ptsc and alum dosages in pH varying VIE

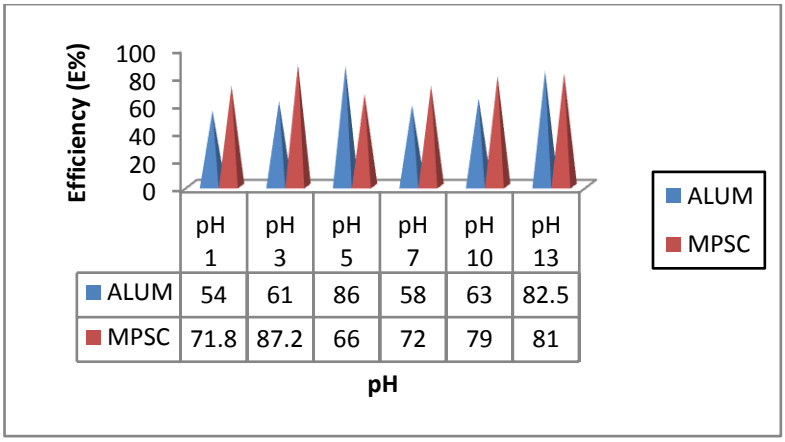

Fig.4.410:Comparative coag-flocculation performance at 40mins for 0.1g/l mpsc and alum dosages in pH varying VIE

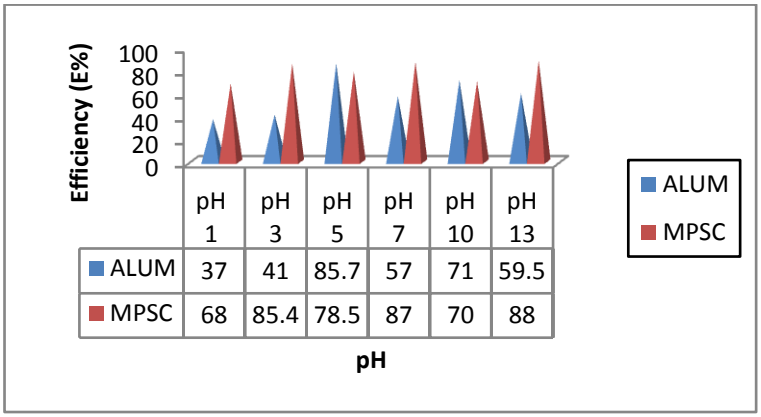

Fig.4.411:Comparative coag-flocculation performance at 40mins for 0.2g/l mpsc and alum dosages in pH varying VIE

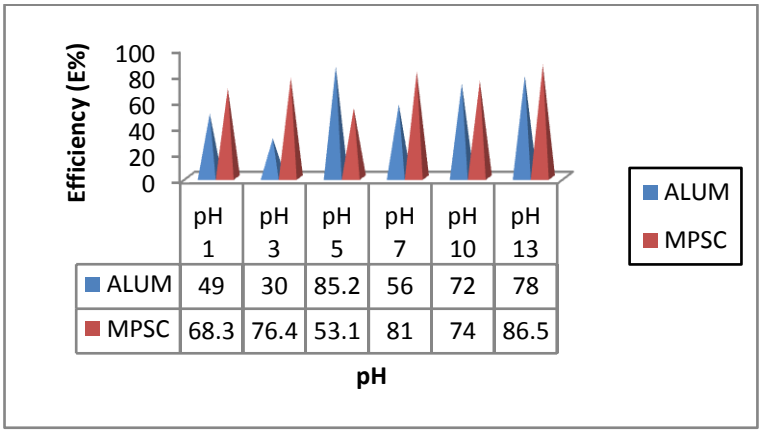

Fig.4.412:Comparative coag-flocculation performance at 40mins for 0.3g/l mpsc and alum dosages in pH varying VIE

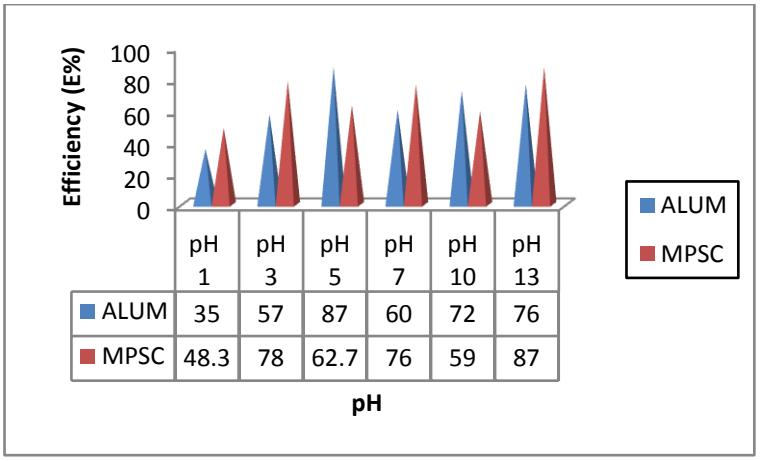

Fig.4.413:Comparative coag-flocculation performance at 40mins for 0.4g/l mpsc and alum dosages in pH varying VIE

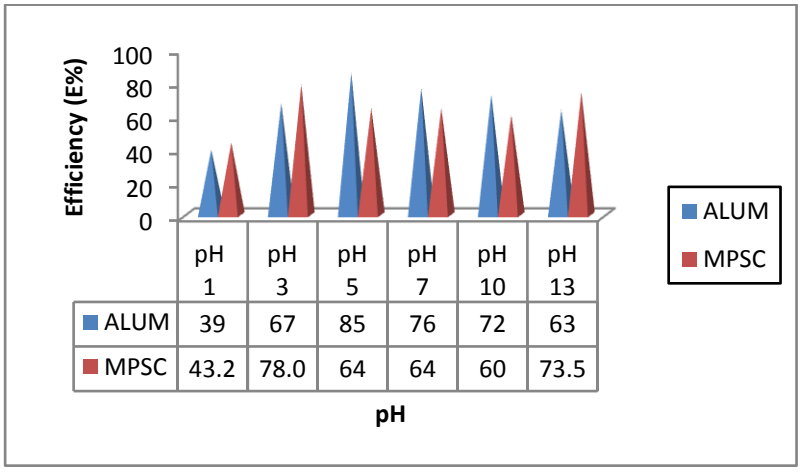

Fig.4.414:Comparative coag-flocculation performance at 40mins for 0.5g/l mpsc and alum dosages in pH varying VIE

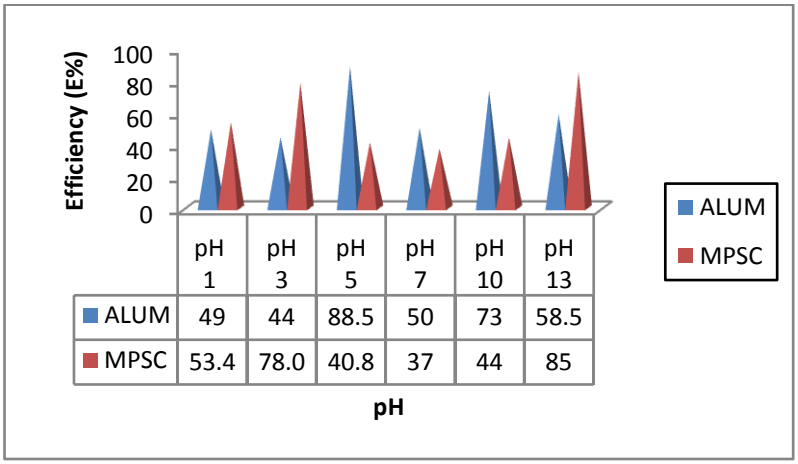

Fig.4.415:Comparative coag-flocculation performance at 40mins for 0.6g/l mpsc and alum dosages in pH varying VIE

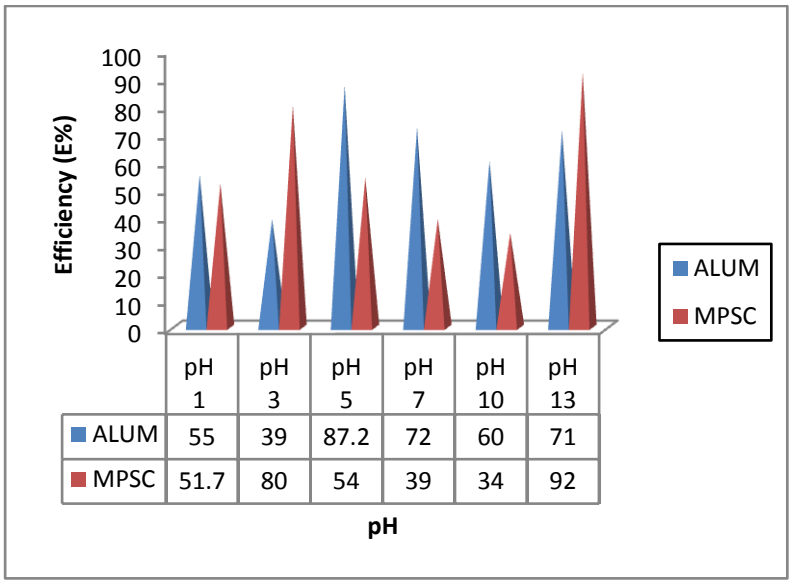

Fig.4.416:Comparative coag-flocculation performance at 40mins for 0.7g/l mpsc and alum dosages in pH varying VIE

4.2: RESULTS AND DISCUSSION ON ADSORPTION

4.2.1: Characterization of the Adsorbents and Wastewaters (PIE and VIE)

The characterization results of the adsorbents are presented in tables 4.146. The parameters considered for the adsorbents characterization are: % yield, % weight Loss, surface area, total pore volume, bulk density, % Ash content, Iodine number, oil content and moisture content. All the adsorbents were activated with 60% H_2SO_4.

Table 4.146 show that the surface area and pore volume of the adsorbents are as follows: 1016.0100cm^2/g, 161.1200cm^2/g, 45.4000cm^2/g 156.4000cm^2/g, 1658.0000cm^2/g and 0.3200, $3.9962x10^{-5}$,0.0630, 0.2300, 0.6600 for BFHA, RHA, LATERITE, UCA and MSA respectively. Observation from table 4.146 indicate that the adsorbent with high adsorption capacity (i.e MSA) had highest value of surface area (1658.00cm^2/g) and total pore volume (0.6600). The higher surface area recorded for the most active adsorbent is an indication that much organic by products and minerals present in the activated carbon surface were removed during activation(Dubinin, 1964).

Conversely, the low yield observed for the adsorbents could be attributed to the sulphuric acid attack on the aliphatic and aromatic species present in the substrate. This results in relatively high devolatilisation rate of the substrate leading to the fragmentation of its char–activated particles. These observed developments of the char–activated structure were confirmed by the significant increase in the surface area of char carbon based adsorbents over non charred based adsorbents (Wannapeera, et al, 2008)

The higher pore volume obtained for carbon char based adsorbents could be attributed to the immediate release of the volatiles from inside of the particles or substrates under a rapid heating up during carbonization process prior to activation (Wannapeera, et al, 2008). This effect was more pronounced in MSA following highest pore volume recorded compared to others. This may be explained by the more rapid devolatilisation of MSA resulting in more extensive volatile explosion and pores creation. Also, the ash content increased much with the carbon char based adsorbent due to much higher reduction of volatile matter in the carbon on activation.

The characterization results of the PIE and VIE before and after adsorption are presented in tables 4.147 and 4.148. The characterization results of the PIE before and after adsorption indicate a reduction from 794.0000 to 4.3510 NTU, 20.5000 to

2.0050mg/l, 5.7500 to 3.3500mg/l, 155.000 to 36.200mg/l, 295.000 to 185.000mg/l for turbidity, TSS, TDS, BOD_5 and COD respectively. For the VIE, the reduction is from 4.9200 to 4.8000, 38.00 to 0.00 NTU, 220.00 to 47.368mg/l, 550.000 to 225.000mg/l, 45.0000 to 5.60mg/l for pH, turbidity, BOD_5, COD, TSS respectively. Though the reduction were not limited to these parameters aforementioned, there is reduction in the following parameters after the adsorption for both PIE and VIE; total hardness, Ca^{2+} hardness, mg^{2+} hardness, Cl^-, DO, and total acidity.

One remarkable feature is the absence of microbes before and after adsorption treatment, showing that the biocoagulants used prior to adsorption were very effective in the removal of microbes. However,it should be noted that among the parameters tested for BOD and COD values did not meet WHO standard for drinking water, but BOD $\leq$ 100.00mg/l and COD $\leq$ 150.00mg/l values posses no restrictions to irrigation use (Carter,1993;Alberta Environment,1984).

Table 4.146 : Characterization result of adsorbents

Parameter	BFHA	RHA	LATERITE	UCA	MSA
% yield	42.0200	47.3670	4.4000	5.6798	31.2101
% Wt. Loss	16.5671	20.3456	5.9120	3.5700	18.5670
Surface area (cm^2/g)	1016.0100	161.1200	45.4000	156.4000	1658.0000
Total pore volume	0.3200	$3.9962x10^{-5}$	0.0630	0.2300	0.6600
Bulk density (g/cm^2)	0.3010	0.0541	0.0480	0.1420	0.0950
% Ash content	5.2123	17.3670	0.9400	1.0000	3.2000
Iodine number (mg/g)	42.4000	1270.0000	68.2430	16.5340	298.3534
Oil content (%)	0.0125	0.0110	Nil	Nil	0.500
Moisture content (%)	8.9501	9.5200	8.600	8.3200	24.4000

Table 4. 147 : Characterization of PIE and VIE before and after adsorption

Parameter	Before Adsorption		After Adsorption		WHO
	PIE	VIE	PIE	VIE	Standard
pH	5.9800	4.9200	6.1000	4.8000	7.000-8.000
Temperature (^oC)	26.5000	27.0000	26.2000	26.9000	-
E. Conductivity ($\mu m/m^2$)	10.4600	8.7400	9.5500	9.3200	1250.0000
Phenol (mg/l)	nil	nil	nil	nil	-
Total Hardness (mg/l)	3730.0000	45.0000	3700.000	40.000	500.000

Ca Hardness (mg/l)	200.0000	12.5000	186.0000	11.9000	100.000
Mg hardness (mg/l)	3530.0000	32.5000	3520.000	29.000	100.000
Chlorides (mg/l)	5.5000	25.0000	4.6520	23.000	200.000
Dissolved oxygen (mg/l)	2.9500	4.6200	2.7000	3.9500	-
Turbidity (NTU)	794.0000	38.000	4.3510	nil	5.0000
Iron fe^{2}+ (mg/l)	nil	0.0300	nil	nil	0.3000
Nitrates (mg/l)	nil	nil	nil	nil	3.0000
Total acidity (mg/l)	0.0200	1.1000	nil	nil	-
TDS (mg/l)	5.7500	nil	3.3500	nil	50.000
TSS (mg/l)	20.5000	45.000	2.0050	5.6000	50.000
Oil & grease (mg/l)	nil	2.5000	nil	1.0000	-
Total viable count (cfu/ml)	nil	nil	nil	nil	-
Total coliform (MPN/100ml)	nil	nil	nil	nil	3/100ml
Pseudomonas aeruginosa(MPN/ml)	nil	nil	nil	nil	nil

Table 4.148: Characterization of COD and BOD for VIE and PIE before and after adsorption

Parameter	Before adsorption		After adsorption		WHO Standard
	PIE	**VIE**	**PIE**	**VIE**	
COD (mg/l)	295.00	550.00	185.000	225.500	50.000
BOD_5(mg/l)	155.00	220.00	36.200	47.368	20.000

4.2.2 Instrumental Characterization of Adsorbents

The char activated carbon adsorbent of BFHA, RHA, MSA and non char activated adsorbents of LATERITE and UCA, were further characterized via FTIR, XRD and SEM analyses, respectively. To study the surface chemistry of each of them which will aid in elucidating the presence of functional groups, chemical compositions of the minerals and surface physical morphology prevalent in these adsorbents .

4.2.2.1 FTIR results of char activated carbon

The FTIR spectroscopic study of the produced carbon are shown in plates 4.1, 4.2 and 4.3. The stretching signals or vibration are appreciable due to the availability of various constituents.

The FTIR absorbance spectra patterns exhibits 18, 14 and 22 discernable peaks for plates 4.1, 4.2, and 4.3 respectively recorded for frequency of 4000cm^{-1} to 5000cm$^{-1.}$ In the IR results presented in plates 1 and 3, the Si – O stretching vibrations were observed at 913.32cm^{-1} and 616.28cm^{-1} respectively showing the presence of quartz for both charred activated carbons from BFHA and RHA). A strong band at 3800.86cm^{-1} and 3952.28cm^{-1} indicate the possibility of hydroxyl groups linkage. The BFHA and RHA charred carbon exhibits a distinct broad band peak in the regions of 1603.86cm^{-1} to 1878.73cm^{-1} and 1610.61cm^{-1} to 1887.41cm^{-1} as shown in plates 4.1 and 4.3. These broad bands are attributed to high concentration of anti-symmetrical Si-O-Si or Si-O–O stretching mode as a result of existing alumina and silica containing minerals within the adsorbents (Prasdhan, 2011; Calzaferri and Imhof, 1996). Comparing the broad band of plates 1 and 4, show that in plate 1, there is band intensity reduction around 1878.73cm^{-1} attributed to the stretching of hydroxyl groups (O – H band) of BFHA which was partially substituted by SOX groups during sulphuric acid activation; whereas plate 4.3 witnessed increased transmittance of the bands between 1610.61cm^{-1} to 1887.41cm^{-1}, attributed to the Si – O bending.

For plate 4.2, the sample showed three major absorbance band at 3419.9 – 3781.57cm^{-1}, 2919.36 – 3223.16cm^{-1}, 1600.01 – 2351.30cm^{-1} and 486.08 – 1042.56cm^{-1}. The band at 3781.57cm^{-1} is attributed to the surface hydroxyl groups and chemisorbed water. The band at 3419.9, 3223.16 and 2919.39cm^{-1} were ascribed to C – H stretching vibrations of methyl groups on the surface and to a co-ordinated H-bridges. Bands at 2351.50, 1600.01 and 1042.56cm^{-1} are assigned to C = O stretching frequency, and to lithium, magnesium, cobalt, scandium groups, respectively. The band at 486.08cm^{-1} is attributed to the presence of metal – halogen bond.

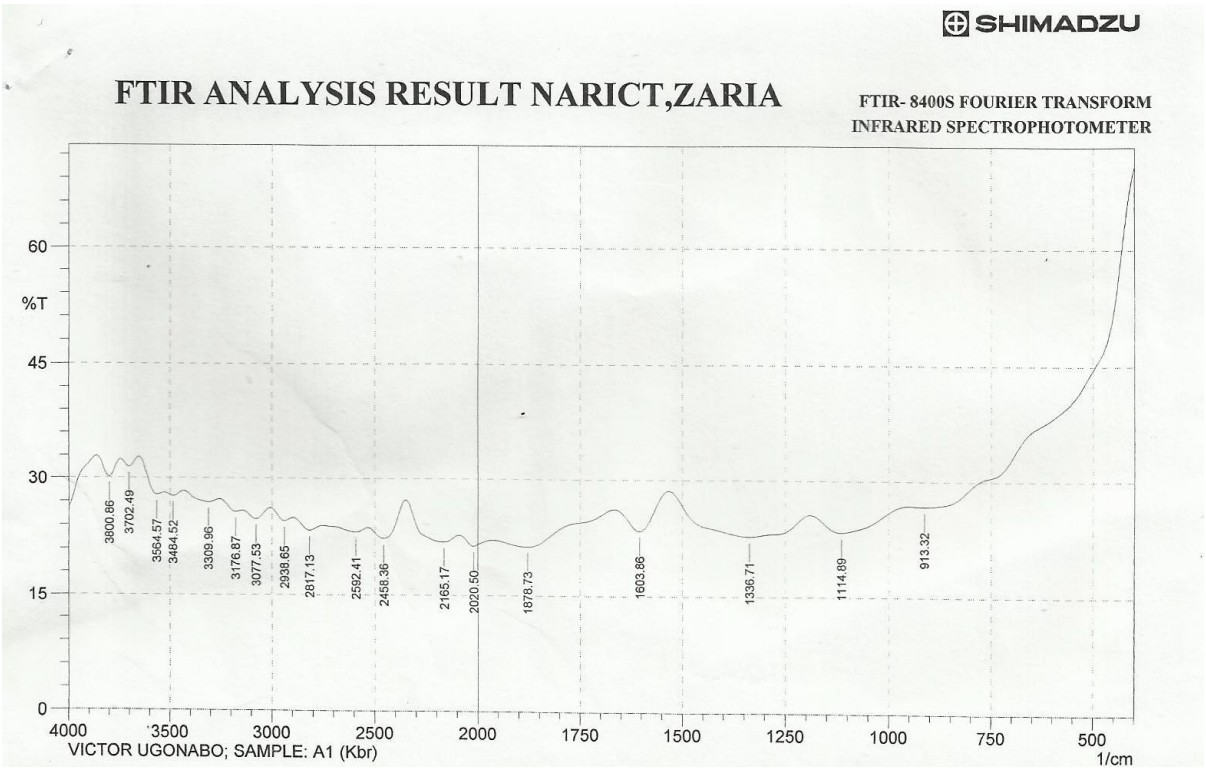

Plate 4.1: FTIR spectrum obtained from BFHA activated carbon**.**

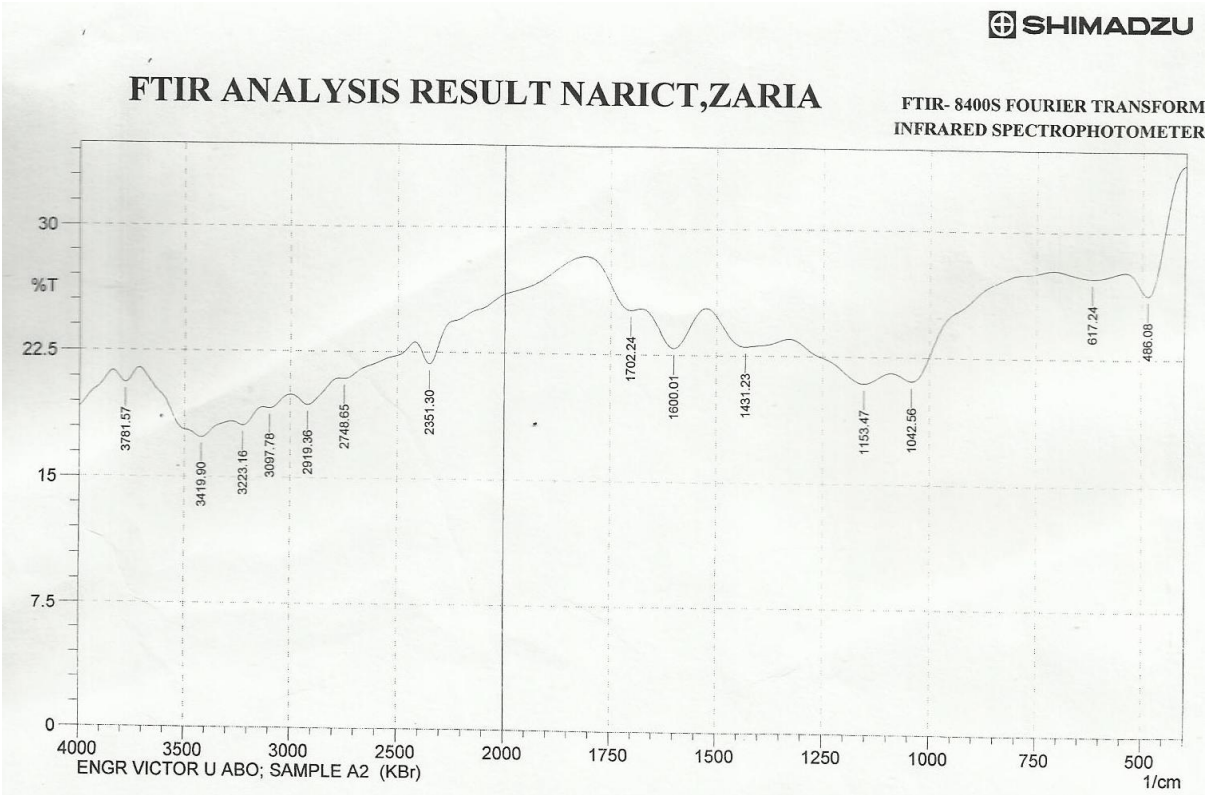

Plate 4.2: FTIR spectrum obtained from MSA activated carbon.

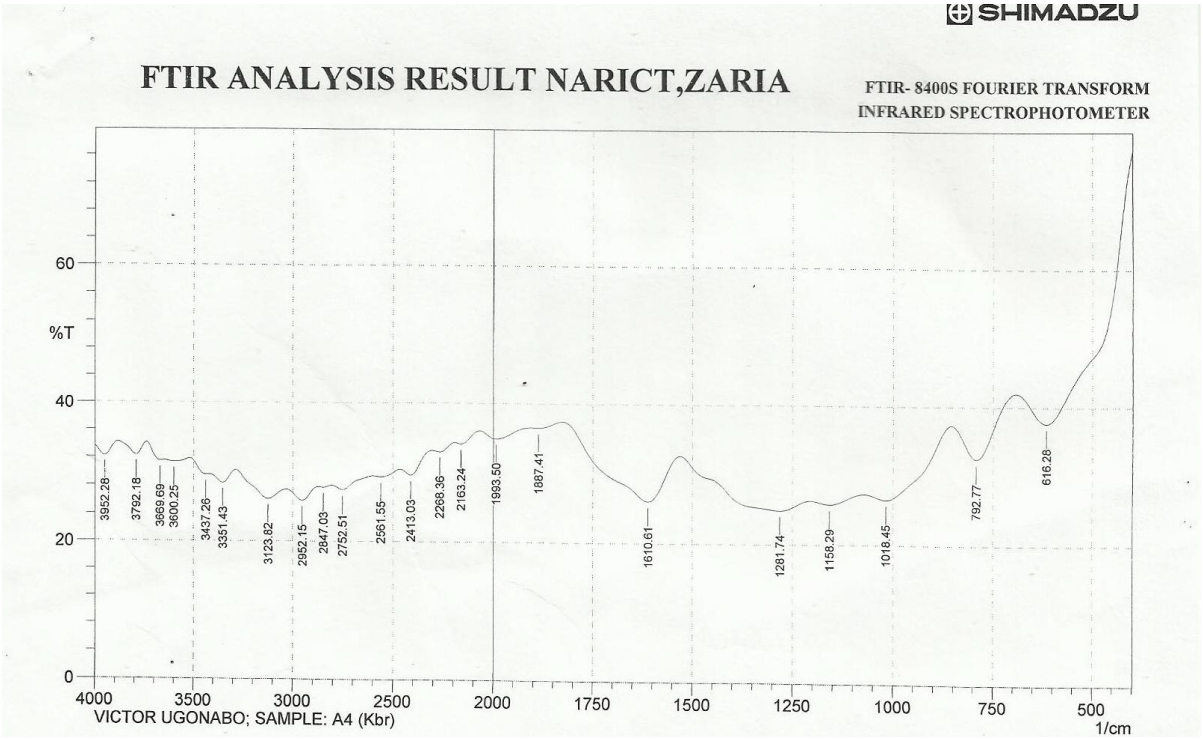

Plate 4.3: FTIR spectrum obtained from RHA activated carbon.

4.2.2.2 FTIR results of laterite and Ukpor clay

The Fourier Transform infra-red FTIR results on activated Laterite and Ukpor clay (Kaolinite) are presented in plates 4.4 and 4.5, respectively. Just like in the previous plates, the observed bands in the range of 4000 – 500 cm^{-1} have been assigned. The discernable band peaks worthy of note are recorded at 3661.01 – 3437.26cm^{-1} and 3973.49 – 3471.98 cm^{-1} for plates 4.4 and 4.5, respectively, indicating the presence of O – H stretching vibrations. Plates 3 and 5 show high Si – O stretching groups, indicating strong presence of quartz only in plate 3. Also most of the bands in plates 4.4 and 4.5, show presence of kaolinite. In plate 4.5, the presence of bands 3973.49 cm^{-1}, 3909.84 cm^{-1}, 3684.16 cm^{-1}, 3576.14 cm^{-1}, 3471.98 cm^{-1} 3384.22 cm^{-1}, 3246.31 cm^{-1}, 3129.61 cm^{-1} 2980.12 cm^{-1}, 2904.89 cm^{-1} indicate the presence of Zaherite. The formation of bands at 569.98 cm^{-1} and 678.00 cm^{-1} indicate the possibility of the presence of kaolin/alumina.

The maximum peaks recorded at 3661.1 cm^{-1}, threshold of 34.26 and 3973.49 cm^{-1}, threshold of 40.14 for plates 4.4 and 4.5 respectively show the presence of Si – O – Si and Al – O – H bends in the samples.

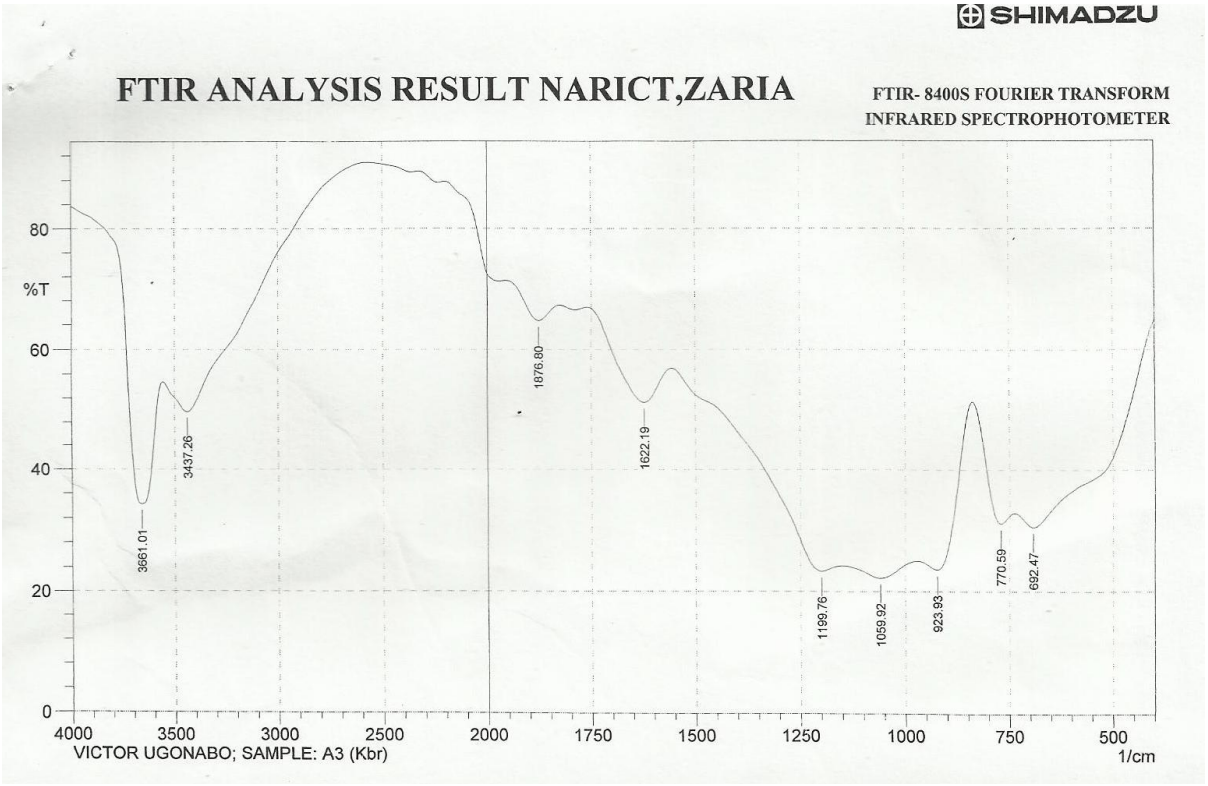

Plate 4.4: FTIR spectrum obtained from activated LATERITE.

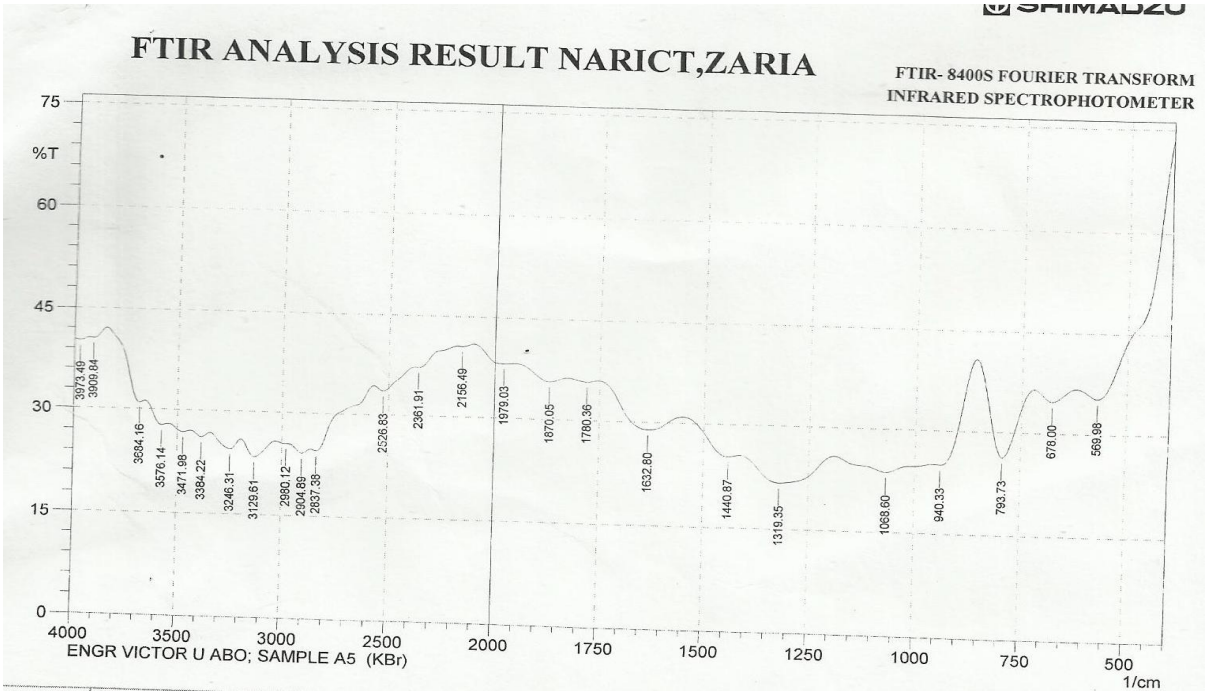

Plate 4.5: FTIR spectrum obtained from activated UCA.

4.2.2.3 XRD results on char activated carbon

The XRD characterization was performed to know the chemical compositions of the minerals that are present in the samples.

The X – ray diffractograms are presented in plates 4.6, 4.7 and 4.9 supported by the corresponding interplanar spacing presented in tables 4.149 to 4.150.

The XRD spectra presented in plate 4.6 showed thirteen peaks at scattering angle of 2θ = 20.8; 26.6°, 36.5 °, 39.4 °, 40.3 °, 42.4 °,, 45.8 °, 50.1 °, 54.8 °, 59.9 °, 67.7 °, 68.8 °,, 77.6 °, with varying relative intensity. The inter planar spacing presented in table 4.147, indicate that peak position two (the maximum peak recorded) has the highest relative intensity of 100% signifying high concentration of quartz and silicate minerals. Peak position thirteen, showed least presence of quartz and silicate mineral. Plate 9, six clear peaks are observed at 2θ = 20.8 °, 26.6 °, 42.4 °, 50.1 °, 59.9 °, 68.2 ° . The interplanar spacing presented in table 4.151 confirmed peak position two to have the highest intensity of 100% followed by peak position one. This is a reflection of where the inherent minerals (silicate, quartz etc) in the sample are found more.

In plate 4.7, the maximum peak position is highlighted at 23° implying that high amount of constituent minerals such as cellulose, the halogens, magnesium, lithium

are located at this point 0.00 displacement, depicting that the atomic structure of charred activated carbon from mango seed (MSA) is a primitive lattice structure. Thus, the diffraction pattern indicates the crystalline nature of MSA.

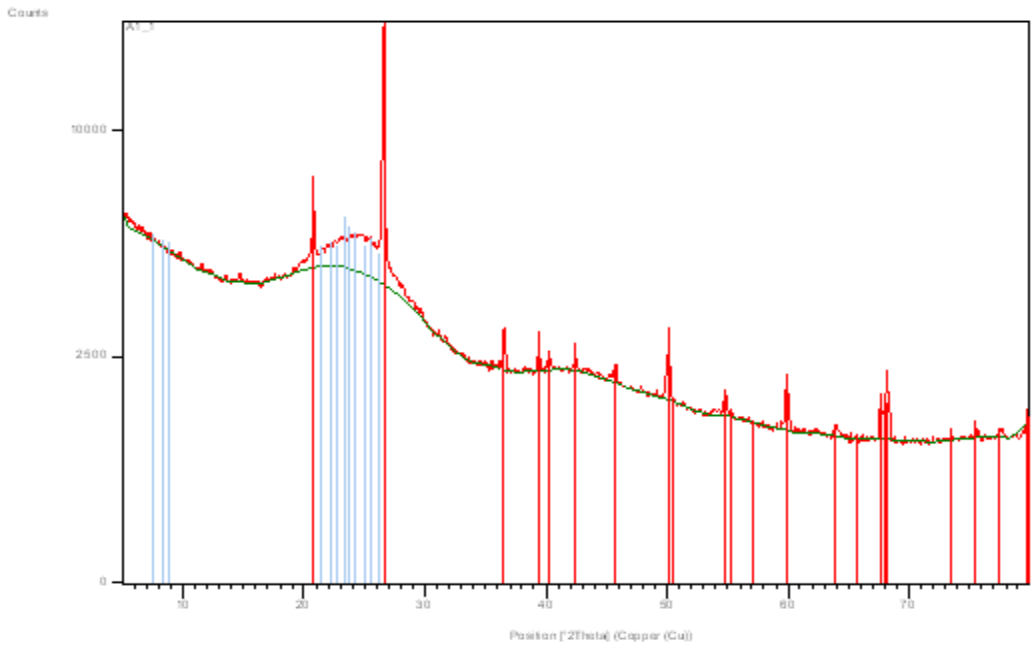

Plate 4.6 : XRD pattern of BFHA

Table 4.149: Inter spatial planes between atomic lattices of BFHA

Pos.[°2Th.]	Height[cts]	FWHM[°2Th.]	d-spacing[Å]	Rel.Int.[%]
20.7920	1924.02	0.1978	4.27229	17.38
26.5826	11073.43	0.1978	3.35333	100.00
36.5184	1004.72	0.1978	2.46057	9.07
39.4040	410.95	0.2637	2.28678	3.71
40.2712	266.80	0.2637	2.23951	2.41
42.3894	282.23	0.3956	2.13238	2.55
45.7521	407.86	0.1978	1.98317	3.68
50.1176	1026.77	0.2637	1.82019	9.27
54.8063	406.26	0.2637	1.67505	3.67
59.9146	852.10	0.2637	1.54387	7.70
67.6640	732.00	0.1978	1.38468	6.61
68.1724	1194.56	0.1978	1.37559	10.79
77.5862	127.59	0.4824	1.22951	1.15

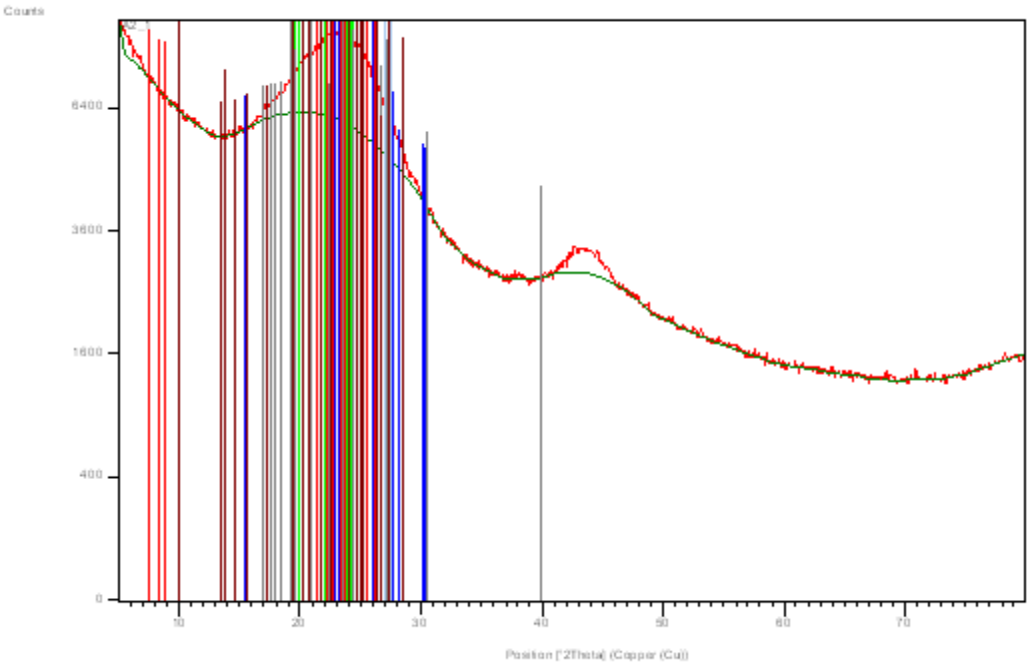

Plate 4.7: XRD pattern of MSA

Table 4.150: XRD pattern list of MSA

Visible	Ref.Code	Score	Compound Name	Displ.[°2Th]	Scale Fac.	Chem. Formula
*	00-026-1652	85	Cobalt phenanthrol	0.000	1.229	C36 H24 Cl2 Co N6 ..
*	00-042-0144	72	Lithium Scandium	0.000	1.226	Li3 Sc2 As3 O12
*	00-048-2061	96	7-chloro-5-(2-chlo..	0.000	1.027	C15 H10 Cl2 N2 O2
*	00-055-1919	74	Magnesium bis(o-ph..	0.000	1.343	C24 H16 Cl2 Mg N4 O8
	00-037-1240	76	á-Gd (Re O4)3	0.000	1.207	Gd (Re O4) 3

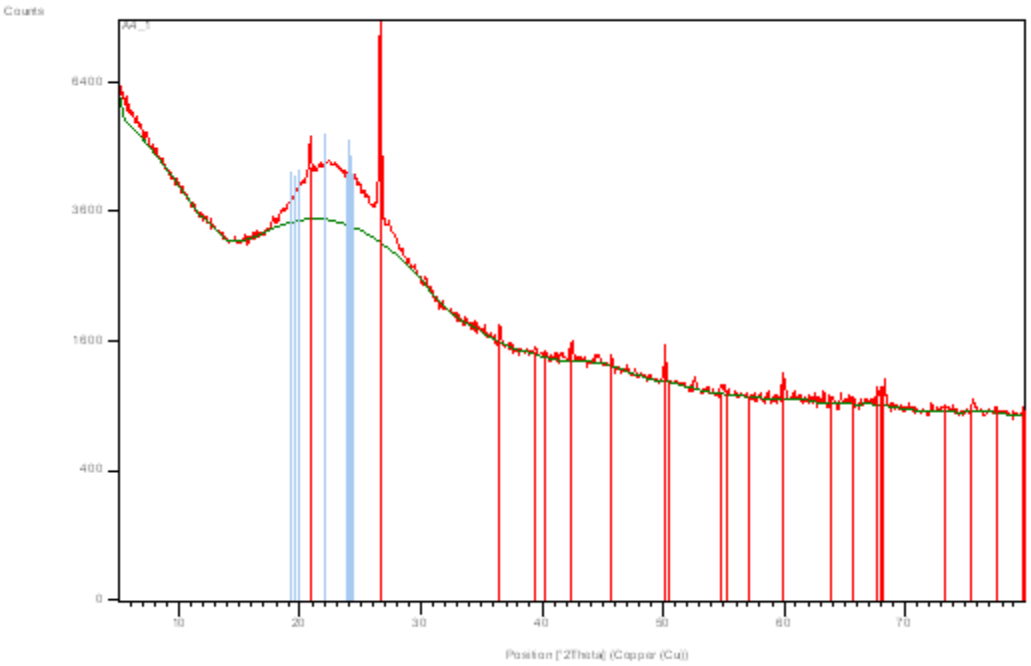

Plate 4.8 : XRD pattern of RHA

Table 5.151: Inter spatial planes between atomic lattices of RHA

Pos.[°2Th.]	Height[cts]	FWHM[°2Th.]	d-spacing[Å]	Rel.Int.[%]
20.8334	1674.62	0.1978	4.26390	31.41
26.6337	5330.89	0.1978	3.34701	100.00
42.4337	214.86	0.2637	2.13025	4.03
50.1459	202.54	0.2637	1.81923	3.80
59.9078	247.92	0.1978	1.54403	4.65
68.2482	183.64	0.8040	1.37311	3.44

4.2.2.4 XRD of activated laterite and Ukpor clay

The XRD shown in plates 4.8 and 4.10 supported by the corresponding interplannar spacing presented in tables 4.151 and 4.152, indicate that, silica oxide, alumina, kaolinite are present in major quantities while other minerals; quartz and Zaherite are present in trace amounts. This confirms the chemical analysis of the samples.

In plate 4.8, twenty four clear peak positions are assigned due to its different reflections and planes. The maximum and minimum peak positions are recorded at

angle 2θ= 26.6 °, and 65.8 °, with corresponding intensity. The minimum peak position signifies locations where you have high concentration of the trace minerals.

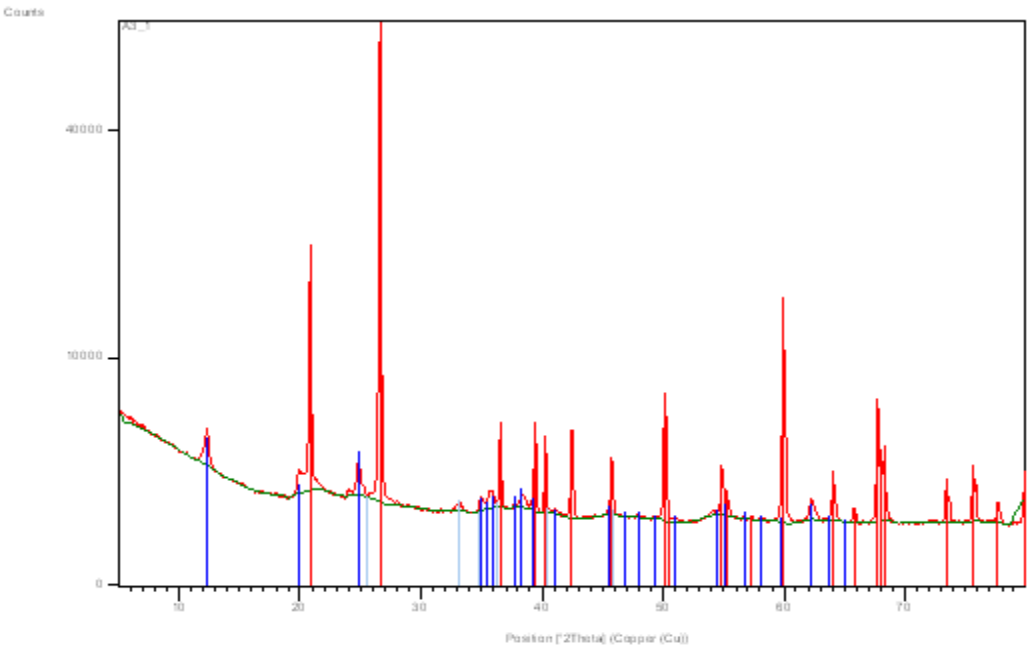

Plate 4.9 : XRD pattern of LATERITE

Table 4.152: Inter spatial planes between atomic lattices of LATERITE

Pos.[°2Th.]	Height[cts]	FWHM[°2Th.]	d-spacing[Å]	Rel.Int.[%]
12.3148	2060.49	0.2637	7.18756	3.40
19.8837	920.78	0.1978	4.46536	1.52
20.8408	20631.68	0.1978	4.26240	34.09
24.8623	1539.95	0.2637	3.58131	2.54
26.6125	60519.72	0.1978	3.34963	100.00
33.1381	300.99	0.5274	2.70342	0.50
34.9698	404.86	0.2637	2.56591	0.67
35.9160	547.42	0.3956	2.50044	0.90
36.5208	3682.21	0.1978	2.46042	6.08
38.4139	453.87	0.3296	2.34341	0.75
39.4491	3788.48	0.1978	2.28427	6.26
40.2872	3298.93	0.1978	2.23866	5.45

42.4602	3962.08	0.1978	2.12899	6.55
45.7820	2156.65	0.1978	1.98195	3.56
50.1445	6193.35	0.1978	1.81927	10.23
54.8729	1650.31	0.1978	1.67317	2.73
59.9773	11490.97	0.2637	1.54240	18.99
62.2482	597.81	0.2637	1.49148	0.99
64.0541	1748.32	0.1978	1.45372	2.89
65.8430	209.44	0.2637	1.41849	0.35
67.7085	5114.40	0.1978	1.38388	8.45
73.4289	1370.64	0.2637	1.28956	2.26
75.6076	2068.00	0.3296	1.25773	3.42
77.6163	635.33	0.2412	1.22911	1.05

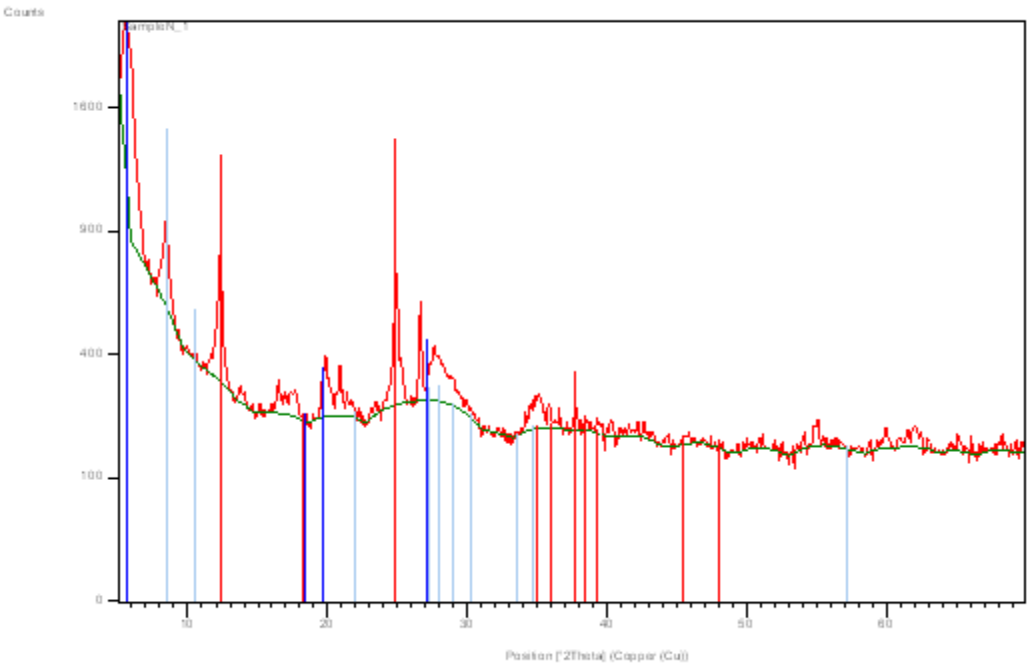

Plate 4.10 : XRD pattern of UCA

Table 4.153: Inter spatial planes between atomic lattices of UCA

Pos.[°2Th.]	Height[cts]	FWHM[°2Th.]	d-spacing[Å]	Rel.Int.[%]
5.5308	1203.51	0.4133	15.97910	100.00
8.4494	407.03	0.3306	10.46501	33.82
12.3127	500.46	0.3306	7.18875	41.58
19.7932	146.50	0.3306	4.48557	12.17
24.8794	452.43	0.3306	3.57889	37.59
26.6350	326.32	0.2480	3.34685	27.11
27.5859	149.27	0.6612	3.23360	12.40

4.2.2.5 SEM analysis of activated Adsorbents

SEM technique was employed to study the effect of activation on adsorbents porosity development. SEM studies were carried out for BFHA, RHA, MSA based char activated carbon and activated LATERITE, UCA adsorbents respectively. SEM images of the samples were obtained by Zeiss EVO(R) MA15 EDX/WDS and presented in plates 4.11 – 4.15. The images on the plates, show irregular and heterogeneous surface morphology, and appear varieties of pores in different widths, though this is more pronounced in plates 4.11, 4.12, 4.14. The presence of more irregular surface could be due to a more complex network of pores. This supports the notion that increasing H_2SO_4 soaking temperature at a higher impregnation ratio can intensify the attack of the acid on the botanical structure, hence altering the surface morphology of char based activated carbon (Wannapeera, et al, 2008). This activation process is dependent on the nature of the raw materials, which is mainly composed of cellulose as can be seen in the samples presented in plates 4.11, 4.12 and 4.14. Due to the electrolytic action of activation agent, cellulose undergoes swelling, prompting the lateral bonds breakdown resulting in the inter–and intra-micelle voids increase under the effect of chemical reactions (Malik, et al; 2006; Smisek and Cerny, 1970). Consequently this will lead to dehydration, decomposition of organic matter occurrence, causing high porosity of activated carbon under the effect of chemical activation.

The morphological change of MSA char was clearly different from others. The extensive widening of pores and changes in particle geometry were clearly observed for

MSA char. These behaviors are likely due to low lignin and high cellulose contents. The low lignin content is responsible for the weak structure of the biomass cell wall

(Wannapeera, et al, 2008; Saka, 2000) . Among the five samples studied MSA chars were generally most reactive while non char activated adsorbent were the least reactive. This is understandable because the structure is composed of compact lattice of Kaolinite, quartz and Zeharite while the biomass (MSA) high reactivity could be attributed to high proportion of chemical component of each biomass, especially cellulose and lignin (Wannapeera, et al, 2008; Saka, 2000).

Finally, observation from the micrographs presented in plates 4.11– 4.15 show that activation play key role in transforming inert carbon porosity development which is largely responsible for the extent of surface area and adsorptive capacity of carbon more especially in plates 4.12 which has proved to be best among other adsorbents studied.

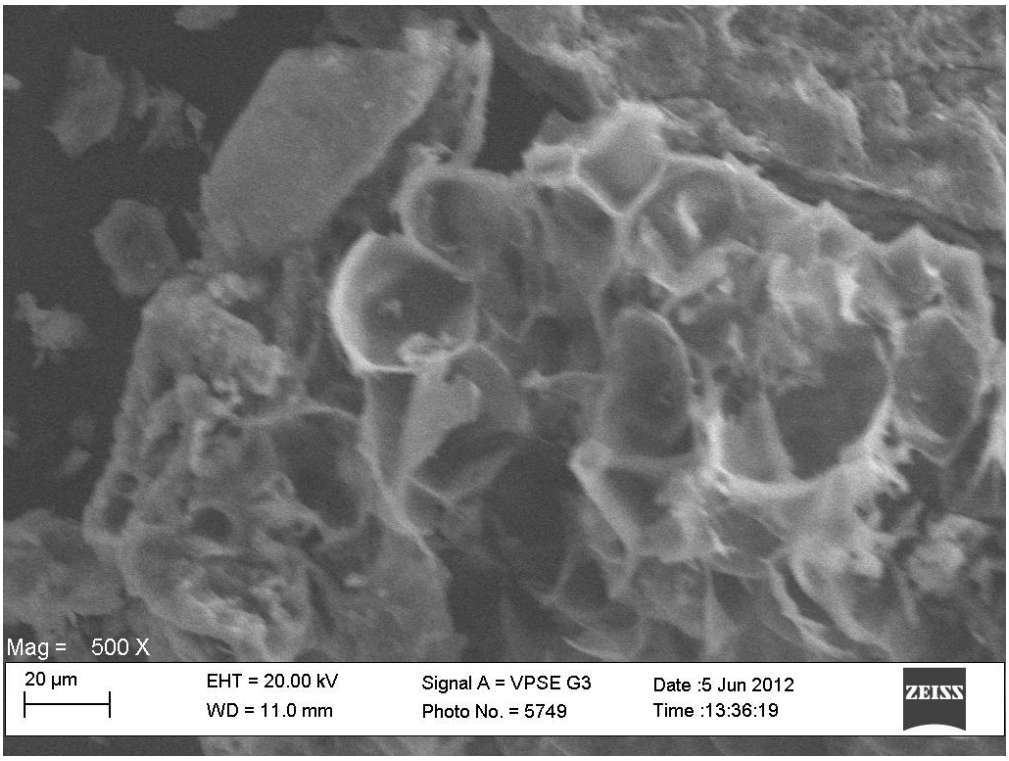

Plate 4.11: SEM image of BFHA activated carbon at 500 times magnification

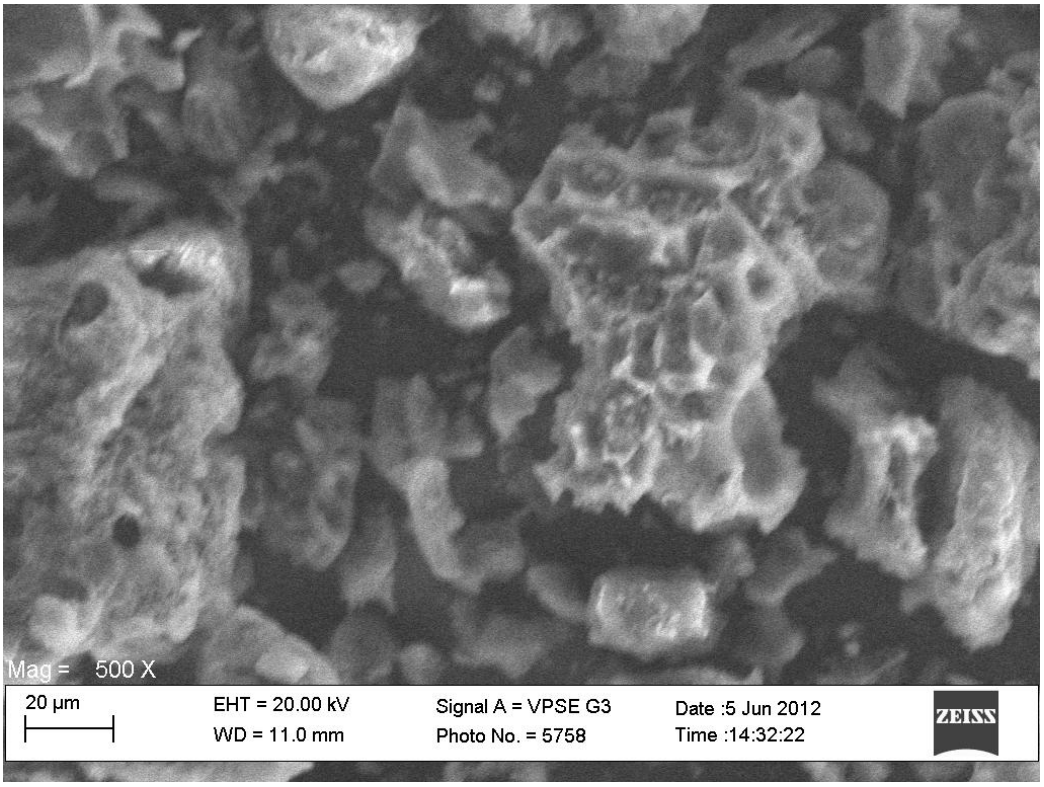

Plate 4.12: SEM image of MSA activated carbon at 500 times magnification

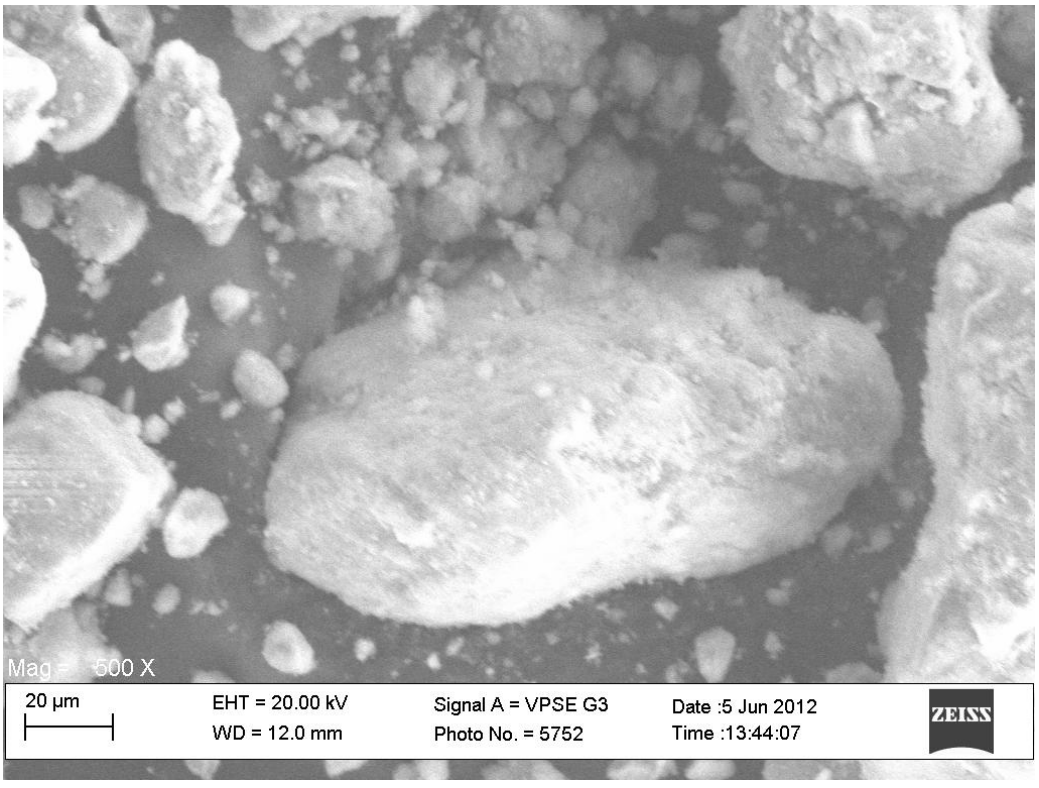

Plate 4.13: SEM image of activated LATERITE at 500 times magnification

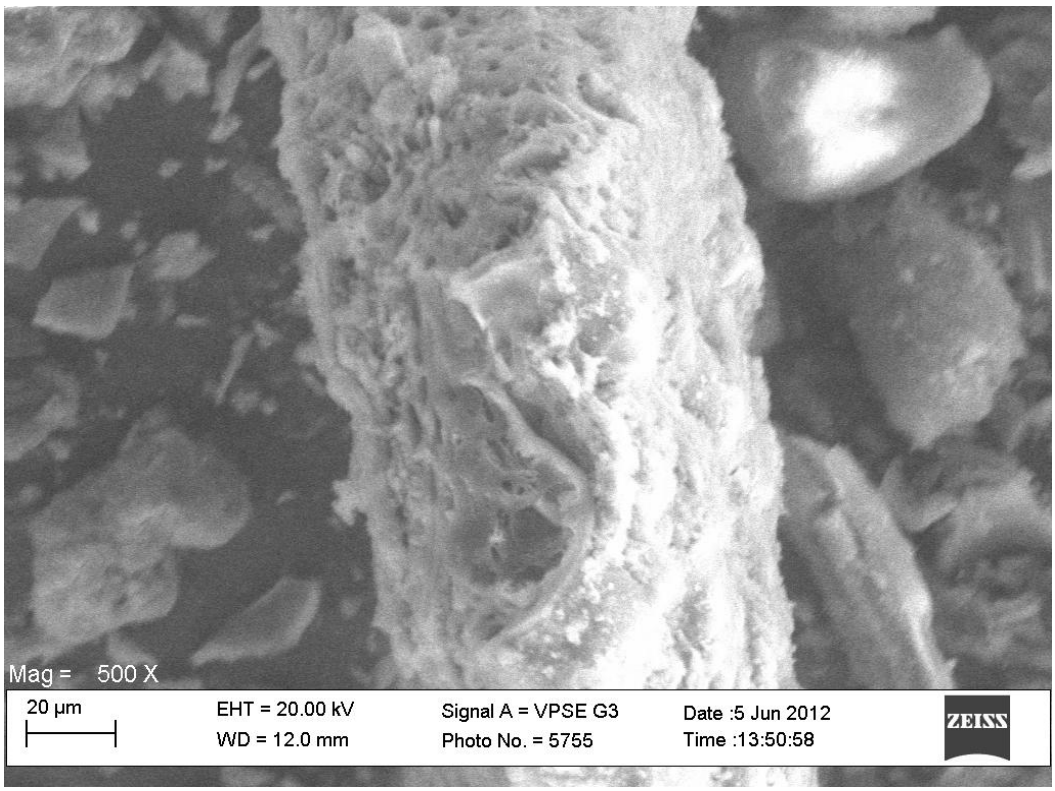

Plate 4.14: SEM image of RHA activated carbon at 500 times magnification

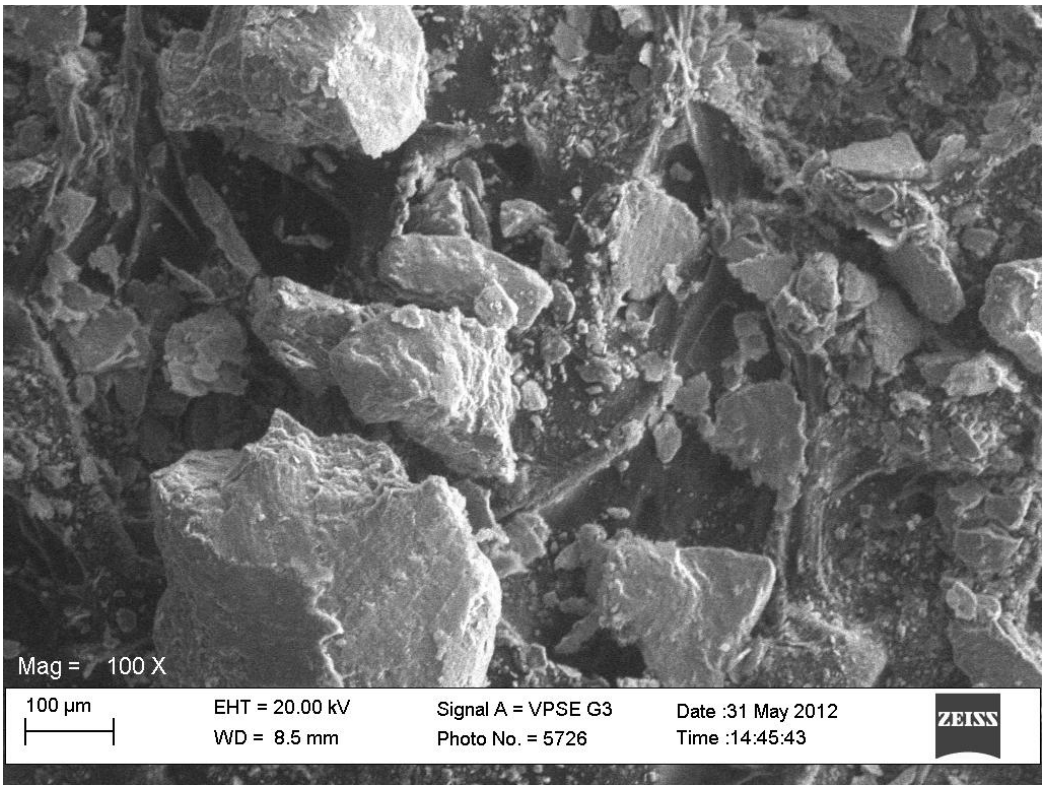

Plate 4.15: SEM image of activated UCA at 100 times magnification

4.2.3 PERCENTAGE REMOVAL OF ADSORBATE FOR VARYING ADSORBE NT CONCENTRATION IN PIE AND VIE.

This presents the effect of time in adsorbate percentage removal for PIE and VIE at varying adsorbent dosages. The studies were conducted at varying stirring time; 5 to 60mins, at adsorbent mass concentration of 0.2, 0.4, 0.6, 0.8 and 1.0g/l. The adsorbents employed are BFHA, RHA, LATERITE, UCA and MSA. The results for PIE and VIE are presented in figures 4.417 to 4.466

The remarkable features existing amongst the figures in this section is the fact that % adsorbate removal increases with both time and adsorbent mass concentration. This phenomenon explains why the lowest % removal is recorded for 0.2g/l and increases progressively to that of 1.0g/l and corresponding maximum time of 60mins. This increase is because at the higher dose of the adsorbent with increased surface area, more adsorption sites are available causing higher removal of TDSS (Wannapeera, et al, 2008).

In case of PIE it can be observed that the % removal of TDSS by different adsorbents is enhanced because the TDSS particles are dissociated and the attractive interactions predominates except for UCA at pH 6 where dispersive/repulsive interactions is prevalent as shown in figure 4.433.The strong interaction between the surface of the adsorbents and TDSS is very apparent in figure 4.432 where the results show minimal variation in % removal with respect to both time and dosages. The closeness of the graphs suggest that the effect of van der waals and electrostatic interactions cannot be neglected and indeed they appear to be dominant. Hence it illustrates the ability of the adsorbent to uptake all TDSS at various doses and time; indicating that the amount of adsorbate (TDSS) removed remain approximately near same (Gang , 2007: Krozel , 1993).

The results for the VIE are presented in figures 4.441 to 4.466. With the exceptions of figures 4.455 and figure. 4.456, all other figures show a similar trend as observed in figure 4.433 of PIE, of having relatively scattered graphs, suggesting less dissociation of the TDSS into radicals, coupled with the fact that VIE does not contain as much TDSS as there are in PIE. The implication is that some portions of the exchangeable sites will remain bare at the end of the adsorption process.

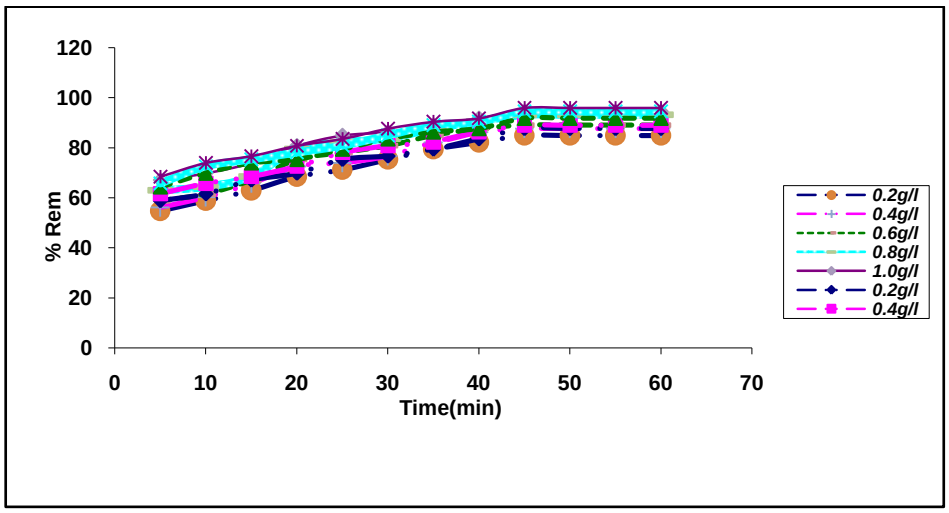

Fig. 4.417: %Removal of adsorbate from PIE for varying BFHA dosage and pH 2

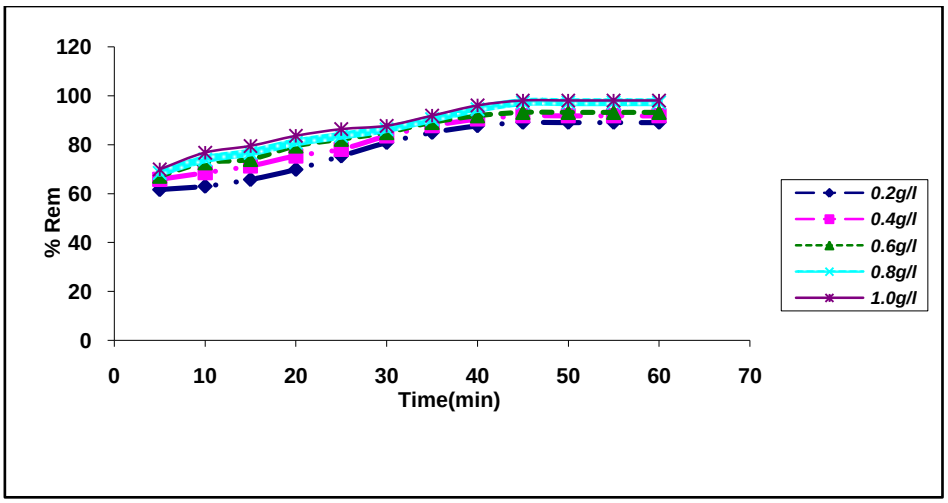

Fig.4.418 : %Removal of adsorbate from PIE for varying BFHA dosage and pH 4

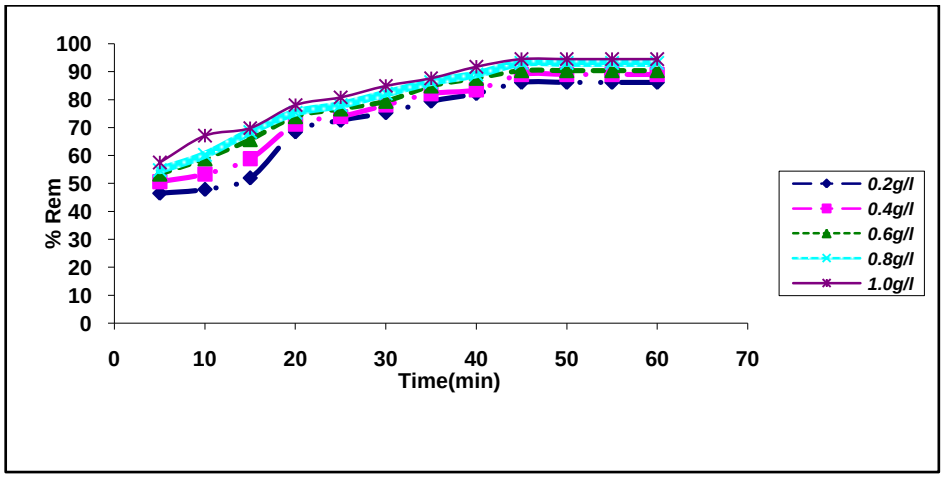

Fig.4.419 : %Removal of adsorbate from PIE for varying BFHA dosage and pH 6

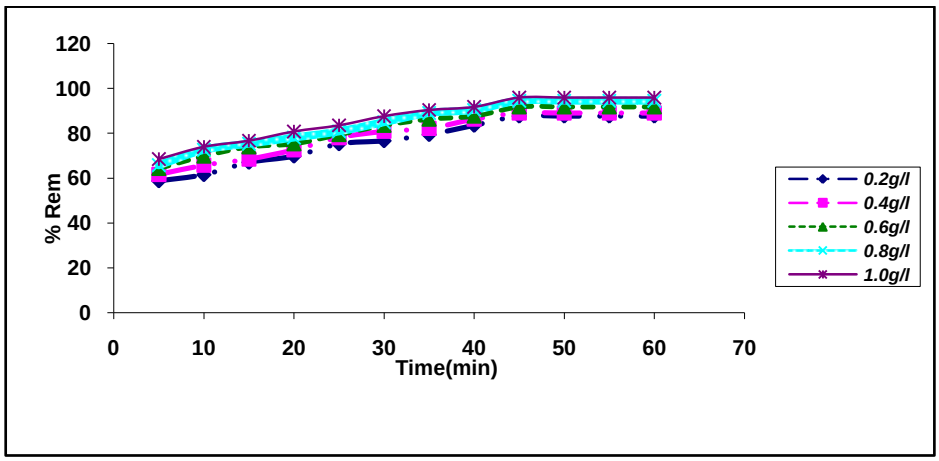

Fig.4.420 : %Removal of adsorbate from PIE for varying BFHA dosage and pH 8

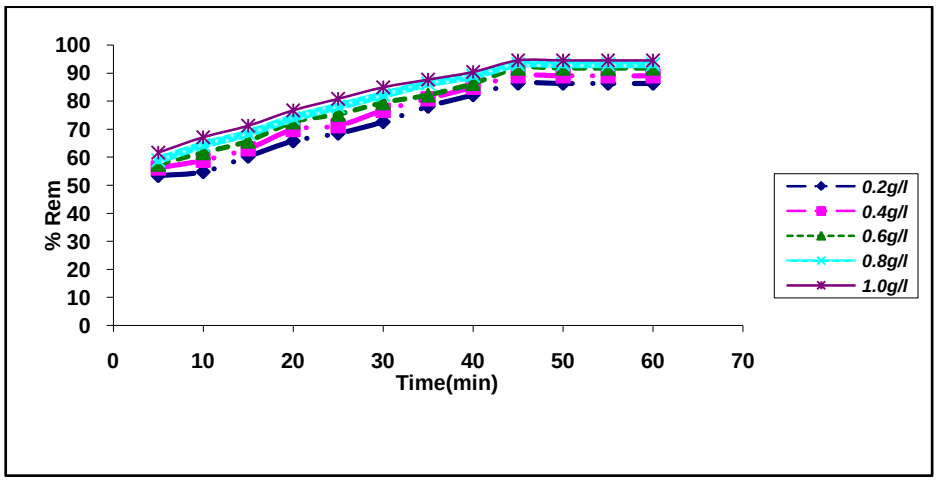

Fig.4.421 : %Removal of adsorbate from PIE for varying BFHA dosage and pH 10

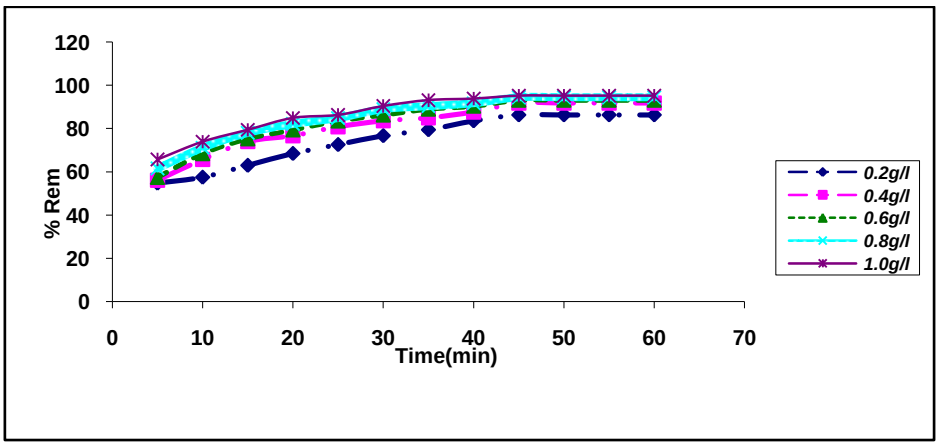

Fig.4.422 : %Removal of adsorbate from PIE for varying RHA dosage and pH 2

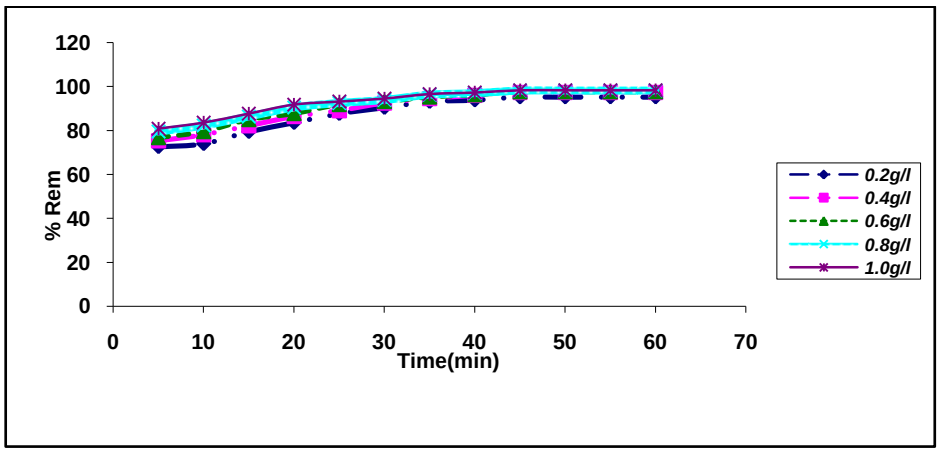

Fig.4.423 : %Removal of adsorbate from PIE for varying RHA dosage and pH 4

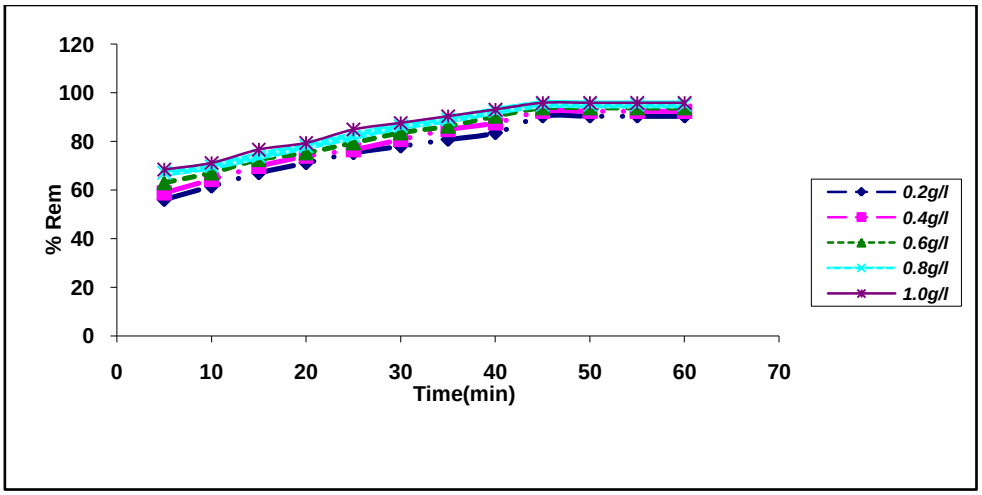

Fig.4.424 : %Removal of adsorbate from PIE for varying RHA dosage and pH 6

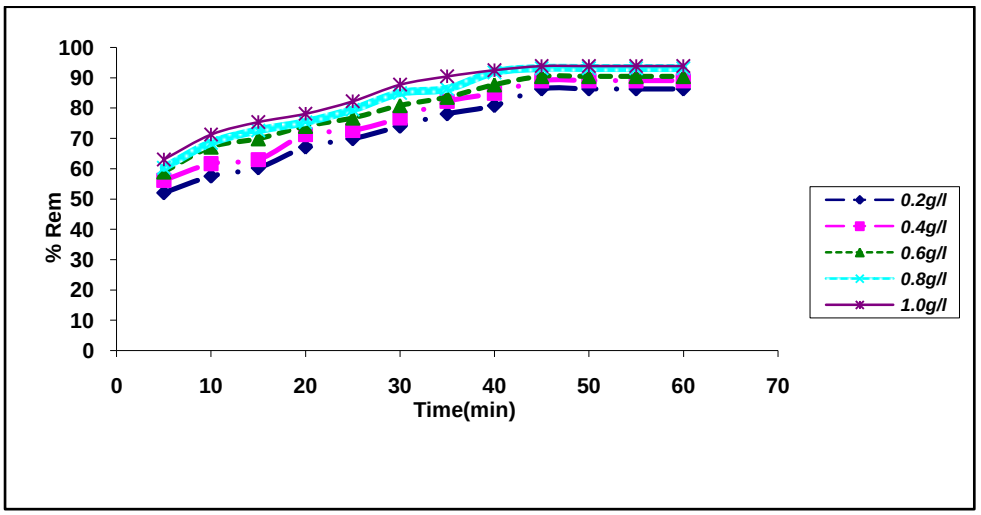

Fig.4.425 : %Removal of adsorbate from PIE for varying RHA dosage and pH 8

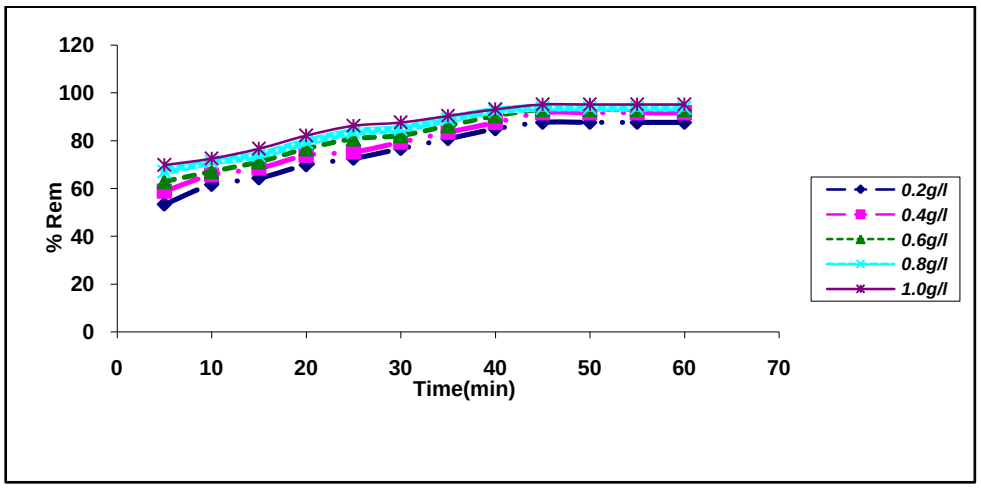

Fig.4.426 : %Removal of adsorbate from PIE for varying RHA dosage and pH 10

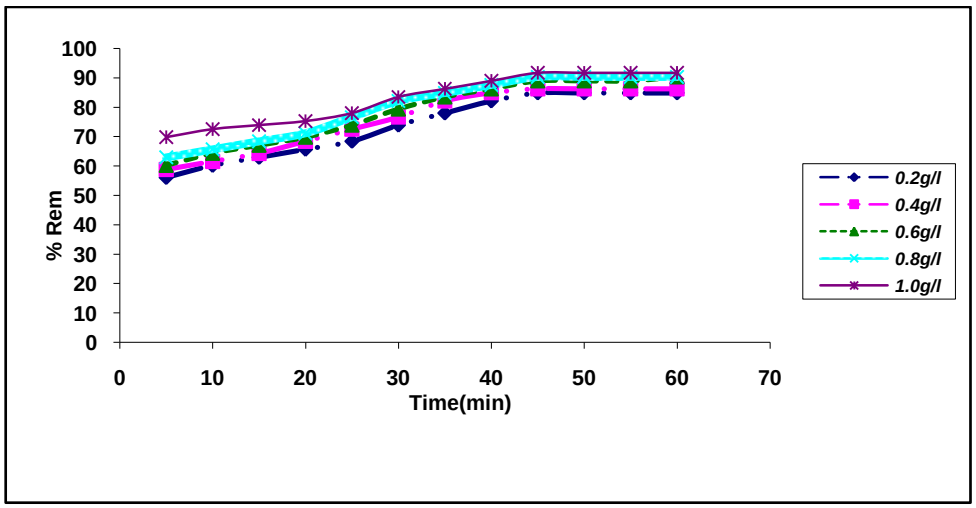

Fig.4.427 : %Removal of adsorbate from PIE for varyingLaterite dosage and pH 2

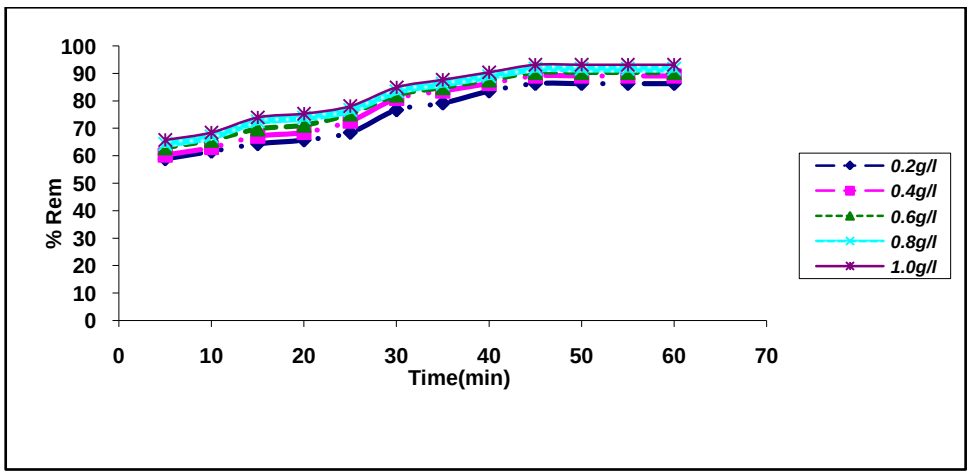

Fig.4.428 : %Removal of adsorbate from PIE for varying Laterite dosage and pH 4

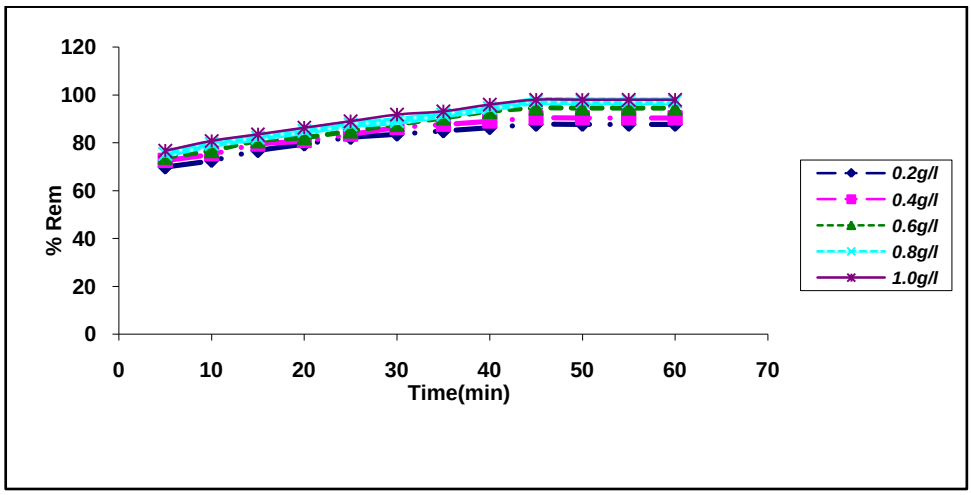

Fig.4.429 : %Removal of adsorbate from PIE for varying Laterite dosage and pH 6

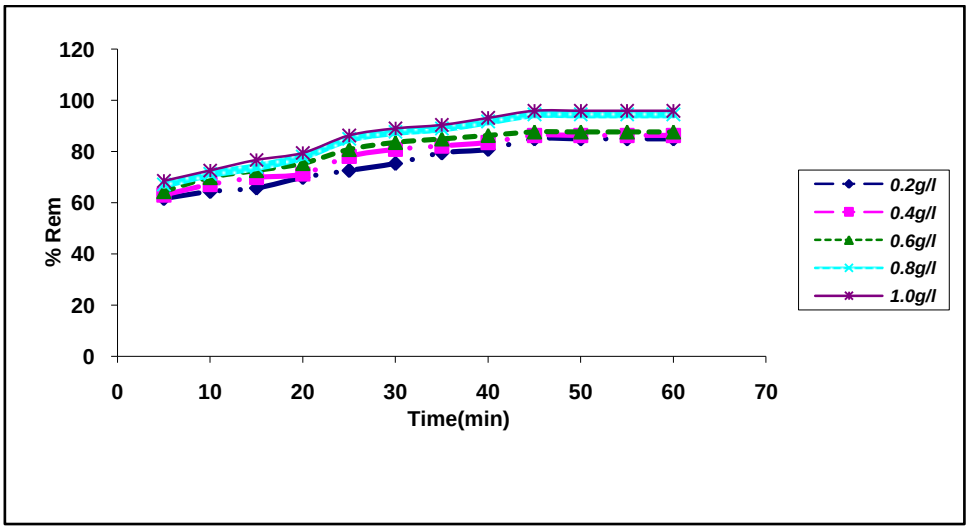

Fig.4.430 : %Removal of adsorbate from PIE for varying Laterite dosage and pH 8

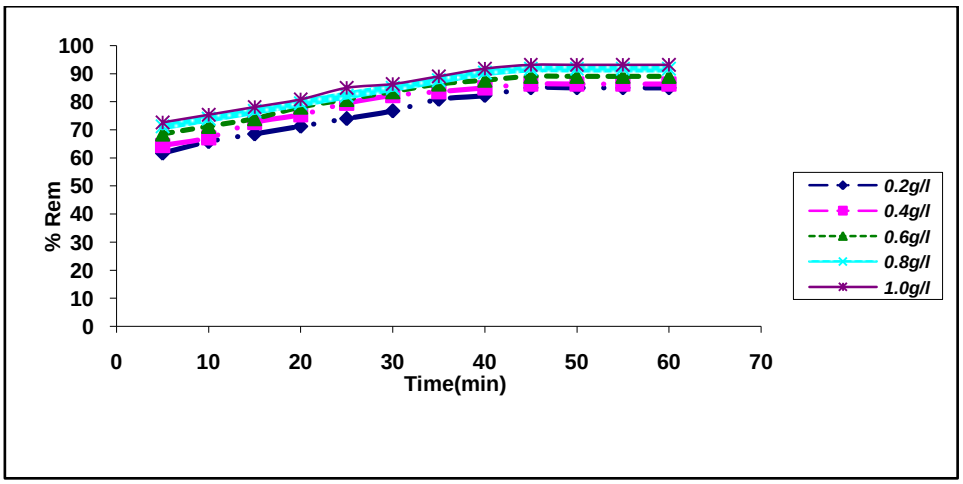

Fig.4.431 : %Removal of adsorbate from PIE for varying Laterite dosage and pH 10

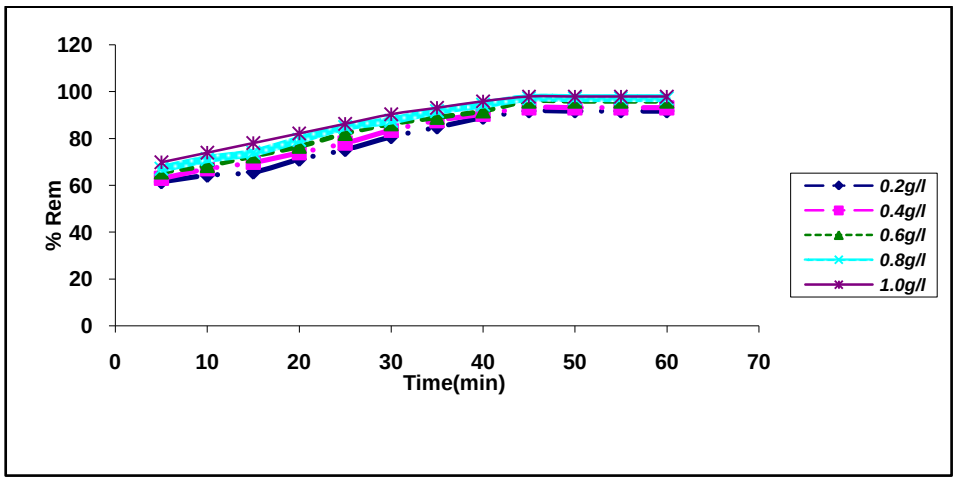

Fig.4.432: %Removal of adsorbate from PIE for varying UCA dosage and pH 2

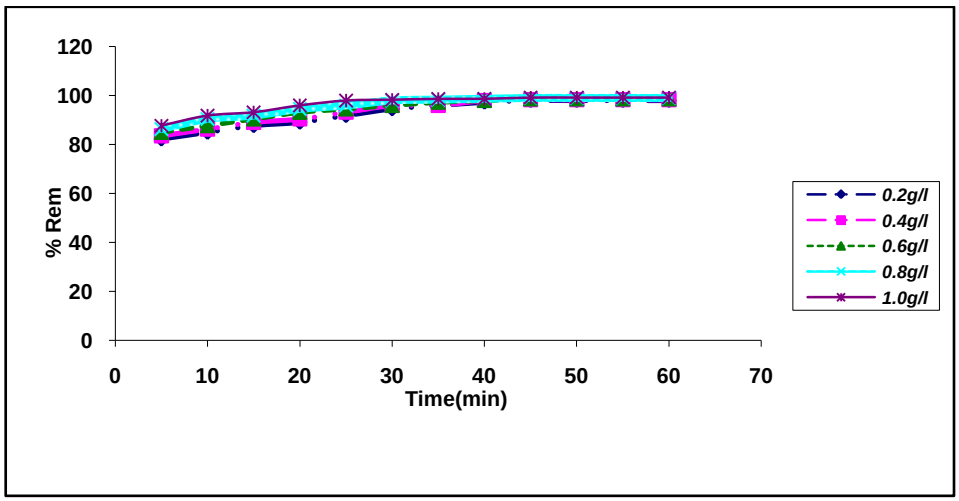

Fig.4.433: %Removal of adsorbate from PIE for varying UCA dosage and pH 4

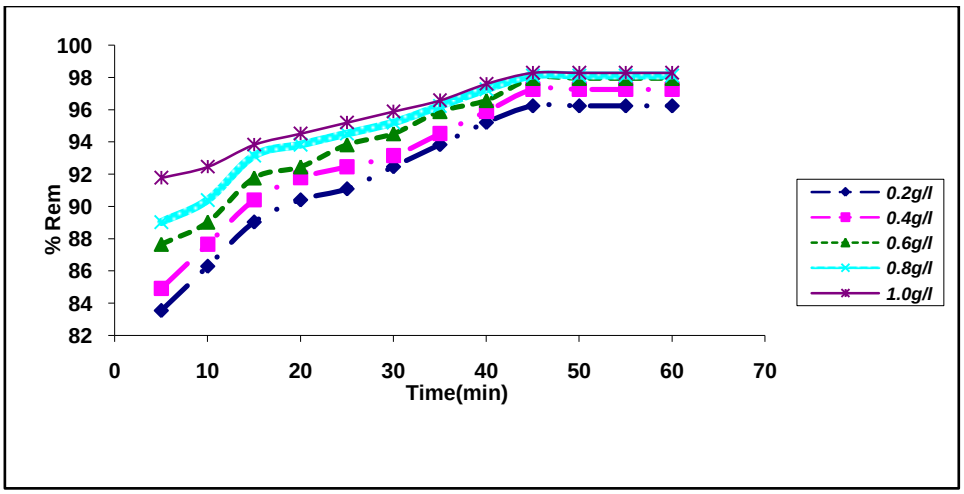

Fig.4.434: %Removal of adsorbate from PIE for varying UCA dosage and pH 6

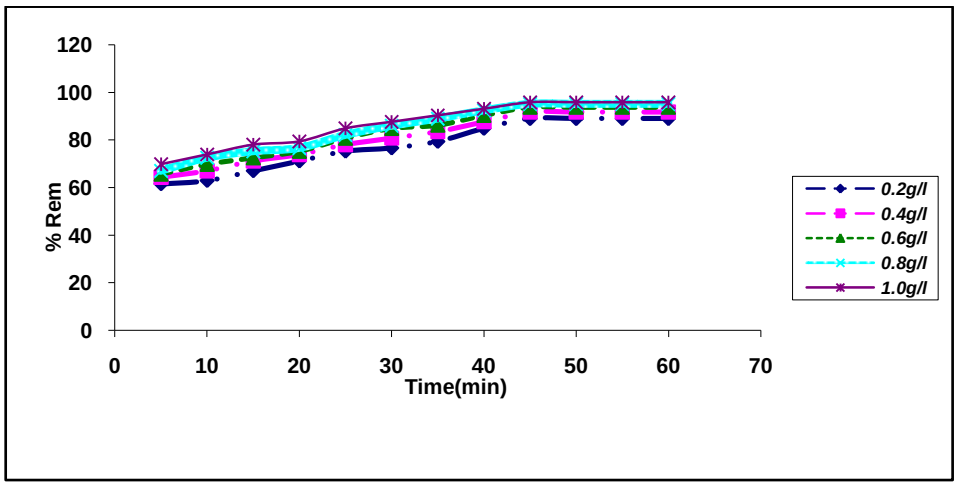

Fig.4.435: %Removal of adsorbate from PIE for varying UCA dosage and pH 8

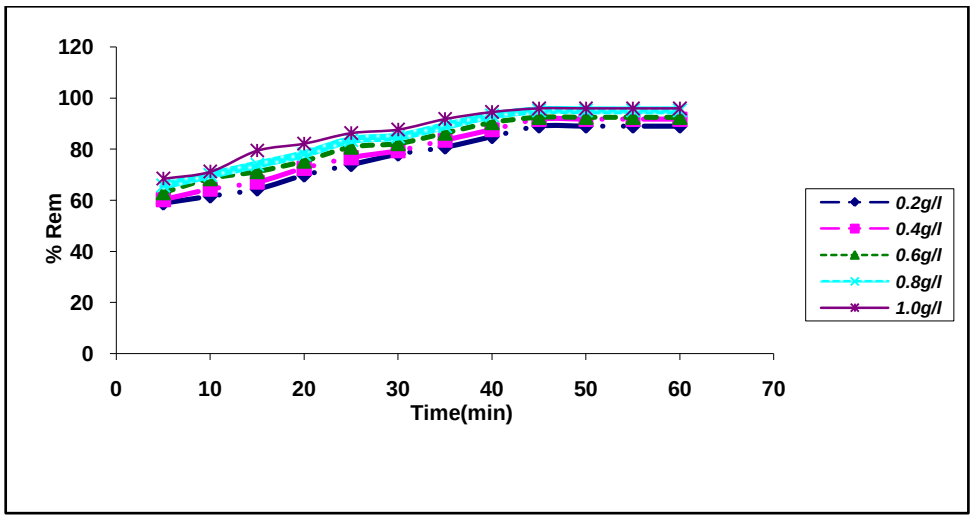

Fig.4.436: %Removal of adsorbate from PIE for varying UCA dosage and pH 10

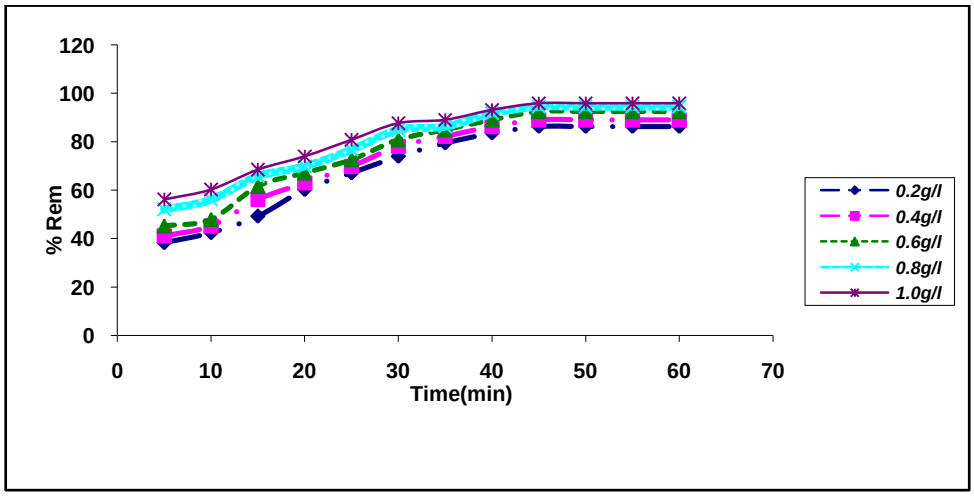

Fig.4.437 : %Removal of adsorbate from PIE for varying MSA dosage and pH 2

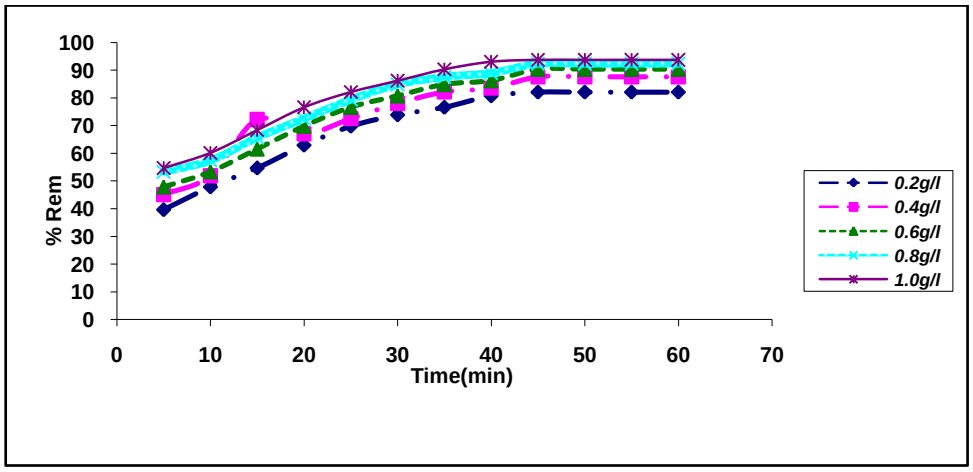

Fig.4.438 : %Removal of adsorbate from PIE for varying MSA dosage and pH 4

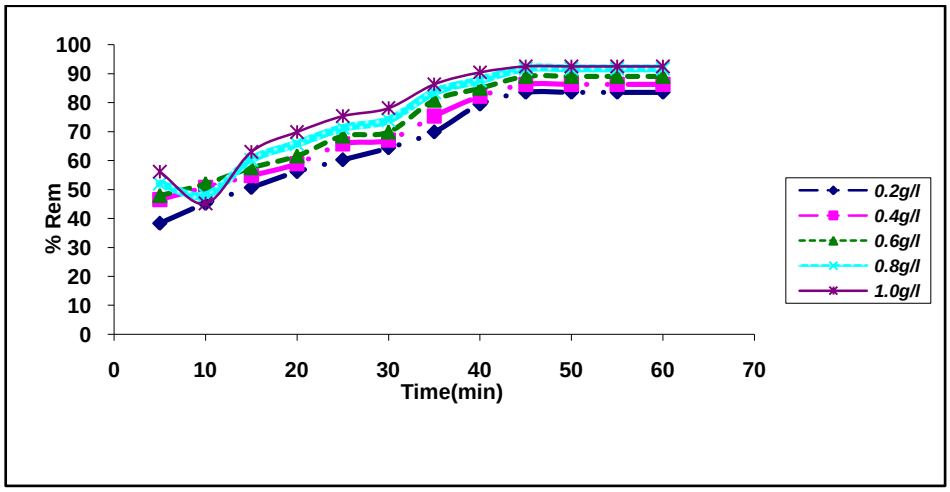

Fig.4.439 : %Removal of adsorbate from PIE for varying MSA dosage and pH 6

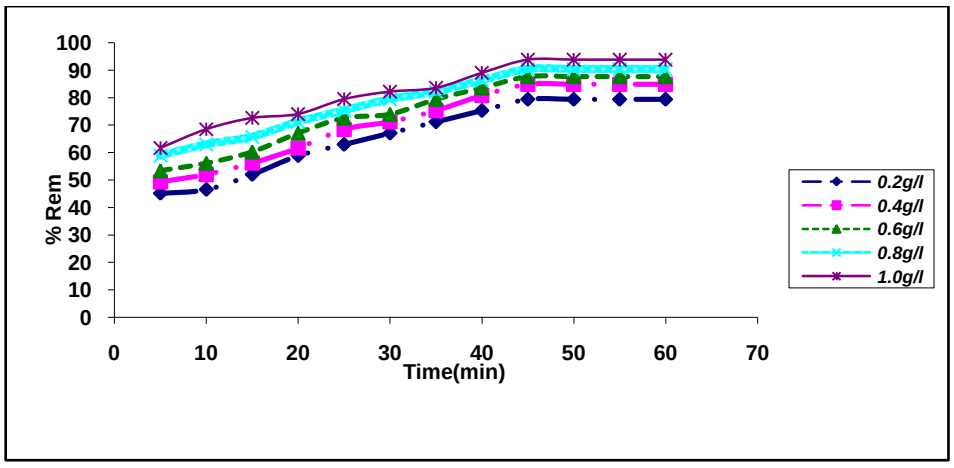

Fig.4.440 : %Removal of adsorbate from PIE for varying MSA dosage and pH 8

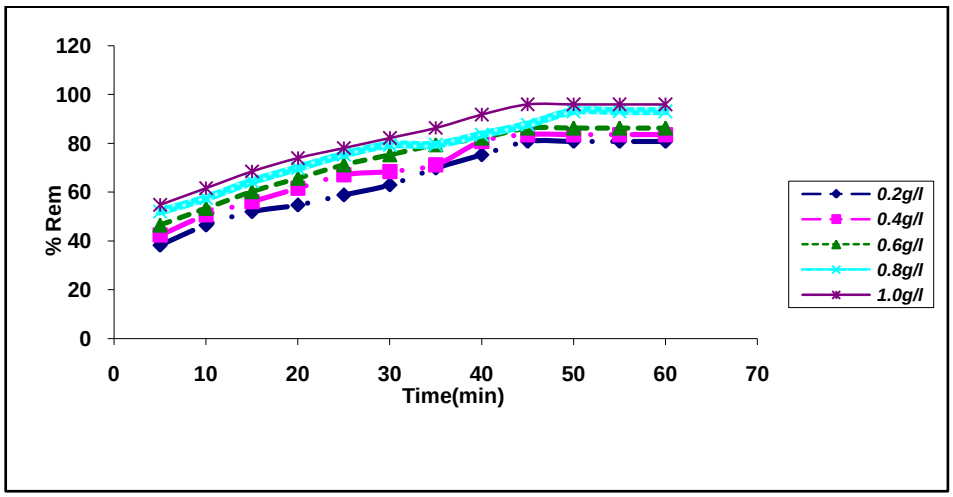

Fig.4.441 : %Removal of adsorbate from PIE for varying MSA dosage and pH 10

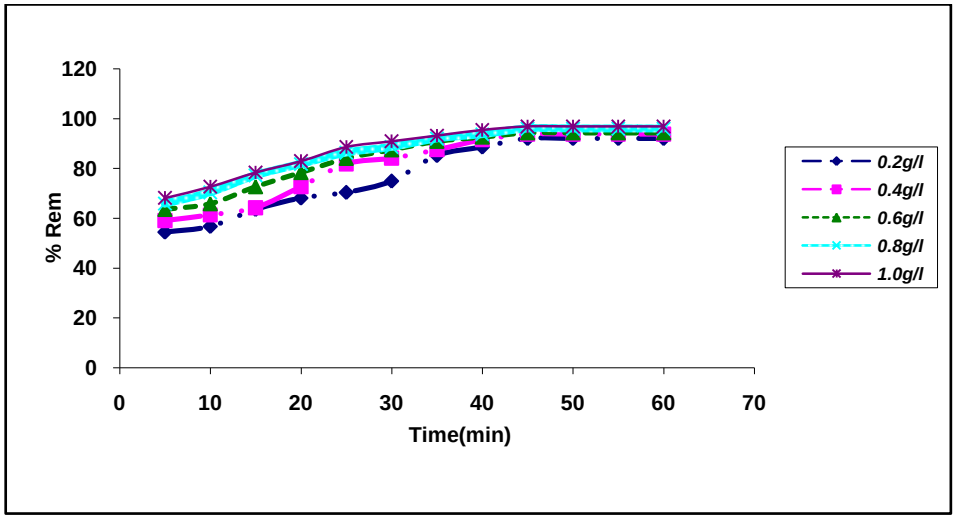

Fig.4.442: %Removal of adsorbate from VIE for varying BFHA dosage and pH 2

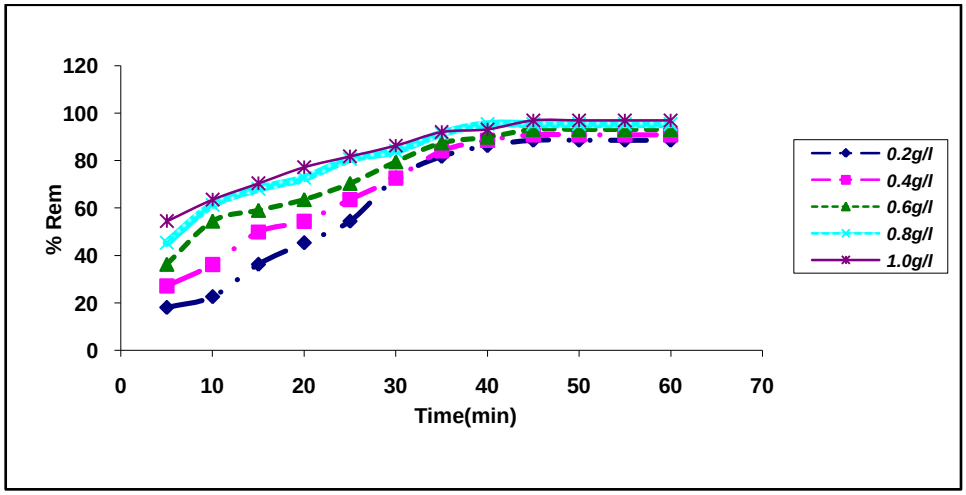

Fig.4.443: %Removal of adsorbate from VIE for varying BFHA dosage and pH 4

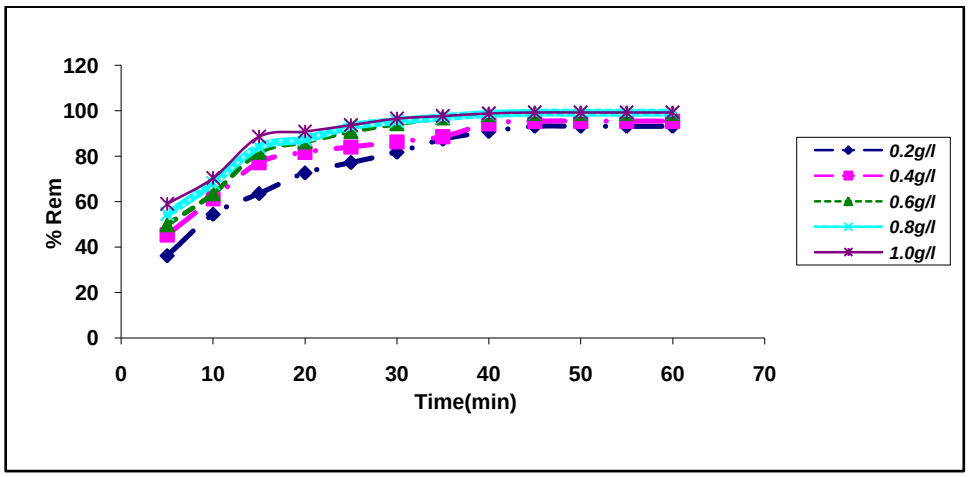

Fig.4.444: %Removal of adsorbate from VIE for varying BFHA dosage and pH 6

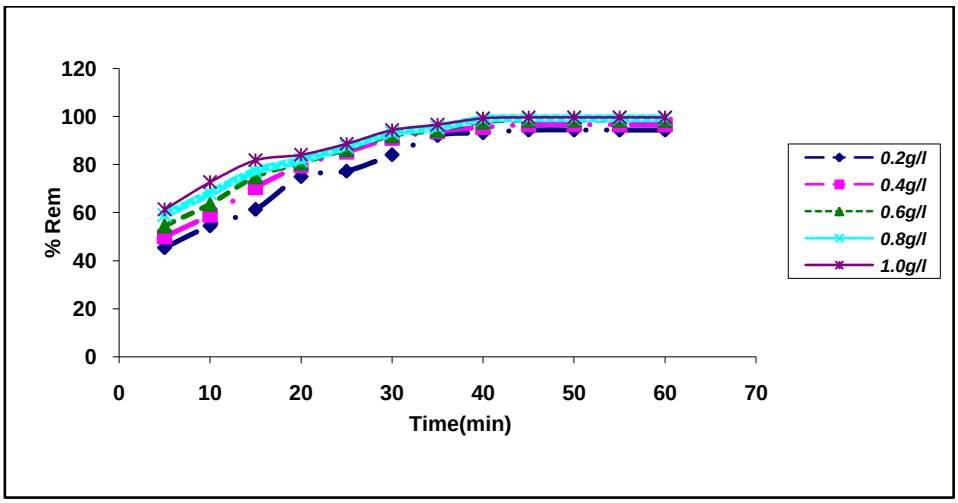

Fig.4.445: %Removal of adsorbate from VIE for varying BFHA dosage and pH 8

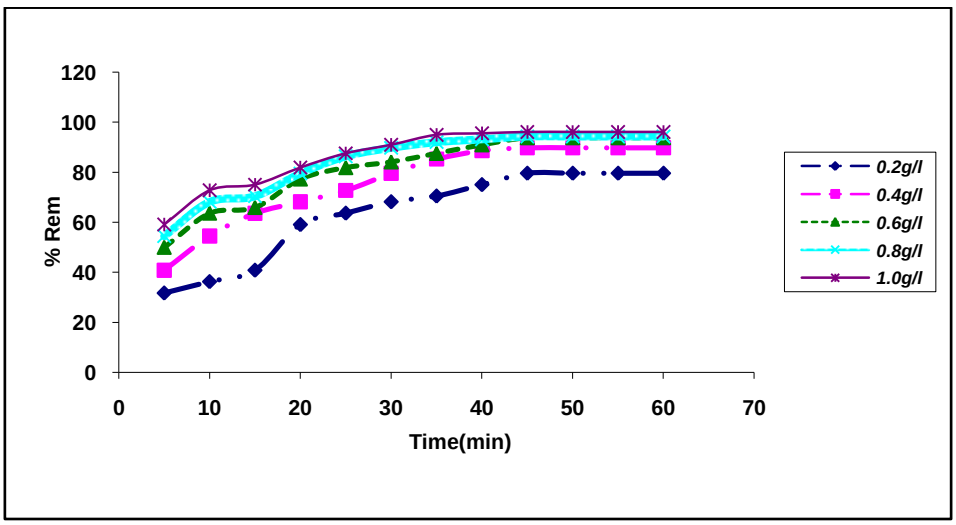

Fig.4.446: %Removal of adsorbate from VIE for varying BFHA dosage and pH 10

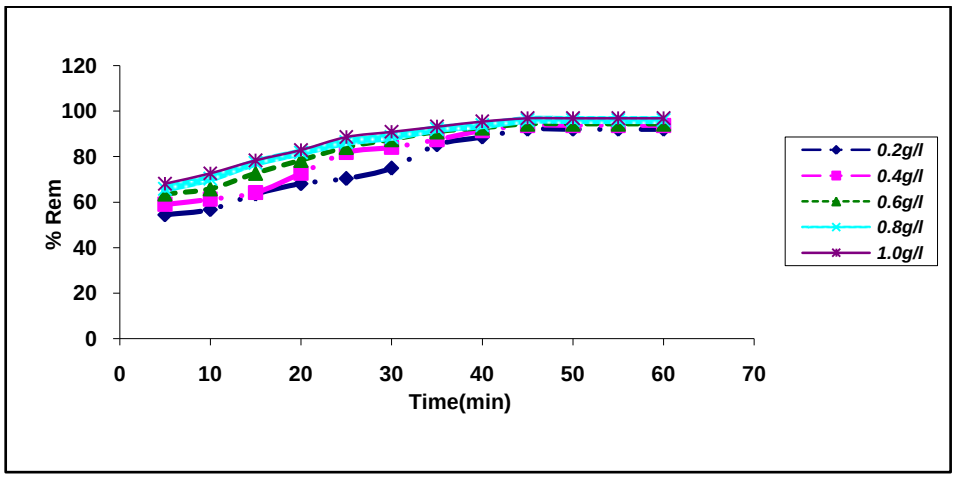

Fig.4.447: %Removal of adsorbate from VIE for varying RHA dosage and pH 2

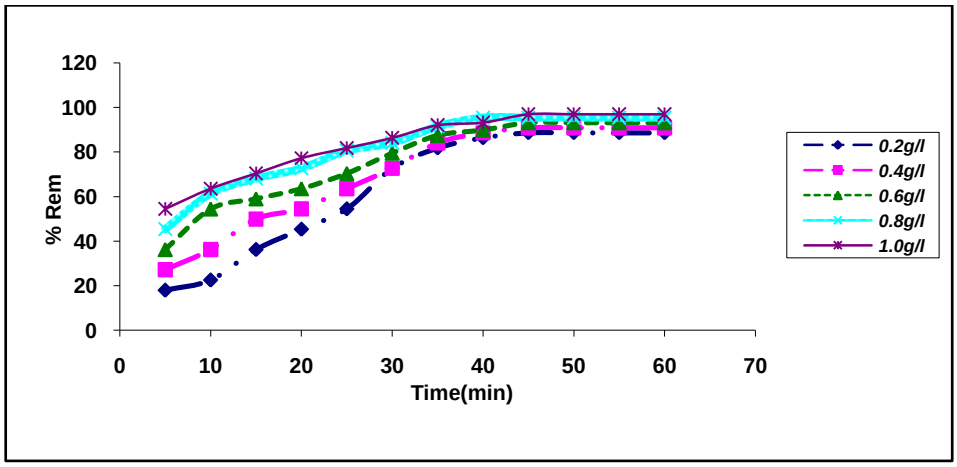

Fig.4.448: %Removal of adsorbate from VIE for varying RHA dosage and pH 4

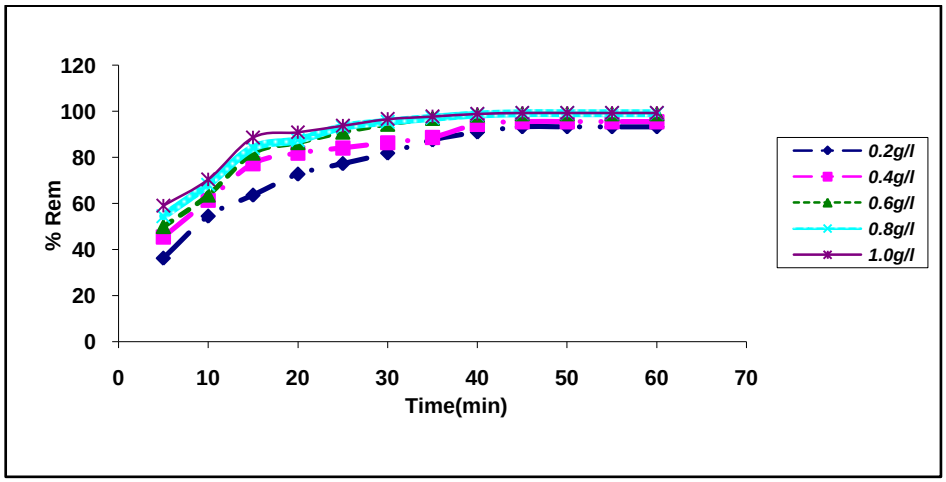

Fig.4.449: %Removal of adsorbate from VIE for varying RHA dosage and pH 6

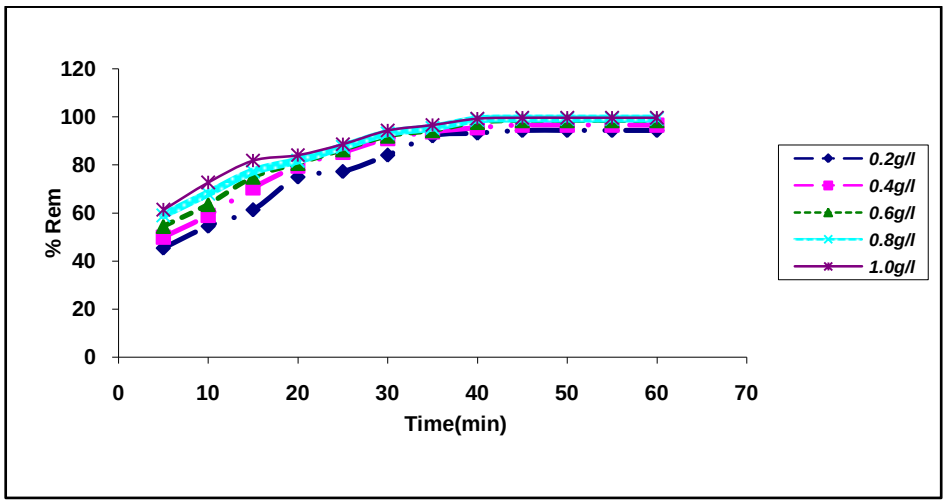

Fig.4.450: %Removal of adsorbate from VIE for varying RHA dosage and pH 8

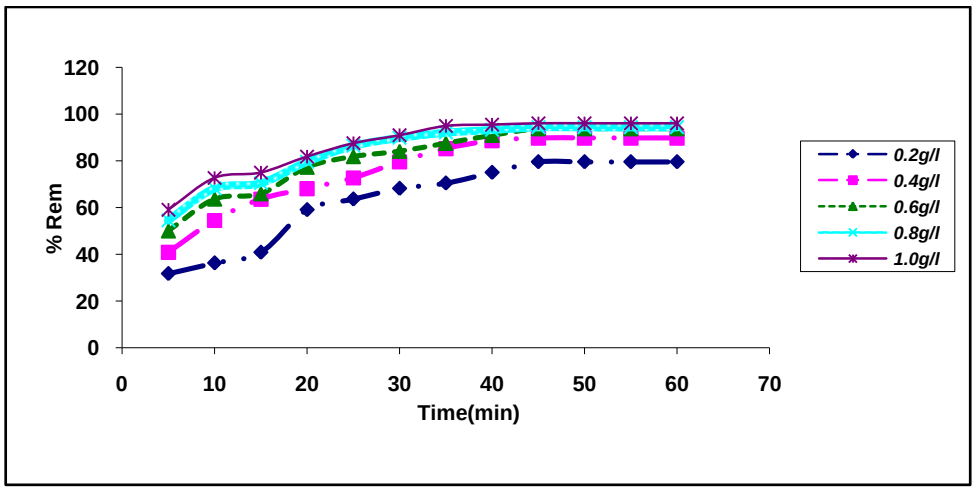

Fig.4.451: %Removal of adsorbate from VIE for varying RHA dosage and pH 10

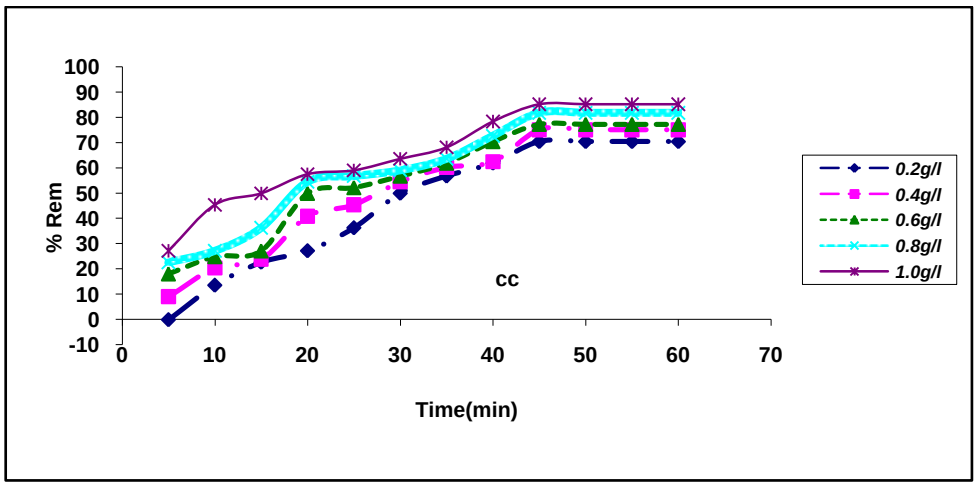

Fig.4.452: %Removal of adsorbate from VIE for varying laterite dosage and pH 2

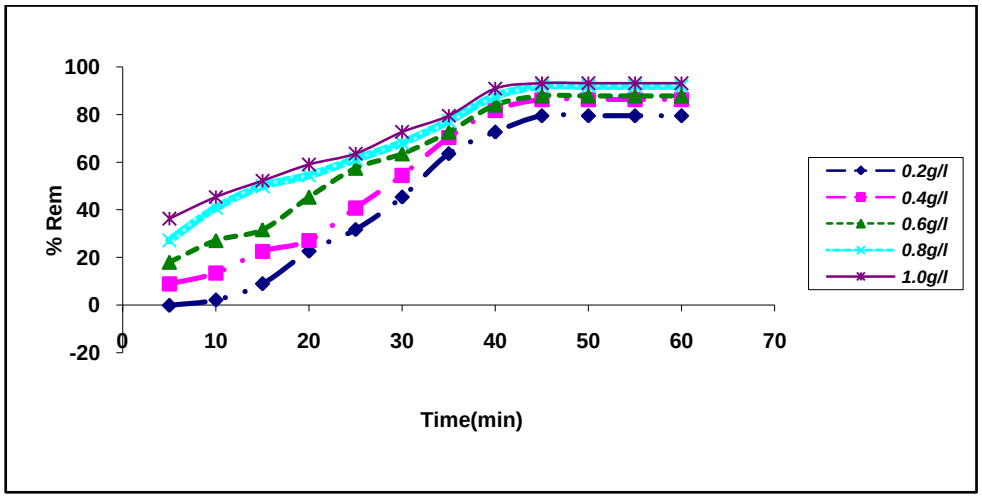

Fig.4.453: %Removal of adsorbate from VIE for varying laterite dosage and pH 4

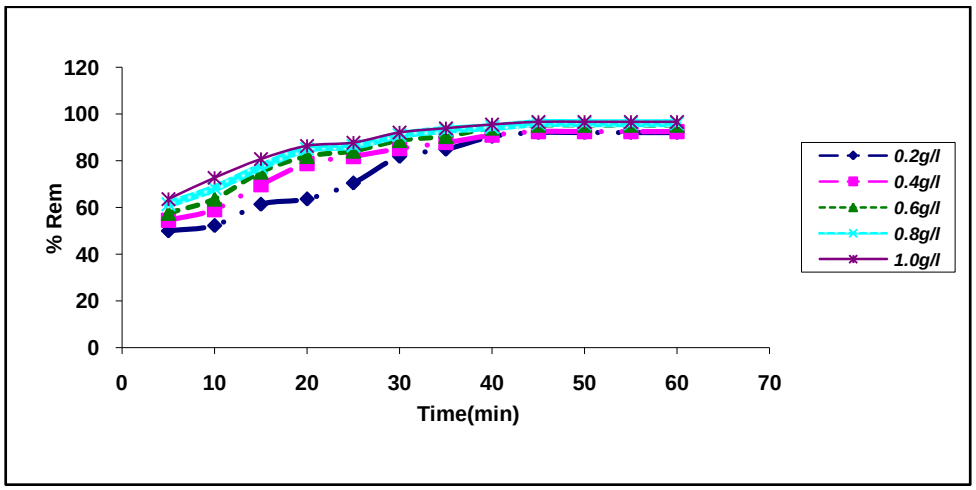

Fig.4.454: %Removal of adsorbate from VIE for varying laterite dosage and pH 6

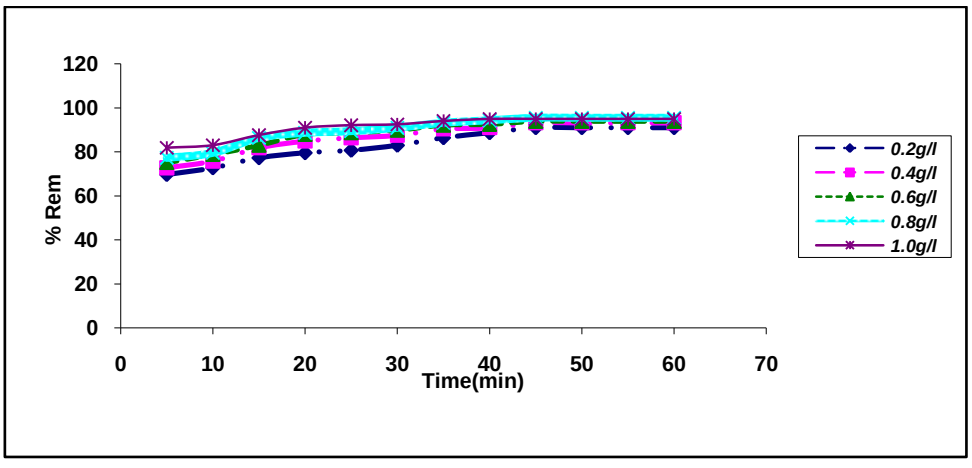

Fig.4.455: %Removal of adsorbate from VIE for varying laterite dosage and pH 8

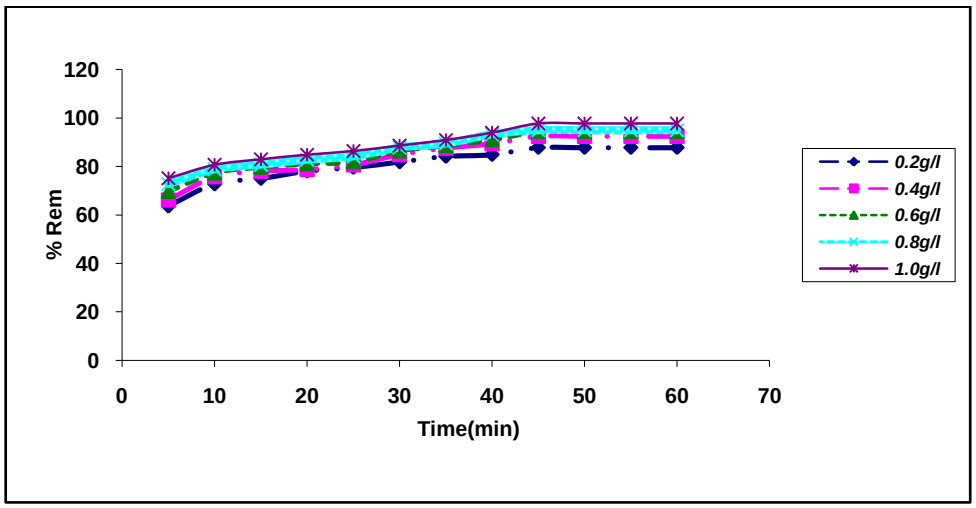

Fig.4.456: %Removal of adsorbate from VIE for varying laterite dosage and pH 10

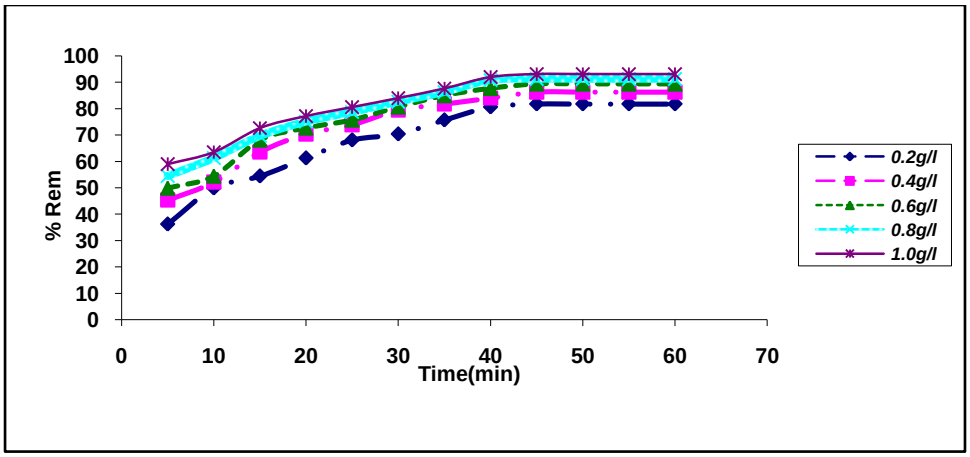

Fig.4.457: %Removal of adsorbate from VIE for varying UCA dosage and pH 2

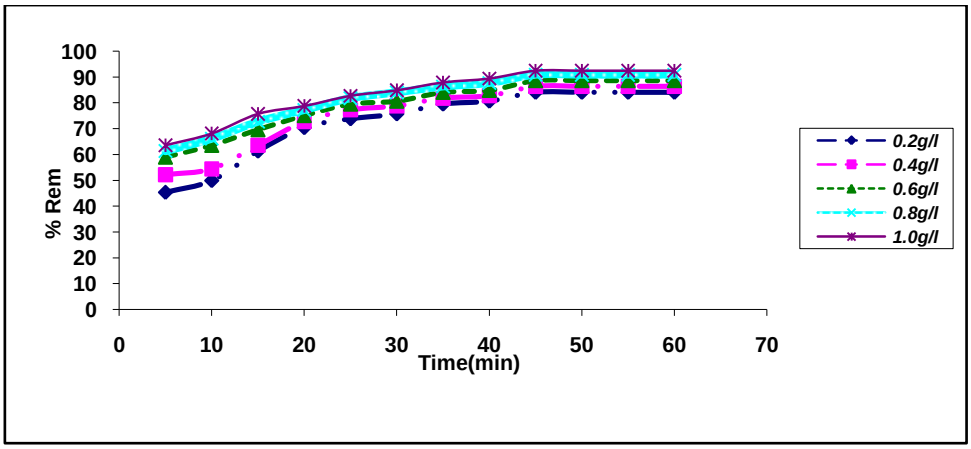

Fig.4.458: %Removal of adsorbate from VIE for varying UCA dosage and pH 4

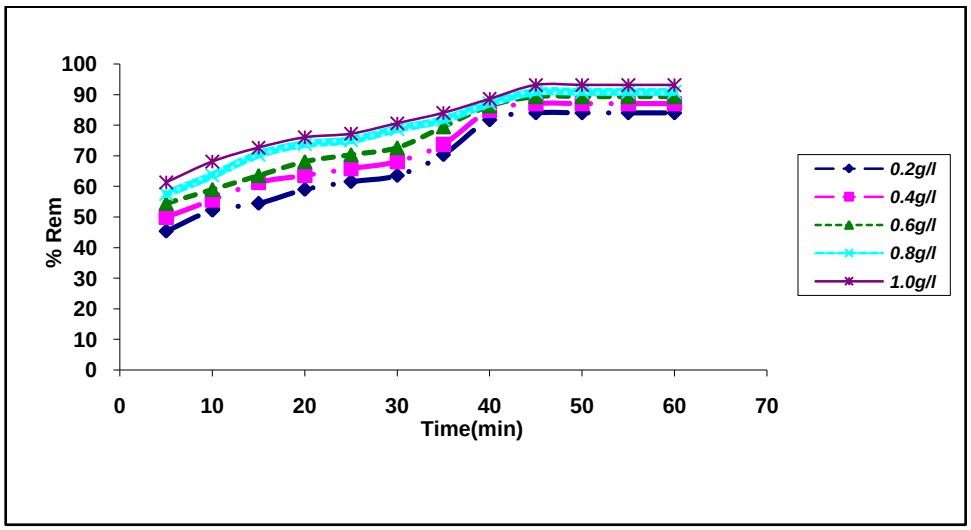

Fig.4.459: %Removal of adsorbate from VIE for varying UCA dosage and pH 6

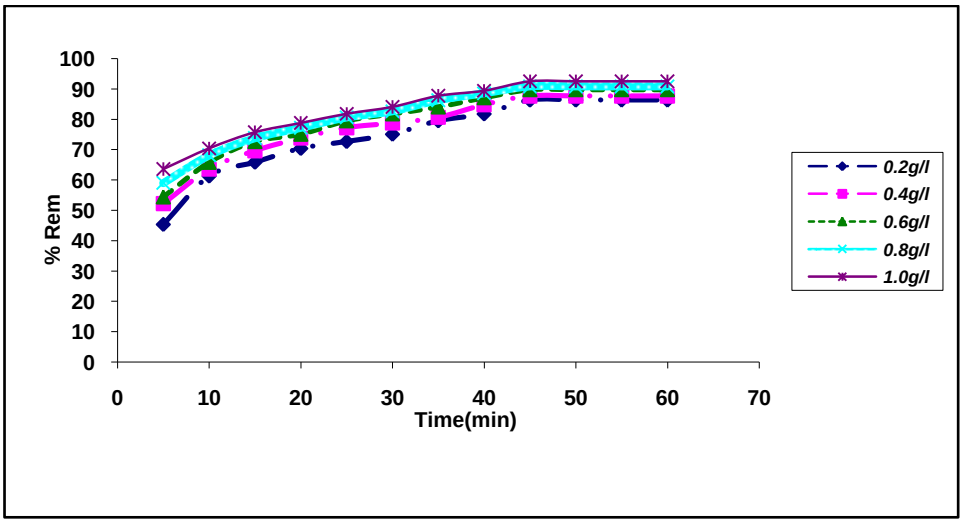

Fig.4.460:%Removal of adsorbate from VIE for varying UCA dosage and pH 8

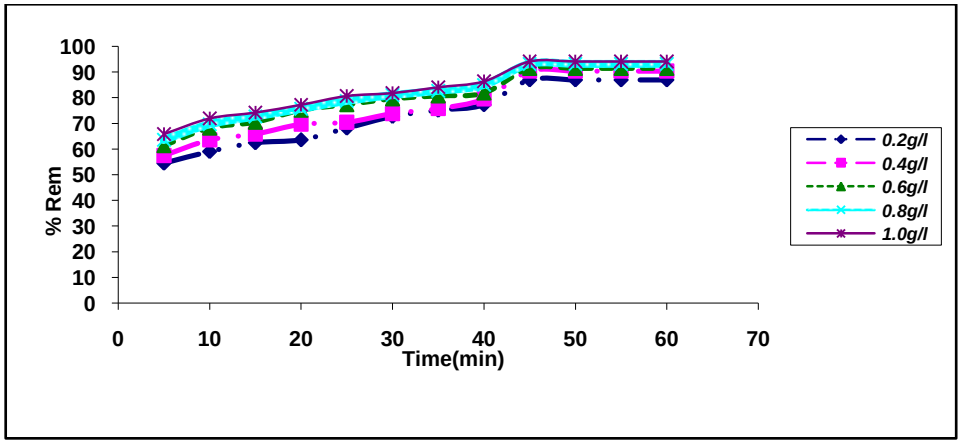

Fig.4.461:%Removal of adsorbate from VIE for varying UCA dosage and pH 10

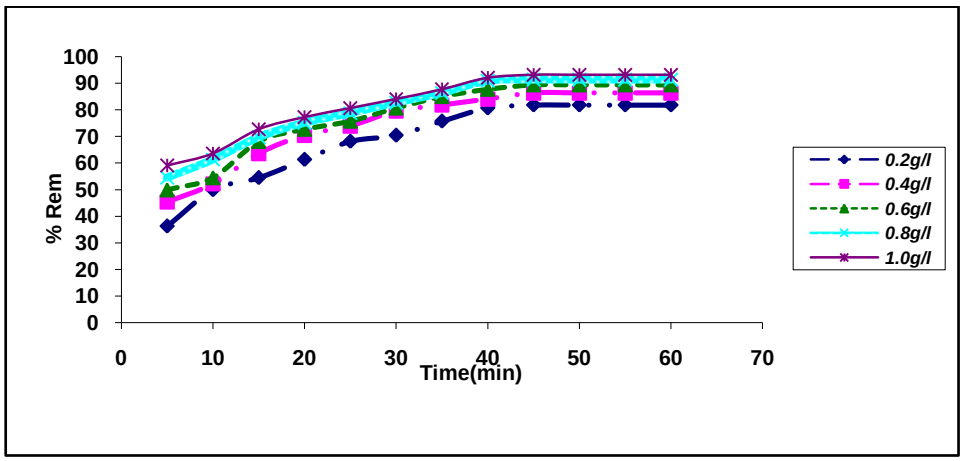

Fig.4.462: %Removal of adsorbate from VIE for varying MSA dosage and pH 2

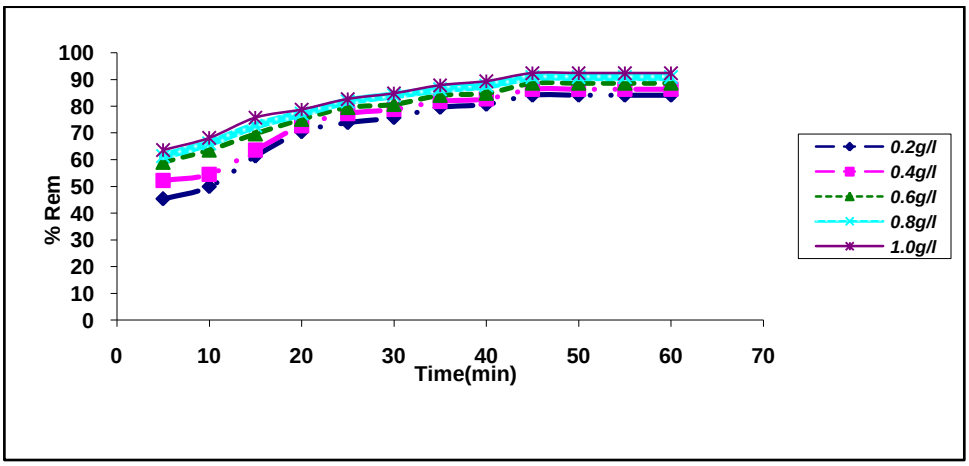

Fig.4.463: %Removal of adsorbate from VIE for varying MSA dosage and pH 4

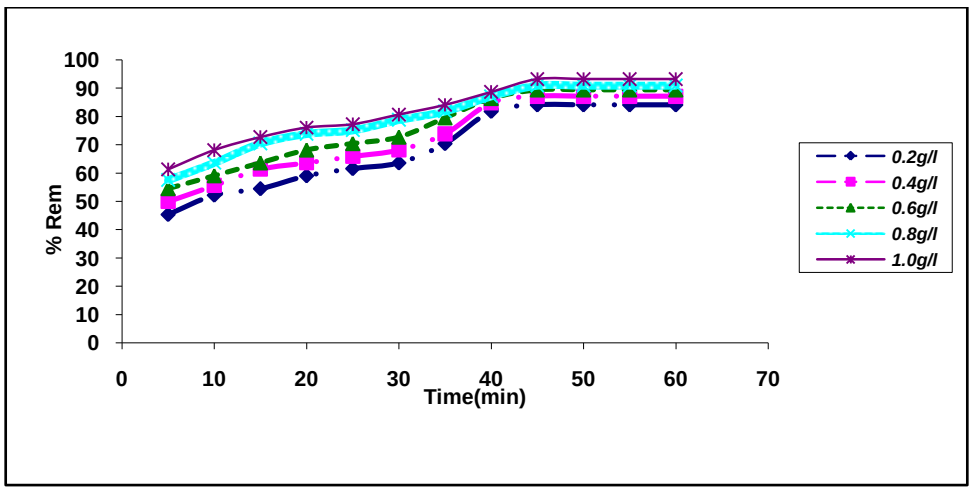

Fig.4.464: %Removal of adsorbate from VIE for varying MSA dosage and pH 6

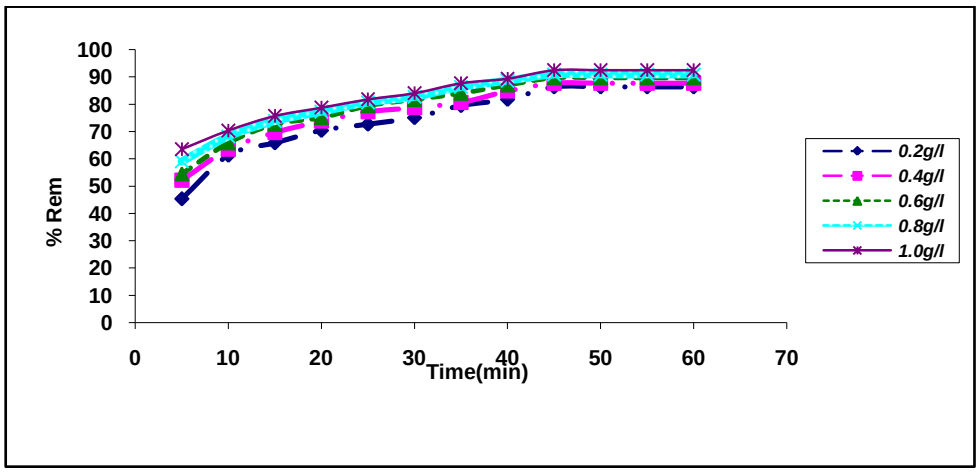

Fig.4.465: %Removal of adsorbate from VIE for varying MSA dosage and pH 8

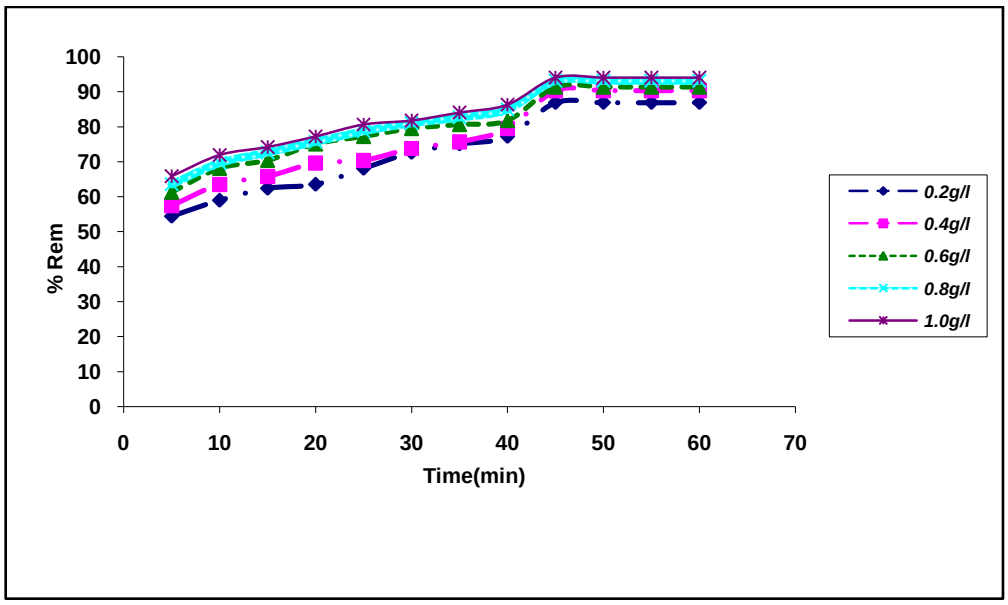

Fig.4.466: %Removal of adsorbate from VIE for varying MSA dosage and pH 10

4.2.4 Adsorption Capacity for varying Adsorbent Concentration in PIE and VIE

This section presents the effect of time and adsorbent concentration on adsorption capacity for PIE and VIE . As previously stated, the adsorbent concentrations and adsorbents under consideration are 0.2, 0.4, 0.6, 0.8 and 1.0g/l, BFHA, RHA, LATERITE, UCA and MSA respectively. The graphical illustration of the results for PIE and VIE are presented in figs. 4.467 to 4.476

The general observation from figures. 4.467 to 4.476, show that adsorption capacity q_t (mg/g) increased with increase in agitation time and adsorbent mass until it gets to a point where the variation of q_t with time is inconsequential to adsorbent concentrations

for both PIE and VIE. The implication of these results is that, there is rapid adsorption of adsorbate within the first 5 mins after which the adsorbate uptake increases progressively at a relatively low increment. The rapid inccrement in q_t for 0.2g/l dose illustrates low presence of exchangeable sites when compared with other doses. Moreover, the results presented in the figures show that increase in adsorbent concentration increased the adsorbate uptake, which might be as a result of increase in surface area of the adsorbent. (Wannapeera, et al, 2008). Hence more active sites are made available for adsorbate uptake. The reverse is obtained for low dose adsorbent as demonstrated in the figures.

In the case of PIE, the results are presented in figures. 4.467 to 4.471. All the figures have similar trend, with 1.0g/l dose having highest q_t greater than 188mg/g for all the adsorbent. However, the maximum q_t for PIE is 197.80mg/g.

For the VIE, the results are presented in figures. 4.472 to 4.476. It is observed that the q_t obtained for PIE is higher than the one obtained for VIE. The maximum q_t for VIE is 182.03mg/g while the minimum is 8.33mg/g for all the adsorbents. The same reason as observed in PIE accounts for the similar behaviors witnessed for VIE. Generally, in both cases, the curves are smooth and continuous leading to saturation.

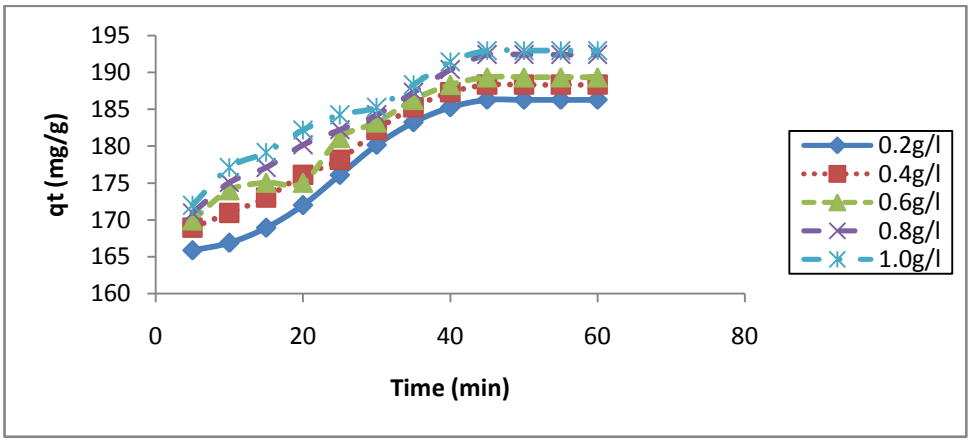

Fig.4.467 :Adsorption capacity for varying BFHA conc. in PIE

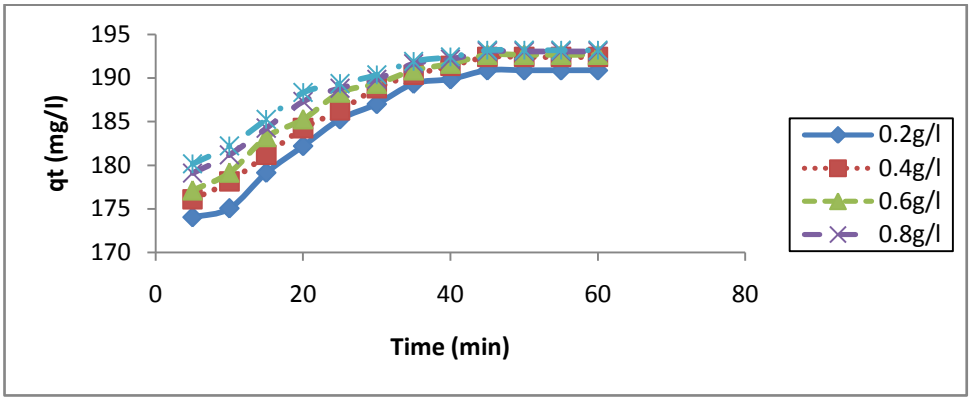

Fig.4.468: Adsorption capacity for varying RHA conc. in PIE

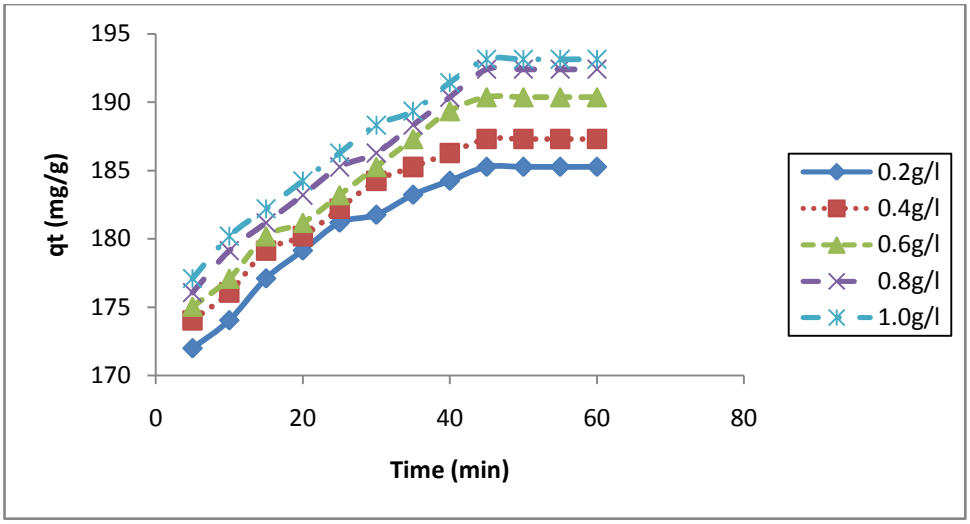

Fig.4.469: Adsorption capacity for varying LATERITE conc. in PIE

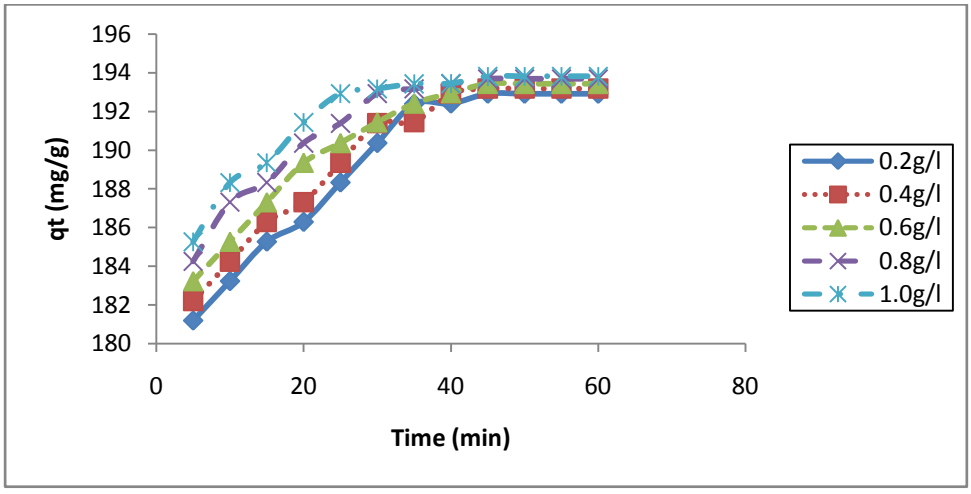

Fig.4.470: Adsorption capacity for varying UCA conc. in PIE

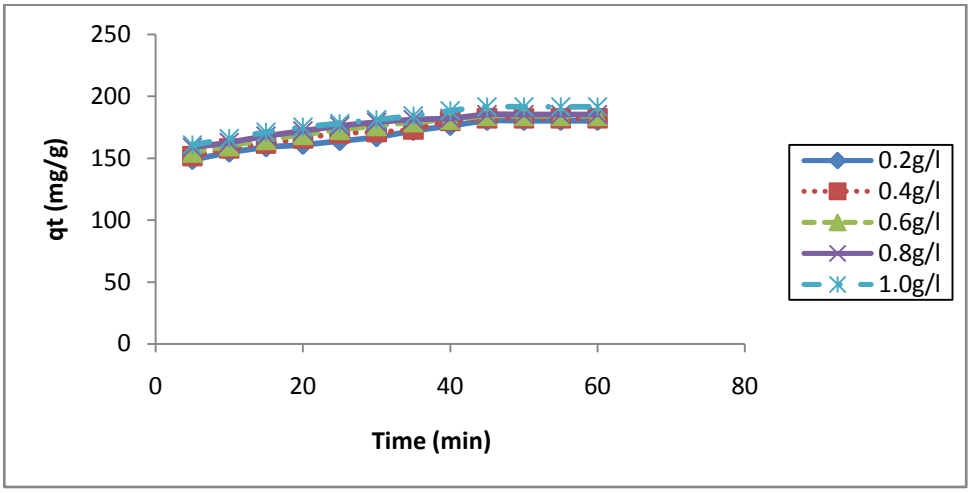

Fig.4.471: Adsorption capacity for varying MSA conc. in PIE

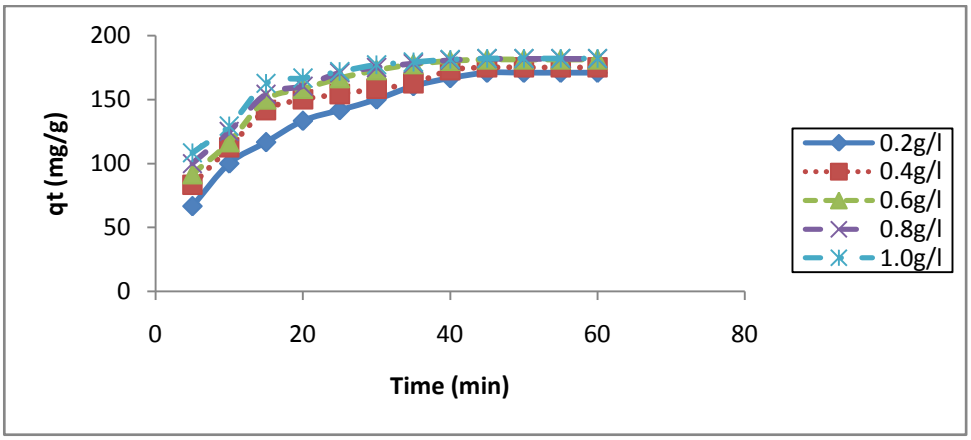

Fig.4.472: Adsorption capacity for varying BFHA conc. in VIE

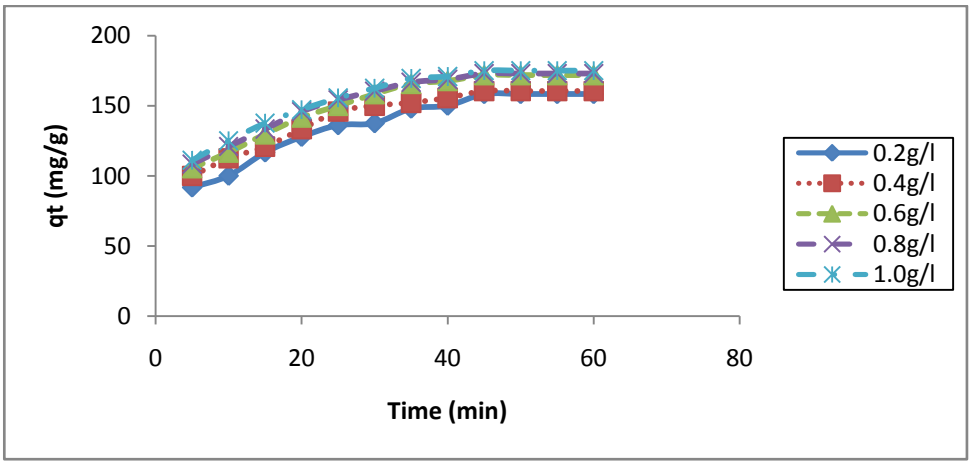

Fig.4.473: Adsorption capacity for varying RHA conc. in VIE

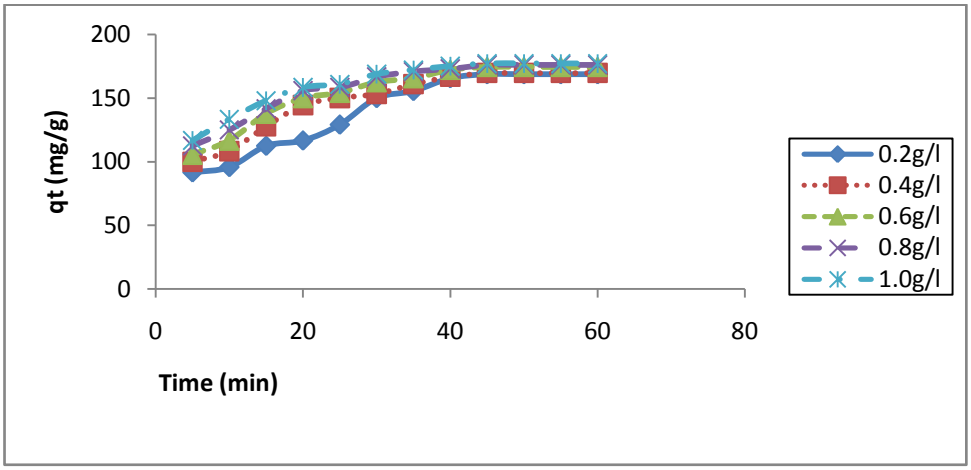

Fig.4.474: Adsorption capacity for varying LATERITE conc. in VIE

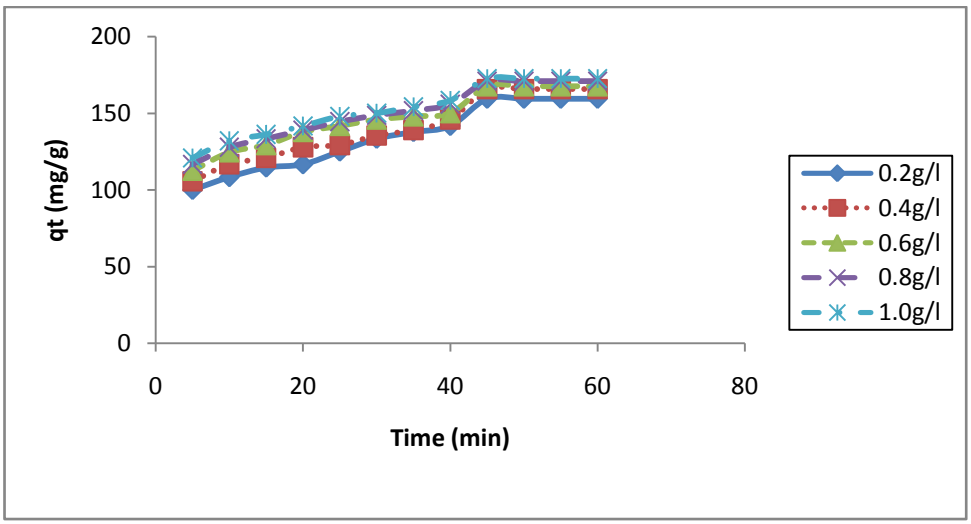

Fig.4.475 :Adsorption capacity for varying UCA conc. in VIE

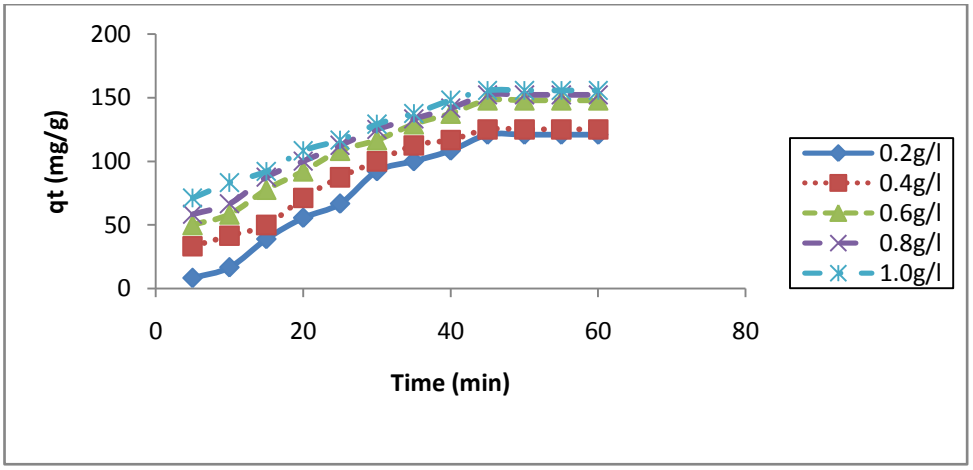

Fig.4.476 :Adsorption capacity for varying MSA conc. in VIE

4.2.5 Adsorption Isotherm

Adsorption isotherm describes the equilibrium relationship between the concentration of adsorbate and adsorption capacity of adsorbent. The experimental data of TDSS adsorption on the various adsorbents at 25^0C were fitted in Langmuir, Freundich and Temkin isotherm models for both PIE and VIE. The adsorption studies were carried out at fixed initial concentration of adsorbate by varying adsorbent dosage. The isotherm results/plots are presented for PIE and VIE with respect to BFHA, RHA, LATERITE, UCA and MSA.

4.2.5.1 Adsorption isotherm for PIE and VIE

The evaluated isotherm parameters for Langmuir, freundlich and Temkin models are presented in tables 4.154 and 4.155, the associated isotherm plots are presented in figs 4.477 to 4.479 and 4.480 to 4.481 for PIE and VIE respectively. The detailed discussion is presented in sections 4.2.5.2 to 4.2.5.4

4.2.5.2 Langmuir isotherm for PIE and VIE

The Langmuir isotherm is the simplest theoretical model for monolayer adsorption with uniform energy along the homogeneous adsorbent surface. It has been widely used to describe the activated carbon adsorption of volatile organic compounds (Pei and Zhang 2012; Yang, 2003C). The Langmuir isotherm is graphically expressed in figures.4.476 and 4.479 for PIE and VIE respectively. The parameters evaluated from the plots are K_L (l/mg), q_{max} (mg/g), and R^2, K_L is Langmuir equilibrium constants, related to the energy of adsorption. q_{max} is the maximum amount of adsorbate adsorbed per unit mass of adsorbate to form a complete monolayer on the surface at the equilibrium adsorbate concentration. The parameters K_L and q_{max} have been calculated from the slope and intercept respectively. Critical observation on tables 4.154 and 4.155, indicate that the maximum values of q_{max} are 1.2500 and 1.4286 mg/g for PIE and VIE, respectively. Also the tables show values for R_L, which is separation factor, indicating the nature of the adsorption process. In this study R_L = 0, indicating that the process is reversible, hence the adsorption does not follow Langmuir isotherm.

4.2.5.3 Freunlich isotherm for PIE and VIE

The freundlich isotherm is an empirical equation suited for non-ideal systems with highly heterogeneous surfaces. It does not lead to formation of a monolayer (Soto, et al, 2011; Dabrowski, et al; 2005). The Freundlich equation provides a plot of $\ln q_e$ against lnCe, from thence K_f and 1/n can be evaluated from the intercept and slope of the plot. Where K_f and n are related to the adsorption capacity and adorption intensity, respectively. K_f has the unit of mg/g, n is dimensionless (Lin, et al; 2011).

The Freundlich plots are presented in figures 4.477 and 4.480 for PIE and VIE, respectively, for the various adsorbents. The related parameters are posted in the 6 – 8 columns of tables 4.154 and 4.155 for PIE and VIE respectively, the values of $n > 1$ for LATERITE, MSA and $n < 1$ for BFHA, RHA and UCA in PIE, indicating favorable and unfavorable adsorption conditions, respectively. Whereas in VIE favorable adsorption process is achieved for BFHA, RHA and LATERITE.

4.2.5.4 Temkin isotherm for PIE and VIE.

The Temkin Isotherm, like freundlich is one of the earliest reported isotherm. It assumes that the heat of adsorption decreases linearly with increasing coverage due to adsorbate and adsorbent interactions.

The Temkin model is represented graphically by potting q_e against ln Ce presented in figures. 4.478 to 4.481 fo PIE and VIE . From thence the parameters (b_T and K_T) of interest weEre calculated from the slope and intercept. These Temkin parameters b_T (kJ/mol) and k_T (l/g) were obtained to study the heat of adsorption and adsorption potential of the process at equilibrium. k_T is the equilibrium binding constant and corresponds to the maximum binding energy, whereas, b_T is a constant related to the heat of adsorption. The value of b_T and k_T are posted in columns 9 and 10 of tables 4.152 and 4.153 for PIE and VIE. The b_T values greater than eight suggest a high level of interaction between the adsorbate and adsorbent for all cases in PIE, whereas in VIE it is only BFHA that meets the requirement while the rest indicate weak adsorbate/adsorbent interaction showing that the process would be physiosorption (Ali, et al; 2011; Theivarasu and MyLsamy, 2010). The highest values of b_T are 23.3337 and 10.4539 kJ/mol for the PIE (MSA) and VIE (BFHA) respectively. The implication of these results is that ion-exchange mechanism is favored more at 23.3337 kJ/mol. Similarly, the values k_T obtained for both cases are

generally satisfactory, but the higher the value, the more the affinity of the adsorbate towards the adsorbent interface. This phenomenon suggests that for k_T = 19.5994 kJ/mol for VIE (MSA), high level of interaction between adsorbate and adsorbent is expected.

Table 4.154 Batch adsorption parameters for PIE

Adsorbent Langmuir isotherm					Freundlich Isotherm				Temkin Isotherm	
	K_L (l/mg)	Q_{max} (mg/g)	R_L	R^2	K_F(mg/g)	n	R^2	b_T(KJ/mg)	K_TL/g	R^2
BFHA	1.9873	1.2500	+0.0000	0.9015	0.0968	0.7760	0.8384	12.6860	3.2871	0.6843
RHA	4.9759	0.0303	+0.0000	0.9867	0.0881	0.6894	0.9932	10.2054	2.8800	0.9695
Laterite	1.9960	0.0333	0.0000	0.9188	0.0195	1.4051	0.8871	22.0405	0.9647	0.7338
UCA	2.4131	0.0270	0.0000	0.9749	0.0070	0.5919	0.9244	8.5664	0.5578	0.7764
MSA	8.0438	0.0270	0.0000	0.7831	0.0361	1.3535	0.7312	23.3337	1.9854	0.5633

Table 4.155 Batch adsorption parameters for VIE

Adsorbent Langmuir isotherm					Freundlich Isotherm				Temkin isotherm	
	K_L (l/mg)	Q_{max} (mg/g)	R_L	R^2	K_F(mg/g)	n	R^2	b_T(KJ/mg)	K_TL/g	R^2
BFHA	1.6835	0.0909	0.0000	0.9440	0.0058	1.7790	0.9107	10.4539	0.6290	0.8220
RHA	7.6394	1.4286	0.0000	0.9837	0.0184	1.1515	0.8854	7.1876	2.5995	0.7300
Laterite	4.1459	0.0833	0.0000	0.7742	0.0248	1.1211	0.8548	7.0146	3.5612	0.7440
UCA	4.4395	0.0400	0.0000	0.9861	0.6192	0.5188	0.9712	3.2277	9.5487	0.8840
MSA	5.6603	1.1111	0.0000	0.9045	0.4652	0.7687	0.8409	6.0179	19.5994	0.7280

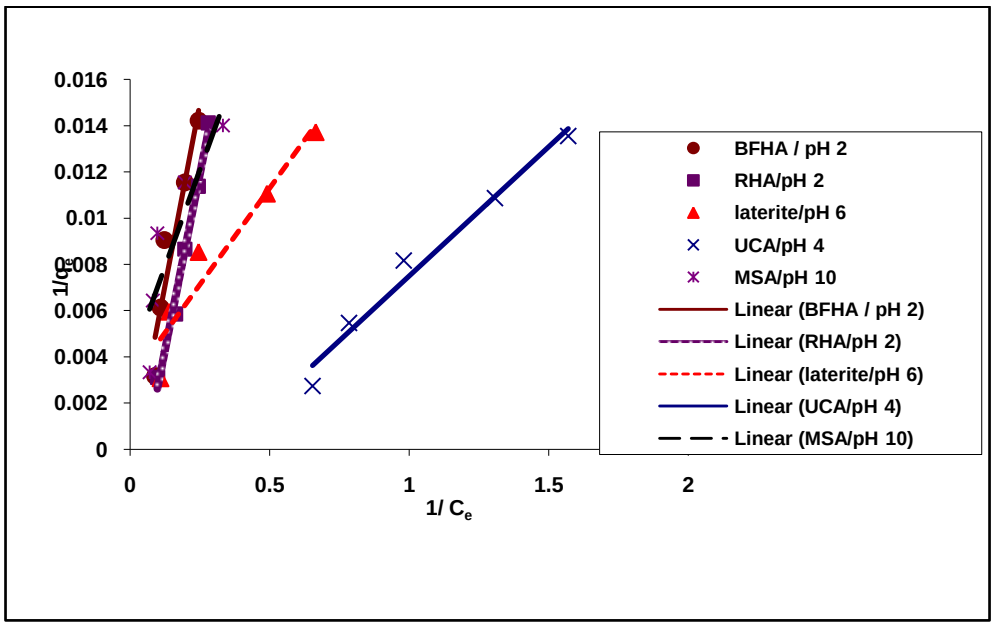

Fig. 4.477 : Langmuir isotherm plot of PIE for various adsorbents

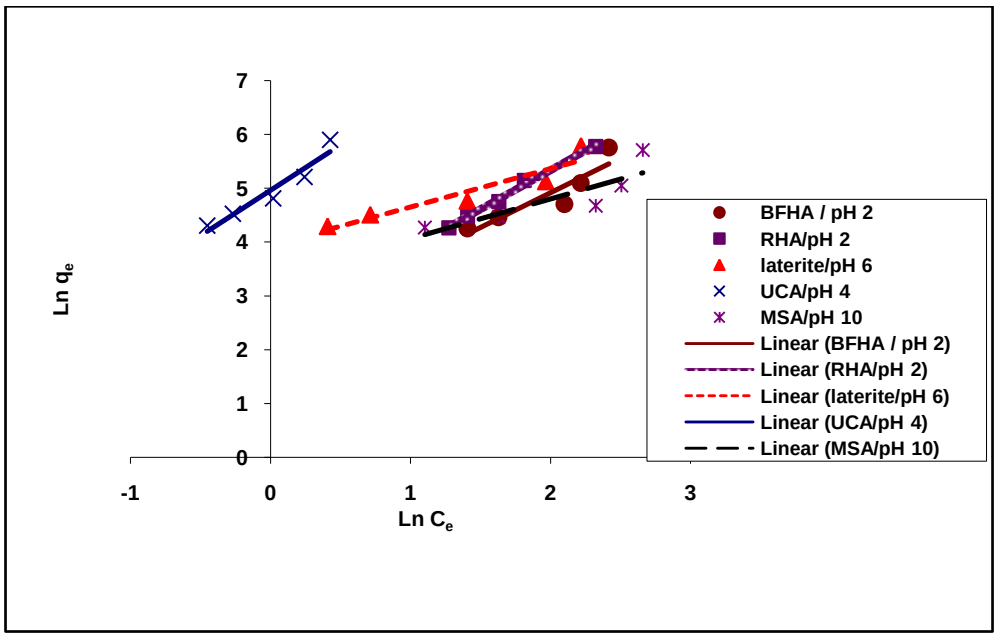

Fig.4.478 : Freundlich isotherm plot of PIE for various adsorbents

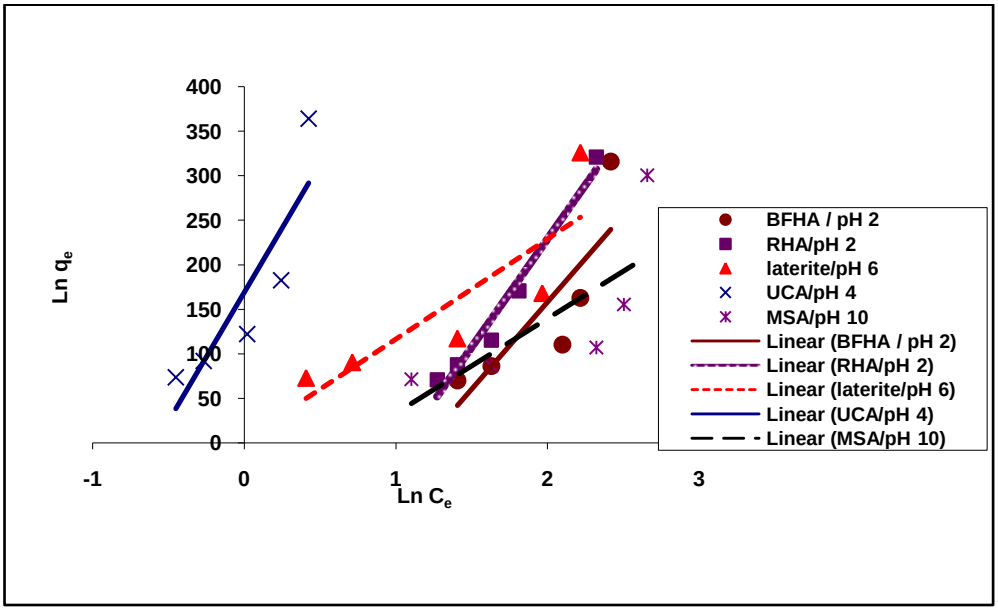

Fig.4.479 : Temkin isotherm plot of PIE for various adsorbents

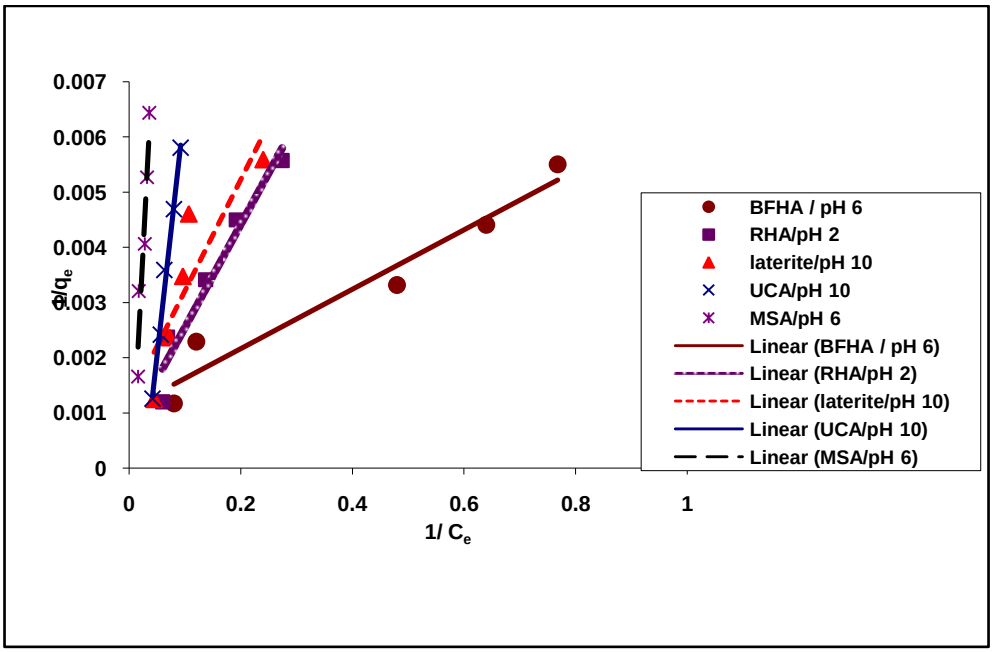

Fig. 4.480 : Langmuir isotherm plot of VIE for various adsorbents

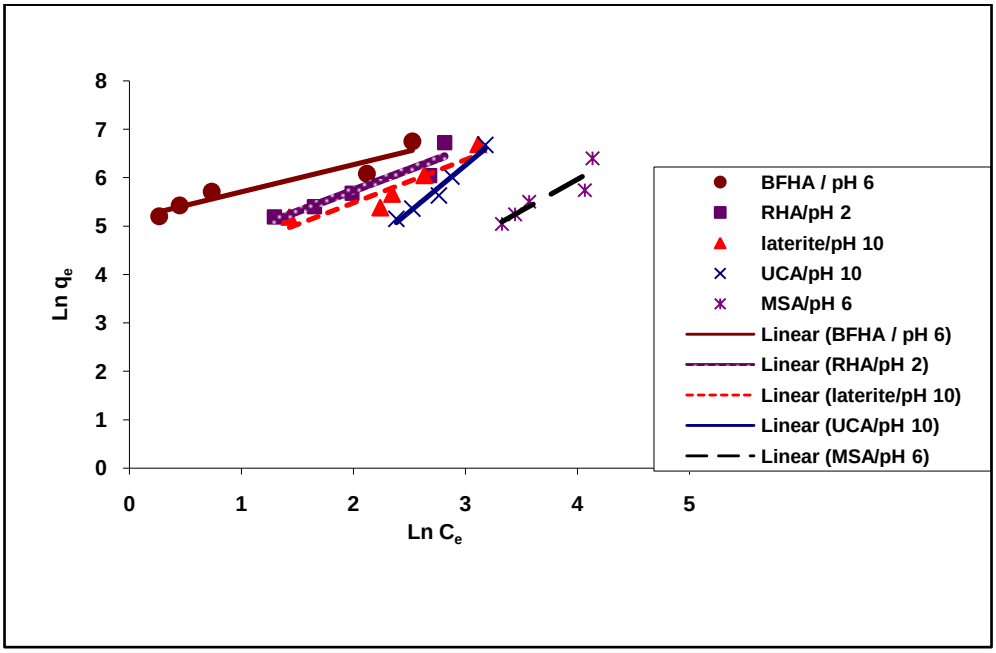

Fig.4.481 : Freundlich isotherm plot of VIE for various adsorbents

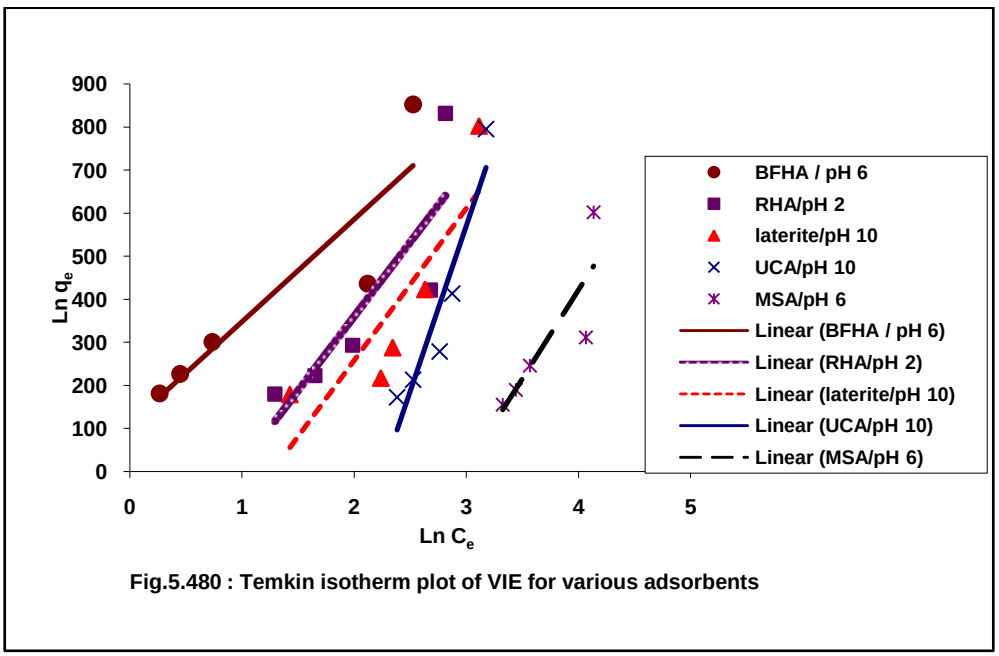

Fig.5.480 : Temkin isotherm plot of VIE for various adsorbents

Fig.4.482 : Temkin isotherm plot of VIE for various adsorbents

4.2.6 Adsorption Kinetics

Kinetics of adsorption describes the solute uptake rate, which in turn governs the residcence time of adsorption reaction. Many kinetic models have been proposed to explain the mechanism of this solute uptake rate (adsorption). The rate and mechanism of adsorption is controlled by physical or chemical properties of adsorbent, such as temperature, pH of medium, and nature of adsorbate. These models are important in the design and optimization of water and wastewater treatment process. For the purposes of this work, the following models were employed: Bhattacharya and Venkobachar (BVM); pseudo first order (PFO); Pseudo second order (PSO) and Elovich. The detailed discussion for PIE and VIE are shown in sections: 4.2.6.1 and 4.2.6.2.

4.2.6.1 Adsorption kinetics related to PIE

The above mentioned four models were used to analyse the primary adsorption kinetic data obtained from the experiment. The linear plots describing the various models are shown in figures. 4.483 to 4.490 for 25^0C and 35^0C temperatures. The associated kinetic parameters have been calculated from the intercepts and the slopes of the respective linear plots and presented in tables 4.154 to 4.157

A comparative analysis of the various kinetic plots based on the coefficient of determination (R^2) for the models as presented in tables 4.154 to 4.157, show that high R^2 values in the range of 0.93333 to 0.9979 for all adsorbent at both temperatures. This is an indication that adsorption of TDSS on these adsorbent can be described by these models. However, the R^2 values of 0.9979 obtained at lower temperature (25^0C), indicate that the adsorption kinetics is better expressed by BVM and PFO.

Table 4.156 Kinetics parameters for BVM at varying temperature of PIE

Adsorbents	25^0C		35^0C	
	$K_B(min^{-1})$	R^2	$K_B(min^{-1})$	R^2
BFHA	-0.0529	0.9667	-0.0327	0.9744
RHA	-0.0692	0.9801	-0.0370	0.9333
Laterite	-0.04761	0.9817	-6.839E-02	0.9554
UCA	-0.1089	0.9623	-0.04613	0.9633
MSA	-0.0437	0.9979	-0.0315	0.9726

Table 4.157 Kinetics parameters for PFO at varying temperature of PIE

Adsorbents	25^0C			35^0C		
	$K_1(min^{-1})$	Q_e(mg/g)	R^2	$K_1(min^{-1})$	Q_e(mg/g)	R^2
BFHA	0.0529	0.0339	0.9667	0.0327	0.0254	0.9744
RHA	0.0692	0.0313	0.9801	0.0370	0.0238	0.9333
Laterite	0.0476	0.0476	0.9817	0.0684	0.0400	0.9554
UCA	0.1098	0.0581	0.9623	0.0461	0.0635	0.09633
MSA	0.0437	0.0256	0.9979	0.0315	0.0277	0.9726

Table 4.158 Kinetics parameters for PSO at varying temperature of PIE

Adsorbents	25^0C			35^0C		
	K_2(g/mg min^{-1})	Q_e(mg/g)	R^2	K_2(g/mg min^{-1})	Q_e(mg/g)	R^2
BFHA	0.3012	13.8122	0.9894	0.0970	29.0698	0.9944
RHA	0.2442	15.9490	0.9968	0.1876	20.4082	0.9841
Laterite	0.3810	10.2881	0.9923	0.1851	17.1821	0.9935
UCA	**0.7141**	**6.0864**	**0.9951**	**0.7099**	**6.3171**	**0.9855**
MSA	0.0949	30.6748	0.9967	0.0901	29.3255	0.9950

Table 4.159 Kinetics parameters of ELOVICH model at varying temperature of PIE

Adsorbents	25^0C			35^0C		
	B(mg/g. min^{-1})	x(mg/g/min)	R^2	B(mg/g. min^{-1})	x(mg/g/min)	R^2
BFHA	0.1163	3.1022	0.9100	0.0984	5.6209	0.9603
RHA	0.0980	2.4235	0.9920	0.0971	4.0572	0.8592
Laterite	0.1643	3.9142	0.9658	0.1406	6.0934	0.9468
UCA	0.2199	3.1081	0.9816	0.2339	4.9600	0.9021
MSA	0.0870	4.5304	0.9772	0.1087	7.1800	0.9547

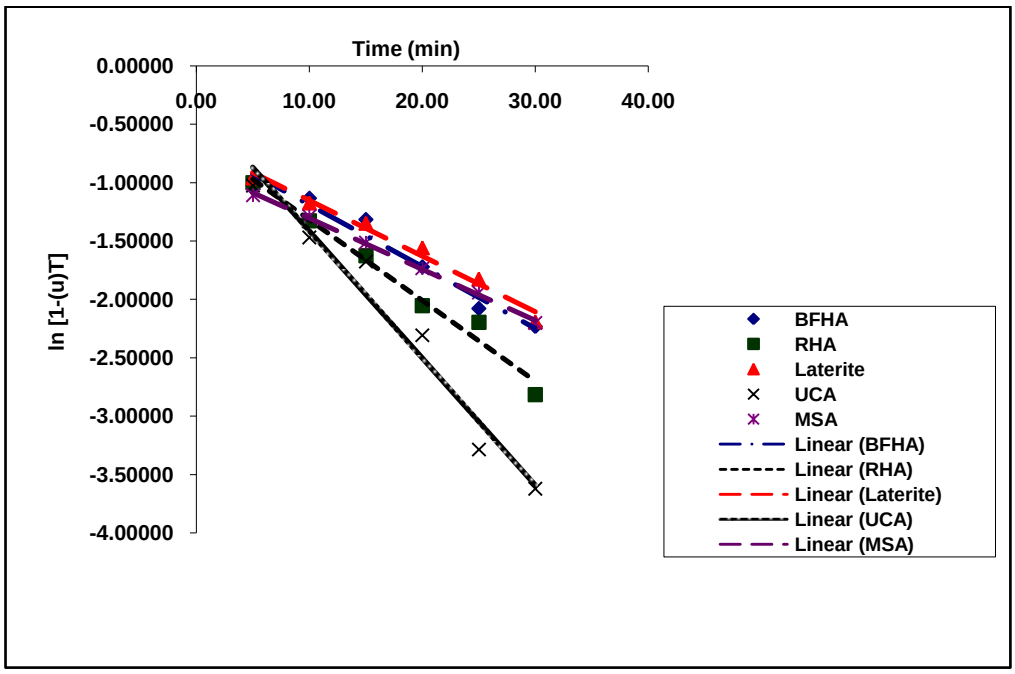

Fig.4.483 : BVM kinetic plot for various adsorbents in PIE at 25°C

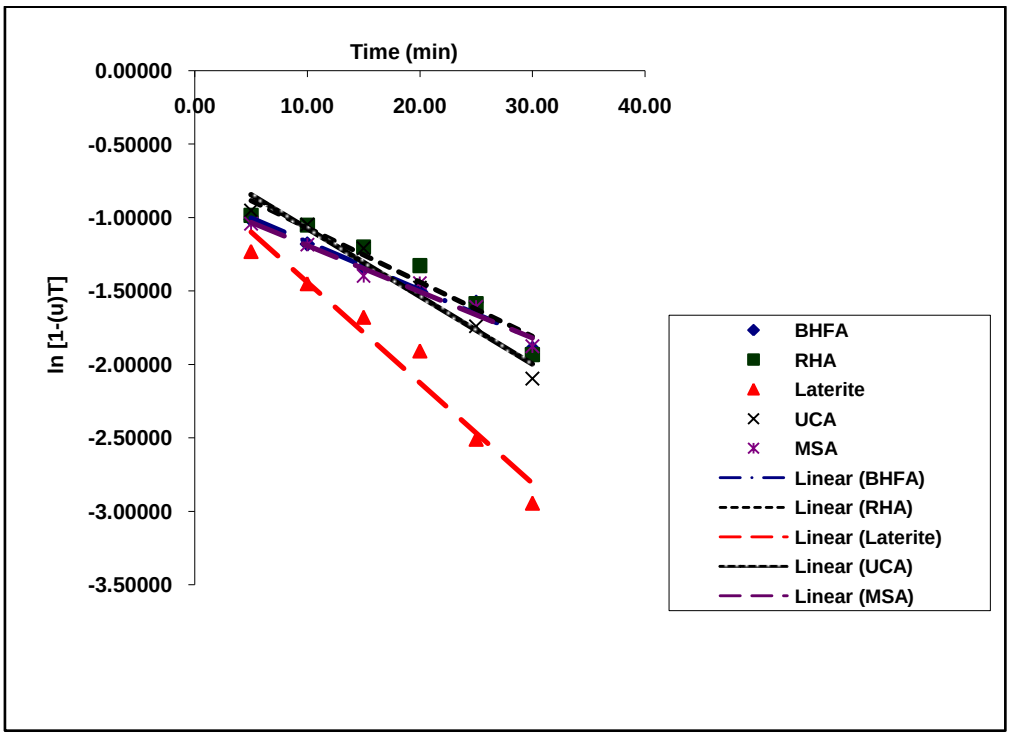

Fig .4.484 : BVM kinetic plot for various adsorbents in PIE at 35°C

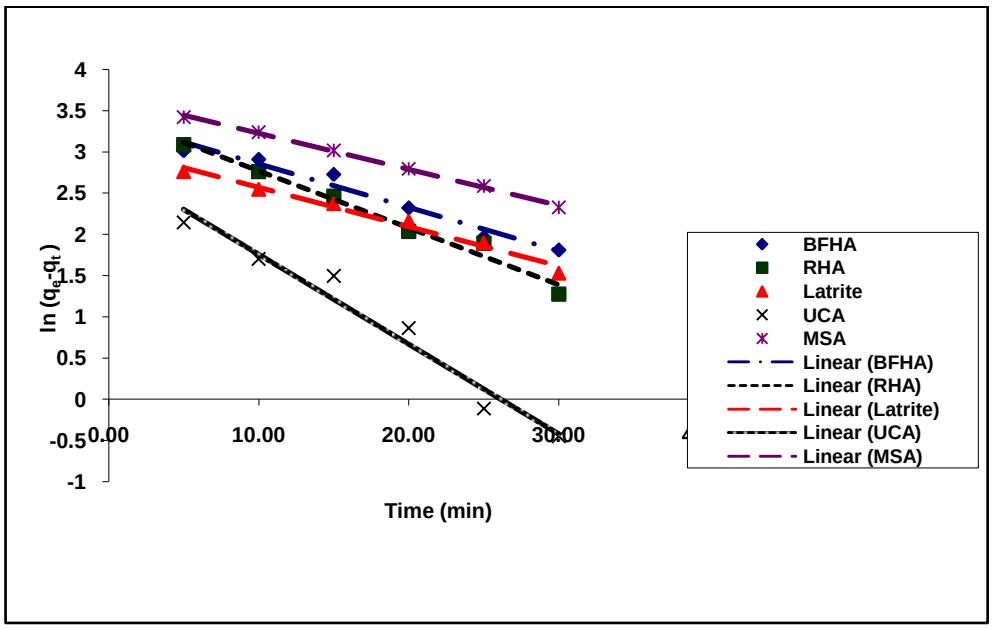

Fig. 4.485:Kinetic plot of Pseudo First Order for various adsorbents in PIE at 25°C

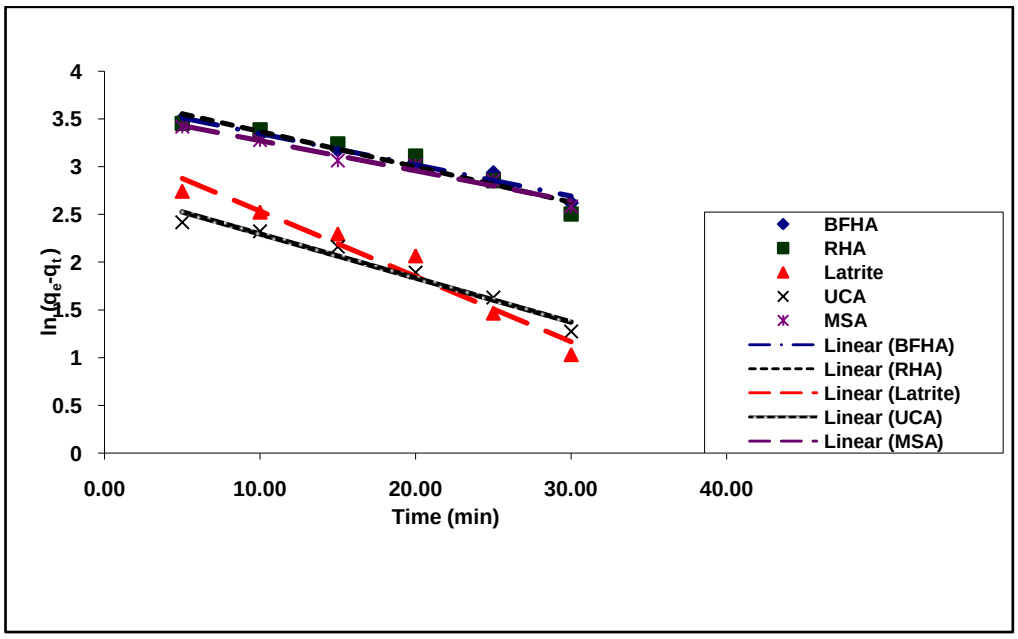

Fig.4.486 :Kinetic plot of Pseudo First Order for various adsorbents in PIE at 35°C

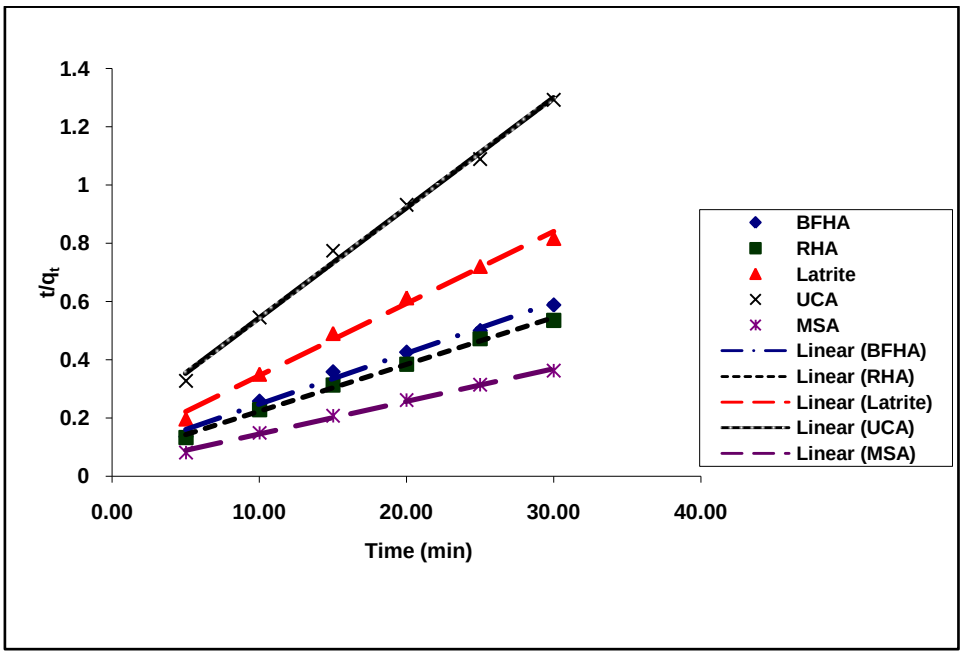

Fig. 4.487:Kinetic plot of Pseudo Second Order for various adsorbents in PIE at 25°C

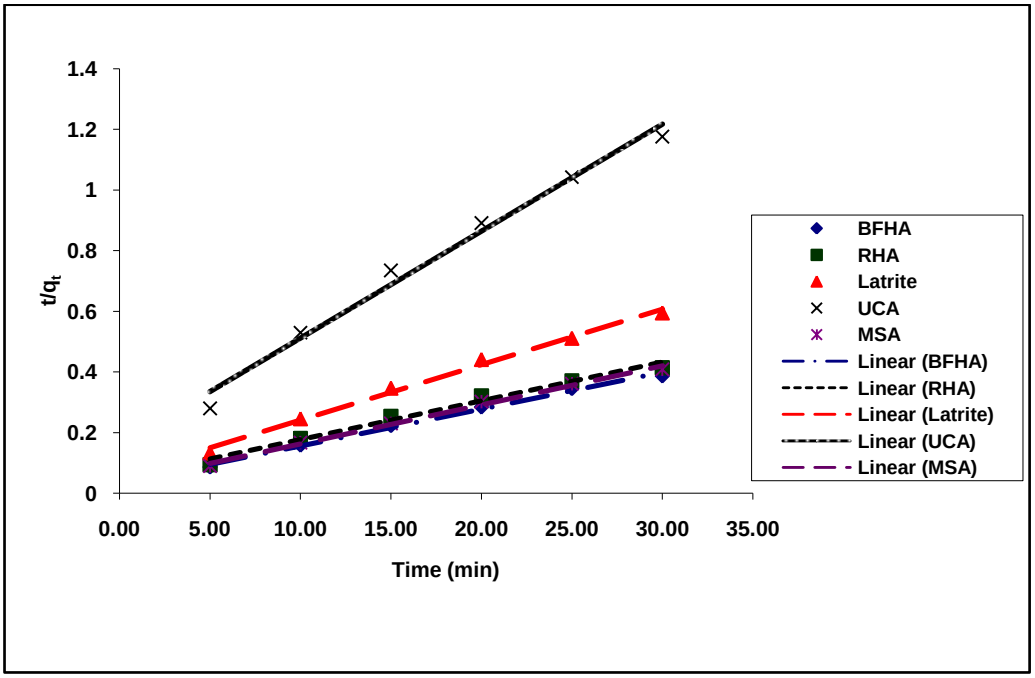

Fig.4.488:Kinetic plot of Pseudo Second Order for various adsorbents in PIE at 35°C

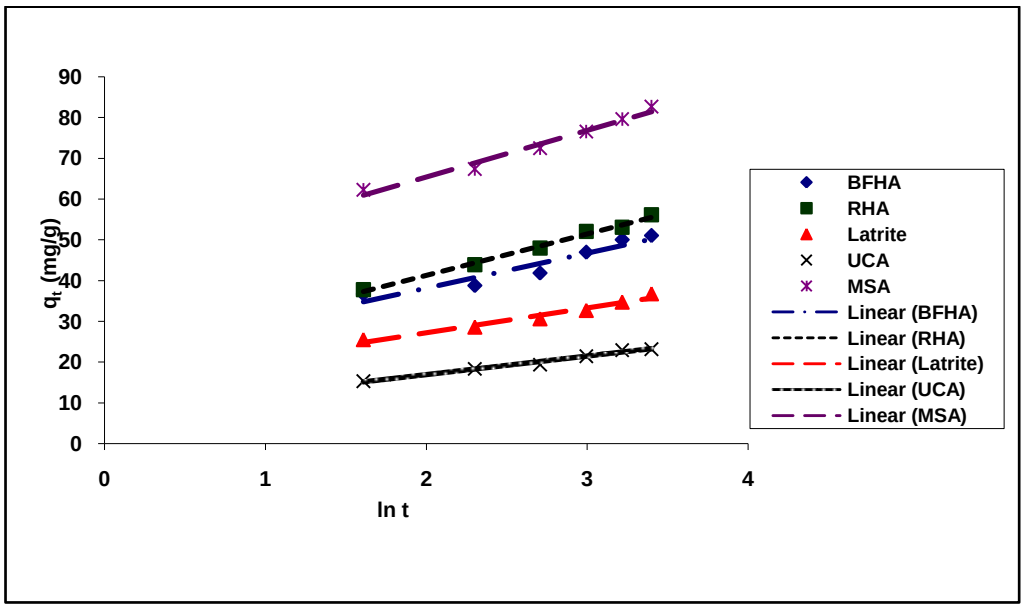

Fig.4.489:Kinetic plot of Elovich for various adsorbents in PIE at 25°C

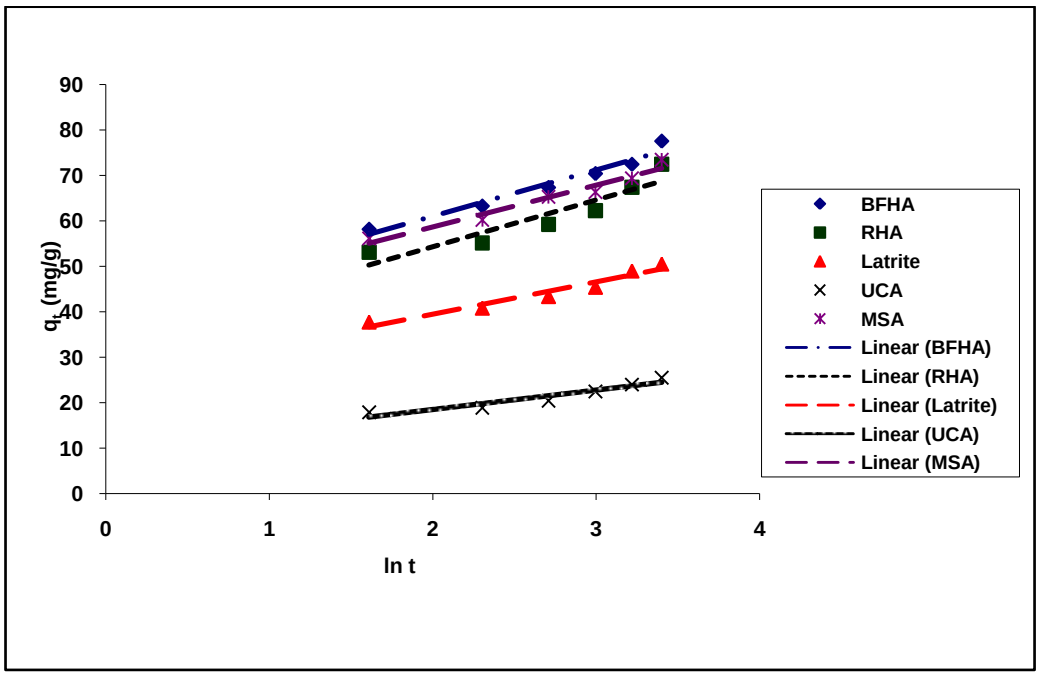

Fig.4.490 :Kinetic plot of Elovich for various adsorbents in PIE at 35°C

4.2.6.2 Adsorption kinetics in respect of VIE.

The linearised form of the equations were plotted as shown in the figures 4.490 to 4.497. The peculiar kinetic parameters have been evaluated from the slopes and intercepts of the various linear plots and shown in tables 4.160 to 4.163. The kinetic data were analysed by fitting into BVM, PFO, PSO and Elovich at the temperatures of 25^0C and 35^0C to ascertain its validity.

The results presented on tables 4.160 to 4.163, indicate that Elovich model best describe the process, having recorded the highest R^2 at a lower temperature of 25^0C. This suggests that the adsorption process for PIE and VIE were enhanced at low operating temperature. It should be emphasized that R^2 recorded by other models are satisfactory (0.7869 to 0.9977).

Table 4.160 Kinetics parameters for BVM at varying temperature of VIE

Adsorbents	25^0C		35^0C	
	$K_B(min^{-1})$	R^2	$K_B(min^{-1})$	R^2
BFHA	-0.1068	0.9740	-0.0375	0.8844
RHA	-0.0850	0.9977	-0.0775	0.9324
Laterite	-0.0337	0.9815	-0.0014	0.9567
UCA	-0.0333	0.9868	-0.0547	0.9851
MSA	-0.0455	0.9688	-0.0748	0.9364

Table 4.161 Kinetics parameters for PFO at varying temperature of VIE

Adsorbents	25^0C			35^0C		
	$K_1(min^{-1})$	Q_e(mg/g)	R^2	$K_1(min^{-1})$	Q_e(mg/g)	R^2
BFHA	0.1069	0.0078	0.9740	0.0375	0.0065	0.8844
RHA	0.0850	0.0105	0.9977	0.0775	0.0036	0.9324
Laterite	0.0337	0.0216	0.9815	0.0808	0.0060	0.9660
UCA	0.0222	0.0135	0.9868	0.0547	0.0049	0.9851
MSA	0.0455	0.0088	0.9688	0.0748	0.0038	0.9364

Table 4.162: Kinetics parameters for PSO at varying temperature of VIE

Adsorbents	25^0C			35^0C		
	K_2(g/mg min^{-1})	Q_e(mg/g)	R^2	K_2(g/mg min^{-1})	Q_e(mg/g)	R^2
BFHA	0.0802	52.6316	0.09965	0.0301	105.2632	0.9840
RHA	0.0672	53.4759	0.9993	0.0655	83.3333	0.9715
Laterite	0.0658	39.3701	0.9980	0.0826	58.8235	0.9905
UCA	0.2120	21.0970	0.9947	0.0861	63.2911	0.9942
MSA	0.0562	64.1026	0.9910	0.0336	119.0476	0.9896

Table 4.163 :Kinetics parameters of ELOVICH model at varying temperature of VIE

Adsorbents	25^0C			35^0C		
	B(mg/g. min^{-1})	x(mg/g/min)	R^2	B(mg/g. min^{-1})	x(mg/g/min)	R^2
BFHA	0.0247	1.4878	0.9555	0.0277	3.7947	0.7869
RHA	1.0000	0.0000	1.0000	0.0131	1.4566	0.8527
Laterite	0.0761	4.3982	0.9926	0.0207	1.5339	0.9355
UCA	0.0614	1.8250	0.9858	0.0117	1.2020	0.9864
MSA	0.0316	2.4537	0.9296	0.0139	1.8043	0.9380

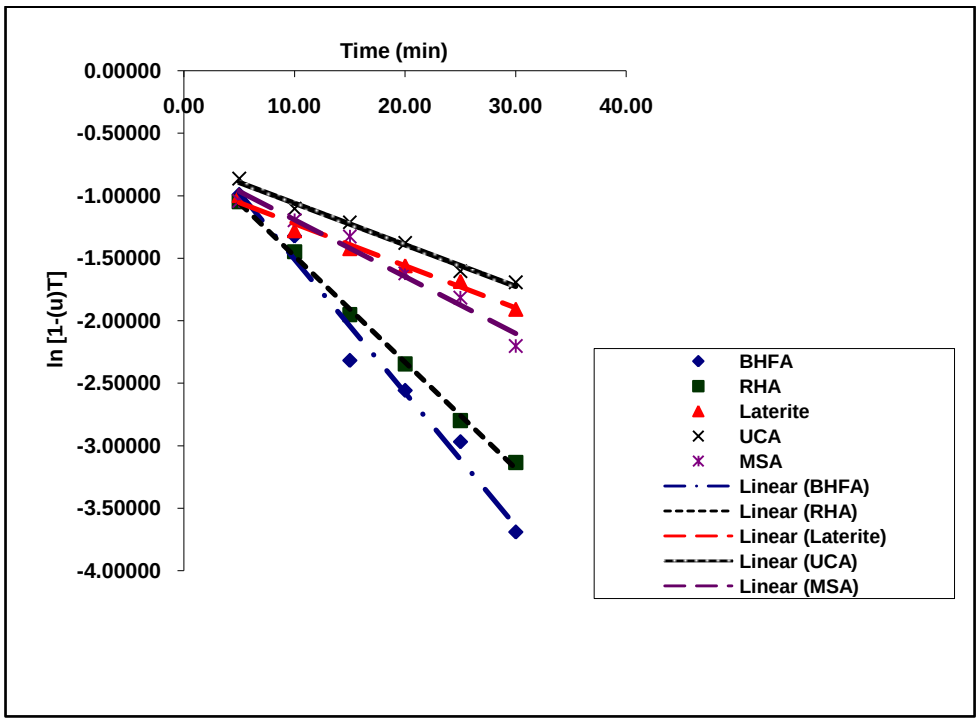

Fig.4.491 :BVM kinetic plot for various adsorbents in VIE at 25°C

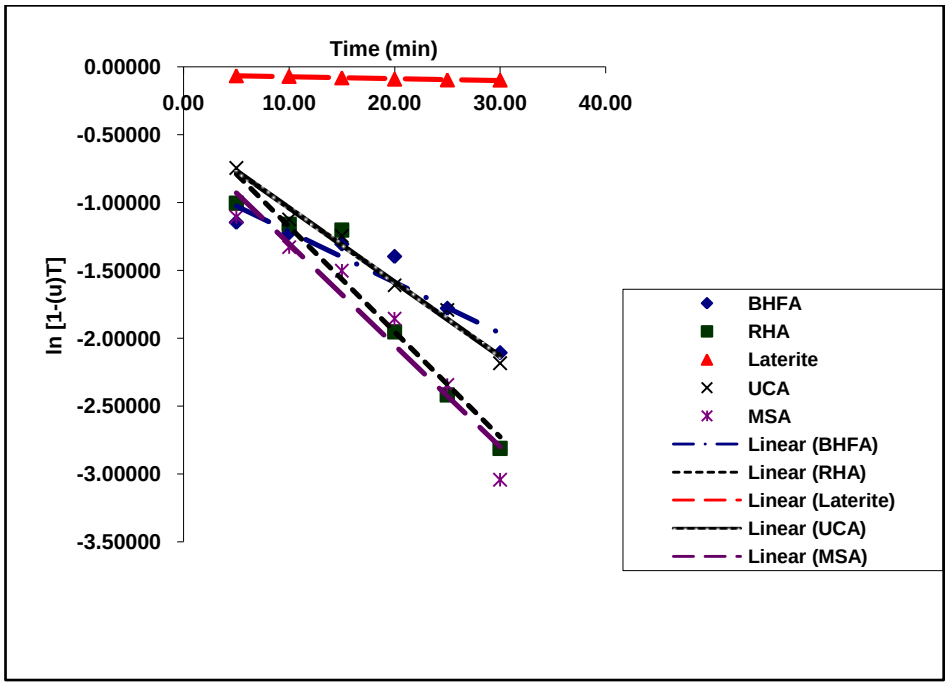

Fig.4.492 : BVM kinetic plot for various adsorbents in VIE at 35°C

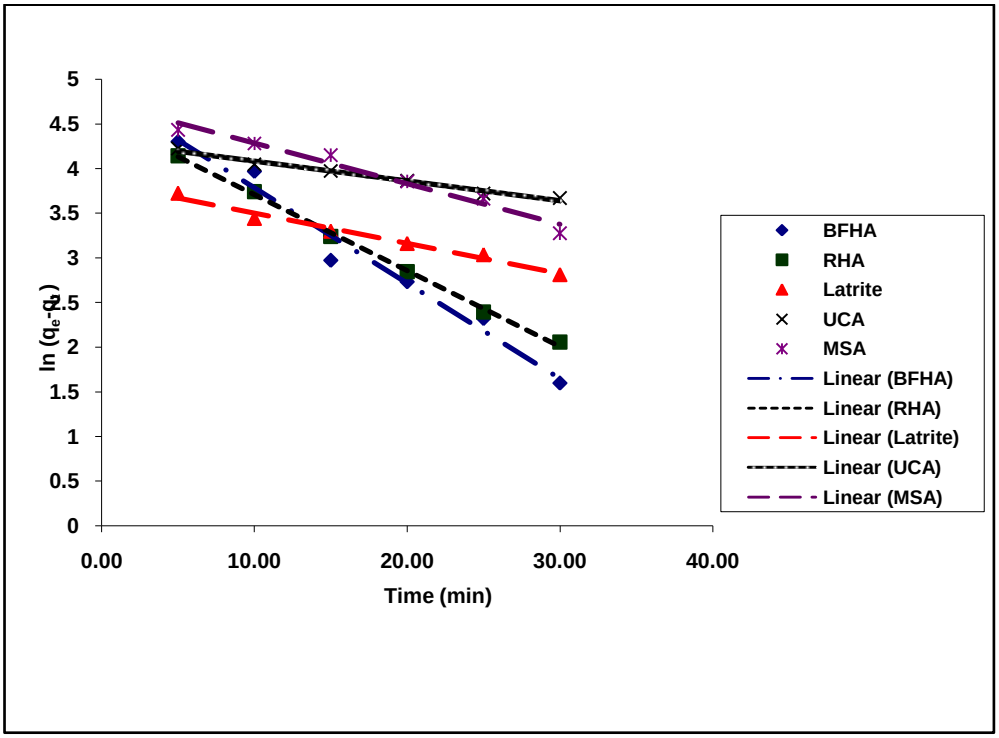

Fig.4.493: Kinetic plot of Pseudo First Order for various adsorbents in VIE at 25°C

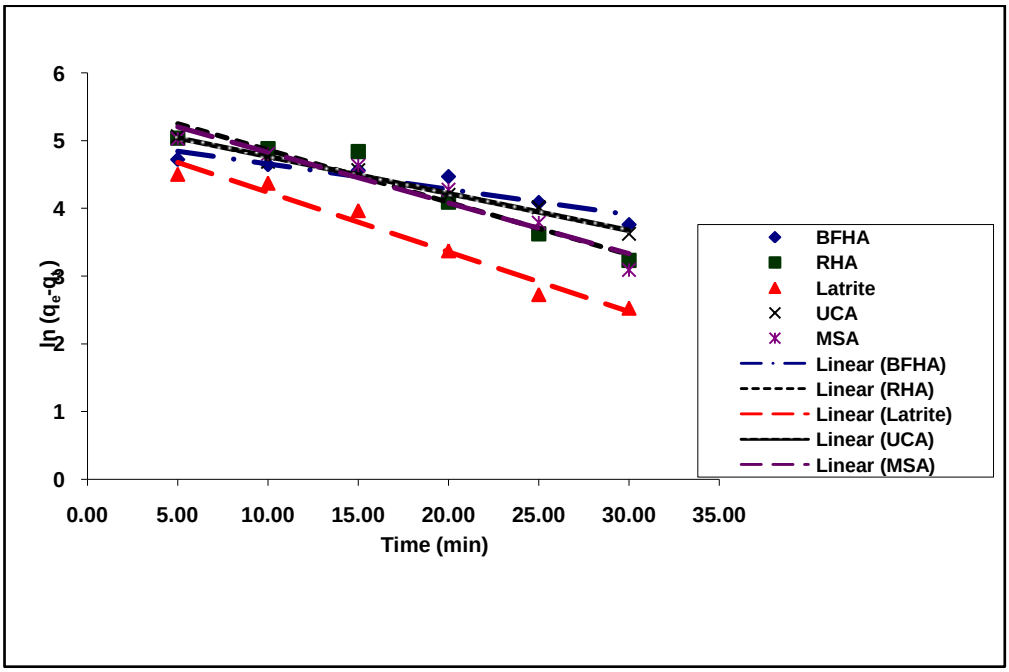

Fig.4.494: Kinetic plot of Pseudo First Order for various adsorbents in VIE at 35°C

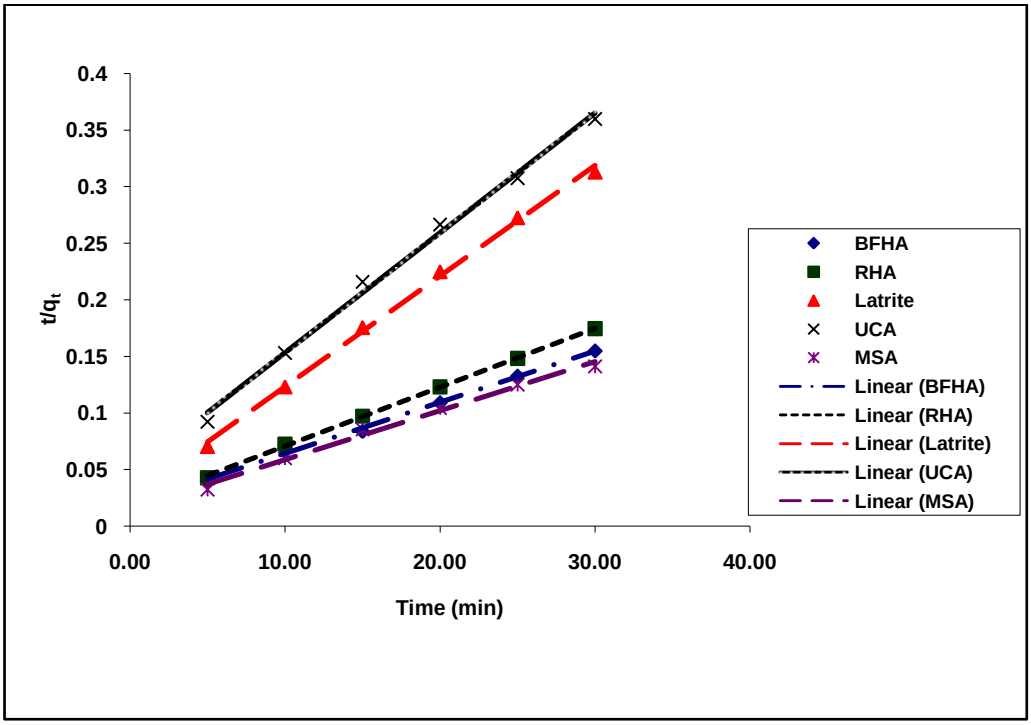

Fig.4.495: Kinetic plot of Pseudo Second Order for various adsorbents in VIE at 25°C

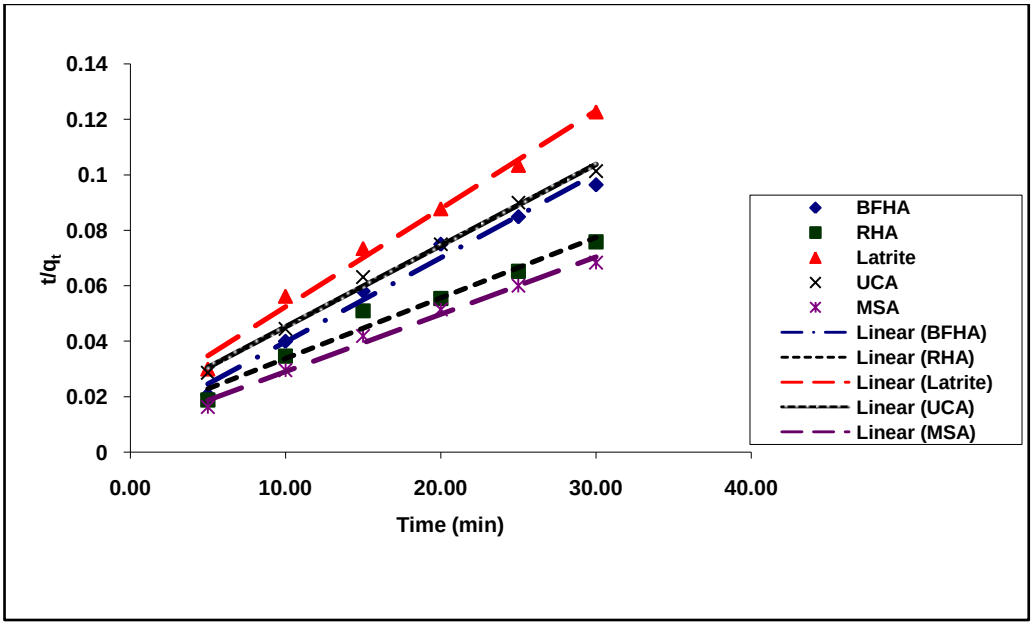

Fig.4.496:Kinetic plot of Pseudo Second Order for various adsorbents in VIE at 35°C

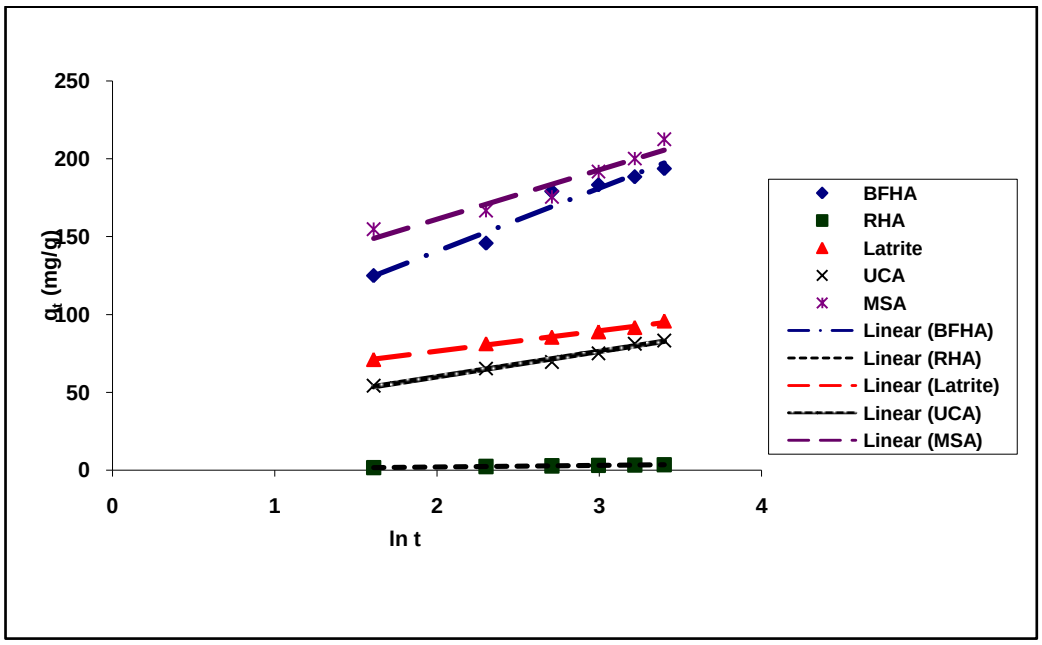

Fig.4.497 :Elovich kinetic plot for various adsorbents in VIE at 25°C

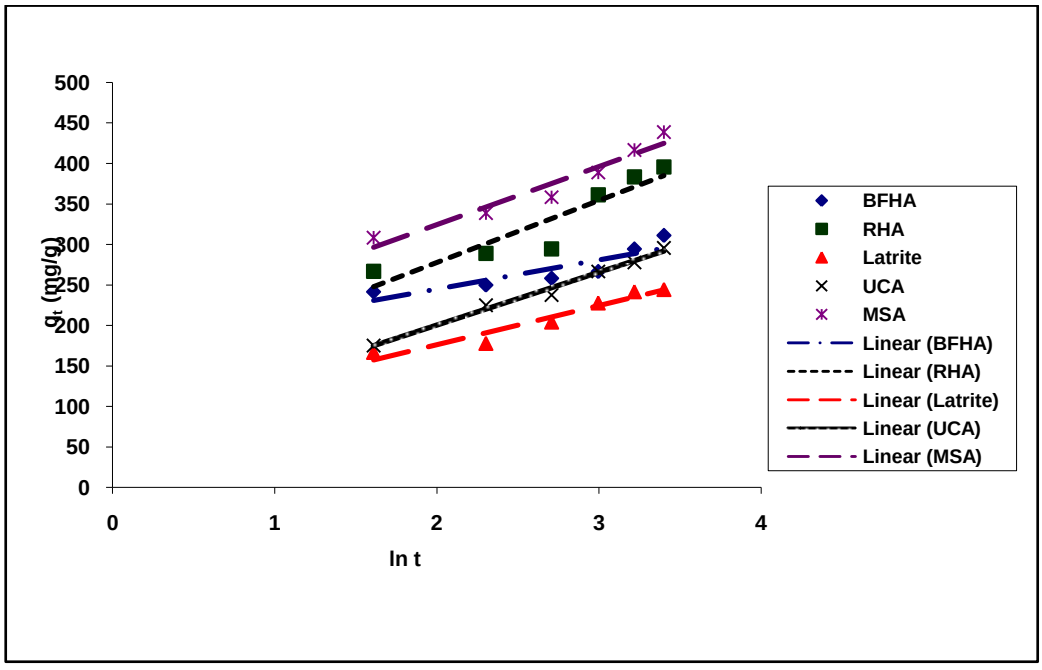

Fig. 4.498 : Elovich Kinetic plot for various adsorbents in VIE at 35°C

4.2.7 Adsorption Thermodynamics

The values of thermodynamic parameters are important for adsorption process. Data peculiar to adsorption of TDSS inherent in PIE and VIE onto BFHA, RHA, LATERITE, UCA and MSA at 25^0 and 35^0C were analyzed to obtain the values of thermodynamic parameters such as change in free energy (ΔG^0), enthalpy change (ΔH^0) and entropy change (ΔS^0).

The negative values of (ΔG^0), indicate the feasibility and spontaneous nature of the adsorption process. The positive value (ΔH^0) confirms the endothermic nature of the adsorption process. The positive value of (ΔS^0) shows the increased affinity of the adsorbate towards the adsorbent. The positive values of Ea, and ΔH^0 are indication of the presence of an energy barrier in the adsorption process (Haque,et al., 1968). In addition, the positive value of (ΔS^0) is an evidence of increased randomness at the solid/solution interface during the adsorption (Manju and Anirudhan, 1996). Generally, the activation energy for physisorption is between 5 – 40kj/mol while that for chemisorption is between 40 – 800kj/mol (Menkiti, 2010). The detailed discussions are presented for PIE and VIE below.

4.2.7.1 Adsorption Thermodynamics perculiar to PIE and VIE

The isotherms data related to adsorption of TDSS onto BFHA, RHA, LATERITE, UCA, MSA at 25^0C and 35^0C were analysed to obtain the values of the thermodynamic parameters. Free energy change (ΔG^0), enthalpy change (ΔH^0) and entropy change (ΔS^0) for the adsorption process were calculated using equations 2.48 to 2.50 and the computed value for the parameters are presented in tables 4.164 to 4.167

The values of ΔG^0 decreased for all the various adsorbents in both PIE and VIE. This is an evidence that the adsorption of TDSS on the various adsorbent were more effective at a higher temperature. However, the thermodynamic results show that the adsorption` were more favorable at higher temperature. The entire adsorption process is endothermic in nature as demonstrated by good affinity of the TDSS towards the adsorbent. Also increase in feasibility of adsorption at elevated temperatures was shown by the increase in the value of ΔG^0 with temperature, thus affirming the endothermic nature of adsorption. The positive values of ΔH^0 also collaborated this statement.

In general, the value of ΔG^0 for physisorption is between -20 and 0 kJ/mol, and that for chemisorption is between -400 and -80kj/mol (Liu, et al., 2010). The values of ΔG^0 obtained in this work were in the range of neither physisorption nor chemisorptions, indicating that the adsorption of TDSS on the various adsorbents in all cases involves the other adsorption process such as ion exchange. (Lin, et al; 2011).

Table 4.164: Adsorption Thermodynamic parameters of various adsorbents for PIE at 25°C

Adsorbent	K_{L1} (l/mg)	ΔG^0 (Kj/mol)	ΔH^0 (Kj/mol)	ΔS^0(J/mol.K)
BFHA	1.9873	-1701.5393	44111.4694	153.7349
RHA	4.9759	-3975.5275	61933.6067	221.1716
Laterite	1.9960	-1712.3619	48072.9186	167.0647
UCA	2.4131	-2182.5235	49737.5663	174.2285
MSA	8.0438	-5165.4938	66677.6181	241.0843

Table 4.165: Adsorption Thermodynamic parameters of various adsorbents for PIE at 35°C

Adsorbent	K_{L2} (l/mg)	ΔG^0 (Kj/mol)	ΔH^0 (Kj/mol)	ΔS^0(J/mol.K)
BFHA	3.2790	-3040.9441	44111.4694	153.0923
RHA	7.2151	-5060.4177	61933.6067	217.5131
Laterite	2.9940	-2808.1031	48072.9186	165.1981
UCA	3.8610	-3459.3330	49737.5663	172.7172
MSA	10.8591	-6107.3069	66677.6181	236.3147

Table 4.166: Adsorption Thermodynamic parameters of various adsorbents for VIE at 25°C

Adsorbent	K_{L1} (l/mg)	ΔG^0 (Kj/mol)	ΔH^0 (Kj/mol)	ΔS^0(J/mol.K)
BFHA	1.6835	-1290.5052	37783.2388	131.1199
RHA	7.6394	-5037.6944	67558.1044	243.6101
Laterite	4.1459	-3523.4044	60474.4769	214.7580
UCA	4.4395	-3692.9245	58944.3300	210.1921
MSA	5.6603	-4294.8138	60005.6201	215.7733

Table 4.167: Adsorption Thermodynamic parameters of various adsorbents for VIE at 35°C

Adsorbent	K_{L2} (l/mg)	ΔG^0 (Kj/mol)	ΔH^0 (Kj/mol)	ΔS^0(J/mol.K)
BFHA	2.8620	-2692.6416	37783.2388	131.4152
RHA	9.9312	-5878.5787	67558.1044	243.4308
Laterite	6.0116	-4593.1259	60474.4769	211.2585
UCA	6.8812	-4939.8352	58944.3300	207.4161
MSA	9.0565	-5642.4847	60005.6201	213.1432

4.2.8 Adsorption Optimization of Statistically Designed Experiment

This section presents adsorption optimization with the corresponding surface contour (3D) plots obtained from central composite design (CCD) of the experiment. For each of the design matrix, three variables, 17 experiments, double replications, 3 centre points and 6 stars points were involved. The table of model coefficients are presented in tables B_1 and B_2 respectively of the appendix B

The optimization results of the local adsorbents with objective of minimizing the quantity of adsorbate in both PIE and VIE are presented in tables 4.168 and 4.169, respectively. For each matrix of the design, the limits for varying factors are same for the adsorbents. Observation from the tables show that for tables 4.168 and 4.169, minimal adsorbate of 29.4796 mg/l and 100.8290 mg/l are recorded for PIE and VIE, respectively. In addition, optimal values of the coded values obtained were converted to real values.

The representative surface contour (3D) plots of the most efficient adsorbent were presented in figures. 4.499 to 4.501 and 4.502 to 4.504 for PIE and VIE, respectively. The figures demonstrate in three dimensions the three way interaction/relationship among two independent and single dependent variables. The independent variables in this study are combination of adsorbent mass and pH; stirring time and pH; stirring time and adsorbent mass. Whereas the dependent variable is the single process response (adsorbent uptake) during the adsorption process.

The surface/contour plots indicate areas of optimal adsorption. From figures. 4.498, 4.499, 4.500, 4.501, 4.502 and 4.503, the optimal adsorbent uptake occurred at 14.000 mg/l, 10.00 mg/l, 5.00 mg/l, 50.00 mg/l, 20.00 mg/l and 20.00 mg/l for PIE and VIE, respectively.

In addition the results obtained from the experiments were shown in tables 4.170 to 4.179. The tables indicate that the coefficients of first order real terms variable (pH, Adsorbent mass, stirring time), interactive terms pH/ adsorbent mass; pH / Stirring time; adsorbent mass / Stirring time) and quadratic interaction pH^2, adsorbent $mass^2$, stirring $time^2$) proved to be significant since all the values obtained are far less than 0.05. This is supported by large F-values obtained in all the experiments. The results affirmed that there is significant model correlation between the variables and process response.

The high R^2 values presented in the tables indicate minimal amount of the total variation in the response predicted by the model. A high R^2 value, close to one is desirable and reasonable agreement with adjusted R^2 is a condition. A high R^2 ensures a satisfactory adjustment of the multivariable polynomial model to the experimental data (Menkiti, et al; 2012). This allows for the presentation of the CCD model and DOE procedures as a consistent statistical method for analyzing the work under study at the conditions of the experiment. ANOVA discussions on the adequacy of model as it concerns individual adsorbents in removing/reducing TDSS inherent in PIE and VIE media is done in subsequent sections.

Table 4.168 Optimum data for Adsorption Process Model Wrt. Various Adsorbent In PIE

Adsorbent	x_1(pH)		X_2(Adsorbent Mass)		X_3 (Stirring time)		Y_u(TDSSmg/l) uptake	Y_{cv} (mg/l)
	CV*	RV**	CV*	RV**(g)	CV*	RV**(min)		
BFHA	1.0000	10.0000	-1.0000	0.2000	-1.0000	5.0000	35.8176	35.0806
RHA	-1.0000	2.0000	-1.0000	0.2000	-1.0000	5.0000	33.3372	33.2112
LATERITE	-1.0000	2.0000	-1.0000	0.2000	-1.0000	5.0000	31.0350	30.9508
UCA	1.0000	10.0000	-1.0000	0.2000	-1.0000	5.0000	29.4796	28.8900
MSA	0.4328	7.6312	-1.0000	0.2000	-1.0000	5.0000	45.663	44.5121

Table 4.169 Optimum Data For Adsorption Process Model Wrt. Various Adsorbent In VIE

Adsorbent	x_1(pH)		X_2(Adsorbent Mass)		X_3 (Stirring time)		Y_u(TDSSmg/l) uptake	Y_{cv} (mg/l)
	CV*	RV**	CV*	RV**(g)	CV*	RV**(min)		
BFHA	1.0000	10.0000	-1.0000	0.2000	-1.0000	5.0000	126.9092	25.8290
RHA	-1.0000	2.0000	-1.0000	0.2000	-1.0000	5.0000	100.8290	101.2311
LATERITE	-1.0000	2.0000	-1.0000	0.2000	-1.0000	5.0000	176.5640	175.7932
UCA	-1.0000	2.0000	-1.0000	0.2000	-1.0000	5.0000	113.6578	114.8356
MSA	-1.0000	2.0000	-1.0000	0.2000	-1.0000	5.0000	250.8341	251.4562

4.2.8.1 ANOVA discussion on LATERITE adsorbent in PIE

The most significant linear term is stirring time, while the least significant is pH. All the interaction terms were not significant. The quadratic terms of pH and stirring time were significant as presented in table 4.170. The model accuracy is validated by the value of R^2 and adjusted R^2, which is further amplified by closeness of the values. The model equation is given as; $Y=8.6580-0.19608_{pH}-2.5524_{Ads.mass}-9.2663_{stir.time}+0.79274_{pH*Ads.mss}-0.50175_{pH*stirring}-1.785_{Ads.mass*stir.time}+3.8357_{pH}{}^{\wedge 2}+3.0183_{Ads.mass}{}^{\wedge 2}$

$+3.3957_{stir.time}{}^{\wedge 2}$ (4.18)

Deleting parameters that are not significant gives;

$Y=8.6580-2.5534_{Ads.mass}-9.2663_{stir.time}+3.8357_{pH}{}^{\wedge 2}$

$+3.395_{stir.time}{}^{\wedge 2}$ (4.19)

Table 4.170: Analysis of Variance of Statistically Designed Adsorption Experiment for LATERITE in PIE

Variables	Coefficients	Se	tstat	P-avlue	Remarks
Constant	8.6580	1.0124	8.5516	5.9407e-5	
pH	-0.19608	0.73428	-0.26704	0.79713	Not Significant
Adsorbent mass	-2.5524	0.69314	-3.6824	0.0078352	Significant
Stirring Time	-9.2663	0.71184	-13.017	3.6762e-6	Significant
pH*Ads. Mass	0.79274	0.76964	1.03	0.33727	Not Significant
pH*Set. Time	-0.50175	0.79586	-0.63045	0.54842	Not Significant
Ads. mass *Stir. Time	-0.1785	0.79586	-0.22428	0.82894	Not Significant
pH^2	3.8357	1.5751	2.4353	0.045071	Significant
Ads.mass^2	3.0183	1.514	1.9936	0.086434	Not Significant
Stir. Time^2	3.3957	1.3257	2.5614	0.037474	Significant
	R^2 = 0.9719	Adj. R^2= 0.9375	MSE = 5.0672		

4.2.8.2 ANOVA discussion on BFHA in PIE

From the result posted in table 4.171, stirring time, adsorbent mass and quadratic term of stirring time are significant while their interactions and other quadratic terms are not significant. Thus, the final model equation is given as follow;

$Y=14.424-3.2394_{Ads.mass}-11.593_{stair.time}+5.3363_{stair.time}{}^{\wedge 2}$. (4.20)

The model is adequate to predict the behavior of BFHA as adsorbent. The model fit has an R^2 greater than 98%, very close to the Adj. R^2 > 96%. The linear effect of stirring time is more prominent than its quadratic effect.

Table 4.171**:** Analysis of Variance of Statistically Designed Adsorption Experiment for BFHA in PIE

Variables	Coefficients	Se	tstat	P-avlue	Remarks
Constant	14.424	0.84169	17.136	5.6558e-7	
pH	0.3683	0.61044	0.60334	0.56531	Not Significant
Adsorbent mass	-3.2394	0.57624	-5.2616	0.00079778	Significant
Stirring Time	-11.593	0.59179	-19.59	2.2545e-7	Significant
pH*Adsorbent mass	0.13058	0.63984	0.20408	0.8441	Not Significant
pH*Stir. Time	-1.0551	0.66164	-1.5947	0.15481	Not Significant
Ads.mass*Stir. Time	0.26987	0.66164	0.40789	0.69554	Not Significant
pH^2	-0.58574	1.3094	-0.44733	0.66815	Not Significant
Adsorbent mass^2	0.24796	1.2587	0.197	0.84942	Not Significant
Stir. Time^2	5.3363	1.1021	4.8417	0.001874	Significant
	R^2 = 0.9849	Adj. R^2= 0.9656	MSE = 3.5021		

4.2.8.3 ANOVA discussion on UCA in PIE.

Table 4.172, show that the linear term of stirring time quadratic of pH are significant. Thus, all the effects of linear terms, interaction and other quadratic terms were not significant. Hence they are excluded from the final model equation of fit.

$$Y=3.6878-9.5212_{stir.time}+7.7867_{pH\wedge 2} \quad (4.21)$$

Table 4.172**:** Analysis of Variance of Statistically Designed Adsorption Experiment for UCA in PIE

Variables	Coefficients	Se	tstat	P-avlue	Remarks
Constant	3.6878	1.6366	2.2533	0.58911	
pH	1.0503	1.187	0.88487	0.40559	Not Significant
Adsorbent mass	-2.4313	1.1205	-2.1699	0.066623	Not Significant
Stirring Time	-9.5212	1.1507	-8.2744	7.3447e-5	Significant
pH*Adsorbent mass	-0.58473	1.2441	-0.47	0.65265	Not Significant
pH*Stirring Time	-0.06625	1.2865	-0.051496	0.96037	Not Significant
Ads. mass*Stir. Time	0.2795	1.2865	0.21726	0.83421	Not Significant
pH^2	7.7867	2.5461	3.0583	0.018367	Significant
Adsorbent mass^2	0.88261	2.4474	0.36063	0.72901	Not Significant
Stirring. Time^2	3.1892	2.143	1.4882	0.1803	Not Significant
	R^2 = 0.9388	Adj. R^2= 0.8602	MSE = 13.2408		

4.2.8.4 ANOVA discussion on RHA in PIE

The most significant linear term is stirring time closely followed by adsorbent mass, while pH is the least. Also their interaction and quadratic effects with the exception of stirring time were not significant. The high value of R^2 and closeness to Adj. R^2 supports the adequacy of the model. The insignificant parameters were excluded from the final model fit equation.

$$Y=11.443-3.9872_{Ads.mass}-10.817_{stir.time}+5.0086_{stir.time\wedge 2} \quad (4.22)$$

Table 4.173**:** Analysis of Variance of Statistically Designed Adsorption Experiment for RHA in PIE

Variables	Coefficients	Se	tstat	P-avlue	Remarks
Constant	11.443	0.4313	26.531	2.7675e-8	
pH	-0.26702	0.3128	-0.85363	0.42156	Not Significant
Adsorbent mass	-3.9872	0.29528	-13.503	2.8696e-6	Significant
Stirring Time	-10.817	0.30324	-35.672	3.5322e-9	Significant
pH*Adsorbent mass	-0.11118	0.32787	-0.33911	0.74448	Not Significant
pH*Stir. Time	-0.07675	0.33904	-0.22638	0.82738	Not Significant
Ads. mass *Stir. Time	0.75875	0.33904	2.238	0.060259	Not Significant
pH^2	1.0287	0.67097	1.5331	0.16912	Not Significant
Adsorbent mass^2	0.21481	0.64497	0.33306	0.74884	Not Significant
Stirring Time^2	5.0086	0.56476	8.8685	4.6936e-5	Significant
	R^2 = 0.9957	Adj. R^2= 0.9902	MSE = 0.9196		

4.2.8.5 ANOVA discussion on MSA in PIE

The result posted in table 4.174, show that all the effects of linear parameter were significant. However, most significant is stirring time. Thus, a change in stirring time has the most effect on the effectiveness of the adsorbent in reducing the TDSS. Also the interaction effects of pH and adsorbent mass with quadratic effect of stirring time are significant. Thus, the model equation is given as;

$Y=18.351+0.56944_{pH}-4.9973_{Ads.mass}-15.651_{stir.time}-0.31379_{pH*ads.mass}+0.1285_{pH*stir.time}$

$+0.56775_{ads.mass*stir.\ time}-0.872_{pH\wedge 2}$

$+0.54288_{ads.mass\wedge 2}+5.3907_{stir.time\wedge 2}$ (4.23)

Deleting variables that are not significant gives;

$Y=18.351+0.56944_{pH}-49973_{ads.time}-15.651_{stir.\ time}$

$+0.56775_{ads.mass}*_{stir.time}+5.3907_{stir.time\wedge 2}$ (4.24)

Table 4.174: Analysis of Variance of Statistically Designed Adsorption Experiment for MSA in PIE

Variables	Coefficients	Se	tstat	P-avlue	Remarks
Constant	18.351	0.3475	52.807	2.2883e-10	
pH	0.56944	0.25203	2.2595	0.058378	Significant
Adsorbent mass	-4.9973	0.23791	-21.005	1.3939e-7	Significant
Stirring Time	-15.651	0.24433	-64.059	5.9347e-11	Significant
pH*Adsorbent mass	-0.31379	0.26416	-1.1879	0.27362	Not Significant
pH*Stir. Time	0.1285	0.27316	0.47041	0.65236	Not Significant
Ads. mass *Stir. Time	0.56775	0.27316	2.0784	0.076263	Not Significant
pH^2	-0.872	0.54061	-1.6130	0.15078	Not Significant
Adsorbent mass^2	0.54288	0.51965	1.0447	0.33089	Not Significant
Stir. Time^2	5.3907	0.45503	11.847	6.93e-6	Significant
	R^2 = 0.9985	Adj. R^2= 0.9967	MSE = 0.5969		

4.2.8.6 ANOVA discussion on BFHA in VIE.

The quadratic model equation obtained for the removal of TDSS from VIE using BFHA is shown as follows;

$$Y_{TDSS}=12.094+8.7895pH-12.623_{ads.mass}-36.32_{stir.time}-7.1104_{pH*ads.mass}-4.5939_{pH*stir.time}+5.0714_{ads.mass*stir.time}+6.3805_{pH\wedge 2}+4.9235_{ads.mass\wedge 2}+29.003_{stir.time\wedge 2} \quad (4.25)$$

The equation indicate that all the main factor effects except pH have negative effect on the percentage removal, that is their decrease causes a corresponding decrease in the percentage removal (Y), while the quadratic terms have positive effect on the percentage removal as can be observed from the equation with positive coefficients. The equation after removing the insignificant parameters becomes;

$$Y=12.094+8.7895_{pH}-12.623_{ads.mass}-36.32_{stir.time}-7.1104_{pH*ads.\ mass}+29.003_{stir.time\wedge 2} \quad (4.26)$$

Table 4.175: Analysis of Variance of Statistically Designed Adsorption Experiment for BFHA in VIE

Variables	Coefficients	Se	tstat	P-avlue	Remarks
Constant	12.094	3.706	3.2634	0.0138	
pH	8.7895	2.6877	3.2702	0.01367	Significant
Adsorbent mass	-12.623	2.5372	-4.9751	0.0016098	Significant
Stirring Time	-36.32	2.6056	-13.939	2.3137e-6	Significant
pH*Adsorbent mass	-7.1104	2.8172	-2.5239	0.039582	Significant
pH*Stir. Time	-4.5939	2.9132	-1.5769	0.15882	Not Significant
Ads. mass*Stir. Time	5.0714	2.9132	1.7408	0.12525	Not Significant
pH^2	6.3805	5.7653	1.1067	0.305	Not Significant
Adsorbent mass^2	4.9235	5.5419	0.88842	0.40381	Not Significant
Stirring Time^2	29.003	4.8527	5.9767	0.00055502	Significant
	R^2 = 9785	Adj. R^2= 0.9508	MSE = 67.8926		

4.2.8.7 ANOVA discussion on RHA in VIE.

The quadratic model equation obtained using RHA for the removal of TDSS from VIE is shown below;

$$Y=24.19+0.43714_{pH}-10.943_{ads.mass}-30.864_{stir.time}+1.6212_{pH*ads.mass}$$
$$+5.5383_{pH*stir.time}+4.835_{ads.mass*stir.time}+1.0954_{pH\wedge 2}+2.5612_{ads.mass\wedge 2}$$
$$+19.618_{stir.time\wedge 2} \quad (4.27)$$

Table 4.176 show that smaller the P-value the more significant is the correspondent coefficient. Thus, the model equation with the significant coefficients is shown below;

$$Y=24.19-10.943_{ads.mass}-30.864_{stir.time}+5.5383_{pH*stir.time}$$
$$+4.835_{ads.mass*stir.time}+19.618_{stir.time\wedge 2} \quad (4.28)$$

Table 4.176: Analysis of Variance of Statistically Designed Adsorption Experiment for RHA in VIE

Variables	Coefficients	Se	tstat	Pvalue	Remarks
Constant	24.19	1.7103	14.144	2.0953e-6	
pH	0.43714	1.2404	0.35243	0.73489	Not Significant
Adsorbent mass	-10.943	1.1709	-9.3457	3.3362e-5	Significant
Stirring Time	-30.864	1.2025	-25.668	3.4817e-8	Significant
pH*Ads. mass	1.6212	1.3001	1.247	0.2525	Not Significant
pH*Stir. Time	5.5383	1.3444	4.1195	0.0044623	Significant
Ads. mass*Stir. Time	4.835	1.3444	3.5964	0.0087817	Significant
pH^2	1.0954	2.6606	0.41169	0.69288	Not Significant
Adsorbent mass^2	2.5612	2.5575	1.0015	0.34996	Not Significant
Stirring Time^2	19.618	2.2395	8.7602	5.0831e-5	Significant
	R^2 = 0.9925	Adj. R^2= 0.9829	MSE = 14.4592		

4.2.8.8 ANOVA discussion on LATERITE in VIE

The test for the significant of the coefficients (any coefficient with P<0.05 is considered significant), indicated that all the linear terms (main effects) and quadratic terms excluding adsorbent mass$\wedge^2$ were significant. Also only the interaction term of pH and stirring time is significant as showed in table 4.177. Thus, the equation after removing the insignificant coefficients becomes;

$Y=23.466-31.991_{pH}-12.76_{ads.mass}-38.541_{stir.time}+4.1181_{pH*ads.mass}$

$+18.122_{pH*stir.time}+2.8761_{ads.mass*stir.time}+31.16_{pH\wedge^2}-2.5112_{ads.mass\wedge^2}$

$+16.041 stir.time_{\wedge^2}$. (4.29)

Table 4.177: Analysis of Variance of Statistically Designed Adsorption Experiment for LATERITE in VIE

Variables	Coefficients	Se	tstat	P-avlue	Remarks
Constant	23.466	2.9023	8.0852	8.5182e-5	
pH	-31.991	2.1049	-15.199	1.2848e-6	Significant
Adsorbent mass	-12.76	1.987	-6.4217	0.00035979	Significant
Stirring Time	-38.541	2.0406	-18.887	2.8998e-7	Significant
pH*Ads. mass	4.1181	2.2063	1.8666	0.1042	Not Significant
pH*Stir. Time	18.122	2.2815	7.9432	9.5386e-5	Significant
Ads.*Stir. Time	2.8761	2.2815	1.2607	0.24783	Not Significant
pH^2	31.16	4.5151	6.9012	0.00023107	Significant
Adsorbent mass^2	-2.5112	4.3401	-0.5786	0.58099	Not Significant
Stirring Time^2	16.041	3.8004	4.2208	0.0039325	Significant
	R^2 = 0.9918	Adj. R^2= 0.9812	MSE = 41.6402		

4.2.8.9 ANOVA discussion on UCA in VIE

Table 4.178, show that all the linear terms, and their interactions were significant. However, stirring time is the most significant process parameter and equally the stirring time is the most significant factor among the quadratic terms. After removing the insignificant coefficients, the model equation becomes;

$Y=43.559-6.1186_{pH}-12.456_{ads.mass}-31.932_{stir.time}+3.5258_{pH*ads.mass}$

$+3.8934_{pH*stir.time}+9.2901$ (4.30)

Table 4.178: Analysis of Variance of Statistically Designed Adsorption Experiment for UCA in VIE

Variables	Coefficients	Se	tstat	P-avlue	Remarks
Constant	43.559	1.1116	39.188	1.8348e-9	
pH	-6.1186	0.80615	-7.5898	0.00012736	Significant
Adsorbent mass	-12.456	0.76099	-16.368	7.7444e-7	Significant
Stirring Time	-31.932	0.78152	-40.858	1.3714e-9	Significant
pH*Ads. mass	3.5258	0.84498	4.1727	0.0041753	Significant
pH*Stir. Time	3.8934	0.87377	4.4558	0.0029508	Significant
Ads. mass*Stir. Time	3.1986	0.87377	3.6607	0.0080627	Significant
pH^2	-1.6026	1.7292	-0.92674	0.3849	Not Significant
Adsorbent mass^2	1.2869	1.6622	0.77418	0.46416	Not Significant
Stirring Time^2	9.2901	1.4555	6.3827	0.00037337	Significant
	R^2 = 0.9967	Adj. R^2= 0.9925	MSE = 6.1078		

4.2.8.10 ANOVA discussion on MSA in VIE

The second order polynomial regression equation that represent the model equation for the removal of TDSS from VIE using MSA adsorbent is shown below;

$$Y=62.787-16.786_{pH}-19.835_{ads.mass}-64.562_{stir.time}+13.303_{pH*ads.mass}$$
$$+9.9003_{pH*stir.time}+2.3308_{ads.mass*stir.time}+37.000_{pH\wedge 2}+3.721_{ads.mass\wedge 2}$$
$$+20.609_{stir.time\wedge 2} \quad (4.31)$$

The equation represents the quantitative effect of the parameters (pH, ads.mass and stir.time) upon the response Y. Positive sign in front of the terms indicates interaction effect while negative sign indicates opposing effect of the parameters. Table 4.177, show that all the linear and the quadratic terms except adsorbent mass $\wedge^2$ were significant. Also from the table 4.179, it can be stated that only the interaction of pH and adsorbent mass is significant. Based on this, the insignificant terms of the model are removed reducing the model equation to the following;

$$Y=62.787-16.786_{pH}-19.835_{ads.mass}-64.562_{stir.time}+13.303_{pH*ads.mass}$$
$$+37.000_{pH\wedge 2}+20.609_{stir.time\wedge 2} \quad (4.32)$$

Table 4.179: Analysis of Variance of Statistically Designed Adsorption Experiment for MSA in VIE

Variables	Coefficients	Se	tstat	P-avlue	Remarks
Constant	62.787	6.8676	9.1405	3.8508e-5	
pH	-16.786	4.9807	-3.3701	0.011919	Significant
Adsorbent mass	-19.835	4.7017	-4.2188	0.0039426	Significant
Stirring Time	-64.562	4.8286	-13.371	3.0672e-6	Significant
pH*Ads. mass	13.303	5.2206	2.5482	0.038205	Significant
pH*Stir. Time	9.9003	5.3985	1.8339	0.10932	Not Significant
Ads. mass*Stir. Time	2.3308	5.3985	0.43174	0.67892	Not Significant
pH^2	37	10.684	3.4631	0.010503	Significant
Adsorbent mass^2	3.721	10.27	0.36232	0.7278	Not Significant
Stirring Time^2	20.609	8.9927	2.2918	0.055662	Significant
	R^2 = 0.9744	Adj. R^2= 0.9414	MSE = 233.1494		

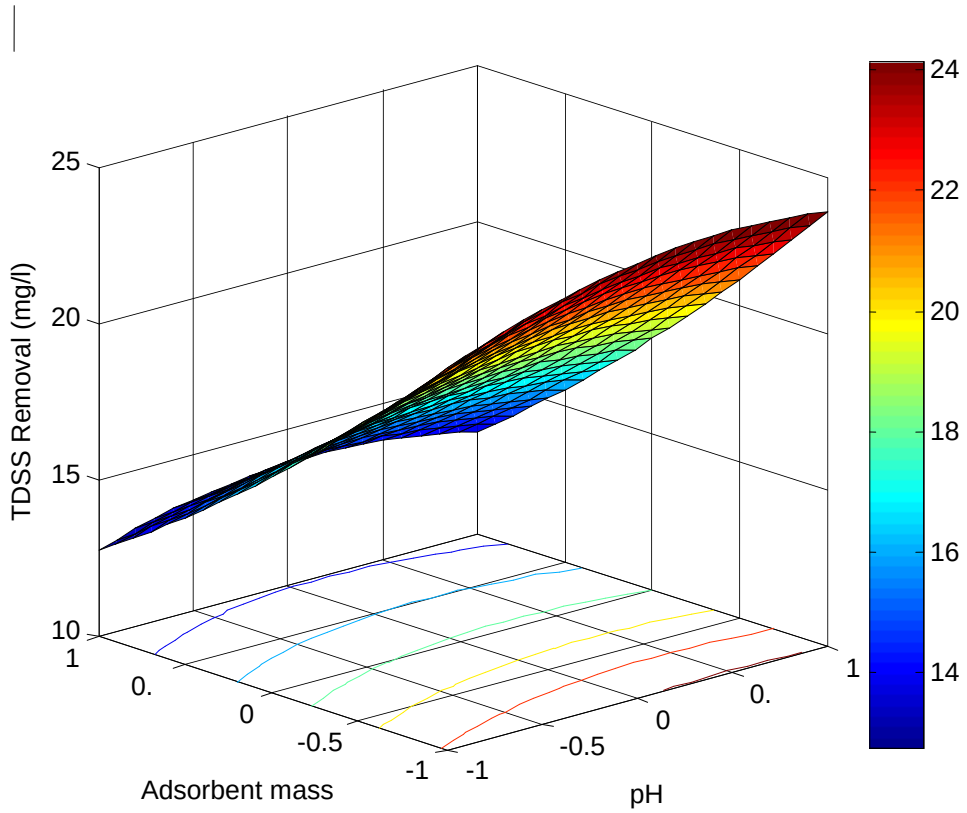

Fig.4.499 :Adsorption surface/contour plots for MSA in PIE showing interaction effects of Adsorbent mass and pH.

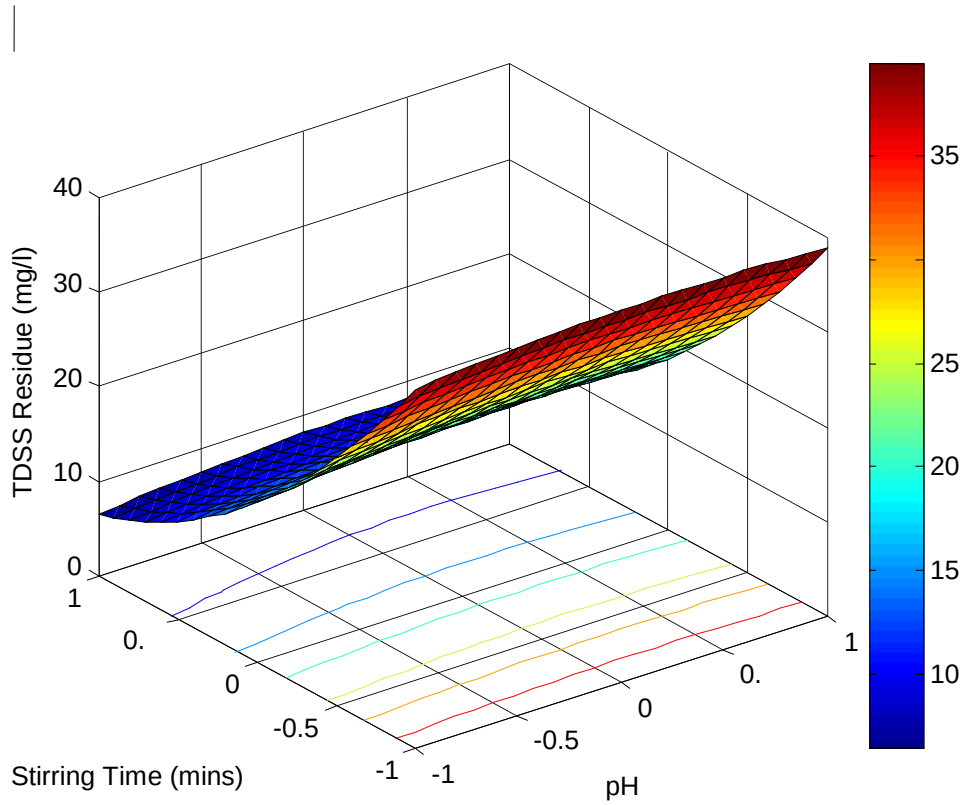

Fig.4.500: Adsorption surface/contour plots for MSA in PIE showing interaction effects of stirring time and pH.

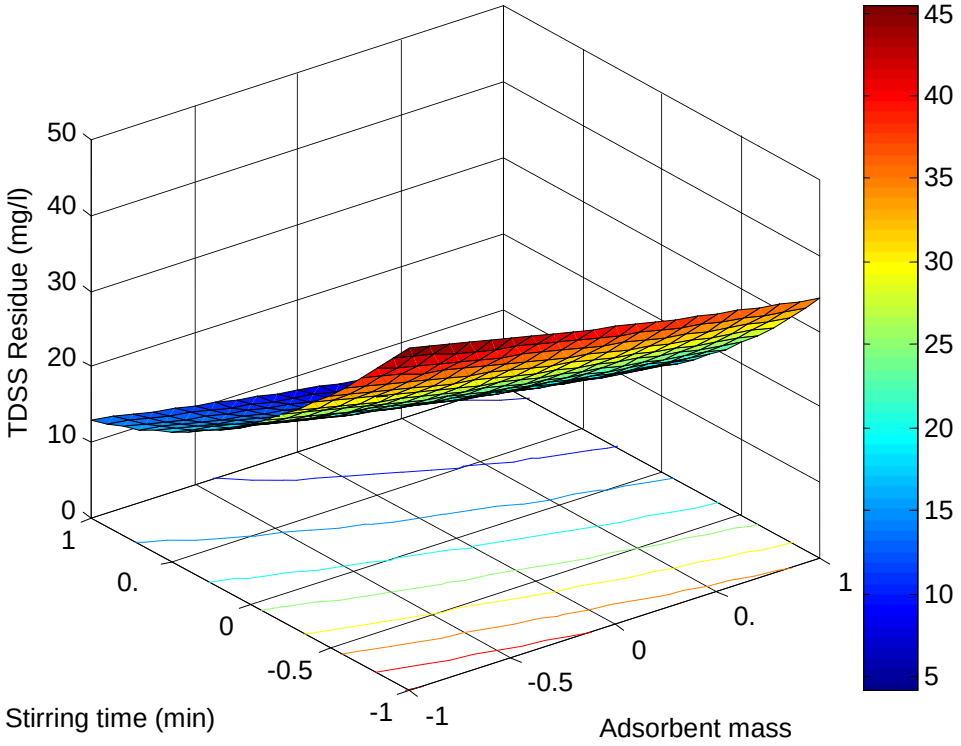

Fig.4.501 :Adsorption surface/contour plots for MSA in PIE showing interaction effects of Stirring time andAdsorbent mass

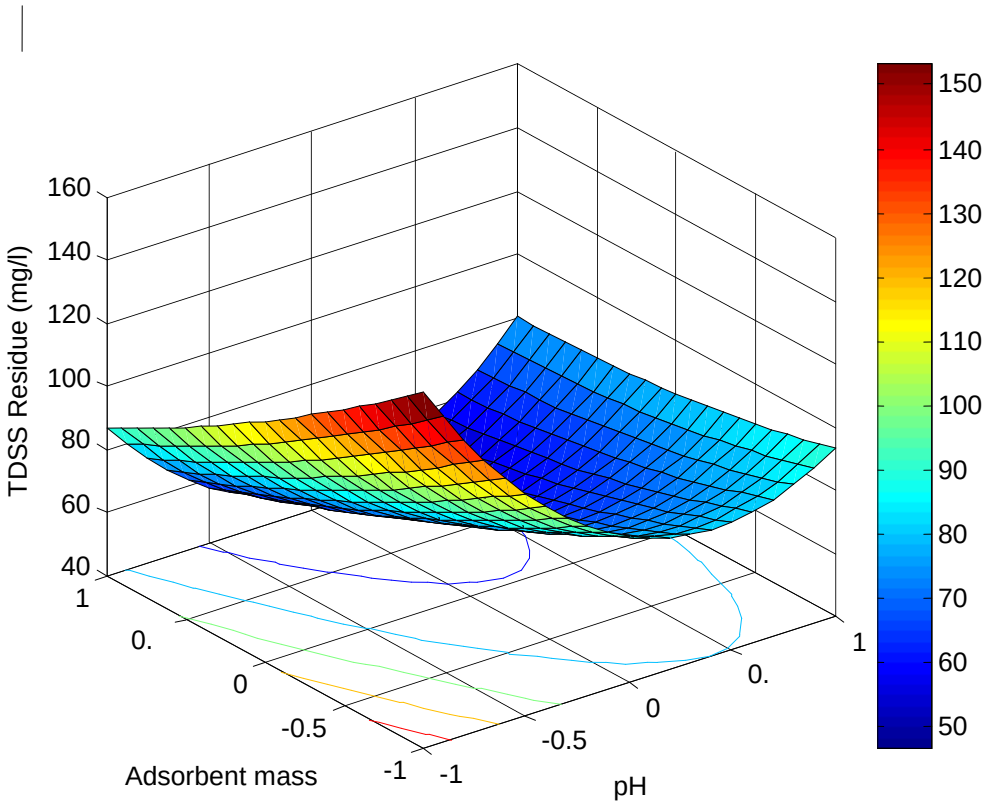

Fig.4.502 :Adsorption surface/contour plots for MSA in VIE showing interaction effects of Adsorbent mass and pH

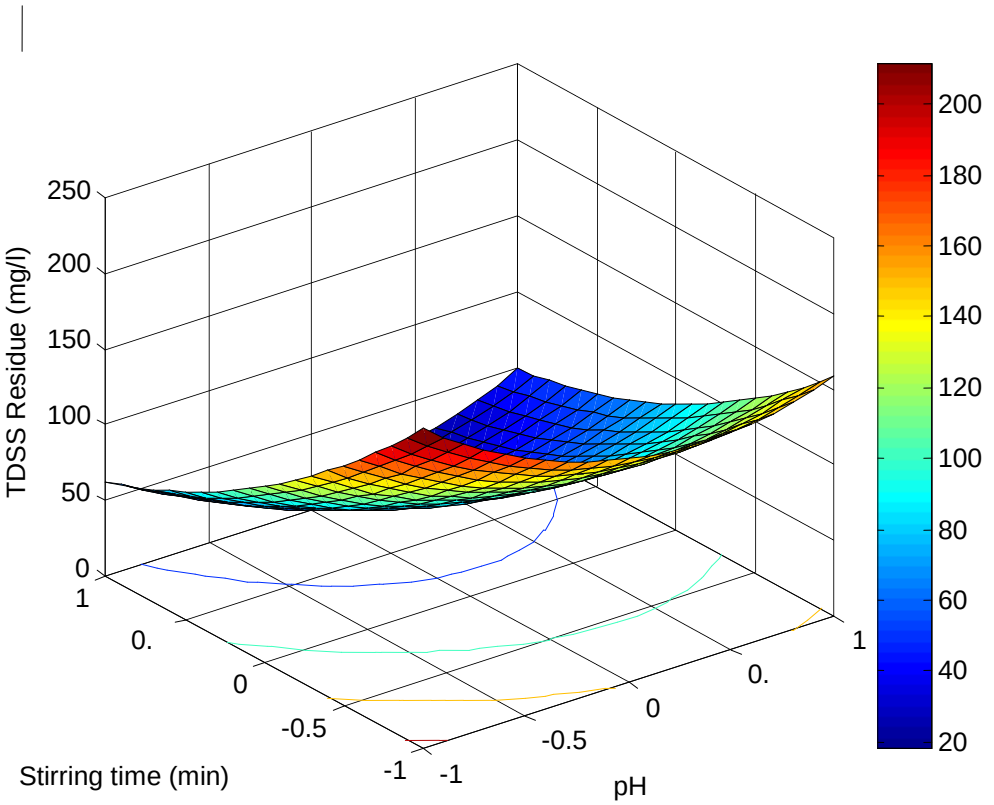

Fig.4.503 :Adsorption surface/contour plots for MSA in VIE showing interaction effects of Stirring time and pH

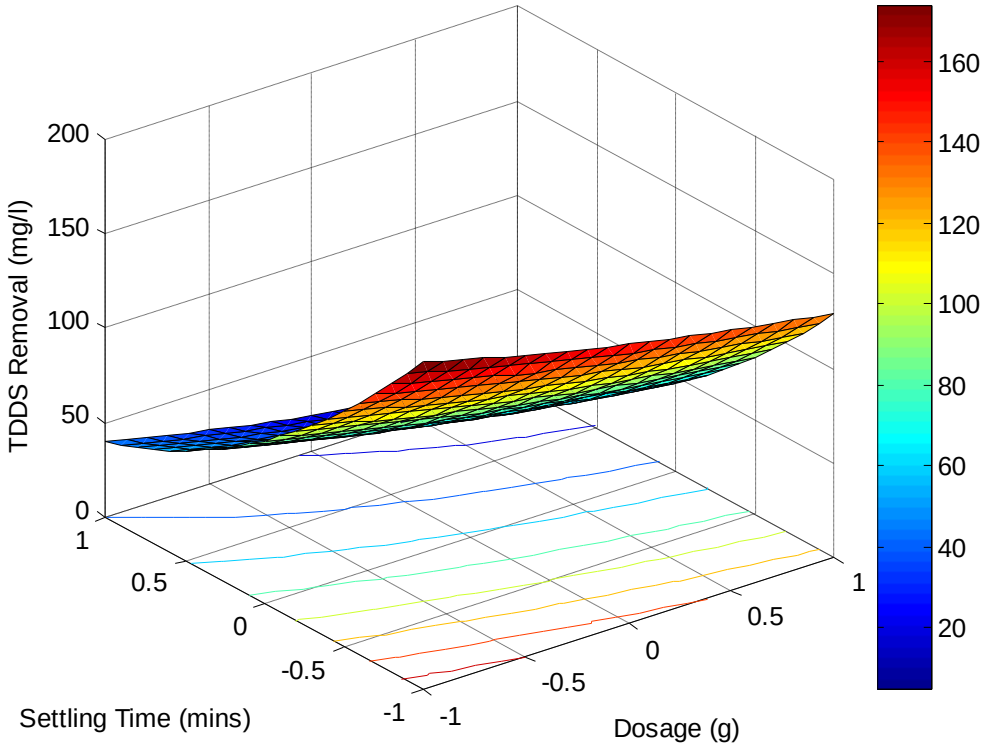

Fig.4.504 :Adsorption surface/contour plots for MSA in VIE showing interaction effects of Stirring time and Adsorbent mass

4.2.9: Comparative Percentage Adsorbate Removal for PIE and VIE

These results are presented in figures. 4.505 to 4.508 for PIE and VIE. The comparism of the various adsorbent with commercially procured one are carried out at temperatures of $25^{o}C$ and $35^{0}C$. Figures 4.505 and 4.506 demonstrates the performance of each of the adsorbent at the temperature of $25^{o}C$ and $35^{o}C$.

Figure 4.505, show that the best performance is recorded for MSA at both temperatures followed by BFHA and CACA for the temperatures of $25^{o}C$ and $35^{o}C$, respectively. This phenomenon supports the values obtained from tables 4.168 and 4.169.

For the VIE, the comparism is presented in fig. 4.506, for all the adsorbents at $25^{o}C$ and $35^{o}C$. The highest performance is achieved by MSA followed by laterite and CACA at both temperatures. The least performance comes from RHA followed by UCA at temperature of $25^{o}C$ and $35^{o}C$. This is also in accordance with the result obtained from table 4.169, showing the optimum data for adsorbent process model for VIE. The results presented in figures. 4.505 and 4.506 is a clear evidence that % removal strongly depended on the amount of initial adsorbate concentration. Higher initial adsorbate concentration translate to higher % removal. It is pertinent to note that the margin of difference in % adsorbate removal among the various adsorbents is negligible at the end of 40^{th} minute of adsorption at both temperatures more especially in PIE. This is an indication that any of the locally sourced adsorbents studied can be successfully used for water treatment in place of commercial ones.

Figures 4.507 and 4.508, show the comparative removal efficiency of the various adsorbents at end of 40 mins. The result presented in these figures show a similar trend as earlier explained previously. The same reason as above is adduced for the observed trend.

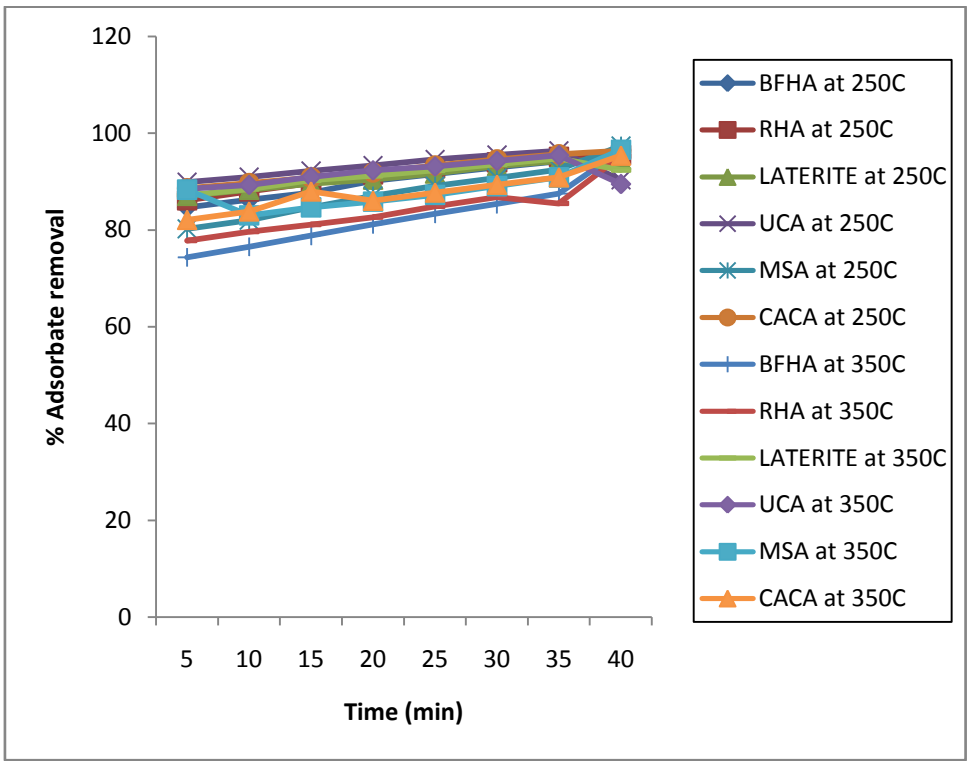

Fig.4.505 :Comparative % adsorbate removal profile for various adsorbents in PIE at 25^0C and 35^0C

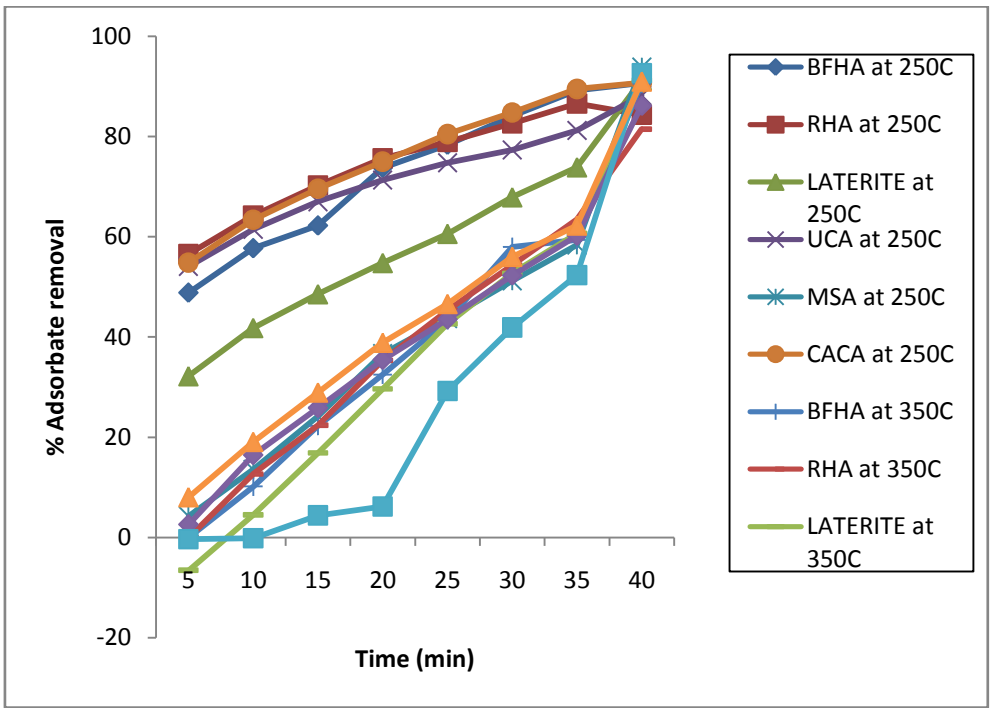

Fig.4.506 :Comparative % adsorbate removal profile for the various adsorbents in VIE at 25^0C and 35^0C

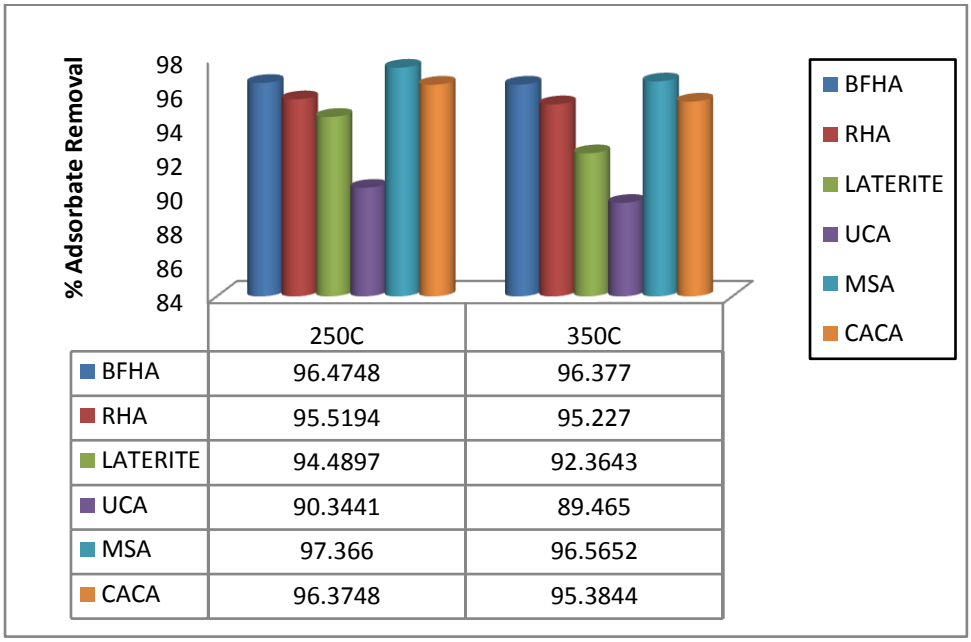

	250C	350C
BFHA	96.4748	96.377
RHA	95.5194	95.227
LATERITE	94.4897	92.3643
UCA	90.3441	89.465
MSA	97.366	96.5652
CACA	96.3748	95.3844

Fig.4.507 :Comparative adsorption performance at 40min for various adsorbent in PIE

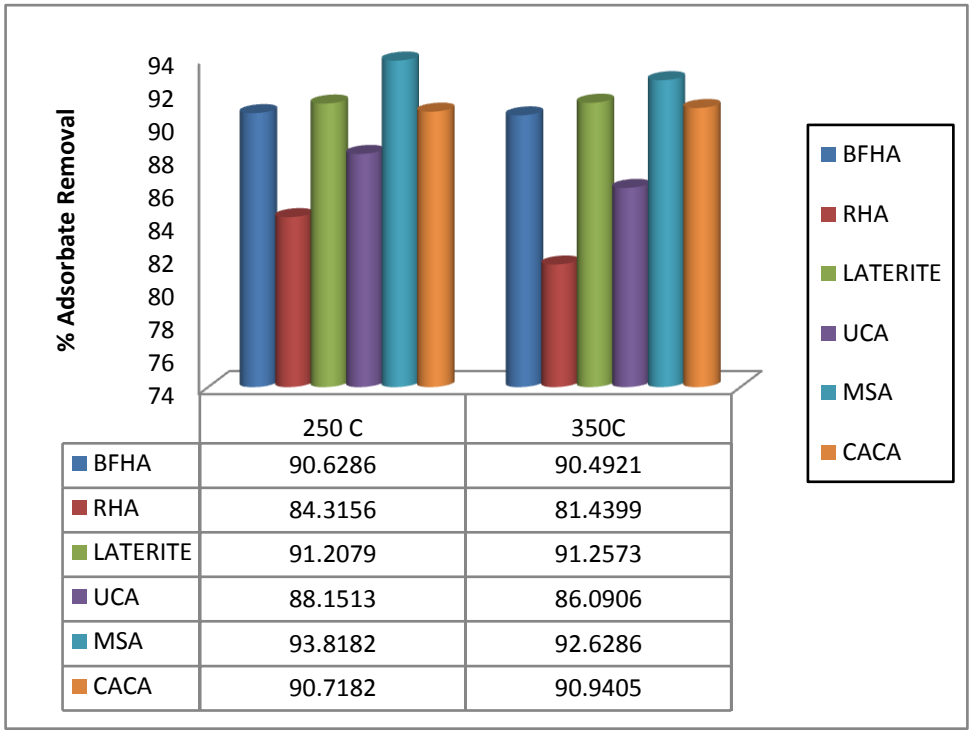

	250 C	350C
BFHA	90.6286	90.4921
RHA	84.3156	81.4399
LATERITE	91.2079	91.2573
UCA	88.1513	86.0906
MSA	93.8182	92.6286
CACA	90.7182	90.9405

Fig.4.508 :Comparative adsorption performance at 40min for various adsorbent in VIE

CHAPTER FIVE

CONCLUSION AND RECOMMENDATION

5.1 CONCLUSION

The investigation on the potentials for using different local coag-flocculants and adsorbents sequentially in the removal/reduction of pollutants (Total dissolved and suspended solids, TDSS) from pharmaceutical and vegetable oil industry wastewater has been carried out with the following conclusions.

The characterization result of the wastewater at the end of the study showed 100% removal of oil and grease, biological parameters and significant reduction in total suspended solid, total dissolved solids, turbidity, biochemical oxygen demand, chemical oxygen demand and dissolved oxygen. Proximate analysis of coag-flocculants and adsorbents showed that *Pleurotus tuberregium sclerotium* (PTSC) and *Magnifera indica* seed (MSA) have highest protein content and highest surface area. Instrumental analysis of carbon and non carbons indicates presence of complex bio-mass/numerous functional groups, crystalline lattice and morphological changes in particle pores and geometry.

The coag-flocculation performance indicates that the process is influenced by settling time and pH at maximum coag-flocculation constant (K) and low coag-flocculation period ($\tau_{1/2}$). The adsorbate removal efficiency is a function of stirring time and adsorbent mass. Pseudo second order best described the kinetics of the adsorption process.

Statistical analysis of coag-flocculation and adsorption process showed that amongst the process variables considered the process was most affected by time.

The adsorption data were best fitted to Freundlich isotherm model.The thermodynamic parameters show that the adsorption process was favourable, endothermic and spontaneous in nature translating to high affinity of adsobate towards the solution-solid interface.

Within the ambit of the experiment, the level of reduction of total dissolved and suspended solids concentration in the wastewater gives strong indication that the coag-flocculants and adsorbents used in the study have high potency for viable scalable application of the treatment scheme

5.2 RECOMMENDATION

Based on the outcome of the study PTSC is recommended as the coagulant for coag-flocculation process and MSA activated with sulphuric acid (H_2S0_4) as adsorbent in batch adsorption. Selection and identification of an appropriate low cost natural materials is one of the key issues to achieve the maximum removal of specific pollutants depending upon the coagulant–TDSS and adsorbent-adsorbate(TDSS) characteristics. The conditions for the production of low cost adsorbents after surface modification for higher uptake of pollutants need to be optimized. Cost factor should not be ignored. Low production cost with higher removal efficiency of adsorbents would make the process economical and efficient. The Effectiveness of the treatment depends not only on the properties of the coag-flocculant, adsorbents and adsorbates, but also on various environmental conditions and process variables used for coag-flocculation and adsorption processes, e.g pH, dosage, settling time stirring time, temperature, existence of competing organic or inorganic compounds in solution, initial concentration of TDSS and particle size of adsorbents etc. These parameters should also be taken into account while examing the potential of low cost natural materials(Coag-flocculants and adsorbents).

However, further studies may be necessary in the following areas:

(a) In order to appreciate the actual integrated effect and to apply the findings for treatment plant systems, pilot to full-scale studies are required to check their feasibility at industrial level.

(b) The mechanism of antimicrobial effect of coagulants and the ranges of microorganisms over which it is effective, are important for further investigations. The coagulants were effective on coliform count and pseudomonas aeruginosa. This could be due to the conformation of the protein. Therefore a study of the structure of the protein may be required to explain the mechanism or mode of action.

(c) A study on the removal of other contaminants than total dissolved and suspended solids (TDSS), such as heavy metals and phosphorus can be carried out to assess its wider application.

(d) Regeneration studies need to be performed with the pollutants-laden adsorbent to recover the adsorbate as well as adsorbent. It will enhance the economic feasibility of the process.

5.3 CONTRIBUTION TO KNOWLEDGE

1. The researcher postulates the validity of t≤40 as maximum period in a Brownian microkinetic aggregation.
2. Most of works on coag-flocculation treatments on pharmaceutical and refined vegetable oil wastewater did not delve into the kinetics of the processes. This work has successfully provided useful information and kinetic data for the processes.
3. Establishment of effectiveness of PTSC, MPSC and SSC over Alum even at its pH domain.
4. Statistical models for the coag-flocculation and adsorption treatments of pharmaceutical and refined vegetable oil wastewaters via optimum process.
5. Improvement on the theoretical model developed by previous researchers, such as Von Smoluchowski, Menkiti and others.
6. Establishment of effectiveness of MSA derived activated carbon over commercial activated carbon for TDSS removal.

REFERENCES

Abbot and Van Ness (1972): Schaum's Outline of Theory and Problems of Thermodynamics, MC Craw – Hill, New York.

Adamson Arthur W.(1990); Physical Chemistry of Surfaces: fifth edition. New York :John Wiley & Sons Inc.

Ajila, C.M and Prasada, R.U.J. (2008). Protection against hydrogen peroxide induced Oxidative Damage in Rat Erythrocytes by Magnifera Indica. Peel extract" Food Chem. Toxicol. 46(1): 303-9.

Akoroda, M.O. (1990). "Ethnobotany of Telfairia Occidentalis (Curcurbitacae) among Igbos of Nigeria" Economic Botany: 29-39.

Alberta Environment(1984); A practical guide to municipal wastewater irrigation. D Discussions and Guidelines, Edmonton Alberta.

Ali, S. Z., Athar, M., Salman, M. and Din, M.I.(2011). Simultaneous removal of Pb(11) and CU(11) from aqueous solutions by adsorption on Triticum aestivum – a green approach. Hydrol. Current Rcs. 2: 118. Dol. 10.4172/2157 – 7587 – 1000118.

Aloko, D.F and Adebayo, G.A., (2007). Production and characterization of Activated Carbon from Agricultural Waste (Rice-husk and corn-cob). Journal of Engineering and Applied Sciences, 2(2), 440 – 444.

Al-Samawi, A.A., and Shokrala, E.M. (1996). An investigation into an indigenous natural coagulant. Journal Environ. Sci. Health A 31(8): 1881-1897.

Altundogan, H.S., Altundogan, S., Tumen, F and Bildik, M. (2000); Arsenic removal from aqueous solutions by adsorption on red mud. Waste management, 20 761 – 767.

AOAC (1989): Official Methods Analysis, Association of Official Analytical Chemists Washington DC. 14th edition.

AOAC (1993); Official Methods of Analysis, Association of Official Analytical Chemists, Washington DC. 14th edition.

APHA and AWWA (1985): Standard Method for the Examination of Water Effluent, New York, USA.

Aqua Ben. Co. (2001); What are coagulants and flocculants? USA

ASTM (1994): American Standard for Testing Material, Philadelphia USA.

Austine, G.T. (1984); Shreve's chemical process industries'Chemical Engineering series. 5th Ed. 137.

AWWA (1984); American Water Works Association; Standard Method for the Examination of Water Effluent, New York, USA

AWWA (1992); American Water Works Association; Standard Method for the Examination of Water Effluent, New York, USA.

Baarlsurd K.G and Henriskens (1994); Measurement of Suspended Matter in Stream Water, JAWWA, Syracus, USA.

Babu,B.V and Gupta, S (2004) "Modeling and Simulation for Dynamics of Packed Bed Adsorption",proceedings of international symposium and 57th annual session of IICHE in association with AICHE (CHEMCON 2004), Mumbai, December 27 – 30,.

Badifu, G.I.O (1993) "Food potentials of some conventional Oliseeds grown in Nigeria- a brief Review." Plants foods for Human Nutrition 43(3), 211-224

Bagwel, T., Henry H.B. and Kenneth M.B (2001); Handbook of Public water supply, 2nd Edition, HDR Engineering Inc. new York, USA.

Bautista, L.F.,Martinez, M and Aracil, J.(2003)."Adsorption of-Amylase in a fixed Bed: Operating Efficiency and Kinetic Modeling," AICHE Journal, 49 (10), 2631 – 2641

Bolto, B. (1995). Soluble Polymers in Water Purification. Progress in polymer Science, 20, 987-1041.

Bratby, J.(2006). Coagulation and Flocculation in Water and WasteWater Treatment. IWA Publishing, London, Seattle.

Brunauer, S, Deming, L.S, Deming, W.S. and Teller, E.J., (1938). Journal of American Chemical Society, 621 1723.

Buser, H.R, Muller M.D and Theobald N. (1998a): Occurrence of the Pharmaceutical Drug Clofibric Acid and the Herbicide Meco Prop in various Swiss Lakes and in the Northsea. Environ Sci. Technol; 32(1): 188.

Buser, H.R,Poiger,T and Muller, M.D (1998b): Occurrence and Fate of the Pharmaceutical Drug Diclofenac in Surface Waters: Rapid Photodegradation in a Lake. Environ. Sci. Technol. 32 (22): 344a

Buser H.R; Poige, T and Muller, M.D (1999): Occurrence and Environmental Behavious of the Chival Pharmaceutical Drug Ibuprofen in Surface Waters and in WasteWater. Environ. Sci. Technol. 33 (15): 2529.

Chumee, J. (2008). Characterization of platinum-iron Catalyst supported on MCM-41 Synthesized with Rice Husk Silica and their performance for phenol hydroxylation Sci. Technol. Adv. Mater.

Cal, M.p. Larson, S.M and Rood, M.J (1994), "Experimental and Modeled Results Describing the Adsorption of Acetone and Benzene onto Activated Carbon fibres, Environmental progress, Vol. 13, No 1,

Calzaferri, G. and Imhof, R (1996). In situ attenuated total reflection FTIR investigation of H_2O, $HSiCL_3$ and $CO_2(CO)_8$ on ZnSe in the range 600 – 4000cm^{-1}. Spectrochimica Acta part A; Molecular and Biomolecular Spectroscopy, 52, 23-28.

Campell H.A (2005); Surfactants: Detergents Chemistry, New Zealand,

Carter, M .R.(1993); Soil sampling and methods of analysis science.Ottawa, Ontario

Cooper, R.A. (2001). Personal Communication, Bio VIr Laboratories, Benicia, CA. Coughlin Robert W. and Ezra Fouad; Role of Surface Acidity in the Adsorption of Organic Pollutants on the Surface of Carbon. Environmental Science and Technology Vol. 2, No. 4, PP 291 – 297,

Coughlin R.W and Ezra, F. (1968). Role of surface Acidity in the Adsorption of organic pollutants on the surface of Carbon Environmental science and Technology Vol. No.4, pp 291-297

Cronin E.M. (1998): Adsorption of Acetone Onto Activated carbon cloth at elevated Temperatures, M.Sc. thesis, Civil and Engineering, University of LLLinois at Urbana Champaign, USA.

Dabrowski, .A (2001), Adsorption from theory to practice. Advances in colloid and interface science Vol. 93, PP. 135 -224,

Dubinin, M.M. (1964); Integrated Study of the porous Structure of Activated Carbon from Carbonized Sucrose, Carbon, 2:261.

Dabrowski, A., Podkoscielny, P., Hubicki, Z and Barczak, M. (2005). Adsorption of Phenolic Compounds by activated carbona critical review. Chemosphere 5, 1049 – 1070.

Danov, D.K., Kralchevsky, P. A and Ivanov, I.B (2001); Dynamic Process in Surfactants Stabilized Emulsion, Faculty of Chemistry, University of Sofia.

Debnath, S and Ghosh, U. C. (2008): Kinetics, isolation and thermodynamics for Cr(III) and Cr(VI) adsorption from aqueous solution by crystalline hydrous titanium oxide, J. Chem. Thermodynamics, 40:67-77.

Department of the Army U.S Army Corps of Engineers (2001), Engineering and Design Adsorption Design Guide. Design Guide No. 1110 – 1-2.

Devika, D.B. (1995). "Mango's wide influence in Indian culture" New strait Times. Retrieved, September 2013.

Diaz, A., Rincon, N., Escorihuela, A. Fernandez, N., Chacin, E and Foster, C.F (1999). A preliminary evaluation of turbidity removal by natural coagulants indigenous to Venezuela: Process Biochemistry: 35:391-395.

Dioha, I.J., Tunga, A.M and Onuegbu, T.U. (2005); Bulletin of science Association of Nigeria. Volume 26.

E.E.A.A (2002); Egyptian Environmental Affairs Agency, Egyptian pollution Abatement project (EPAP) Industrial wastewater Treatment plants inspection procedures manual May 2002.

Eaton, A; Closceril and Greenberg. A (1998); Standard Methods for the Examination of Water and WasteWater. USA, ALPHA, AWWA, WEF.

Edema, M.O., Omemu, A. M., and Fapetu, O.M. (2001). Microbiology and physicochemical Analysis of Different Sources of Drinking Water in Abeokuta.Nig. j. Mic. 15(1), 57-61.

FEPA (1992): Environmental Impact Assessment decree No 86 of 1992; Federal Environmental Protection Agency Lagos, Nigeria pg 1 – 18.

Egwaikhide P.A., Akporhobour, E.E and Okieimen, F.E. (2007); Utilization of Coconut Fibre Carbon in the Removal of Soluble Petroleum Fraction Polluted Water-International Journal of Physical Sciences. Volume 2 (2).

Faust, S.O. and Asman, M.A (1987). Adsorption process for water treatment, Butter worth London. P. 15.

Fernandez – Kim, S. (2004). Physiochemical and functional properties of Crayfish Chitosan as as affected by Different Processing Protocols, M.Sc. Thesis: Department food science. Louisiana State University and Agricultural College , USA, 1-99

Fridriskhsberg, D.A. (1984); A course in Colloid Chemistry, Mir Publishers, Moscow, Russia.

Gassenschmidt, U., Jany, K.K., Tauscher, B and Niebergall, H. (1995). Isolation and Characterization of a Flocculating Protein from Moringa Oleifera Lam. BBA Bio-Chemica et Biophysica Acta. 1243, 477-481.

Gabremichael, A.K.(2004). Moringa seed and pumice as alternative natural materials for drinking water treatment TRITA - LWR PHD1013KTH Land and water Resources Engineering.

Giami, S(2003). "Effect of Gerumination on Bread Making properties of wheat-fluted pumkin (Telfaira occidentalis) seed flour blends. Plant foods for Human Nutrition, 58, 1-9.

Greenberg, A.E Clesceri, L.S and Eaton, A.D, (1992); Standard Method for the Examination of Water and WasteWater APHA & AWWA, 18th Edition, Washington, D.C.

Gregg, S.J and Sing, K.S.W (1982) Adsorption, Surface Area, and porosity, 2nd Ed. Academic, Press, London,

Gunaratna, K.R, Garcia, B., Anderson, S and Dalhammar, G (2007): Screening and evaluation of natural coagulants for water treatment. Water science and technology-water supply 7(5/6), 19

Gang F. (2007). Evaluation and performance of a Tannin-based polymer as a Coagulant in Water Treatment. Ph.D Thesis Submitted to Department of Civil and Environmental Engineering Imperial college London.

Han, M & lawer D.F (1992); The (relative) Insignificance of G.M Flocculation; JAWWA, Vol. 82; No 11, PP 65 – 75, USA.

Haque R., Lindstrom S.T. Freed V.H. and Sexton R. (1968). Kinetic Study of the Sorption of 2,4-D on some Clay. Environ. Sci. Technol., 2:207-211.

Hassler, J. W. (1988); Active carbon, Marcel Deecker Inc. New York, 174.

Haydn, H. M, (1960), Clay: In industrial minerals and Rocks, AIME, PP: 259 – 284.

Heberer T.H and Stan H.J (1997): Determination of Clofibric Acid and N-(phenlsulfonyl) – Sarcosine in Sewage, river and Drinking Water Int. J. Environ. Anal Chem; 67:113.

Helmut, H., Egelhaefsu, S.U., Borkovec, M., Schurtenberger, P and Stcher, H (1996); Coagulation Rate Measurements of colloidal particles by simultaneous static and Dynamic light scattering, Langmuir (1996), 12, 5541 – 5549, Switzerland.

Hennery, M.P., Donlon, B.A., Lens, P.N and Colleran, E.M (1996): "Use of Anaerobic Hybrid Reactors for Treatment of Synthetic Pharmaceutical WasteWater containing Organic Solvents". J. Chem. Tech. Biotechnol. 66: 251 – 264

Hutchison, P.R. and Healy, T.W (1990). Surface and Colloid Chemistry in Natural Water and Water Treatment Plenum press, New York.

Ho, Y. S and Mckay (2000); The kinetics of the sorption of divalent metal ions onto sphagnum moss peat. Water Res. 34: 735-742.

Holtholf, H., Egeihaafsu, S.U., Borkovec, M., Schurtenberger, P and Sticher, H (1996): Coagulation Rate Measurement of Colloid Particles by simultaneous. Static and dynamic light scattering Langmuir 12, Pp 5541-5547.

Horsefall, J.M. and Sp.ff, A.L. (2005). Ewulibrium sorption study of $AL^{3+,}$ Co^{2+} and Ag^{+} in aqueous solution by fluted pumpkin (Telfaria Occidentalis Hook) wast biomass Acta. Chim,Slor, 52, 174-181.

Hunter, R. J. (1993). Introduction to Modern Colloid Science, 4th Oxford University Press, New York, 33 – 38; 289 – 290.

Igwe, J.C and Abia, A.A. (2007); Adsorption kinetics and interparticulate diffusivities for bioremediation of Co(11), Fe(11) and Cu(11) ions from waste water using modified and unmodified maize Cob; international Journal of physical Sci. 2(5): 119-127.

Illinois Annual Air Duality Report (1996): Illinois Environmental protection Agency, IEPA/APC/97 – 005, June 1997..

Isikhuemhen, O. S and Okhuoya, J.A (1996). Cultivation of Pleurotus tuberregium(Fr.) Singer for production of Edible Sclerotia on Agricultural wastes. Mushroom products, Royse (ed). Penn State University ISBN1-883956- 01-3

Jahn, S.A. (2001). Drinking water from Chinese Rivers: Challenges of Clarification. Journal of Water supply Res. Technol. 50: 15-27.

Jatto, E.O; Asia, I.O, Egbon, E.E., Otutu, J. O., Chukwuedo, M.E and Ewansila, C.J (2010) :Treatment of WasteWater from Food Industry using Snail Shell. Academia Areana, 2(1), 32 – 36.

Jatto, E.O. (2013). "Kinetic studies of wastewater Treatment from Rubber factory using snail shell. Journal Article. New York Science Journal, 25-33.

Jiang, J.E. and Graham, J.D. (1998); Pre-Polymerized Inorganic and Phosphorus Removal by Coagulation. A Review. Water Res. Dept. of CVE. Imperial College of Science, Technology & Medicine, London.

Jin, Y. (2005). Use of high Rosolution photographic Technique for studying coagulation/flocculation in water treatment. M.Sc Thesis, University of Saskatchewan, Saskatoon, Canada.

Katzenschlager, R., Evans, A., Manson, A., Patsalos, P.N., Ratmarai, N., Walt, H; Tmimmermann, I; Van Der Giessen, R; Less, A.J (2004) "Mucuns pruriens in Parkinson's diseases: a double blind clinical and pharmacological study. Journal of Neurology. Neurosugery & phychiatry 75(12): 1672-7.

Knorr, D (1991). Recovery and Utilization of Chitin and Chitosan in food Processing waste Management, Food Technology. 114-122

Kostermans, A.J.H.G and Bompard, J.M. (1993). The Mango: Their Botany, Nomenclature, Horticulture and Utilization.

Langmuir, I. (1918):Langmuir, 1918. The adsorption of gases on plane surfaces of glass, mica and platinum. Journal of the American Chemical Society, 40,1361 –1403.

Lentech, (2005); Lentech Water Treatment and Air Purification Holding B.V; Rotter Damseweg

Lin, J., Zhan, Y., Zhu, Z and Xing, Y. (2011). Adsorption of tannic acid from aqueous solution onto surfactant – modified Zeolite. Journal of Hazardous Materials, 193, 102 – 111.

Liu, Q.S., Zheng, T., Wang, P, Jiang, J. P and Li, N. (2010). Adsorption Isotherm, kinetic and mechanism studies of some substituted phenols on activated carbon fibers. Chem.. Eng. J. 157, 348 – 356.

Lawal, R.O. (1992). The Effect of a Single Oral dose of polyphenols obtained from the outercoat of the Fruit of Treculia Africa in protein-deficient Rats. Food chemistry, 44, 5, 321-323.

LV, S., Zhang, Y., Liu, T.T.X., Ttu, L., Yang, K., Steinmann, P., Chen, Z., Wang, L.Y., Utzinger, J.R and Zhou, X. N.(2009). "Invasive Snails and an Emerging Infectious Disease: Results from the first National Survey on Angiostrongylus Vantonensis in China". In knight, Matty. Plos Neglected Tropical Diseases 3(2): 368.

Ma, Q.Y., Traina, S.J., Logan, S.J and Ryan, J.A (1994). Effects of NO_3^-, CL^-, F^-, $SO_4^{2,}$ and CO_3^{2-} on Pb^{2+} Immobilization by Hydroxyapatite. Environ. Sci. Technol., 28, 408 – 418.

Mallevialle, J., Bruchet, A. and Fiessinger, F. (1984). How safe are Organic polymers in Water Treatments. Journal of American Water Works Association, 76, 87-93.

Mair, R. M., Pepper, I. I and Gerba, C.P (2000). Environmental Microbiology, Academic Press, A Harcourt Science and Technology Company, San Diego, CA.

Manju G.N. and Anirudhan T.S. The Removal of Mercury in WasteWater with Polymer-Coated Hydrous Iron (III) Oxide Having Carboxylate Functional Groups

Malik, R., Ramteke, D.S and Wate, S.R. (2006) Physico-chemical and Surface Characterization of Adsorbent prepared from Groundnut Shell by Zncl2 activation and its ability to adsorb colour. Indian Journal of Chemical Technology, 13, 319 – 328.

Mc Graw Hill; Concise Encyclopedia of Science and Technology, Volume 2, 3rd Edition.

Menkiti M. C. Aneke, M.C., Onukwuli, O. D. (2012). Optimization and kinetics of Coag-flocculation of coal effluent by crab extract via response surface methodological analysis. Journal of Nigerian Society of Chemical Engineers, 27(1), 61 -80.

Menkiti, M. C. and Onukwuli, O. D. (2010) Coag-flocculation Studies of Moringa Oleifera Coagulant (MOC) in Brewery Effluent: Nephelometric Approach. Journal of American Science, 6(12), 788 – 806.

Menkiti, M.C (2010). Sequential Treatments of Coal Watery and Brewery Effluents by Biocoag-flocculation and Activated Carbon Adsorption. A Ph.D dissertation presented to the Department of Chemical Engineering, Nnamdi Azikiwe University, Awka.

Miller P.E and Westra P. (2004); How Surfactants work, Colorado State University, USA

Montgomery, J.M. (1985). Water Treatment, principles and Design, John Wiley and Sons, New York, 116.

Muhammad, S. (2007): Pharmaceutical WasteWater Treatment: A physicochemical Study. Journal of Research (Science), Bahauddin Zakanya University, Multan, Pakistan, Vol 18, No 2, PP 125 – 134.

Ndabigengesere A. Narasiah, K.S and Talbot B.G. (1995): Active agent mechanisms of coagulation of Turbid water using Moringa Oleifera, Water Res. 29(2): 703-710

Nwanna, E.E (2008). "Antioxidant and Hepatoprotective properties of Telfairia Occidentalis Leaf (fluted pumpkin) "Thesis and Dissertations (Biochemistry). In web. 17 Nov. 2013.

Nuga, O.O. and Ofodile E.A.U. (2010). Potentials of Treculia Africana Decne-an endangered species of Southern Nigeria. Journal of Agriculture and Social Research No.2

Nwabueze, T.U and Uchendu, C.B. (2011). African Breadfruit (Treculia Africana). Seed as Adjunct in Ethanol production-European Journal of Food Research and Review 1(1): 15, 22

O'Melia, C.R (1978); Coagulation in WasteWater Treatment Plant Design, Ann Arbor Science, Ann Arbor, MI.

Otto, W.F. (2008)."Silica" in Ullmann's Encylopedia of Industrial Chemistry, Weinherim: Wiley-UCH.

Ogundana, S.k and Fagade, O. (1981). The Nutritive Value of some Nigerian Edible Mushroom. In Mushroom Science xi, proceedings of the Eleventh International Scientific Congress on the Cultivation of EdibleFfungi, Australia, 123-131.

Okoli, B.E and Mgbeogu, C.M. (1983). "Fluted pumpkin, Telfairia Occidentalis West Africa Vegetable Crop" School Biological Science University of Port-Harcourt 37(2)

Okoye, A.I.(2009): Production of Low Cost Activated Carbon from locally available Agricultural Wastes, M. Sc. Thesis, University of Nigeria Nsukka, 21-35

Okieimen F.E., Okieimen, C.O and Wuana, R.A (2007); Preparation and Characterization of Chemical Society of Nigeria, Volume 32 (1).

Ozacar, M. and Sengil, I.A. (2000): Effectiveness of tannins obtained from Velonia as a coagulant aid for dewatering of sludge. Water Res. 34(4): 1407-1412.

Patel R and Suresh, S. 2008. Kinetic and equilibrium Studies on the biosorption of reactive block 5 dye by Aspergillus foetide. Bioresources Technology 99.51-88,

Patrick, J.W and Edward Arnold (1995); Porosity in Carbons Hodder Headline Publishers, London,.

Pei, J. J and Zhang, J. S. (2012). Determination of Adsorption Isotherm and Diffusion Coefficient of Toluene on Activated Carbon at Low Concentrations. Building and Environment 48, 66 – 76.

Perkins, W. (1988); Surfactants – A primer, ATI Publication, USA.

Perry R.H and Green D.W. (1999); Perry's Chemical Engineers Handbook, 7th Edition. New York McGraw Hill Inc. 16-4 to 16-16

PFRA, (2003). Prairie farm Rehabilitation Administration Bulletin Canada.

Pimental, P.M (2008), "kinetics and thermodynamics of Cu(11) adsorption on oil shale wastes" duel processing Technology. 89, 62-67.

Pope, J.P (2003). Activated Carbon and Some Applications for the Remediation of Soil and GroundWater Pollution. Available (online): http:www.cee.vt.edu/program_areas/environmental/teach/gwprimer/group 23/web page. Htm. Accessed December 6.

Pradhan, S. (2011). Production and Characterization of Activated Carbon produced from a Suitable Industrial Sludge. B.Tech. project submitted to Department of Chemical Engineering of National Instution of Technology Rourkela.

Prasad, M., Saxena, S., Amritphale, S.S and Chandra, N (2000), Kinetics and Isotherms for Aqueous Lead Adsorption by Natural Minerals. Ind. Eng. Chem. Res. 39 (8), 3034 – 3037.

Pratt, K.C and Christoverson, V (1982). Hydrogenation of Model Hydrogen – Donor System Using Activated Red ud catalyst. Fuel, 61, 460 – 462.

Reynolds, T.D and Richards, P.A (1996); Unit Operation and Process in Environmental Engineering; 2nd Ed; PWS Publishing Company, Canada.

Richardson, J.F, Harker, J.H and Backhurst, J.R (2003). Coulson and Richardson's Chemical Engineering 5th Edition, volume 2, 146-189.

Rosen, M.J (2004); Surfactants and Interfacial Phenomena, 3rd Ed. John Wiley, U.K.

Roussy, J., Van. Vooren, M., Guilbal, E. (2004). Chitosan for the coagulation and flocculation of mineral colloids. Journal of Dispersion Science and Technology., 25(5), 663 – 677.

Rowson, B., Warren, B and Nigereza, C.(2010). "Terrestrial Mollusks of Pemba Island, Zanzibar, and its status as an "Oceanic" Island" Zookeys, 70.

Reddy, V.B. (2008). Cowhage evoked itch is mediated by a novel cysterie Protease a ligand of propease- Activated Receptors Neuro -Sci., 28 (17) 4331-4335.

Stackelberg, P.E., Furlong E.T., Meyer, M.T., Zaugg, S.D., Henderson, A.K and Reissman, D.B. (2004): Persistence of Pharmaceutical Compounds and other Organic WasteWater Contaminants in a Conventional Drinking Water-Treatment Plant. Science of the Total Environment 329:99 – 113

Saka, S. (2000). Chemical Composition and Distribution. Wood and Cellulosic Chemistry, D. N – S. Hon and N. Shiraishi, editor, 2nd edition, Revised and Expanded, Marcel Dekker Ltd., New York, 51 – 82.

Skelley, P.E., Dixon, W.N and Hodges, G. (2011). Giant African Land Snail and Giant South American Snails Field Recognition. Florida Department of Agriculture and Consumer Services Gainesville, Florida.

Sanks, R.L (1979); Water Treatment Plant Design, Ann Arbor Science Publishers Inc; Ann Arbor

Sanghi, R and Bhattacharya, B. (2005). Comparative Evaluation of Natural Polydectrolytes Psyllium and chitosan as coagulant Aids for Decolourization of Dye Solution. Water Qual. Res.J. Canada. 40,1, 97-101.

Shiqo, S.J and Akashi, K. (1977). Phosphate Removal from Aqueous Solution from Activated Red Mud. Journal Water Pollution Control Federation, 49:2, 280 – 285.

Soleimani, M and Kaghazachi (2008); Activated hard shell of apricot stones: A promising adsorbent in gold recovery, Chinese journal of Chem. Engrg 16(1): 112-118.

Smisek, M. and Cerny, S. (1970). Active Carbon Manufacture Properties and Application Elservier publishing Company, Amsterdein.

Smoluchowski, Von. (1917); Versucheiner Mathematischen Theorie der koagulation skinetic kolloider lousungen. Z. phys. Chem. 92: 129 – 168.

Soto, M. L., Moure, A. Dominguez, H and Parajo, J. C. (2011). Recovery, Concentration and purification of phenolic Compounds by Adsorption. A Review. Journal of Food Engineering. 105, 1 – 27.

Stochi, E. (1990); Industrial Chemistry, Vol. 1, Ellis Horwood, New York.

Suidan, M.T (1988); Coagulation and Flocculation, Env. Engineering Unit Operation and Unit Process Lab. Manual, 4th Ed. Assoc. of Environmental Engineering professors, Canada.

Stewart, R.H. (2011). The Corchorus (Jute) Malvacae Info. Retrieved from Wikipedia September, 10, 2011.

Swift, D.L and Friedlanders, S.K (1964); The Coagulation of Hydrosols by Brownian Motion and Laminar Shear Flow, J. Coll. Scic. 19:21, Canada

Tchobangoglous, R.H (1998): Analysis Techniques for Water Examination. Journal of the Institute of Engineers, India (online serial), 98 (3) Available http//app.gov.sg.articles.asp.

Tchobanoglous,G, Burton,F.L.,Stensel, D.H. (2003); Waste Water Engineering Treatment and Reuse, 4th Ed. Tata McGraw Hill, New Delhi, 4th Ed.42-55.

Tchobanoglous G. and Schroeder (1985). Water Quality: Characteristics, Modeling, Modifcation, Addison-Wesley Publishing Company, Reading, M.A.

Terlizzi, S.D (1994); Introduction to Coagulation and Flocculation of WasteWater, Environmental System project, USA.

Theivarasu, C and Mylsamy, S. (2010). Equilibrium and Kinetic Adsorption Studies of Rhodamine – B from Aqueous Solutions Using Cocoa (Theobroma cacao) Shell as a new Adsorbent. International Journal of Engineering Science and Technology. 2, 6284 – 6292.

Thomas, D.N. Judd, S.J and Fawcett, N (1999); Flocculation Modeling: A Review. Water Research, No 33, (7) USA.

Treybals, R.E. (1980). Mass Transfer operations. 3rd. Ed. Mc Graw Hitt. New York; 581-582

Tripathi, P.N., Chaudhuri, M. Bokil, S.D. (1976). Nimali Seeds – a natural occurring coagulant. Indian Journal of Environmental Health, 18(4): 272-281.

Van Zanten J.H and Elimelechi, M (1992); Determination of Absolute Coagulation Rate Constant by Multiangle Light Scattering; Journal of Colloids and Interface Science, Vol. 154, No 1, USA.

Wannapeera, J., Worasu W.N and Pipatmanomai, S. (2008). Product Yields and Characteristics of Rice Husk, Rice Straw and Corncob during fast pyrolysis in a drop – Tube/Fixed –Bed Reactor. Song K. Lanakarin J. Sci. Technol. 30 (3), 393 – 404.

Weber, W.J., Morris J.C (1963); Kinetics of Adsorption on Carbon from Solution. J. sanit. Eng. DIV Am. Soc. CIV. Eng. 89:31-60.

Wright, J.K and Hordon, B.K. (1993); RIVPACS – A technique for Evaluating the Biological Quality of Rivers in U.K, European Water Pollution Control, U.K Pp 8, 15 – 25.

WSSA,(1992); Water Service Association of Australia, Assessment of Coagulants for Water Treatment, Report No 14, Australia.

WST (2005); About Coagulation and Flocculation; Information Bulleting, U.S.A.

Walker, M. (2009). Chimps use cleavers and anvils as tools to Crop Food. BBC News. Retrieved, 24th December 2009.

Walt, H., Timmermann, I., Van Der Giessen, R and Lees, A.J. (2004) "Mucuna pruriens in Parkinson disease: A double Blind Clinical and pharmacological Study. Journal of Neurology. Neurosurgery psychiatry 75(12): 1672-7.

Whittock, B.A., Karol, K.G and Alverson, W.S (2003). Here Chloroplast DNA Sequence confirm the placement of the Enigmatic Oceanopapaver within Corchorus (Gireviodeae: Malvaceae, S.I, formerly Tiliaceae) International Journal of plant Sciences, 164, 35-41.

Yan .J. (2005); Use of High Resolution photographic Technique for studying Coagulation/flocculation in Water Treatment, M.Sc Thesis, Dept. of civil and Geological Engineering, University of Saskatchewan, Saskatoon, Canada.

Yang, R.T. (2003c). Adorbents: Fundamentals and Application. Hoboken NJ: Wiley Interscience;

Zhang. J.J. and Li, X, y (2003); Modeling Particle – Size Distribution Dynamics in a Flocculation System. Journal of American Institute of Chemical Engineering, 49 (7); 1870, USA.

APPENDICES

APPENDIX A: THEORETICAL PRINCIPLES AND MODEL DEVELOPMENT

COAG-FLOCCULATION MODEL DEVELOPMENT

For a homogeneous aggregating particles (i, j) in equilibrium state with negligible influence of gravitational, buoyancy, drag, van der Waals and repulsive forces: (Abbot and Van Ness, 1972, Hunter, 1993., Menkiti and Onukwuli, 2010).

$$\mu_i = \boldsymbol{U_i}\left(\frac{\delta(n_u)}{\delta(n_i)}\right) \boldsymbol{nS, nV, n_j} \quad \textbf{(1)}$$

Also

$$\mu_i = \tau_i = \left(\frac{\delta(n_c)}{\delta((n_i)}\right) \boldsymbol{p, T, n_j} = \textbf{a constant} \quad (2)$$

Thus $\mu_i = G_i = O$ (3)

For a homogeneous phase solutions

$\mu_i = \mu_i + RT \ln C_i$ (4)

In a case where drag force (f_d) predominants there is a shift from the equilibrium state

Thus $f_d = -\frac{K_B T}{C_i} \frac{dC_i}{dx} \frac{d}{dx}$ (5)

Note that Boltzman Constant (K_B) = Molar gas constant per particle i.e.

$K_B = \frac{R}{n}$

For a single particle component say i, n = 1, $K_B = R$ (6)

Substituting equation (6) into (4), yields

$\mu_i = \mu_i + K_B T \ln C_i$ (7)

Where:

μ_i is chemical potential of component i

U_i is internal energy of component i

G_i is Gibb's free energy of component i.

n_i is the number of moles of component i

n_j is the number of moles of component j, indicating that all moles numbers are held constant except the i^{th} .

n is the number of particles

T is absolute temperature

C_i is concentration of particle component i

X is diffusion distance

f_d is viscous drag force

R is molar gas constant

K_B is Boltzman constant (molar gas constant per particle)

Substituting equation (7) into (5), gives

$$f_d = -\frac{d}{dx}(\mu_i^o + K_B T \ln C_i) \quad (8)$$

$$f_d = -\frac{K_B T}{dx} \quad (9)$$

But from ficks law

$$D^1 = -\frac{f_d}{B}\frac{C}{(dc/dx)} \quad (10)$$

Where D^1 is diffusion coefficient

B is friction factor

Comparing equations (9) and (10) yields Einstein's equation

$$D^1 = \frac{K_B T}{B} \quad (11)$$

The general model for microkinetic coagulation-flocculation of mono dispersed particle under the influence of Brownian motion is given by Von Smoluchowski, 1917.

$$r_k = \frac{dN_k}{dt} = \frac{1}{2}\sum_{I+j=k}\alpha\beta(v_{i,\ Vj})\, ni\ nj \ - \sum_{i=1}\alpha\beta(v_{i,\ Vj})\, ni\ nj \quad (12)$$

Where $r_k = \frac{dN_k}{dt}$ is the rate of change of concentration of particle size K (*Conc./time*)

α is the fraction of collisions that result in particle attachment.

β is a function of coagulation-flocculation transport for Brownian, Shear and differential sedimentation mechanisms

The value of β for transport mechanism is given as (Von Smoluchowski, 1917).

$$\beta_{BR} = \frac{8}{3}\varepsilon_p \frac{K_B T}{\eta} \quad (13)$$

Where ε_p is collision efficiency

η is the viscousity of effluent medium

K_B is boltzman's constant (*J/K*)

T is absolute temperature (*K*)

The general equation representing aggregation rate of particles is obtained by solving the combination of equation (12) and (13) to yield

$$-\frac{dN_t}{dt} = KN_t^{\alpha} \quad (14)$$

Where N_t is total particle concentration at time *t*, $N_t = \sum n_t$ (*mass/volume*)

K is the α[th] order coagulation-flocculation constant

α is the order of coagulation-flocculation

And $k = ½\ \beta_{BR}$ (15)

Also $\beta_{BR} = 2\ \varepsilon_p\ K_R$ (16)

Combining equations (14), (15) and (16) yields

$$-\frac{dN_t}{dt} = \varepsilon_p\ K_R\ N_t^{\alpha} \quad (17)$$

Where K_R is the Von Smoluchowski rate constant for rapid coagulation (FridKhberg, 1984)

But $K_R = 8\pi R_o D^1$ (18)

Where R_o is particle radius

D^1 is diffusion coefficient for intending flocculating particles *i* and *j*

$$R_p = R_i + R_j \quad (19)$$

Where R_p is relative particle radius for R_i and R_j

Putting $R_i = R_o$ and $R_j = R_o$

Equation (19) transposes to $R_p = 2R_o$ (20)

Recall from equation (11)

$$D^1 = \frac{k_B T}{B}$$

And from stokes equation $B = \frac{F}{V}$ (21)

Where K_B – is Boltzman's constant (*J/K*)

T – is absolute temperature (*K*)

$V-$ is the velocity acquired by potential aggregating particles under the influence of stiochastic force (as result of heat and stirring of the system).

But for a solid sphere of radius R_o , the stokes equation gives

$$B = 6\pi\eta R_o \quad (22)$$

Where η is viscosity of coagulating and flocculating medium.

Combing equations (17) to (22) produce:

$$-\frac{dN_t}{dt} = \frac{4}{3}\varepsilon_p \frac{K_B T}{\eta} N_t^{\alpha} \quad (23)$$

Comparing equations (14) and (23) show that

$$K = \frac{4}{3}\varepsilon_p \frac{K_B T}{\eta} \quad (24)$$

For microkinetic aggregation, α theoretically equals 2 (Hunter, 1993, Menkiti and Onukwuli, 2010)

From fick's law,

$$J_f = D^1\ 4\pi\ R_p^{\ 2} \frac{dN_t}{dR} \quad (25)$$

Where J_f is flux

Re-arranging and integrating equation (25) at initial conditions $N_t = 0,\ R = 2R_o$.

$$\frac{J_t}{4\pi}\frac{dR_p}{R_p^2}\int_o^{R_p} dR_p = \int_{N_o}^{N_t} d\,N_t \quad (26)$$

Thus $J_f = 8\pi D^1 R_o N_o$ (27)

Generally, for particle of same size under the influence of Brownian motion.

The initial rate of coag-flocculation is

$$-\frac{dN_t}{dt} = J_t\ \varepsilon_p\ N_o \quad (28)$$

Substituting equations (21), (22) and (27) into (28) yields

$$-\frac{dN_t}{dt} = \frac{4}{3}\varepsilon_p \frac{k_B T}{\eta} N_o^2 \quad (29)$$

Similarly

$$-\frac{dN_t}{dt} = \frac{4}{3}\varepsilon_p \frac{k_B T}{\eta} N_t^2 \quad \text{at t > o}$$

Hence equation (29) has confirmed α =2

For α =2, equation (14) transposed to

$$\frac{dN_t}{dt} = KN_t^{\alpha} \quad (30)$$

Re-arranging and integrating equation (30) yields

Integrating

$$\int_{N_o}^{N_t} \frac{dN_t}{N_t} = -K\int_0^t dt \quad (31)$$

Thus $$\frac{1}{N_t} = Kt + \frac{1}{N_o} \quad (32)$$

Plot of $\frac{1}{N}$ vs t gives a slope of K and intercept of $\frac{1}{N_o}$

On evaluation of equation (32), $\tau_{1/2}$ (Coagulation period) can be determined.

$$N_t = \frac{N_o}{1 + \left(\frac{t}{\frac{1}{NoK}}\right)} \quad (33)$$

Where $\tau = \left(\frac{1}{NoK}\right)$ (34)

Substituting equation (34) into (33) yields

$$N_t = \frac{N_o}{1 + \left(\frac{t}{\tau}\right)} \quad (35)$$

As $t = \tau$ equation (34) transpose to;

$$N_t = \frac{N_o}{2} \quad (36)$$

Similarly

$N_t = 0.5N_o$

As $N_o \rightarrow 0.5\ N_o$; $\tau \rightarrow \frac{\tau}{2}$,

Hence equation (33) becomes

$$\frac{\tau}{2} = (0.5N_oK)^{-1} \quad (37)$$

For a coagulation period, where total number of concentration N_t is halves, solving equation (12) results in the general expression for particle of m^{th} order.

$$\frac{N_m(t)}{N_o} = \frac{\left[\frac{KN_o t}{2}\right]^{m-1}}{\left[1 + \frac{KN_o t}{2}\right]^{m+1}} \quad (38)$$

Recall; $\frac{\tau}{2} = \frac{NoK}{2}$ or $(0.5N_oK)^{-1}$

For single particle (m = 1)

$$\frac{N_1 t}{N_o} = \frac{1}{\left(1 + \left[\frac{KN_o t}{2}\right]\right)^2} \quad (39)$$

$$\therefore N_1 t = N_o \frac{1}{\left(1 + \left[\frac{KN_o t}{2}\right]\right)^2} \quad (40)$$

For double particles (m = 2)

$$\frac{N_2 t}{N_o} = \frac{\left[\frac{KN_o t}{2}\right]^2}{\left(1 + \left[\frac{KN_o t}{2}\right]\right)^3} \quad (41)$$

$$\therefore N_2 t = N_o \left[\frac{KN_o t}{2}\right]^2 \Big/ \left(1 + \left(\frac{KN_o t}{2}\right)\right)^3 \quad (42)$$

For triple particles (m = 3)

$$\frac{N_3 t}{N_o} = \left[\frac{KN_o t}{2}\right]^3 \Big/ \left(1 + \left(\frac{KN_o t}{2}\right)\right)^4 \quad (43)$$

$$\therefore N_3 t = N_o \left[\frac{KN_o t}{2}\right]^3 \Big/ \left(1 + \left(\frac{KN_o t}{2}\right)\right)^4 \quad (44)$$

Finally, the evaluation of coag-flocculation efficiency or coag-flocculant performance of the process was obtained by applying the relation below.

$$E_{I,j}(\%) = \left(\frac{N_o - N_t}{N_o}\right) x\,100 \quad (45)$$

APPENDIX B: PRESENTATION OF EFFICIENCY TABLES FOR PIE

Table B1: Efficiency of SSC in PIE at varying dosage and pH of 1 (To = 920 mg/l)

2	26.52	44.78	40.00	48.70	58.70	64.35	62.17
4	81.30	59.57	58.70	72.17	59.35	78.59	62.61
6	86.97	70.00	85.65	83.91	65.22	84.78	63.04
10	83.91	71.74	86.09	84.78	67.83	87.39	63.91
20	86.52	74.78	87.83	86.52	67.39	88.70	68.7
30	86.09	76.96	89.13	87.83	72.61	88.70	69.57
40	85.22	77.39	90.00	87.39	66.96	90.43	70.87

TableB2: Efficiency of SSC in PIE at varying dosage and pH of 5 (To = 1840 mg/l)

Time (Mins)	E_1(%)	E_2(%)	E_3(%)	E_4(%)	E_5(%)	E_6(%)	E_7(%)
2	59.78	60.65	54.78	59.78	41.74	36.96	23.91
4	60.43	60.87	55.22	60.00	45.00	41.30	26.96
6	60.87	60.65	56.09	60.43	46.52	43.30	31.30
10	60.00	69.53	58.48	60.65	46.96	42.83	35.43
20	59.57	61.74	60.43	68.48	51.96	56.85	39.57
30	60.00	65.00	58.04	61.52	59.78	57.17	43.92
40	66.96	64.78	58.26	50.65	60.65	51.30	46.30

Table B3:Efficiency of SSC in PIE at varying dosage and pH of 7 (To = 1380 mg/l)

Time (Mins)	E_1(%)	E_2(%)	E_3(%)	E_4(%)	E_5(%)	E_6(%)	E_7(%)
2	71.88	57.83	54.35	22.61	19.28	23.91	25.80
4	76.38	65.36	68.12	25.07	41.59	40.43	42.03
6	77.39	73.48	70.87	42.32	52.32	57.25	57.25
10	80.72	76.23	77.25	55.51	65.94	63.48	67,97
20	83.91	82.61	81.01	68.99	75.51	73.77	78.84
30	85.80	84.06	83.48	74.49	79.57	76.81	82.17
40	87.35	85.65	85.22	77.10	81.13	79.13	84.35

Table B4: Efficiency of SSC in PIE at varying dosage and pH of 10 (To = 1380 mg/l)

Time (Mins)	E_1(%)	E_2(%)	E_3(%)	E_4(%)	E_5(%)	E_6(%)	E_7(%)
2	52.46	25.80	46.67	25.36	20.72	13.33	24.78
4	66.96	60.87	59.86	45.80	41.01	30.29	45.36
6	76.81	70.00	66.23	55.65	59.28	41.74	58.55
10	80.87	74.35	69.86	63.77	69.42	62.90	71.88
20	84.35	80.14	74.78	68.99	75.22	66.81	78.99
30	85.51	81.30	77.10	72.32	77.97	72.03	83.48
40	86.38	82.17	77.39	74.06	79.57	73.04	83.19

Table B5: Efficiency of SSC in PIE at varying dosage and pH of 13 (To = 2070 mg/l)

Time (Mins)	E_1(%)	E_2(%)	E_3(%)	E_4(%)	E_5(%)	E_6(%)	E_7(%)
2	38.36	34.40	35.27	21.55	31.01	25.22	13.72
4	85.12	73.43	69.18	55.56	63.77	49.95	33.43
6	86.67	86.38	81.45	66.76	72.37	57.29	41.55
10	88.31	88.50	82.32	69.18	75.65	56.04	43.86
20	87.63	89.57	82.42	73.53	76.43	61.55	48.60
30	90.82	89.76	84.54	76.14	80.00	64.35	50.92
40	89.57	91.30	85.70	77.78	81.16	68.21	52.27

APPENDIX C: PRESENTATION OF EFFICIENCY TABLES FOR VIE

Table C1: Performance Efficiency of MPSC in VIE at Varying dosage and pH of 1 (To = 1380 mg/l)

Time (Mins)	E_1(%)	E_2(%)	E_3(%)	E_4(%)	E_5(%)	E_6(%)	E_7(%)
2	72.33	76.67	70.33	38.00	46.33	42.67	44.00
4	77.67	73.67	71.67	46.67	55.33	46.67	46.67
6	74.33	72.33	73.00	55.00	62.67	55.00	52.67
10	74.33	77.00	75.33	62.00	68.67	61.33	61.00
20	80.33	72.00	76.33	67.00	67.67	65.33	64.67
30	97.55	76.67	77.67	68.33	63.67	69.00	66.67
40	81.67	68.67	79.33	66.33	63.00	69.67	68.67

Table C2: Performance Efficiency of MPSC in VIE at Varying dosage and pH of 3 (To = 1380 mg/l)

Time (Mins)	E_1(%)	E_2(%)	E_3(%)	E_4(%)	E_5(%)	E_6(%)	E_7(%)
2	69.67	59.33	53.33	39.33	32.00	21.83	22.33
4	76.33	64.33	60.33	54.33	43.33	39.00	51.67
6	81.67	68.67	69.00	62.00	66.67	63.33	72.33
10	81.67	73.67	72.33	73.33	74.00	70.67	81.33
20	84.33	80.33	77.33	79.33	79.67	79.00	81.33
30	86.00	83.00	76.00	79.67	80.00	77.33	80.67
40	88.00	86.33	73.33	77.67	79.33	79.33	76.32

Table C3: Performance Efficiency of MPSC in VIE at Varying dosage and pH of 5 (To = 920 mg/l)

Time (Mins)	E_1(%)	E_2(%)	E_3(%)	E_4(%)	E_5(%)	E_6(%)	E_7(%)
2	56.50	57.25	34.50	33.75	31.75	26.00	13.00
4	60.25	69.75	42.50	43.50	45.00	29.00	16.09
6	60.50	73.75	48.75	51.00	48.25	31.25	33.50
10	64.25	75.75	51.50	52.00	58.50	34.75	37.50
20	69.50	77.50	52.75	61.25	64.00	33.75	47.25
30	65.75	75.00	46.00	55.25	61.50	36.00	54.00
40	63.50	75.00	49.25	62.75	59.50	39.75	54.00

Table C4: Performance Efficiency of MPSC in VIE at Varying dosage and pH of 7 (To = 920 mg/l)

Time (Mins)	E_1(%)	E_2(%)	E_3(%)	E_4(%)	E_5(%)	E_6(%)	E_7(%)
2	76.00	90.50	84.50	80.00	44.50	29.50	19.50
4	75.00	91.00	87.00	84.00	52.50	39.00	42.50
6	77.50	91.00	89.50	86.50	62.50	45.00	48.00
10	82.50	92.50	90.00	87.00	74.50	50.50	51.50
20	80.00	90.50	91.50	90.50	78.50	55.00	55.50
30	81.50	90.50	91.50	90.00	81.50	59.00	58.00
40	86.00	90.50	90.50	88.00	77.50	68.50	69.50

Table C5: Performance Efficiency of MPSC in VIE at Varying dosage and pH of 10 (To = 920 mg/l)

Time (Mins)	E_1(%)	E_2(%)	E_3(%)	E_4(%)	E_5(%)	E_6(%)	E_7(%)
2	84.50	70.00	72.50	57.00	53.50	48.00	12.50
4	87.00	75.00	78.00	60.00	65.00	44.50	26.00
6	88.00	77.50	80.50	65.00	69.00	47.50	45.00
10	88.00	81.00	83.00	68.50	71.50	58.50	45.00
20	88.50	83.00	86.00	74.00	75.50	68.00	58.00
30	89.50	84.00	86.50	77.50	79.00	69.50	64.00
40	89.50	85.00	87.00	79.50	80.00	72.00	67.00

Table C6: Performance Efficiency of MPSC in VIE at Varying dosage and pH of 13 (To = 460 mg/l)

Time (Mins)	E_1(%)	E_2(%)	E_3(%)	E_4(%)	E_5(%)	E_6(%)	E_7(%)
2	70.00	81.00	66.00	66.00	62.00	60.00	87.50
4	73.00	81.00	72.00	73.50	63.00	62.50	88.00
6	78.00	84.00	77.00	74.50	64.50	71.50	91.00
10	78.00	85.00	84.50	83.00	70.00	73.00	91.00
20	80.00	86.00	82.50	84.50	69.00	79.50	94.50
30	82.00	87.00	85.50	86.50	72.50	82.50	91.50
40	81.00	88.00	86.50	87.00	73.50	85.00	94.50

APPENDIX D: COMPARATIVE ADSORPTION TABLES FOR PIE AND VIE

PIE

	BFHA at 25^{0}C	RHA at 25^{0}C	LATERITE at 25^{0}C	UCA at 25^{0}C	MSA at 25^{0}C	CACA at 25^{0}C	BFHA at 35^{0}C	RHA at 35^{0}C	LATERITE at 35^{0}C	UCA at 35^{0}C	MSA at 35^{0}C	CACA at 35^{0}C
5	84.6762	86.0932	87.0397	89.8695	80.2156	88.6007	74.3276	77.8006	87.1322	88.4859	88.3193	82.0882
10	86.2505	87.9297	88.2973	90.9474	81.9956	89.6837	76.5315	79.6383	88.4286	89.2699	82.997	83.8392
15	87.72	89.6616	89.5415	92.2067	84.6764	90.826	78.7986	81.1078	90.2652	90.9474	84.6218	87.9742
20	90.1339	91.445	90.3963	93.3377	87.0357	91.826	81.1604	82.6295	91.1572	92.2856	85.8309	86.0408
25	91.5477	92.758	91.656	94.5685	89.0854	93.3238	83.3644	84.8861	92.3119	93.0992	87.2277	87.7431
30	92.8995	94.0172	93.1778	95.4997	90.7637	94.574	85.3585	86.749	93.5713	94.24	89.0573	89.3724
35	94.1749	95.145	94.2167	96.3789	92.4487	95.671	87.4838	85.4635	94.7782	95.4213	90.8425	90.8994
40	96.475	95.519	94.49	90.3441	97.366	96.375	96.377	95.227	92.364	89.465	96.565	95.384

VIE

	BFHA at 25^{0}C	RHA at 25^{0}C	LATERITE at 25^{0}C	UCA at 25^{0}C	MSA at 25^{0}C	CACA at 25^{0}C	BFHA at 35^{0}C	RHA at 35^{0}C	LATERITE at 35^{0}C	UCA at 35^{0}C	MSA at 35^{0}C	CACA at 35^{0}C
5	48.8633	56.5907	32.2102	54.0913	4.2966	54.8484	-0.0091	-0.0055	-6.5473	2.6132	-0.3189	8.0677
10	57.727	64.2421	41.8181	61.5145	13.6145	63.4089	10.1661	12.6786	4.5299	16.4543	-0.132	19.0899
15	62.2496	70.2271	48.5562	67.0074	24.2208	69.5831	22.2752	22.4205	16.8633	25.8484	4.4245	28.939
20	73.7496	75.6437	54.7722	71.3209	36.6663	74.9772	32.4592	35.3176	29.6362	35.436	6.1818	38.8635
25	78.3508	78.9016	60.5903	74.7769	43.6634	80.4761	43.3331	45.3407	42.6592	43.5254	29.2292	46.5941
30	84.0906	82.5942	67.8785	77.324	51.1909	84.7726	57.9467	54.2938	52.712	52.2723	41.8999	55.9998
35	89.1475	86.5527	73.8556	81.1955	58.36	89.4885	59.3329	63.4648	60.6463	60.1889	52.3692	62.2343
40	90.629	84.316	91.208	88.151	93.818	90.718	90.4921	81.44	91.257	86.091	92.629	90.941

APPENDIX E: PRESENTATION OF POLYNOMIAL COEFFICENTS

Table E1: Coeffluents of process models for DOE and various coag-flocculants in PIE.

Sample	b_o	b_1	b_2	b_3	b_{12}	b_{13}	b_{23}	b_{11}	b_{22}	b_{33}
MPSC	341.6690	-166.5500	106.9000	-273.6000	-350.8750	-11.1875	30.1250	-9.0458	-24677.7079	92236.2411
SSC	355.9577	297.0000	291.4000	-876.4500	297.1250	-575.8125	-763.8750	1212.7040	-7284.9980	1358907.0820
TOSC	415.3239	48.0500	546.000	-896.4000	118.5000	-94.8750	- 240.7500	399339.4429	-85927.4247	57863.9657
PTSC	338.1338	-23.6500	276.7000	-1035.000	-1.2500	-397.1250	-772.5000	9004.2639	24580.4701	95.582.3260
ALUM	842.6338	-30.7000	174.9000	-227.7000	65.1250	-9.9384	13.1250	-117895.5402	14588.1949	58526.4476

Table E2: Coeffluents of process models for DOE and various coag-flocculants in VIE.

Sample	b_o	b_1	b_2	b_3	b_{12}	b_{13}	b_{23}	b_{11}	b_{22}	b_{33}
MPSC	158.81130	-191.1800	122.6300	-249.9750	-178.4124	143.5314	-147.8628	2838.7903	3482.2509	15280.8907
SSC	319.7937	207.2300	116.8200	-239.2350	51.5876	-254.1936	-96.8622	2106.6815	-3113.9525	692.7845
COSC	603.8208	62.9060	578.8780	-501.0480	18.3226	17.9964	-836.0928	-16547.3491	-35881.0729	629944.6098
TOSC	676.4683	179.5100	1040.1600	-370.2450	332.1874	505.7814	-306,2628	47151.0825	1205573.2560	1534987.1910
PTSC	269.2197	-51.9950	16.1500	-161.8500	6.8624	101.8314	-341.4378	-6.2976	-9943.8961	141900.2531
ALUM	172.9430	-48.4800	27.0400	-111.9750	65.7500	- 63.5250	-45.4500	385.6236	6.1236	1192.7946

APPENDIX F: PRESENTATION OF POLYNOMIAL COEFFICENTS

Table F1: Coefficients of process models for DOE and various adsorbents in PIE.

Sample	b_o	b_1	b_2	b_3	b_{12}	b_{13}	b_{23}	b_{11}	b_{22}	b_{33}
BFHA	14.4240	0.3683	-3.2394	-11.5930	0.1306	-1.0551	0.2699	-0.5857	0.2480	5.3363
RHA	11.4430	-0.2670	-3.9872	-10.8170	-0.1112	-0.0768	0.7588	1.0287	0.2148	5.0086
LATERITE	8.6580	-0.19608	-2.5524	-9.2663	0.79274	-0.50175	-0.1785	3.8357	3.0183	3.3957
UCA	3.6878	1.0503	-2.4313	-9.5212	-0.5847	-0.0663	0.2795	7.7867	0.8826	3.1892
MSA	18.3510	0.5694	-4.9973	-15.6510	-0.3138	0.1285	0.5678	-0.8720	0.5429	5.3907

Table F2: Coefficients of process models for DOE and various adsorbents in VIE.

Sample	b_o	b_1	b_2	b_3	b_{12}	b_{13}	b_{23}	b_{11}	b_{22}	b_{33}
BFHA	12.0940	8.7895	-12.6230	-36.3200	-7.1104	-4.5939	5.0714	6.3805	4.9235	29.0030
RHA	24.1900	0.4371	-10.9430	-30.864	1.6212	5.5383	4.8350	1.0954	2.5612	19.6180
LATERITE	23.4660	-31.9910	-12.7600	-38.5410	4.1181	18.1220	2.8761	31.1600	-2.5112	16.041
UCA	43.5590	-6.1186	-12.4560	-31.9320	3.5258	3.8934	3.1986	-1.6026	1.2869	9.2901
MSA	67.787	-16.7860	-19.8350	-64.5620	13.3030	9.9003	2.3308	37.0000	3.7210	20.6090

APPENDIX G: PRESENTATION OF STATISTICAL MODEL EQUATIONS

Table G1: Statistical tests and model for DOE and various coag-flocculants in PIE

Sample	Pval	Fstat	Model Equations
SSC	0.0004371	18.533	y=355.9577+297.0000*x1+145.7000*x2-292.1500*x3+148.5625*x1.*x2 191.9375*x1.*x3+127.3125*x2.*x3+34.8239*x1.^2-42.6761*x2.^2+388.5739*x3.^2;
PTSC	0.045954	3.805	y=338.1338-23.6500*x1+138.3500*x2-345.0000*x3-0.6250*x1.*x2-132.3750*x1.*x3-128.750*x2.*x3+94.8908*x1.^2+78.3908*x2.^2+91.6408*x3.^2;
MPSC	0.017053	5.5564	y=341.6690-166.5500*x1+53.4500*x2-273.6000*0-175.4375*x1.*x2-11.1875*x1*0+15.0625*x2*0-3.0458*x1.^2-78.5458*x2.^2+303.7042*0^2;
ALUM	0.49328	1.0352	y=842.6338-30.700*x1+87.4500*x2-75.900*x3+32.56250*x1.*x2-3.3128*x1.*x3+2.18750*x2.*x3-343.3592*x1.^2+60.3908*x2.^2+80.6408*x3.^2;

Table G2: Statistical tests and model for DOE and various coag-flocculants in VIE

Sample	Pval	Fstat	Model Equations
SSC	0.0013473	13.043	y=319.7937+207.2300*x1+58.410*x2-79.7450*x3+25.7938*x1.*x2-84.7312*x1.*x3-16.1437*x2.*x3+45.8986*x1.^2-27.9014*x2.^2+8.7736*x3.^2;
PTSC	0.12324	2.4695	y=269.2197-51.9950*x1+8.0750*x2-53.9500*x3+3.4312*x1.*x2+33.9438*x1.*x3-56.9063*x2.*x3-2.5095*x1.^2-49.8595*x2.^2+125.5655*x3.^2;
MPSC	0.0038723	9.2696	y=158.8113-191.1800*x1+61.3150*x2-83.3250*x3-89.2062*x1.*x2+47.8438*x1.*x3-24.6438*x2.*x3+53.2803*x1.^2+29.5053*x2.^2+41.2053*x3.^2;
ALUM	0.16754	2.1171	y=172.9430-48.4800*x1+13.52*x2-37.3250*x3+32.875*x1.*x2-21.175*x1.*x3-7.575*x2.*x3+19.6373*x1.^2+1.2373*x2.^2+11.5123*x3.^2;